ACTA CHIMICA

ACADEMIAE SCIENTIARUM HUNGARICAE

TOMUS 108 FASCICULUS 1

AKADÉMIAI KIADÓ, BUDAPEST

1981

ACTA CHIM. ACAD. SCI. HUNG. ACASA2 108 (1) 1–101 (1981)

ACTA CHIMICA

A MAGYAR TUDOMÁNYOS AKADÉMIA KÉMIAI TUDOMÁNYOK OSZTÁLYÁNAK IDEGEN NYELVŰ KÖZLEMÉNYEI

Acta Chimica is a journal for the publication of papers on all aspects of chemistry in English, German, French and Russian.

Acta Chimica is published in 3 volumes per year. Each volume consists of 4 issues of varying size.

Manuscripts should be sent to

Acta Chimica
Budapest, P.O. Box 67, H-1450, Hungary

Correspondence with the editors should be sent to the same address. Manuscripts are not returned to the authors.

Hungarian subscribers should order from Akadémiai Kiadó, 1363 Budapest, P.O. Box 24. Account No. 215 11488.

Orders from other countries are to be sent to "Kultura" Foreign Trading Company (H-1389 Budapest 62, P.O. Box 149. Account No. 218 10990) or its representatives abroad.

ACTA CHIMICA

ACADEMIAE SCIENTIARUM HUNGARICAE

TOMUS 108

AKADÉMIAI KIADÓ, BUDAPEST

1981

ACTA CHIMICA

TOMUS 108

Fasciculus 1
Fasciculus 2
Fasciculus 3
Fasciculus 4

INDEX

Acta Chimica Academiae Scientiarum Hungaricae, Tomus 108 (1), pp. 1—7 (1981)

KINETISCHE UNTERSUCHUNG DER SOLVOLYSEBESTÄNDIGKEIT VON KALIUMDIPHENYLDISELENOPHOSPHAT

A. I. Busev, N. T. Jacimirskaja und P. Nenning*

(Chemische Fakultät der Lomonossov-Universität Moskau und Sektion Chemie der Karl-Marx-Universität Leipzig)

Eingegangen am 7. März 1980

Zur Veröffentlichung angenommen am 29. Juli 1980**

In dieser Arbeit wird die Solvolyse von Kaliumdiphenyldiselenophosphat diskutiert. Nach Charakteristik des Reagenz' durch NMR- und IR-Spektren wird die Dissoziationskonstante der Diphenyldiselenophosphorsäure zu $(1{,}0 \pm 0{,}1) \cdot 10^{-2}$ mol /L in CH_3OH bzw. $(2{,}8 \pm 0{,}6) \cdot 10^{-2}$ mol/L in C_2H_5OH indirekt bestimmt. Der Solvolysemechanismus der Diaryldiselenophosphate wird angegeben.

Kaliumdiphenyldiselenophosphat $(C_6H_5O)_2P(Se)SeK$ (DSP) ist ein neues, selenhaltiges organisches Reagenz — vergleichbar Salzen der Dithiophosphorsäuren [1—5], die in der Analytik weit verbreitet sind und zur extraktionsphotometrischen Bestimmung einer Reihe von Elementen benutzt werden. Es ist bekannt, daß in aliphatischen Alkoholen in der Wärme und in Anwesenheit geringer Mengen Salzsäure eine Umesterung von Diaryldiselenophosphaten stattfindet [6]. Sehr wahrscheinlich finden analoge Prozesse auch in wäßrigen Lösungen statt.

Nun ist aber die spektrophotometrische und extraktionsphotometrische Bestimmung einer Reihe Elemente unter Verwendung von Diphenyldiselenophosphat nur in Anwesenheit von Mineralsäuren möglich. Deshalb ist die Kinetik der säurekatalysierten Solvolyse des Reagenzes in aliphatischen Alkoholen von Interesse. Auf der Grundlage der von uns erhaltenen Ergebnisse können Schlüsse gezogen werden über den Mechanismus der Solvolyse der Diaryldiselenophosphate, auch kann indirekt die Dissoziationskonstante der Diphenyldiselenophosphorsäure bestimmt werden, die wegen deren Instabilität [6] nicht unmittelbar gemessen werden kann.

Experimenteller Teil

Methanol und Äthanol werden nach [7] gereinigt. Der Wassergehalt der Lösungsmittel wird IR-spektroskopisch bestimmt. Methanol und Äthanol enthalten $\leq 0{,}05\%$ bzw. $0{,}1\%$ H_2O. Das Kaliumdiphenyldiselenophosphat wurde für uns am Lehrstuhl für organische Chemie der Staatsuniversität Lwow hergestellt. Es wird aus Aceton mit Benzol umgefällt [*F* 170 °C (Z.)], seine Konzentration in Lösung wird jodometrisch bestimmt.

Die Absorbanz der Lösungen wird am HITACHI EPS-3 gemessen in thermostatierter Kammer bei 25 °C. IR-Spektren liefert das IR 10, bei Verwendung von KBr-Tabletten. NMR-Spektren werden aufgenommen am WH 90 in D_2O.

* Korrespondenz bitte an diesen Autor richten.

** Die endgültige Form angenommen am 12. Dezember 1980.

Das NMR-Spektrum des Kaliumdiphenyldiselenophosphates (DSP) in D_2O bei 90 Megeherz ist ein Singulett bei $\delta = 2{,}6$ ppm, bezogen auf Wasser und 7,6 ppm, bezogen auf Tetrai methylsilan. Diese Adsorption kann Protonen der Phenylringe zugeschrieben werden, für da- ein Resonanzsignal im Gebiet $\delta = 6{,}5-8{,}0$ ppm typisch ist [8].

Im IR-Spektrum des DSP fallen zwei Absorptionsbanden im Bereich 610—520 cm^{-1} auf. Nach [9—12] sind diese zwei Banden der asymmetrischen und der symmetrischen Schwingung der >P-(Se)Se-Gruppe des Diphenyldiselenophosphates zuzuordnen. Das Auftreten dieser Frequenzen ist durch die zwei Resonanzformen

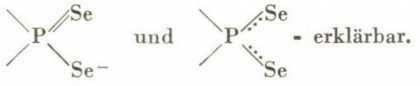

- erklärbar.

Eine ähnliche Resonanz beobachtet man beim Diäthyldiselenophosphat und *O*, *O*-Dimethyldithiophosphat.

Ergebnisse

Abb. 1 zeigt die Veränderung des Adsorptionsspektrums einer DSP-Lösung in Äthanol, die 0,15 *M* an HCl ist, in Abhängigkeit von der Zeit. Mit Zeitablauf wächst der Produktanteil, der bei 275 nm ein Adsorptionsmaximum

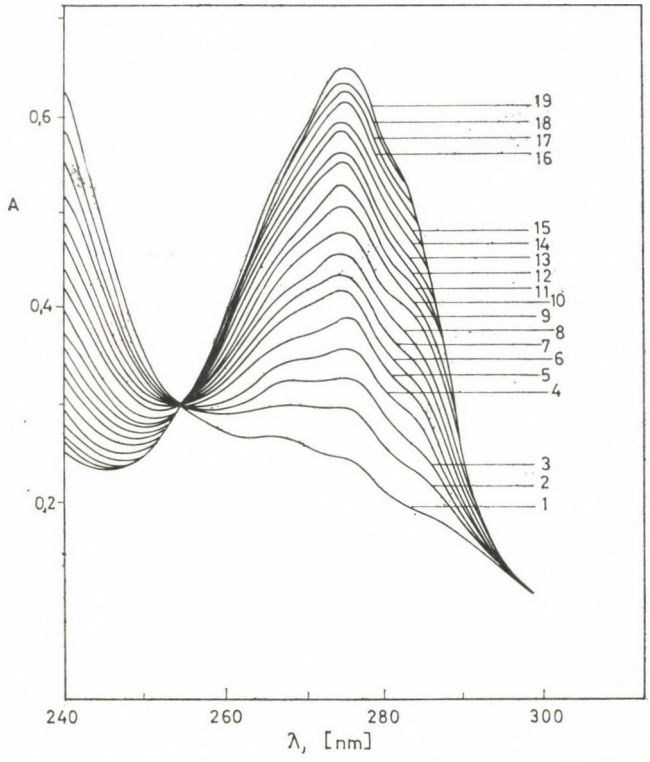

Abb. 1. Absorptionsspektren einer äthanolischen Kaliumdiphenyldiselenophosphatlösung ($1 \cdot 10^{-4}$ mol/L; 0,15 *M* an HCl) nach 1) 2; 2) 4,5; 3) 6,1; 4) 8,3; 5) 10,5; 6) 12,1; 7) 14,8; 8) 15,5; 9) 17,2; 10) 20,5; 11) 22,5; 12) 25,3; 13) 27,3; 14) 31,1; 15) 34,4; 16) 40,4; 17) 44,6; 18) 45,2; 19) 59,5 min nach Herstellen der Lösung

hat. Die Adsorptionsbande entspricht nach Lage und Form der des Phenols in Äthanol ($\lambda = 275$ nm, $\varepsilon = 2 \cdot 10^3$). Das wiederum stimmt mit Ergebnissen aus [6] überein, wo gezeigt wird, daß in saurem Medium eine Umesterung von Diaryldiselenophosphaten stattfindet. Analog läuft eine derartige Reaktion auch in Methanol und *tert.*-Butanol ab, wie wir festgestellt haben.

Die von uns ermittelte Zerfallskinetik des DSP in Methanol und Äthanol bei unterschiedlicher HCl-Konzentration zeigt eine befriedigende Übereinstimmung der Meßwerte mit Gleichung 2, die eine Reaktionskinetik 1. Ordnung beschreibt und weist darauf hin, daß dieser Prozeß ein pseudomonomolekularer Zerfall des DSP ist.

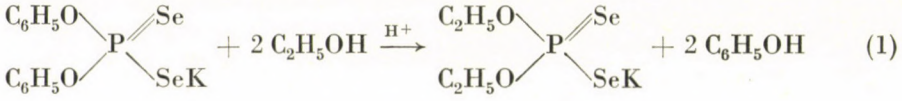

(1)

$$\lg \frac{A_\infty - A_0}{A_\infty - A_x} = \frac{1}{2{,}3} \cdot k_b \cdot t, \qquad (2)$$

wo

k_b = beobachtete Geschwindigkeitskonstante,
A_0 = Absorbanz zu Reaktionsbeginn,
A_∞ = Absorbanz zu Reaktionsende,
A_x = Absorbanz zur Zeit t.

Die Berechnung der Geschwindigkeitskonstanten k_b erfolgte einmal aus den Anfangsgeschwindigkeiten v_0 unter Verwendung der Gleichung

$$k_b = \frac{v_0}{[L_0]\Delta\varepsilon} \qquad L_0 = \text{Diphenyldiselenophosphat} \qquad (3)$$

oder grafisch nach Gleichung (2) ($k_b \sim \operatorname{tg} \alpha$). Die erhaltenen Werte für k_b sind unterschiedlich für verschiedene HCl-Konzentrationen. Die Abhängigkeit k_b von der HCl-Konzentration in CH_3OH und C_2H_5OH zeigen die Abb. 2 und 3. Der Kurvenverlauf entspricht der Protonisierung der Anionenform des DSP nach folgendem Schema:

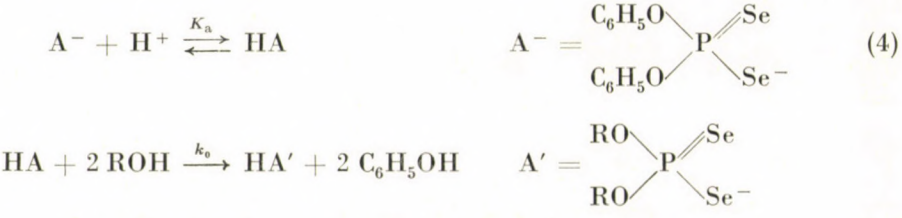

(4)

K_a = Dissoziationskonstante HA,
k_0 = Geschwindigkeitskonstante des Zerfalls der protonisierten Form

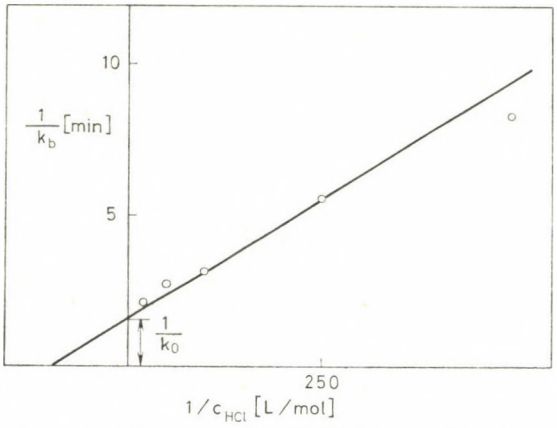

Abb. 2. Abhängigkeit k_b von c_{HCl} in CH_3OH in den Koordinaten der Gl. 6

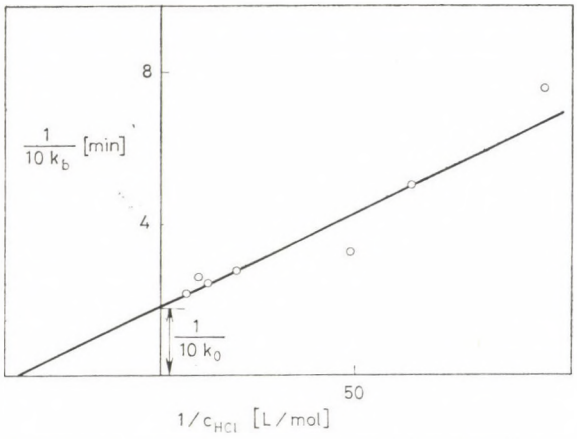

Abb. 3. Abhängigkeit k_b von c_{HCl} in C_2H_5OH in den Koordinaten der Gl. 6

des DSP — nach Pseudo — 1. Ordnung (k_0 schließt dabei konstante Lösungsmittelkonzentration ein).

In Abwesenheit von Säuren erfolgt praktisch keine Umesterung des Diphenyldiselenophosphatanions in Analogie zur Hydrolyse von Dialkyl- und Dibenzylphosphaten [14, 15]. Die Hydrolysegeschwindigkeit ist hier proportional der Konzentration der Neutralteilchen $(MeO)_2P(O)OH$ und $(ArCH_2O)_2P(O)OH$, während die Monoanionen $(MeO)_2P(O)O^-$ und $(ArCH_2O)_2P(O)O^-$ praktisch nicht hydrolysieren. Mit markierten Isotopen wurde festgestellt, daß für Arylphosphate die Hydrolyse zum Bruch der P—O-Bindung führt [15]:

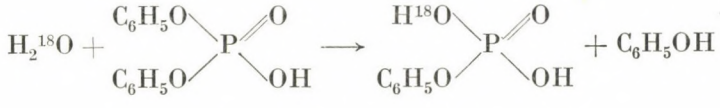

Die Gleichung zu (4) lautet:

$$k_b = \frac{k_0 [HCl]}{K_a + [HCl]} \tag{5}$$

oder linearisiert:

$$\frac{1}{k_b} = \frac{1}{k_0} + \frac{K_a}{k_0} \cdot \frac{1}{[HCl]}. \tag{6}$$

Aus der in Abb. 2 und 3 gezeigten experimentell ermittelten Abhängigkeit k_b von der HCl-Konzentration kann die Dissoziationskonstante der Diphenyldiselenophosphorsäure errechnet werden. Für CH_3OH und C_2H_5OH ist $K_a =$ $= (1{,}0 \pm 0{,}1) \cdot 10^{-2}$ mol/L bzw. $(2{,}8 \pm 0{,}6) \cdot 10^{-2}$ mol/L.

Bei der Diskussion des Solvolysemechanismus des Diphenyldiselenophosphats ist die Möglichkeit eines innermolekularen Protonenübergangs vom Selen zum Sauerstoff in Analogie zur bekannten Reaktion für Phosphorsäureester [16—19] in Betracht zu ziehen. In diesem Fall käme für die Umesterung ein monomolekularer Zerfall mit synchroner Protonisierung des Sauerstoffatoms der Substituenten in Frage:

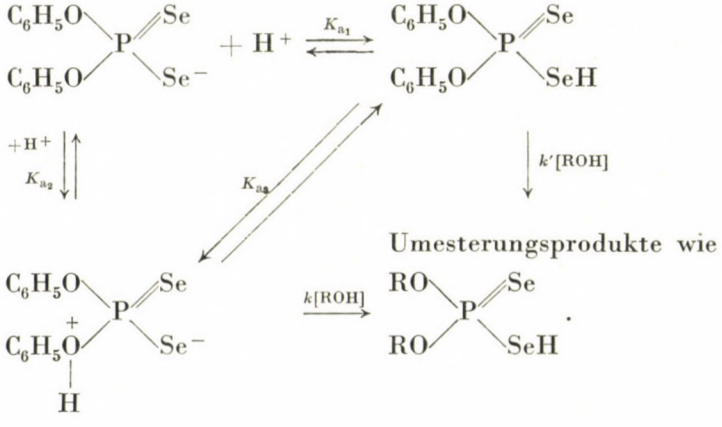

(7)

Nach Schema (7) kann k_b berechnet werden.

$$k_b = \frac{[ROH]\left(\frac{k' + k \cdot K_{a_3}}{1 + K_{a_3}}\right)[H^+]}{\frac{K_{a_1}}{1 + K_{a_3}} + [H^+]}. \tag{8}$$

Die Gleichung (8) zeigt folgendes. Wenn der Protonenübergang nach den Gleichungen (4) und (7) gering ist, d. h. wenn $K_{a_3} \ll 1$, dann ist $K_a = K_{a_1}$ und den wesentlichsten Beitrag zur Reaktion leistet der monomolekulare Zer-

fall von $(RO)_2P\begin{matrix}\diagup\!\!\!=Se\\ \diagdown SeH\end{matrix}$, der sehr wahrscheinlich durch einen nucleophilen Angriff eines aliphatischen Alkohols auf das Phosphoratom erfolgt. Unter dieser Voraussetzung ist ein Vergleich von K_a mit den Konstanten der entsprechenden schwefel- und sauerstoffhaltigen Säuren möglich.

Der pK_a-Wert des Liganden in Äthanol beträgt 1,5; der entsprechende pK_a-Wert der Diphenyldithiophosphorsäure ist 2,66 in 80%igem Äthanol [20]. Wie zu erwarten, ist die Diphenyldiselenophosphorsäure stärker als die entsprechenden schwefel- und sauerstoffhaltigen Analoga.

Allein es ist bekannt, daß die «harten» Sauerstoffatome den «harten» Protonen stärker verwandt sind als die «weichen» Selenatome [21]. Deshalb ist zu erwarten, daß in Wirklichkeit K_{a_3} wesentlich größer ist. Wenn äußerstenfalls $K_{a_3} \gg 1$, ist

$K_a = \dfrac{K_{a_1}}{K_{a_3}} = K_{a_2}$, d. h. die beobachtete Dissoziationskonstante wird hauptsächlich die Protonisierung des Sauerstoffatoms wiedergeben und den wesentlichen Beitrag zu ihrem Zahlenwert leistet der Zerfall der Zwitterionenform des Reagenzes ($k_{0,\,\text{scheinbar}} = k$). In diesem Fall wäre in Analogie zu den sauerstoffhaltigen Phosphorsäureestern [15] anzunehmen, daß die P—O-Bindung gelöst wird. Beide Mechanismen berücksichtigen den Einfluß des Alkohols auf die Reaktionsgeschwindigkeit. Die leichte Solvolyse des DSP in verdünnten Säuren (Halbwertszeit $\tau_{1/2}$ in CH_3OH, 0,01 mol/L HCl, beträgt 3 min) ist bei analytischen Arbeiten zu beachten.

LITERATUR

[1] Bode, H., Arnswald, W.: Z. anal. Chem., **185,** 99, 179 (1962); **193,** 415 (1970)
[2] Handley, Th. H., Dean, J. A.: Analyt. Chemistry, **34,** 1312 (1962); **35,** 991, 1163 (1963)
[3] Handley, Th. H.: Talanta, **12,** 893 (1965)
[4] Busev, A. I., Ivanjutin, M. I.: Trudy Komm. analit. chim. akad. nauk SSSR, **11,** 172 (1960)
[5] Busev, A. I., Ivanjutin, M. I.: J. analyt. Chem. (UdSSR), **11,** 523 (1956)
[6] Semljanski, N. I., Dsikovskaja, L. M., Turkevic, P. V., Vaskin, A. P.: J. allgem. Chemie (UdSSR), **46,** 1475 (1976)
[7] Weissberger, A., Proskauer, E., Riddis, D., Tups, E.: Organische Lösungsmittel (russ.), Moskau, Verlag für ausländische Literatur, 1958
[8] Bhacca, N. S., Williams, D. H.: Applications of NMR spectroscopy in organic chemistry, Holden-Day Inc., San Francisco, London, Amsterdam, 1964
[9] Kudchadker, M. V., Zingaro, R. A., Irgolic, K. J.: Canad. J. Chem., **46,** 1415 (1968)
[10] Jørgensen, C. K.: Molec. Phys., **2,** 309 (1959)
[11] Krishnan, V., Zingaro, R. A.: Inorg. Chem.. **8,** 2337 (1969)
[12] Zingaro, R. A.: Inorg. Chem., **2,** 192 (1963)
[13] Coppens, P., MacGillavry, C. H., Hovenkamp, S. G., Douwes, H.: Acta Cryst., **15,** 765 (1962)
[14] Bunton, C. A., Mhala, M. M., Oldham, K. G., Vernon, C. A.: J. Chem. Soc., **1960,** 3293
[15] Kumamoto, J., Westheimer, F. H.: JACS, **77,** 2515 (1955)

[16] BUNTON, C. A., LLEWELLYN, D. R., OLDHAM, K. G., VERNON, C. A.: J. Chem. Soc., **1958,** 3574
[17] BUTCHER, W. W., WESTHEIMER, F. H.: JACS, **77,** 2420 (1955)
[18] KIRBY, A. J., VARVOGLIS, A. G.: JACS, **89,** 415 (1967)
[19] KIRBY, A. J., WARREN, S. G.: The organic chemistry of phosphorus, Elsevier Amsterdam, London, New York 1967
[20] KABACNIK, M. I., MASTRJUKOVA, T. A., BALUJEVA, G. A., KUGUCEVA, E. E., SCHIPOV, A. E., MELENTJEVA, T. A.: J. allgemeine Chemie (UdSSR), **31,** 140 (1961)
[21] BASOLO, F., PEARSON, R. G.: Mechanism of Inorganic reactions, J. Wiley & Sons Inc., New York, London, Sidney 1967

Alexei Ivanovic BUSEV
Natalja Timofejevna JACIMIRSKAJA
Chemische Fakultät der Lomonossov-Universität Moskau

Peter NENNING
Sektion Chemie der Karl-Marx-Universität Leipzig, 7010 Leipzig, Liebigstraße 18., DDR

Acta Chimica Academiae Scientiarum Hungaricae, Tomus 108 (1), pp. 9–12 (1981)

TERNARY COPPER(II) COMPLEXES OF SOME PURINE DERIVATIVES USING NITRILOTRIACETIC ACID AS A PRIMARY LIGAND

R. GHOSE and K. DEY*

(*Chemical Laboratories, University of Allahabad, Allahabad*-211002, *India*)

Received June 12, 1980

Accepted for publication September 3, 1980

Ternary complexes of the type Cu-NTA-L have been investigated potentiometrically, where NTA is nitrilotriacetic acid; L is adenine, hypoxanthine, xanthine, tuanosine or xanthosine. Measurements were made in aqueous medium at 25° maintaining the ionic strength at 0.1. Binary complexes have also been examined under identical experimental conditions. The formation constants of the ternary complexes as compared to those of the corresponding binary complexes are also discussed.

Introduction

In view of the biological importance of the purines, considerable work on the formation of copper(II) complexes in solution with purine derivatives as ligands, has been reported, which has excellently been reviewed by IZATT *et al.* [1]. The stability constants of adenine and thioguanine complexes with a variety of cations have been described from these laboratories [2]. In earlier publications [3, 4] mixed ligand complexes involving the purines, and 2,2'-bipyridine or 1,10-phenanthroline have been reported. In the present work, nitrilotriacetic acid (NTA) has been used as a primary ligand for studying mixed ligand complex formation of Cu(II) with adenine (ADN), hypoxanthine (HXNT), xanthine (XNT), guanosine (GNS), and xanthosine (XNS) as secondary ligands Ni(II), Co(II), Mn(II) and Zn(II) yield opacity/turbidity and/or precipitation with the ligands and studies in solution were, therefore, not possible.

The structures of the various purines studied are given in the next page.

Results and Discussion

Calculations

To determine the formation constant of the mixed ligand complex the method of GOLDBERG [5] for binary complexes was modified for application to biligand complex formation [3]. Various parameters *viz.* $\bar{n}_H$, the average number of protons bound per free ligand ion; $\bar{n}$, average number of secondary

* To whom correspondence should be addressed.

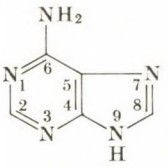

ADN

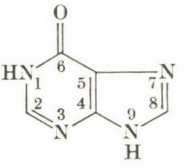

HXNT

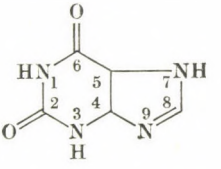

XNT

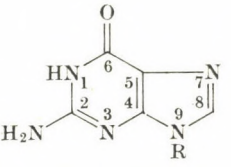

GNS

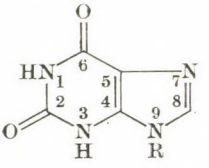

XNS

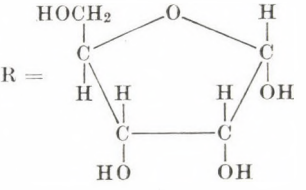

Ribose

ligands attached per $(CuNTA)^-$ complex ion; [L], free secondary ligand concentration were calculated employing the titration curves D and E *(vide infra)*.

SCHWARZENBACH *et al.* [6] observed that in 1 : 1 mixtures of a bivalent metal ion and NTA, the species is entirely $[M(NTA)]^-$, and they measured the formation constants of the $[M(NTA)]^-$ complex. It has been reported [7] that in Cu(II)—NTA system $[Cu(NTA)OH]^{2-}$ forms in an alkaline medium, but below pH 12; above pH 12 more OH^- ions get associated. The values of the formation constant obtained from the titration curves in this work (figs omitted), are reported in Table I. These are in general agreement with literature values. The associated water of copper nitrilotriacetate complex $[Cu(NTA)(H_2O)]^-$ is replaced by bidentate ligands, which are purine derivatives, during the ternary complex formation. The values of the formation constants are reported in Table I. The formation constants of the binary complexes have also been determined under the same experimental conditions as those of the ternary complexes and a comparison has been made. The values obtained here are in agreement with the constants reported earlier (Table I).

Table I

Formation constants of various complexes

Ligand	M/MNTA	Formation constants						Ref.
		Present work (25°, $\mu = 0.1$)			Literature values (25°, $\mu = 0.1$)			
		$\log K_1^*$	$\log K_2^+$	$\log K_3$	$\log K_1^*$	$\log K_2^+$	$\log K_3$	
NTA	H^+	9.60±0.01	2.45±0.02	1.78±0.01	9.65	2.48	1.8	[8]
	Cu^{2+}	12.80±0.01	—	—	12.94	—	—	[8]
ADN	H^+	9.40±0.01	4.45±0.01	—	9.83[a]	4.25[a]	—	[9]
		—	—	—	9.32[b]	4.22[b]	—	[2]
	Cu^{2+}	6.77±0.02	5.80±0.01	—	6.56[a]	5.60[a]	—	[9]
	$(CuNTA)^-$	3.77±0.02	—	—	—	—	—	—
HXNT	H^+	8.90±0.01	—	—	8.94	2.98	—	[9]
	Cu^{2+}	5.80±0.01	—	—	6.20[a]	—	—	[9]
	$(CuNTA)^-$	3.30±0.02	—	—	—	—	—	—
XNT	H^+	7.51±0.01	—	—	7.70[a]	—	—	[10]
	Cu^{2+}	—	—	—	—	—	—	—
	$(CuNTA)^-$	3.27±0.02	—	—	—	—	—	—
GNS	H^+	9.70±0.01	—	—	9.30[c]	—	—	[9]
	Cu^{2+}	5.32±0.02	—	—	6.00[c]	—	—	[9]
	$(CuNTA)^-$	3.31±0.02	—	—	—	—	—	—
XNS	H^+	5.73±0.01	—	—	5.67[c]	—	—	[9]
	Cu^{2+}	3.42±0.02	—	—	3.40[c]	—	—	[9]
	$(CuNTA)^-$	—	—	—	—	—	—	—

* $\log K_{MNTA}$ in case of formation of MNTA
$\log K_{ML}$ in case of formation of ML
$\log K_{MNTAL}$ in case of formation of MNTAL
\+ $\log K_{ML_2}$ in case of formation of ML_2

[a] at 20°, $\mu = 0.1$
[b] at 30°, $\mu = 0.1$
[c] at 20°, $\mu = 0.01$

It is noted that $\log K_{CuNTAL}$ is smaller than the first formation constant $\log K_{CuL}$ and even less than $\log K_{CuL_2}$ (in case of ADN). This may be ascribed to coulombic interactions between various ligand anionic species present. In the formation of the ternary complexes there is repulsion between one negative charge of the secondary ligand anion and three negative charges of the NTA anions. On the other hand, in the formation of CuL_2, L^- reacts with CuL^+ and there is an attractive force. Obviously, the repulsive force in the formation of Cu(NTA)L would make it less stable than CuL_2 and hence $\log K_{CuNTAL} < \log K_{CuL_2}$. The following relationship becomes obvious: $\log K_{CuL} > \log K_{CuL_2} > \log K_{CuNTAL}$.

Experimental

Materials

Reagent grade chemicals were used. Solutions of Zn(II), Cu(II), Ni(II), Co(II), and Mn(II) nitrates were prepared and standardized by complexometric titration [11]. A stock solution of NTA (Koch-Light) was prepared by dissolving accurately a weighed amount in hot water *(ca.* 40°), under vigorous shaking. Fresh solutions of ADN (E. Merck), HXNT (Reanal, Budapest), XNT (Reanal, Budapest), GNS (E. Merck), XNS (E. Merck), MCP (Fluka), TGN (Koch-Light) were prepared in 0.02 *M* alkali hydroxide.

Standard solutions of 0.2 *M* KOH, 0.02 *M* HNO_3 and 1.0 *M* KNO_3 were prepared as usual.

Procedure

An Elico pH meter (Model LI-10) reading with a precision of 0.02 pH units, with glass (EK-62 A) and calomel electrode assembly was used for pH-measurements. Calibration of pH meter was done with 0.05 *M* potassium hydrogen phthalate buffer.

To study the ternary complexes, five titrations were performed at 25°. The titrated solutions were as follows:

A. Nitric acid + potassium nitrate.
B. Mixture A + NTA.
C. Mixture B + metal nitrate solution.
D. Mixture A + secondary ligand.
E. Mixture C + secondary ligand.

The volume of each solution was 50 mL. In mixture C three equivalents of H^+ are liberated as a result of the complexation reaction. Hence in mixture D three equivalents of nitric acid were added to compensate for the reaction in C. The overall concentrations of the various solutions were: acid — 0.004 *M*; KNO_3 — 0.1 *M*; NTA — 0.002 *M*; metal nitrate — 0.002 *M*; secondary ligand — 0.002 *M*. Mixtures A, B, C, D and E were titrated potentiometrically against 0.2 *M* KOH as usual and the corresponding titration curves were obtained (25°, $\mu = 0.1$).

*

The authors are thankful for the award of a research associateship of the University Grant Commission, New Delhi, to RG.

REFERENCES

[1] Izatt, R. M., Christensen, J., Rytting, J. H.: Chem. Revs., **71,** 439 (1971)
[2] Nayan, R., Dey, A. K.: J. Indian Chem. Soc., **50,** 98 (1973)
[3] Ghose, R., Chattopadhyaya, M. C., Dey, A. K.: Indian J. Chem. (Communicated)
[4] Ghose, R., Ghose, A. K., Dey, A. K.: J. Indian Chem. Soc. (In press)
[5] Goldberg, D. E.: J. Chem. Educ., **39,** 328 (1962); **40,** 341 (1963)
[6] Schwarzenbach, G., Anderegg, G., Schneider, W., Senn, H.: Helv. Chim. Acta, **38,** 1147 (1955)
[7] Hopgood, D., Angelici, R. J.: J. Am. Chem. Soc., **90,** 2508 (1968)
[8] Critical Stability Constants, Ed. A. E. Martell, and R. M. Smith, Plenum Press, New York and London
[9] Albert, A.: Biochem. J., **54,** 646 (1953)
[10] Ogston, A. G.: J. Chem. Soc., **1935,** 1376
[11] Flaschka, H. A.: EDTA Titrations, Pergamon, Oxford, 2nd Ed., 1964

Ranjana Ghose, Arun K. Dey
Chemical Labs, University of Allahabad, Allahabad-211002, India

Acta Chimica Academiae Scientiarum Hungaricae, Tomus 108 (1), pp. 13–25 (1981)

COMPLEXES OF Co(II), Ni(II), Cu(II) AND Zn(II) WITH 3-HYDROXY-2-NAPHTHOYL HYDRAZONES OF SOME AROMATIC ALDEHYDES

M. M. OSMAN* and G. Y. ALI

(*Chemistry Department, Faculty of Science, Alexandria University, Alexandria, Egypt*)

Received July 3, 1980

Accepted for publication September 3, 1980

3-Hydroxy-2-naphthoyl hydrazones of benzaldehyde, *p*-chlorobenzaldehyde, *p*-nitrobenzaldehyde, vaniline, *o*-vaniline and salicylaldehyde together with their metal complexes have been prepared. All compounds have been characterized by chemical analysis and i.r. spectra; also by ^{1}H NMR for ligands and by electronic spectral and magnetic measurements for the complexes. Except for copper chelate with vaniline hydroxynaphthoyl hydrazone, copper and zinc compounds with *o*-vaniline and salicylaldehyde derivatives, complexes of general formula $M^{2+}(L)_2^-$ have been isolated, where M stands for Co, Ni, Cu and Zn; L^- represents deprotonated monovalent didentate or tridentate ligands. Only copper forms with vaniline derivative $Cu^{2+}L^-(OAc)^-$ where OAc^- is the acetate ion. Both Cu(II) and Zn(II) form with *o*-vaniline and salicylaldehyde naphthoyl hydrazones dimeric complexes of general formula $M(L)^{2-}$, where L^{2-} represents divalent tridentate ligand anion. The cobalt and nickel complexes, except that with vaniline hydroxynaphthoyl hydrazone, are octahedral. The latter has diamagnetic square environment. Copper and zinc compounds have square planar and distorted tetrahedral structures, respectively.

Introduction

The copper and nickel complexes with aldehydes aroyl hydrazones (1 : 1 metal to ligand compounds) become recently of industrial importance as coloring pigments of plastics [1]. Although a lot of work has been done on complexation by many aliphatic and aromatic aroyl and acyl hydrazones [2—17], no attempt has been, however, made to study the coordination chemistry of Schiff bases derived from 3-hydroxy-2-naphthoic acid hydrazide and carbonyl compounds. It was deemed desirable to prepare and study this acid hydrazones of benzaldehyde, *p*-chlorobenzaldehyde, *p*-nitrobenzaldehyde, vaniline, *o*-vaniline and salicylaldehyde; and their metal complexes with Co(II), Ni(II), Cu(II) and Zn(II).

Experimental

Preparation of the ligands

The following method was used for preparation of the ligands by direct condensation of 3-hydroxy-2-naphthoic acid hydrazide with the appropriate aldehyde. The acid hydrazide has been firstly prepared by standard methods [18].

A solution of the aldehyde (0.1 mole) in a least volume of hot ethanol was then added under stirring to a hot solution of the acid hydrazide (0.1 mole) in ethanol. The reaction mix-

* To whom correspondence should be addressed.

ture was refluxed on a water bath for 30 minutes. A yellowish product was precipitated, filtered, washed with hot ethanol and ether; and dried in vacuo at 60 °C (P_2O_5). Further purification of the ligand was done by recrystallisation from ethanol.

The ligands are hereafter referred to as "B3H2NHz, *p*-ClB3H2NHz, *p*-NO_2B3H2NHz, V3H2NHz, *o*-V3H2NHz and S3H2NHz" in the abbreviated form for the 3-hydroxy-2-naphthoyl hydrazones of benzaldehyde, *p*-chlorobenzaldehyde, *p*-nitrobenzaldehyde, vaniline, *o*-vaniline and salicylaldehyde, respectively.

Preparation of the metal complexes

All complexes were generally prepared as follows. A solution of the metal acetate (10 mmole) in 20 mL hot ethanol or methanol was added under stirring to a hot solution of the ligand (20 mmole) in 100 mL of ethanol. The complex was immediately precipitated and was digested on a water bath for 30 minutes. It was hot-filtered, washed with hot ethanol and ether, and dried in vacuo at 60 °C (P_2O_5). All complexes were insoluble in water and common organic solvents.

Analysis and physical measurements

The chemical analysis of carbon and nitrogen were done by the microanalytical techniques in the Faculty of Science, University of Cairo; and Elnasr Co. for medical chemicals, Egypt. The estimation of metals were carried out by standard complexometric titrations.

The i.r. spectra of the ligands and their complexes were done on a Unicam SP 200 infra-red spectrophotometer in the range 4000—400 cm^{-1} using potassium bromide pellets of the sample.

The ^1H NMR spectra of the organic ligands in deuterated dimethylsulfoxide were recorded at 25 °C on a Perkin-Elmer R 20-B spectrophotometer. Tetramethyl silane was used as an internal standard. The magnetic susceptibility of the complexes were determined at room temperature with a Guoy balance using cobalt(II)-tetrathiocyanato-mercurate(II) as a standard. Diamagnetic corrections were also calculated. The measurements were done in the Physics Department, Faculty of Science. Alexandria.

The absorption spectra of the complexes as nujol mull were carried out on a manual Unicam SP 600 spectrophotometer in the range of 400—1000 nm.

Results and Discussion

The analytical data of the ligands and their metal complexes are listed in Table I. The results are compatible with the suggested stoichiometries. In all complexes with B3H2NHz, *p*-ClB3H2NHz, *p*-NO_2B3H2NHz and V3H2NHz the complexed species of the ligand is the monovalent anion. Only in the case of the V3H2NHz copper complex one acetate ion enters into the coordination sphere. The complex-forming species of *o*-V3H2NHz and S3H-2NHz is, however, either the monovalent anion in case of Co(II) and Ni(II) or the divalent anion with Cu(II) and Zn(II). The ^1H NMR and i.r. measurements of the free ligands shown in Tables II and III, respectively, are not at variance with their suggested formulation. The i.r. will be discussed later in comparison with that of metal chelates.

The ^1H NMR spectra show for all phenolic protons peaks, which lie at a relatively lower magnetic field than that normally expected for a phenolic substituent. This indicate that these hydroxyl groups are hydrogen-bonded in DMSO. The phenolic group of the acid hydrazone moiety is proposed to form a 6-membered chelate ring with the (—NH—N=) group. On the other hand, the phenolic group in the aldehyde residue is presumably linked either

Table I

Analytical data, colour and m.p. of ligands and their metal complexes

Compound	Colour (M.P. °C)*	M% Found (Cal.)	N% Found (Cal.)	C% Found (Cal.)
B3H2NHz	y.			
($C_{18}H_{14}O_2N_2$)	(222—23)		9.50	74.23
			(9.95)	(74.47)
Co(B3H2NHz)$_2$	d. yellow	9.41	8.65	67.94
		(9.24)	(8.79)	(67.82)
Ni(B3H2NHz)$_2$	b. yellow	9.40	8.49	67.80
		9.21)	(8.79)	(67.84)
Cu(B3H2NHz)$_2$	p. green	10.10	8.63	67.30
		(9.90)	(8.73)	(67.33)
Zn(B3H2NHz)$_2$	p. yellow	10.18	8.68	66.90
		(10.15)	(8.70)	(67.14)
p-ClB3H2NHz	y.			
($C_{18}H_{13}O_2N_2Cl$)	(254—55)		8.52	66.78
			(8.63)	(66.57)
Co(*p*-ClB3H2NHz)$_2$	yellow	8.25	7.64	61.33
		(8.34)	(7.93)	(61.20)
Ni(*p*-ClB3H2NHz)$_2$	yellow	8.14	7.93	61.30
		(8.31)	(7.93)	(61.22)
Cu(*p*-ClB3H2NHz)$_2$	green	8.79	7.73	60.84
		(8.94)	(7.88)	(60.81)
Zn(*p*-ClB3H2NHz)$_2$	yellow	9.42	7.41	60.80
		(9.17)	(7.86)	(60.65)
p-NO$_2$B3H2NHz	yellow			
($C_{18}H_{13}O_4N_3$)	(260—61)		12.30	64.14
			(12.53)	(64.47)
Co(*p*-NO$_2$B3H2NHz)$_2$	orange	7.88	11.89	59.19
		(8.10)	(11.55)	(59.43)
Ni(*p*-NO$_2$B3H2NHz)$_2$	orange	8.40	10.90	59.63
		(8.07)	(11.56)	(59.44)
Cu(*p*-NO$_2$B3H2NHz)$_2$	y. green	9.00	11.50	59.20
		(8.68)	(11.48)	(59.05)
Zn(*p*-NO$_2$B3H2NHz)$_2$	orange	8.63	11.22	59.12
		(8.91)	(11.45)	(58.91)
V3H2NHz	y.			
($C_{19}H_{16}O_4N_2$)	(175—76)		8.33	67.55
			(8.33)	(67.85)

Table I (contd.)

Compound	Colour (M.P. °C)*	M% Found (Cal.)	N% Found (Cal.)	C% Found (Cal.)
$Co(V3H2NHz)_2 \cdot 2H_2O$	brown	7.76	7.72	59.95
		(7.70)	(7.32)	(59.61)
$Ni(V3H2NHz)_2$	orange	8.36	7.78	62.82
		(8.05)	(7.68)	(62.57)
$Cu(V3H2NHz) \cdot OAc$	green	13.51	6.62	55.11
		(13.88)	(6.12)	(55.08)
$Zn(V3H2NHz)_2$	yellow	8.91	7.63	61.90
		(8.88)	(7.61)	(62.01)
S3H2NHz	y.			
($C_{18}H_{14}O_3N_2$)	> 300		8.89	70.46
			(9.15)	(70.58)
$Co(S3H2NHz)_2$	orange	8.62	8.32	64.52
		(8.80)	(8.37)	(64.58)
$Ni(S3H2NHz)_2$	p. green	8.59	8.17	64.70
		(8.77)	(8.37)	(64.60)
Cu(S3H2NHz)	green	17.51	7.75	58.68
		(17.27)	(7.62)	(58.77)
Zn(S3H2NHz)	yellow	17.37	7.77	58.37
		(17.69)	(7.58)	(58.48)
o-V3H2NHz	y.			
($C_{19}H_{16}O_4N_2$)	(258—59)		8.49	67.60
			(8.33)	(67.85)
$Co(o\text{-}V3H2NHz)_2$	y. brown	8.30	7.70	62.60
		(8.08)	(7.70)	(62.55)
$Ni(o\text{-}V3H2NHz)_2$	y. green	7.82	7.62	62.40
		(8.05)	(7.68)	(62.57)
Cu(*o*-V3H2NHz)	green	15.67	6.70	57.55
		(15.97)	(7.04)	(57.35)
Zn(*o*-V3H2NHz)	yellow	15.92	6.73	57.03
		(16.36)	(7.01)	(57.09)

y = yellowish, d = dark, b = brownish, p = pale
* m.p. uncorrected

Table II

^1H NMR peaks of the aldehydes-3-hydroxy-2-naphthoyl hydrazones in DMSO at 25 °C in p.p.m.

Compound	Assignment					
	N=CH	O—CH_3	aromatic protons	—OH		—NH
B3H2NHz	3.20	—	7.02—7.80	8.24	—	10.90
p-ClB3H2NHz	3.28	—	7.04—8.00	8.24	—	11.30
p-NO_2B3H2NHz	3.30	—	7.10—8.30	8.40	—	11.50
S3H2NHz	3.20	—	6.70—7.68	8.38	8.62	11.20
o-V3H2NHz	3.22	3.70	6.66—7.86	8.36	8.62	10.82
V3H2NHz	3.24	3.66	6.66—7.86	8.24	8.36	11.72

Table III

Infrared spectra of the ligands and their metal complexes

Compound	Assignment				
	$\nu(OH)_f$ $\nu(OH)_d$	ν(NH)	ν(am. I)	ν(C=N)	δ(OH) in pl.
B3H2NHz	— 3490b	3260— 3080m	1680s	1660m	1180m
$Co(B3H2NHz)_2$	— 3490b	—	—	1633m	1175m
$Ni(B3H2NHz)_2$	— 3490b	—	—	1640m	1180m
$Cu(B3H2NHz)_2$	— 3490b	—	—	1635m	1175m
$Zn(B3H2NHz)_2$	— 3490b	—	—	1630m	1175m
p-ClB3H2NHz	— 3400b	3200— 3100w	1645s	1640m	1170m
$Co(p\text{-}ClB3H2NHz)_2$	— 3400b	—	—	1635m	1175m
$Ni(p\text{-}ClB3H2NHz)_2$	— 3400b	—	—	1640m	1175m
$Cu(p\text{-}ClB3H2NHz)_2$	— 3390b	—	—	1635m	1175m
$Zn(p\text{-}ClB3H2NHz)_2$	— 3400b	—	—	1635m	1175m
p-NO_2B3H2NHz	— 3450b	3230— 3120w	1660s	1640m	1175m
$Co(p\text{-}NO_2B3H2NHz)_2$	— 3450b	—	—	1630m	1170m
$Ni(p\text{-}NO_2B3H2NHz)_2$	— 3450	—	—	1630m	1175m
$Cu(p\text{-}NO_2B3H2NHz)_2$	— 3455	—	—	1630m	1175m
$Zn(p\text{-}NO_2B3H2NHz)_2$	— 3450b	—	—	1635m	1175m

Table III (contd.)

Compound	Assignment				
	ν(OH)$_f$ ν(OH)$_d$	ν(NH)	ν(am. I)	ν(C=N)	δ(OH) in pl.
V3H2NHz	3650m 3450b	3200m	1680s	1660s	1180m
Co(V3H2NHz)$_2$ · 2H$_2$O	3600m 3300b	—	—	1645s	1180m
Ni(V3H2NHz)$_2$	3660m 3450b	—	—	1645s	1180m
Cu(V3H2NHz)OAc	3660m 3450b	—	—	1650m	1180m
Zn(V3H2NHz)$_2$	3660m 3450b	—	—	1650m	1180m
o-V3H2NHz	— 3450b	3200— 3070w	1665s	1635m	1180m
Co(*o*-V3H2NHz)$_2$	— 3450b	3200— 3070w	1645m	1620m	1180w
Ni(*o*-V3H2NHz)$_2$	— 3450b	3200— 3070	1645m	1620m	1180m
Cu(*o*-V3H2NHz)	— 3450b	—	—	1620m	1185m
Zn(*o*-V3H2NHz)	— 3450b	—	—	1620m	1185m
S3H2NHz	— 3450b	3200— 3080w	1660s	1630m	1170m
Co(S3H2NHz)$_2$	— 3450b	3200— 3080w	1640m	1615m	1170m
Ni(S3H2NHz)$_2$	— 3450b	3200— 3080w	1640m	1615m	1170m
Cu(S3H2NHz)	— 3450b	—	—	1615m	1175m
Zn(S3H2NHz)	— 3450b	—	—	1615m	1175m

f = free, d = bonded, am. = amide, in pl. = in plane, b = broad, s = strong, m = medium, w = weak

to —NH—N= in *o*-V3H2NHz and S3H2NHz or to the methoxyl group in case of V3H2NHz. This conclusion could be drawn from the relative peak position of these hydroxyl groups in the aldehyde moiety, which support the fact that the hydrogen bonding ability of the phenolic group towards the methoxy group is less pronounced than that towards the nitrogen atom of the (—NH—N=) residue. The ^{1}H NMR peak observed at 11.27 $\pm$ 0.45 p.p.m., which is tentatively assigned to an exchangeable imino proton indicates that all the aldehydes-3-hydroxy-2-naphthoyl hydrazones exist in DMSO solution as an enol—keto tautomeric equilibrium. The structure of these hydrazones in DMSO can accordingly be represented as follows:

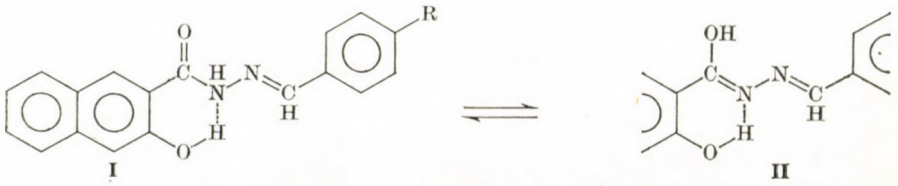

I II

B3H2NHz, *p*-ClB3H2NHz and *p*-NO_2B3H2NHz

(R=H, Cl or NO_2)

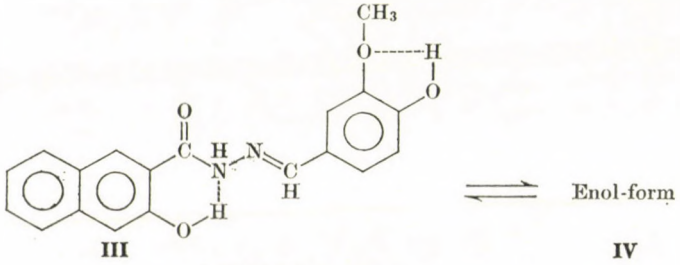

III IV

V3H2NHz

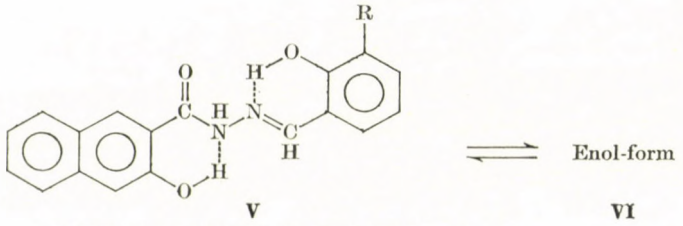

V VI

o-V3H2NHz and S3H2NHz; R=H_3CO or H

In solids, the i.r. spectra show that all hydrazones are present in the keto-form. Well-defined ligand bands at 3400—3490 and 1175 $\pm$ 5 cm^{-1} are attributed to stretching and O—H in plane deformation modes of the phenolic substituent, respectively. The stretching vibration modes of the NH group lie in the region 3070—3260 cm^{-1}. The observed lowering in the ν(OH) and ν(NH) frequencies suggest that these groups are hydrogen bonded. V3H2NHz exhibits, however, an additional band at 3650 cm^{-1}, which is tentatively assigned to the free para-phenolic substituent. The ν(OH) at 3400—3490 cm^{-1} persists in all metal chelates. It seems that one phenolic group at least is not involved in the complex formation. Since B3H2NHz, *p*-ClB3H2NHz and *p*-NO_2B3H2NHz contain the phenol substituent only in the naphthalene ring, we can conclude that this group remains unactive site for coordination with metal ions. The presence of this free hydroxyl group in complexes has also

been confirmed by its chemical reaction in dimethylformamide with iron(III)-chloride solution.

The general features of the i.r. spectra of all metal chelates with B3H2NHz, *p*-ClB3H2NHz, *p*-NO_2B3H2NHz and V3H2NHz are similar. The ligand ν(C=N) stretching vibration is negatively shifted on complexation. Both ligand ν(NH) and ν(amide I) disappear in the complexes. Coordination of the metal ions with these ligands occurs, therefore, through the azomethine nitrogen and enolate oxygen atoms. The i.r. spectra of the metal complexes with *o*-V3H2NHz and S3H2NHz can simply be differentiated into two groups. The first includes that of nickel and cobal chelates while the second has the copper and zinc complexes. In nickel and cobalt chelates, the ligands ν(C=N) and ν(amide I) are negatively shifted while ν(NH) remains unchanged. This suggests that both metal ions are linked through the carbonyl oxygen and azomethine nitrogen atoms. The charge balance is compatible with participation of the *ortho*-phenolate oxygen in coordination with the cations. On the other hand, the absence of any absorption bands due to ν(NH) and ν(amide I) in addition to the negative shift of the ligand ν(C=N) in the complexes of copper and zinc with *o*-V3H2NHz and S3H2NHz suggests that the complexed ligand is the divalent tridentate anion. The coordination sites are both the enolate and phenolate oxygens together with the azomethine nitrogen atom.

The magnetic and spectral data of the cobalt, nickel and copper complexes are given in Table IV. The magnetic moments of the cobalt(II) chelates are between 4.76 and 5.04 B.M. These values are consistent with a high-spin octahedral geometry. The electronic spectra of the cobalt compounds also confirm the octahedral environment. The weak bands observed in the regions 530—560 and 620—660 nm are tentatively assigned to the crystal field transitions $^4T_{1g}(F) \rightarrow {}^4T_{1g}(P)$ and $^4T_{1g}(F) \rightarrow {}^4A_{2g}$, respectively. The broad band in the region 935—975 nm is assigned to the transition $^4T_{1g}(F) \rightarrow {}^4T_{2g}$. The proposed octahedral structure for $Co(B3H2NHz)_2$, $Co(p\text{-}ClB3H2NHz)_2$ and $Co(p\text{-}NO_2B3H2NHz)_2$ is contradicting with the stoichiometry of these compounds and with the bidentate nature of the complex-forming agent. These are in favour of 4-coordinate geometry. The tendency of the cobalt ion to expand its coordination number from 4 to 6 may, however, be attributed to molecular association between the cobalt ion in one molecule and both nitrogen and oxygen atoms in another molecule. Polymeric structures, insoluble in the usual organic solvents, are accordingly formed. A similar structure has also been reported for (Co(II)-bis-(acetylacetonate) [19].

The magnetic moments of all nickel complexes, except for the diamagnetic $Ni(V3H2NHz)_2$, lie in the region of 2.86—3.19 B.M. These values indicate an octahedral geometry. The electronic spectra of the compounds also confirm the octahedral structure. They show two main bands in the regions 633 ± 8 and 955 ± 20 nm, which may be assigned to the transitions

Table IV

Electronic spectra and magnetic moments at room temperature of complexes with aldehyde-3-hydroxy-2-naphthoyl hydrazones

Compound	Absorption bands, nm	μ_{eff}, B.M.
$Co(B3H2NHz)_2$	540 sh, 650, 975	4.76
$Co(p\text{-}ClB3H2NHz)_2$	545, 620, 970	5.04
$Co(p\text{-}NO_2B3H2NHz)_2$	535 sh, 635, 960	4.89
$Co(V3H2NHz)_2 \cdot 2H_2O$	550 sh, 630 sh, 965	4.60
$Co(S3H2NHz)_2$	530 sh, 620 sh, 935	4.82
$Co(o\text{-}V3H2NHz)_2$	550 sh, 640, 960	4.77
$Ni(B3H2NHz)_2$	630, (730, 835), 940	2.86
$Ni(p\text{-}ClB3H2NHz)_2$	625, (705, 825), 945	3.16
$Ni(p\text{-}NO_2B3H2NHz)_2$	635, (700, 820), 975	3.18
$Ni(V3H2NHz)_2$	440 s, 610 sh, 780	diamag.
$Ni(S3H2NHz)_2$	640, (690, 825), 935	3.12
$Ni(o\text{-}V3H2NHz)_2$	640 sh, (690, 840), 960	3.18
$Cu(B3H2NHz)_2$	655 b, 725 sh, 905	1.82
$Cu(p\text{-}ClB3H2NHz)_2$	685 b, 880	1.91
$Cu(p\text{-}NO_2B3H2NHz)_2$	670 b, 860	1.76
Cu(V3H2NHz)OAc	660 b, 745	1.44
Cu(S3H2NHz)	670 b, 750 sh, 905	1.60
Cu(*o*-V3H2NHz)	680 sh, 755 sh, 900	1.45

b = broad, sh = shoulder, s = strong

$^3A_{2g} \rightarrow {}^3T_{1g}(F)$ and $^3A_{2g} \rightarrow {}^3T_{2g}$, respectively. The weak bands or shoulders observed in the region 690—840 nm are probably attributed to the transitions $^3A_{2g} \rightarrow {}^1E_g(D)$ and $^3A_{2g} \rightarrow {}^1E_g(G)$ [20]. Polymeric 6-coordinate octahedral structures due to molecular association are also suggested for $Ni(B3H2NHz)_2$, $Ni(p\text{-}ClB3H2NHz)_2$ and $Ni(p\text{-}NO_2B3H2NHz)_2$. Formation of such polymeric complexes has been confirmed by X-ray studies on nickel(II)-bis(acetylacetonate) [19]. The diamagnetism and electronic spectrum of $Ni(V3H2NHz)_2$ agree with a square planar geometry. The spectrum shows an intense band at 440 nm which is assigned to the $^1A_{1g} \rightarrow {}^1E_g$ transition. The weak shoulder and the absorption band at 610 and 780 nm may be attributed to the $^1A_{1g} \rightarrow {}^1A_{2g}$ and $^1A_{1g} \rightarrow {}^3E_g$, respectively.

The magnetic moments of $Cu(B3H2NHz)_2$, $Cu(p\text{-}ClB3H2NHz)_2$ and $Cu(p\text{-}NO_2B3H2NHz)_2$ are consistent with the values expected for copper(II) compounds. Subnormal magnetic moments are, however, found for Cu(*o*-V3H2NHz), Cu(S3H2NHz) and Cu(V3H2NHz) OAc. The low magnetic

moment values of the first two complexes may be explained by the super-exchange mechanism [21] or/and spin-spin interaction between two copper ions [22]. Dimeric structures **VII** and **VIII** are suggested for Cu(*o*-V3H2NHz) and Cu(S3H2NHz). It is difficult to decide without complete X-ray work whether this dimerization takes place through direct Cu-Cu interaction or super-exchange phenomenon. A dimeric structure may also be proposed for Cu(V3H-2NHz) OAc. The molecular association hereby is presumably achieved

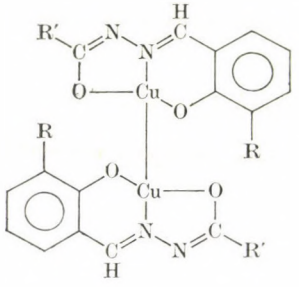

VII

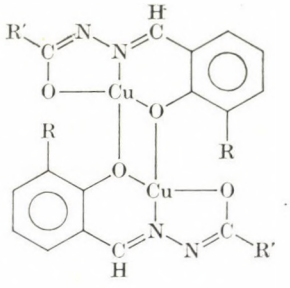

VIII

Cu(S3H2NHz) and Cu(*o*-V3H2NHz)

(R = H or OCH_3, R' = 2-OH—$C_{10}H_7$)

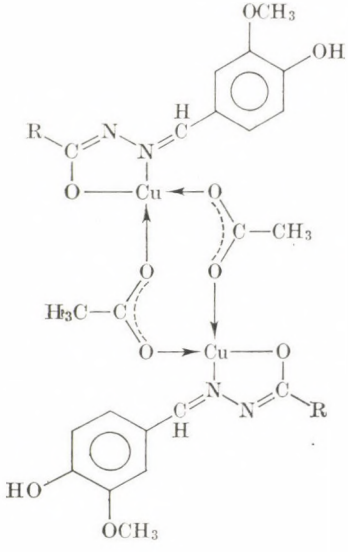

IX

Cu(V3H2NHz)OAc

(R = 2-OH—$C_{10}H_7$)

through the bridge-acting acetate ion (**IX**). The electronic spectra of all copper complexes are compatible with square planar structure. They show a broad band centered at 655—685 nm, which is assigned to the transition $^2B_{1g} \rightarrow {}^2E_g$. In addition two weak bands or shoulders are observed at 725—755 and 860—905 nm. These may be attributed to the transitions $^2B_{1g} \rightarrow {}^2B_{2g}$ and $^2B_{1g} \rightarrow \rightarrow {}^2A_{1g}$, respectively.

Zinc forms 1 : 2 metal to ligand complexes with all ligands except for the tridentate *o*-V3H2NHz and S3H2NHz, whereby 1 : 1 chelates are formed. Dimeric structures, similar to that of copper compounds (**IX**), are suggested for Zn(*o*-V3H2NHz) and Zn(S3H2NHz). All the yellow zinc complexes are assumed to have distorted tetrahedral environment.

REFERENCES

[1] L'Eplatenier, F., Vuitel, L. (Ciba-Geigy AG.): Ger. Offen. 2,556,473; C. A., **85,** 110096y (1976)
[2] Morton, R. A., Ali, H., Calloway, T. C.: J. Chem. Soc., **1934,** 883
[3] Mellor, D. P., Craig, D. P.: Proc. Roy. Soc., **74,** 475 (1940)
[4] Sacconi, L.: J. Amer. Chem. Soc., **74,** 4503 (1952); **76,** 3400 (1954)
[5] Nagano, K., Kinoshita, H., Hirakawa, A.: Chem. Pharm. Bull., Tokyo, **12,** 1198 (1964)
[6] Sacconi, L., Pasletti, P., Maggio, F.: J. Amer. Chem. Soc., **79,** 4067 (1957)
[7] Dato, H.: Bull. Chem. Soc., Japan, **31,** 1056 (1958); **33,** 202 (1960)
[8] Katiyar, S. S., Tandon, S. N.: J. Indian Chem. Soc., **41** (3), 219 (1964)
[9] Vasilikiotis, G. S., Tossidis, T. A.: Microchemical J., **14,** 380 (1969)
[10] Elsayed, L., Iskander, M. F.: J. Inorg. Nucl. Chem., **33,** 435 (1971)
[11] Vasilikiotis, G. S., Kouitzis, Th. A.: Microchemical J., **18,** 85 (1973)
[12] Dutta, R. L., Sen Gupta, G. P.: J. Indian. Chem. Soc., **49** (10), 919 (1972)
[13] Agarwal, R. C., Narang, K. K.: Inorg. Chem. Acta, **9,** 137 (1974)
[14] Iskaner, M. F., Elaggan, A. M., Refaat, L. S., Elsayed, L.: Inorg. Chem. Acta, **1975,** 14
[15] Pelizzi, C., Predieri, G.: Gazz. Chim. Ital., **105,** 413 (1975)
[16] Domiano, P., Musatti, A., Nardelli, M., Pelizzi, C.: J. Chem. Soc., **1975,** 295
[17] Biradar, N. S., Havinale, B. R.: Inorg. Chem. Acta, **17,** 157 (1976)
[18] Franzen, H., Eichler, T.: J. Pr., **78,** 164 (1889)
[19] Cotton, F. A., Wilkinson, G.: "Advanced Inorganic Chemistry," Interscience, 1972
[20] Lever, A. B. P.: "Inorganic Electronic Spectroscopy," Elsevier, 1968
[21] Barclay, G. A., Harris, C. M., Hoskins, B. F., Kokot, E.: Proc. Chem. Soc., **1961,** 264
[22] Barclay, G. A., Hoskins, B. F.: J. Chem. Soc., **1965,** 1979

Maher Mohamed Osman, Gamila Yousef Ali — Chemistry Department Faculty of Science, Alexandria University, Alexandria, Egypt

Acta Chimica Academiae Scientiarum Hungaricae, Tomus 108 (1), pp. 25–30 (1981)

ON THE CORRELATION BETWEEN ELECTRONEGATIVITY AND MOLECULAR PARAMETERS

T. V. RAMAKRISHNA RAO, G. T. NAIDU and R. RAMAKRISHNA REDDY

(*Department of Physics, S. V. University, Post-Graduate Centre, Anantapur-515003, A. P. India*)

Received November 23, 1979

In revised form July 28, 1980

Accepted for publication September 11, 1980

The mean electronegativities which are satisfactory approximations for the equalized ones can be brought into a close correlation with the simplest molecular parameters. The force constants of diatomic molecules MgO, CaO, SrO, SiO, SiS, TiO, NO^+, P_2^+, SO, SeO and TeO or of simple isolated bonds can be expressed by means of the equalized electronegativities, bond orders, bond strengths and interatomic distances. The performance of the LENNARD-JONES parameters has been tested with the potential function proposed by SZŐKE in calculating $\omega_e x_e$ and α_e, and found to be excellent. The role of the electronegativity in constructing the potential energy functions proves the validity of the assumption that there is a close connection between electronegativity and the energy relations of the molecules.

Introduction

Electronegativity was introduced into theoretical chemistry by PAULING. This is the energy by which an atom attracts an electron or electrons belonging to another atom, for establishing a bond. The concept of equalized electronegativity was introduced by SANDERSON [1] into valence theory and was later extended to orbital electronegativities. The main aim of the present study is to use electronegativities as physicochemical parameters in addition to other spectroscopic constants. The present paper deals with the calculations of the force constants, LENNARD-JONES parameters, anharmonicity and rotational-vibrational coupling constants. As has been pointed out by SZŐKE [2], all electronegativity scales give schematic values, therefore, when checking on the maximal errors of K_e, $\omega_e x_e$ and α_e, the certainty of the D_e is important. In continuation of the work on the estimation of the dissociation energy D_e for these molecules, we took up the present investigation of the performance of the LENNARD-JONES parameters for calculating molecular constants as proposed by SZŐKE. The D_e values estimated by the authors [3—7] are used in the evaluation of K_e, $\omega_e x_e$ and α_e constants, confirming the correctness of the D_e values. As is well known, the potential energy is a function of internuclear distance, but the exact shape of the curve depends on the dis-

sociation energy. The force constants and the mean electronegativities have the lowest values in diatomic cases. In the case of diatomic molecules there is a relationship between the force constants and the bond strengths. The relations of the parameters characterizing the bond strength, given as the proportionality constant d, can, in first approximation, be considered constant within the individual groups.

In order to verify the above and for the evaluation of K_e, $\omega_e x_e$ and α_e, the authors adopted the electronegativity function proposed by SZŐKE [8]. The criterion for recalculating the $\omega_e x_e$ and α_e terms is that the LENNARD-JONES parameters must be of the same magnitude in the given bond type using the concept of mean electronegativity and also to prove the correctness of the proposed function.

Estimation of d values and the behaviour of other parameters

The relationship between the force constant and internuclear distance, the mean value of the electronegativities and dissociation energy was introduced by SZŐKE [8] as

$$\bar{K}_e = d\varepsilon \bar{D}_e^{1/2} r_e^{-1} \tag{1}$$

where $\bar{K}_e$ is the force constant reduced to unit bond order, $\varepsilon = (X_A X_B)^{1/2}$ is the mean value of the electronegativities of the atoms forming the bond, D_e is the dissociation energy similarly reduced to unit bond order; r_e is the internuclear distance. This equation has been well established by SZŐKE [2, 9, 10] and employed for the evaluation of the equalized electronegativities by molecular parameters. The electronegativities are taken from PAULING.

Table I shows the parameters of some diatomic molecules as well as the corresponding d values according to Eq. (1).

The molecular ions are formed by removal of a bonding or an antibonding electron. If a bonding electron is removed, the force constant, the dissociation energy and the reciprocal interatomic distance will diminish. If an antibonding electron is removed, these characteristic values will increase. It is very regrettable that the cases occurring in the literature are not always so unequivocal and it is very hard to distinguish between experimental error and an anomaly. The situation occurs with P_2^+ where we have obtained 4.121 mdyn/A for the force constant instead of the value of 5.56 in P_2 [2]. A similar fact has been observed by SZŐKE [2] in the case of HF^+ and OH^+.

The criterion for the validity of Eq. (1) is that within an individual group of molecules d is constant. The average values for the above sequence are 0.341, 0.388, 0.417 and 0.376, respectively. In a class of similar molecules, such as oxides, fluorides *etc.*, it is clear that the molecular parameters must

Table I

Parameters of diatomic molecules

Molecule	K_e (N/m)	r_e (nm)	D_e^* (10^{-16} kJ)	$(\varepsilon = (e_i e_j)^{1/2}$	N	d
MgO	3.483	0.1749	5.975	2.05	2	0.320
CaO	3.619	0.1822	7.017	1.87	2	0.349
SrO	3.402	0.1919	6.739	1.87	2	0.355
SiO	9.238	0.1509	12.922	2.51	3	0.405
SiS	4.939	0.1928	10.907	2.12	3	0.360
TiO	7.193	0.1620	11.255	2.29	3	0.400
NO^+	24.858	0.1602	17.229	3.24	3	0.780
P_2^+	4.121	0.1984	8.267	2.10	2.5	0.352
SO	8.295	0.1481	8.615	2.96	2	0.373
SeO	6.565	0.1641	6.878	2.89	2	0.375
TeO	5.327	0.1825	6.044	2.71	2	0.385

* Dissociation energies taken from the author's data.

vary in a periodic fashion as a function of the atomic number. Figure 1 shows the plot of internuclear distances r_e (dotted line) and force constants K_e (solid line) in the ground states of the some diatomic oxide molecules. The curve of the r_e values has a minimum within each period. The force constants show a behaviour opposite to that of the internuclear distances (Fig. 1) and

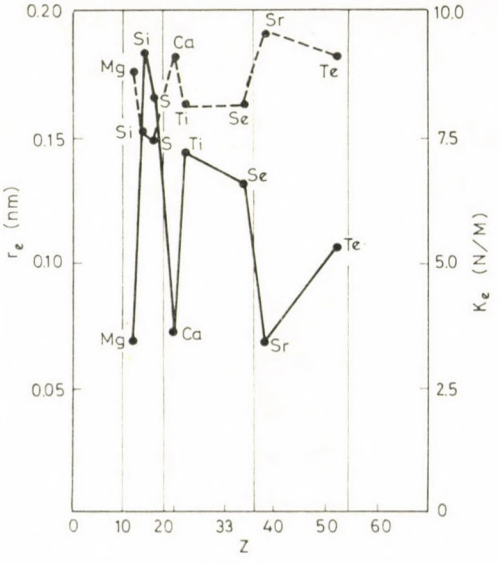

Fig. 1

they reach a maximum within each period. The inverse behaviour of internuclear distance and the force constant is qualitatively in agreement with theoretical expectations, *i.e.* with increasing strength of binding the potential minimum is shifted to smaller r values. At the same time the minimum becomes narrower, that is, the force constant K_e and therefore the vibrational frequency ω_e increases.

Validity of the LENNARD-JONES parameters for the evaluation of $\omega_e x_e$ and α_e

In general, the potential energy functions do not describe the lower and higher energy levels with the same accuracy. In order to justify the above, a supplementary term is useful when employing electronegativity. In order to study the performance of the LENNARD-JONES parameters, we have chosen the equation proposed by SZŐKE [8] as

$$U = D_e \left(1 - e^{\frac{\nu(r - r_e)^2}{r}}\right) [1 + af(r)] . \tag{2}$$

In Eq. (2) the other parameters have their usual spectroscopic meaning and a denotes the LENNARD-JONES parameter. ν can be defined as

$$\nu = d \left(\frac{e_i e_j}{D_e}\right)^{1/2} \tag{3}$$

where d is a proportionality constant, and e_i, e_j are the electronegativities.

It is common practice in the literature to correlate same properties of the proposed function with those of other functions and verify how far the function is suitable to reproduce the spectroscopic constants which are not involved in the function. An interesting assumption introduced by SZŐKE is that

$$(I_i^{\text{red}} I_j^{\text{red}})^{1/2} = b \left[\frac{e_i e_j}{D_e}\right]^{1/2} + C . \tag{4}$$

The function proposed by SZŐKE and LIPPINCOTT can be simultaneously valid when the above assumption holds approximately (b is a proportionality constant) in the present set of molecules. The assumption expresses that the electronegativities can be used as physico-chemical parameters in addition to spectroscopic constants.

By analogy of the equations given by LIPPINCOTT, SCHROEDER and DUNHAM, also introducing the Van der Vaals terms, the equations for the

determination of $\omega_e x_e$, α_e, ab and b are as follows

$$\omega_e x_e = 1.5\, B_e \left[0.25 + \frac{\nu r_e}{2} + ab(\nu r_e)^{1/2} + \left(\frac{a^2 b^2}{1.6} - \frac{ab^2}{2} \right) 2\, \nu r_e \right] \tag{5}$$

$$\frac{\omega_e \alpha_e}{6\, B_e^2} = ab(\nu r_e)^{1/2} \tag{6}$$

and

$$b = \frac{\frac{5}{4}\left[1 - \frac{\alpha_e \omega_e}{6\, B_e^2} \right]^2 - \frac{2\, \omega_e x_e}{3\, B_e} - 1 + \frac{\nu r_e}{2} - \frac{3}{2} ab(\nu r_e)^{1/2}}{ab \cdot \nu r_e} . \tag{7}$$

The details are given elsewhere [9, 10]. The ab, b and $\omega_e x_e$ and α_e values have been calculated for some diatomic molecules and the results are shown in Table II. The average values of ab's (0.669, 0.665, 0.681, 0.642) and that of b's (0.803, 0.974, 0.980, 1.103) for different molecular groups were used in calculating the $\omega_e x_e$ and α_e values.

The standard deviations in the estimated $\omega_e x_e$ and α_e values from that of the experimental values, as seen from the Table II, are 3.4 and 3.6, respectively.

Table II

Molecule	ab	b	$\omega_e x_e$ (cm^{-1}) Cal.	$\omega_e x_e$ (cm^{-1}) Expt.	α_e (cm^{-1}) Cal.	α_e (cm^{-1}) Expt.
MgO	0.661	0.947	5.820	5.180	0.00503	0.00500
CaO	0.709	0.831	5.265	5.280	0.00326	0.00335
SrO	0.637	0.631	3.956	3.960	0.00198	0.00204
SiO	0.693	1.017	5.900	5.920	0.00482	0.00504
SiS	0.687	1.035	2.669	2.577	0.00146	0.00150
TiO	0.617	0.872	4.378	4.497	0.00323	0.00301
NO^+	0.657	0.963	16.666	16.449	0.02448	0.01901
P^+	0.705	0.997	2.660	2.740	0.00159	0.00151
SO	0.650	0.101	6.020	5.700	0.00565	0.00560
SeO	0.626	1.126	4.587	4.520	0.00334	0.00330
TeO	0.650	1.084	3.855	4.000	0.00234	0.00237
		Standard deviation		0.186	0.00071	

From these studies, it can be concluded that the performance of the LENNARD-JONES parameters for the evaluation of $\omega_e x_e$ and α_e are justified using the concept of mean electronegativity.

*

The authors wish to express their thanks to Prof. S. SZŐKE (Central Research Institute for Chemistry of the Hungarian Academy of Sciences, Budapest) for providing the necessary data and thanks are due to Prof. S. V. J. LAKSHMAN and Prof. S. V. SUBRAHMANYAM for their interest in the present work.

REFERENCES

[1] SANDERSON, R. T.: Science, **114,** 670 (1951)
[2] SZŐKE, S.: Acta Chim. Acad. Sci. Hung., **68,** 345 (1970)
[3] LAKSHMAN, S. V. J., RAMAKRISHNA RAO, T. V., THIMMA NAIDU, G.: Pramana, **7,** 369 (1976)
[4] LAKSHMAN, S. V. J., RAMAKRISHNA RAO, T. V., THIMMA NAIDU, G.: Curr. Sci., **47,** 7 (1978)
[5] RAMAKRISHNA RAO, T. V., RAMAKRISHNA REDDY, R.: Physica, **95C,** 412 (1978)
[6] RAMAKRISHNA RAO, T. V., RAMAKRISHNA REDDY, R.: Proc. Indian Acad. Sci., **88,** 257 (1979)
[7] LAKSHMAN, S. V. J., RAMAKRISHNA RAO, T. V., NAIDU, G. T.: Indian J. Pure and Appl. Phys., **15,** 834 (1977)
[8] SZŐKE, S.: Acta Chim. Acad. Sci. Hung., **51,** 183 (1967)
[9] SZŐKE, S., BAITZ, E.: Acta Chim. Acad. Sci. Hung., **57,** 129 (1968)
[10] SZŐKE, S.: Acta Chim. Acad. Sci. Hung., **58,** 399 (1968)

Γ. V. RAMAKRISHNA RAO, G. T. NAIDU, R. RAMAKRISHNA REDDY
Department of Physics, S. V. University, Post-Graduate Centre, Anantapur-515003, A.P. India

Acta Chimica Academiae Scientiarum Hungaricae, Tomus 108 (1), pp. 31—35 (1981)

NEW SIMPLE SYNTHESIS OF UNSYMMETRICAL DISULFIDE

D. GUPTA*

(Chemical Laboratories, University of Rajasthan, Jaipur-302004 India)

Received April 28, 1980

In revised form August 15, 1980

Accepted for publication September 17, 1980

Unsymmetrical disulfides from the co-photolysis of mixtures of symmetrical alkyl disulfides is reported. Rates have been obtained for 35 combinations of C_2 to C_{10} alkyl disulfides and their isomers. An equilibrium is attained after relatively short irradiation periods in cyclohexane.

The effectiveness of disulfides as radiation protectors [1, 2] and their derivatives as antioxidants [3] is well known. Molecules containing the disulfide linkage are believed to be a key point of attack when biological systems are irradiated with UV light. They are used as a chain transfer agent in free radical polymerisation. Several disulfides have been found to shorten the latency phase and to increase the growth of virus stains in cell cultures [4].

There are various methods reported in the literature which use activated sulfenyl derivatives to synthesize unsymmetrical disulfides. The common active sulfenyl derivatives are sulfenyl halide [5], sulfenyl thiocyanate [6], sulfenyl hydrazide [7], sulfenyl thiocarbonate [8], sulfenimide [9], thiosulfate [10], thiosulfonate [11], thiol sulfinate [12] and alkyl thiodialkyl sulfonium salts [13]. Sulfur monochloride with active methylene compounds, Grignard reagents, alkenes or arenes can give disulfides and chlorodithio compounds, but other products as well [14]. OAE and co-workers [15] have reported that unsymmetrical disulfides can be obtained by treating thionitrites with thiols. All the methods reported so far involve two or three steps to synthesize unsymmetrical disulfide. We wish to report an easy and less cumbersome method for its synthesis by photolysing disulfides. An equilibrium is attained after relatively short periods in cyclohexane.

Experimental

All experiments were carried out at room temperature, 20 ± 3° with samples thoroughly degassed by alternate freeze-pump thaw cycles utilizing a simple high vacuum system. The reaction cell was a quartz tube, 6 mm of that contains 250 μl of equimolar mixture of disulfide (RSSR + R'SSR'). The light source was a Hanovia 306-20 medium pressure mercury lamp with Vycor 7910 filter to eliminate wavelength less than 230 nm. The position of the lamp was fixed to have constant light intensity throughout the experiments, which was

* For correspondence: B-63, University Marg, Jaipur-302004, India.

measured by a detector attached to a LIMS 920 photometer. All the symmetrical disulfides were of commercial grade and were used after purification by fractional distillation. At the end of the reaction, the reaction mixture was analyzed by thermal conductivity or by flame ionization gas chromatography using tricresyl phosphate and Apiezon-M columns. A blank mixture of disulfide was always passed through the gas chromatograph to check for initial concentrations and to detect the extent of any thermal reaction. The extent of thermal reaction was invariably less than 0.5% of the photo-chemical processes. The formation of unsymmetrical disulfide was confirmed by comparing their glc [16] and mass spectra [17] with samples which were obtained by the methods described earlier [18, 19]. The eluted unsymmetrical disulfide fraction was trapped in liq. N_2 (−196 °C).

Results and Discussion

Preliminary investigations showed that in agreement with previous reports [19, 20], photolysis of mixtures of neat RSSR + R′SSR′ yields the unsymmetrical disulfide. The rate of production of RSSR' is exceptionally large in cyclohexane and decreases with increasing exposure time and becomes constant after short irradiation periods. Further irradiation did not alter the proportion of the three disulfides present, concluding that the equilibrium is attained. It is also observed that the photochemical equilibrium is attained relatively after short irradiation period in cyclohexane contrary to the work of HARALDSON *et al.* [21].

The data for equimolar mixtures of straight chain dialkyl disulfides are shown in Table I. The initial rate of unsymmetrical disulfide is the lowest for diethyl disulfide—dipentyl disulfide system. Significant decreases in the rate of unsymmetrical disulfide formation was observed when one of the disulfide was changed from dipropyl to diisopropyl disulfide *(cf.* Table II). However, when both disulfide had isoalkyl groups, the observed rate of unsymmetrical disulfide formation were very much higher. Exceptionally high rates are also observed for diethyl-dipropyl disulfide system in which the reaction is completed in less than a minute. The results of the series of experiments in which various C_2 to C_{10} disulfide were co-photolysed with dibutyl, diisobutyl, disecbutyl and ditertbutyl disulfide are shown in Table III. It is apparent that

Table I

Initial rates of unsymmetrical disulfide (RSSR′) *formation for straight chain dialkyl disulfides*

RSSR + R′SSR′ in cyclohexane	Rate of RSSR′ formation, % min^{-1}							
	R′ = C_2H_5		*n*-C_3H_7		*n*-C_4H_9		*n*-C_5H_{11}	
	|0.1|	|0.01|	|0.1|	|0.01|	|0.1|	|0.01|	|0.1|	|0.01|
R=CH_3	3.8	20.6	3.0	21.0	0.6	3.4	0.4	1.6
C_2H_5	—	—	10.2	100	0.95	5.0	0.18	1.45
n-C_3H_7	—	—	—	—	1.2	6.0	0.31	3.0
n-C_4H_9	—	—	—	—	—	—	0.22	1.65

Table II

Initial rates of unsymmetrical disulfide (RSSR') *formation for dipropyl disulfide* (R'SSR' + RSSR) *mixtures*

RSSR + R'SSR' in cyclohexane	Rate of RSSR' formation, % min^{-1}			
	R' = *n*-C_3H_7		R' = *iso*-C_3H_7	
	|0.1|	|0.01|	|0.1|	|0.01|
R=CH_3	3.0	21	0.78	2.7
C_2H_5	10.2	100	4.7	18.9
n-C_4H_9	1.2	6.0	0.34	1.2
iso-C_4H_9	0.35	2.5	4.4	25.7
sec-C_4H_9	5.0	27.5	3.2	10.5
n-C_5H_{11}	0.31	3.0	0.09	0.58
iso-C_5H_{11}	0.38	2.3	3.8	13.0

Table III

Initial rates of unsymmetrical disulfide (RSSR') *formation for dibutyl disulfide* (R'SSR' + RSSR) *mixtures*

RSSR + R'SSR' in cyclohexane	Rates of RSSR' formation, % min^{-1}							
	R' = *n*-C_4H_9		*iso*-C_4H_9		*sec*-C_4H_9		*tert*-C_4H_9	
	|0.1|	|0.01|	|0.1|	|0.01|	|0.1|	|0.01|	|0.1|	|0.01|
R=CH_3	0.6	3.4	0.44	3.0	0.9	5.0	0.039	0.205
C_2H_5	0.95	5.0	0.3	2.1	4.6	30	0.034	0.18
n-C_3H_7	1.2	6.0	0.35	2.5	5.0	27.5	—	—
iso-C_3H_7	0.34	1.2	4.4	25.7	3.2	10.5	—	—
n-C_5H_{11}	0.22	1.6	0.16	1.6	0.14	0.80	0.0267	0.12
iso-C_5H_{11}	0.3	1.9	11.9	85.1	0.14	0.86	0.033	0.14

the rate of unsymmetrical disulfide formation is significantly lower for the mixtures containing ditertbutyl disulfide compared to those of other disulfide.

In addition to the data listed in Table I, II, III, the rates of unsymmetrical disulfide formation for dimethyl disulfide-diisopentyl disulfide and diethyl disulfide—diisopentyl disulfide mixtures were also obtained. The values are 0.40, 0.38% min^{-1} in 0.1 cyclohexane and 2.0, 2.1% min^{-1} in 0.01 cyclohexane, respectively.

The observation that unsymmetrical disulfide is the only co-photolysis product and that photolysis of disulfide alone does not result in product formation leads to the conclusion that the C—S bond fission does not occur to a great extent as compared to S—S bond cleavage in agreement with the

earlier work [18—26]. The accumulated evidence thus strongly indicates that the only significant primary process in the condensed phase photolysis must be the homolytic rupture of the S—S bond producing thiyl radicals.

Since no reactions other than those leading to unsymmetrical disulfide formation occur after 12 hrs irradiation, the mechanism applicable to the photostationary state thus presumably consists only of the three reversible processes (1—3).

$$RSSR + h\nu \rightleftharpoons 2\ RS \tag{1}$$

$$R'SSR' + h\nu \rightleftharpoons 2\ R'S \tag{2}$$

$$RSSR' + h\nu \rightleftharpoons RS + R'S \tag{3}$$

The concentration of unsymmetrical disulfide increases in the system until it effectively competes for the absorption of light and its own photolysis becomes an important source of thiyl radicals. After some characteristic exposure time, a photostationary state will be attained as described earlier [27] for dimethyl—diethyl, diethyl—dipropyl and dimethyl—dipropyl disulfide systems.

The unsymmetrical disulfide formation can occur only *via* the following processes

$$RS + R'SSR' \rightarrow RSSR' + R'S \tag{4}$$

$$RS + R'S \rightarrow RSSR' \tag{5}$$

The overall mechanism can be represented by a simple equilibrium

$$RSSR + R'SSR' \underset{h\nu}{\overset{h\nu}{\rightleftharpoons}} 2\ RSSR'. \tag{6}$$

The data of Table III show that the rate of unsymmetrical disulfide formation is the lowest for RSSR—ditertbutyl disulfide mixtures. The behaviour of ditertbutyl disulfide appears to be quite different from other disulfides. The data indicate that the attack of thiyl radicals on disulfide molecule is decreased substantially when the sulfur atoms are significantly sterically hindered. The reduced sensitivity of rates of radical reactions for ditertbutyl disulfide systems compared to other disulfides is consistent with the observation made by PRYOR *et al.* [22] and OHTA *et al.* [28] for phenyl radicals. Further studies are underway to prepare and investigate the effect of higher molecular weight disulfide of biological importance on exchange reaction.

*

The author is thankful to University of Saskatchewan, Saskatoon, Canada for providing the necessary research facilities and to Dr. B. C. JOSHI for the valuable suggestions

REFERENCES

[1] Bac, Z. M.: Chemical protection against ionization radiation, Thomas Spring Field, 1965.
[2] Hollaender, A., Doherty, D. G.: Radiation damage and sulphhydryl compounds, International Atomic Energy Viena, 1969
[3] Ingold, K. V.: Chem. Rev., **61,** 563 (1961)
[4] Augusti, K. T., Benaim, M. E.: Clinica Chimica Acta, **60,** 121 (1975)
[5] Endo, T., Tasai, H., Ishigami, T.: Chemistry Letters, **1975,** 913
[6] Hiskey, R. G., Carroll, F. I., Babb, R. M., Bledsoe, J. C., Puckett, R. T., Roberta, B. W.: J. Org. Chem., **26,** 1152 (1961)
[7] Mukaiyama, T., Takahashi, K.: Tetrahedron Letters, **1968,** 5907
[8] Brols, S. G., Pilot, J. F., Barnum, H. W.: J. Am. Chem. Soc., **92,** 7629 (1970)
[9] Boustany, K. S., Sulivan, A. B.: Tetrahedron Letters, **1970,** 3547
[10] Klayman, D. A., Shine, R. G.: Quart Rep. Sulfur Chem., **3,** 231 (1968)
[11] Field, L., Harle, H., Owen, T. C., Ferretti, A.: J. Org. Chem., **29,** 1632 (1954)
[12] Small, L. D., Bailey, J. H., Cavallito, Ch. J.: J. Am. Chem. Soc., **69,** 1710 (1947)
[13] Dubs, P., Stussi, R.: Helv. Chim. Acta, **59,** 1307 (1976)
[14] Reid, E. E.: Organic Chemistry of Bivalent Sulfur, Vol. **III,** Chemical Publishing Co., New York, 1960
[15] Oae, S., Kim, Y. H., Fukushima, D., Takate, T.: Chemistry Letters, **1977,** 893
[16] Gupta, D.: Chem. Anal. (Warsaw), **329,** 221 (1980)
[17] Gupta, D.: unpublished work
[18] Birch, S. F., Cullum, T. V., Dean, R. A.: J. Inst. Petrol, **39,** 206 (1953)
[19] Gupta, D.: Ind. J. Chem. (In press)
[20] Sayamol, K., Knight, A. R.: Can. J. Chem., **46,** 999 (1968)
[21] Haraldson, L., Olanfer, G. I., Sunner, S., Varde, E.: Acta Chem. Scand., **14,** 1509 (1960)
[22] Pryor, W. A., Platt, P. K.: J. Am. Chem. Soc., **85,** 1496 (1963)
[23] Milligan, B., Rivett, D. E., Savige, W. E.: Aust. J. Chem., **16,** 1020 (1963)
[24] Pryor, W. A., Guard, H.: J. Am. Chem. Soc., **86,** 1150 (1964)
[25] Rosengren, K. J.: Acta Chem. Scand., **16,** 1401 (1962)
[26] Guryanova, E. N.: Quart. Rep. Sulfur Chem., **5,** 113 (1970)
[27] Gupta, D.: Ind. J. Chem. (In press)
[28] Fujisawa, T., Ohta, H.: Bull. Chem. Soc., **49,** 2341 (1976)

Dinesh Gupta B-63, University Marg, Jaipur-302004, India

Acta Chimica Academiae Scientiarum Hungaricae, Tomus 108 (1), pp. 37—42 (1981)

OXYGENATION OF *N*-SUBSTITUTED *o*-PHENYLENEDIAMINES IN THE PRESENCE OF COPPER(I) CHLORIDE IN PYRIDINE

É. BALOGH-HERGOVICH, G. BODNÁR and G. SPEIER

(*Department of Organic Chemistry, Veszprém University of Chemical Engineering and Research Group for Petrochemistry, Hungarian Academy of Sciences, Veszprém*)

Received June 30, 1980

Accepted for publication September 17, 1980

Depending on the *N*-substituents, *o*-phenylenediamines react in the system Cu(I) halide / amine / O_2, through radicals or nitrene intermediates, to give (*a*) *cis-cis*-muconitriles (through *o*-dinitrenes); (*b*) with insertion of nitrenes into the C—H bond; or (*c*) with coupling of the nitrenes to diazo compounds.

Introduction

Copper(I) halide/amine/O_2 systems are versatile reagents in important oxidation reactions such as the oxidative coupling of terminal acetylenes to diacetylenes [1, 2], thiols to disulfides [3], and phenols to diphenoquinones and polyethers [4]. The oxidation of aromatic amines with molecular oxygen activated by metal salts is a well established reaction. *o*-Phenylenediamine (**1a**) is oxidized in the presence of ferric chloride [5—9] to 2,3-diaminophenazine or 2-amino-3-oxophenazine. Aniline is coupled to azobenzene [10] and 2-aminodiphenylamine is oxidized to 2-amino-3,5-dihydro-5-phenyl-3-phenyliminophenazine [11] by dioxygen in the cuprous chloride/pyridine system. Compound **1a** has also been oxidized to *cis,cis*-muconitrile (**4**) by using a stoichiometric amount of nickel peroxide [12], lead tetraacetate [13], and by dioxygen catalyzed by cuprous chloride in pyridine [14]. This ring cleavage resembles the enzymic reaction of pyrocatechase yielding *cis,cis*-muconic acid from the isoelectronic catechol [15]. Since knowledge is scarce about the copper-dioxygen complex(es) [16—18] formed in the CuCl(py)O_2 system and the mechanism of the formation of *cis,cis*-muconononitrile from *o*-phenylenediamine, we undertook a systematic study of the effect of different substituents and the role of the degree and mode of substitution on the nitrogen atoms of **1** on the products of these copper-catalyzed oxygenations, in order to obtain a better insight into the mechanism of such reactions.

Results and Discussion

A number of *N*-substituted *o*-phenylenediamines were prepared and allowed to react with dioxygen in the presence of CuCl in pyridine.

The results and the possible reaction paths proposed are shown in Schemes 1 and 2. If both N-atoms of the *o*-phenylenediamine derivative (**1**)

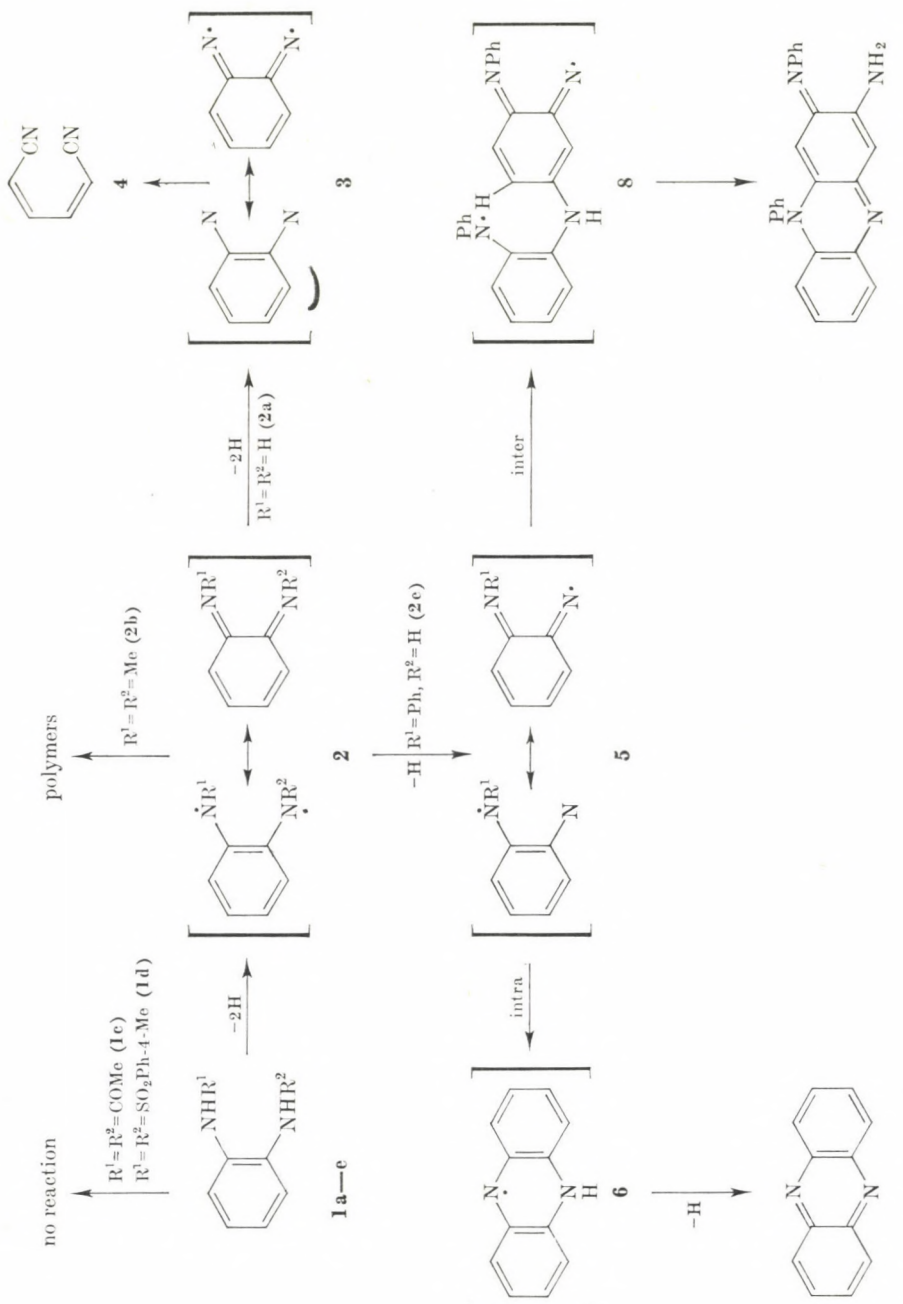
no reaction
R¹=R²=COMe (1c)
R¹=R²=SO₂Ph-4-Me (1d)
polymers
R¹=R²=Me (2b)
1a—e
−2H
2
−2H
R¹=R²=H (2a)
3
4
−H
R¹=Ph, R²=H (2e)
5
inter
8
9
intra
6
−H
7

Scheme 1

bear at least one hydrogenatom, like in **1a-b** and **1e**, the *o*-diimine (**2a**) or the substituted *o*-diimines **2b**, **2e** were obtained by a two-electron oxidation step. A further two-electron oxidation of **2a** leads probably to the dinitrene **3**, which then rearranges to *cis,cis*-muconononitrile (**4**). Compound **4** is also formed by pyrolysis [19] or photolysis [20] of *o*-diazidobenzene under different conditions, and the intermediacy of the dinitrene **3** was assumed on the basis of analogous reactions of several azidobenzenes [21]. *N,N'*-Dimethyl-*o*-benzodiimine (**2b**) could neither be oxidized further, nor isolated from the reaction mixture. The reason for this, we believe, is the easy polymerization of this class of compounds. From the monosubstituted derivative, *N*-phenyl-*o*-phenylenediamine (**1e**), the two-electron oxidized product **2e** undergoes a further H-abstraction (one-electron oxidation) resulting in the intermediate radical **5**, from which in an *intra*molecular nitrene insertion reaction the radical **6** is formed, ending up in phenazine (**7**) through a subsequent one electron-oxidation. The radical **5** may also react in an *inter*molecular fashion giving probably the diradical **8**, from which, by coupling and hydrogen migration, the three-electron oxidation product **9** is formed in 26% yield. Interestingly, the *N,N'*-disubstituted acyl (**1c**) and tosyl (**1d**) derivatives do not react with dioxygen in the presence of copper(I) chloride in pyridine. This can be explained with the strong electron-withdrawing character of the substituents.

If one of the N-atoms of *o*-phenylenediamine is disubstituted (**1f—g**), the oxygenation reactions take a different course. In these compounds one of the amino groups attached to the benzene ring is insusceptible to oxidation (the inertness of tertiary amines against oxygenation is well documented). This structural feature prevents the formation of diimine intermediates of type **2**. Compounds **1f** and **1g** are, however, readily transformed to **10f** and **10g** by a two-electron oxidation step. These *o*-substituted nitrenes, depending on the substituents of the neighbouring amino group, may dimerize as in the case of **10f** to the azo compound **11** (yield: 36%), or nitrene insertion may take place into the C—H bond of the benzylidene group of **10g** giving 2-phenylbenzimidazole (**12**). Compound **12** could also be prepared from the *o*-azidoanil of benzaldehyde at 130—150 °C in a good yield, assumedly through nitrene insertion [22, 23]. Under the conditions of the reaction **12** is oxidatively coupled to 1,1'-bis(2-phenylbenzimidazole) (**13**).

With tetrasubstituted derivatives such as tetramethyl-*o*-phenylenediamine (**1h**) or *N,N'*-dibenzylidene-*o*-phenylenediamine (**1i**) no oxygenation was observed in the CuCl/py system.

From the reactions in Schemes 1 and 2 the conclusion may be drawn that the copper dioxygen complex formed from copper(I) chloride, pyridine and dioxygen abstracts hydrogens successively from the *o*-phenylenediamine derivatives giving radicals or nitrene intermediates, which then react in an *intra* or *inter*molecular fashion practically in three ways:

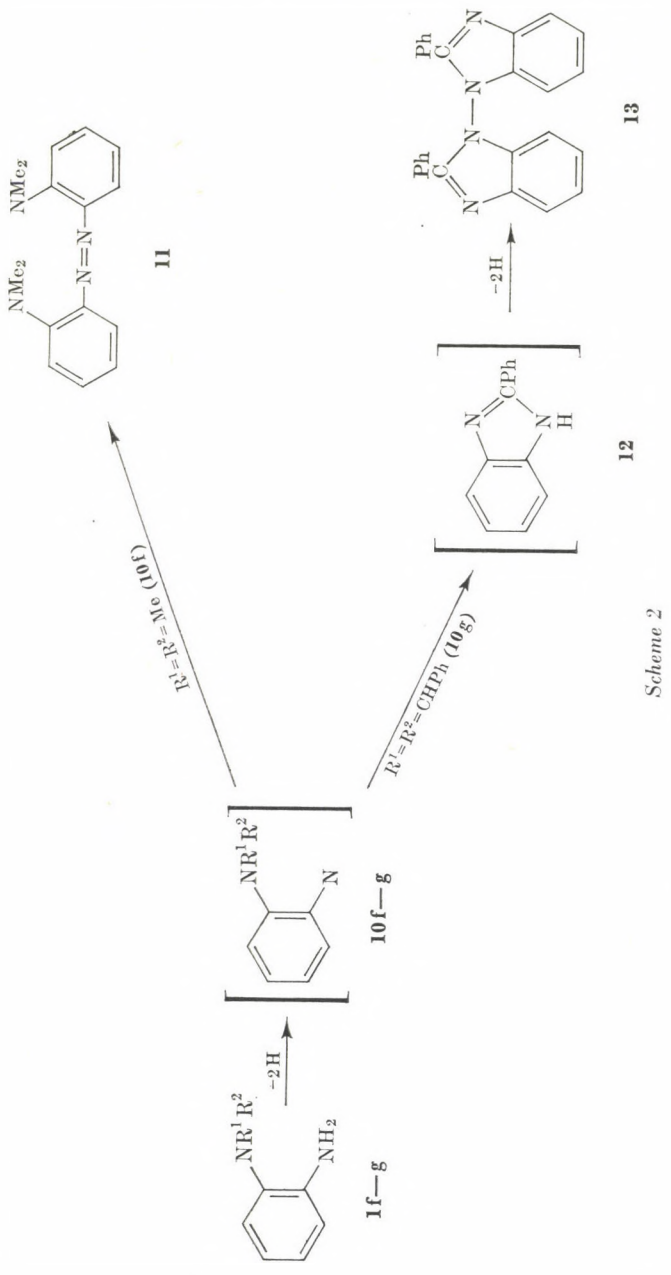
NMe2
NMe2
N=N
11
Ph
C
N
N
Ph
C
N
N
N
13
R¹=R²=Me (10f)
R¹=R²=CHPh (10g)
CPh
N
N
H
12
NR¹R²
N
10f—g
NR¹R²
NH2
1f—g
-2H
-2H

Scheme 2

(i) ring splitting of *o*-dinitrenes (**3**) to *cis,cis*-muconononitrile (**4**);

(ii) insertion of nitrenes into the C—H bond, *e.g.* the reactions of **5**, **8**, and **10g**;

(iii) the coupling of nitrenes to diazo compounds, the reaction of **10f** to **11**.

Compounds, where no hydrogens are attached to the nitrogen in the *o*-phenylenediamine derivatives showed inertness in these reactions.

Experimental

Materials and methods

N,N'-Ditosyl-*o*-phenylenediamine (**1d**) [24], *N,N'*-diacetyl-*o*-phenylenediamine (**1c**) [25], and *N*-benzylidene-*o*-phenylenediamine (**1g**) [26] were synthesized from *o*-phenylenediamine by known methods. *N,N'*-Dimethyl-*o*-phenylenediamine (**1b**) was prepared from **1d** according to [27]. *N*-Phenyl-*o*-phenylenediamine (**1e**) and *N,N*-dimethyl-*o*-phenylenediamine (**1f**) were obtained by the method of SCHOPF [28] and BAMBERGER [29], respectively. The solvents were dried and distilled before use. Pyridine was dried over potassium hydroxide. Copper(I) chloride (REANAL) was purified with potassium sulfite solution and dried in vacuum.

IR spectra were run on ZEISS UR 20 and SPECORD 75IR instruments. A SPECORD UV-VIS spectrophotometer and a VARIAN T 60, with TMS as internal standard, were used for recording the UV, VIS and ^{1}H-NMR spectra. The mass spectra were taken on a VARIAN MAT 111 GC-MS spectrometer using an ionization energy of 70 eV.

Oxidation of 2-aminodiphenylamine (1c)

Copper(I) chloride (2.0 g; 20 mmoles) was dissolved in 10 mL of dry pyridine and stirred under dioxygen until no more of the gas was consumed (the O_2-uptake was about 5 mmoles during 1 h). To this solution 1.84 g (10 mmoles) of 2-aminodiphenylamine (**1c**), dissolved in 10 mL of pyridine, was slowly added, with stirring. After the oxygen absorption ceased, the pyridine was evaporated in vacuum, the residue extracted with ether and separated by TLC (silica gel, CH_2Cl_2) to give 0.48 g of phenazine (**7**), [MS (*m/e*): 180 (M^+)], identical spectrum with an authentic sample [30]; λ_{max} (EtOH) 360 nm [31]), and 0.52 g of 2-amino-3,5-dihydro-5-phenyl-3-phenyliminophenazine (**9**), identical with an authentic sample [11].

Oxidation of *N,N*-dimethyl-*o*-phenylenediamine (1f)

The reaction with 1.36 g (10 mmoles) of **1f** was carried out as above, and the dry residue purified by TLC (silica gel, CH_2Cl_2) to give 0.48 g of 2,2'-bis(dimethylamino)azobenzene (**11**).

MS (*m/e*): 268 (M^+), m.p. 76—77 °C.

UV: λ_{max} (EtOH): 462 mm (ε = 3280), identical with the literature data [32].

Oxidation of *N*-benzylidene-*o*-phenylenediamine (1g)

The reaction was carried out with 1.96 g (10 mmoles) of **1g** in the usual way. After the extraction with ether the dry residue was recrystallized from ethanol to give **13** as white crystals. Yield: 42%, m.p. 196 °C.

$C_{26}H_{18}N_4$ (386.44). Calcd. C 80.8; H 4.7; N 14.5. Found C 80.4; H 4.6; N 14.2%.

IR (KBr): ν (C=N) 1615, ν (C—N) 1340 cm^{-1}.

UV (EtOH): λ_{max} = 204 (18 600), 240 (5730), 294 nm (8320).

^{1}H-NMR (CCl_4): δ 7.15 ppm (16 H, m, ArH), 7.85 (2H, m, ArH).

MS (*m/e*): 386 (M^+); 193 (M-$C_6H_4N_2CC_6H_5$).

*

The authors are grateful to Prof. L. MARKÓ for his interest throughout this work.

REFERENCES

[1] See, *e.g.*, HAY, A. S.: J. Org. Chem., **25,** 1275 (1960)
[2] RAPHAEL, R. A.: Acetylene Compounds in Organic Synthesis, p. 127. Acad. Press Inc., New York, 1955
[3] BROOKS, B. W., SMITH, R. M.: Chem. Ind., **1973,** 326
[4] FERINGA, B., WYNBERG, A.: Tetrahedron Lett., **1977,** 4447, and references cited therein
[5] GRIESS, P.: J. Prakt. Chem., **3,** 142 (1860)
[6] RUDOLPH, C.: Chem. Ber., **12,** 2211 (1879)
[7] WIESINGER, F.: Ann., **224,** 353 (1884)
[8] FISCHER, E. O., HEPP, E.: Chem. Ber., **23,** 2789 (1890)
[9] ULLMANN, F., MAUTHNER, F.: Chem. Ber., **35,** 4302 (1902)
[10] KINOSHITA, K.: Bull. Chem. Soc. Japan, **32,** 777 (1959)
[11] ALLEN, L. T., SWAN, G. A.: J. Chem. Soc., **1965,** 3892
[12] NAKAGAWA, K., ONOUE, H.: Chem. Commun., **1965,** 396
[13] NAKAGAWA, K., ONOUE, H.: Tetrahedron Lett., **1965,** 1433
[14] KAJIMOTO, T., TAKAHASHI, M., TSUJI, J.: J. Org. Chem., **41,** 1389 (1976)
[15] HAYAISHI, O., KATAGIRI, M., ROTHBERG, S.: J. Am. Chem. Soc., **77,** 5450 (1955)
[16] KRAMER, C. E., DAVIES, G., DAVIES, R. B., SLAVEN, R. W.: J. C. S. Chem. Commun., **1975,** 606
[17] ROGIČ, M. M., DEMMIN, T. R.: J. Am. Chem. Soc., **100,** 5472 (1978)
[18] BODEK, I., DAVIES, G.: Inorg. Chim. Acta, **27,** 213 (1978)
[19] HALL, J. H.: J. Am. Chem. Soc., **87,** 1147 (1965)
[20] RIGAUDY, J., IGIER, C., BARCELO, J.: Tetrahedron Lett., **1979,** 1837
[21] SMOLINSKY, G., WASSERMAN, E., YAGER, W. A.: J. Am. Chem. Soc., **84,** 3220 (1962)
[22] KRBECHEK, L. O., TAKIMOTO, H.: J. Org. Chem., **29,** 3630 (1964)
[23] HALL, J. H., KAMM, D. R.: J. Org. Chem., **30,** 2092 (1965)
[24] STETTER, H.: Chem. Ber., **86,** 161 (1953)
[25] BISTRZYCKI, A., ULFFERS, F.: Chem. Ber., **23,** 1878 (1830)
[26] HINSBERG, O., KOLLER, P.: Chem. Ber., **29,** 1497 (1896)
[27] CHEESEMAN, G. W. H.: J. Chem. Soc., **1955,** 3308
[28] SCHOPF, M.: Chem. Ber., **23,** 1843 (1890)
[29] BAMBERGER, E., TSCHIRNER, F.: Chem. Ber., **32,** 1905 (1899)
[30] EGUCHI, S.: Bull. Chem. Soc. Japan, **51,** 1128 (1978)
[31] BADGER, G. M., PEARCE, R. S.: J. Chem. Soc., **1951,** 3199
[32] PRICE, R.: J. Chem. Soc. A, **4,** 521 (1967)

Éva BALOGH-HERGOVICH, Gábor SPEIER } H-8201 Veszprém, Schönherz Z. u. 8.

György BODNÁR H-3346 Bélapátfalva, Lt. 16. 1/1.

Acta Chimica Academiae Scientiarum Hungaricae, Tomus 108 (1), pp. 43—49 (1981)

PREPARATION AND CHARACTERIZATION OF BIS-π-CYCLOPENTADIENYL AND BIS-π-INDENYL MOLYBDENUM(VI)-OXO-DICHLORIDE WITH OXIMES

S. K. SENGUPTA[1]* and S. KUMAR[2]

([1]*Department of Chemistry, University of Gorakhpur, Gorakhpur* 273001 *(U.P.) India,*
[2]*Department of Chemistry, University of Delhi, Delhi*-11007, *India*)

Received July 28, 1980

Accepted for publication September 17, 1980

The reactions of bis-π-cyclopentadienyl and bis-π-indenyl molybdenum(VI)-oxo-dichloride with the hydroxy oximes (OxH_2) *viz.* salicylaldoxime ($SOxH_2$), 2-hydroxy-5-methylacetophenoneoxime ($AOxH_2$), 2-hydroxy-1-naphthaldioxime ($NOxH_2$) and with dioximes ($Ox'H_2$) *viz.* α-benzildioxime ($BOx'H_2$), dimethylglyoxime ($DOx'H_2$) and 2,6-diacetylpyridinedioxime ($POx'H_2$) have been studied in tetrahydrofurane in the presence of triethylamine at room temperature. The complexes isolated of the types $[(\pi\text{-}C_5H_5)_2$ or $(\pi\text{-}C_9H_7)_2MoO(Ox)]$ and $[(\pi\text{-}C_5H_5)_2$ or $(\pi\text{-}C_9H_7)_2MoO(Ox'H)Cl]$, have been characterized by elemental analyses, i.r. and electronic spectra, electrical conductance and magnetic measurements.

Introduction

Although oximes are widely recognized as versatile ligands and a number of complexes with various transition metals have been studied in detail and have been reviewed recently [1], much remains to be learned about the type of structures that are formed. In general, the oxime function is known [2] to coordinate in four ways:

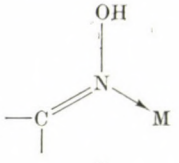

I

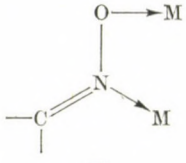

II

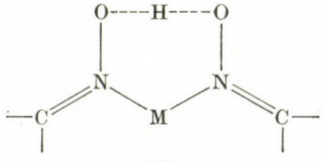

III

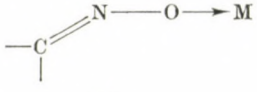

IV

Coordination modes **I** and **III** are observed most frequently, although it should be noted that the oxime function is a poor donor unless it is a part of a chelate ring. The interest in such complexes continues because of their interesting

* To whom correspondence should be addressed.

structural aspects and analytical applications. However, there is no reference in the literature regarding the preparation and characterization of oxime derivatives of bis-π-cyclopentadienyl and bis-π-indenyl molybdenum(VI)-oxo-dichloride. It is, therefore, considered of interest to study the reactions of bis-π-cyclopentadienyl and bis-π-indenyl molybdenum(VI)-oxo-dichloride with different oximes in different molar ratios in non-aqueous media.

Experimental

Special precautions were taken to exclude moisture and all operations were carried out under anhydrous condition. Bis-π-cyclopentadienyl molybdenum(VI)-oxo-dichloride and bis-π-indenyl molybdenum(VI)-oxo-dichloride were prepared by the method reported earlier [3, 4]. Oximes were prepared by known methods [5]. THF (BDH) was dried by storage over sodium wire overnight and was then boiled under reflux until it gave a blue colouration with benzophenone. It was finally dried by distilling over $LiAlH_4$. *n*-Hexane was dried by distilling over sodium wire.

Preparation of the complexes

All the complexes were prepared by a similar procedure. The appropriate oxime (1 mole) was added to a solution of bis-π-cyclopentadienyl or bis-π-indenyl molybdenum(VI)-oxo-dichloride (1 mole) in dry THF (50 mL). To this, triethylamine (2 mole in hydroxyoximes and 1 mole in dioximes) was added, the mixture was stirred for 30—35 hrs., then dried under pressure and the product was crystallized from *n*-hexane. The reactions of bis-π-cyclopentadienyl or bis-π-indenyl molybdenum(VI)-oxo-dichloride with dioximes in 1 : 2 molar ratio, respectively, in the presence of 2 mole of triethylamine, have also been studied but in such cases also 1 : 1 products could have been isolated.

Elemental analyses and physical measurements

The carbon and hydrogen analyses were carried out at the Microanalytical Division of Central Drug Research Institute, Lucknow, and Department of Chemistry, Banaras Hindu University, Varanasi (India). Molybdenum was measured as 8-hydroxyquinolate. Nitrogen was estimated by Kjeldahl's method and chlorine as silver chloride.

Infrared spectra in KBr pellets were recorded on a Perkin–Elmer-621 and Beckmann Acculab-9 spectrophotometer, electronic spectra in tetrahydrofurane on a Perkin–Elmer-4000 A and on Cary-14 spectrophotometer. The magnetic susceptibility measurements were carried out by Gouy's method using mercury tetrathiocyanocobaltate(II) as calibrant. Electrical conductance measurements were carried out in nitrobenzene on a Beckmann conductivity Bridge Model RC-18A.

Results and Discussion

A systematic study of reaction of bis-π-cyclopentadienyl molybdenum-(VI)-oxo-dichloride or bis-π-indenyl molybdenum(VI)-oxo-dichloride (1 mole) with hydroxyoximes (1 mole) in the presence of triethylamine (2 mole) yielded complexes of the type $[(\pi\text{-}C_5H_5)_2$ or $(\pi\text{-}C_9H_7)_2MoO(Ox)]$ where $[OX]^{2-}$ represents the anion of corresponding oximes:

$$(\pi\text{-}C_5H_5)_2MoOCl_2 + OxH_2 + 2\ Et_3N \xrightarrow[30\ °C]{THF}$$

$$\longrightarrow [(\pi\text{-}C_5H_5)_2MoO(OX)] + 2\ Et_3N \cdot HCl$$

$$(\pi\text{-}C_9H_7)_2MoOCl_2 + OxH_2 + 2\ Et_3N \xrightarrow[30\ °C]{THF}$$

$$\longrightarrow [(\pi\text{-}C_9H_7)_2MoO(OX)] + 2\ Et_3N \cdot HCl.$$

These complexes are soluble in benzene, tetrahydrofuran, chloroform, dimethyl formamide, nitrobenzene and dimethyl sulfoxide. Analytical data are given in Table I.

Reactions of bis-π-cyclopentadienyl molybdenum(VI)-oxo-dichloride and bis-π-indenyl molybdenum(VI)-oxo-dichloride (1 mole) with dioximes ($Ox'H_2$) (1 mole) in tetrahydrofurane in the presence of triethylamine (1 mole) yielded complexes of the type $[(\pi\text{-}C_5H_5)_2$ or $(\pi\text{-}C_9H_7)_2MoO(Ox'H)Cl]$ where $[Ox'H]^{1-}$ represents the anion of the corresponding oxime.

$$(\pi\text{-}C_5H_5)_2MoOCl_2 + Ox'H_2 + Et_3N \xrightarrow[30°C]{THF}$$

$$\rightarrow [(\pi\text{-}C_5H_5)_2MoO(Ox'H)Cl] + Et_3N \cdot HCl$$

$$(\pi\text{-}C_9H_7)_2MoOCl_2 + Ox'H_2 + Et_3N \xrightarrow[30\,°C]{THF}$$

$$\rightarrow [(\pi\text{-}C_9H_7)_2MoO(Ox'H)Cl] + Et_3N \cdot HCl.$$

These complexes are soluble in nitrobenzene, dimethyl formamide and dimethyl sulfoxide, sparingly soluble in tetrahydrofurane and insoluble in benzene and chloroform. Analytical data are given in Table I.

All these oximato complexes are susceptible to hydrolysis and decompose on heating above 180°. Electrical conductance measured in nitrobenzene show them to be essentially non-electrolytes.

Magnetic and electronic spectral studies

Magnetic susceptibilities measured at room temperature by Gouy's method proved the expected diamagnetic nature of the complexes. The electronic spectra recorded in tetrahydrofurane show a band at *ca.* 34 000—34 500 cm^{-1}. The electronic spectra of ligands also show this band, indicating that this is due to internal transition of ligand and may be assigned to $\pi \rightarrow \pi^*$ transition of ($\rangle C{=}N$) group.

Infrared spectra

The important i.r. frequencies are given in Table II. The infrared spectra of the ligands exhibit a broad band at *ca.* 3300—3250 cm^{-1} assigned to ν(OH), which vanishes in the spectra of complexes of hydroxyoximes indicating that both the OH group coordinate to metal atom through deprotonation. However, in the spectra of complexes derived from dioximes, this band shifts at 3400 cm^{-1}. In these complexes, the precipitation of $Et_3N \cdot HCl$ during the preparation of complexes and also the estimation of chloride indicate the involvement of only one OH group to the metal atom through deprotonation.

Table I

*Analytical data of the complexes**

Compound	Calculated %					Found %				
	C	H	N	Cl	M	C	H	N	Cl	M
1	2	3	4	5	6	7	8	9	10	11
$[(\pi-C_5H_5)_2MoO(SOx)]$	54.1	3.9	3.7	—	25.4	53.9	3.7	3.6	—	25.4
$[(\pi-C_5H_5)_2MoO(AOx)]$	56.3	4.6	3.4	—	23.6	56.2	4.6	3.4	—	23.4
$[(\pi-C_5H_5)_2MoO(NOx)]$	59.0	3.9	3.2	—	22.4	58.7	3.5	3.0	—	22.0
$[(\pi-C_5H_5)_2MoO(BOx'H)Cl]$	55.5	4.4	4.4	6.8	18.1	55.3	4.1	4.2	6.5	18.0
$[(\pi-C_5H_5)_2MoO(DOx'H)Cl]$	42.8	4.3	7.1	7.1	24.4	42.6	4.0	7.0	8.7	24.0
$[(\pi-C_5H_5)_2MoO(POx'H)Cl]$	46.4	4.2	8.9	7.5	20.0	46.3	4.2	8.8	7.5	20.0
$[(\pi-C_9H_7)_2MoO(SOx)]$	62.9	3.9	2.9	—	20.0	62.5	3.4	2.7	—	19.7
$[(\pi-C_9H_7)_2MoO(AOx)]$	64.1	4.5	2.7	—	19.0	64.0	4.3	2.4	—	18.4
$[(\pi-C_9H_7)_2MoO(NOx)]$	66.0	3.9	2.6	—	18.2	65.6	3.7	2.4	—	18.0
$[(\pi-C_9H_7)_2MoO(BOx'H)Cl]$	62.0	4.3	4.5	5.7	15.3	61.8	4.0	4.4	5.6	15.3
$[(\pi-C_9H_7)_2MoO(DOx'H)Cl]$	53.5	4.2	5.6	7.0	19.4	53.3	4.0	5.5	7.0	19.0
$[(\pi-C_9H_7)_2MoO(POx'H)Cl]$	56.8	4.2	7.3	6.2	16.8	56.5	4.1	7.2	6.0	16.6

* where $SOxH_2 = C_7H_7NO_2$, $AOxH_2 = C_9H_{11}NO_2$, $NOxH_2 = C_{11}H_9NO_2$, $BOx'H_2 = C_{14}H_{12}N_2O_2$, $DOx'H_2 = C_4H_8N_2O_2$, $POx'H_2 = C_9H_{11}N_3O_2$.

Table II

Important infrared spectral bands (in cm^{-1}) with assignments

Compound	νOH	νC=N	ν(N—O)	ν(C—O) phenolic δ(N—O)	8a or 8b	6a	16b	ν(Mo—Py)	ν(Mo—N)	ν(Mo—O) phenolic
$[(\pi-C_5H_5)_2MoO(SOx)]$	—	1560s	1200s, 930s	1290s	—	—	—	—	360w	480w
$[(\pi-C_5H_5)_2MoO(AOx)]$	—	1550m	1190m, 935m	1280m	—	—	—	—	375w	470m
$[(\pi-C_5H_5)_2(MoONOx)]$	—	1550m	1200m, 940s	1280m	—	—	—	—	375m	470w
$[(\pi-C_5H_5)_2MoO(BOxH)Cl]$	3400mb	1555s	1190m, 940s	1275m	—	—	—	—	370w, 365m	—
$[(\pi-C_5H_5)_2MoO(DOx'H)Cl]$	3420mb	1540m	1185s, 930m	1270b	—	—	—	—	375m, 360w	—
$[(\pi-C_5H_5)_2MoO(POx'H)Cl]$	3400mb	1540m	1195m, 940m	1280m	1585s	630m 615sh	410s	285w	370w, 350w	—
$[(\pi-C_9H_7)_2MoO(SOx)]$	—	1560s	1200s, 930s	1290s	—	—	—	—	360w	480m
$[(\pi-C_9H_7)_2MoO(AOx)]$	—	1555m	1195m, 930m	1280m	—	—	—	—	370w	480m
$[(\pi-C_9H_7)_2MoO(NOx)]$	—	1560s	1185m, 935m	1285mb	—	—	—	—	375m	475w
$[(\pi-C_9H_7)_2MoO(BOx'H)Cl]$	3400b	1550m	1190m, 940s	1270m	—	—	—	—	370w, 360w	—
$[(\pi-C_9H_7)_2MoO(DOx'H)Cl]$	3400mb	1540m	1195m, 930m	1280m	—	—	—	—	375w, 350w	—
$[(\pi-C_9H_7)_2MoO(POx'H)Cl]$	3400b	1540m	1190m, 935m	1275m	1580s	628m, 610sh	415m	280w	370w, 350w	—

The medium band appearing at *ca.* 1610 cm^{-1} in the ligands due to $\nu(C=N)$ shifts to lower frequency *ca.* 1560—1550 cm^{-1}. The lowering of the $\nu(C=N)$ frequency indicates that the C=N bond order decreases and that the nitrogen atom coordinates to molybdenum [6]. The large $\nu(C=N)$ shifts from the normal value of 1610 cm^{-1} to 1560—1550 cm^{-1} appears to be due to resonance, conjugation or coupling with C=C and with hydrogen bonds [6]. The bands in the 1200—1185 and 940—930 cm^{-1} regions in the complexes are attributed [6] to a $\nu(N-O)$ vibration.

In addition to above the pyridine ring vibrations, in the ligand 2,6-diacetylpyridine dioxime, appear at 1580 cm^{-1} (8a or 8b, ring deformation), 620 cm^{-1} (6a, an in-plane deformation) and 400 cm^{-1} (16b, out-of-plane deformation). In the complexes, these bands show upward shift ($\sim$ 10 cm^{-1}) and splitting of 6a band has also been observed. The upward shift and splitting of 6a band are consistent [7—9] with the pyridine nitrogen coordination. The band due to $\nu(Mo-Py)$ is located at *ca.* 285—280 cm^{-1}.

In the infrared spectra of bis-π-cyclopentadienyl molybdenum(VI) derivatives the presence of $C_5H_5^-$ ring in these compounds is inferred by the absorption bands [10] at *ca.* 3000 cm^{-1} (C—H stretching), at *ca.* 1150 and 1025 cm^{-1} (C—H, in-plane deformation) and at 860—840 cm^{-1} (C—H, out-of-plane deformation). Sharp and strong absorption bands in the region 1460—1440 cm^{-1} indicate the C—C stretching (asymmetric ring breathing), and also the π-bonding of the ring with the molybdenum oxo-group. The presence of indenyl group is indicated by the usual peaks due to $C_5H_5^-$ ring. The absorption bands due to phenyl part [10] of the indenyl group appeared at 1600 and 1450 cm^{-1} (C—C stretching), at *ca.* 1380 and 750 cm^{-1} (C—H, in-plane and out-of-plane deformations, respectively). A band at 710 cm^{-1} may be due to the methylene rocking vibration (since indene itself shows an absorption band at *ca.* 700 cm^{-1}).

In addition to above, a very sharp band at *ca.* 980 cm^{-1} in all the complexes is due to Mo=O stretching frequencies [11].

Thus, on the basis of elemental analyses, electrical conductance, infrared and electronic spectra, the following structures are assigned for the complexes (see in the next page).

*

Research facilities provided by Prof. S. C. TRIPATHI enabling the work to be carried out at the Organometallic Laboratory, Chemistry Department, University of Gorakhpur, are greatly appreciated.

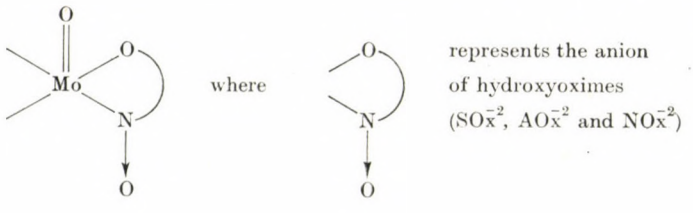

(I)

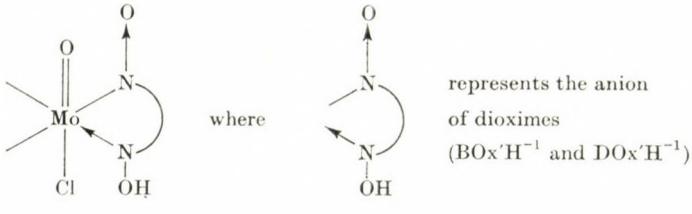

(II)

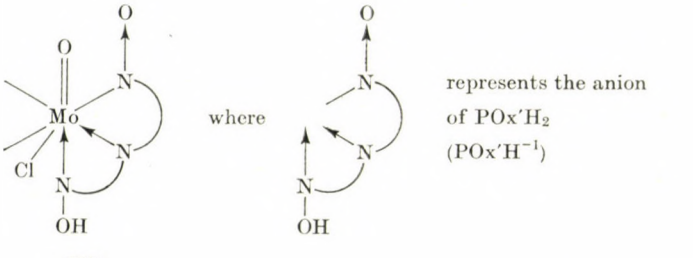

(III)

REFERENCES

[1] MEHROTRA, R. C., RAI, A. K., SINGH, A., BOHRA, R.: Inorg. Chim. Acta Revs., **13,** 91 (1975)
[2] CHAKRAVORTY, A.: Coord. Chem. Rev., **13,** 1 (1974)
[3] ANAND, S. P., MULTANI, R. K., JAIN, B. D.: J. Organometal. Chem., **24,** 428 (1970)
[4] ANAND, S. P., MULTANI, R. K., JAIN, B. D.: Curr. Sci., **37,** 487 (1968)
[5] PRAKASH, S.: Ph. D. Thesis, University of Delhi, 1970; VOGEL, A. I.: "A Text Book of Practical Organic Chemistry," Longman Green, London, 1948
[6] BIRADAR, N. S., MAHALE, V. B.: J. Less. Common Mets., **31,** 159 (1973)
[7] MADDEN, D. P., NELSON, S. M.: J. Chem. Soc. A, **1968,** 2342
[8] MODDEN, D. P., DAMOTA, M. M., NELSON, S. M.: J. Chem. Soc. A, **1970,** 890
[9] FERRARO, J. R.: "Low Frequency Vibrations of Inorganic and Coordination Compounds," Plenum, New York, 1971
[10] NAKAMOTO, K.: "Infrared Spectra of Inorganic and Coordination Compounds," Wiley Interscience, New York, 1970
[11] ADAMS, D. M.: "Metal Ligand and Related Vibration," E. Arnold, London, 1967

S. K. SENGUPTA — Department of Chemistry, University of Gorakhpur, Gorakhpur-273001 (U.P.), India

Shyam KUMAR — Department of Chemistry, University of Delhi, Delhi-110007, India

Acta Chimica Academiae Scientiarum Hungaricae, Tomus 108 (1), pp. 51—54 (1981)

POLARIZABILITIES AND SUSCEPTIBILITIES OF HOMOLOGOUS *TRANS*-4-ETHOXY-4'-*n*-ALKANOYL-OXYAZOBENZENES

V. R. MURTHY and R. N. V. RANGA REDDY

(Molecular Biophysics Laboratory, Department of Physics S.V.U. Autonomous Post-Graduate Centre, Anantapur-515003, India)

Received July 17, 1980

Accepted for publication September 30, 1980

The mean polarizabilities of homologous series of nematogenic *trans*-4-ethoxy-4'-*n*-alkanoylazobenzenes have been evaluated by using the modified Lippincott δ-function potential model [1, 2]. From the evaluated polarizabilities, the diamagnetic susceptibilities of these liquid crystals are calculated using the method of RAO and MURTHY [3]. The results are discussed in relation to the ones obtained from the refractivity method and PASCAL's method.

Introduction

The steric structures of polymers, biopolymers and liquid crystals has been studied by various physical methods like X-ray diffraction, NMR, ORD and CD. Recently attempts have been made by RAO *et al.* [4] and MURTHY *et al.* [5—8] to use mean polarizability as a technique to investigate the stereochemistry of these macromolecules. They have studied the polarizabilities of a few polymers and biopolymers and have successfully applied polarizability in the conformational analysis of biopolymers [9]. Recently MURTHY *et al.* [1, 2, 10, 11] have also evaluated the polarizabilities of a few liquid crystal systems with the idea of using them for conformational studies.

The present investigation deals with the evaluation of mean polarizabilities of a homologous series of the nematogenic 4-ethoxy-4'-*n*-alkanoyloxyazobenzenes $CH_3CH_2O-C_6H_4N=NC_6H_4OC(=O)(CH_2)_nCH_3$ for $n = 3$ to 12 using a method based on the Lippincott δ-function potential model modified recently by MURTHY and REDDY [1, 2]. The mean diamagnetic susceptibilities of these liquid crystals are also evaluated from the polarizability data using the method of Rao and Murthy.

Method

The equations for calculating the mean polarizability in terms of the parallel bond component ($\Sigma \alpha_{\|p}$), perpendicular bond contribution ($\Sigma 2\alpha_{\perp}$) and no-bond region electron contribution ($\Sigma \alpha_{\|n}$) are

$$\alpha_1 = 1/3\,(\Sigma \alpha_{\|p} + \Sigma \alpha_{\|n} + \Sigma 2\alpha_{\perp}). \qquad (1)$$

Where

$$\Sigma \alpha_{\|p} = \frac{4nA \exp{(T - T_c)/T_c}}{a_0} \left[\frac{R^2}{4} + \frac{1}{2C_R^2}\right]^2 \cdot \exp\left[\frac{-(X_1 - X_2)^2}{4}\right] \tag{2}$$

$$\Sigma \alpha_{\|n} = \Sigma f_j \alpha_j \tag{3}$$

and

$$\Sigma 2\alpha_{\perp} = n_{df}\left[\frac{\Sigma X_j^2 \alpha_j}{\Sigma X_j^2}\right]. \tag{4}$$

The mean polarizability in the liquid crystalline phase (α) is

$$\alpha = \alpha_1\left[1 - \frac{m}{\varrho_1}(T_c - T)\right] \tag{5}$$

where m is the slope of the ϱ *versus* t plot, ϱ_1 is the density of the liquid crystal in the liquid phase, α_1 is the mean polarizability in the liquid phase and T_c is the transition temperature.

The significance of the various terms in the above equations is explained in Ref. [1, 2]. The bond lengths used in the evaluation of mean polarizability were taken from Ref. [12]. The values of A and C_R were taken from our previous work [13, 14]. The density data for these system were taken from Ref. [15].

The semi-empirical relation derived by RAO and MURTHY between diamagnetic susceptibility and polarizability can be written as

$$-\chi = (\gamma_m \sigma')\alpha \tag{6}$$

Here $\gamma = (0.9)^n$ reveals the unsaturation state of the molecule with n denoting the number of unsaturated bonds and rings present in the molecule. σ' is the degree of covalency of the characteristic group and is given as

$$\sigma' = [\sigma_1^{1/n_1} \sigma_2^{1/n_2} \ldots \sigma_p^{1/n_p}]^{1/2}$$

where $\sigma_1, \sigma_2, \ldots, \sigma_p$ are Pauling's percent covalency characters of the bonds present in the characteristic group. $n_1, n_2, \ldots, n_p$ are the bond orders of the various bonds in the characteristic group. m is a constant equal to 0.72×10^{19}.

Using Eqs (5) and (6) the mean polarizabilities and mean diamagnetic susceptibilities of the homologous series of *trans*-4-ethoxy-4'-*n*-alkanoyloxyazobenzenes have been determined. In order to have a comparison, the mean polarizabilities of these liquid crystals were also calculated from the refractivity method [16]. The mean diamagnetic susceptibilities of these liquid crystals were determined by PASCAL's method [17, 18]. The results are presented in Tables I and II.

Table I

Polarizabilities (X 10^{23} cm^3) *of* $CH_3CH_2O-C_6H_4N=NC_6H_4OC(=O)(CH_2)_nCH_3$

n	$\Sigma\alpha_{\|\|p}$	$\Sigma\alpha_{\|\|n}$	$\Sigma 2\alpha_{\perp}$	$m\times10^4$	α	α^*
3	6.053	0.128	4.320	10.07	3.492	3.752
4	6.450	0.128	4.547	9.13	3.685	4.020
5	6.846	0.128	4.695	8.62	3.789	4.191
6	7.242	0.128	4.921	9.38	4.013	4.293
7	7.639	0.128	5.146	9.49	4.214	4.533
8	8.035	0.128	5.372	9.51	4.402	4.637
9	8.431	0.128	5.597	9.70	4.609	4.813
10	8.828	0.128	5.823	9.92	4.816	4.902
11	9.224	0.128	6.049	9.76	5.024	5.152
12	9.620	0.128	6.774	10.25	5.486	5.304

* Estimated by the refractivity method

Table II

Diamagnetic susceptibilities (X10^5 CGS *Units) of* $CH_3CH_2OC_6H_4N=NC_6H_4OC(=O)(CH_2)_nCH_3$

n	$-\chi$	$-\chi^*$
3	19.178	19.257
4	20.314	20.443
5	21.131	21.629
6	22.446	22.815
7	23.582	24.001
8	24.748	25.187
9	25.853	26.373
10	26.989	27.559
11	28.125	28.745
12	29.260	29.931

* Estimated by PASCAL's method

Conclusion

The results in Tables I and II permit to draw the following conclusions. The polarizabilities of all the ten liquid crystals as calculated from the modified Lippincott δ-function model agree very well with the values obtained from the refractivity method. This suggests the applicability of our method, which

serves as an a priori method of obtaining estimated polarizabilities without recourse to experimental methods. The same conclusion can be drawn in the case of susceptibility measurements too. While no direct proof for our calculations from experiments could be obtained, indirect evidence for its validity is provided by PASCAL's method, whose correctness has already been established [19, 20].

*

The authors thank Prof. S. V. SUBRAHMANYAM, Head, Department of Physics, for his keen interest in this work.

REFERENCES

[1] MURTHY, V. R., NAIDU, S. V., RANGA REDDY, R. N. V.: Mol. Cryst. Liq. Cryst., **59**, 27 (1980)
[2] MURTHY, V. R., RANGA REDDY, R. N. V.: Acta Phys. Acad. Sci. Hung., **48**, 107 (1980)
[3] RAO, B. P., MURTHY, V. R., SUBBAIAH, D. V., NAIDU, S. V.: Acta Ciencia Indica, **5**, 118 (1979)
[4] RAO, B. P., MURTHY, V. R., SUBBAIAH, D. V.: Ind. J. Biochem. Biophy., **14**, 181 (1977)
[5] MURTHY, V. R., SUBBAIAH, D. V., NAIDU, S. V.: Ind. J. Biochem. Biophy., **16**, 43 (1979)
[6] MURTHY, V. R., NAIDU, S. V.: JQSRT, **19**, 551 (1978)
[7] MURTHY, V. R., NAIDU, S. V.: Acta Ciencia Indica, **5**, 124 (1979)
[8] MURTHY, V. R., SUBBAIAH, D. V., NAIDU, S. V.: Ind. Chem. J., **1**, 1 (1977)
[9] MURTHY, V. R.: Ind. J. Biochem. Biophy., **16**, 32 (1979)
[10] MURTHY, V. R., RANGA REDDY, R. N. V.: Acta Ciencia Indica, **6**, 21 (1980)
[11] MURTHY, V. R., RANGA REDDY, R. N. V.: JQSRT (In press)
[12] Handbook of Physics and Chemistry, Chem. Rubber Publ. Co., 1979
[13] RAO, B. P., MURTHY, V. R.: Curr. Sci., **41**, 15 (1972)
[14] RAO, B. P., MURTHY, V. R., SUBBAIAH, D. V.: Ind. J. Pure Appl. Phy., **14**, 276 (1979)
[15] VAN HECKE, G. R., SANTARSIERO, B. D., THEODORE, L. J.: Mol. Cryst. Liq. Cryst., **45**, 1 (1978)
[16] ADAMSKI, P., DYLIK, A.: Mol. Cryst. Liq. Cryst., **35**, 337 (1976)
[17] PASCAL, P.: Ann. Chem. Phys., **19**, 5 (1910)
[18] PACAULT, A.: Rev. Sci. Acad. Sci. Paris, **84**, 169 (1946); **86**, 38 (1948)
[19] de JEU, W. H., CLAASSEN, W. A. P.: J. Chem. Phys., **68**, 102 (1978)
[20] BAHADUR, B.: J. Chem. Phys., **67**, 3272 (1977)

V. R. MURTHY
R. N. V. RANGA REDDY
S. V. U. Autonomous Post-Graduate Centre,
Anantapur-515003, INDIA

Acta Chimica Academiae Scientiarum Hungaricae, Tomus 108 (1), pp. 55–73 (1981)

FORCE FIELD AND DIPOLE MOMENT DERIVATIVES OF ETHYLENE FROM A COMBINATION OF *AB INITIO* QUANTUM CHEMICAL AND EXPERIMENTAL INFORMATION

G. FOGARASI and P. PULAY

(*Eötvös L. University, Department of General and Inorganic Chemistry, Budapest*)*

Received July 1, 1980

Accepted for publication October 13, 1980

The quadratic and the most important cubic force constants as well as the dipole moment derivatives of ethylene have been calculated *ab initio* at the Hartree-Fock level, using a large spd basis function set and for comparison a smaller sp basis set. The *ab initio* harmonic force field was scaled with 6 empirical scale factors by optimizing the latter on the experimental frequencies. The final force field reproduces all available experimental data as precisely as does the most sophisticated experimental force field and is considered as the more reliable one in the cases of the few discrepancies. The infrared intensities are moderately well reproduced by the sp basis set; the polarization functions improve the results significantly.

Introduction

Ethylene is one of the few molecules for which highly detailed studies have been carried out, both experimentally and theoretically, for the determination of the general harmonic force field. For many years, the basic problem concerned the A_g symmetry species in which there are two basically different sets of force constants, both of which reproduce the frequency data of several isotopic species equally well. This problem was first solved in 1971 in an experimental study by MCKEAN and DUNCAN [1] based on ^{13}C frequency shifts in CH_2CD_2 and, simultaneously, in an *ab initio* study by PULAY and MEYER [2]. Later on, the excellent work of DUNCAN, MCKEAN and MALLINSON [3], based on 55 experimental data including ^{13}C frequency shifts and Coriolis constants, resulted in one of the most sophisticated force field determinations ever made (quoted as D-M-M force field in this paper). Recent *ab initio* calculations by BLOM and ALTONA [4] scaled on the experimental frequencies, gave a force field (B-A force field in the following) which confirms the experimental one in almost every respect; still, in spite of the excellent general agreement, there are also some disturbing small discrepancies in the finer details.

Recently, we have started systematic studies for the determination of molecular force constants (as well as dipole moment derivatives and geo-

* During part of this work G. F. was visiting research associate at the Department of Chemistry, University of Texas, Austin, Texas.

metries) from the combined information of *ab initio* quantum chemical calculations on the SCF level and experimental data [5]. Results on ethylene will be presented here.

The main purpose of this study is to investigate the basis set effect. We have carried out calculations with a large spd basis which, from the point of view of force constants, represent results close to the Hartree-Fock limit. These will be compared with results obtained with moderate sp basis function sets. In addition, we want to analyze the small discrepancies mentioned above between the experimental and theoretical force field.

Computational details

The calculations have been carried out by the force (gradient) method [6], using the *ab initio* gradient program TEXAS [7]. Our general practice for force constant calculations is described in [5]. The large, spd basis was essentially the 6—31G** basis developed in POPLE's group [8, 9], with two minor deviations which should be insignificant for the results: for hydrogen, the exponents were scaled uniquely by 1.15, rather than using two different scaling factors; for carbon, their original atomic exponents were used without scaling. Otherwise the basis was exactly taken from [8, 9]. Specifically the exponents of the polarization functions were $\alpha_d(C) = 0.8$, $\alpha_p(H) = 1.1$. For the comparative sp basis set calculations our standard Gaussian 4—21 basis [5] was used which is similar to the widely applied 4—31G basis [10] with a slight reduction: the first contraction in the valence shell contains only two functions instead of three; this is more economical and gives very similar results.

The original quantum mechanical calculations were carried out around the following reference geometry: $R(CC) = 1.339$ Å (133.9 pm), $r(CH) =$ $= 1.085$ Å (108.5 pm), $\beta(CCH) = 121.1°$. As suggested by BLOM and ALTONA [11] and advocated also by us [5], the ideal reference geometry should be an empirically corrected theoretical geometry, which is considered as the best estimate of the true equilibrium geometry. For ethylene this is: $R(CC) =$ $= 1.334$ Å (133.4 pm), $r(CH) = 1.078$ Å (107.8 pm), $\beta(CCH) = = 122.0°$ (see section on geometry, below). Thus, the original force constants were transformed to this geometry, using the anharmonic force constants obtained in our calculations.* For the latter, all f_{iii} and f_{iij} type terms are available, except the f_{ijk} terms. The lack of these latter, generally smaller, cubic terms and of the higher terms should only insignificantly influence the transformation.

* This is done by a small computer program in the following way: the more complete potential which includes the cubic terms is written in analytic form and the second derivatives of this function are evaluated at the new geometry.

In accordance with the recommendations of [5], local symmetry coordinates were used in the vibrational analysis. They are defined in Fig. 1 and Table I.

Table I

Definition of local symmetry coordinates[a)]

$S_1 = R$; $S_2 = r_1 + r_2$; $S_3 = r_3 + r_4$; $S_4 = r_1 - r_2$; $S_5 = r_3 - r_4$; $S_6 = 2\alpha_1 - \beta_1 - \beta_2$;
$S_7 = 2\alpha_2 - \beta_3 - \beta_4$; $S_8 = \beta_1 - \beta_2$; $S_9 = \beta_3 - \beta_4$; $S_{10} = \Theta_{2341}$; $S_{11} = \Theta_{1652}$;
$S_{12} = \tau_{3126} + \tau_{4125} + \tau_{3125} + \tau_{4126}$

a) See also Fig. 1.

Normalization factors are omitted in the table; each coordinate is normalized in the usual way by $(\Sigma c_i^2)^{-1/2}$

Θ is an out-of-plane and τ a torsional coordinate as defined in: WILSON, E. B., Jr., DECIUS, J. C., CROSS, P. C., Molecular Vibrations, McGraw-Hill, New York, 1955. Θ thus describes the angle of the C=C bond with the CH_2 plane (wagging). In both waggings, the CH_2 groups bend towards the positive z direction.

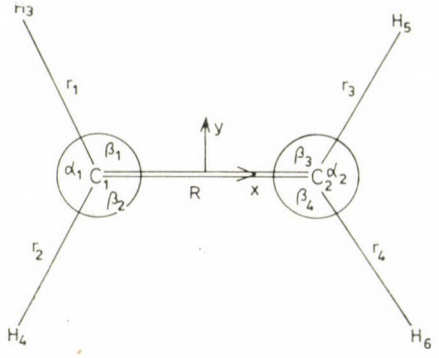

Fig. 1. Definition of internal coordinates for ethylene

It is now generally established that the theoretical diagonal force constants, as calculated at the SCF level, are systematically overestimated by 10—30 percent and the off-diagonal terms are obtained with comparable accuracy, the deviations being less systematic. Although this accuracy is not sufficient for a pure theoretical determination of the force field, the theoretical information can be very successfully combined with the experimental data. In some earlier calculations by us [12] and by BOTSCHWINA *et al.* [13—15] the coupling terms were taken from the theory and the diagonal terms fitted to the experimental frequencies. In another procedure, as practiced by BLOM and ALTONA [11] and in our semiempirical calculations [16], the force constants are grouped according to their types, with a separate scale factor for each group and the complete force field is scaled on the experimental frequencies. In the practice of BLOM and ALTONA all coupling constants represent

one single group with a common factor. In our procedure, if F_{ii} and F_{jj} are scaled by c_i and c_j, then $\sqrt{c_i c_j}$ is used for F_{ij}. This procedure was used in the present study, too. Neither of the two methods can be laid on a strict theoretical basis, but scaling the smaller interaction terms is not a crucial point anyway: the main effect of both procedures is to scale down the dominant diagonal force constants. In favour of our procedure, one may mention that it is invariant to certain transformations of the vibrational coordinates, notably to symmetrization of individual internal coordinates.

Results and discussion

Geometry

Although, it was already included in our general paper [5], for completeness we quote here the theoretical geometry obtained with the two different basis function sets and compare it with 4—31G results [17, 18] as well as with the experimental results of DUNCAN [19]. In addition, in column 5 of Table II

Table II

The geometry of ethylene[a]

	4—21	4—31G[b]	6—31G**	exp.[c]	scaled 4—21
C=C	1.312	1.316	1.318	1.334	1.334
C—H	1.073	1.073	1.077	1.081	1.078
CCH	122.0	122.0	121.7	121.3	122.0

a) Bond lengths in Å $= 10^{-10}$ m, bond angle in degree.
b) Refs. [17, 18]. c) Ref. [19].

the corrected 4—21 geometry is given, which is considered as a good estimate of the true equilibrium geometry. The correction is based on systematic deviations observed in the 4—21 calculations on a number of molecules, as indicated in [5] and as will be discussed in more detail in a separate paper. Both the 4—21 and the 6—31G** harmonic force constants, to be given, refer to this geometry as reference.

Force constants

The quantum mechanically calculated force constants were scaled on the experimental frequencies as described above. In the first stages of the fitting procedure, three scaling factors were used according to a rough separation of the various types of vibrations: stretchings, in-plane bendings and out-

of-plane deformations. This gave already a fairly good reproduction of the experimental frequencies. Our final aim is, however, to obtain a force field which is as reliable as possible thus making a critical discussion of the experimental results justified. For this purpose all of the types of coordinates were separated, leading to 6 scaling factors. These were optimized in a least square procedure by fitting them simultaneously to the vibrational frequencies of C_2H_4, C_2D_4 and CH_2CD_2. The frequencies were those corrected for anharmonicity and were taken from DUNCAN *et al.* [3], except ω_5 and ω_6 which will be discussed below.

The final scaling factors are given in Table III. The final force constants, obtained after scaling, are compared with the B-A [4] and D-M-M [3] force fields in Table IV.

Table III

Scale factors for the force constants

	4—21	6—31G**
CH stretch.	0.9346	0.9077
CC stretch.	0.9043	0.8679
sym. def.	0.8241	0.8622
rocking	0.8487	0.9028
wagging	0.7499	0.7958
twist	0.8097	0.8406

Before going into details of the force constants, two points in the assignment of the parent molecule C_2H_4 are worth discussing.

For the B_{1g} CH stretching mode, the assignment $\nu_5 = 3102.5$ cm^{-1}, $\omega_5 = 3231.9$ cm^{-1} was used in the D-M-M force field. Later, however, this mode was reassigned to $\nu_5 = 3083.2$ cm^{-1} [20] which gives after anharmonicity correction $\omega_5 = 3212$ cm^{-1}. We used the latter value in the fitting procedure. BLOM and ALTONA already pointed out [4] that their 4—31G *ab initio* calculation favored this latter assignment. As can be seen from Table V, an excellent fit is obtained for the reassigned value also in our calculations, both with the 4—21 and with the 6—31G** force fields. Thus, independent of the basis set, all theoretical results definitely confirm the reassignment.

The other questionable point is the B_{1g} rocking mode which has never been observed in the vapor phase. The assignment used in [3], $\nu_6 = 1220$, $\omega_6 = 1245$ cm^{-1} is based on a combination band. Based on their calculated frequencies, BLOM and ALTONA suggested [4] an alternate assignment of $\nu_6 = 1236$ cm^{-1} (giving $\omega_6 = 1261$ cm^{-1}) which is a weak band in the Raman spectrum of the liquid. We carried out the fitting with both assignments:

Table IV

Force constants of ethylene[a]

Description	$F_{i,j}$	present[b]		B-A[c] 4—31G	D-M-M[d] exp.
		4—21	6—31G**		
CC str.	$F_{1,1}$	9.351	9.152	9.311	9.395
CH_2 sym. str.	$F_{2,2}$	5.606	5.601	5.609	5.620
CH_2 as. str.	$F_{4,4}$	5.547	5.537	5.546	5.575
CH_2 sym. def.	$F_{6,6}$	0.467	0.470	0.468	0.470
CH_2 rock	$F_{8,8}$	0.560 (0.570)[e]	0.558	0.573	0.572
CH_2 wagg	$F_{10,10}$	0.267 (0.258)[e]	0.268	0.257	0.257
torsion	$F_{12,12}$	0.135 (0.139)[e]	0.135	0.139	0.139
CC str./CH_2 sym. str.	$F_{1,2}$	0.112	0.123	0.106	0.257
CC str./CH_2 sym. def.	$F_{1,6}$	−0.220	−0.190	−0.223	−0.222
CH_2 sym. str./sym. str.	$F_{2,3}$	0.011	0.009	0.010	0.017
CH_2 sym. str./sym. def.	$F_{2,6}$	0.093	0.087	0.082	0.018
CH_2 sym. str./sym. def.	$F_{2,7}$	−0.013	−0.016	−0.013	−0.074
CH_2 sym. def./sym. def.	$F_{6,7}$	0.017	0.018	0.019	0.018
CH_2 as. str./as. str.	$F_{4,5}$	0.022	0.019	0.020	−0.082
CH_2 as. str./rock	$F_{4,8}$	0.161	0.123	0.155	0.111
CH_2 as. str./rock	$F_{4,9}$	−0.055	−0.060	−0.059	−0.285
CH_2 rock/rock	$F_{8,9}$	−0.086	−0.093	−0.088	−0.087
CH_2 wagg/wagg	$F_{10,11}$	0.035	0.039	0.039	0.039

a) Units are consistent with energy measured in aJ, stretching coordinates in Å = 0.1 nm and bending coordinates in radian.

b) *Ab initio* results, scaled by the factors given in Table III.

c) Scaled *ab initio* results from BLOM and ALTONA [4].

d) Experimental results from DUNCAN, MCKEAN and MALLINSON [3].

e) The considerable deviations of the rocking, wagging and torsional force constants from the D-M-M and B-A values are the consequence of different geometry. To show this, the scaling of the 4—21 force constants was also carried out using the G matrix evaluated at the D-M-M geometry. These values are given in parentheses.

as Table V shows the reproduction is indeed somewhat better with $\omega_6 =$ $= 1261$ cm^{-1}, but the results are less conclusive than was the case with ω_5. (As to the other theoretical frequencies, the reassignment of ω_6, which affects mainly the rocking force constant, has noticeable effect only on ω_6 and ω_{10}. Their values for both assignments are included in Table V.)

As a somewhat arbitrary choice, we have accepted the reassignment also for the rocking mode and our final scale factors and force constants refer to the reassigned values $\omega_5 = 3212$, $\omega_6 = 1261$ cm^{-1}.

When discussing the force field, the first general observation from Table IV is the very good agreement of all the three theoretical results with each other as well as with the D-M-M values. Two important conclusions can

Table V

Experimental (harmonic) and calculated frequencies (cm^{-1})[a]

	ω_i	C_2H_4					C_2D_4					CH_2CD_2				
		exp.	*A*	*B*	*C*	*D*	exp.	*A*	*B*	*C*	*D*	exp.	*A*	*B*	*C*	*D*
	1	3152	3157	3154	3155	3158	2330	2335	2333	2330	2332	3145	3147	3145	3145	3147
A_g	2	1655	1658	1669	1657	1658	1539	1536	1535	1537	1541	1609	1610	1618	1609	1608
	3	1370	1369	1356	1367	1371	1000	1000	998	998	1000	1047	1045	1044	1043	1043
A_u	4	1044	1043	1043	1045	1044	738	738	738	739	738	903	903	903	905	904
B_{1g}	5	3212	3210	3212	3215	3229	2381	2391	2396	2398	2389	2408	2400	2403	2407	2402
	6	1245[b] 1261[c]	1253 1257	1258 1263	1262	1249	1028	1021 1024	1024 1027	1027	1024	1164	1165 1168	1168 1172	1173	1166
B_{1u}	7	969	955	962	967	967	731	722	727	732	731	763	762	764	764	764
B_{2g}	8	959	973	967	962	962	798	804	799	794	794	963	965	964	964	964
B_{2u}	9	3234	3239	3236	3243	3232	2418	2410	2409	2415	2413	3223	3225	3225	3229	3230
	10	843	842 845	835 838	849	844	—	605 608	600 602	610	605	699	698 700	692 694	703	697
B_{3u}	11	3147	3136	3136	3135	3136	2266	2266	2266	2263	2264	2298	2302	2301	2298	2300
	12	1473	1476	1479	1469	1472	1094	1093	1095	1089	1091	1411	1410	1403	1406	1414

[a] exp.: experimental values taken from [3]; *A*: obtained with the present 4 –21 force field; *B*: obtained with the present 6 –31G** force field; *C*: BLOM and ALTONA [4]; *D*: D-M-M force field [3];
[b] assignment used in [3]. [c] proposed assignment from [4], the second row for ω_6 and ω_{10} refers to this.

be drawn from a comparison of the theoretical force fields. First, considering that we applied a slightly different scaling procedure than that used by BLOM and ALTONA [4], the agreement with their results shows that the exact form of scaling is not a crucial point. (As to the differences in some diagonal terms, see the remarks below.) Secondly, it is very reassuring that the final force constants are almost independent of the basis set. While this is not surprising for the two similar sp basis sets, it is the more significant that even the inclusion of polarization functions does not change the results. Of course, this refers to the scaled values; the original *ab initio* values differ considerably, as can be calculated back from the scaling factors of Table III.

For the diagonal force constants, the agreement with the experimentally derived D-M-M values is generally excellent, the deviations being 1 per cent or less. One should realize that the larger differences in the rocking, wagging and torsional force constants are the consequence of different geometry (this refers also to the B-A values): if the same *ab initio* values are scaled using the D-M-M **G** matrix, the agreement is excellent, see Table IV. (In fact, the torsion is a one dimensional mode so that the corresponding force constant is uniquely defined by the experimental frequencies, independent of the starting *ab initio* value.) Note that this geometry effect causes comparable *relative* changes in the relevant coupling terms. However, a few per cent uncertainty in these small constants is insignificant and it does not explain the much greater discrepancies to be discussed further below.

Although the dependence of the force constants on the, to some extent always uncertain, selection of the geometry is obvious, it is usually left out of consideration because other uncertainty factors predominate. This problem should be born in mind, however, if high quality results are compared.

Concerning the diagonal force constants, there is one more, finer detail: the 6—31G** value of the CC stretching constant $F_{1,1}$ is about 2 per cent smaller than in other results. Although this is still compatible with the 1 per cent experimental uncertainty in the frequencies, it seemed worthwhile to analyze it in detail. It turns out that the underlying problem is not with $F_{1,1}$ itself but with the CC str./CH_2 sym. def. coupling term, $F_{1,6}$ which, as can be seen from Table IV, is 0.03 smaller in absolute value than in other results. While such a small deviation is usually negligible, in the present case $F_{1,6}$ couples two near-degenerate zeroth-order (as if there were no coupling either in G or F) frequencies ω_2 and ω_3 which thus become extremely sensitive to it. With smaller $F_{1,6}$ ω_2 becomes too high so that the fitting procedure tries to compensate for this by lowering $F_{1,1}$. This was explicitly proved by varying $F_{1,6}$ as an independent parameter. In this case $F_{1,6}$ converged to -0.219, $F_{1,1}$ to 9.34 and $F_{6,6}$ to 0.467. Whatever is the best estimate of the true value of $F_{1,6}$, -0.19 or -0.22, the small difference is certainly insignificant from the physical point of view.

Turning now to the discussion of the complete force field, including all coupling terms, some general considerations seem appropriate. All three scaled theoretical force fields agree with the D-M-M results in general very well, except for just a few coupling constants. Noteworthy is the discrepancy in the CC str./CH_2 sym. str. ($F_{1,2}$) and the CH_2 as.str./CH_2 rock' ($F_{4,9}$) terms. One should realize the basic difference between the two approaches. In the purely experimental determination, 55 data points were fitted by 18 parameters. Although the ratio of number of data points to number of parameters is relatively high, there may be still too much flexibility in the fitting procedure, with the result that some parameters remain ill-determined. On the other hand, our scaling procedure contains only 6 parameters. This, together with the starting *ab initio* values places a very strict restriction upon the final theoretical force field.

Of great importance is the observation that the deviations occur randomly. Obviously, it is just the experimental force field in which random errors can be expected: due to the different sensitivity of the individual force constants to the experimental data, if one of the latter is strongly perturbed by some anharmonicity effect, the result may be a force constant matrix in which a few elements are ill-determined, while all others are correct. On the other hand, it is reasonable to assume that the theoretical force field is well balanced, *i.e.* if the majority of force constants are correct, as judged by experiment, then the remaining ones are also correct within comparable accuracy.

We discuss first the in-plane force field, in the light of the frequencies. As can be seen from Table V, their reproduction is as good as by the D-M-M field, fitted directly to the experimental data. In the CH (CD) stretching region, the A_g, B_{1g} and B_{2u} frequencies are in fact better reproduced than could be expected from the 1 per cent experimental uncertainty, as accepted by DUNCAN *et al.* [31]. Thus, their estimation of anharmonicity was apparently excellent. The B_{3u} ω_{11} mode in C_2H_4 is also reproduced within 0.3 per cent, but it is noticeable that it comes out systematically too low by 11—12 cm^{-1} in all calculations, including the D-M-M one, while it is excellently reproduced in the isotopic molecules. Considering that the accepted experimental value of $\nu_{11} = 3021$ cm^{-1} (giving $\omega_{11} = 3147$ cm^{-1}) contains a large correction for Fermi resonance [3] (the directly measured band center is at 2988.6 cm^{-1} [21]), it seems that this correction was slightly overestimated.

In the more interesting medium frequency range, the maximum deviation of the 4—21 results from the experimental frequencies of C_2H_4, C_2D_4 and CH_2CD_2 is 4 cm^{-1} (!) (with the $\omega_6 = 1261$ cm^{-1} assignment being accepted; it is 8 cm^{-1} with the original assignment). In the 6—31G** results somewhat larger deviations are observed for ω_2 and ω_3 in C_2H_4 (14 cm^{-1}). These are due to the slightly different value of the CC str./CH_2 sym.def. coupling, as was

discussed above. Even these are, however, well acceptable, especially if one realizes that ω_2 is rather uncertain, containing a Fermi resonance correction of 7 cm^{-1} [3].

While such an excellent reproduction of the 27 in-plane frequencies would not sufficiently prove the correctness of an experimental force field, it is certainly a very strong argument for the reliability of our results. We used only 4 (in-plane) adjustable parameters so that the final force field is still basically fixed by the *ab initio* calculations. Nevertheless, it seemed appropriate to check the reproduction of the remaining experimental data. This is the more interesting because, contrary to the experimental force field, these were not used in our fitting procedure. Table VI and Table VII show the frequency shifts of the ^{13}C isotopic forms and the Coriolis coupling constants, respectively.

Table VI

^{13}C *frequency shifts* (cm^{-1})

Isotope		exp.[a]	D-M-M[b]	4—21[c]	4—31G[d]	6—31G**[c]
$H_2{}^{12}C^{13}CH_2$	$\Delta\omega_2$	22.0 (1.0)	22.1	21.6	21.7	20.6
	$\Delta\omega_3$	6.8 (0.3)	6.9	7.1	7.2	8.0
	$\Delta\omega_{12}$	3.1 (0.1)	3.1	3.1	3.2	3.1
$D_2{}^{12}C^{13}CD_2$	$\Delta\omega_9$	6.4 (0.5)	6.4	5.3	5.1	4.2
	$\Delta\omega_{11}$	4.1 (0.2)	4.1	4.2	4.0	4.3
	$\Delta\omega_{12}$	3.9 (0.1)	3.9	3.8	3.8	3.8
$H_2{}^{12}C^{13}CD_2$	$\Delta\omega_2$	14.2 (1.0)	13.7	13.0	13.4	12.1
	$\Delta\omega_5$	19.0 (1.0)[e]	17.7	18.5	19.0	18.9
	$\Delta\omega_{11}$	12.7 (0.7)	12.8	13.3	12.8	13.2
$H_2{}^{13}C^{13}CH_2$	$\Delta\omega_{12}$	5.9 (0.3)	5.9	5.8	5.9	5.8
$D_2{}^{13}C^{13}CD_2$	$\Delta\omega_{11}$	7.4 (0.4)	7.2	7.4	7.1	7.5
	$\Delta\omega_{12}$	6.7 (—)	7.2	7.1	7.2	7.1
$H_2{}^{13}C^{12}CD_2$	$\Delta\omega_1$	6.5 (0.5)	6.3	6.5	6.2	6.5
	$\Delta\omega_2$	26.2 (0.6)	26.5	25.9	26.1	25.0
	$\Delta\omega_9$	13.7 (1.0)[e]	12.6	13.0	13.3	13.2

[a] Experimental data corrected for anharmonicity [3], with uncertainties in parentheses.
[b] Reproduction of the data by the experimentally derived force field [3].
[c] Present results. [d] Ref. [4].
[e] Contrary to [3], these were also corrected for anharmonicity, see text.

Table VII

Coriolis coupling constants of C_2H_4

i, j in $\zeta_{i,j}$	exp.[a]		D-M-M[b]	4—21[c]	6—31G**[c]
1, 5	0.065	(0.01)	0.065	0.059	0.070
3, 6	0.4	(0.1)	0.36	0.356	0.375
4, 10	0.90	(0.02)	0.89	0.859	0.863
6, 8	0.61	(0.05)	0.58	0.559	0.552
7, 10	0.44	(0.02)	0.46	0.512	0.505
9, 11	0.04	(0.04)	0.09	0.036	0.044

[a] Experimental values (with uncertainty in parentheses) taken over from [3].
[b] Reproduction of the data by the experimentally derived force field [3].
[c] Present results, with the scaled force fields of Table IV.

We can now discuss the main discrepancies in the coupling constants on the basis of the complete experimental data. The CC str./CH_2 sym. str. ($F_{1,2}$) interaction term is 0.11—0.12 in all theoretical results while its D-M-M value is 0.257, significantly larger. According to DUNCAN *et al.* [3], $F_{1,2}$ is mainly defined by the ^{13}C shifts $\Delta\omega_2(C_2H_4)$ and $\Delta\omega_1$, $\Delta\omega_{11}(CH_2CD_2)$. As can be seen, the theoretical force fields reproduce these data very well, it is only the 6—31G** value of $\Delta\omega_2$ which is slightly outside the experimental range. We have checked that the latter minor discrepancy comes from the differences in $F_{1,1}$ and $F_{1,6}$ discussed above. Thus, it is proved that all relevant data can be reproduced also with the lower value of $F_{1,2}$ and we see no reason to doubt that the theoretical result is the correct one.

Two other remarkable discrepancies concern $F_{4,8}$ and, in a more pronounced way, $F_{4,9}$. In terms of our local semisymmetry coordinates the physical difference can be seen very clearly. Taking the theoretical values, the coupling of the CH_2 as. stretch. with the rocking on the same carbon atom is significantly larger than that with the rocking on the other carbon atom. The D-M-M values show just the opposite trend. Although there is no exact theoretical argument for either results, intuitively the *ab initio* result is certainly more plausible.

As the experimental information is directly related to symmetry species, it seemed appropriate to analyze this problem in more detail in terms of symmetry coordinates, rather than in our local coordinates. The relevant terms are then the symmetry coupling force constants $F^{sym}_{5,6}$ (B_{1g} species) and $F^{sym}_{9,10}$ (B_{2u} species), as defined and given in Table VIII.

The sensitivity of these interaction constants to the input data is analyzed in [3]. According to this, among the ^{13}C shifts it is $\Delta\omega_9(C_2D_2)$ and $\Delta\omega_5$, $\Delta\omega_9(CH_2CD_2)$ which are most important in fixing both coupling constants.

Table VIII

CH_2 as. str./rock interaction constants in terms of symmetry coordinates[a]

Symmetry force const.	D-M-M[b]	4—21[c]	4—31G[d]	6—31G**[c]
$F^{sym}_{5,6} = F_{4,8} - F_{4,9}$	0.396	0.216	0.214	0.182
$F^{sym}_{9,10} = F_{4,8} + F_{4,9}$	−0.174	0.106	0.096	0.062

[a] Standard symmetry coordinates, which agree with those of [3], except that deformation coordinates are not scaled by r_0. For units see Table IV.
[b] Ref. [3]. [c] Present results. [d] Ref. [4].

Among the Coriolis data, $\zeta_{6,8}$ is sensitive to $F^{sym}_{5,6}$, while $\zeta_{7,10}$ and $\zeta_{4,10}$ are sensitive to $F^{sym}_{9,10}$. An important observation of the authors is that, among these, $\Delta\omega_5$ and $\Delta\omega_9$ of CH_2CD_2 are in conflict with the others, as well as with several frequency data. They suggested tentatively that crystal site symmetry may cause some weak Fermi resonances and due to these uncertainties they used no anharmonicity correction for $\Delta\omega_5$ and $\Delta\omega_9$, *i.e.* sacrificed their exact reproduction for the sake of the other data.

This separate handling of $\Delta\omega_5$ and $\Delta\omega_9$ seemed unnecessary in our calculations, and we applied the usual anharmonicity correction. Accepting the analysis in Appendix I. of [3], either from Dennison's rule or from the anharmonicity data based on overtones, this correction is about $+1$ cm^{-1} for both frequencies. These corrected values are given in our Table VI.

With these corrected values, both $\Delta\omega_5$ and $\Delta\omega_9$ of CH_2CD_2 are well reproduced by the theoretical force fields, but $\Delta\omega_9$ of C_2D_4 comes out too small. The situation is opposite with the D-M-M field: this reproduces $\Delta\omega_9$, but gives less satisfactory agreement for the other two shifts. Unfortunately, it is impossible to make a definite choice: $\Delta\omega_9(C_2D_4)$ is, as can be judged by comparing its 4—21 and 6—31G** value, extremely sensitive to the force field, so that it is not justifiable to predict it theoretically. On the other hand, in our opinion it is rather uncertain experimentally, too. It was measured in the pure crystal only (and not in solid solution), so that crystal field effects cannot be ruled out completely (the subject of debate being frequency differences of the order of 1 cm^{-1}).

As to the Coriolis constants, $\zeta_{6,8}$ which determines $F^{sym}_{5,6}$ is reproduced within the quoted uncertainty. For $F^{sym}_{9,10}$ the important data are $\zeta_{4,10}$ and $\zeta_{7,10}$. The first one is calculated just outside the experimental range, for the latter the deviation is larger. Considering, however, that uncertainties of a ζ constant are always rough estimates, both calculated values seem acceptable. The reliability of our force field is also supported by the fact that the other three ζ constants are excellently reproduced. Specifically, we reproduce $\zeta_{9,11}$, which is not the case with the D-M-M field. Although $\zeta_{9,11}$ is very un-

certain experimentally, realizing that its value of 0.04 was given as an upper limit in [21], the D-M-M value of 0.09 is definitely too large.

As to the frequencies, mentioned in [3] as being in conflict with $\Delta\omega_5$ and $\Delta\omega_9$, we see no contradiction, all of them are reproduced by the theoretical force fields within experimental uncertainty.

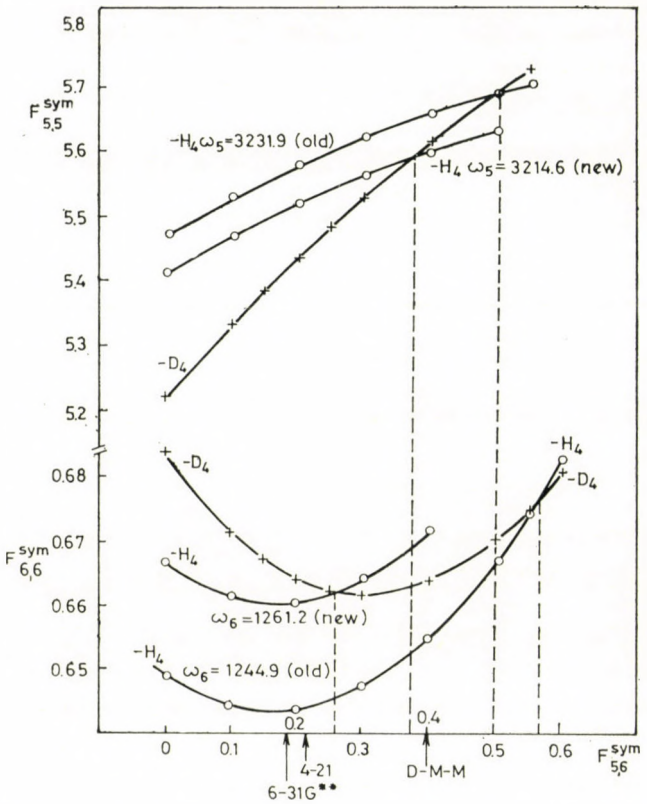

Fig. 2. Force constant display graph for the symmetry species B_{1g} of C_2H_4 and C_2D_4

A separate question in connection with $F^{sym}_{5,6}$ is the reassignment of ω_5 and ω_6 in C_2H_4, as discussed above. It seemed interesting to analyze, how this influences the coupling constant. In Fig. 2 the force constant display graphs for the B_{1g} species of C_2H_4 and C_2D_4 are shown. As can be seen, from the (original) frequencies alone 0.50—0.56 would follow for $F^{sym}_{5,6}$. The final D-M-M value, fitted to these and several other data, is only 0.40. Clearly, if these frequencies, as being uncertain, were left out of consideration, the remaining data would predict a value significantly below 0.40. The fact that the new values of both ω_5 and, especially, ω_6 shift the coupling constant to lower values, is a good argument for the correctness of the reassignments. Also, in view of

these considerations the theoretical value of 0.18—0.22 seems much more reliable now.

With the discrepancy in $F^{sym}_{9,10}$ in mind, a similar analysis would also be interesting for the B_{2u} species. Here, however, there are no reliable data for ω_{10} of C_2D_4. Just to get a better insight, we have constructed the display graphs for two trial values, $\omega_{10} = 600$ and 606 cm^{-1}, respectively, based on the calculated results. As Fig. 3 shows, $F^{sym}_{9,10}$ is extremely sensitive to small uncertainties in both ω_9 and ω_{10} which shows the dangers of an experimental determination. The theoretical value seems very well acceptable.

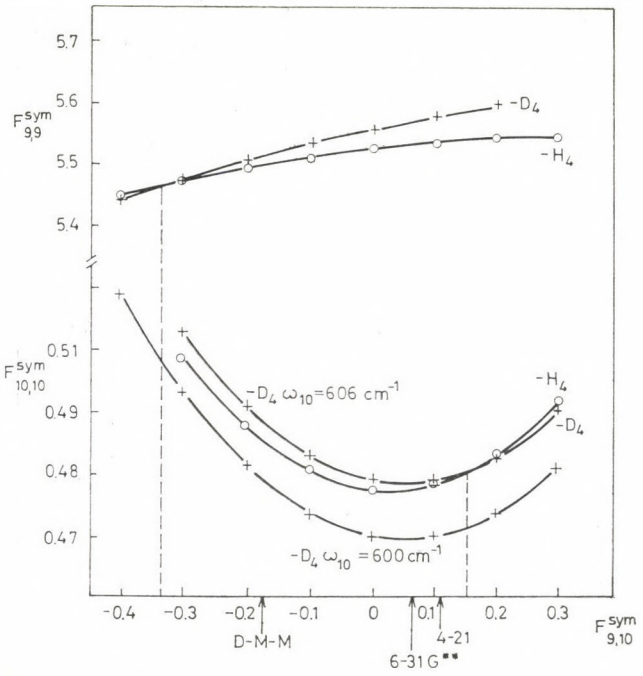

Fig. 3. Force constant display graph for the symmetry species B_{2u} of C_2H_4 and C_2D_4

The out-of-plane force constants

Finally, the out-of-plane force field should be discussed briefly. This leaves much less problem for debate, as the three modes factorize into one-dimensional symmetry blocks so that, apart from the uncertainty in the geometry discussed above, the experimental force field is uniquely determined. Thus, the primary reason for including the out-of-plane field in the investigation was to obtain the scaling factors which are hoped to be transferable to similar molecules. Our study on butadiene, acrolein and glyoxal, which is in progress, confirms this [22].

In the present context the only noticeable point is the fact that both the 4—21 and the 6—31G** force field interchange the sequence of the two, very close lying, wagging modes ω_7 and ω_8. Obviously, the determining quantity is the ratio of the wagging/wagging' coupling to the wagging diagonal constant (and, actually, this is what remains fixed by the ab initio result in our scaling procedure). It can be calculated that, with the **G** matrix in our geometry, the sequence reverses at the ratio of 0.150, while our value is 0.134 and 0.148, respectively, in the 4—21 and the 6—31G** force field. For the coupling this means only a difference of a few thousandths of aJ. Thus, the theoretical value is physically very accurate, in spite of its inability to reproduce correctly this extremely sensitive splitting.

Cubic force constants

Anharmonic calculations of vibrational spectra are becoming more and more important. For ethylene, MACHIDA and TANAKA [23] have published a simplified empirical anharmonic force field based on Morse potential for the individual bonds. It seemed worthwhile to make our *ab initio* results available for future calculations. In fact, an analysis of ethylene using *ab initio* anharmonic force constants is already in progress by BLOM [24]. From our calculations, the most important, f_{iii} and f_{iij} type, cubic terms can be evaluated from the forces. They are given in Table IX. To conserve space, only the best quality, 6—31G** results are given.

Table IX

6-31G** *cubic force constants*[a]

$RRR = -56.1$; $RRr = -0.27$; $RR\beta = -0.41$
$rrr = -32.7$; $rrR = +0.15$; $r_1r_1\beta_1 = -0.00$; $r_1r_1\beta_2 = -0.16$; $r_1r_1\beta_3 = +0.06$;
$r_1r_1\beta_4 = -0.02$; $r_1r_1r_2 = -0.17$; $r_1r_1r_3 = -0.06$; $r_1r_1r_4 = +0.10$
$\beta\beta\beta = -0.25$; $\beta_1\beta_1\beta_2 = +0.55$; $\beta_1\beta_1\beta_3 = -0.08$; $\beta_1\beta_1\beta_4 = -0.08$; $\beta\beta R = -0.52$;
$\beta_1\beta_1r_1 = -0.26$; $\beta_1\beta_1r_2 = -0.20$; $\beta_1\beta_1r_3 = -0.00$; $\beta_1\beta_1r_4 = -0.08$;
$\Theta\Theta R = -0.50$; $\Theta_1\Theta_1r_1 = -0.06$; $\Theta_1\Theta_1r_3 = -0.02$; $\Theta_1\Theta_1\beta_1 = +0.06$; $\Theta_1\Theta_1\beta_3 = -0.05$;
$\tau\tau R = -0.14$; $\tau\tau r = -0.016$; $\tau\tau\beta = -0.012$

[a] Direct calculated values without any adjustment, obtained around the geometry: $R(CC) = 1.339$ Å, $r(CH) = 1.085$ Å, (Å $= 10^{-10}$ m) $\beta(CCH) = 121.1°$. f_{ijk} ($i \neq j \neq k$) type terms have not been calculated. For simpler notation, only the subscript is used, *e.g.* RRR stands for f_{RRR}. R, r and β are individual internal coordinates here, defined in Fig. 1. Θ_1, Θ_2 and τ are equivalent to S_{10}, S_{11} and S_{12}, respectively, defined in Table I. Units are consistent with energy measured in aJ, stretching coordinates in Å $= 10^{-10}$ m and bendings in radian.

Dipole moment derivatives

From the dipole moments in the distorted geometries, the corresponding derivatives can be evaluated numerically. They are given in Table X, compared with other results. For a comparison with the direct observables, the intensities themselves are compiled in Table XI for C_2H_4 and C_2D_4.

Table X

Dipole moment derivatives, with respect to local symmetry coordinates[a]

	Experimental		Theoretical				
	A[b]	B[c]	73/3+1[d]	4—21[e]	4—31G[f]	6—31G[g]	6—31G**[e]
$\partial\mu_x/\partial S_2$ (sym. str.)	+.427	+.447	+.557	+.426	+.511	+.522	+.445
$\partial\mu_x/\partial S_6$ (sym. def.)	−.165	+.197	+.211	+.151	+.183	+.189	+.201
$\partial\mu_y/\partial S_4$ (as. str.)	−.512	−.522	−.641	−.587	−.667	−.677	−.537
$\partial\mu_y/\partial S_8$ (rock.)	−.185	−.021	−.035	−.104	−.101	−.123	−.056
$\partial\mu_z/\partial S_{10}$ (wagg.)	−.684	+.691	+.866	+.829	+.924	+.931 (+.780) (+.691)	+.855

[a] Dipole moment measured in $D \simeq 3.33564 \times 10^{-30}$ Cm, stretching coordinates in Å = $= 10^{-10}$ m, bendings in radian.

Signs are consistent with the direction of the x, y and z axes given in Fig. 1 and the definition of coordinates in Table I, and the dipole moment vector showing from positive to negative charge. [b] The original experimental study [26]. Note that only the relative signs are determined by experiment, the absolute signs were just proposed, based on bond theory considerations. [c] Reinterpreted experimental values [25]. Signs based on *ab initio* calculations. [d] Ref. [25]. [e] Present results, calculated around the geometry: R(CC) = 1.339 Å, r(CH) = 1.085 Å, β(CCH) = $= 121.1°$. [f] Ref. [4], calculated around R(CC) = 1.338 Å, r(CH) = 1.084 Å, β(CCH) = 121.0°. [g] Ref. [18], calculated around the theoretical geometry. Values in parentheses: basis set extended by bond functions.

Table XI

Infrared absolute intensities (km · mol^{-1})

Symm.	Mode	C_2H_4			C_2D_4		
		exp.[a]		4—21	6—31G**	exp.[b]	4—21	6—31G**
B_{1u}	ω_7	81.3	(79.8)	103	109	41.7	58.9	62.7
B_{2u}	ω_9	24.9		31.8	26.8	12.2	17.3	14.7
	ω_{10}	0.20	(0.53)	0.68	0.21	0.04	0.37	0.12
B_{3u}	ω_{11}	13.5		15.0	16.1	7.6	7.1	7.4
	ω_{12}	9.8		5.2	9.4	5.2	3.0	5.4

[a] The reinterpreted values of [25] are accepted here; in parentheses the original values of [26].

[b] From [26].

First, a brief discussion of the experimental derivatives seems necessary. We have accepted here the analysis of [25], which differs from the original one [26] in two ways: the 950 cm^{-1} region was reinterpreted, which leads to slightly different intensities A_7 and A_{10}. More importantly, the form of the normal vibrations was determined from the D-M-M force field which drastically reduces the magnitude of the rocking derivative as compared to [26]. Furthermore, as it is well known, a basic uncertainty in the experimental results arises from the fact that only the absolute values of $\partial\mu/\partial Q_i$ are determined by the measured intensities. Within one symmetry species, different *relative* signs of $\partial\mu/\partial Q_i$ give different $\partial\mu/\partial S_i$. (Q denotes normal coordinates, S stands for symmetry coordinates.) The correct choice may be selected on the basis of isotope data (even then, obviously, the absolute signs of $\partial\mu/\partial S_i$ remain indeterminate, as all signs can be reversed). As to the relative signs, GOLIKE *et al.* [26] accepted identical signs (symbolized by $++$) in species B_{2u} and opposite signs ($+-$) in B_{3u}, with the remark that the ($+-$) sign combination in B_{2u} cannot be ruled out completely. It can now be finally established that the accepted choice in B_{2u} was correct. With recent reliable force fields — either the D-M-M or the present one — if opposite signs are assumed for the $\partial\mu/\partial Q_i$ derivatives, this leads to opposite signs for the $\partial\mu/\partial S_i$ values, while all theoretical results show clearly that they have the same (negative) sign.

On the other hand, the relative sign combination ($+-$) in B_{3u}, used in the experimental study [26] was the wrong choice: it leads to opposite signs for the symm. stretching and the sym. def. derivatives, which is unacceptable on the basis of the quantum mechanical results.

Taking thus the reinterpreted experimental values as the basis of comparison, one can draw the following conclusions. The wagging (out-of-plane) derivative is somewhat overestimated in all theoretical calculations, except in one which used bond functions in the basis set [18]. The result is, however, very sensitive to the form of polarization functions and the better balanced 6—31G** basis gives again too high a value. The consistency of the overestimation indicates that it might be an electron correlation effect, although good SCF calculations using soft polarization functions would be needed to substantiate this conclusion. Note that there is also a considerable experimental uncertainty: the wagging derivative showed differences up to 10 per cent, depending on the isotope from which it was determined [26].

The in-plane derivatives obtained with the sp basis sets are reasonable to the extent that a semiquantitative prediction of the intensities is already possible at this level. The polarized, 6—31G** basis works excellently; the calculated values agree with the experimental ones within a few per cent, *i.e.* within experimental uncertainty. It is only the very small rocking derivative for which the percentage error seems larger. However, its value derived

from the intensities is extremely sensitive to the force field, so that we consider the quantum mechanical result as the more reliable one.

Finally, it is interesting to investigate the direction (absolute sign) of the dipole moment derivatives. All theoretical results show that for the stretching modes the CH bond behaves formally as having C^+H^- partial charges, while in the bending modes, including the wagging, C^-H^+ formal charges appear. It is noticeable that the same behaviour was observed in methane (see footnote to Table VI in [5]).

In terms of the bond-moment hypothesis this means that the μ_{CH} bond moment is positive (positive charge on hydrogen) while its derivative ε_{CH} with respect to the CH distance is negative. In the pioneer experimental work [26] the apparent anomaly that either μ or ε must change sign between the B_{2u} and B_{3u} symmetry species, led to complex speculations. It is now clear that this was caused by the unfortunate choice of signs in B_{3u}. Note also that their suggested sign for the wagging derivative (Fig. 7 in [26]) was also incorrect. The theoretical results are consistent throughout the three symmetry species.

*

This material is based in part upon work supported by the U.S. National Science Foundation under Grant No. INT-7819341 and by the Hungarian Institute for Cultural Relations as part of the cooperative research program of the Eötvös L. University and the University of Texas. It has also been supported in part by a grant from The Robert A. Welch Foundation.

Note: After we finished the manuscript of this study, Prof. J. L. DUNCAN sent us the manuscript of a recent work by DUNCAN and HAMILTON describing their improved determination of the ethylene force field, based on 116 experimental data. It was reassuring to see that in all cases where significant changes occurred as compared to the original D-M-M field, the new values came closer to the *ab initio* values. More specifically, the agreement is much better now for the CC str./CH_2 sym. str. coupling constant as well as for the CH_2 as. str./rock. constant $F^{sym}_{5,6}$ (B_{1g} species); however, the discrepancy in the other CH_2 as. str./rock. interaction $F^{sym}_{9,10}$ (B_{2u}) is still present.

REFERENCES

[1] MCKEAN, D. C., DUNCAN, J. L.: Spectrochim. Acta, Part A, **27,** 1879 (1971)
[2] PULAY, P., MEYER, W.: J. Mol. Spectrosc., **40,** 59 (1971)
[3] DUNCAN, J. L., MCKEAN, D. C., MALLINSON, P. D.: J. Mol. Spectrosc., **45,** 221 (1973)
[4] BLOM, C. E., ALTONA, C.: Mol. Phys., **34,** 177 (1977)
[5] PULAY, P., FOGARASI, G., PANG, F., BOGGS, J. E.: J. Am. Chem. Soc., **101,** 2550 (1979)
[6] PULAY, P.: Mol. Phys., **17,** 197 (1969); and, in: H. F. SCHAEFER, III (Ed.), Modern Theoretical Chemistry, Vol. 4., Plenum Press, New York, 1977, pp. 153—185.
[7] PULAY, P.: Theor. Chim. Acta, **50,** 299 (1979)
[8] HEHRE, W. J., DITCHFIELD, R., POPLE, J. A.: J. Chem. Phys., **56,** 2257 (1972)
[9] HARIHARAN, P. C., POPLE, J. A.: Theor. Chim. Acta, **28,** 213 (1973)
[10] DITCHFIELD, R., HEHRE, W. J., POPLE, J. A.: J. Chem. Phys., **54,** 724 (1971)
[11] BLOM, C. E., ALTONA, C.: Mol. Phys., **31,** 1377 (1976)
[12] FOGARASI, G., PULAY, P., MOLT, K., SAWODNY, W.: Mol. Phys., **33,** 1565 (1977)
[13] BOTSCHWINA, P.: Chem. Phys. Lett., **29,** 98 (1974)
[14] BOTSCHWINA, P.: Chem. Phys. Lett., **29,** 580 (1974)

[15] BLEICHER, W., BOTSCHWINA, P.: Mol. Phys., **30,** 1029 (1974)
[16] FOGARASI, G., PULAY, P.: J. Mol. Struct., **39,** 275 (1977) and references therein
[17] BLOM, C. E., SLINGERLAND, P. J., ALTONA, C.: Mol. Phys., **31,** 1359 (1976)
[18] WIBERG, K. B., WENDOLOSKI, J. J.: J. Am. Chem. Soc., **98,** 5465 (1976)
[19] DUNCAN, J. L.: Mol. Phys., **28,** 1177 (1974)
[20] DUNCAN, J. L., HEGELUND, F., FOSTER, R. B., HILLS, G. W., JONES, W. J.: J. Mol. Spectrosc., **61,** 470 (1976)
[21] VAN LERBERGHE, D., WRIGHT, I. J., DUNCAN, J. L.: J. Mol. Spectrosc., **42,** 251 (1972)
[22] PULAY, P., VARGHA, A., FOGARASI, G.: to be published
[23] MACHIDA, K., TANAKA, Y.: J. Chem. Phys., **61,** 5040 (1974)
[24] BLOM, C. E.: private communication
[25] JALSOVSZKY, Gy., PULAY, P.: J. Mol. Struct., **26,** 277 (1975)
[26] GOLIKE, R. C., MILLS, I. M., PERSON, W. B., CRAWFORD Jr., B.: J. Chem. Phys., **25,** 1266 (1956)

Géza FOGARASI
Péter PULAY
H-1088 Budapest, Múzeum krt. 6—8., Hungary

Acta Chimica Academiae Scientiarum Hungaricae, Tomus 108 (1), pp. 75—83 (1981)

STRUCTURAL INFORMATION ON COPPER(I) COMPLEXES OF SOME PYRIDINE DERIVATIVES FROM THEIR FAR INFRARED SPECTRA

M. A. S. GOHER* and M. DRÁTOVSKÝ**

(*Department of Chemistry, Faculty of Science, Alexandria University, Alexandria, Egypt*)

Received August 12, 1980

Accepted for publication October 13, 1980

The far infrared spectra (500—50 cm^{-1}) of a variety of diamagnetic copper(I) complexes of some pyridine derivatives have been measured. Tentative assignments of the stretching Cu—X and Cu—N vibrations are given. IR results suggest distorted tetrahedral geometry for L_3CuX complexes. The results given here suggest different structures for L_2CuX complexes depending on the nature of the substituent group in pyridine ring. Monomeric, C_{2v}, or dimeric structures are formulated for complexes derived from ligands with electron releasing or attracting groups, respectively. Polymeric structures are proposed for LCuX complexes.

Introduction

MALIK [1, 2] has suggested a monomeric structure for 1 : 1 copper(I) complexes derived from pyridine and other related ligands. On the other hand, a higher coordination number than two for bis(amine)copper(I) perchlorate complexes has been suggested by LEWIN *et al.* [3] on the basis of their lower frequencies. However, RASTON and WHITE [4] have studied the structure of pyridine-copper(I) iodide by X-ray analysis. This adduct consists of the well known tetrahedral tetrameric unit Cu_4I_4. It is the only example which has been studied and no structural information is available for any other copper(I) halide complexes of pyridine and its derivatives.

Recently we have been interested in the study of copper(I) complexes derived from pyridinecarboxylic acids and their derivatives [5, 6]. As copper(I), being d^{10} ion, does not show d-d transitions and therefore the stereochemistry of its complexes can not be derived from their electronic spectra, and in order to gain structural information on some copper(I) complexes we measured their far infrared spectra. In this paper we report the lower frequencies in the region 500—50 cm^{-1} for copper(I) complexes derived from pyridinecarboxylic acid esters and other pyridine derivatives.

Experimental

The complexes have been prepared according to the method described previously [5, 6] and their purity was checked by elemental analyses (Table I). Magnetic measurements, reflectance spectra, X-ray powder patterns, microanalyses of C, H and N, and conductivity measurements were carried out as given previously [5, 6].

* Tho whom correspondence should be addressed.

** Department of Inorganic Chemistry, Charles University, 12 840 Prague, Czechoslovakia.

Table I

Analytical data

Complex	Colour	Analysis: % Found/Required			
		Cu	C	H	N
(EtIN)CuCl	yellow cryst.	25.55	38.27	3.74	5.42
	powder	25.40	38.41	3.63	5.60
(EtIN)CuBr	yellow cryst.	21.74	32.60	2.98	4.56
	powder	21.56	32.61	3.08	4.75
(EtIN)CuI	yellow	18.75	27.74	2.74	4.00
	powder	18.60	28.12	2.65	4.10
(EtIN)CuCN	yellow	26.60	44.43	3.84	11.38
	powder	26.40	44.81	3.77	11.61
(EtIN)CuSCN	pale yellow	23.23	39.32	3.47	10.42
	powder	23.30	39.44	3.33	10.26
(MeIN)CuBr	yellow cryst.	22.33	30.03	2.55	5.02
	powder	22.64	29.96	2.51	4.99
(MeIN)CuI	yellow	19.42	25.78	2.06	4.18
	powder	19.39	25.66	2.15	4.27
(MeIN)CuCN	yellow	28.24	42.67	3.21	12.17
	powder	28.03	42.38	3.11	12.35
(MeIN)CuSCN	pale yellow	24.76	37.50	2.85	10.72
	powder	24.56	37.15	2.70	10.81
$(EtIN)_2CuBr$	pale brown	14.42	43.32	4.03	6.04
	powder	14.25	43.11	4.07	6.28
$(MeIN)_2CuCl$	red brown cryst.	17.25	44.25	3.87	7.37
	powder	17.02	44.05	3.78	7.50
$(MeIN)_2CuBr$	brown cryst.	15.37	40.12	3.52	6.32
	powder	15.21	40.25	3.38	6.70
$(MeIN)_2CuI$	red orange	13.87	36.35	3.17	5.82
	cryst. powder	13.67	36.18	3.03	6.02
$(2,4\text{-lut})_2CuBr$	yellow cryst.	17.55	45.96	5.16	7.72
	powder	17.76	46.99	5.07	7.82
$(2,4\text{-lut})_2CuClO_4$	white cryst.	16.98	44.22	4.83	7.42
	powder	16.84	44.56	4.80	7.42
$(2,5\text{-lut})_2CuBr$	yellow cryst.	17.45	46.33	5.27	7.64
	powder	17.76	46.99	5.04	7.82
$(EtIN)_3CuCl$	red brown	11.62	52.33	4.97	7.52
	crystals	11.50	52.18	4.92	7.60
$(EtIN)_3CuBr$	red brown	10.68	48.37	4.66	6.89
	cryst. powder	10.64	48.29	4.56	7.04
$(2,5\text{-lut})_3CuClO_4$	light brown	13.01	51.88	5.74	8.46
	powder	13.13	52.06	5.62	8.67
$(EtIN)_4CuClO_4$	red orange	8.39	50.39	4.92	7.18
	crystals	8.28	50.07	4.73	7.30
$(MeIN)_4CuClO_4$	red orange	9.12	47.00	4.08	7.67
	crystals	8.93	47.27	3.97	7.87

Abbreviations; MeIN: methyl isonicotinate, EtIN: ethyl isonicotinate, lut: lutidine

The IR spectra in the regions 4000—400 cm^{-1} and 500—50 cm^{-1} were measured on a UR-20 (Zeiss, Jena) and a Perkin-Elmer 325 spectrophotometer. The solid samples were measured as nujol mulls and/or KBr pellets, and liquid ligands as capillary films. Spectra in the region 400—50 cm^{-1}, were obtained for samples as pressed discs in polyethylene using a RIIC, FS-620 interferometer, the requisite calculations being performed on an IBM computer.

Results and Discussion

The vibration frequencies (500—50 cm^{-1}) for both ligands and their copper(I) complexes are collected in Table II. Because the complexes dissociate in organic solvents like alcohols, acetone, chloroform, *etc.*, and therefore their solutions contain varieties of species, we were not able to measure their solution spectra.

Table II

Far infrared spectra

Compound	Vibrations (cm^{-1})
EtIN	334vs, 270s, 194vs
(EtIN)CuCl	365m, 285s, 220vs, 190s, 150s, 118m, 98m
(EtIN)CuBr	354vs, 282vs, 218s, 176s, 142s, 112s
(EtIN)CuI	352s, 282s, 212s, 156m, 136s, 116w, 98m, 76wm
(EtIN)CuCN	348s, 298s, 210vs, 172s, 162s, 132m
(EtIN)CuSCN	346vs, 272vs, 218vs, 196s, 162m, 124m, 106m
$(EtIN)_2CuBr$	350s, 280s, 224ms, 204ms, 180m, 148m, 120m, 80m
$(EtIN)_3CuCl$	356ms, 308s, 282s, 234ms, 212s, 196s, 156m, 144m, 114m, 74m
$(EtIN)_3CuBr$	348vs, 324m, 278vs, 222s, 210s, 188m, 150s, 120m, 76m, 56m
$(EtIN)_4CuClO_4$	346s, 274s, 206s, 160m
MeIN	358s, 334vs, 218vs, 170vs
(MeIN)CuBr	378s, 330vs, 224vs, 160ms, 112s, b
(MeIN)CuI	372vs, 335vs, 230vs, 142s, 98s, b
(MeIN)CuCN	374s, 345vs, 230s, 220s, 164m
(MeIN)CuSCN	370s, 340s, 232s, 200s, 170ms, 120m
$(MeIN)_2CuCl$	386w, 336s, 226ms, 198m, 180s, 100m, 88m
$(MeIN)_2CuBr$	380wm, 336vs, 234vs, 198s, 154m, 136s, 112s
$(MeIN)_2CuI$	377m, 340vs, 226vs, 202m, 144ms, 124s, 96m
$(MeIN)_4CuClO_4$	372m, 330vs, 230vs, 150ms
$(2,4\text{-lut})_2CuBr$	442vs, 427s, 294wm, 251m, 240m, 215m
$(2,4\text{-lut})_2CuClO_4$	448vs, 434m, 316wm, 266s, 207m
$(2,5\text{-lut})_2CuBr$	435ms, 370w, 314ms, 246ms, 166ms, 150vs
$(2,5\text{-lut})_3CuClO_4$	440w, 408w, 378w, 312m, 162ms, 96vs, 74s

Far IR spectroscopy has been used to study copper(II) halide complexes of substituted pyridines [7]. For copper-nitrogen, the stretching frequency was observed in the range 230—270 cm^{-1}, for copper-chloride it was 230—330 cm^{-1} and for copper-bromide the range was 190—260 cm^{-1}. Previous studies [8, 9] have shown that the assignments of $\nu M-X$ and $\nu M-N$ in pyridine derivative systems, ML_mX_n, are reasonable. Thus $\nu Cu-X$ may be identified by their shifts to lower frequencies when X is progressively changes from chloride to iodide and by comparison with perchlorates of copper(I) complexes of the same ligands. The bands which are relatively insensitive to change in halogen are tentatively assigned as copper-nitrogen stretching vibrations. Also, the work of WONG and BREWER [10] on the isoelectronic Zn(II) complex with methyl isonicotinate (MeIN) has been considered. They assigned the two bands observed at 230 and 203 cm^{-1} in its spectrum as zinc-nitrogen stretching vibrations in accordance with the calculated ones.

Metal-halogen and metal-nitrogen vibrations of complexes of the type under consideration are often IR active and can therefore be utilized for structural investigations. A general feature of the spectra is the shift of the fundamental modes of the ligands, as expected [9]. The spectra of all complexes are well characterized. In order to facilitate comparison, the copper-halogen and copper-nitrogen stretching frequencies are given in Table III.

L_4CuClO_4 complexes: Tetrahedral geometry has been revealed for $[L_4Cu]^+$ where L is pyridine by X-ray analysis [11]. For such geometry, T_d symmetry, one stretching and one bending copper-nitrogen vibration frequencies are expected. Infrared spectra in the region 4000—400 cm^{-1} as well as conductivity measurements have revealed the ionic nature of $(EtIN)_4CuClO_4$ and $(MeIN)_4CuClO_4$ complexes both in the solid state and in solutions, respectively. For these two complexes only one band in the region 200—230 cm^{-1} associated with the copper-nitrogen stretching vibration is observed. Around 150—160 cm^{-1} another band is also observed and tentatively assigned as the copper-nitrogen bending frequency. The observation of these two bands is in contrast with that reported for other L_4CuClO_4 complexes, where L is pyridine, 4-picoline and quinoline [3], which are transparent in the region 600—170 cm^{-1}. We prepared the tetrakis(pyridine)copper(I) perchlorate complex. Its colour, analysis, IR spectrum above 600 cm^{-1}, and other physical data are very close to those given by LEWIN *et al.* [3]. The far infrared spectrum of the complex prepared by us showed that it is transparent only in the range 170—375 cm^{-1}, and three bands at 170, 158 and 108 cm^{-1} are observed. In order to be certain that this transparency is not due to the cation $[(pyridine)_4Cu]^+$, we prepared and measured the spectrum of pyridine-copper(I) iodide adduct. Here too we found that it is transparent in the region 190—375 cm^{-1}, and three bands at 172, 144 and 82 cm^{-1} together with a shoulder at 190 cm^{-1} are observed.

Table III

Copper-halogen and copper-nitrogen stretching frequencies (cm^{-1})

Complex	νCu—X	νCu—N
$(EtIN)_3CuCl$	234	308, 212, 196
$(EtIN)_3CuBr$	188	324, 222, 210
$(EtIN)_2CuBr$	182, 148	224, 204
(EtIN)CuCl	190, 150	220
(EtIN)CuBr	178, 142	216
(EtIN)CuI	156, 136	212
(EtIN)CuCN		210
(EtIN)CuSCN		218
$(EtIN)_4CuClO_4$		206
$(MeIN)_2CuCl$	180, 140	226, 198
$(MeIN)_2CuBr$	154, 136	234, 196
$(MeIN)_2CuI$	140, 124	226, 202
(MeIN)CuBr	160, 108	224
(MeIN)CuI	142, 96	230
(MeIN)CuCN		230, 220
(MeIN)CuSCN		232, 200
$(MeIN)_4CuClO_4$		230
$(2,4\text{-lut})_2CuBr$	240	294, 251
$(2,4\text{-lut})_2CuClO_4$		316, 266
$(2,5\text{-lut})_2CuBr$	246	314
$(2,5\text{-lut})_3CuClO_4$		312

L_3CuX complexes: Two complexes of this formula — $(EtIN)_3CuX$ (X = Cl or Br) — are examined. X-ray powder diffractogramme reveals the isomorphism of these two compounds. These tris(amine)copper(I) halide complexes exhibited similar reflectance spectra to that of the cation $[(EtIN)_4Cu]^+$ (Figures 1 and 2).

Complexes of this formula have been frequently formulated as a tetrahedral or approximate tetrahedral [12]. Assuming C_{3v} symmetry, one νCu—X (A_1) and two νCu—N (A; and E) stretching bands are expected. As seen from Tables II and III, only one band can be attributed to νCu—X stretching for $(EtIN)_3CuX$ complexes since it is absent from the spectra of $(EtIN)_4CuClO_4$. This band appears at 234 cm^{-1} for the chloride and at 188 cm^{-1} for the bromide complex. It was pointed out [13] that the presence of copper(I)—chloride stretching absorption above 200 cm^{-1} strongly implies that halogen atoms are non bridging. Thus monomeric structure may be assigned to these 1 : 3

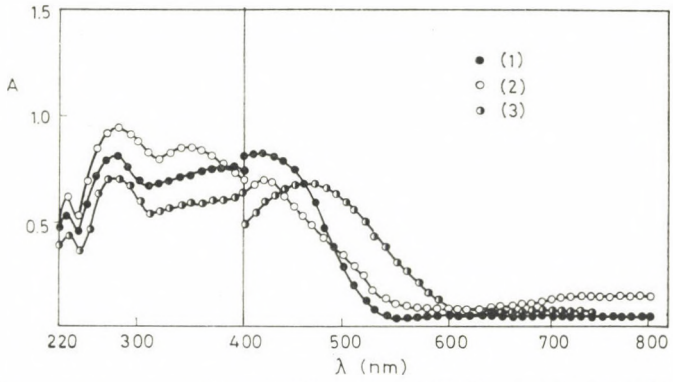

Fig. 1 Reflectance spectra of (1) $(EtIN)_3CuCl$, (2) $(EtIN)_4CuClO_4$, (3) $(MeIN)_2CuBr$

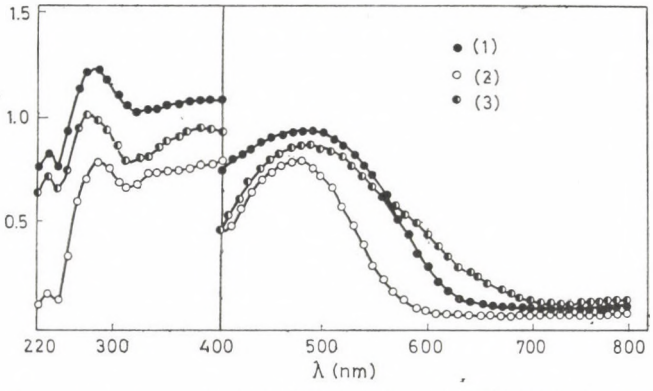

Fig. 2 Reflectance spectra of (1) $(MeIN)_3CuClO_4$, (2) (MeIN)CuI, (3) $(MeIN)_4CuClO_4$

complexes. The νCu(I)—Br/νCu(I)—Cl ratio being 0.79 compares well with the ratio 0.77 given by WONG and BREWER [10]. The values given here for νCu(I)—Cl and νCu(I)—Br are much lower than the corresponding stretching vibrations observed for tris(3-picoline)copper(I) halide complexes. In this latter case, νCu(I)—Cl and νCu(I)—Br were observed at 294 and 225 cm^{-1}, respectively [14]. This indicates stronger copper-halogen bond in 3-picoline complexes than in the EtIN ones. As expected two bands associated with copper-nitrogen stretching vibrations are observed in the range 190—230 cm^{-1} for both complexes in accordance with C_{3v} symmetry. However, another strong band is observed at 308 cm^{-1} in the spectrum of the chloride complex and at 324 cm^{-1} in that of the bromide one. This band is absent from the spectra of all other complexes derived from the same ligand. LEWIN *et al.* [3] have assigned two bands, in some cases more, in the region 425—250 cm^{-1}, as copper-nitrogen stretching vibrations for copper(I) complexes derived from

other pyridine derivatives. The separation between these two bands exceeds in some cases 100 cm^{-1}. Therefore we assigned the band which appeared around 308—324 cm^{-1} as copper-nitrogen stretching vibrations. The appearance of more than two bands associated with copper-nitrogen stretching vibrations suggest that these tris(amine)copper(I) halide complexes do not possess local C_{3v} symmetry around copper cation.

L_2CuX complexes: The assignment of structures to complexes of this formula has generally caused difficulty [14]. They have been frequently formulated as three coordinate monomers, halogen bridged dimers or ionic compounds containing the anion $[CuX_2]^-$. The complexes described here must be of the first two since they gave non-conducting solutions in chloroform and acetone. X-ray diffraction revealed the isomorphism of $(MeIN)_2CuX$ (X = Cl, Br and I) complexes.

Monomeric structure **I** for these 1 : 2 complexes with C_{2v} symmetry requires one νCu—X (A_1) and two νCu—N ($A_1 + B_2$) to be IR-active. On the other hand, dimeric structure **II** requires two bridging νCu—X and two νCu—N

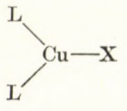

I

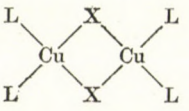

II

to be IR-active. According to the data given here in Table III, we can distinguish between two types of L_2CuX complexes mentioned here. Of the first type are those derived from methyl and ethyl isonicotinates, *i.e.* ligands with electron attracting substituents in the pyridine ring. In this case two bands below 200 cm^{-1} are sensitive to halogen and therefore assigned as bridging copper-halogen stretching vibrations since they are absent from spectra of the perchlorates of copper(I) complexes derived from the same ligands. In the region 200—240 cm^{-1} two bands associated with copper-nitrogen stretching vibrations are observed in accordance with the dimeric formula **II**.

Of the second type complex are those derived from lutidines, *i.e.* ligands with electron attracting groups. The appearance of one band associated with the terminal copper-halogen stretching vibrations suggest tri-coordinated monomeric structure **I** for these bis complexes. Table III shows that two bands associated with copper-nitrogen stretching vibrations are observed, suggesting that the copper(I) cation possesses local C_{2v} symmetry in these complexes. The higher stretching frequency observed here for these copper(I) salts when compared with copper(II) salts must be indicative of a strong copper-nitrogen bonds. This in turn may be due to the sp^2 hybridization of the tri-coordinated copper(I).

It was pointed out [15] that for a given oxidation state of a metal, the metal-halogen stretching frequencies decrease as the coordination number of the metal increases. This may explain why the terminal copper-bromide vibrations of the monomeric 1 : 2 complexes appear at higher frequencies when compared to that of monomeric 1 : 3 complexes of EtIN. This reflects the general tendency for longer bond lengths in metal complexes of higher coordination number.

LCuX complexes: The complexes reported here of this general formula gave non-conducting solutions in chloroform or acetone, and their reflectance spectra are very similar to those of cations $[L_3Cu]^+$ derived from the same ligands as seen from Fig. 2. X-ray powder diffractions showed that the halide complexes are isomorphous.

Above 200 cm^{-1} no bands could be attributable to copper(I)—chloride stretching vibrations. However, as seen from Table II and III, two bands below 200 cm^{-1} are sensitive to change of the halogen, and therefore assigned as bridging copper(I)—halogen stretching frequencies. In the region 200—240 cm^{-1}, only one band associated with copper-nitrogen stretching frequency is observed. These results suggest dimeric structure $[LCuX]_2$ for these 1 : 2 halide complexes, in which copper(I) ion is trigonally coordinated. The formulation given here is in contrast with the linear geometry proposed for 1 : 1 copper(I) halide complexes of pyridine and other related ligands [1, 2]. It also differs from that given for 1 : 1 copper(I) halides of lutidines and *sym*-collidine. In the latter case the terminal copper-halogen stretching vibrations were observed [16]. However, the structure of $[(py)CuI]_4$ revealed the existence of the tetrahedral unit Cu_4I_4 [4]. The spectrum of pyridine-copper(I) adduct prepared by us is so similar to that of $(py)_4CuClO_4$ that we could not identify the copper-iodide frequencies. Because tetrameric formulation have been revealed for LCuI complexes derived from ligands other than pyridine, *e.g.* piperidine [17], morpholine [18], polymeric structures for the 1 : 1 copper(I) halide complexes under consideration can not be ruled out.

REFERENCES

[1] MOLIK, A. U.: Z. Anorg. Allg. Chem., **344,** 107 (1966)
[2] MALIK, A. U.: J. Inorg. Nucl. Chem., **29,** 2106 (1967)
[3] LEWIN, A. H., COHEN, I. A., MICHL, R. J.: J. Inorg. Nucl. Chem., **36,** 1951 (1974)
[4] RASTON, C. I., WHITE, A. H.: J. Chem. Soc., **1976,** 2153
[5] GOHER, M. A. S., DRÁTOVSKY, M.: Coll. Czech. Chem. Commun., **26,** 40 (1975); J. Inorg. Nucl. Chem., **38,** 1269 (1976)
[6] GOHER, M. A. S.: Can. J. Chem., **53,** 2657 (1975)
[7] HATFIELD, W. E., WHYMAN, R.: In Transition Metal Chemistry (Edited by CARLIN, R. L.), Marcel Dekker, New York (1969)
[8] CLARK, R. J. H., WILLIAMS, C. S.: Inorg. Chem., **4,** 350 (1965); Spectrochim. Acta, **22,** 1081 (1966)
[9] FRANK, C. W., ROGERS, L. B.: Inorg. Chem., **5,** 615 (1966)

[10] WONG, P. T. T., BREWER, D. G.: Can. J. Chem., **47,** 4589 (1969)
[11] LEWIN, A. H., MICHL, R. J., GANIS, P., LEPORE, U., ANITAVILE, G.: Chem. Commun., **1971,** 1400
[12] LIPPARD, S. J., PALENIK, G. J.: Inorg. Chem., **10,** 1322 (1971)
[13] PATILLON, F., GUERCHAIS, J. E., GOODGAME, M. L.: J. Chem. Soc., **1973,** 1209
[14] NYHOLM, R. S.: J. Chem. Soc., **1952,** 1257
[15] FINCH, A., GATES, P. N., RADCLIFFE, K., DICKSON, F. N., BENTLEY, F. F.: Chemical Application of Far Infrared Spectroscopy, Academic Press, London and New York, 134 (1970)
[16] GOHER, M. A. S.: Acta Chim. Acad. Sci. Hung., **99,** 307 (1979)
[17] SCHRAMM, V.: personal communication
[18] SCHRAMM, V., FISCHER, K. F.: Naturwiss., **61,** 500 (1974)

Mohamed A. S. GOHER, Milan DRÁTOVSKÝ
Department of Chemistry, Faculty of Science, Alexandria University, Alexandria, Egypt.

Acta Chimica Academiae Scientiarum Hungaricae, Tomus 108 (1), pp. 85—90 (1981)

ISENTROPIC COMPRESSIBILITIES OF TERNARY MIXTURES CONTAINING METHYLETHYLKETONE, *n*-ALKANOLS AND AN ALKANE

G. R. NAIDU and P. R. NAIDU*

(*Department of Chemistry, College of Engineering, Sri Venkateswara University, Tirupati* 517 502, *India*)

Received June 9, 1980

In revised form September 26, 1980

Accepted for publication November 1, 1980

Isentropic compressibilities of four ternary mixtures, which included methylethylketone and *n*-heptane as common components and a homologous series of *n*-alkanols as non-common components, were measured at 303.15 K. The alkanols employed were 1-propanol, 1-butanol, 1-pentanol and 1-hexanol. Isentropic compressibilities of five binary mixtures of *n*-heptane with 1-propanol, 1-butanol, 1-pentanol, 1-hexanol and methylethylketone were measured at 303.15 K. The deviation in isentropic compressibility is positive in two systems; both positive and negative deviations are observed in the remaining two systems.

Introduction

A survey of the literature shows that only few attempts have been made to study isentropic compressibilities of ternary mixtures of non electrolytes though data were collected for a large number of binary mixtures. Experimental results of ternary mixtures, when compared with those of corresponding binary, will throw light on change in interspace between molecules arising due to the addition of a third component to a binary system. Further, the third component brings a change both in the nature and degree of interaction between molecules of components. With a view to study these factors, isentropic compressibilities for four ternary mixtures with *n*-heptane and methylethylketone as common components and a homologous series of *n*-alkanols as non-common components were measured at 303.15 K. The non-common components were 1-propanol, 1-butanol, 1-pentanol and 1-hexanol. While *n*-heptane is capable of exerting structure breaking effect on self-associated alkanols, methylethylketone would be able to exert both structure breaking and structure making effects. Hence the systems chosen afford an opportunity to study the relative strengths of structure breaking and structure making effects in terms of isentropic compressibility-composition relations.

* To whom correspondence should be addressed.

Experimental

Purification of materials

The alcohols (B.D.H.) were purified by the method described by RAO and NAIDU [1]. 1-Propanol, 1-butanol, 1-pentanol and 1-hexanol were refluxed over lime for 5 h and then fractionated using a fractionating column that contained thirty theoretical plates. Methylethylketone (B.D.H.) was purified by the method, described by REDDY and NAIDU [2]. The sample was dried over anhydrous potassium carbonate and finally distilled. *n*-Heptane (England B.D.H.) was dried over sodium hydroxide pellets for several days and finally fractionated. The purities of the liquids were checked by comparing the measured densities with those reported in the literature [3]. The data are given in Table I. Densities were measured using a bi-capillary pycnometer described by RAO [4].

Table I

Densities of pure substances at 303.15 *K*

	Present work ρ/g cm^{-3}	Literature P/g cm^{-3}
Methylethylketone	0.79449	0.79452
n-Heptane	0.67504	0.67510
1-Propanol	0.79562	0.79567
1-Butanol	0.80202	0.80206
1-Pentanol	0.80762	0.80764
1-Hexanol	0.81198	0.81201

Isentropic compressibilities were computed from ultrasonic sound velocity and density using the relation

$$\varkappa_{S_{123}} = u^{-2}\, \rho^{-1} \tag{1}$$

where $\varkappa_{S_{123}}$, u and ρ denote isentropic compressibility, sound velocity and density, respectively, of a ternary mixture. The values of $\varkappa_{S_{123}}$ were accurate to ± 2 TPa. Ultrasonic sound velocities were measured with a single crystal ultrasonic interferometer at a frequency of 2 MHz and the values were accurate to $\pm 0.15\%$. The densities for ternary mixtures were calculated from experimental V^{E}_{123} included in an earlier communication [5]. The relation

$$P = \frac{x_1 M_1 + x_2 M_2 + x_3 M_3}{V + V^{E}_{123}} \tag{2}$$

was used in these calculations, x_1, x_2, x_3 and M_1, M_2, M_3 denote the mole fractions and molecular weights of methylethylketone, 1-alkanol and *n*-heptane, respectively, V and V^{E}_{123} denote molar volume and excess volume, respectively. Isentropic compressibilities of binary mixtures: methylethylketone with *n*-heptane and *n*-heptane with 1-propanol, 1-butanol, 1-pentanol and 1-hexanol were also computed in a similar manner.

Results and Discussion

The deviation in isentropic compressibility, $K_{S_{123}}$ for a ternary mixture is computed from the relation

$$K_{S_{123}} = \varkappa_{S_{123}} - \varkappa^{id}_{S_{123}} \tag{3}$$

where $\varkappa_{S_{123}}$ and $\varkappa^{id}_{S_{123}}$ are isentropic compressibilities of the real mixture and an ideal mixture, respectively. The ideal isentropic compressibility is calculated using the equation

$$\varkappa^{id}_{S_{123}} = \Phi_1 \varkappa_{S_1} + \Phi_2 \varkappa_{S_2} + \Phi_3 \varkappa_{S} \tag{4}$$

Table II

Experimental values for the isentropic compressibility of ternary systems: Methylethylketone(1) + 1-alkanol(2) + n-heptane(3) at 303.15 K

Φ_1	Φ_2	ρ/g cm^{-3}	u/ms^{-1}	$\frac{\kappa_{s123}}{\text{TPa}^{-1}}$	$\frac{K_{s123}}{\text{TPa}^{-1}}$
		Methylethylketone(1) + 1-propanol(2) + *n*-heptane(3)			
0.7155	0.1018	0.77039	1151	980	12
0.6850	0.1232	0.76905	1153	978	9
0.5983	0.2389	0.77329	1156	968	10
0.4785	0.3415	0.77142	1158	967	8
0.4516	0.3392	0.76752	1155	976	9
0.3267	0.4617	0.76763	1156	975	11
0.2307	0.6046	0.77406	1165	952	6
0.1187	0.7026	0.77255	1167	951	4
		Methylethylketone(1) + 1-butanol(2) + *n*-heptane(3)			
0.7422	0.1202	0.77786	1162	952	6
0.7228	0.1032	0.77219	1157	967	8
0.5993	0.2266	0.77368	1164	954	6
0.4869	0.2972	0.76918	1165	958	4
0.2894	0.5002	0.77229	1175	938	4
0.2268	0.5970	0.77737	1184	918	2
0.1159	0.7107	0.77825	1189	909	4
0.1130	0.7596	0.78432	1196	891	3
		Methylethylketone(1) + 1-pentanol(2) + *n*-heptane(3)			
0.7060	0.1165	0.77255	1164	955	2
0.5788	0.2432	0.77450	1173	939	3
0.4761	0.3055	0.77038	1175	940	1
0.3748	0.4342	0.77634	1189	911	−3
0.2982	0.4846	0.77385	1191	910	−3
0.2254	0.6169	0.78335	1208	875	−5
0.1204	0.7036	0.78231	1214	867	−6
0.1002	0.7580	0.78724	1222	850	−6
		Methylethylketone(1) + 1-hexanol(2) + *n*-heptane(3)			
0.7412	0.1248	0.77904	1168	941	5
0.6041	0.2330	0.77739	1178	927	2
0.4805	0.3024	0.77200	1183	926	−2
0.4216	0.3858	0.77693	1194	903	−3
0.3471	0.4381	0.77536	1199	897	−4
0.2961	0.4925	0.77699	1204	888	−5
0.2188	0.6243	0.78629	1225	848	−7
0.1096	0.7493	0.79027	1242	820	−9

where Φ_1, Φ_2, Φ_3 and $\varkappa_{s_1}$, $\varkappa_{s_2}$, $\varkappa_{s_3}$ are volume fractions and isentropic compressibilities of methylethylketone, an alkanol and *n*-heptane, respectively. The results are included in Table II.

The binary data: methylethylketone with *n*-heptane and *n*-heptane with 1-propanol, 1-butanol, 1-pentanol and 1-hexanol are given in Table III along with excess volumes. The deviation in isentropic compressibility of these binary mixtures are also graphically presented in Fig. 1. The values of K_s and

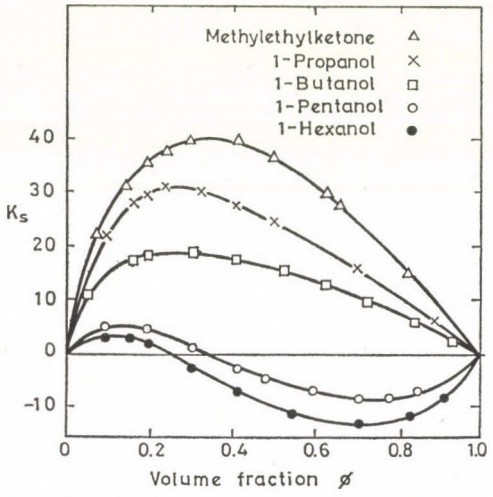

Fig. 1. Plot of K_s as a function of volume fraction for methylethylketone(1) + *n*-heptane(2) and 1-alkanol(1) + *n*-heptane(2) at 303.15 K

excess volumes for binary mixtures of methylethylketone with four alcohols are reported to be within the experimental error [6]. Hence the data are not included here.

The results included in Tables II and III indicate that the non-ideal behaviour of the four ternary systems is parallel to that of four binary ones made up of *n*-heptane and the four alcohols. This is expected since the K_s values and excess volumes are within the experimental error in the binary mixtures of methylethylketone with four alcohols. It is very difficult to understand the origin of deviation in isentropic compressibility. However, one can qualitatively explain the size and magnitude of deviation in terms of molecular interaction. The data of the four ternary mixtures and the binary data included in Table II suggest that the addition of either *n*-heptane or a mixture of *n*-heptane and methylethylketone brings about depolymerization of hydrogen bonded aggregates of alcohols over the whole range of composition. In the remaining two systems depolymerization occurs in mixtures rich in heptane-ketone mixtures. On the other hand, in mixtures rich in 1-pentanol and 1-hexanol the depolymerization is outweighed by effect of interstitial accommodation of *n*-heptane and methylethylketone molecules in the alcohol polymers.

Table III

Experimental values for the isentropic compressibility of binary systems at 303.15 *K*

Φ	ρ/g cm^{-3}	u/ms^{-1}	$\frac{\varkappa_s}{\text{TPa}^{-1}}$	$\frac{K_s}{\text{TPa}^{-1}}$	$\frac{V^E}{\text{cm}^3\,\text{mol}^{-1}}$
$\Phi\ C_3H_7OH + (1-\Phi)C_7H_{16}$					
0.0000	0.67504	1112	1198		
0.0902	0.68479	1107	1192	22	0.223
0.1554	0.69215	1108	1187	28	0.305
0.1868	0.69582	1109	1169	30	0.318
0.2302	0.70087	1110	1158	31	0.338
0.3247	0.71209	1116	1127	30	0.336
0.4119	0.72268	1123	1097	27	0.300
0.5037	0.73387	1131	1067	24	0.264
0.6909	0.75716	1150	999	16	0.145
0.8777	0.78028	1173	931	7	0.057
1.0000	0.79562	1190	887		
$\Phi\ C_4H_9OH + (1-\Phi)C_7H_{16}$					
0.0000	0.67504	1112	1198		
0.0508	0.68122	1110	1191	11	0.090
0.1563	0.69383	1116	1157	17	0.210
0.1884	0.69779	1118	1147	18	0.226
0.3009	0.71198	1127	1106	18	0.230
0.4074	0.72352	1139	1066	17	0.210
0.5202	0.73998	1150	1022	15	0.170
0.6178	0.75251	1162	984	12	0.142
0.7197	0.76564	1176	945	10	0.106
0.8320	0.78018	1193	900	6	0.062
0.9251	0.79226	1209	863	3	0.022
1.0000	0.80202	1224	832		
$\Phi\ C_5H_{11}OH + (1-\Phi)C_7H_{16}$					
0.0000	0.67504	1112	1198		
0.1010	0.68777	1120	1159	4	0.146
0.1988	0.70056	1130	1118	3	0.170
0.3059	0.71481	1142	1072	1	0.151
0.4135	0.72923	1157	1024	−3	0.116
0.4837	0.73876	1168	922	−5	0.076
0.5920	0.75343	1185	945	−7	0.017
0.6979	0.76773	1202	901	−8	−0.024
0.7653	0.77675	1215	872	−9	−0.038
0.8378	0.78638	1227	844	−7	−0.042
1.0000	0.80762	1257	784		

Table III (contd.)

Φ	ρ/g cm^{-3}	u/ms^{-1}	$\frac{\varkappa_s}{\text{TPa}^{-1}}$	$\frac{K_s}{\text{TPa}^{-1}}$	$\frac{V^E}{\text{cm}^3\,\text{mol}^{-1}}$
$\Phi\ C_6H_{13}OH + (1-\Phi)C_7H_{16}$					
0.0000	0.67504	1112	1198		
0.0905	0.68725	1120	1160	3	0.046
0.1530	0.69576	1126	1134	3	0.050
0.1956	0.70164	1132	1112	2	0.042
0.3023	0.71639	1148	1059	−3	0.010
0.4120	0.73161	1166	1005	−7	−0.026
0.5357	0.74869	1189	944	−12	−0.054
0.7023	0.77167	1222	868	−13	−0.073
0.8246	0.78837	1250	813	−12	−0.066
0.9128	0.80029	1267	778	−7	−0.043
1.0000	0.81198	1285	746		
$\Phi\ CH_3COC_2H_5 + (1-\Phi)C_7H_{16}$					
0.0000	0.67504	1112	1198		
0.0735	0.68353	1104	1200	22	0.350
0.1329	0.68717	1105	1192	31	0.545
0.1750	0.68999	1106	1184	35	0.645
0.2352	0.69818	1107	1169	37	0.730
0.2937	0.70574	1108	1154	38	0.775
0.4088	0.71904	1112	1125	40	0.790
0.5008	0.73005	1119	1094	36	0.740
0.6122	0.74370	1128	1056	29	0.635
0.6464	0.74800	1131	1045	27	0.590
0.8090	0.76898	1148	987	15	0.340
1.0000	0.79446	1170	920		

REFERENCES

[1] Rao, M. V. P., Naidu, P. R.: Can. J. Chem., **52,** 788 (1974)
[2] Reddy, K. S., Naidu, P. R.: Can. J. Chem., **55,** 76 (1977)
[3] Timmermans, J.: Physico-chemical Constants of Pure Organic Compounds. Elsevier, New York, 1950
[4] Rao, M. V. P.: Ph. D. Thesis. Sri Venkateswara University, India, 1974
[5] Naidu, G. R., Naidu, P. R.: Can. J. Chem. (communicated)
[6] Reddy, K. S., Naidu, P. R.: J. Chem. Thermodynamics, **10,** 201 (1978)

G. R. Naidu, P. R. Naidu
Department of Chemistry, College of Engineering,
S. V. University, Tirupati 517502, India.

Acta Chimica Academiae Scientiarum Hungaricae, Tomus 108 (1), pp. 91—98 (1981)

REACTIONS OF MONO- AND DIARYLIDENECYCLOALKANONES WITH THIOUREA AND AMMONIUM THIOCYANATE, IV*

AROMATIZATION OF 2-ALKYLMERCAPTO-4-PHENYL-8--BENZYLIDENE-3,4,5,6,7,8-HEXAHYDROQUINAZOLINES

T. LÓRÁND[1], D. SZABÓ[1], A. FÖLDESI[2] and A. NESZMÉLYI[3]

([1]*Chemical Institute, Medical University, Pécs,*
[2]*Central Theoretical Laboratory, Medical University, Pécs, and*
[3]*Central Chemical Research Institute, Hungarian Academy of Sciences, Budapest*)

Received May 14, 1980

In revised form September 2, 1980

Accepted for publication November 11, 1980

2-Alkylmercapto-4-phenyl-8-benzylidene-3,4,5,6,7,8-hexahydroquinazolines (**III a—f**) and their salts (**IIa—f**) can be aromatized by singlet oxygen or alkaline $K_3[Fe(CN)_6]$ oxidation reactions to obtain 2-alkylmercapto-4-phenyl-8-benzylidene-5,6,7,8-tetrahydroquinazolines (**IVa—f**). The structures of **IVa—f** were confirmed by UV, IR, ^{1}H-NMR and ^{13}C-NMR spectroscopy.

In previous papers we described the synthesis of some 3,4,5,6,7,8-hexahydro-2(1*H*)-quinazolinethiones (**I**) and their *S*-alkyl derivatives (**IIa—d**) [1, 2]; later on homologues with a higher number of carbon atoms (**IIe—f**) were also synthesized (see Experimental).

In the present paper the partial aromatization of **IIa—f** will be discussed.

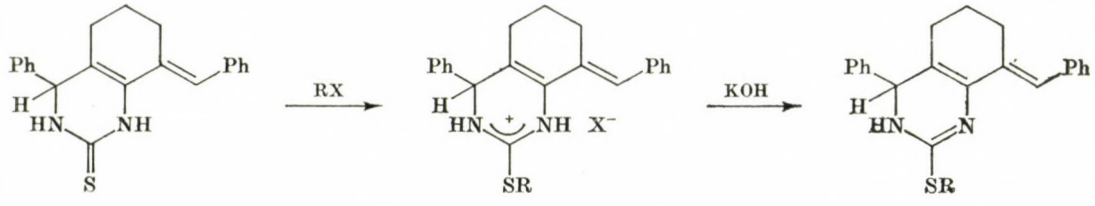

I

IIa (R = CH_3, X = I)
b (R = C_2H_5, X = Br)
c (R = C_3H_7, X = I)
d (R = C_4H_9, X = Br)
e (R = C_5H_{11}, X = Br)
f (R = C_6H_{13}, X = Br)

IIIa (R = CH_3)
b (R = C_2H_5)
c (R = C_3H_7)
d (R = C_4H_9)
e (R = C_5H_{11})
f (R = C_6H_{13})

Fig. 1

* Part III, see Ref. [2].

Table I

Compound R	Compound X	M.p., °C	Formula, M.w., Yield, %	UV (ethanol) λ_{max} (nm)	UV (ethanol) log ε	IR, cm^{-1} (KBr pellets)	^{1}H-NMR, δ ppm ($CDCl_3$)
IIe		155–160	$C_{26}H_{31}BrN_2S$	240	4.78	3250–2400 NH, =NH$^+$	0.7 t 3H CH_3
$(CH_2)_4CH_3$	Br		483.53	278	5.03	1650 νC=N	0.9–3.7 m 14H CH_2, SCH_2
			36	327	4.59		5.3 s 1H CH
							7.0–7.8 m 11H Ar, =CH
							10.3–10.7 s 2H =NH^{+a}
IIf		134–142	$C_{27}H_{33}BrN_2S$	239	4.46	3300–2400 NH, =NH$^+$	0.8 t 3H CH_3
$(CH_2)_5CH_3$	Br		497.56	277	4.70	1650 νC=N	0.9–3.7 m 16H CH_2, SCH_2
			62	328	4.23		5.3 s 1H CH
							7.1–7.7 m 11H Ar, =CH
							10.3–10.7 s 2H =NH^{+a}
IIIe		104–110	$C_{26}H_{30}N_2S$	238	4.30	3370 νNH	0.9 t 3H CH_3
$(CH_2)_4CH_3$	—		402.61	278	4.55	1620 νC=N	1.1–3.3 m 14 H CH_2, SCH_2
			84	325	4.13		4.7–5.1 s 2H NH, CH^b
							7.0–7.7 m 11H Ar, =CH
IIIf		87–94	$C_{27}H_{32}N_2S$	237	4.33	3375 νNH	0.8 t 3H CH_3,
$(CH_2)_5CH_3$	—		416.64	277	4.58	1620 νC=N	0.9–3.3 m 16H CH_2, SCH_2
			66	329	4.22		4.5–5.0 s 2H NH, CH^b
							7.0–7.8 m 11H Ar, =CH

[a] Disappears on the effect of D_2O

[b] The CH signal is overlapping the NH signal, on the effect of D_2O the value of the integral decreased

When the preparation of the corresponding bases was attempted from the salts **IIc—d**, in some cases the product was other than the **IIIc—d** derivative expected. In the ^{1}H-NMR spectrum of the substance obtained from **IId** the signals of the CH and NH protons assumed to be at positions 4 and 3, respectively, were absent, showing that the heterocyclic ring must have aromatic character. Since the spontaneous formation of **IVd** in the alkaline reaction mixture occurred in very poor yield only (14%), a suitable oxidation method was to be found to prepare the aromatic derivatives of **IIIa—f**. Chromic acid and H_2O_2 were tried unsuccessfully. Since in the previous case the dehydrogenation was suspected to be due to the effect of O_2 dissolved in methanol, the reaction was tried in alkaline medium (KOH, methanol) while sucking air through the solution. This method also failed.

Recently several papers have dealt with oxidations by singlet oxygen [3—5]. This can be prepared very advantageously by the photochemical method using methylene blue sensitizer [6]. Compound **IIa—f** was dissolved in methanol containing KOH and a very slight amount of methylene blue, and exposed to the radiation of sun; in this way **IVa—f** were prepared in acceptable yields. (Similar results were achieved when using an UV lamp as the light source.) When the above experiment was effected in N_2 atmosphere, no aromatization could be observed, which confirms the mechanism involving the action of singlet oxygen.

GIRKE [7, 8] achieved the aromatization of partially saturated pyrimidines and quinazolines by means of potassium hexacyanoferrate in satisfactory yields. This method gave in our experiments substances of higher purity than those obtained previously. In certain cases, when starting from the corresponding bases, the aromatic products could again be obtained (see Experimental) in satisfactory yields.

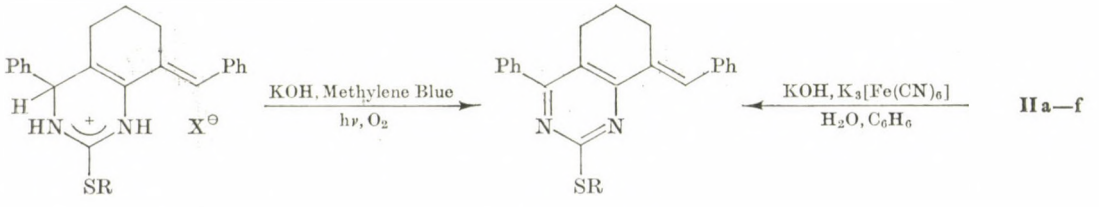

IIa—f

IVa (R = CH_3)
b (R = C_2H_5)
c (R = C_3H_7)
d (R = C_4H_9)
e (R = C_5H_{11})
f (R = C_6H_{13})

Fig. 2

Table II

Compound R	M.p., °C	Formula, M.w., Yield, %	UV (ethanol)		IR, cm^{-1} (KBr pellets)	^{1}H-NMR, δ ppm ($CDCl_3$)
			λ_{max} (nm)	log ε		
IVa CH_3	123—128	$C_{22}H_{20}N_2S$ 344.48 73[a] 61[b]	223 264 350	4.22 4.38 4.06	1520, 1530 $\nu C{=}C_{Ar}$[c]	1.4—1.9, 2.5—3.1 m 6H CH_2 2.6 s 3H SCH_3[d] 6.9—7.7 m 10H Ar 8.2 t 1H =CH
IVb C_2H_5	80—84	$C_{23}H_{22}N_2S$ 358.51 15[a] 13[b]	263 351	4.40 3.99	1515 $\nu C{=}C_{Ar}$[c]	1.4 t 3H CH_3[d] 1.2—2.0, 2.5—3.1 m 6H CH_2 3.16 q 2H SCH_2 J=6Hz 7.1—7.6 m 10H Ar 8.2 t 1H =CH
IVc C_3H_7	90—95	$C_{24}H_{24}N_2S$ 372.53 48[a] 46[b] 54[e]	223 265 352	4.24 4.39 4.00	1520 $\nu C{=}C_{Ar}$[c]	1.05 t 3H CH_3 1.4—2.2, 2.5—3.0 m 8H CH_2 3.2 t[f] 2H SCH_2 7.1—7.7 m 10H Ar 8.2 t 1H =CH
IVd C_4H_9	106—113	$C_{25}H_{26}N_2S$ 386.57 41[a] 39[b]	222 264 352	4.22 4.37 3.99	1520, 1530 $\nu C{=}C_{Ar}$[c]	1.0 t 3H CH_3 1.2—2.1, 2.5—3.1 m 10H CH_2 3.2 t[f] 2H SCH_2 7.1—7.7 m 10H Ar 8.2 t 1H =CH
IVe C_5H_{11}	88—92	$C_{26}H_{28}N_2S$ 400.60 17[a] 41[g]	224 264 351	4.25 4.38 4.01	1520, 1530 $\nu C{=}C_{Ar}$[c]	0.9 t 3H CH_3 1.1—2.2, 2.5—3.0 m 12H CH_2 3.2 t[f] 2H SCH_2 6.9—7.9 m 10H Ar 8.3 t 1H =CH

IVf C_6H_{13}	96—100	$C_{27}H_{30}N_2S$ 414.62 46[a] 35[b]	222 264 351	4.25 4.39 4.02	1520 1530 } $\nu C{=}C_{Ar}$[c]	0.9 1.1—2.2 2.6—3.1 3.2 7.0—7.8 8.3	t m t[f] m t	3H CH_3 14H CH_2 2H SCH_2 10H Ar 1H =CH

[a] according to method *A*;
[b] according to method *B*;
[c] very intense doublet or multiplet band;
[d] the signal of the methyl group overlaps that of the methylenes;
[e] from **IIIc**, by method *A*;
[f] in first-order approximation;
[g] from **IIIe**, by method *A*.

The structures of the products were confirmed by IR, ^{1}H-NMR, ^{13}C-NMR and UV spectroscopic methods.

The sharp ν NH band characteristic of the starting material **IIIa—f** (3360—3380 cm^{-1}) is absent in **IVa—f**, while a skeletal vibration of the hetero-aromatic ring appears as a new band in the range between 1520 and 1530 cm^{-1}. (Exact assignment of these bands is difficult, since there are three aromatic rings in the molecule.)

In the ^{1}H-NMR spectra (Table II) the absence of the CH proton at site 4 indicates the occurrence of aromatization most strikingly (**IIIa—f**: δ 4.9) [2]. The only olefin proton in the molecules suffered a paramagnetic shift of 0.6—0.7 ppm (δ 8.2 ppm) as compared with the starting bases (**IIIa—f**); this can probably be attributed to the shielding and conjugation effect of the hetero-aromatic ring. This signal exhibits a triplet character (allyl coupling with a methylene group). In these spectra, a significant change can be observed in the signal assigned to the SCH_2 group. In **IIIa—f**, a complex multiplet can be assigned to the *S*-methylene group [2], while in **IVa—f** this signal is significantly simpler, owing to the higher symmetry of the molecule. In the spectra of the aromatic compounds **IVa—f**, the shift data for the $5CH_2$ and $7CH_2$ protons are nearly identical (δ 2.5—3.0 ppm), while the shifts of the same methylene protons in the starting bases are δ 1.4—2.1 ppm ($5CH_2$) and δ 2.5—2.9 ppm ($7CH_2$). The carbon atom at site 4 is in sp^2 hybrid state as a result of the aromatization, thus this phenyl group lies in the plane of the molecule, which explains the identical shifts of the $5CH_2$ and $7CH_2$ ring protons mentioned above. The high difference between the shifts of the same protons in the starting bases (**IIIa—f**) confirms the *axial* position of the C-4 phenyl substituent. This is also indicated by the fact that aromatization takes place relatively readily; the substituent with high space requirement leaves the unfavourable *axial* position to become coplanar with the molecule.

The assignments of the ^{13}C-NMR spectrum of **IVd** is shown in Fig. 3. It is noteworthy that, as compared with the ^{13}C-NMR spectrum of the starting material **I** [1], the aromatic character of the hetero ring is reflected in the shifts of the C-2, C-4, C-4a and C-8a carbon atoms. The character of the C-8, C-8 α double bond remained essentially unchanged. Thus the rotational freedom of the phenyl ring in the benzal group can be considered to be similar to that in **I**. The phenyl group attached to C-4 is not involved in a significant delocalization either. The *trans* character of the benzal group is also retained.

The appearance of the new chromomorphic system results in significant changes in the UV spectra, too (Table II), as compared with the starting substances **IIIa—f**. In **IIIa—f** there are three characteristic maxima [2]. Each of them is shifted as a result of aromatization. In compounds **IIId** and **IVd** the following changes can be observed: **IIId** $\lambda_1 = 237$ nm, $\lambda_2 = 276$ nm, $\lambda_3 = 325$ nm; **IVd** $\lambda_1 = 222$ nm, $\lambda_2 = 264$ nm, $\lambda_3 = 352$ nm.

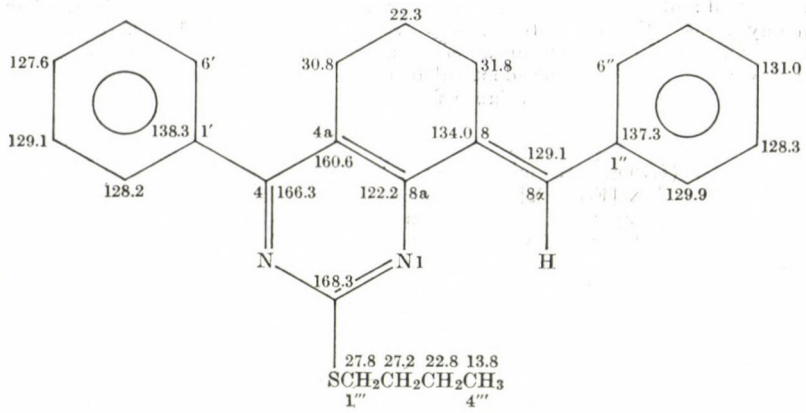

IVd

Fig. 3

The experimental results support the earlier observation [7, 8] that dihydropyrimidines and quinazolines can easily be dehydrogenated. The reaction presumably takes place according to a radical mechanism, which is favoured by the relatively high stability of the radical of benzyl type formed transitionally [9].

Experimental

Of the spectra discussed, the IR spectra were recorded with a Specord F5 instrument; the PMR spectra were obtained with a Perkin-Elmer R-12 (60 MHz) spectrometer. The ^{13}C-NMR spectrum of **IVd** was recorded with a Varian XL-100-15 FT (25.16 MHz) instrument in $CDCl_3$, at room temperature, the internal standard being TMS. The UV spectra were taken with a Perkin-Elmer 402 spectrophotometer. The UV lamp used for irradiation, was Analysenlampe, Hanau, λ 366 nm, 125 watts. In the reactions, outside illumination was employed, the reaction time was, on the average, 12 hours.

The elemental analysis data of the compounds were within the limits of experimental error.

Syntheses of the starting materials (**IIa—d**) have been reported [2]. The preparation of 2-pentylmercapto-4-phenyl-8-benzylidene-3,4,5,6,7,8-hexahydroquinazoline hydrobromide (**IIe**) and 2-hexylmercapto-4-phenyl-8-benzylidene-3,4,5,6,7,8-hexahydroquinazoline hydrobromide (**IIf**) from **I** was achieved by using pentyl or hexyl bromide, respectively; the corresponding bases were liberated with potassium hydroxide yielding **IIIe—f** [2].

Other data for **IIe—f** and **IIIe—f** are shown in Table I.

2-Methylmercapto-4-phenyl-8-benzylidene-5,6,7,8-tetrahydroquinazoline (IVa)

Method A

Compound **IIa** (4.76 g; 0.01 mole) was dissolved in methanol (100 mL) and a solution of potassium hydroxide (1.12 g; 0.02 mole) in methanol (40 mL) was added. Methylene blue (5 mg) was added to the solution which was then exposed to sunshine in an Erlenmeyer flask (ERGON) for 12 h. The course of the reaction was monitored by TLC (adsorbent: Kieselgel GF_{254} nach Stahl, Merck; developing mixture: benzene-ethyl acetate 10 : 1; detection with iodine; R_f values: **IIIb** 0.66, **IVb** 0.79). At the end of the reaction a colourless precipitate separated, this was filtered off, washed with methanol then with water until neutral and recrystallized from methanol. The mother liquor of the reaction was evaporated to dryness, the oily residue was dissolved in benzene and washed with 10% hydrochloric acid and with

water until neutral and colourless, then dried over anhydrous magnesium sulfate. After standing for one day, the solution was filtered, evaporated to dryness and the residue was recrystallized from methanol. The products obtained as a precipitate from the reaction mixture and in the latter way were found to be identical in all respects. (Compound **IVa** was isolated in a similar manner, when using an UV lamp for irradiation.

Method B

Compound **IIa** (4.76 g; 0.01 mole) was suspended in water (70 mL); potassium hydroxide (1.12 g; 0.02 mole) and $K_3[Fe(CN)_6]$ (7 g; 0.021 mole) were added to the suspension, which was then covered with a layer of benzene (60 mL). The reaction mixture was stirred for 22 h, then $K_3[Fe(CN)_6]$ (2 g; 0.006 mole) was added again, and stirring was continued for 3 h more. The completion of the reaction was checked by TLC. At the end of the reaction the benzene phase was separated, the aqueous phase extracted with benzene (2×100 mL), and the combined benzene phases were washed with water until colourless and neutral. The solution was dried over anhydrous magnesium sulfate, filtered next day and evaporated to dryness. The residue was crystallized from methanol.

The analogous compounds **IVb**—**f** were obtained in a similar manner by methods *A* or *B* from **IIb**—**f**. These methods were also employed in the aromatization reactions starting from the corresponding bases (**IIIc**, **IIIe**) (see Table II).

Other data of **IVa**—**f** are shown in Table II.

*

The authors' thanks are due to Dr. R. OHMACHT and Mrs. M. OTT for the analyses, to Dr. R. OHMACHT for the IR spectra, to Mrs. Gy. HALÁSZ for the UV spectra and to Miss E. MÁTRAI, Mrs. E. BLESZITY and Miss H. TENCZ for technical assistance.

REFERENCES

[1] LÓRÁND, T., SZABÓ, D.: Acta Chim. Acad. Sci. Hung., **93,** 51 (1977)
[2] LÓRÁND, T., SZABÓ, D., FÖLDESI, A.: Acta Chim. Acad. Sci. Hung., **104,** 147 (1980)
[3] FOOTE, C. S., WEXLER, S.: J. Am. Chem. Soc., **86,** 3879 (1964)
[4] FOOTE, C. S., WEXLER, S., ANDO, W., HIGGINS, R.: J. Am. Chem. Soc., **90,** 975 (1968)
[5] MURRAY, R. W., KAPLAN, M. L.: J. Am. Chem. Soc., **91,** 5358 (1969)
[6] COTTON, F. A., WILKINSON, G.: Advanced Inorganic Chemistry, 3rd ed. p. 412. Wiley and Sons, New York, London, Sydney, Toronto, 1972
[7] GIRKE, W. P. K.: Ber., **112,** 1 (1979)
[8] GIRKE, W. P. K.: Ber., **112,** 1348 (1979)
[9] MORRISON, R. T., BOYD, R. N.: Organic Chemistry, 3rd ed. p. 388. Allyn and Bacon, Boston, London, Sydney, Toronto, 1973

Tamás LÓRÁND
Dezső SZABÓ
András FÖLDESI
H-7643 Pécs, Szigeti út 12.

András NESZMÉLYI H-1525 Budapest, Pusztaszeri út 57—69. Hungary

RECENSIONES

G. A. Somorjai and M. A. Van Hove: *Adsorbed monolayers on solid surfaces*

Springer Verlag, 1979

This monograph has been published by Springer Verlag and it is No. 38 in the series of "Structure and Bonding".

This book gives an excellent summary on the interaction between adsorbed monolayers and solid surfaces starting with the principle of monolayer adsorption, and of the ordering of adsorbed monolayer. The causes, the degree of ordering, and the temperature dependence of surface irregularities are given.

In the last decade many new methods have been developed based on physical methods applied to solid surfaces. In the fourth chapter a brief summary of all methods used so far shows the applicability, the limitations, *etc.*, of these experimental techniques.

These methods are divided into five subgroups: Methods sensitive to a) atomic geometry at surfaces; b) electronic structure and geometry of surfaces; c) electron distribution at surfaces; d) chemical composition at surfaces; and f) vibrational structure of surfaces. The reader who is not familiar with all these methods can easily understand the principle of Low Energy Electron Diffraction (LEED), Reflection High Energy Electron Diffraction (RHEED), Field Ion Microscopy (FIM), surface Sensitive Extended X-ray Absorption Fine Structure (SEXAFS), *etc.* UV and X-ray photoemission spectroscopy (UPS and XPS) are included in the second subgroup and information about the electron structure of the surface can be collected by these methods. Auger electron spectroscopy (AES) and Secondary Ion Mass Spectroscopy (SIMS) are the tools to measure quantitatively surface compositions. Infrared (IR) and High Resolution Electron Energy Loss Spectroscopy (HREELS) are very powerful methods to study the structure of the adsorbed layer.

Data on different adsorbates are given in chapter 5, including the ordering and literature citations.

The book is finished by a summary of the surface crystallography of ordered monolayers of atoms and of ordered multiatomic and molecular monolayers.

The book may serve as a handbook for everyone who is working in the field of surface chemistry either from a fundamental aspect or in connection with heterogeneous catalysis.

L. Guczi

Lecture Notes in Chemistry, Vol. 11

F. A. Gianturco: *The Transfer of Molecular Energies by Collision: Recent Quantum Treatments*

Springer-Verlag, Berlin, Heidelberg, New York, 1979, 327 pp.

Results from crossed molecular beam studies, use of lasers for state selected excitation of molecules, increased use of molecular spectroscopy in kinetic experiments have contributed considerably in recent years to our knowledge of chemistry at a microscopic level. At the same time significant progress has been made in developing reliable theoretical treatments for the calculation of probabilities and cross sections for various channels in reactive collisions and non-reactive inelastic encounters. This volume provides the presentation of the theoretical and computational aspects of the simplest type of energy transfer, namely of the con-

version of translational energy into rotational and vibrational energy in encounters of atoms and simple molecules in their ground electronic state.

The working formalism required to deal with quantum mechanical scattering is introduced in Chapter *1*. The next chapter provides a clear presentation of generally used *ab initio* potential energy hypersurface calculation methods, computational techniques and some recent applications. Approximate treatments are reviewed only briefly. A detailed description of the theory of three-dimensional atom-molecule and molecule-molecule encounters resulting in the conversion of translational energy into rotational and vibrational excitation is given in Chapter *3*. The formulation of the theory presented by the author adopts a fully quantum mechanical approach based on the Schrödinger equation. The drawback of the rigorous *ab initio* treatments is that their application is restricted today to light systems and to low collision energies. Approximations suggested in recent years to reduce the dimensionality of the coupled-channel (CC) equations are discussed in Chapter *4*. The importance of such approximate treatments comes from the expectation that they may allow the calculation of cross sections for more sophisticated systems at various collision energies. Text proceeds with a survey of numerical procedures available for the solution of the CC equations (Chapter *5*), and ends with a short discussion of the relationship between computed cross sections and experimental quantities obtained from relaxation phenomena (Chapter *6*).

This volume consists of an up-to-date and well balanced presentation of the theory, the computational techniques and the numerical procedures related to the subject. Readers possessing a good knowledge in quantum chemistry and familiar with the basic elements of the subject discussed, will find the volume very useful. Experimentalists and graduate students with little experience in the areas mentioned, may find difficulties in reading the book.

T. BÉRCES

W. KLEMM, R. HOPPE: *Anorganische Chemie*

Sammlung Göschen de Gruyter

Walter de Gruyter, Berlin—New York, 1980. 328 p.

Dieses auf drei Jahrzehnte zurückblickende, in 16 Auflagen erschienene Buch diente und dient dem Ziel, einen kurzen Überblick über das Gebiet der anorganischen Chemie zu bieten und ist vor allem für Hochschulstudenten mit Chemie als Nebenfach, für Mittelschulschüler und für Leser mit Mittelschulbildung und Interesse für Chemie bestimmt.

Das Buch entspricht dem Ziel; zum Verständnis sind die Kenntnisse ausreichend, die weltweit in den Mittelschulen vermittelt werden.

Der Wert der vorliegenden Auflage wird dadurch erhöht, daß das SI-System konsequent angewendet wird. Dadurch ergänzt bzw. korrigiert das Buch jene Handbücher und Hochschullehrbücher, die früher herausgegeben wurden, jedoch zur Zeit noch im Gebrauch sind.

Neben der Anwendung des SI-Systems bringt die 16. Auflage vor allem in zwei Beziehungen Neues. Absatz XXXIII enthält einen recht brauchbaren Überblick über die mittels verschiedener Strukturprüfmethoden zu erhaltenden Informationen. Auch die Diskussion der technischen Probleme wurde — der Entwicklung der Industrieverfahren entsprechend — wesentlich modernisiert.

B. CSÁKVÁRI

Lecture Notes in Chemistry, Vol. 18

Stefan G. CHRISTOV: *The Statistical and Collision Theory of Chemical Reactions*

Springer-Verlag, Berlin—Heidelberg—New York, 1980. 322 pages

The author is the former director of the Institute of Physical Chemistry of the Bulgarian Academy of Sciences, member of the Bulgarian Academy of Sciences. In this book he gives a survey of high standard on the results obtained in the field of quantum-mechanical treatment of chemical reactions and the possibilities of further development.

The main concept of the book is that atomic and molecular properties, as well as the knowledge of the electronic structure enable us to understand the elementary steps of chemical processes.

The increasing amounts of information in the last decade initiated scientists to develop new methods for calculating the potential energies of reacting systems, reaction cross-sections and reaction rate constants. The basic problems can be solved in an exact manner only for the simplest chemical reactions on the basis of quantum-mechanical and statistical physics. For this reason, various approximations have been made for the simplification of complex problems. The aim of the book is to discuss in detail the correlations between the different theories, possibly on the basis of uniform aspects. The author does not deal with computer techniques for the solution of this task. However, uniformity demands the clear definition of principles and the correct formulation of theories.

Approximate theories as *e.g.* the classical collision theory or the semiclassical theory of transition states introduce simplifying conditions and apply corrections (steric factor, transmission coefficient), which are in general not well-defined for the approximation of experimental results. Therefore, it seems to be more reliable to narrow the conditions and to give more precise definitions.

The book sets out from an equation based on a general collision theory which, under certain conditions, can be transformed into the equations of either the classical collision theory, or various statistical theories. Thus these conditions can be defined more precisely and the limits of validity can be better studied.

In Chapter *1*, "The Potential Energy of Reacting Systems", methods are surveyed, suitable for the calculation of potential energy surfaces, with special reference to the relationship between electronic structure and reactivity.

Chapter *2*, "Dynamics of Molecular Collisions", is somewhat longer. It deals with the calculation methods of reaction cross-sections of electronic adiabatic and non-adiabatic reactions, but several approximate methods useful for practical applications are also mentioned.

Chapter *3*, "General Theory of Reaction Rates", is the most important part of the book. This chapter tries to present the various reaction rate theories from a uniform aspect.

Finally, Chapter 4 "Application of Reaction Rate Theories", illustrates the present capabilities of these theories.

Chapter *1* (29 pages) discusses the following topics: Adiabatic Approximation, Corrections in the Adiabatic Approximation, and Potential Energy Surfaces.

Chapter *2* (85 pages) treats Time-dependent and Time-independent Collision Theories, Transition Probability and Reaction Cross-section, Classical Trajectory Calculations, Quantum-mechanical Calculations, Quasi-classical Calculations and Non-adiabatic Transitions in Chemical Reactions.

Chapter *3* (105 pages) includes Formulation of Reaction Rates According to Collision Theory, Classical and Semiclassical Approximations, Adiabatic Statistical Theory of Reaction Rates, Calculation of the Transmission Coefficient and the Tunnelling Correction, and General Consequences of Rate Equations.

Chapter *4* (87 pages) discusses several unimolecular and bimolecular gas- and liquid-phase reactions.

Among gas-phase reactions only the reactions of isoenergetic particles can be treated accurately, in the liquid-phase mainly reactions with electron exchange, and in one case with proton exchange are discussed. The subject is completed with electrode kinetic and biological problems selected from the literature.

The book can serve two different purposes: the physicochemist can obtain a survey about the up-to-date stand and possibilities of this theory without getting lost in quantitative details, and on the other hand, it can supply a good start for scientists intending to work in this difficult field.

The book is prepared by rotaprint technique with the inevitable typing mistakes, which are, fortunately, not distorting the sense.

The author does not use a uniform nomenclature, designations and the SI units.

The text contains 30 line figures and 200 references, of which 25 are the works by the author.

Gy. VARSÁNYI

INDEX

PHYSICAL AND INORGANIC CHEMISTRY

ORGANIC CHEMISTRY

Printed in Hungary

A kiadásért felel az Akadémiai Kiadó igazgatója — Műszaki szerkesztő: Rózsa Katalin

A kézirat a nyomdába érkezett: 1981 II. 12. — Terjedelem 9 (A/5) ív, 21 ábra

81.9300 Akadémiai Nyomda, Budapest — Felelős vezető: Bernát György

Les Acta Chimica paraissent en français, allemand, anglais et russe et publient des mémoires du domaine des sciences chimiques.

Les Acta Chimica sont publiés sous forme de fascicules. Quatre fascicules seront réunis en un volume (3 volumes par an).

On est prié d'envoyer les manuscrits destinés à la rédaction à l'adresse suivante:

Acta Chimica
Budapest, P.O.B. 67, H-1450, Hongrie

Toute correspondance doit être envoyée à cette même adresse.

La rédaction ne rend pas de manuscript.

Abonnement en Hongrie à l'Akadémiai Kiadó (1363 Budapest, P.O.B. 24, C. C. B. 215 11488), à l'étranger à l'Entreprise du Commerce Extérieur « Kultura » (H-1389 Budapest 62, P.O.B. 149. Compte-courant No. 218 10990) ou chez représentants à l'étranger.

Die Acta Chimica veröffentlichen Abhandlungen aus dem Bereich der chemischen Wissenschaften in deutscher, englischer, französischer und russischer Sprache.

Die Acta Chimica erscheinen in Heften wechselnden Umfanges. Vier Hefte bilden einen Band. Jährlich erscheinen 3 Bände.

Die zur Veröffentlichung bestimmten Manuskripte sind an folgende Adresse zu senden:

Acta Chimica
Budapest, Postfach 67, H-1450, Ungarn

An die gleiche Anschrift ist jede für die Redaktion bestimmte Korrespondenz zu richten:

Manuskripte werden nicht zurückerstattet.

Bestellbar für das Inland bei Akadémiai Kiadó (1363 Budapest, Postfach 24, Bankkonto Nr. 215 11488), für das Ausland bei »Kultura« Aussenhandelsunternehmen (H-1389 Budapest 62, P.O.B. 149. Bankkonto Nr. 218 10990) oder seinen Auslandsvertretungen.

«Acta Chimica» издают статики по химии на русском, английском, французском и немецком языках.

«Acta Chimica» выходит отдельными выпусками разного объекта, 4 выпуска составхяют один том и за год выходят 3 тома.

Предназначенные для публикации рукописи следует направлять по адресу:

Acta Chimica
Budapest, P.O.B. 67, H-1450, ВНР

Всякую корреспонденцию в редакцию направляйте по этому же адресу.

Редакция рукописей не возвращает.

Отечественные подписчики направляйте свои заявки по адресу Издательства Академии Наук (1363 Budapest, P.O.B. 24, Текущей счет 215 11488), а иностранные подписчики через организацию по внешней торговые «Kultura» (H-1389 Budapest 62, P.O.B 149. Текущий счет 218 10990) или через ее заграничные представительства и уполномеченных.

Reviews of the Hungarian Academy of Sciences are obtainable at the following addresses:

AUSTRALIA
C B.D. LIBRARY AND SUBSCRIPTION SERVICE. Box 4886, G.P.O., *Sydney N.S.W. 2001*
COSMOS BOOKSHOP, 145 Ackland Street, *St. Kilda (Melbourne), Victoria 3182*

AUSTRIA
GLOBUS, Höchstädtplatz 3, *1200 Wien XX*

BELGIUM
OFFICE INTERNATIONAL DE LIBRAIRIE, 30 Avenue Marnix, *1050 Bruxelles*
LIBRARIE DU MONDE ENTIER, 162 Rue du Midi, *1000 Bruxelles*

BULGARIA
HEMUS, Bulvar Ruski 6, *Sofia*

CANADA
PANNONIA BOOKS, P.O. Box 1017, Postal Station "B", *Toronto, Ontario M5T 2T8*

CHINA
CNPICOR, Periodical Department, P.O. Box 50, *Peking*

CZECHOSLOVAKIA
MAD'ARSKÁ KULTURA, Národni tr'da 22, *115 33 Praha*
PNS DOVOZ TISKU, Vinohradská 46, *Praha 2*
PNS DOVOZ TLACE, *Bratislava 2*

DENMARK
EJNAR MUNKSGAARD, Norregade 6, *1165 Copenhagen*

FINLAND
AKATEEMINEN KIRJAKAUPPA, P.O. Box 128, *SF-00101 Helsinki 10*

FRANCE
EUROPERIODIQUES S.A., 31 Avenue de Versailles, *78170 La Celle St. Cloud*
LIBRAIRIE LAVOISIER, 11 rue Lavoisier *75008 Paris*
OFFICE INTERNATIONAL DE DOCUMENTATION ET LIBRAIRIE, 48 rue Gay-Lussac, *75240 Paris Cedex 05*

GERMAN DEMOCRATIC REPUBLIC
HAUS DER UNGARISCHEN KULTUR, Karl-Liebknecht-Strasse 9, DDR-*102 Berlin*
DEUTSCHE POST ZEITUNGSVERTRIEBSAMT, Strasse der Pariser Kommüne 3—4, *DDR-104 Berlin*

GERMAN FEDERAL REPUBLIC
KUNST UND WISSEN ERICH BIEBER, Postfach 46, *7000 Stuttgart 1*

GREAT BRITAIN
BLACKWELL'S PERIODICALS DIVISION, Hythe Bridge Street, *Oxford OX1 2ET*
BUMPUS, HALDANE AND MAXWELL LTD., Cower Works, *Olney Bucks MK46 4BN*
COLLET'S HOLDINGS LTD., Denington Estate, *Wellingborough, Northants NN8 2QT*
WM. DAWSON AND SONS LTD., Cannon House, *Folkestone, Kent CT19 5EE*
H. K. LEWIS AND CO., 136 Gower Street, *London WC1E 3BS*

GREECE
KOSTARAKIS BROTHERS, International Booksellers, 2 Hippokratous Street, *Athens-143*

HOLLAND
MEULENHOFF-BRUNA B.V., Beulingstraat 2, *Amsterdam*
9—11, *Den Haag*
SWETS SUBSCRIPTION SERVICE 347b Heereewg, *Lisse*

INDIA
ALLIED PUBLISHING PRIVATE LTD., 13/14 Asaf Ali Road, *New Delhi 110001*
150 B-6 Mount Road, *Madras 600002*
INTERNATIONAL BOOK HOUSE PVT. LTD., Madame Cama Road, *Bombay 400069*
THE STATE TRADING CORPORATION OF INDIA LTD., Books Import Division, Chandralok, 36 Janpath, *New Delhi 110001*

ITALY
EUGENIO CARLUCCI, P.O. Box 252, *70100 Bari*
INTERSCIENTIA, Via Mazzé 28, *10149 Torino*
LIBERIA COMMISSIONARIA SANSONI, Via Lamarmora 45, *50121 Firenze*
SANTO VANASIA, Via M. Macchi 58, *20124 Milano*
D. E. A., Via Lima 28, *00198 Roma*

JAPAN
KINOKUNIYA BOOK-STORE CO. LTD., 17-7 Shinjuku-ku 3 chome. Shinjuku-ku, *Tokyo 160-91*
MARUZEN COMPANY LTD., Book Department, P.O. Box 5050 Tokyo International, *Tokyo 100-61*
NAUKA LTD. IMPORT DEPARTMENT, 2-40-19 Minami Ikebukuro, Toshima-ku, *Tokyo 171*

KOREA
CHULPANMUL, *Phenjan*

NORWAY
TANUM-CAMMERMEYER, Karl Johansgatan 41—43, *1000 Oslo*

POLAND
WEGIERSKI INSTYTUT KULTURY, Marszalkowska 80, *Warszawa*
CKP I W ul. Towarowa 28 *00-958 Warszawa*

ROUMANIA
D. E. P., *Bucuresti*
ROMLIBRI, Str. Biserica Amzei 7, *Bucuresti*

SOVIET UNION
SOJUZPETCHATJ — IMPORT, *Moscow*
and the post offices in each town
MEZHDUNARODNAYA KNIGA, Moscow G-*200*

SPAIN
DIAZ DE SANTOS, Lagasca 95, *Madrid 6*

SWEDEN
ALMQVIST AND WIÓSELL, Gamla Brogatan 26, *101 20 Stockholm*
GUMPERTS UNIVERSITETSBOKHANDEL AB, Box 346, *401 25 Göteborg 1*

SWITZERLAND
KARGER LIBRI AG, Petersgraben 31, *4011 Basel*

USA
EBSCO SUBSCRIPTION SERVICES, P.O. Box 1943, *Birmingham, Alabama 35201*
F. W. FAXON COMPANY, INC., 15 Southwest Park, *Westwood, Mass. 02090*
THE MOORE-COTTRELL SUBSCRIPTION AGENCIES, *North Cohocton, N. Y. 14868*
READ-MORE PUBLICATIONS, INC., 140 Cedar Street, *New York, N. Y. 10006*
STECHERT-MACMILLAN, INC., 7250 Westfield Avenue, *Pennsauken N. J. 08110*

VIETNAM
XUNHASABA, 42, Hai Ba Trung, *Hanoi*

YUGOSLAVIA
JUGOSLAVENSKA KNJIGA, Terazije 27, *Beograd*
FORUM, Vojvode Misica 1, *21000 Novi Sad*

15. X. 1981. HU ISSN 0001-5407 Index: 26.007

ACTA CHIMICA

ACADEMIAE SCIENTIARUM HUNGARICAE

TOMUS 108 FASCICULUS 2

AKADÉMIAI KIADÓ, BUDAPEST

1981

ACTA CHIM. ACAD. SCI. HUNG. ACASA2 108 (2) 103–214 (1981)

ACTA CHIMICA

A MAGYAR TUDOMÁNYOS AKADÉMIA KÉMIAI TUDOMÁNYOK OSZTÁLYÁNAK IDEGEN NYELVŰ KÖZLEMÉNYEI

Acta Chimica is a journal for the publication of papers on all aspects of chemistry in English, German, French and Russian.

Acta Chimica is published in 3 volumes per year. Each volume consists of 4 issues of varying size

Manuscripts should be sent to

Acta Chimica
Budapest, P.O. Box 67, H-1450, Hungary

Correspondence with the editors should be sent to the same address. Manuscripts are not returned to the authors.

Hungarian subscribers should order from Akadémiai Kiadó, 1363 Budapest, P.O. Box 24. Account No. 215 11488.

Orders from other countries are to be sent to "Kultura" Foreign Trading Company (H-1389 Budapest 62, P.O. Box 149. Account No. 218 10990) or its representatives abroad.

Acta Chimica Academiae Scientiarum Hungaricae, Tomus 108 (2), pp. 103—110 (1981)

INTERACTION STUDIES IN BINARY LIQUID MIXTURES FROM VISCOSITY MEASUREMENTS

R. MISHRA

(Department of Chemistry, P.B. Degree College, Affil. Avadh University, Pratapgarth City — 230 002, U.P., India)

Received November 27, 1979

In revised form August 21, 1980

Accepted for publication October 13, 1980*

A comparison of viscosities evaluated from KATTI and CHAUDHRI's relation and from FRENKEL's relation has been made in three binary liquid mixtures with cyclohexane as a common component *viz.* cyclohexane-phenol, cyclohexane-*p*-cresol and cyclohexane-*o*-chlorophenol over a wide range of compositions at 30 °C. FRENKEL's relation underestimates the viscosity values whereas the results obtained from KATTI and CHAUDHRI's relation are in excellent agreement with the experimental values. The excess free energy of mixing, strength of interaction parameter and interaction energy term have also been computed and the interactions explained.

Introduction

Interaction studies in liquid mixtures have been a matter of sufficient interest during the last few decades [1—12]. Most of the attempts made so far give only a qualitative treatment of intermolecular interactions. However, only a few attempts [13—18] have been made to predict intermolecular interactions quantitatively. In the present communication theoretical evaluation of viscosity (η) has been made for three binary liquid mixtures; cyclohexane-phenol, cyclohexane-*p*-cresol and cyclohexane-*o*-chlorophenol (hereafter these three systems are simply stated as I, II and III, respectively) using KATTI and CHAUDHRI's relation [13 and also FRENKEL's relation [19]. Furthermore, excess free energy of mixing ($\alpha \cdot \Delta F_m$), interaction parameter (d) and interaction energy term ($W_{vis.}$) have been computed using viscosity data. In order to carry out calculations experimental measurements due to RAMAN *et al.* [20] were used. The viscosities and molar volumes were measured with an accuracy of ± 0.001 and ± 0.01, respectively. In the present investigation, the spread of experimental and calculated data is well established upto second place of the decimal as may be seen later on in the results and discussion part of this paper.

* In final form accepted March 6, 1981

Theoretical

A well-known relation [21] between the free energy of activation (ΔF^*) and energy of vaporization (ΔE) is given by.

$$\Delta F^* = \Delta E/2.45 \tag{1}$$

The actual value of the fluidity $\Phi_{m(a)}$ is expressed by the following relation due to EYRING *et al.* [21],

$$\Phi_{m(a)} = \frac{V_m}{hN} \cdot e^{\left[-\left\{\sum_{i=1}^{2} x_i \cdot \Delta E_i/2.45 - \Delta F_m/2.45\right\}/RT\right]}. \tag{2}$$

Where V_m, h, N, ΔF_m, R and T stand for molar volume of the mixture, Planck' constant, Avogadro constant, free energy of mixing, gas constant and absolute temperature, respectively. x_i and ΔE_i stand for mole fraction and energy of vaporization of component 'i' in the mixture. The fraction (1/2.45) of the free energy of mixing in the above equation is represented by the letter α and different workers [16, 22, 23] gave different values for it.

Rewriting equation (2) in terms of viscosity $\eta_{m(a)}$ of the mixture and taking logarithms on both sides one gets,

$$\ln \eta_{m(a)} + \ln \left(\frac{V_m}{hN}\right) = \sum_{i=1}^{2} x_i \cdot \Delta E_i/2.45\, RT - \alpha \cdot \Delta F_m/RT. \tag{3}$$

In the light of EYRING's equation [21] for the fluidity of ideal mixtures, the viscosity of an ideal mixture $\eta_{m(i)}$ is given by the relation,

$$\ln \eta_{m(i)} + \ln \left(\frac{V_m}{hN}\right) = \sum_{i=1}^{2} x_i \cdot \Delta E_i/2.45\, RT. \tag{4}$$

From Eqs (3) and (4) the following expression is obtained,

$$\alpha \cdot \Delta F_m = -RT[\ln \eta_{m(a)} - \ln \eta_{m(i)}]. \tag{5}$$

Thus $\alpha \cdot \Delta F_m$ can be evaluated from Eq. (5) using the viscosity data. GRÜNBERG and NISSAM [24] have given the following relation for the viscosity of non-ideal mixtures,

$$\ln \eta_{m(a)} = \sum_{i=1}^{2} x_i \ln \eta_i + x_1 \cdot x_2 d. \tag{6}$$

Where η_i stands for the viscosity of component i in the mixture. From Eqs (5) and (6), interaction parameter (d) can be obtained, thus,

$$d = -\left[\frac{1}{x_1 \cdot x_2} \cdot \frac{\alpha \cdot \Delta F_m}{RT}\right] \tag{7}$$

$\eta_{m(a)}$ from KATTI and CHAUDHRI's relation [13] is given by,

$$\ln \eta_{m(a)} \cdot V_m = \sum_{i=1}^{2} x_i \ln \eta_i V_i + x_1 x_2 \cdot W_{vis.}/RT. \tag{8}$$

Also, $\eta_{m(a)}$ from FRENKEL's relation [19] is calculated as follows,

$$\log \eta_{m(a)} = \sum_{i=1}^{2} x_i^2 \log \eta_i + 2 x_1 x_2 \log \eta_{1\,2} \tag{9}$$

$\eta_{1\,2}$ stands for the viscosity of the mixture at equimolar composition.

An inspection of Eqs (8) and (9) shows that the factor $W_{vis.}$ and $\eta_{1\,2}$ have been added, respectively, to account for the non-ideality in the mixture. Moreover, both parameters are explicitly in the respective equations. This makes possible to compare the relative merits of both the equations. A theoretical outlook shows that the advantageous feature of Eq. (8) over (9) lies in the fact that the factor $\eta_{1\,2}$ has been taken as the value of viscosity at equimolar composition of the mixture and it will be constant for that mixture at the particular temperature whereas factor $W_{vis.}$ varies with the composition of the mixture. Consequently better agreement with experimental values is expected from Eq. (8) than that from Eq. (9). However, actual state of affairs will be discussed later on in the results and discussion part of the present paper.

Assuming that Eq. (9) enables the estimation of $W_{vis.}$ from a knowledge of experimental viscosity data, following expression may also be derived from Eqs (6) and (8).

$$W_{vis.} = \frac{RT}{x_1 x_2} \ln \frac{V_m}{V_1^{x_1} \cdot V_2^{x_2}} + x_1 x_2 \cdot d. \tag{10}$$

The quantity $\Delta \log (\eta w)$ is given by,

$$[\Delta \log (\eta V)]_{exp.} = [\log (\eta_m \cdot V_m)]_{exp.} - \sum_{i=1}^{2} x_i \log \eta_i V_i \tag{11}$$

$$[\Delta \log (\eta V)]_{calcd.} = [\log (\eta_m \cdot V_m)]_{calcd.} - \sum_{i=1}^{2} x_i \log \eta_i V_i. \tag{12}$$

where η_m stands for the viscosity of the mixture and other symbols have their usual meanings. In order to make a comparison between FRENKEL's relation and KATTI and CHAUDHRI's relation, η_m values evaluated from both the relations were separately substituted in Eq. (12) and $[\Delta \log [\eta V)]_{calcd.}$ values so obtained were compared with $[\Delta \log (\eta V)]_{expt.}$ values.

Results and Discussion

Tables I and II enlist the values of viscosity η and molar volume V for pure liquids and liquid mixtures, respectively. $\Delta \log (\eta V)$ values evaluated from KATTI and CHAUDHRI's relation and from FRENKEL's relation have

Table I

Viscosity and molar volume values for pure liquids, at 30 °C

Liquid	η 10^{-3} kg m^{-1} s^{-1}	V 10^{-6} m^3 mole^{-1}
Cyclohexane	0.801	109.46
Phenol	6.944	88.31
p-Cresol	10.440	105.29
o-Chlorophenol	2.998	102.73

also been compared with experimental $\Delta \log (\eta V)$ values in Table II. Values of interaction parameter (d), excess free energy of mixing ($\alpha \cdot \Delta F_m$) and interaction energy terms (W_{vis}) are listed in Table III. An inspection of Table III (Column 3) shows that the variation of $\alpha \cdot \Delta F_m$ for all the mixtures are almost symmetrical. The positive magnitudes of $\alpha \cdot \Delta F_m$ values are largest for the system III and lowest for the system I. This observation may be rationalized in terms of the internal flexibility of cyclohexane providing more favourable accomodation to a less associated liquid within available volume in its liquid structure. Of course, phenol in system I, in comparison to *p*-cresol and *o*-chlorophenol in systems II and III, respectively, is a highly associated liquid forming larger molecular aggregates. High degree of association in phenol is due to stronger intermolecular hydrogen bonding between its molecules whereas, in case of *p*-cresol, the electron releasing substituent ($-CH_3$ group) due to its $+I$ effect reductes the extent of intermolecular hydrogen bonding by accentuating the electron density on oxygen atom in $-OH$ group and in the case of *o*-chlorophenol, intramolecular hydrogen bonding set up between the electronegative chlorine atom and hydrogen atom of $-OH$ group prevents significantly the formation of intermolecular hydrogen bonding. Obviously, from Tables II and III, it may also be observed that at equimolecular compositions, maximum positive magnitudes of $\alpha \cdot \Delta F_m$ are accompanied by the maximum negative magnitudes the quantity $\Delta \log (\eta \cdot V)$. Columns 2 and 4 of Table III show that both, the negative magnitudes of interaction parameter d and interaction energy term (W_{vis}), follow an exactly similar trend of variation with the composition.

Nigam *et al.* [16] and Ram Moorthy [17] observed that if $d > 0$ and large in magnitude, strong specific interaction is indicated. If $d > 0$ but not very large in magnitude, weak specific interactions are present. If $d < 0$ and large in magnitude, there are no specific interactions. All the systems under present study belong to non-polar weakly polar type system. An examination of Table III (Column 2) shows that the values of d are negative for all the systems, the negative magnitude being largest in system III. Also, the negative magnitude of d, in system I (except at $x_1 = 0.2824$ and 0.5905) and system II

Table II

Viscosity (η), molar volume (V) and Δ log (ηC) values for binary liquid mixtures at 30 °C

x_1	η 10^{-3} kg m^{-1} s^{-1}				V 10^{-6} m^3 mole^{-1}		$\Delta \log (\eta V)$		
	Exp.	Ideal	Calcd. by Eq. (8) (Ref. [13])	Calcd. by Eq. (9) (Ref. [19])	Exp.	Calcd.	Exp.	Calcd. by using Ref. [13]	Calcd. by using Ref. [19]
I Cyclohexane — phenol mixtures ($\eta_{12} = 1.472 \times 10^{-3}$ kg m^{-1} s^{-1})									
0.0815	5.517	5.823	5.517	5.425	89.81	90.04	−0.024	−0.023	−0.031
0.2049	3.870	4.461	3.870	3.824	92.43	92.64	−0.061	−0.060	−0.065
0.2824	3.177	3.773	3.177	3.118	93.97	94.28	−0.074	−0.073	−0.081
0.4033	2.326	2.906	2.326	2.317	96.58	96.84	−0.096	−0.094	−0.096
0.5012	1.864	2.353	1.864	1.860	99.01	98.90	−0.098	−0.099	−0.099
0.5905	1.552	1.939	1.552	1.544	100.88	100.80	−0.094	−0.094	−0.097
0.7019	1.255	1.525	1.255	1.252	103.15	103.15	−0.083	−0.083	−0.084
0.7969	1.066	1.242	1.066	1.066	105.24	105.16	−0.065	−0.065	−0.065
0.8953	0.898	1.004	0.898	0.918	107.28	107.25	−0.047	−0.048	−0.038
II Cyclohexane-*p*-cresol mixtures ($\eta_{12} = 1.752 \times 10^{-3}$ kg m^{-1} s^{-1})									
0.1014	7.352	8.047	7.352	7.343	105.69	105.71	−0.039	−0.039	−0.040
0.1683	5.440	6.777	5.440	5.889	105.75	105.99	−0.096	−0.095	−0.061
0.3021	4.004	4.806	4.004	3.890	106.57	106.55	−0.079	−0.079	−0.092
0.3949	2.988	3.787	2.988	2.980	107.30	106.94	−0.101	−0.103	−0.104
0.5007	2.250	2.886	2.250	2.247	107.40	107.38	−0.108	−0.108	−0.109
0.6007	1.732	2.233	1.732	1.756	107.73	107.80	−0.111	−0.110	−0.104
0.7004	1.350	1.728	1.350	1.401	108.64	108.21	−0.106	−0.107	−0.091
0.7973	1.110	1.348	1.110	1.147	108.96	108.62	−0.083	−0.084	−0.070
0.8999	0.909	1.035	0.909	0.946	109.24	109.04	−0.056	−0.057	−0.039
III Cyclohexane-*o*-chlorophenol mixtures ($\eta_{12} = 0.8772 \times 10^{-3}$ kg m^{-1} s^{-1})									
0.1078	2.275	2.600	2.275	2.331	103.32	103.46	−0.059	−0.058	−0.047
0.2025	1.996	2.295	1.996	1.909	104.03	104.08	−0.061	−0.060	−0.079
0.3072	1.622	1.999	1.622	1.569	104.98	104.80	−0.089	−0.091	−0.105
0.4048	1.331	1.757	1.331	1.336	105.78	105.45	−0.121	−0.120	−0.119
0.6046	1.032	1.350	1.032	1.028	107.27	106.80	−0.114	−0.116	−0.118
0.6564	0.981	1.260	0.981	0.975	107.38	107.15	−0.103	−0.109	−0.111
0.7542	0.881	1.108	0.881	0.897	108.11	107.81	−0.098	−0.099	−0.092
0.8969	0.795	0.918	0.795	0.826	109.13	108.77	−0.061	−0.062	−0.046

Table III

Values of interaction parameter (d), excess free energy of mixing ($\alpha \cdot \Delta F_m$) and interaction energy term ($W_{vis.}$) for binary liquid mixtures at 30 °C

x_1	d	$\alpha \cdot \Delta F_m$ 10^{-3} kcal mole^{-1}	W_{vis} 10^{-3} kcal mole^{-1}
		I Cyclohexane — phenol	
0.0815	−0.7210	32.51	−418.15
0.2049	−0.8720	85.52	−510.48
0.2824	−0.8486	103.53	−496.57
0.4033	−0.9248	133.99	−542.77
0.5012	−0.9315	140.20	−546.99
0.5905	−0.9212	134.11	−540.95
0.7019	−0.9299	117.14	−546.63
0.7969	−0.9427	91.86	−554.27
0.8953	−1.1892	67.12	−702.89
		II Cyclohexane-*p*-cresol	
0.1014	−0.9910	54.34	−596.29
0.1683	−1.5696	132.27	−944.33
0.3021	−0.8661	109.94	−521.06
0.3949	−0.9918	142.69	−596.55
0.5007	−0.9960	149.91	−599.21
0.6007	−1.0581	152.80	−636.49
0.7004	−1.1771	148.71	−708.35
0.7973	−1.1998	116.74	−721.94
0.8999	−1.4454	78.39	−869.56
		III Cyclohexane-*o*-chlorophenol	
0.1078	−1.3895	80.46	−835.27
0.2025	−0.8636	83.96	−519.05
0.3072	−0.9807	125.66	−589.25
0.4048	−1.1521	167.13	−692.47
0.6046	−1.1221	161.50	−674.39
0.6564	−1.1109	150.84	−667.62
0.7542	−1.2350	137.84	−742.32
0.8969	−1.5493	86.25	−931.55

(except at $x_1 = 0.1683$ and 0.3021) increases regularly with an increase in concentration of cyclohexane whereas in system III such a regular increase is not observed. This shows that any type of interaction that may be possible in these three systems is most pronounced in system I, less in system II and least in system III.

RAMAN *et al.* [20] have treated $W_{vis.}$ as a composition-independent parameter. An inspection of column 4 of Table III reveals that $W_{vis.}$ is a composition dependent parameter contrary to the observations made by them [20].

An inspection of Columns 8, 9 and 10 of Table II makes it possible to compare the relative merits of FRENKEL's relation and KATTI and CHAUDHRI's relation in terms of the quantity $\Delta \log (\eta V)$. The deviation between theoretical and experimental values using KATTI and CHAUDHRI's relation lies in the range of 0.12—7.41 per cent for system I whereas FRENKEL's relation shows the deviation of 0.46—9.19 per cent. In case of system II, the deviation shown by KATTI and CHAUDHRI's relation lies around 1.83 per cent while FRENKEL's relation shows an appreciable amount of deviation ranging from 0.83—25.68 per cent. The range of deviation shown by KATTI and CHAUDHRI's relation for system III lies around 0.41—5.43 per cent whereas FRENKEL's relation shows deviations in the range of 1.67—30.7 per cent. A comparative look over the range of deviations in the light of intermolecular interactions discussed above shows that the range of deviations shown by both the relations in case of system I is almost similar in magnitude whereas in systems II and III the magnitudes of deviations differ significantly. It concludes that in case of systems where there are appreciable amount of interactions present, both the relations are equally applicable while in the case of the systems where interactions are not well pronounced FRENKEL's relation is less accurate in the evaluation of theoretical values. This is probably due to the fact the introduction of the term η_{12} in Eq. (9) is more appropriate to account higher degree of interaction and this term should be excluded or a smaller value for η_{12} should be chosen in case of systems where there are only very weak interactions present. Choice of η_{12} at equimolecular composition for all the mixtures is not always advisable. Moreover, the advantageous feature of KATTI and CHAUDHRI's relation over FRENKEL's relation lies in the fact that $W_{vis.}$ is a composition dependent parameter which takes into account the extent of interactions.

Conclusion

On the basis of above discussions, it may be concluded that KATTI and CHAUDHRI's relation gives better agreement with the experimental values than FRENKEL's relation. Furthermore, a qualitative as well as a quantitative estimation of intermolecular interactions is possible from viscosity measurements.

However, the approach is quite unable to predict exactly the nature of interactions present in the systems under study and further work in the field is needed.

*

The author is highly thankful to Dr. R. L. MISRA for useful discussions. He is also grateful to Dr. J. D. PANDEY for his kind interest.

REFERENCES

[1] GUGGENHEIM, E. A.: Mixtures. Oxford University Press, Oxford, 1952
[2] REDDY, K. C., SUBRAHMANYAM, S. V., BHIMSENACHAR, J.: J. Phys. Soc. Japan, **19**, 559 (1964)
[3] NAIDU, P. R., KRISHNAN, V. R.: J. Phys. Soc. Japan, **20**, 1554 (1965)
[4] RASTOGI, R. P., JAGANNATH, MISHRA, J.: J. Phys. Chem., **71**, 1277 (1967)
[5] NIGAM, R. K., SINGH, P. P.: Trans Faraday Soc., **65**, 950 (1969)
[6] HYDER KHAN, V., SUBRAHMANYAM, S. V.: Trans. Faraday Soc., **67**, 2282 (1971)
[7] JAIN, D. V. S., ALSTAIR, M., PETHRICK, A.: Trans. Faraday Soc., **70**, 1293 (1974)
[8] DELMAS, G., TURRELL, S.: Trans. Faraday Soc., **70**, 572 (1974)
[9] CALADO, C. G., GERALD, A. G., STAVELY, L. A. K.: Trans. Faraday Soc., **70**, 1445 (1974)
[10] PRAKASH, S., PRASAD, N., SINGH, R., PRAKASH, O.: Acustica, **34**, 121 (1975)
[11] PANDEY, J. D., MISHRA, R. L.: Acustica, **36**, 342 (1977)
[12] PANDEY, J. D., MISHRA, R. L.: Acustica, **40**, 335 (1978)
[13] KATTI, P. K., CHAUDHRI, M. M.: J. Chem. and Engineering Data, **9**, 1442 (1964)
[14] KATTI, P. K., CHAUDHRI, M. M., PRAKASH, O.: J. Chem. and Engineering Data, **11**, 593 (1966)
[15] NIGAM, R. K., MAHL, B. S.: Ind. J. Chem., **9**, 1225 (1971)
[16] NIGAM, R. K., DHILLON, M. S.: Ind. J. Chem., **8**, 1260 (1971)
[17] RAM MOORTHY, K.: Ind. J. Pure and Appl. Physics, **11**, 554 (1973)
[18] MISHRA, R. L., PANDEY, J. D.: Ind. J. Pure and Appl. Physics, **15**, 870 (1977)
[19] FRENKEL: Petroleum (London), **9**, 27 (1946)
[20] RAMAN, F. K., NAIDU, P. R., KRISHNAN, V. R.: Aust. J. Chem., **21**, 2717 (1968)
[21] GLASSTONE, S., LAIDLER, K. J., EYRING, H.: The theory of rate processes. McGraw-Hill, New York, 1941
[22] ROOSEVEARE, W. E., POWELL, R. E., EYRING, H.: J. Appl. Phys. **12**, 324 (1968)
[23] KRISHNA, M. R. V., LADHA, G. S.: Ind. Eng. Chem., **7**, 324 (1968)
[24] GRÜNBERG, L., NISSAN, A. H.: Nature, Lond., **164**, 799 (1949)

Ramacharya MISHRA
Department of Chemistry,
P.B. Degree College (Affil. Avadh University),
Pratapgarth City — 230 002, U.P., India

Acta Chimica Academiae Scientiarum Hungaricae, Tomus 108 (2), pp. 111—124 (1981)

MECHANICAL-RHEOLOGICAL STUDIES ON POLYMER NETWORKS, II

EFFECT OF MOLECULAR MASS AND MOLECULAR MASS DISTRIBUTION OF THE STARTING POLYMER ON THE MECHANICAL PROPERTIES

F. HORKAY[1] and M. NAGY[2]

([1]*National Institute of Occupational Health, Budapest,*
[2]*Department of Colloid Science, Eötvös Loránd University, Budapest*)

Received October 1, 1980

Accepted for publication November 11, 1980

Mechanical investigations (unidirectional compression) were carried out on poly(vinyl alcohol) hydrogels prepared from polymers of different relative molecular mass and relative molecular mass distribution.

In accordance with earlier experimental results, it was found that $K_1 \nu_{el}^* q_0^{-2/3}$ considerably increases with increasing volume fraction of the polymer and that the value of the topological factor, $K_1 q_0^{-2/3}$, is independent of the degree of cross-linking also in the case when polymers of different molecular mass and molecular mass distribution are used.

It has been established that the efficiency of network formation increases with increasing relative molecular mass of the primary polymer chains.

It has been concluded that in the reference state of the gel chain dimensions can be fairly well approximated by relationships valid for dilute polymer solutions.

Moreover, investigations showed that the mechanical properties of the gels are decisively determined by the quantity of the elastically active network chains while the role of pendant chains — at least in the case of unidirectional compression — can be neglected.

Introduction

In the first part of this series the effect of a few fundamental parameters characteristic of networks, such as the concentration of the initial polymer solution, the medium of cross-linking, the chemical nature of the cross-linking agent and the degree of cross-linking on the mechanical properties of chemically cross-linked poly(vinyl alcohol) hydrogels has been discussed.

The present communication deals with the effect of the relative molecular mass and the relative molecular mass distribution of the starting polymer on the mechanical characteristics of the gels determined macroscopically.

Theoretical

On the basis of the statistical thermodynamic theory of rubber elasticity, the change of Helmholtz energy in the case of unidirectional deformation of homogeneous, isotropic, swollen networks can be written in the following

form [1, 2]:

$$\Delta A_{el} - \Delta A_{el}^{i} = \frac{kTK_1 \nu_{el}}{2} \left(\frac{q_i}{q_0}\right)^{2/3} \left[\Lambda_x^2 + 2\frac{V}{V_i}\Lambda_x^{-2} - 3\right] - kTK_2 \ln \frac{V}{V_i} \qquad (1)$$

where K_1 and K_2 are constants, ν_{el} is the number of elastically active network chains in the system, V_i the volume of the isotropic, undeformed network, q_i its volume degree of swelling, V the volume of the deformed network, and q_0 the so-called reference degree of swelling. Λ_x means the ratio of deformation in the direction of force (if L_{Vx} is the length of the undeformed and L_x that of the deformed sample measured in the direction of the x-axis, then $\Lambda_x = L_x/L_{Vx}$), k is Boltzmann's constant and T the temperature.

If the volume is not changed by deformation, Eq. (1) gives for the force (f) the following relationship:

$$f = \left(\frac{\partial(\Delta A_{el} - \Delta A_{el}^{i})}{\partial L_x}\right)_{T,V} = \frac{RT K_1 \nu_{el}^{*} V_d}{L_{Vx}} \left(\frac{q_i}{q_0}\right)^{2/3} (\Lambda_x - \Lambda_x^{-2}). \qquad (2)$$

Here, ν_{el}^{*} is the concentration of the elastically active network chains in the dry network, and V_d is the volume of the dry gel.

The value of K_1 in the equations is determined mainly by the steric structure of the gel. According to the WALL—FLORY—HERMANS theory, generally accepted today, for ideal networks $K_1 = 1$. Several authors relate K_1 to the number of network chains starting from one junction point (functionality, $\bar{f}$). According to the calculations of DUISER, STAVERMAN and GRAESSLEY [3, 4]:

$$K_1 = \frac{\bar{f} - 2}{\bar{f}}.$$

In the case of cross-linking in the polymer solution by taking into consideration of the network defects only the pendant chains, the so-called terminal chains, the value of ν_{el}^{*} can be calculated from the relationship [5]:

$$\nu_{el}^{*} = \nu^{*}\left(1 - \frac{2d_2}{\overline{M}_n \nu^{*}}\right) = \nu^{*}\left(1 - \frac{2\overline{M}_c}{\overline{M}_n}\right). \qquad (3)$$

In Eq. (3) ν^{*} is the number of moles of network chains per unit dry volume of the gel, d_2 the density of the polymer, $\overline{M}_n$ is the molecular mass of the polymer in the starting solution, $\overline{M}_c$ the average relative molecular mass of the network chains. The theoretical calculation of other network defects (entanglements, intramolecular cyclization, unreacted functionalities, *etc.*) can not be regarded as solved, they depend strongly on the individual properties of the given system.

The estimation of the parameter q_0 causes further difficulties. According to theoretical considerations,

$$q_0^{2/3} = \frac{\langle r^2 \rangle_{os}}{\langle r^2 \rangle_d}$$

where $\langle r^2 \rangle_{os}$ is the mean square end-to-end distance of the network chains in the so-called reference state of the swollen network, while $\langle r^2 \rangle_d$ is the mean square end-to-end distance of the network chains in the dry state. The reference state is that state of the network in which the network chains do not exert any force on the junction points.

The reference degree of swelling, q_0, is also called the memory parameter, because on the basis of the relationship

$$q_0^{2/3} = \frac{\langle r^2 \rangle_{os}}{\langle r^2 \rangle_d} = \frac{\langle r^2 \rangle_{os}}{\langle r^2 \rangle_c} \frac{\langle r^2 \rangle_c}{\langle r^2 \rangle_d} = \frac{\langle r^2 \rangle_{os}}{\langle r^2 \rangle_c} q_c^{2/3} \tag{4}$$

it is correlated with q_c, *i.e.* that volume degree of swelling, at which gel preparation occured [2]. In Eq. (4) $\langle r^2 \rangle_c$ is the mean square end-to-end distance of the network chains after cross-linking at the volume of gel formation. If we assume that the chains are of equilibrium conformation in the initial polymer solution, further that in the case of cross-linking at constant volume in the same solvent, chain dimensions do not change (*i.e.* $\langle r^2 \rangle_{os} = \langle r^2 \rangle_c$), then $q_0 = q_c$. However, this approximation is arbitrary, because the formation of the cross-links may be accompanied by a strong deformation of the chains.

It follows even from this brief survey that experimentally only the value of product $K_1 \nu_{el}^* q_0^{-2/3}$ can be determined unambiguously by using Eq. (2). To obtain information on the molecular quantities characteristic of gels, further assumptions must be made, which take into consideration also the properties of the real system investigated.

Experimental

Materials and methods

For our investigations Kuraray Poval 420 (Japan) poly(vinyl alcohol) (PVA) was used. The acetate content of the product was hydrolyzed in methanol — water mixture with an excess of NaOH, then fractionated with *n*-propanol (Reanal, anal. grade). Four fractions were prepared in this way, and the parts of low and high relative molecular mass were then separated, similarly with *n*-propanol, from these solutions. Samples of medium relative molecular mass (marked fraction II, III, IV and V) were used for further investigations. Fraction I was prepared in a similar way from Mowiol 4—88 (Hoechst, GFR).

The characteristics of the fractions were determined by viscosimetry at 303 ± 0.1 K. Intrinsic viscosities were determined from the axial sections of the $\frac{\eta_{sp}}{c}$ *vs.* c functions, extrapolated to $c = 0$. In the measurements, the concentration of the PVA solutions was varied between 0.2 and 0.9 g/100 cm³. The relative average molecular mass of the single fractions was calculated through the relationship [6]

$$[\eta]_{303} = 4.28 \times 10^{-4} \overline{M}_w^{0.64}$$

Table I

Intrinsic viscosity and relative molecular mass of PVA fractions

Symbol of fraction	$[\eta]_{303}$ (100 $cm^3 \times g^{-1}$)	$\overline{M}_w$
I	0.26	22 300
II	0.45	52 600
III	0.70	102 700
IV	0.84	139 600
V	1.50	345 500

Table II

Relative molecular mass of polydisperse systems

Symbol of system	$\overline{M}_w$	$\overline{M}_n$	$PF = \frac{\overline{M}_w}{\overline{M}_n} - 1$
PD 1	95 400	60 000	0.59
PD 2	199 000	91 300	1.18
PD 3	302 700	190 600	0.59
PD I	69 500	25 800	1.69
PD II	184 000	41 900	3.39
PD III	298 300	110 900	1.69

(Table I). According to our earlier results [7], the fractionation process used by us gives a relative molecular mass distribution, which can be considered as rather narrow. The depedence of the mechanical properties of the gels on the relative molecular mass and on the molecular mass distribution of the primary polymer chains has been studied. Polydisperse systems were prepared by the mixing of the fractions.

Three mixtures were prepared from fractions I and V, and three from fractions II and V; in both cases the degree of polydispersity $\left(PF = \frac{\overline{M}_w}{\overline{M}_n} - 1\right)$ of one of the mixtures was maximal (marked with PD II and PD 2), while that of the other two mixtures $PF = \frac{PF_{max}}{2}$ (marked PD I, PD III and PD 1, PD 3). Gels marked with PD I, PD II, PD III were prepared from the mixtures of fractions I and V, those marked with PD 1, PD 2 and PD 3 from mixtures of fractions II and V. The relative molecular masses of the mixtures marked with PD are contained in Table II. Our investigations were carried out on gels of various degree of cross-linking (dc: 50,100, 200 and 400), cross-linked at 9.0 wt.% polymer concentration with glutaric aldehyde (GDA). The degree of cross-linking is the molar ratio of the monomer and the cross-linking agent.

Gels were prepared from the PVA solution at 298 $\pm$ 0.1 K, in special dismountable frames, suitable for the preparation of cylindrical specimens.

For mechanical investigations the apparatus of our own design described earlier has been used, which is suitable for the high-precision determination of force-deformation functions in unidirectional compression [8].

The degree of swelling of the gels was changed by the equilibrium swelling-degree decreasing method developed by us (modified deswelling technique) [9].

All the investigations were carried out at 298 $\pm$ 0.1 K.

All the measurement points were calculated from the arithmetic mean of at least three measurements. Reproducibility generally was within 5 rel. %.

Results and Discussion

Mechanical measurements were evaluated on the basis of the phenomenologically deductible, completely generalized MOONEY—RIVLIN equation [10, 11]. From this, the following relationship can be derived for force in the case of unidirectional stretching or compression:

$$f = 2C_1(\Lambda_x - \Lambda_x^{-2}) + 2C_2(1 - \Lambda_x^{-3}). \tag{5}$$

In Eq. (5) C_1 and C_2 are constants, their values depend only on molecular parameters characteristic of the structure of the network and on temperature. For ideal networks $2C_1$ is equal to the term $\frac{K_1 \nu_{el}^* RT V_d}{L_{Vx}} \left(\frac{q_i}{q_0}\right)^{2/3}$ of Eq. (2), while C_2 is zero.

In accordance with our earlier investigations in similar systems, it was found that for all the gels $C_2 = 0$, within the limits of experimental error [12].

Information on the effect of the relative molecular mass of the primary polymer chains on network formation can be obtained if the average change in the value of $2C_1$ caused by unit quantity of the cross-linking agent is investigated as a function of the molecular mass of the polymer (Fig. 1). The value of c_{GDA} in the figure was calculated by subtracting from the total quantity of the cross-linking agent introduced into the system the quantity needed for the cross-linking of independent chains, because this quantity, depending on the relative molecular mass of the macromolecules in the starting polymer, does not take part in the formation of elastically active network chains. It can be established that the efficiency of cross-linking process increases with increasing relative molecular mass of the polymer. Presumably, this is due to reasons of solution structure. Since PVA is a polymer with a tendency for crystallization, and according to experiences in conjunction with our samples this tendency for crystallization decreases with increasing molecular mass,

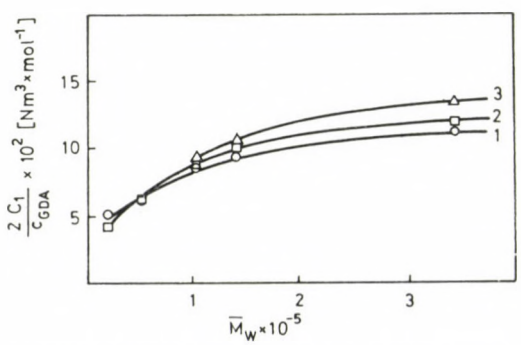

Fig. 1. Variation of $2C_1/c_{GDA}$ with the relative molecular mass of the polymer; dc: (1) 100; (2) 200; (3) 400

presumably the segment distribution is less homogeneous in polymer solutions of lower relative molecular mass. One part of the cross-linking agent added to systems containing such associations fixes the structure already formed in the solution. Moreover, it can be established that the extent of change decreases with increasing molecular mass. When using polymers of sufficiently large molecular mass, it can be assumed that the efficiency of network formation becomes independent of the molecular mass of the polymer.

From the value of $2C_1$ the product $K_1 v_{el}^* q_0^{-2/3}$ in Eq. (2) can be calculated, containing the molecular parameters characteristic of the gel, which are independent of the degree of swelling. It became apparent already from earlier investigations that for PVA gels, contrary to theory, $K_1 v_{el}^* q_0^{-2/3}$ is not constant,

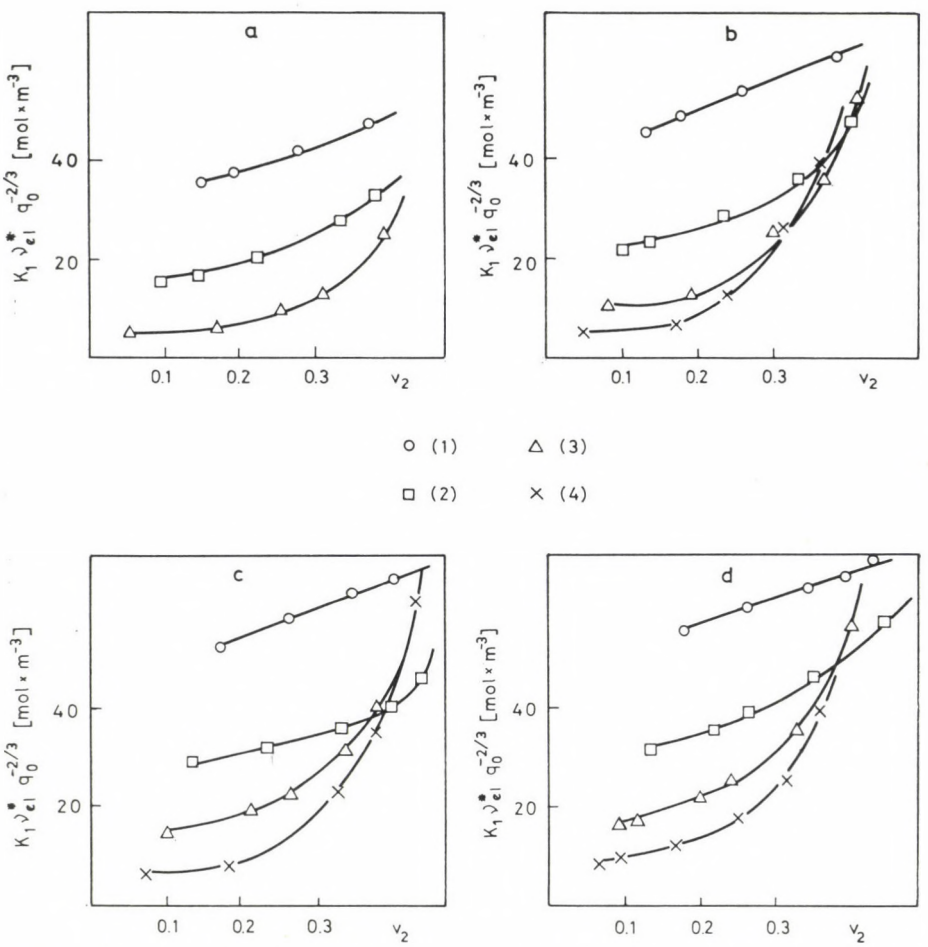

Fig. 2. $K_1 v_{el}^* q_0^{-2/3}$ *vs.* v_2 functions for PVA gels; a) fraction II; b) fraction III; c) fraction IV; d) fraction V; dc: (1) 50; (2) 100; (3) 200; (4) 400

but increases with increasing volume fraction of the polymer ($v_2 = q_i^{-1}$); first to a small extent, then above volume fractions of 0.3—0.4 very steeply [12]. The same phenomenon was observed also in systems prepared from polymers of different relative molecular mass or different relative molecular mass distribution (Figs 2 and 3). Moreover, it can be established from Fig. 3d that at the same degree of cross-linking the course of the $K_1 \nu_{el}^* q_0^{-2/3}$ *vs.* v_2 functions is generally less steep for polydisperse systems.

To eliminate intermolecular interactions, increasing with decreasing degree of swelling, the product $K_1 \nu_{el}^* q_0^{-2/3}$, characteristic of the gel, has been determined by the process used earlier, from the value of the function extrapolated to infinite degree of swelling (Table III).

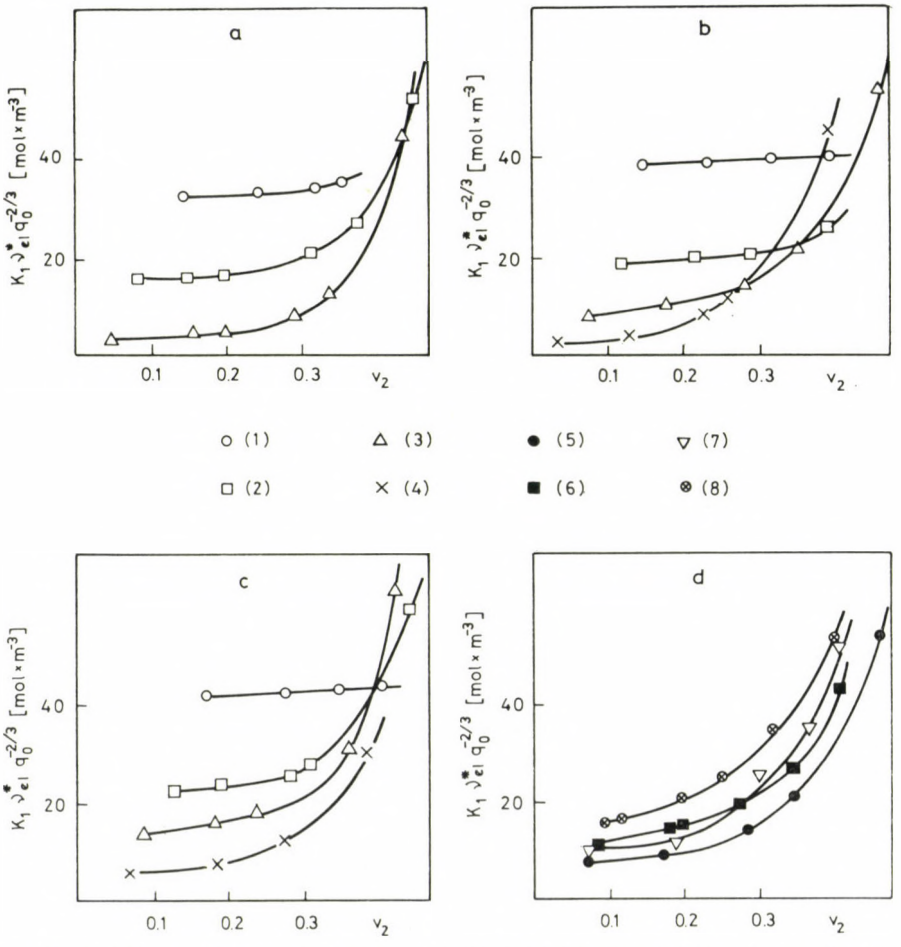

Fig. 3. $K_1 \nu_{el}^* q_0^{-2/3}$ *vs.* v_2 functions for PVA gels a) PD I; b) PD II; c) PD III; dc: (1) 50; (2) 100; (3) 200; (4) 400; d) dc: 200; (5) PD II; (6) PD 2; (7) fraction III; (8) fraction V

Table III

$K_1 \nu_{el}^* q_0^{-2/3}$ ($v_2 \to 0$) values of PVA gels

Symbol of system	$K_1 \nu_{el}^* q_0^{-2/3}$ (mol × m^{-3})			
	Degree of cross-linking			
	50	100	200	400
I	26.5	10.0	2.5	—
II	32.0	13.5	5.5	—
III	37.0	19.7	9.0	4.0
IV	42.5	22.0	11.0	5.0
V	47.5	25.5	12.5	6.5
PD 1	38.0	16.0	7.0	—
PD 2	41.5	20.5	8.5	4.0
PD 3	45.5	23.0	12.5	6.0
PD I	32.9	14.5	4.0	—
PD II	37.0	17.0	7.0	2.5
PD III	41.0	22.0	12.0	5.0

Plotting the $K_1 \nu_{el}^* q_0^{-2/3}$ values as a function of the quantity of the elastically active network chains (ν_{el}^*) contained in unit volume of the dry network, information is obtained on the topological factor $K_1 q_0^{-2/3}$ (Figs 4, 5; Table IV). It can be established from the figures that the larger the relative molecular mass of the primary polymer, the higher is the value of the topological factor. This can be easily seen from Fig. 5, where, in spite of the differences in $\left(\frac{\bar{M}_w}{\bar{M}_n} - 1\right)$ the order PD I < PD II < PD III is valid. It becomes also evident from the

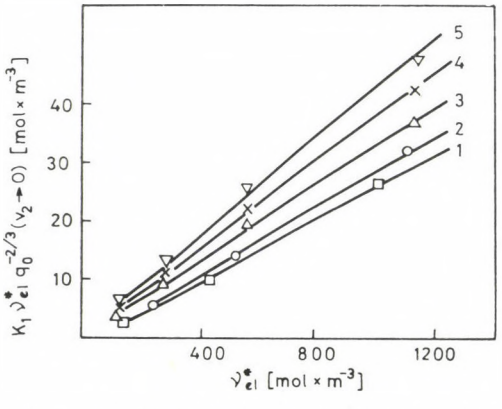

Fig. 4. Determination of the value of $K_1 q_0^{-2/3}$ (topological factor). (1) fraction I; (2) fraction II; (3) fraction III; (4) fraction IV; (5) fraction V

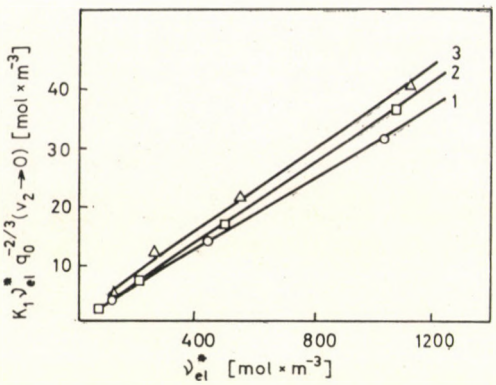

Fig. 5. Determination of the value of $K_1 q_0^{-2/3}$ (topological factor). (1) PD I; (2) PD II; (3) PD III

figures that in accordance with our earlier observations $K_1 q_0^{-2/3}$ is independent of the degree of cross-linking [12]. In Table IV the values obtained for the K_1 and q_0 parameters at different conditions are summarized. It can be seen that in each case both K_1 and q_0 differ considerably from values expected on the basis of theory.

In view of the fact that both ν^*_{el} and $q_0^{-2/3}$ are functions of the relative molecular mass ($\overline{M}_c$) of the network chains, it seemed worth to investigate the change of the product $K_1 \nu^*_{el} q_0^{-2/3}$ with $\overline{M}_c$ (Figs 6, 7). It can be established from the figures that the functions log $K_1 \nu^*_{el} q_0^{-2/3}$ *vs.* log $\overline{M}_c$ are, for all the systems, straight lines with negative slopes. The slopes (m) of the straight lines vary between -1.0 and -1.2.

Table IV

K_1 and q_0 values of PVA gels

Symbol of system	$K_1 q_0^{-2/3}$	K_1 ($q_0 = q_c$)	q_0 ($K_1 = 1$)	q_0 ($K_1 = 0.5$)
I	0.028	0.161	213.4	75.5
II	0.030	0.173	192.5	68.0
III	0.033	0.190	166.8	58.9
IV	0.038	0.219	135.0	47.7
V	0.043	0.248	112.1	39.7
PD 1	0.034	0.196	159.5	56.4
PD 2	0.037	0.214	140.5	49.7
PD 3	0.040	0.230	125.0	44.2
PD I	0.031	0.179	183.2	64.8
PD II	0.034	0.196	159.5	56.4
PD III	0.036	0.207	146.4	51.8

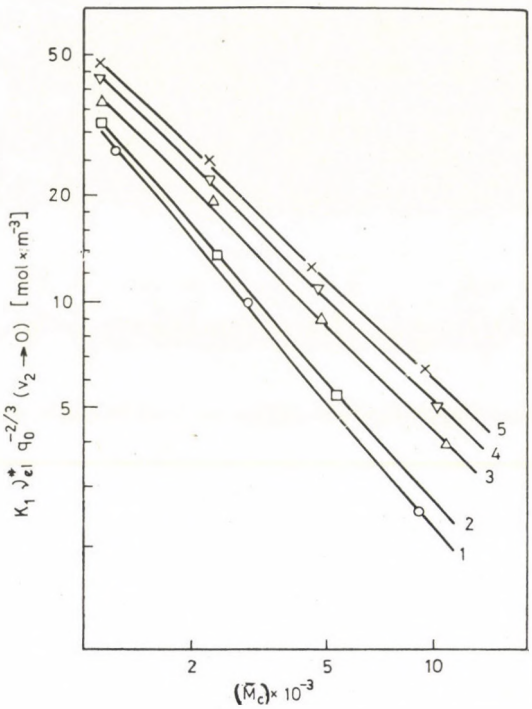

Fig. 6. log $K_1 \nu_{el}^* q_0^{-2/3}$ *vs.* log $\overline{M}_c$ functions. (1) fraction I; (2) fraction II; (3) fraction III; (4) fraction IV; (5) fraction V

Under certain arbitrary assumptions, the value of m can be calculated also theoretically. The fact that very high q_0 values have been obtained for the systems investigated indicates that the reference state of the gels lies in the region of dilute solution. In this range, using the FLORY—FOX and the KUHN—MARK—HOUWINK equations, chain dimensions in the reference state can be expressed in a simple form [13, 14, 15]:

$$KM^a = \Phi \frac{\alpha^3 \langle r^2 \rangle_{os}^{3/2}}{M} \tag{6}$$

where K and a are constants of the KUHN—MARK—HOUWINK equation, α is the expansion factor and Φ is FLORY's constant.

On the other hand, $\langle r^2 \rangle_d$ can be calculated on the basis of purely geometrical considerations if the quantity of the cross-linking agent added to the system is known:

$$\langle r^2 \rangle_d = \left[\frac{2 \overline{M}_c}{N_A d_2} \right]^{2/3}, \tag{7}$$

where N_A is the Avogadro number.

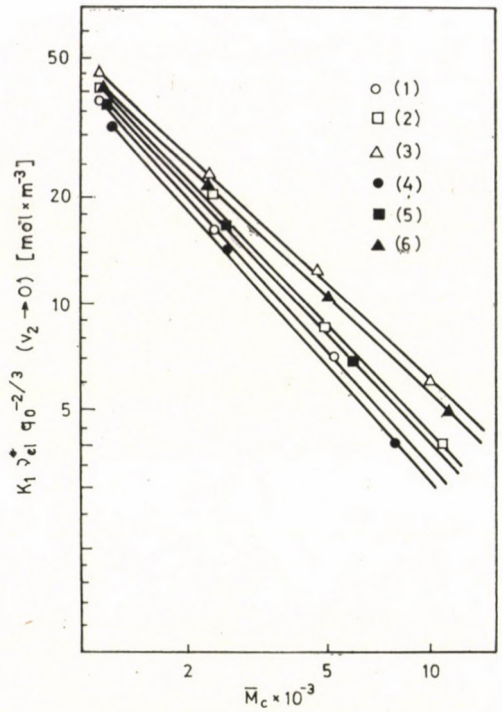

Fig. 7. log $K_1 \nu^*_{el} q_0^{-2/3}$ *vs.* log $\bar{M}_c$ functions. (1) PD 1; (2) PD 2; (3) PD 3; (4) PD I; (5) PD II; (6) PD III

From Eqs (6) and (7) we obtain:

$$q_0^{-2/3} = \frac{\langle r^2 \rangle_d}{\langle r^2 \rangle_{os}} = \left(\frac{2 \Phi \alpha^3}{N_A d_2 K} \right)^{2/3} \bar{M}_c^{-(2/3)a}.$$

In consideration of the facts that for PVA solutions α increases exponentially with the 0.1th power of the relative molecular mass [7], and that for ideal networks $\nu^*_{el} = \dfrac{d_2}{\bar{M}_c}$, the product $K_1 \nu^*_{el} q_0^{-2/3}$ can be written in the form $C \bar{M}_c^{-1.23}$.

Though the calculated exponent differs from those determined experimentally, this is indeed not suprising in view of the simplifying assumptions made (use of relationships relevant to solutions of infinite dilution, calculation of $\bar{M}_c$ on the basis of the chemical reaction, disregarding network defects, *etc.*).

It should be emphasized that there is no substantial difference between the functions for gels prepared from fractionated and from polydisperse polymer samples, which indicates in accordance with experimental results already mentioned that the mechanical properties of networks are determined primarily by the quantity of the elastically active network chains contained in unit

volume. Thus, in the case of unidirectional compression terminal chains (pendant chains) do not substantially contribute to the elastic work needed for the production of deformation.

It can be said on the basis of Figs 6 and 7, and the relatively small difference between the calculated and the experimental m values, that in the systems investigated the chain dimensions in the reference state — at least as concerns the character of their dependence on $\overline{M}_c$ — can be fairly well approximated with relationships relevant to dilute polymer solutions.

For the further investigation of the properties of gels the so-called scaling concept offers a possibility [16]. According to a scaling law, the elastic modulus (E) and the polymer concentration of the gel in swelling equilibrium (c_e) are in the following relationship with one another:

$$E \propto c_e^{2.25}$$

where $E = RTK_1 v_{el}^* q_0^{-2/3} q_i^{-1/3}$.

The E and c_e values of the PVA gels are contained in Table V. In the case of logarithmic plotting, points belonging together lie in good approximation along the same straight line (Fig. 8). The slope of the straight line, 2.1, is close to the theoretical value, which is particularly noteworthy in consideration of the substantial deviation of the PVA networks from the ideal model system.

Table V

c_e and E values of PVA gels

Degree of cross-linking	Symbol of fractions									
	I		II		III		IV		V	
	c_e (g cm^{-3})	$E\times10^{-4}$ (N m^{-2})	c_e (g cm^{-3})	$E\times10^{-4}$ (N m^{-2})	c_e (g cm^{-3})	$E\times10^{-4}$ (N m^{-2})	c_e (g cm^{-3})	$E\times10^{-4}$ (N m^{-2})	c_e (g cm^{-3})	$E\times10^{-4}$ (N m^{-2})
50	0.146	3.25	0.162	4.12	0.171	5.34	0.178	6.18	0.182	6.74
100	0.088	1.02	0.099	1.38	0.114	2.44	0.125	2.89	0.137	3.30
200	0.038	0.19	0.057	0.49	0.074	0.91	0.089	1.22	0.093	1.45
400	—	—	—	—	0.048	0.42	0.056	0.52	0.058	0.62

It also becomes apparent from the figure that within the limits of experimental error the exponent is independent of the quantity of terminal chains contained in the system.

This finding is in contradiction with recent experimental results obtained for poly(dimethylsiloxane) and polystyrene gels, according to which the exponent increases considerably with increasing ratio of pendant chains [17, 18].

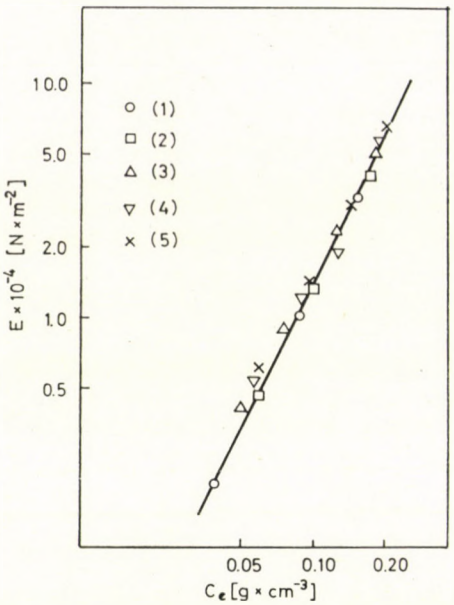

Fig. 8. log E *vs.* log c_e functions for PVA gels; symbols of the fractions: (1) I; (2) II; (3) III; (4) IV; (5) V

To elucidate the nature of several anomalies attributed to crystallization, investigations are carried out on systems of similar steric structure that of the PVA gels studied, where the possibility of crystallization is a priori excluded by the chemical nature of the polymer chains.

*

We wish to thank Dr. János KABAI for support of this work and for reading of the manuscript.

Thanks are due to Mrs. Miklós HERCZEG for her careful experimental work.

REFERENCES

[1] WALL, F. T.: J. Chem. Phys., **10,** 485 (1942)
[2] DUŠEK, K., PRINS, W.: Fortschr. Hochpolym. Forschung, **6,** 1 (1969)
[3] DUISER, J. A., STAVERMAN, A. J.: Physics of Noncrystalline Solids. J. A. PRINS, Ed., North-Holland, 1965
[4] GRAESSLEY, W. W.: Macromolecules, **8,** 186 (1975)
[5] FLORY, P. J.: Principles of Polymer Chemistry. Cornell University Press, Ithaca, New York, 1953
[6] MATSUMOTO, M., OHYANAGI, Y.: Kobunshi Kagaku, **17,** 17 (1960)
[7] NAGY, M.: Kém. Közlemények, **29,** 1 (1968)
[8] HORKAY, F., NAGY, M., ZRINYI, M.: Magy. Kém. Folyóirat, **85,** 513 (1979)
[9] NAGY, M., HORKAY, F.: Acta Chim. Acad. Sci. Hung., **104,** 49 (1980)

[10] MOONEY, M.: J. Appl. Phys., **11,** 582 (1940)
[11] RIVLIN, R. S.: Phil. Trans. Roy. Soc. London, **A240,** 491 (1948)
[12] HORKAY, F., NAGY, M.: Acta Chim. Acad. Sci. Hung., (In press)
[13] FLORY, P. J., FOX, T. G.: J. Polym. Sci., **5,** 745 (1950)
[14] FLORY, P. J., FOX, T. G.: J. Am. Chem. Soc., **73,** 1904 (1951)
[15] BELKEBIR-MRANI, A., HERZ, J. E., REMPP, P.: Macromol. Chem., **178,** 485 (1977)
[16] DAOUD, M., COTTON, J. P., FARNOUX, B., JANNINK, G., SARMA, G., BENOIT, H., DUPLESSIX, R., PICOT, C., de GENNES, P. G.: Macromolecules, **8,** 804 (1975)
[17] MUNCH, J. P., LEMARECHAL, P., CANDAU, S.: J. Phys., Paris, **38,** 1499 (1977)
[18] BASTIDE, J., PICOT, C., CANDAU, S.: J. Polym. Sci., Polym. Phys. Ed., **17,** 1441 (1979)

Ferenc HORKAY H-1096 Budapest, Nagyvárad tér 2.
Miklós NAGY H-1088 Budapest, Puskin u. 11—13.

Acta Chimica Academiae Scientiarum Hungaricae, Tomus 108 (2), pp. 125—133 (1981)

BIPOTENTIOSTAT USED IN THE ROTATING RING DISC ELECTRODE METHOD OF INVESTIGATION

J. FARKAS,[1] L. DOBOS,[2] P. KOVÁCS[1] and L. KISS[1]

([1]*Department of Physical Chemistry and Radiology, Eötvös Loránd University, Budapest,*
[2]*Department of General and Physical Chemistry József Attila University, Szeged*)

Received June 23, 1980

Accepted for publication November 11, 1980

A bipotentiostatic measuring system has been developed for electrochemical kinetic investigations in systems featuring two working electrodes, as *e.g.* the rotating ring disc electrode. The measuring method is described, and the application of the technique is illustrated on hand of a few dynamic measurements.

The rotating ring disc electrode became a widely used tool of investigation in the last decade [1, 2]. Essentially, the soluble intermediates and end products formed at the disc electrode used as working electrode are transported by the well defined convective diffusion to the vicinity of the ring electrode used as an indicator electrode, where they can be detected and determined by a suitably selected method [3, 4, 5]. For example, current-free potential [4] or limiting current [1, 2, 3, 6] can be measured at the appropriately selected indicator electrode, with an instrument park analogous to that of the electrochemical measuring technique used at the working electrode. Measuring technical possibilities and demands may arise, which would require the application of potentiostatic or potentiodynamic measuring techniques at both the disc and the ring electrodes. In this case, using the symbols of the equivalent electric circuit shown in Fig. 1, the potential differences of the electrodes W2-R and W1-R ought to be kept independently of one another at controlled and generally different constant values even if impedances Z_1—Z_4 do change. This task is performed by the bipotentiostats [7, 8].

The block scheme of a bipotentiostat performing such task is shown in Fig. 2. (The marking of electrode connections is the same as in Fig. 1.)

It follows already from the most simple equivalent scheme of electrode impedance shown in Fig. 1 that the current flowing through the two working electrodes (W1, W2) can not be separately measured in the circuit of the counter electrode (A) (where the algebraic sum of the two currents is flowing). Thus, current measuring systems have been located in the circuits of the working electrodes, with the consequence that *none of the electrodes can be connected to zero point.*

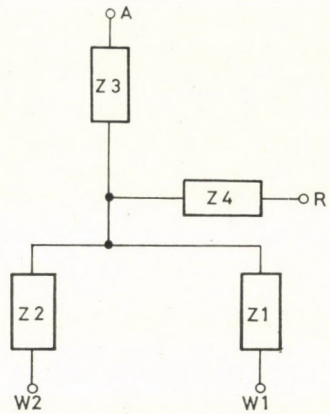

Fig. 1. Electric equivalent of an electrolysis cell with two working electrodes; Z1, Z2, Z3, Z4 — electrode impedances; W1, W2 — working electrodes; R — reference electrode; A — counter electrode

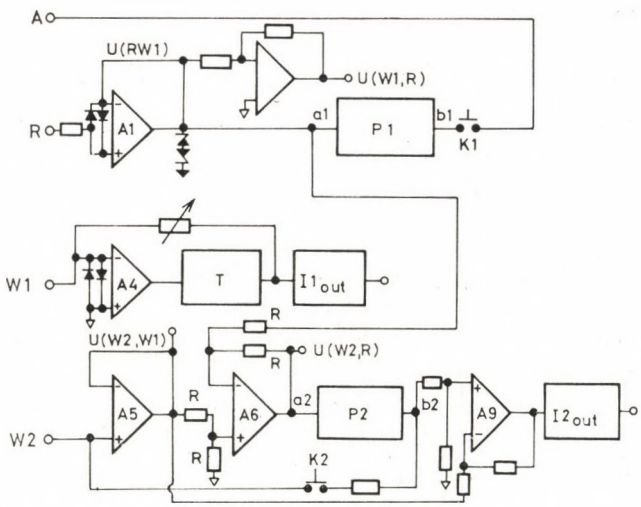

Fig. 2. Block scheme of the bipotentiostat. The marking of the electrode connections is the same as in Fig. 1. For further symbols see text and Figs 3, 4

The unit consisting of A4 (protected) operational amplifier, T power amplifier (feedback to the input; gain = 1) and of the display system $I1_{out}$ serves for the measurement of the current flowing through working electrode W1.

The potential of the working electrode W1 is in this arrangement at quasi earth potential, because the operating voltage established between the inputs of A4 feedback operational amplifier is only of an order of magnitude of 10 μV.

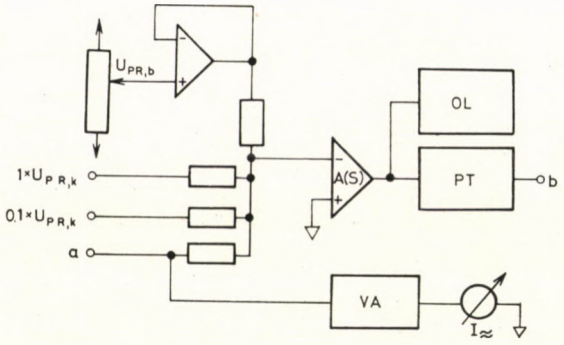

Fig. 3. Schematic diagram of the unit marked in Fig. 2. with P (1)2. $U_{PR,b}$: generation of internal program voltage; $U_{PR,k}$: connections of the external program voltage, A(S) — summation amplifier, OL — overload indicators, PT — power amplifier, VA — high-frequency amplifier, $I_{\approx}$ — high-frequency indicator

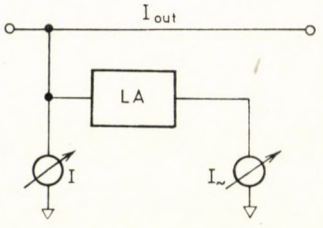

Fig. 4. Circuit diagram of current outputs (I_{out}). I_{out} — direct current output, I — built-in amperometer, LA — low-frequency amplifier, $I_{\sim}$ — low-frequency noise indicator

The circuit built up from units A5, A6, A9, P2 and $I2_{out}$ serves for the measurement of the current flowing through the working electrode W2. The potential difference between the W2-R electrodes can be measured at the output of the operational amplifier A6.

The circuit supplying the electrolyzing current (and power) is the part built up from units A1, P1. The switch K1 switches off the electrolyzing cell from the bipotentiostat. Using an inverter, the potential difference between electrodes W1-R can be measured at the output of the operational amplifier A1.

In open position of switch K2, shown in Fig. 2, a galvanostatic mode of operation can be established over the electrode system W2-A-R.

Units marked in Fig. 2 with P1 (2) generate the external and built-in program voltages (Fig. 3), and comprise the high-frequency noise indicator (VA), the overload indicator (OL) and a power amplifier (PT).

The outputs I1 $(2)_{out}$ (Fig. 4) contain also the noise indicators connected after the low-frequency amplifiers of the bipotentiostat.

It can be seen from the circuit diagrams of Figs 2, 3 and 4 that the output signals proportional to the values of the parameters to be measured (potential differences, current strengths) are ***voltage outputs***, having at the

same time a low output impedance. This feature permits to connect to each output recorders of display systems selected from a wide field.*

After the description of the block diagram and the principle of operation of the bipotentiostat, its application in investigations with the rotating ring disc electrode will be discussed. Without claim for completeness, a circuit diagram will be described, with the aid of which many methods in investigation can be elaborated (Fig. 5). Naturally, by changing the arrangement, several kinds of measurements can be realized.

In the following, the usability of the measuring apparatus will be described on hand of experimental results obtained in the anodic dissolution of copper.

The disc of the rotating ring disc electrode is made of copper, its ring from platinum. Teflon rings are used for their insulation. Electric connection is provided by carbon brushes through bronze rings located at the exchangeable electrode stems.

The electrode is rotated by an asynchronous motor of stable speed of rotation. A V-belt gear provides for changeable connection between the motor and the electrode disc. For the rapid checking of actual speed of rotation a manual tachometer is used. Exact values are established by a measuring equipment, operation on the basis of the circuit diagram shown in Fig. 6.

The essence of the measuring principle is that infrared light, emitted by the photodiode is reflected from a narrow, marked part of the electrode disc. The reflected signal is converted by a photosensor into an electric signal. This signal is fed after amplification and uniformization to the input of a

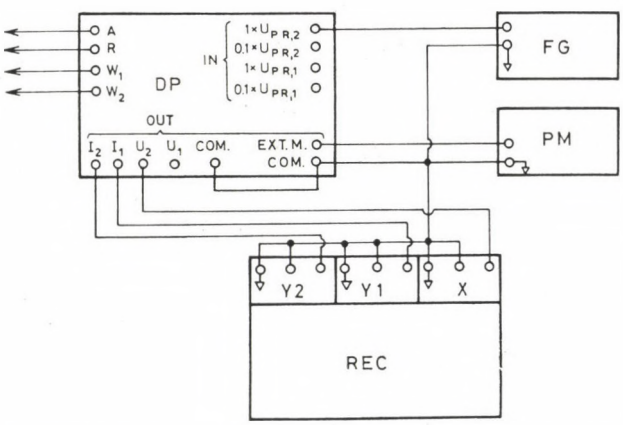

Fig. 5. Circuit diagram of the measuring system. DP — bipotentiostat, FG — function generator, PM — voltmeter, COM — common zero point of the system, EXT.M — connection of external measuring instrument (the other symbols are the same as in Figs 1, 2, and 3)

* We wish to call the attention also to the fact that output circuits designed in this way make possible connection to analogue computers, even in feedback mode of operation [9].

counter, and the number of revolutions per unit time appears directly on the digital display.

Figure 7 shows the schematic drawing of the thermostatable glass apparatus. For thermostating a thermostat Model HAAKE KT 33 is used the temperature is constant within ± 0.1 °C.

The external junction of the platinum wire auxiliary electrode, immersed into the solution, is provided by a mercury contact. The reference electrode,

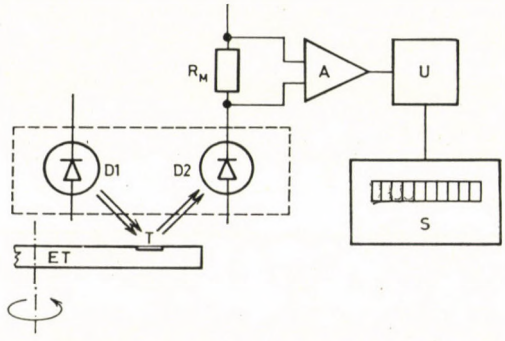

Fig. 6. Scheme of the speed measuring circuit. D1 — photodiode (LED), D2 — photosensor, R_M — loading resistance, ET — electrode-rotating disc, T — mirror strip, A — amplifier, U — signal conditioner, S — counter (with digital display)

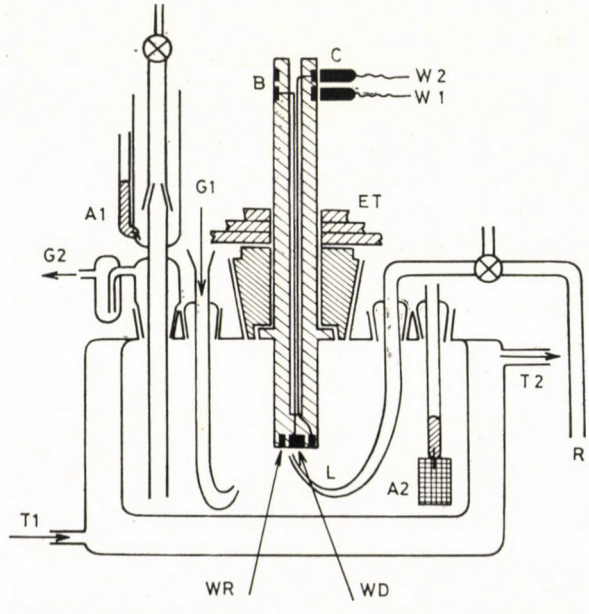

Fig. 7. Thermostatable glass vessel with electrodes. WD — disc electrode, WR — ring electrode, R — reference electrode connection, A1 — external counter electrode, A2 — internal counter electrode, L — Luggin capillary, ET — electrode driving disc, G1, G2 — gas inlet and outlet, T_1, T_2 — inlet and outlet of thermostating liquid, B — bronze rings, C — carbon brushes

which similarly can be thermostated, is a 1.0 mol/dm^3 NaCl calomel electrode. (Potential values given in the following are referred to this electrode.)

The potential of the ring electrode was set in each case to + 600 mV. Thus, the limiting current of the further oxidation of copper (I) ion can be measured at this electrode [10]. The potential of the disc and the ring electrode, respectively, is displayed on the digital instrument of the special purpose bipotentiostat AFKEL 413/1 discussed above, and on the digital voltmeter HIKI TR 1667-A.

In potentiodynamic measurements the continuous change of the potential is performed by a function generator Philips PM 5168, while recording by a double Y-axis plotter Model BRYANS A3, featuring also a logarithmic unit.

Electrolytes needed for the measurements were prepared from *p.a.* perchloric acid and *p.a.* hydrochloric acid with bidistilled water. The total

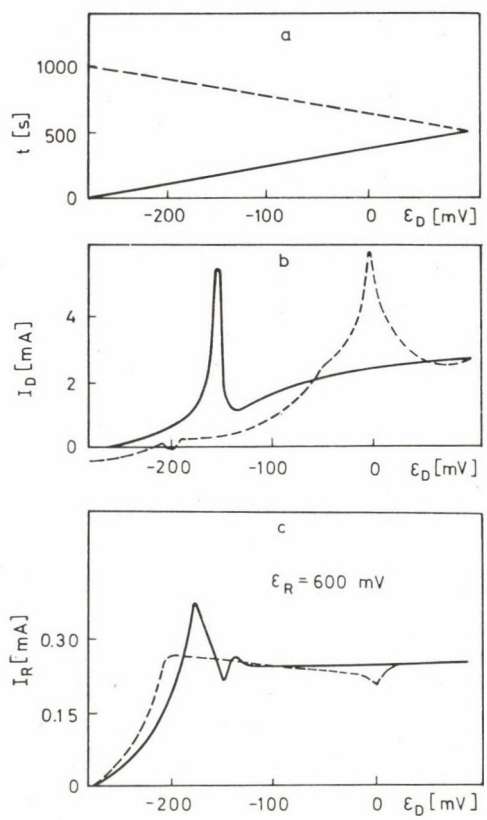

Fig. 8. Potentiodynamic measuring at the copper disc electrode, potentiostatic measurement at the platinum ring electrode. Composition of the solution: 2.9 mol/dm^3 $HClO_4$ + 0.1 mol/dm^3 HCl; temperature of the system 60 °C, electrode speed 520 min^{-1}. ε_D — electrode potential, I_D — current strength at the disc electrode, I_R — current strength at the ring electrode

electrolyte concentration of the solutions was always 3.0 mol/dm^3, *i.e.* 3-x mol/dm^3 $HClO_4$ and x mol/dm^3 HCl. (The value of x was changed between 0.01 and 1.0). The second distillation of once distilled water from alkaline $KMnO_4$ solution removes the predominant part of organic impurities. The quality of water used is continuously controlled by a conductivity cell.

Oxygen is removed from the electrolyte by bubbling through it high purity nitrogen, further purified before the electrolysis cell with a copper-ammonia gas scrubber. The removal of oxygen from the solution requires before each run about 1 hour. (Using auxiliary electrodes A1 and A2, the design of the electrolysis cell makes possible the reductive removal of oxigen dissolved in the electrolyte.) The passing of nitrogen is continued also during the test, and must be stopped only for the period of measurements at a speed of rotation of less than 500 min^{-1}, because in this case bubbling interfers already with measurement.

To ensure an electrode surface of constans quality, definitely needed for reproducible measurement, the electrode is prepared before each measuring

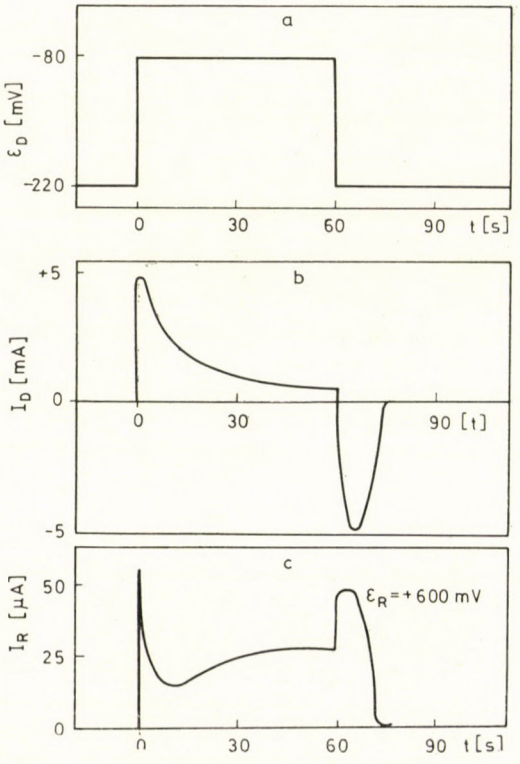

Fig. 9. Double potential step at the copper disc electrode, potentiostatic measurement at the ring electrode. Composition of the solution: 2.97 mol/dm^3 $HClO_4$ + 0.03 mol/dm^3 HCl. Speed of rotation 2000 min^{-1}, temperature 25 °C. Symbols are the same as in Fig. 8

series in an identical way. The regeneration of the surface can be realized by the deposition of a new copper layer after washing with dilute sulfuric acid. Composition of the depositing electrolyte: 0.5 mol/dm^3 $CuSO_4$ and 0.05 mol/dm^3 H_2SO_4. Electrolysis is carried out for 10 minutes at 20 mA, then for further 10 minutes at 2 mA current strength on a surface of 0.25 cm^2, at a speed of rotation of 1060 min^{-1}. According to our experiences, an electrode surface prepared in this way is already suitable for reproducible measurements.

After this description of equipment and methods of preparation needed for the measurements, results obtained at three different measuring technical arrangements will be presented [11].

The series of curves shown in Figs 8a, b, c represents results of potentiodynamic measurements at the disc electrode (at a relatively rapid polarization rate), while potentiostatic measuring technique was used at the ring electrode. For the interpretation of the relatively complicated current–potential curve

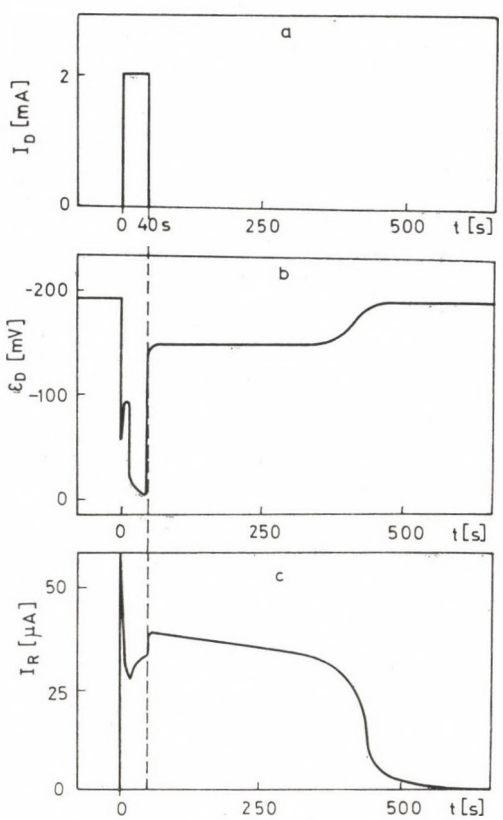

Fig. 10. Double current step at the copper disc electrode, potentiostatic measurement at the ring electrode. Composition of the solution: 2.97 mol/dm^3 $HClO_4$ + 0.03 mol/dm^3 HCl. Speed of rotation 1080 min^{-1}, temperature 25 °C. Symbols are the same as in Fig. 8

measured at the ring electrode offers useful help, because with the exception of the active section here only the chemical dissolution of the deposited CuCl salt layer is measured [6, 11].

In the case of the curves shown in Figs 9a, b, c double potential step was done at the disc electrode, while potentiostatic measuring technique was used at the ring electrode. The decrease in current at the disc electrode after the deposition of the salt layer can be readily observed, while after the adjustment of the current-free potential the cathodic reduction current of the covering salt layer can be measured. Since in this case the Cl^- ion content at the surface of the disc electrode increases (and thus also the rate of the chemical dissolution of the still existing CuCl crystals) — the oxidation limiting current measured at the ring electrode is also increasing.

In the recording of the measuring series shown in Figs 10a, b, c double current step measuring technique was used at the disc electrode, and potentiostatic on the ring electrode, in the same system as described above. The change in time of the potential at the disc electrode can be readily interpreted with the change in time of the oxidation limiting current measured at the ring electrode, the latter curve showing clearly the supersaturation peak before the deposition of the CuCl layer, then the current decrease due to the formation of Cu^{++} complexes, and subsequently in currents-free state the chemical dissolution of the salt layer until the disappearance of the layer.

REFERENCES

[1] Albery, W. J., Hitchman, M. L.: Ring-Disc Electrodes. Oxford University Press, London, 1971
[2] Pleszkov, Ju. V., Filinovszkij, V. Ju.: Vrasajucsijszja diszkovüj electrod. Izd. Nauka, Moscow, 1972
[3] Levics, V. G.: Fiziko-himiszecskaja gidrodinamika Fizmatgiz. Moscow, 1959
[4] Kiss, L., Farkas, J.: Kém. Közlemények, **34,** 261 (1970); Ann. Univ. Sci. Budapest, Sect. Chim., **12,** 123 (1971)
[5] Kiss, L., Farkas, J., Kőrösi, A., Mandl, J.: Acta Chimica (Budapest), **79,** 43 (1973)
[6] Farkas, J.: A forgó gyűrűs korongelektród alkalmazása a fémoldódás tanulmányozására (Application of the rotating ring disc electrode for the study of metal dissolution). Thesis, Budapest, 1971
[7] Bruckenstein, S.: J. Am. Chem. Soc., **90,** 6303 (1968); **90,** 6592 (1968)
[8] Bruckenstein, S., Miller, B.: J. Electrochem. Soc., **117,** 1032 (1970); **117,** 1040 (1970)
[9] Mányai, Gy.: Diploma work, Budapest, 1977
[10] Kiss, L., Farkas, J., Kőrösi, A.: Acta Chim. (Budapest), **68,** 359 (1971)
[11] Kiss, L., Farkas, J., Kőrösi, A.: Acta Chim. (Budapest), **67,** 179 (1971)

József Farkas
Pál Kovács
László Kiss
H-1088 Budapest, Puskin u. 11—13.

László Dobos
H-6701 Szeged, Rerrich B. tér 1.

Acta Chimica Academiae Scientiarum Hungaricae, Tomus 108 (2), pp. 135—145 (1981)

FLAVONOIDS, XXXVI*

REACTION OF 3-ALKYL- OR -ARYLSULFONYLOXYFLAVANONES WITH AMINES. SYNTHESIS OF 3-DIALKYLAMINOFLAVANONES**

T. PATONAY,+ GY. LITKEI and R. BOGNÁR

(*Institute of Organic Chemistry, Kossuth Lajos University, Debrecen*)

Received July 10, 1980

Reactions of 3-alkyl- or -arylsulfonyloxyflavanones (**1a—h**) with primary and tertiary amines gave mixtures of the corresponding flavones (**2a—d**) and aurones (**3a—d**), while with secondary amines, in addition to **2** and **3**, 3-dialkylaminoflavanones (**6—9**) were also obtained. The factors which determine the ratio of products are discussed.

Treatment of the 3-dialkylaminoflavanones **6a** and **7** with DDQ gave 3-dialkylaminoflavones (**10, 11**); treatment with alkali in methanol afforded 2-dialkylamino--2-benzylcoumaran-3-ones (**12, 13**).

Earlier in this series we reported the synthesis of 3-alkyl- and 3-arylsulfonyloxyflavanones, their reactions with azide ions [1], and their usefulness in the preparation of new 3-substituted-flavanones of potential biological activity. In the present communication we wish to report on the reactions of 3-alkyl- or -arylsulfonyloxyflavanones with amines.

Reactions of 3-alkyl- or -arylsulfonyloxyflavanones with primary and tertiary amines

The *trans*-3-alkyl- or -arylsulfonyloxyflavanones (**1a—h**) when treated with triethylamine, isopropylamine or cyclohexylamine in dimethylsulfoxide at room temperature, or refluxed in pyridine, afford a mixture of flavones (**2a—d**) and aurones*** (**3a—d**). No formation of isoflavones could be detected.

* Part XXXV: Gy. LITKEI, T. MESTER, T. PATONAY and R. BOGNÁR: Ann., **1979,** 174

** A part of this work was presented at the Conference of the Hungarian Chemical Society, Sopron, 28—31 August, 1979.

+ To whom correspondence should be addressed

*** An IR spectroscopic investigation revealed the presence of *only* (*Z*)-aurones in the reaction mixture, but after column chromatography the isolated aurones were found to consist of a mixture of the *E* and *Z* isomers. By control experiments it was verified that the *E* compounds appear as a result of $Z \rightleftarrows E$ isomerisation during chromatographic separation in the presence of (visible) light. The UV irradiation-induced $Z \rightarrow E$ isomerization is well known [2, 3]. Studies on this isomerization are in progress.

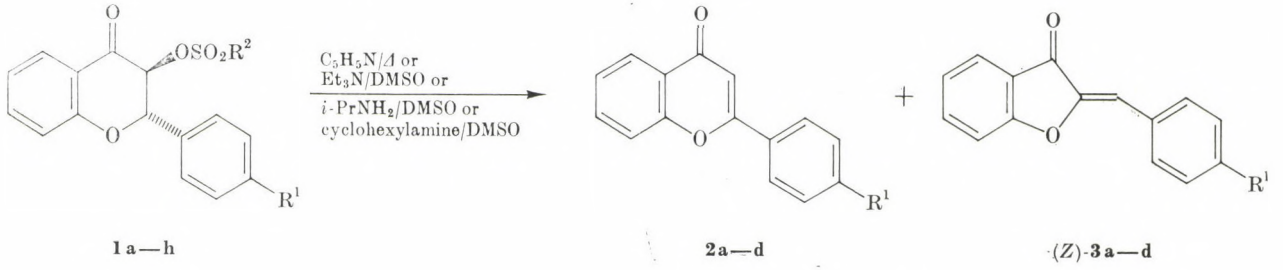

1a—h **2a—d** (*Z*)-**3a—d**

	R^1	R^2
1a	H	Me
1b	OMe	Me
1c	Br	Me
1d	NO_2	Me
1e	H	$PhCH_2$
1f	H	Ph
1g	H	4-Br—C_6H_4
1h	H	4-NO_2—C_6H_4

	R^1
2a, 3a	H
2b, 3b	OMe
2c, 3c	Br
2d, 3d	NO_2

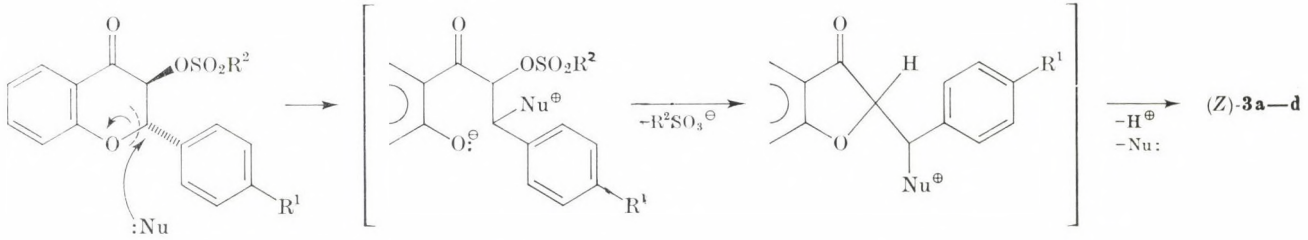

1a—h **4** **5**

The appearence of aurones in the reaction mixture is surprising, because the reaction of 3-bromo-flavanones with nucleophilic agents affords either only flavones by simple β-elimination [4, 5], or isoflavones by aryl migration (in the presence of certain silver salts) [5]. No formation of aurones was observed in the reaction of **1a**—**h** and azide ions [1].

To explain the elimination accompained by ring contraction leading to aurones it is supposed that — parallel to β-elimination leading to flavones — the attack of the nucleophile also occurs at the C-2 carbon atom, affording **4** by ring opening. Recyclization of the intermediate **4** by intramolecular attack at C-3 linked to a good leaving group gives **5**, which is finally transformed to (*Z*)-**3** in a fast elimination step [6].

The aurone/flavone ratio depends not only upon the character of the amine, but also on the leaving group and the other substituents of the flavanone **1a**—**h**.

(1) More aurone is formed in the reaction with primary amines than with tertiary ones. This indicates the importance of steric factors; the smaller primary amines can more easily attack at C-2 carrying the bulky phenyl group, than can the larger tertiary amines.

(2) In the series of 3-mesyloxyflavanones (**1a**—**d**) an increase in the electron-attracting character of the R^1 group causes a decrease in the yield of **3**. This can be attributed to the fact that electron attraction by the R^1 group facilitates β-elimination and also hampers the cleavage of the O-(C-2) bond.

(3) β-Elimination is favoured by the presence of a better leaving group and thus aurone formation is supressed. This tendency is quite noticeable in the case of 4-X-benzenesulfonyloxy groups (**1f**—**1h**).

Reactions of 3-mesyloxyflavanones (1a, b) with secondary amines

The reactions of *trans*-3-mesyloxyflavanone (**1a**) or *trans*-3-mesyloxy-4'-methoxyflavanone (**1b**) with different secondary amines (piperidine, morpholine, diethylamine, *N*-methyl-benzylamine) in dimethylsulfoxide at room temperature give *trans*-3-dialkylaminoflavanones (**6a, b, 7**—**9**), in addition to the corresponding flavones (**2a, b**) and aurones (**3a, b**). Displacement takes place with full retention of the configuration, the isomeric *cis*-3-dialkylaminoflavanones were not detectable. In the reaction of **1** and azide ions also a dominant retention was observed, but it was accompanied by about 15% inversion [1].

The yield of 3-dialkylaminoflavanones depends on the nature of the amine, being *e.g.*, higher with alicyclic amines than with secondary aliphatic amines. This difference may be explained by steric factors [7], but then the lack of

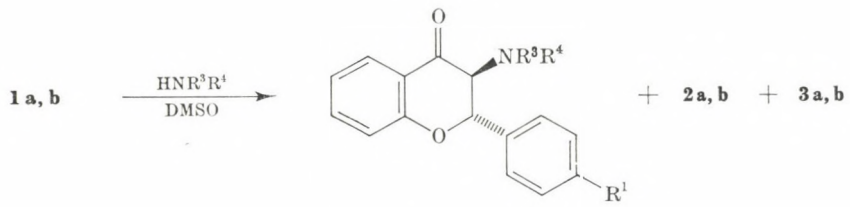

6a, b, 7—9

	R^1	R^3	R^4
6a	H	$-(CH_2)_5-$	
6b	OMe	$-(CH_2)_5-$	
7	H	$-(CH_2)_2O(CH_2)_2-$	
8	H	Et	Et
9	H	Me	$PhCH_2$

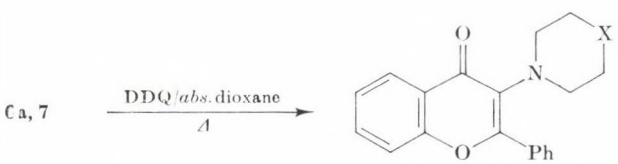

10, 11

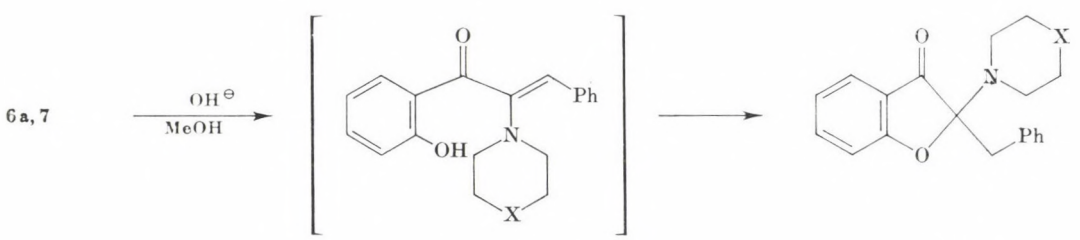

14, 15 **12, 13**

	X
6a, 10, 12, 14	CH_2
7, 11, 13, 15	O

substitution with the smaller primary amines requires another — and still unknown — explanation.

Contrary to the literature [8], we observed no correlation between the yield of 3-dialkylaminoflavanones and the basicity of the amine used.

The 3-dialkylaminoflavanones **6a** and **7** can be transformed to the 3-dialkylaminoflavones **10** and **11** with 2,3-dichloro-5,6-dicyanobenzoquinone (DDQ) according to the method of MATSUURA *et al.* [9]. The treatment of **6a** and **7** with dilute sodium hydroxide in methanol at room temperature gave, by ring-contraction, the 2-dialkylamino-2-benzylcoumaran-3-ones **12** and **13** as the only products, in almost quantitative yield.

The formation of **12** and **13** is assumed to be a result of the recyclization of the 2′-hydroxy-α-dialkylaminochalcones **14** and **15**, which are formed from **6a** and **7** in basic medium. The cyclization of some 2′-OR-α-substituted--chalcones to 2-substituted-2-benzylcoumaran-3-ones in the presence of acids is well known [10], but the transformation of 3-hydroxyflavanones to 2-hydroxy-2-benzylcoumaran-3-ones by alkali in poor yield — presumably *via* 2′,α-dihydroxychalcones — has been reported only in a few cases [11]. The present ring-contraction offers a new method for the synthesis of 2-substituted--2-benzylcoumaran-3-ones.

Further results on the reaction of **1** with other nucleophiles will be published in the near future.

Experimental

All m.p.'s are uncorrected and were determined on a Kofler hot-stage. UV spectra were registrated on a UNICAM SP-800 instrument, IR spectra were recorded with UNICAM SP-200 G and Perkin–Elmer 283 instruments; NMR spectra were obtained on a JEOL MH-100 instrument (internal standard TMS $\delta = 0$ ppm).

All the isolated flavones (**2a—d**) and (*Z*)-aurones (**3a—d**) were identified on the basis of m.p., mixed m.p., TLC investigations and IR spectra.

Transformation of *trans*-3-alkyl- or -arylsulfonyloxyflavanones (1a—h) in hot pyridine

Three mmoles of the *trans*-3-alkyl- or -arylsulfonyloxyflavanone (**1a—h**) [1] was refluxed in dry pyridine (10 mL). The solid product which precipitated after pouring the reaction mixture into dilute hydrochloric acid was filtered off, washed and dried. The product ratio was determined as follows:

Method A

The product mixtures were chromatographed on Kieselgel 40 (Merck) or Kieselgel Woelm (Akt. I.) adsorbents with an eluant system of petroleum ether-ethyl acetate (4 : 1), unless otherwise stated.

Aurones were eluted as a mixture of the *E* and *Z*-isomers; they were separated by repeated crystallization. In the reaction mixture only the (*Z*)-aurones were detected by TLC and IR. Chromatography of pure (*Z*)-**3a** under similar conditions afforded an (*E*)—(*Z*) mixture in a ratio of about 1 : 1 (TLC and IR identification). This ratio was similar to the one observed in the chromatography of the reaction mixtures.

(*E*)-Aurones were identified on the basis of the characteristic differences between their IR spectra and those of the *Z* isomers [2, 13].

Acta Chim. Acad. Sci. Hung. 108, 1981

Table I

Details of the reaction of 3-alkyl- and 3-arylsulfonyloxyflavanones with primary and tertiary amines

Start. compd.	Reagent	Time of reaction	Product determination	4′-R¹-flavone (**2a—d**)			4′-R¹-aurone (**3a—d**)		
				Yield, %	M.p., °C	*Lit.* m.p., °C	Yield, %	M.p., °C[a]	*Lit.* m.p., °C
1a	py/Δ	6h	*A*	84.1	95	97	12.0	108—110	108 [12]
	py/Δ	6h	*B*	88.7	—		10.95	—	
	Et_3N/DMSO	7d	*A*	87.7	96—97		8.6	106—108	
	i-$PrNH_2$/DMSO	3d	*A*	57.5	95—96		32.9	107—108	
	$C_6H_{11}NH_2$/DMSO	4d	*B*	56.6	—		41.9	—	
	Bu_2NH/DMSO	3d	*A*	91.5	96—98		6.2	—	
1b	py/Δ	6h	*A*	62.0	156—158	157—158 [14]	12.5	138—140	138—139 [15]
1c	py/Δ	6h	*A*[b]	81.1	177—179	178 [16]	8.4	170—171	168 [17]
1d	py/Δ	1.5h	c	84.4	235—238	244—246 [18]	1.0	—	207—208 [18]
	Et_3N/DMSO	24h	*A*[b]	91.3	236—239		6.7	207—211	
1e	py/Δ	6h	*B*	88.2	—		8.8	—	
1f	py/Δ	6h	*B*	83.8	—		12.6	—	
1g	py/Δ	6h	*B*	87.9	—		9.6	—	
1h	py/Δ	6h	*B*	91.6	—		5.3	—	

[a] M.p.'s of (*Z*)-aurones. The m.p.'s of the isolated (*E*)-aurones are not characteristic owing to their isomerisation during heating (see References [2] and [19])

[b] Elution with petroleum ether-ethyl acetate (7 : 3)

[c] Recrsytallization from acetone followed by preparative TLC [Kieselgel 60 F_{254}; toluene-ethyl acetate [4 : 1]]

Method B

The spectra of the crude products ($c \sim 0.2$ mg/10 mL, $CHCl_3$) were recorded. The amount of flavone (**2a**), (*Z*)-aurone (**3a**) and 3-hydroxyflavone (which also could be detected by TLC) was calculated from the extinction data measured at $\lambda = 292.5$, 343 and 382 nm wavelengths on the basis of $E_\lambda = l \Sigma \varepsilon_{i,\lambda} c_i$.

Each individual product composition was determined as an average of two independent measurements, the maximal error being $\pm 0.73\%$. The maximum amount of 3-hydroxyflavone was 3.6%. The details of the experiments and spectroscopic data are summarized in Tables I and II.

Table II

IR spectroscopic data of the prepared aurones (cm^{-1})

Compound	*Z*				*E*			
	νC=O	νC=C	νAr—C(=O)	DHF	νC=O	νC=C	νAr—C(=O)	DHF
3a	1712	1657	1297	883	1694	1640	1286	889
3b	1711	1652	1298	885	1702*	1636*	—	—
3c	1717	1660	1297	885	1706	1623	1286	—
3d	1720	1661m	1297	885	1687	1640vw	—	—

DHF: Vibration of the dihydrofuranone skeleton, m: medium, vw: very weak. The spectra were recorded in CCl_4 solution or from TLC plate (denoted by * symbol)

Reaction of *trans*-3-mesyloxyflavanones (1a, b, d) with amines in dimethyl sulfoxide

The *trans*-3-mesyloxyflavanone (**1a, b, d**) (3 mmoles) was treated with 6 mmoles of amine in *abs.* dimethyl sulfoxide (10—15 mL) at room temperature. The reaction mixture was poured into water and then extracted with chloroform or carbon tetrachloride. After drying, the solvent was evaporated and the crude product was separated by one of the method *A*—*D*. (In the reaction of **1a** with cyclohexylamine and of **1d** with triethylamine the reaction mixture was poured into water, the precipitated crude product was filtered off, washed and separated.)

Method C

The crude product was dissolved in carbon tetrachloride and then extracted with dilute hydrochloric acid. The acid phase was made alkaline with ammonium hydroxide and extracted again with diethyl ether. After drying, the ether was evaporated and the residue crystallized from methanol or ethanol to obtain pure 3-dialkylaminoflavanone.

The carbon tetrachloride phase remaining from the extraction with hydrochloric acid was dried, evaporated and chromatographed on a Kieselgel 40 or a Kieselgel Woelm (Akt. I.) column (eluant: petroleum ether-ethyl acetate (4 : 1)).

Method D

The crude product was dissolved in a small quantity of acetone, poured into dilute hydrochloric acid and extracted with diethyl ether. The remaining acidic solution was made alkaline with ammonium hydroxide, extracted with chloroform and evaporated. Crystallization of the residue from ethanol gave pure 3-dialkylaminoflavanone.

Results and characteristics of the new products are given in Tables III and IV.

3-Piperidinoflavone (10)

A solution of **6a** (0.49 mmole) and 2,3-dichloro-5,6-dicyanobenzoquinone (0.66 mmole) in *abs.* dioxane (15 mL) was refluxed for 8hrs. After cooling, the precipitated 2,3-dichloro-5,6-dicyanohydroquinone was filtered off, the solvent was evaporated from the filtrate and the

Table III

Details of the reaction of 3-mesyloxyflavanones with secondary amines

Compound	Time of reaction, days	Product determination	Yield, %	M.p., °C	Formula (Mol. weight)	Analysis		Isolated	
						Calcd.	Found	Flavone, %	Aurone, %
6a	3	*C*	22.0	96—97 149—151[a]	$C_{20}H_{21}NO_2$ (307.40)	C: 78.15 H: 6.89 N: 4.56	C: 78.66 H: 6.88 N: 4.53	43.9	6.7
6b	6	*D*	30.4	108—110.5	$C_{21}H_{23}NO_3$ (337.42)	C: 74.75 H: 6.87 N: 4.15	C: 74.66 H: 6.42 N: 3.96	b	b
7	9	*C*	8.0	135—137 162—164.5[a]	$C_{19}H_{19}NO_3$ (309.37)	C: 73.76 H: 6.19 N: 4.53	C: 73.93 H: 6.38 N: 4.32	69.2	8.1
8	4	*C*	2.7	123—127	$C_{19}H_{21}NO_2$ (295.39)	N: 4.74	N: 4.48	b	b
9	3	*A*	5.1	oil	—	c	c	80.3	11.5

[a] M.p. of picrate. [b] Not isolated. [c] Identified by spectroscopic data.

Table IV

Spectroscopic data of the new trans-3-dialkylaminoflavanones

Compound	IR (KBr), cm^{-1}			^{1}H-NMR ($CDCl_3$)			$J_{2,3}$ Hz
				δ ppm			
	νC=O	νAr—C(=O)	Other characteristic absorptions	H-2	H-3	Other signals	
6a	1692 1679	1290	—	5.48	3.65	2.82, 2.63 (2″, 6″—CH_2) 1.40 (3″, 4″, 5″—CH_2)	9.8
6b	1683	1288	2841 (νOMe) 1253 (ν_{as} C—O—C; OMe) 1035, 1023 (ν_s, C—O—C; OMe)	5.42	3.65	3.82 (OMe) 2.78, 2.62 (2″, 6″—CH_2) 1.36 (3″, 4″, 5″—CH_2)	10.1
7	1689	1292	1006 (νC—O—C; morpholine)	5.53	3.69	3.55 (2″, 2″, 6″—CH_2) 2.84, 2.70 (3″, 5″—CH_2)	9.8
8[a]	1685	1295	2962 (ν_{as} CH_3)	5.23	3.77	2.80, 2.50 (2×CH_2CH_3) 1.79 (2×CH_2CH_3)	11.4
9[b]	1688	1291	2811 (νNMe)	5.45	3.88	3.84, 4.01 (CH_2Ph; J_{AB} = 14.2 Hz) 2.41 (N*Me*)	11.6

[a] The ^{1}H-NMR spectrum was recorded in CCl_4. [b] IR spectrum of neat product

oily residue was separated by preparative TLC [Kieselgel 60 F_{254}; toluene-ethyl acetate (4 : 1)] to obtain pure **10** (54%) as a yellow oil.

IR (neat): 1636 cm^{-1} ($\nu C{=}O$).

^{1}H-NMR ($CDCl_3$): 3.28 (m, 4H, 2″,6″-CH_2), 1.60 ppm (m, 6H, 3″,4″, 5″-CH_2).

Picrate of **10**: M.p. 142—144 °C (ethanol).

$C_{26}H_{22}N_4O_9$ (534.49) Calcd. N 10.48. Found N 9.85%.

3-Morpholinoflavone (11)

A mixture of **7** (0.36 mmole) and 2,3-dichloro-5,6-dicyanobenzoquinone (0.66 mmole) in *abs.* dioxane (10 mL) was refluxed for 18 hrs. Work up in the same manner as described for compound **10** afforded **11** (47.5%), m.p. 175—176.5 °C (methanol).

$C_{19}H_{17}NO_3$ (307.35) Calcd. N 4.56. Found N 4.58%.

IR (CCl_4): 1650 cm^{-1} ($\nu C{=}O$).

^{1}H-NMR ($CDCl_3$): 3.75 (m, 2H,2″,6″ CH_2), 3.20 (m, 4H, 3″, 5″-CH_2).

2-Benzyl-2-piperidinocoumaran-3-one (12)

Compound **6a** (0.325 mmole) was treated with 2*N* sodium hydroxide (1 mL) in methanol (10 mL) at room temperature. After 3 days the precipitated crystals were filtered off and identified as **12** (67%), m.p. 139—140 °C.

The mother liquor was evaporated and the residue recrystallized from ethanol-water (5 : 1) to yield a second crop of **12** (20%), m.p. 141—142 °C.

$C_{20}H_{21}NO_2$ (307.40). Calcd. N 4.56. Found N 4.28%.

^{1}H-NMR ($CDCl_3$): 3.60, 3.21 (AB, 2H, CH_2Ph), 2.90, 2.74 (m, 4H, 2″, 6″-CH_2), 1.62, 1.58 (m, 6H, 3″,4″,5″-CH_2); J_{AB} = 14 Hz.

2-Benzyl-2-morpholinocoumaran-3-one (13)

A mixture of **7** (0.323 mmole) and 2*N* sodium hydroxide (1 mL) was allowed to react in methanol (10 mL) at room temperature. After 5 days the mixture was poured into water and extracted with diethyl ether. After drying, the extract was evaporated. Recrystallization of the residue yielded **13** (71%), m.p., 139—141 °C (aqueous methanol).

$C_{19}H_{19}NO_3$ (309.37). Calcd. N 4.53. Found N 4.44%.

IR (KBr): 1714 cm^{-1} ($\nu C{=}O$).

^{1}H-NMR ($CDCl_3$): 3.80 (m, 4H, 2″, 6″-CH_2), 3.59, 3.24 (AB, 2H, CH_2Ph), 2.90 (m, 4H, 3″,5″-CH_2); J_{AB} = 13.3 Hz.

REFERENCES

[1] Patonay, T., Rákosi, M., Litkei, Gy., Bognár, R.: Ann., **1979**, 162

[2] Hastings, J. S., Heller, H. G.: J. Chem. Soc. Perkin I. **1972**, 2128

[3] Brady, B. A., Kennedy, J. A., O'Sullivan, W. I.: Tetrahedron, **29**, 359 (1973)

[4] Bognár, R., Rákosi, M., Litkei, Gy.: Magyar Kémiai Folyóirat, **68**, 305 (1962)

[5] Pelter, A., Ward, R. S., Balasubramanian, M. J.: J.C.S. Chem. Commun., **1976**, 151

[6] See, *e.g.*, Dean, E. M., Podimuang, V.: J. Chem. Soc., **1965**, 3978; Wong, E.: Chem. Ind. (London,) **1966**, 598

[7] Mosher, H. S.: in Heterocyclic Compounds, Vol. I, p. 667 (Ed. Elderfield, R. C.), Wiley, London, 1950; Gibson, M. S.: in The Chemistry of Amines, p. 46. (Ed. Patai, S.) Interscience, London—New York—Sidney, 1968

[8] Hudson, R. F.: Chimia, **16**, 173 (1962); Jensen, W. B.: Chem. Rev., **78**, 1 (1978) and references cited therein

[9] Matsuura, S., Iinuma, M., Ishikawa, R., Kagei, K.: Chem. Pharm. Bull., **26**, 305 (1978)

[10] Enebäck, C.: Soc. Chim. Fennica Comm. Phys.-Math., **28**, 1 (1963); Litkei, Gy., Bognár, R.: Acta Chim. Acad. Sci. Hung., **77**, 93 (1973); Ferreira, D., Brandt, E. V., Volsteedt, F. du R., Roux, D. G.: J. Chem. Soc. Perkin I, **1975**, 1437 and references cited therein

[11] GRIPENBERG, J.: Acta Chem. Scand., **7**, 1323 (1953); CHOPIN, J., BOUILLANT, M. L.: Compt. rend., **254**, 2699 (1962)
[12] FRIEDLÄNDER, P., NEUDÖRFER, G.: Ber. Dtsch. Chem. Ges., **30**, 1077 (1897)
[13] KUROSAWA, K., HIGUCHI, J.: Bull. Chem. Soc. Japan, **45**, 1132 (1972)
[14] FITZGERALD, D. M., O'SULLIVAN, J. F., PHILBIN, E. M., WHEELER, T. S.: J. Chem. Soc., **1955**, 860
[15] GOWAN, J. E., HAYDEN, P. M., WHEELER, T. S.: J. Chem. Soc., **1955**, 862
[16] CHEN, F.-C., YANG, C.-H.: J. Taiwan Pharm. Assoc., **3**, 39 (1951); Chem. Abstr., **49**, 2432 (1955)
[17] NAGY, E., DINYA, Z.: Unpublished results
[18] REICHEL, L., HEMPEL, G.: Ann., **625**, 184 (1959)
[19] AZZOLINA, O., DESIMONI, G., DI TORO, V., GHISLANDI, V., TACCONI, G.: Gazz. Chim. Ital., **105**, 971 (1975)

Tamás PATONAY
György LITKEI
Rezső BOGNÁR

H-4010 Debrecen, P.O.B. 20.

Acta Chimica Academiae Scientiarum Hungaricae, Tomus 108 (2), pp. 147—159 (1981)

TRANSITION METAL COMPLEXES OF OXIME CONTAINING LIGANDS, XI

MAGNETIC AND SPECTRAL PROPERTIES OF SOME CYCLIC NITROGEN BASES OF SOME METAL COMPLEXES OF PYRIDINE-2-ALDOXIME AND 6-METHYLPYRIDINE-2-ALDOXIME

M. MOHAN* and P. K. VARSHNEY

(*Department of Chemistry, N.R.E.C. College, Khurja (U.P.)-203131 India*)

Received October 6, 1980

Accepted for publication November 17, 1980

Complexes of the type $[M(HL)_2(B)_2]$ (where M = Mn(II), Fe(II), Co(II) or Ni(II), L = pox$^-$, anion of pyridine-2-aldoxime (Hpox) or mpox$^-$, anion of 6-methylpyridine-2-aldoxime (Hmpx) and B = pyridine-2,3,4-picoline or 2,3,4-ethylpyridine) have been synthesized and characterized by analytical, magnetic (300 — 78 °K), infrared and electronic spectral data. A *trans*-symmetrical structure with *N*-coordination of pox$^-$ and mpox$^-$ and pyridines in the *trans- axial* positions has been proposed. Mössbauer spectra also support the proposed structure for iron(III) complexes.

Introduction

Oximes are well known [1] for their chelation behaviour. The chelation is due to the presence of two electron donor atoms, nitrogen and oxygen. The nature of the linkage with the metal ion depends upon the ionization of the proton of the oxime group. Several metal(II) and (III) complexes of Hpox and Hmpox have been studied [1, 2] extensively but the cyclic base adducts of transition metal complexes of Hpox and Hmpox have recieved very little attention. In this paper, we report the synthesis and spectral properties of some cyclic base adducts of manganese(II), iron(II), cobalt(II) and nickel(II) complexes of Hpox and Hmpox.

Experimental

Hydrated manganese(II), cobalt(II) and nickel(II) chlorides, ferrous ammonium sulphate (all reagent grade), pyridine-2-aldoxime and 6-methylpyridine-2-aldoxime (K & K Laboratories, New York) were used without further purification.

Synthesis of Complexes

The following general procedure was used to prepare manganese(II), iron(II), cobalt(II) and nickel(II) cyclic base adducts of Hpox and Hmpox.

The complexes [2] $[M(HL)_2(Cl_2)]$ (where M = Mn(II), Fe(II), Co(II) or Ni(II) and HL = Hpox or Hmpox) (0.03 mole) were mixed with *ca.* 100 cm^3 of appropriate pyridine base

* To whom correspondence should be addressed.

Table I

Analytical data

Complex*	Found (Calcd.) %			
	C	H	N	M
$[Mn(pox)_2(py)_2]$	58.40 (58.29)	4.10 (3.97)	18.62 (18.54)	12.00 (12.12)
$[Mn(pox)_2(\alpha\text{-pic})_2]$	59.75 (59.88)	4.62 (4.57)	17.56 (17.46)	11.62 (11.41)
$[Mn(pox)_2(\beta\text{-pic})_2]$	59.80 (59.88)	4.65 (4.57)	17.66 (17.46)	11.23 (11.41)
$[Mn(pox)_2(\gamma\text{-pic})_2]$	59.80 (59.88)	4.50 (4.57)	17.38 (17.46)	11.05 (11.41)
$[Mn(pox)_2(\alpha\text{-Epy})_2]$	61.12 (61.30)	5.15 (5.10)	16.60 (16.50)	10.88 (10.78)
$[Mn(pox)_2(\beta\text{-Epy})_2]$	61.38 (61.30)	5.25 (5.10)	16.75 (16.50)	10.62 (10.78)
$[Mn(pox)_2(\gamma\text{-Epy})_2]$	61.42 (61.30)	5.30 (5.10)	16.42 (16.50)	10.90 (10.78)
$[Fe(pox)_2(py)_2]$	58.28 (58.17)	3.85 (3.96)	18.48 (18.51)	12.35 (12.29)
$[Fe(pox)_2(\alpha\text{-pic})_2]$	59.92 (59.77)	4.65 (4.56)	17.35 (17.43)	11.65 (11.58)
$[Fe(pox)_2(\beta\text{-pic})_2]$	59.69 (59.77)	4.72 (4.56)	17.49 (17.43)	11.62 (11.58)
$[Fe(pox)_2(\gamma\text{-pic})_2]$	59.85 (59.77)	4.50 (4.56)	17.59 (17.43)	11.48 (11.58)
$[Fe(pox)_2(\alpha\text{-Epy})_2]$	59.97 (61.20)	5.15 (5.10)	16.58 (16.47)	10.85 (10.94)
$[Fe(pox)_2(\beta\text{-Epy})_2]$	60.95 (61.20)	5.18 (5.10)	16.39 (16.47)	10.90 (10.94)
$[Fe(pox)_2(\gamma\text{-Epy})_2]$	61.32 (61.20)	5.02 (5.10)	16.52 (16.47)	10.85 (10.94)
$[Co(pox)_2(py)_2]$	57.65 (57.78)	3.90 (3.93)	18.45 (18.38)	12.95 (12.89)
$[Co(pox)_2(\alpha\text{-pic})_2]$	59.45 (59.39)	4.50 (4.53)	17.40 (17.32)	12.26 (12.14)
$[Co(pox)_2(\beta\text{-pic})_2]$	59.27 (59.39)	4.48 (4.53)	17.28 (17.32)	12.07 (12.14)
$[Co(pox)_2(\gamma\text{-pic})_2]$	59.45 (59.39)	4.60 (4.53)	17.39 (17.32)	12.26 (12.14)
$[Co(pox)_2(\alpha\text{-Epy})_2]$	60.95 (60.83)	5.12 (5.06)	16.48 (16.37)	11.52 (11.48)
$[Co(pox)_2(\beta\text{-Epy})_2]$	60.75 (60.83)	5.00 (5.06)	16.28 (16.37)	11.32 (11.48)
$[Co(pox)_2(\gamma\text{-Epy})_2]$	60.92 (60.83)	5.02 (5.06)	16.48 (16.37)	11.56 (11.48)
$[Ni(pox)_2(py)_2]$	57.92 (57.80)	3.85 (3.94)	18.45 (18.39)	12.69 (12.85)
$[Ni(pox)_2(\alpha\text{-pic})_2]$	59.96 (59.41)	4.60 (4.53)	17.46 (17.33)	12.00 (12.11)
$[Ni(pox)_2(\beta\text{-pic})_2]$	59.35 (59.41)	4.48 (4.53)	17.28 (17.33)	12.24 (12.11)
$[Ni(pox)_2(\gamma\text{-pic})_2]$	59.52 (59.41)	4.62 (4.53)	17.42 (17.33)	12.02 (12.11)
$[Ni(pox)_2(\alpha\text{-Epy})_2]$	60.92 (60.85)	5.12 (5.07)	16.45 (16.38)	11.52 (11.44)
$[Ni(pox)_2(\beta\text{-Epy})_2]$	60.80 (60.85)	5.20 (5.07)	16.30 (16.38)	11.38 (11.44)
$[Ni(pox)_2(\gamma\text{-Epy})_2]$	60.75 (60.85)	5.18 (5.07)	16.48 (16.38)	11.54 (11.44)
$[Mn(mpox)_2(py)_2]$	59.75 (58.63)	4.80 (4.96)	17.50 (17.39)	11.47 (11.36)
$[Mn(mpox)_2(\alpha\text{-pic})_2]$	61.12 (61.06)	5.60 (5.48)	16.58 (16.44)	10.82 (10.74)
$[Mn(mpox)_2(\beta\text{-pic})_2]$	61.20 (61.06)	5.56 (5.48)	16.50 (16.44)	10.89 (10.74)
$[Mn(mpox)_2(\gamma\text{-pic})_2]$	61.25 (61.06)	5.38 (5.48)	16.38 (16.44)	10.80 (10.74)
$[Mn(pmox)_2(\alpha\text{-Epy})_2]$	66.42 (62.34)	5.80 (5.93)	15.62 (15.58)	10.32 (10.18)
$[Mn(mpox)_2(\beta\text{-Epy})_2]$	62.40 (62.34)	5.80 (5.93)	15.50 (15.58)	10.40 (10.18)
$[Mn(mpox)_2(\gamma\text{-Epy})_2]$	62.28 (62.34)	5.75 (5.93)	15.51 (15.58)	10.35 (10.18)
$[Fe(mpox)_2(py)_2]$	60.10 (59.52)	5.10 (4.96)	17.52 (17.36)	11.65 (11.53)
$[Fe(mpox)_2(\alpha\text{-pic})_2]$	61.15 (60.96)	5.40 (5.47)	16.52 (16.41)	10.98 (10.90)

Table I (Contd.)

Complex*	Found (Calcd.) %			
	C	H	N	M
$[Fe(mpox)_2(\beta\text{-pic})_2]$	60.90 (60.96)	5.42 (5.47)	16.60 (16.41)	10.95 (10.90)
$[Fe(mpox)_2(\gamma\text{-pic})_2]$	60.85 (60.96)	5.50 (5.47)	16.58 (16.41)	10.85 (10.90)
$[Fe(mpox)_2(\alpha\text{-Epy})_2]$	62.30 (62.24)	6.10 (5.92)	15.70 (15.56)	10.40 (10.33)
$[Fe(mpox)_2(\beta\text{-Epy})_2]$	62.35 (62.24)	6.12 (5.92)	15.65 (15.56)	10.42 (10.33)
$[Fe(mpox)_2(\gamma\text{-Epy})_2]$	62.40 (62.24)	6.10 (5.92)	15.60 (15.56)	10.45 (10.33)
$[Co(mpox)_2(py)_2]$	59.29 (59.14)	4.85 (4.92)	17.38 (17.25)	12.15 (12.08)
$[Co(mpox)_2(\alpha\text{-pic})_2]$	60.65 (60.59)	5.50 (5.43)	16.50 (16.31)	11.60 (11.43)
$[Co(mpox)_2(\beta\text{-pic})_2]$	60.49 (60.59)	5.38 (5.43)	16.40 (16.31)	11.60 (11.43)
$[Co(mpox)_2(\gamma\text{-pic})_2]$	60.62 (60.59)	5.49 (5.43)	16.45 (16.31)	11.70 (11.43)
$[Co(mpox)_2(\alpha\text{-Epy})_2]$	62.00 (61.88)	5.95 (5.89)	15.56 (15.47)	10.92 (10.84)
$[Co(mpox)_2(\beta\text{-Epy})_2]$	61.96 (61.88)	5.75 (5.89)	15.60 (15.47)	10.90 (10.84)
$[Co(mpox)_2(\gamma\text{-Epy})_2]$	61.79 (61.88)	5.76 (5.89)	15.58 (15.47)	10.75 (10.84)
$[Ni(mpox)_2(py)_2]$	59.29 (59.17)	4.85 (4.93)	17.12 (17.25)	12.20 (12.06)
$[Ni(mpox)_2(\alpha\text{-pic})_2]$	60.75 (60.61)	5.60 (5.44)	16.40 (16.32)	11.52 (11.40)
$[Ni(mpox)_2(\beta\text{-pic})_2]$	60.69 (60.61)	5.62 (5.44)	16.45 (16.32)	11.60 (11.40)
$[Ni(mpox)_2(\gamma\text{-pic})_2]$	60.72 (60.61)	5.70 (5.44)	16.47 (16.32)	11.54 (11.40)
$[Ni(mpox)_2(\alpha\text{-Epy})_2]$	61.98 (61.91)	5.96 (5.89)	15.35 (15.47)	10.89 (10.81)
$[Ni(mpox)_2(\beta\text{-Epy})_2]$	61.85 (61.91)	5.92 (5.89)	15.58 (15.58)	10.92 (10.81)
$[Ni(mpox)_2(\gamma\text{-Epy})_2]$	61.86 (61.91)	5.75 (5.89)	15.60 (15.58)	10.90 (10.81)

* pox^- = anion of pyridine-2-aldoxime; $mpox^-$ = anion of 6-methylpyridine-2-aldoxime; py = pyridine; pic = α-, β-, γ-picolines; Epy = α-, β-, γ-ethylpyridines

and heated to boiling under continuous stirring. Excess of anhydrous potassium carbonate and some amount of sodium hydroxide pellets were added to the reaction mixture and was again heated under continuous stirring for 2—3 hrs. It was soon filtered and the filtrate was allowed to cool at room temperature. The crystals so obtained were recrystallized by dissolving in chloroform, filtered to remove insoluble material and the filtrate was poured into a volume of pyridine base equal to five times the volume of chloroform used. The solution was allowed to stand overnight and the product was collected by filtration, washed with appropriate pyridine base and dried *in vacuo* over P_4O_{10}.

Characterization of Complexes

Molar conductances of 10^{-3} *M* solution of metal(II) complexes were determined at 25 °C using a Toshniwal Conductivity bridge, model CL01/01. Magnetic susceptibilities from room temperature to liquid N_2 temperature were measured on polycrystalline samples by using a standard Gouy's balance. The balance was calibrated with $Hg[Co(NCS)_4)]$. Diffuse reflectance spectra were recorded on a Cary 14 spectrophotometer equipped with a diffuse reflectance accessory using MgO as a reference material. Solution spectra were recorded on the same instrument, using 1-cm silica cells and 10^{-3} *M* solutions. Infrared spectra of free ligands and their complexes were recorded on a Perkin–Elmer 180 spectrophotometer on crystalline solids in CsI. The ^{57}Fe Mössbauer spectra were recorded on polycrystalline samples by using a constant acceleration Mössbauer spectrometer. The spectrometer was equipped with a copper matrix source which was maintained at room temperature and was calibrated with natural iron foil.

Carbon, hydrogen and nitrogen analysis results were obtained through the courtesy of the Microanalytical Division C.D.R.I., Lucknow. The metal(II) content in the complexes was estimated [3] by EDTA titrimetry using Eriochrome Black T as an indicator after destroying the organic residues first with aqua regia and then with *cc.* H_2SO_4. Molecular weights were determined cryoscopically in formamide. The analytical data of the complexes are reported in Table I.

Results and Discussion

All the complexes are quite stable at room temperature and do not exhibit any decomposition after a long period of standing. All the complexes are insoluble in water and slightly soluble in non-polar solvent but soluble in polar solvents. The molar conductance of all the complexes in EtOH at the concentration level of 10^{-3} *M* lie in the range 10—20 mhos · cm^2 · mol^{-1} suggesting [4] their non-ionic nature. Molecular weights of all the complexes in formamide show that they are monomeric complexes.

A summary of the magnetic moments of manganese(II), cobalt(II) and nickel(II) complexes at room temperature and 78 °K are presented in Table II. The iron(II) complexes are diamagnetic in nature. A plot of $1/\chi'_M$ *vs.* *T* for each of the complexes was linear within the experimental uncertainty over the temperature range studied, so no temperature independent paramagnetic correction was included in the calculation of magnetic moments. The values of Weiss constant, Θ were taken from these plots and fall in the range, —8 to —2 K for manganese(II) complexes, *ca.* 6K for cobalt(II) complexes and —8K to —2K for nickel(II) complexes.

The manganese(II) complexes exhibit temperature independent paramagnetic values in the 5.87—5.92 μ_{BM} range. These values are in the range expected for five unpaired electrons with the $^6A_{1g}/(t_{2g}{}^3e_g^2)$ ground term. Although, it is possible that other geometries of manganese(II) could show such magnetic behaviour, the propensity of manganese(II) to form six coordinate octahedral complexes would appear to rule out this possibility.

The cobalt(II) complexes exhibit magnetic moment values in the 4.78—4.60 μ_{BM} range at room temperature. These values are higher than the spin only value of 3.87 μ_{BM} expected for three unpaired electrons but lower than the values of 5.0 μ_{BM} which is generally observed for regular octahedral cobalt(II) complexes. The mechanism which best account for the lower magnetic moment values of cobalt(II) involves partial or wholly quenching of the orbital moment contribution by low symmetry ligand field components. As for other distorted octahedral high-spin cobalt(II) complexes with low-symmetry the magnetic moment values decrease to *ca.* 95% of their room temperature value at liquid N_2 temperature.

The magnetic moment values of nickel(II) complexes fall to *ca.* 95% of their room temperature value of 3.10—2.98 μ_{BM} at liquid N_2 temperature. These values are higher than the spin-only value of 2.83 μ_{BM} expected for two

Table II

Magnetic susceptibility data

Compound	T, K	χ'_M, cgsu	μ_{eff}, μ_B
$[Mn(pox)_2(py)_2]$	298.2	14.475	5.90
	78	54.960	5.88
$[Mn(pox)_2(\alpha\text{-pic})_2]$	299.7	14.450	5.91
	78	55.145	5.89
$[[Mn(pox)_2(\beta\text{-pic})_2]$	297.6	14.455	5.89
	78	54.770	5.87
$[Mn(pox)_2(\gamma\text{-pic})_2]$	298.7	14.350	5.88
	78	54.400	5.85
$[Mn(pox)_2(\alpha\text{-Epy})_2]$	299.5	14.460	5.91
	78	55.330	5.90
$[Mn(pox)_2(\beta\text{-Epy})_2]$	298.7	14.350	5.88
	78	54.770	5.87
$[Mn(pox)_2(\gamma\text{-Epy})_2]$	296.4	14.460	5.91
	78	55.144	5.89
$[Mn(mpox)_2(py)_2]$	297.5	14.560	5.91
	78	55.340	5.90
$[Mn(mpox)_2(\alpha\text{-pic})_2]$	297.6	14.460	5.89
	78	54.960	5.88
$[Mn(mpox)_2(\beta\text{-pic})_2]$	298.4	14.420	5.89
	78	54.770	5.88
$[Mn(mpox)_2(\gamma\text{-pic})_2]$	199.7	14.450	5.91
	78	55.144	5.89
$[Mn(mpox)_2(\alpha\text{-Epy})_2]$	300.0	14.385	5.90
	78	54.960	5.88
$[Mn(mpox)_2(\beta\text{-Epy})_2]$	298.2	14.475	5.90
	78	55.145	5.89
$[Mn(mpox)_2(\gamma\text{-Epy})_2]$	200.0	14.490	5.92
	78	55.340	5.90
$[Co(pox)_2(py)_2]$	297.6	8.625	4.55
	78	31.760	4.47
$[Co(pox)_2(\alpha\text{-pic})_2]$	299.2	8.470	4.52
	78	31.760	4.47
$[Co(pox)_2(\beta\text{-pic})_2]$	300.0	8.630	4.57
	78	31.900	4.48
$[Co(pox)_2(\gamma\text{-pic})_2]$	296.2	8.440	4.60
	78	31.900	4.48
$[Co(pox)_2(\alpha\text{-Epy})_2]$	296.2	8.475	4.50
	78	41.055	4.42
$[Co(pox)_2(\beta\text{-Epy})_2]$	297.2	8.600	4.54
	78	31.480	4.45
$[Co(pox)_2(\gamma\text{-Epy})_2]$	295.7	8.720	4.56
	78	32.050	4.49
$[Co(mpox)_2(py)_2]$	300.0	8.670	4.58
	78	31.760	4.47
$[Co(mpox)_2(\alpha\text{-pic})_2]$	297.4	8.590	4.54
	78	32.045	4.49
$[Co(mpox)_2(\beta\text{-pic})_2]$	295.4	8.730	4.56
	78	32.180	4.50
$[Co(mpox)_2(\gamma\text{-pic})_2]$	295.7	8.720	4.56
	78	31.900	4.48
$[Co(mpox)_2(\alpha\text{-Epy})_2]$	299.2	8.400	4.50
	78	31.060	4.42
$[Co(mpox)_2(\beta\text{-Epy})_2]$	297.4	8.590	4.54
	78	31.760	4.47

Table II (Contd.)

Compound	T, K	χ_M, cgsu	μ_{eff}, μ_B
$[Co(mpox)_2(\gamma\text{-Epy})_2]$	300.0	8.670	4.58
	78	32.045	4.49
$[Ni(pox)_2(PY)_2]$	298.0	3.990	3.10
	78	14.790	3.05
$[Ni(pox)_2(\alpha\text{-pic})_2]$	297.0	3.980	3.09
	78	14.500	3.02
$[Ni(pox)_2(\beta\text{-pic})_2]$	299.0	3.960	3.09
	78	14.210	2.99
$[Ni(pox)_2(\gamma\text{-pic})_2]$	300.0	3.840	3.05
	78	14.210	2.99
$[Ni(pox)_2(\alpha\text{-Epy})_2]$	299.0	3.960	3.09
	78	14.500	3.02
$[Ni(pox)_2(\beta\text{-Epy})_2]$	295.6	3.880	3.04
	78	14.110	2.98
$[Ni(pox)_2(\gamma\text{-Epy})_2]$	297.6	3.900	3.06
	78	14.210	2.99
$[Ni(mpox)_2(py)_2]$	299.2	3.940	3.08
	78	14.310	3.00
$[Ni(mpox)_2(\alpha\text{-pic})_2]$	297.6	4.000	3.10
	78	14.790	3.05
$[Ni(mpox)_2(\beta\text{-pic})_2]$	298.2	3.900	3.06
	78	14.030	2.97
$[Ni(mpox)_2(\gamma\text{-pic})_2]$	296.7	3.920	3.06
	78	14.310	3.00
$[Ni(mpox)_2(\alpha\text{-Epy})_2]$	297.4	3.800	3.02
	78	14.030	2.97
$[Ni(mpox)_2(\beta\text{-Epy})_2]$	297.5	3.960	3.08
	78	14.790	3.05
$[Ni(mpox)_2(\gamma\text{-Epy})_2]$	295.4	3.960	3.07
	78	14.310	3.00

unpaired electrons and are characterized to those reported for tetragonally distorted octahedral nickel(II) complexes [5].

The ^{57}Fe Mössbauer spectra of iron(II) complexes have been measured both at room temperature and liquid N_2 temperature. The values of isomer shift, δ, and quadrupole moment, ΔE_Q, derived from these spectral data are reported in Table III. The isomer shift value measures the total s-electron density at the nucleus and is given by $\delta = \frac{2}{5}\pi Ze^2[R_{ex^2} - R_{gr^2}]\{|\Psi s(0)|_{a^2} - |\Psi s(0)|_{s^2}\}$. Where the quantities have their usual meaning. In iron(II) compound the isomer shift value is in general larger for $^5T_2$ than for $^1A_1$ ground state. This fact has been interpreted [6] in terms of increased covalency of the metal-ligand bond in the $^1A_1$ state, since a larger d-electron delocalization decrease the shielding of core s electrons. The experimental isomer shift values support [6] the presence of $^1A_1$ ground state in low spin iron(II) complexes. The range of isomer shift values can be attributed to the difference in the σ-donor and π-acceptor properties of ligands. Increased d_σ and π-bonding,

Table III

Mössbauer spectral parameters for iron(II) complexes

Compound	T, K	δ^* mm/sec	ΔE_Q mm/sec	Γ_1^{**} mm/sec	Γ_2^{**} mm/sec
[Fe(pox)$_2$(py)$_2$]	*RT*	0.45	0.74	0.24	0.24
	78	0.51	0.70	0.26	0.24
[Fe(pox)$_2$(α-pic)$_2$]	*RT*	0.40	0.56	0.26	0.25
	78	0.48	0.52	0.26	0.26
[Fe(pox)$_2$(β-pic$_2$]	*RT*	0.50	0.77	0.24	0.24
	78	0.57	0.75	0.26	0.24
[Fe(pox)$_2$(γ-pic)$_2$]	*RT*	0.46	0.80	0.27	0.25
	78	0.52	0.77	0.26	0.26
[Fe(pox)$_2$(α-Epy)$_2$]	*RT*	0.38	0.50	0.26	0.25
	78	0.48	0.48	0.24	0.25
[Fe(pox)$_2$(β-Epy)$_2$]	*RT*	0.52	0.79	0.26	0.27
	78	0.59	0.76	0.26	0.28
[Fe(pox)$_2$(γ-Epy)$_2$]	*RT*	0.52	0.82	0.28	0.26
	78	0.56	0.80	0.28	0.28
[Fe(mpox)$_2$(py)$_2$]	*RT*	0.40	0.75	0.25	0.25
	78	0.48	0.71	0.26	0.25
[Fe(mpox)$_2$(α-pic)$_2$]	*RT*	0.45	0.60	0.26	0.26
	78	0.42	0.58	0.26	0.27
[Fe(mpoc)$_2$(β-pic)$_2$]	*RT*	0.50	0.80	0.26	0.25
	78	0.57	0.77	0.26	0.25
[Fe(mpox)$_2$(γ-pic)$_2$]	*RT*	0.54	0.82	0.26	0.25
	78	0.59	0.80	0.26	0.25
[Fe(mpox)$_2$(α-Epy)$_2$]	*RT*	0.33	0.54	0.28	0.25
	78	0.44	0.52	0.28	0.27
[Fe(mpox)$_2$(β-Epy)$_2$]	*RT*	0.52	0.79	0.25	0.25
	78	0.59	0.77	0.26	0.27
[Fe(mpox)$_2$(γ-Epy)$_2$]	*RT*	0.54	0.83	0.26	0.26
	78	0.60	0.81	0.27	0.28

* Relative to natural iron foil

** Full-width at half-maximum for low-velocity line, Γ_1 and for high-velocity line, Γ_2.

both tend to increase the electron density at the nucleus and, consequently decrease the isomer shift. The isomer shift values reported for the present complexes are, in general, higher compared to analogous compounds derived from dimethylglyoxime and 1,2-cyclohexane-dionedioxime, suggesting lower σ-bonding and π-back bonding properties of these ligands.

The quadrupole splitting, ΔE_Q, arises from the interaction of the ^{57}Fe nuclear quadrupole moment Q with an electric field gradient e_q in the region of the nucleus and is given by

$$\Delta E_Q = \frac{1}{2} e_q^2 Q \left(1 + \frac{1}{3}\eta^2\right)^{\frac{1}{2}}$$

where symbols have their usual meaning. From a spherical ground state like $^1A_1(t_{2g}^6)$, a very small electric field gradient and thus a small ΔE_Q will be expected. On the other hand, substantial values of ΔE_Q are obtained from T_2 terms

in the absence of octahedral symmetry. The low values of ΔE_Q as compared with high spin iron(II) complexes further support [6, 7] the presence of $^1A_1$ ground state and a significant distortion from cubic symmetry in the present iron(II) complexes. This distortion may be the result of a cooperative effect of steric factors and of bonding characteristic of the ligands. The ΔE_Q values decrease with increasing σ-bonding and increasing steric contribution but decrease with increasing π-back bonding [8]. In the present case, the nearest neighbour of the iron(II) atom are six nitrogen atoms but the spectra of the complexes vary strongly with different substituents on pyridine. While the substitution of H-atom by alkyl group in β- or γ-position of pyridine has little effect on the shape of the spectrum, the same group in the α-position of the pyridine ligands greatly changes the spectrum. This may be understood as a steric effect. Higher chemical isomer shift values and lower quadrupole splitting lead us to the conclusion that there is a large contribution from lattice to the ΔE_Q in the present complexes. The ΔE_Q values are also less compared to dimethylglyoxime and cyclohexanedione dioxime analogues.

The diffuse reflectance spectra of manganese(II) complexes have been measured at room temperature and exhibit the weak absorption bands in the 18.2—20.0, 22.5—25.5 and 23.0—26.3 kK ranges. These transition bands arising from the sextet quartet $t_{2g}e_g^2$ configuration have been assigned [9] to $^6A_{1g} \rightarrow {}^4T_{1g}(G)$; $^6A_{1g} \rightarrow {}^4T_{2g}(G)$ and $^6A_{1g} \rightarrow {}^4A_{1g}, {}^4E_g(G)$, respectively. The various ligand field parameters (Dq, B, C, β), calculated [9] from these bands, are presented in Table IV, which confirm [9] the octahedral ligand field geometry in these manganese(II) complexes. In addition to the bands mentioned above, the additional bands are observed in the 27.0—40.0 kK range and are common in the spectra of all the metal(II) complexes. These are assigned as intra-ligand electronic transitions.

The diffuse reflectance spectra of iron(II) complexes exhibit an intense band in the region of 16.6—17.9 kK with a weak band at its lower side at *ca.* 9.0 kK. These bands have been assigned [9] to $^1A_{1g} \rightarrow {}^1T_{1g}$ and $^1A_{1g} \rightarrow {}^3T_{1g}$. respectively. Other ligand field transition bands are not observed probably due to overlap by intense charge-transfer bands. Assuming $C = 4B$ the various ligand field parameters (Dq, B, β) have been calculated [8] using the following equations:

$$E(^1A_{1g} \rightarrow {}^1T_{1g}) = 10\,\mathrm{Dq} - C + \frac{86\,B^2}{10\,\mathrm{Dq}} \tag{1}$$

$$E(^1A_{1g} \rightarrow {}^3T_{1g}) = 10\,\mathrm{Dq} - 3\,C + \frac{50\,B^2}{10\,\mathrm{Dq}}. \tag{2}$$

The values are reported in Table V. From the values of β covalency factor, it is clear that there is a regular gradiation as we move down from axial

Table IV

Electronic spectral data of manganese(II) complexes

Compound	$^6A_{1g} \rightarrow {}^4T_{1g}(G)$	$^6A_{1g} \rightarrow {}^4T_{2g}(G)$	$^6A_{1g} \rightarrow {}^4A_{1g}, {}^4E_g(G)$	Dq	B	C	β^*	ν_1^{**}	ν_2^{**}	ν_3^{**}
$[Mn(pox)_2(py)_2]$	18.2	22.5	23.0	0.7	0.6	3.4	0.62	18.06	22.24	23.0
$[Mn(pox)_2(\alpha\text{-pic})_2]$	18.4	22.5	23.2	0.7	0.6	3.45	0.62	18.36	22.54	23.25
$[Mn(pox)_2(\beta\text{-pic})_2]$	18.2	22.7	23.5	0.72	0.62	3.45	0.64	18.31	22.63	23.45
$[Mn(pox)_2(\gamma\text{-pic})_2]$	18.4	22.7	23.6	0.72	0.62	3.47	0.64	18.43	22.75	23.55
$[Mn(pox)_2(\alpha\text{-Epy})_2]$	19.0	23.2	24.6	0.75	0.64	3.6	0.66	19.08	23.54	24.4
$[Mn(pox)_2(\beta\text{-Epy})_2]$	18.8	23.4	24.4	0.78	0.64	3.6	0.66	18.83	23.32	24.4
$[Mn(pox)_2(\gamma\text{-Epy})_2]$	18.8	23.3	24.5	0.8	0.65	3.6	0.67	18.72	23.29	24.5
$[Mn(mpox)_2(py)_2]$	18.5	22.7	23.8	0.73	0.62	3.5	0.64	18.53	22.66	23.7
$[Mn(mpox)_2(\alpha\text{-pic})_2]$	18.3	22.6	23.6	0.74	0.6	3.5	0.62	18.33	22.55	23.5
$[Mn(mpox)_2(\beta\text{-pic})_2]$	19.07	23.4	24.3	0.74	0.62	3.6	0.64	19.04	23.38	24.2
$[Mn(mpox)_2(\gamma\text{-pic})_2]$	19.1	23.3	24.3	0.74	0.62	3.6	0.64	19.04	23.38	24.2
$[Mn(mpox)_2(\alpha\text{-Epy})_2]$	19.2	23.9	24.5	0.8	0.62	3.7	0.64	19.15	23.9	24.7
$[Mn(mpox)_2(\beta\text{-Epy})_2]$	19.5	24.0	25.5	0.82	0.64	3.8	0.66	19.7	24.22	25.4
$[Mn(mpox)_2(\gamma\text{-Epy})_2]$	20.0	25.5	26.3	0.82	0.65	4.0	0.67	20.96	25.54	26.5

* $B_0 = 0.917$ kK; ** Calcd.

Table V

Electronic spectral data of iron(II) complexes

Compound	$^1A_{1g} \rightarrow {}^3T_{1g}$	$^1A_{1g} \rightarrow {}^1T_{1g}$	Dq	B	β^*	ν_1^{**}	ν_2^{**}
$[Fe(pox)_2(py)_2]$	8.98	16.60	1.65	0.78	0.85	8.98	16.55
$[Fe(pox)_2(\alpha\text{-pic})_2]$	8.94	16.8	1.66	0.80	0.87	8.92	16.65
$[Fe(pox)_2(\beta\text{-pic})_2]$	9.4	17.48	1.72	0.82	0.89	9.31	17.3
$[Fe(pox)_2(\gamma\text{-pic})_2]$	9.01	17.2	1.68	0.82	0.89	8.96	16.96
$[Fe(pox)_2(\alpha\text{-Epy})_2]$	9.3	16.96	1.67	0.80	0.87	9.0	16.8
$[Fe(pox)_2(\beta\text{-Epy})_2]$	9.08	17.32	1.69	0.82	0.89	9.05	17.06
$[Fe(pox)_2(\gamma\text{-Epy})_2]$	9.5	17.8	1.74	0.84	0.91	9.34	17.52
$[Fe(mpox)_2(py)_2]$	9.02	16.94	1.66	0.80	0.87	8.92	16.71
$[Fe(mpox)_2(\alpha\text{-pic})_2]$	8.98	17.4	1.68	0.83	0.90	8.9	17.00
$[Fe(mpox)_2(\beta\text{-pic})_2]$	9.25	17.5	1.72	0.84	0.91	9.17	17.36
$[Fe(mpox)_2(\gamma\text{-pic})_2]$	9.3	17.6	1.70	0.84	0.91	8.99	17.20
$[Fe(mpox)_2(\alpha\text{-Epy})_2]$	9.2	17.8	1.73	0.86	0.93	9.11	17.53
$[Fe[mpox)_2(\beta\text{-Epy})_2]$	9.1	17.7	1.72	0.86	0.93	9.03	17.45
$[Fe(mpox)_2(\gamma\text{-Epy})_2]$	9.5	17.9	1.75	0.87	0.94	9.31	17.8

* $B_0 = 0.971$ kK; ** Calcd.

ligands pyridine to ethylpyridines. The complexes $[Fe(L)_2(py)_2]$ have the least value of β (most covalent) while $[Fe(L)_2(\gamma\text{-Epy})_2]$ have maximum value of β (least covalent). This leads to the conclusion that steric hindrance introduced by alkyl groups in the pyridines plays a role in the covalent nature of the complexes.

The diffuse reflectance spectra of cobalt(II) complexes are characteristic [9] of distorted, octahedral, high-spin cobalt(II) complexes and exhibit three ligand field transition bands in the 8.3—9.1, 18.02—19.5 and 20.6—22.4 kK regions in addition to intra-ligand bands. The lowest energy ligand field band is assigned [9] to ν_1, the $^4T_{1g}(F) \rightarrow {}^4T_{2g}(F)$ transition. The band 18.02—19.5 kK is assigned to ν_2, the $^4T_{1g}(F) \rightarrow {}^4A_{2g}(F)$ transition and the band 20.6—22.4 kK is assigned to ν_3, the $^4T_{1g}(F) \rightarrow {}^4T_{1g}(P)$ transition. A least squares fit of these experimental band positions to the electrostatic matrix elements of McClure [10] gives the parameters and calculated values of ν_1, ν_2 and ν_3 and are reported in the Table VI. A Dq value of 1.0 kK is common for octahedral cobalt(II) complexes as is a nephelauxetic parameter, β of 0.8—0.9.

The diffuse reflectance spectra of nickel(II) complexes exhibit the features associated with the spectrum of distorted high-spin, octahedral nickel(II) complexes [11]. The present nickel(II) complexes exhibit two low intensity ligand field bands in the 11.6—12.7 and 18.4—20.24 kK ranges in

Table VI

Electronic spectral data of cobalt(II) complexes

Compound	ν_1	ν_2	ν_3	Dq	B	β^*	ν_1^{**}	ν_2^{**}	ν_3^{**}
$[Co(pox)_2(py)_2]$	8.3	18.02	20.6	0.96	0.89	0.91	8.4	18.025	20.6
$[Co(pox)_2(\alpha\text{-pic})_2]$	8.5	18.02	20.5	0.97	0.89	0.91	8.51	18.21	20.68
$[Co(pox)_2(\beta\text{-pic})_2]$	8.6	18.4	20.7	0.99	0.90	0.92	8.69	18.59	20.99
$[Co(pox)_2(\gamma\text{-pic})_2]$	8.6	18.6	21.2	0.99	0.92	0.94	8.68	18.58	21.27
$[Co(pox)_2(\alpha\text{-Epy})_2]$	8.82	18.5	21.5	1.01	0.94	0.96	8.85	18.96	21.71
$[Co(pox)_2(\beta\text{-Epy})_2]$	8.9	19.2	21.6	1.02	0.94	0.96	8.95	19.15	21.8
$[Co(pox)_2(\gamma\text{-Epy})_2]$	9.0	19.4	21.9	1.03	0.94	0.96	9.04	19.34	21.9
$[Co(mpox)_2(py)_2]$	8.4	17.95	20.8	0.96	0.91	0.93	8.4	18.02	20.85
$[Co(mpox)_2(\alpha\text{-pic})_2]$	8.5	18.2	20.9	0.97	0.92	0.94	8.5	18.2	21.09
$[Co(mpox)_2(\beta\text{-pic})_2]$	8.4	18.0	21.3	0.97	0.94	0.96	8.5	18.18	21.4
$[Co(mpox)_2(\gamma\text{-pic})_2]$	8.6	18.2	21.7	0.99	0.95	0.97	8.67	18.6	21.54
$[Co(mpox)_2(\alpha\text{-Epy})_2]$	8.87	18.7	21.5	1.01	0.95	0.97	8.87	18.97	21.85
$[Co(mpox)_2(\beta\text{-Epy})_2]$	9.0	19.2	22.2	1.04	0.96	0.98	9.12	19.53	22.11
$[Co(mpox)_2(\gamma\text{-Epy})_2]$	9.1	19.5	22.4	1.05	0.96	0.98	9.21	19.72	22.34

* $B_0 = 0.97$ kK; ** Calcd.

Table VII

Electronic spectral data (kK) nickel(II) complexes

Complex	ν_2	ν_1	B	β^*	10 Dq	ν_2^{**}	ν_3^{**}	ν_2/ν_1
$[Ni(pox)_2(py)_2]$	18.4	11.5	0.89	0.82	11.6	18.4	29.66	1.58
$[Ni(pox)_2(\alpha\text{-pic})_2]$	18.57	11.7	0.90	0.83	11.7	18.6	29.9	1.58
$[Ni(pox)_2(\beta\text{-pic})_2]$	18.7	11.8	0.94	0.86	11.8	18.8	30.55	1.58
$[Ni(pox)_2(\gamma\text{-pic})_2]$	18.8	11.9	0.92	0.85	11.9	19.0	30.66	1.58
$[Ni(pox)_2(\alpha\text{-Epy})_2]$	19.2	12.2	0.94	0.86	12.2	19.4	31.33	1.58
$[Ni(pox)_2(\beta\text{-Epy})_2]$	19.78	12.5	0.96	0.88	12.5	19.8	31.99	1.58
$[Ni(pox)_2(\gamma\text{-Epy})_2]$	19.6	12.3	0.95	0.87	12.3	19.64	31.66	1.59
$[Ni(mpox)_2(py)_2]$	18.57	11.7	0.90	0.83	11.7	18.60	29.99	1.58
$[Ni(mpox)_2(\alpha\text{-py})_2]$	18.7	11.96	0.92	0.85	11.96	18.69	30.66	1.56
$[Ni(mpox)_2(\beta\text{-py})_2]$	19.4	12.2	0.94	0.86	12.2	19.4	31.33	1.59
$[Ni(mpox)_2(\gamma\text{-py})_2]$	19.2	12.09	0.93	0.84	12.09	12.22	30.99	1.59
$[Ni(mpox)_2(\alpha\text{-Epy})_2]$	19.8	12.5	0.96	0.88	12.5	19.85	31.99	1.58
$[Ni(mpox)_2(\beta\text{-Epy})_2]$	20.04	12.6	0.97	0.89	12.6	20.0	32.33	1.59
$[Ni(mpox)_2(\gamma\text{-Epy})_2]$	20.24	12.7	0.98	0.90	12.7	20.19	32.66	1.59

* $B_0 = 1.084$ kK; ** Calcd.

addition to intense intra-ligand absorption bands. These bands are assigned to $^3A_{2g}(F) \rightarrow {}^3T_{2g}(F)$ (11.6—12.7 kK) and $^3A_{2g}(F) \rightarrow {}^3T_{1g}$ (18.4—20.24 kK). The presence of very intense intra-ligand transition bands into visible region obscures the weak transition ν_3, $^3A_{2g}(F) \rightarrow {}^3T_{1g}(P)$. By using these assignments, the values of ligand field parameters (Dq, B and β) were calculated by using the expressions of KONIG [12] and are presented in Table VII.

The infrared spectra of free ligands, Hpox and Hmpox differ from that of conventional oximes, which show ν(OH) band of NOH around at 3250 cm^{-1}. This ν(OH) band is replaced by multiple bands between 3194 and 2791 cm^{-1} in Hpox and Hmpox ligands, the strongest of which lies at 2791 cm^{-1}. This implies [13] much stronger intermolecular hydrogen-bonding in Hpox and Hmpox than in other oximes. None of the present complexes exhibits any band in the region 3600—2800 cm^{-1} indicating [14] the ionization of the protons of two NOH groups and Hpox and Hmpox.

The free ligands exhibit the ν(C=N) acyclic and ν(N—O) stretching vibrations at *ca.* 1520 and *ca.* 985 cm^{-1}, respectively. In the present complexes the ν(C=N) acyclic and ν(N—O) stretching frequency are observed at *ca.* 1500 and *ca.* 1200 cm^{-1}, respectively. The greater shifting of the ν(C=N) acyclic stretching towards the low frequency side as compared [2] with other complexes of Hpox and Hmpox, suggesting that the polarity of the nitrogen atom has been increased by the ionization of two protons of NOH groups. The coordination of pyridine nitrogen atom to the metal(II) atom is indicated [15] by shifting and splitting of the ring vibrations as is usually observed for other metal(II) complexes.

In the far infrared region Hpox and Hmpox exhibit the absorption bands at *ca.* 400 s, 380 m, 298 m and 217 mb cm^{-1}. The metal(II) complexes show bands of varying intensity at 400, 390, 360, 310 and 220 cm^{-1} assigned to ligand absorption bands. In addition to these bands, the complexes exhibit the bands at 260 vs, 250 s and 230 m cm^{-1} which are assigned [61] to metal(II)-N(ligand) and M-N(py) vibrations, respectively, suggesting the presence of *trans-* symmetry of these complexes.

*

The authors are thankful to the U.G.C., New Delhi for financial support to one of us (P.K.V.) and to the authorities of T.I.F.R., Bombay, and Delhi University, Delhi for carry out low temperature and room temperature magnetic measurements. Thanks are also due to the authorities of R.S.I.C., I.I.T., Madras and Guru Nanak Dev University, Amritsar for recording Mössbauer reflectance and infrared spectra.

REFERENCES

[1] LINDOY, L. F., LIVINGSTONE, S. E.: Coord. Chem. Rev., **2**, 1973 (1967); CHAKRAVORTHY, A.: Coord. Chem. Rev., **13**, 1 (1974)

[2] MOHAN, M., MITTAL, S. G., KHERA, H. C., SIRIVASTAVA, A. K.: Mh. Chem., **111**, 63 (1980) and references therein

[3] WELCHER, F. J.: The Analytical Uses of EDTA, Van Nostrand, New York, 1958
[4] GEARY, W. J.: Coord. Chem. Rev., **7,** 81 (1971)
[5] EARNSHAW, A.: Introduction to Magnetochemistry, Academic Press, New York, N.Y. 1968
[6] BANCROFT, G. M., PLATT, R. H.: Adv. Inorg. Radiochem., **15,** 59 (1972)
[7] MATHUR, H. B.: Spectroscopy in Inorganic Chemistry, **1,** 347 (1970)
[8] BANCROFT, G. M., MAYS, M. J., PRATER, B. E.: J. Chem. Soc. *A*, **1970,** 956
[9] LEVER, A. B. P.: Inorganic Electronic Spectroscopy, Elsevier, New York, 1968
[10] MCCLURE, D. S.: Treatise on Solid State Chemistry, Vol. **2,** N. B. Hannay, Ed., Plenum Press, New York, N.Y. 1975
[11] FERGUSON, J.: Prog. Inorg. Chem., **12,** 159 (1970)
[12] KONIG, E.: Struct. Bonding (Berlin), **9,** 175 (1971)
[13] KRAUSE, R., COLTHUP, N. S., BUSCH, D. H.: J. Phys. Chem., **65,** 2216 (1961)
[14] HOLMES, F., LEES, G., UNDERHILL, A. E.: J. Chem. Soc. *A*, **1971,** 999; MOHAN, M., PARAMHAMNS, B. D.: Trans. Metal Chem., **5,** 117 (1980)
[15] GILL, N. S., NUTTALL, R. H., SCAIFE, D. E., SHARP, D. W. A.: J. Inorg. Nucl. Chem., **18,** 79 (1961); FIGGINS, P. E., BUSCH, D. H.: J. Phys. Chem. Phys., **38,** 122 (1963); GREEN, J. H. S., KYNASTON, W., PAISLEY, H. M.: Spectrochim. Acta, **19,** 549 (1963); SINHA, S. P.: Spectrochim. Acta, **20,** 879 (1964); GILL, N. S., KINGDON, H. J.: Aust. J. Chem., **19,** 2197 (1966)
[16] FERRARO, J. R.: Low-Frequency Vibrations of Inorganic and Coordination Compounds, Plenum Press, New York 1971

Madan MOHAN
Prem K. VARSHNEY
Department of Chemistry, N.R.E.C. College, Khurja (U.P.) — 203131, India

Acta Chimica Academiae Scientiarum Hungaricae, Tomus 108 (2), pp. 161—165 (1981)

THE USE OF THE HALF NEUTRALIZATION POINT IN THE POTENTIOMETRIC DETERMINATION OF WEAK BASES IN WATER

G. PETHŐ and K. BURGER*

(Department of Inorganic and Analytical Chemistry, Eötvös Loránd University, Budapest)

Received October 17, 1980

Accepted for publication November 17, 1980

The half neutralization point was used for the evaluation of potentiometric titration curves which do not show realistic inflection points at the end-point. Weak bases, measurable otherwise only in non-aqueous media, were determined by this method in water using an acid standard solution.

Many attempts have been made to apply equilibria of weak electrolytes in potentiometric analysis. Most of these [1—5] are based on linearization of titration curves. In our previous paper [6] a procedure was suggested utilizing the fact that the equilibrium reactions can be made to proceed quantitatively by an excess of the reagent standard solution. In this way by plotting the concentration of the reagent consumed (*e.g.*, the bound proton in titration of bases) as a function of the volume of titrant saturation curves are obtained the limiting value of which being equivalent to the concentration (of *e.g.*, a base) to be determined.

Since the excess of any reactant may shift the equilibrium reaction to proceed quantitatively, choosing the half titration point (*e.g.*, the half neutralization point in titrations of weak bases) as the end-point, the excess of the weak base itself assures the quantitative protonation of 50.0% of its concentration. Thus the volume of the standard solution consumed till the half neutralization point in the titration can be used for the calculation of the base concentration.

The mV *vs* cm^3 titrant curves of the acidimetric titration of bases correspond to the lg $[H^+]$ *vs.* C_H curves (where C_H denotes the total acid concentrations added in the course of titration). Performing titrations based on one step reactions in constant ionic medium the titration curves are symmetrical around the half neutralization point according to equilibrium calculations. This was found true also by our measurements. This makes the graphic determination of the half neutralization point possible.

The length of the symmetric part of the titration curve depends on the equilibrium constant (K) of the reaction serving as the basis of the determina-

* To whom correspondence should be addressed.

Table I

The length of the symmetric part of the titration curve around the half neutralization point

K	Total concentrations (M)		Symmetric part ± % around 50.0% titration
	of the unknown	of the titrant	
10^3	0.1	1	± 9
	0.1	0.1	± 7
	0.01	0.1	± 5
	0.01	0.01	± 4
10^4	0.1	0.1	±22
	0.01	0.1	±11
	0.01	0.01	± 9
	0.001	0.01	± 5
10^5	0.1	0.1	±34
	0.01	0.1	±22
	0.01	0.01	±16
	0.001	0.01	± 9
10^6	0.1	0.1	±45
	0.01	0.1	±37
	0.01	0.01	±34
	0.001	0.01	±22

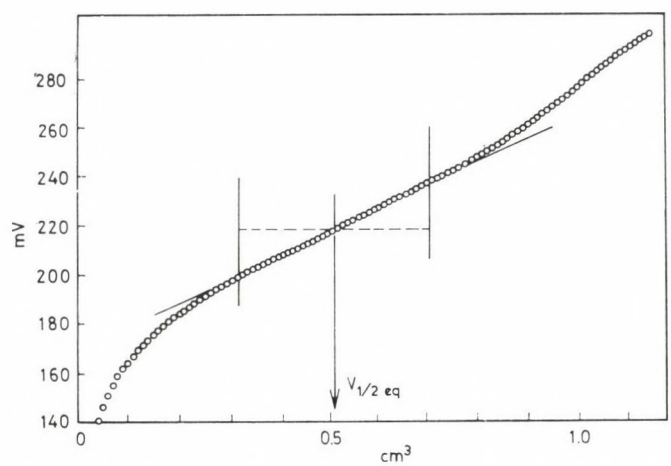

Fig. 1. The potentiometric titration curve of 10.00 cm³ 0.05 *M* nicotinamide in aqueous solution with a 0.5 *M* HCl standard solution

tion and on the total concentrations (Table I). Fitting a straight line to the symmetric part of the titration curve (Fig. 1) the middle point of the fitting section gives the half neutralization point (Evaluation A). Another method (B) for the determination of this point is based on the first derivative of the experimental titration curve (Fig. 2). For these two evaluations the knowledge of K equilibrium constant is not necessary. In the knowledge of K the half titration point can be determined by plotting $\lg K + \lg [H^+]$ *vs.* cm^3 titrant (Evaluation C). The intersection of the x axis in the coordinate system by this line gives the half neutralization point (Fig. 3). (The $\lg [H^+]$ values are calculated from the experimental electromotive force (mV) values.)

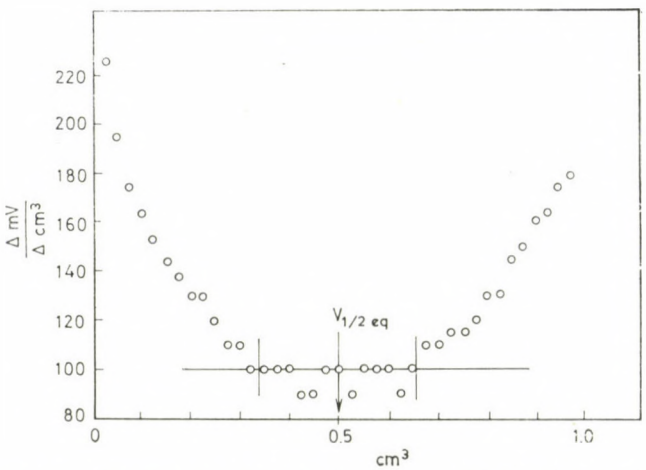

Fig. 2. The first derivative curve of the titration curve of 10.00 cm^3 0.001 M amidopyrine in aqueous solution with 0.01 M HCl standard solution

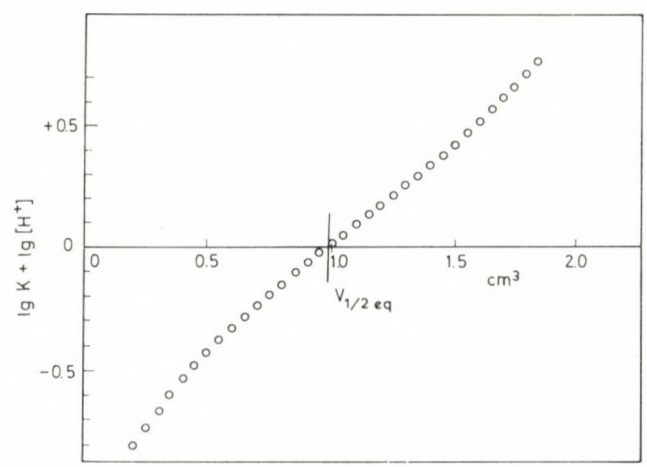

Fig. 3. The $\lg K + \lg [H^+]$ *vs* cm^3 of titrant curve for the titration of 20.00 cm^3 0.001 M sulfacetamide sodium in aqueous solution with 0.01 M HCl standard solution

Table II

The results of the acidimetric titrations of weak bases in aqueous solution

Compound	Calculated concentration (mg cm^{-3})	Evaluation A			Evaluation B			Evaluation C		
		Measured concentration (mg cm^{-3})	Observed total error (Δ%)	Standard deviation of error (%)	Measured concentration (mg cm^{-3})	Observed total error (Δ%)	Standard deviation of error (%)	Measured concentration (mg cm^{-3})	Observed total error (Δ%)	Standard deviation of error (%)
Calcium lactate	*15.42	16.04	+4.01	±0.57	16.18	+4.95	±0.25	15.23	−1.22	±0.22
	*7.710	7.874	+2.13	±0.22	7.830	+1.56	±1.63	7.496	−2.78	±0.23
Nicotinamide	*23.66	24.04	+1.60	±0.86	23.74	+0.33	±0.96	23.71	+0.18	±0.87
	*11.83	11.96	+1.14	±1.20	11.97	+1.15	±1.03	11.80	−0.77	±0.17
	*5.915	6.043	+2.17	±0.41	5.973	+0.98	±0.92	6.030	+1.94	±0.84
Amidopyrine	*22.82	23.11	+1.27	±1.05	22.65	−0.76	±1.60	23.01	+0.85	±0.69
	**2.282	2.241	−1.80	±2.01	2.288	+0.26	±0.90	2.305	+1.00	±0.98
	***0.2282	0.2277	−0.24	±2.30	0.2272	−0.43	±1.29	0.2202	−3.53	±0.97
Sulfacetamide sodium	*25.45	25.10	−1.37	±1.15	25.33	+0.33	±0.69	25.27	−0.72	±1.08
	**2.545	2.532	−0.51	±1.38	2.533	−0.46	±1.85	2.576	+1.21	±0.94
	***0.2545	0.2555	+0.41	±1.37	0.2569	+0.95	±1.19	0.2537	−0.33	±0.06

* Standard solution: 0.5 *M* HCl
** Standard solution: 0.1 *M* HCl
*** Standard solution: 0.01 *M* HCl

This latter method has the disadvantage of being sensitive to the eventual error of the ionic strength and temperature dependent K values. In the knowledge of exact K values, however, it has the advantage to give reliable results in more diluted solutions, since for the evaluation no broad symmetric section round the half neutralization point of the titration curve is needed.

To show the practical application, accuracy and reproducibility of these evaluation methods the results of the potentiometric titration of weak bases in water (measurable otherwise only in non-aqueous media) are presented in Table II.

Experimental

The amount given in Table II of the compound to be measured have been dissolved in a sodium chloride solution to get a solution of 1.0 M ionic strength. The acid standard solution was also set to 1.0 M ionic strength with sodium chloride. The titrations have been performed by a Radiometer ABU 12 automatic burette (precision ± 0.001 cm^3) using an Orion Research digital ionalyzer model 701 A and Orion pH glass electrode (91-01-00) and a Radiometer calomel electrode (K 100) in a Wilhelm bridge [7] as reference. The accuracy and reproducibility of the results is shown by the data in Table II.

REFERENCES

[1] GRAN, G.: Acta Chem. Scand., **4,** 559 (1950); Analyst, **77,** 661 (1952)
[2] INGMAN, F., STILL, E.: Talanta, **13,** 1431 (1966)
[3] BUFFLE, J.: Anal. Chim. Acta, **59,** 439 (1972)
[4] BUFFLE, J., PATHASARATHY, N., MONNIER, D.: Anal. Chim. Acta, **59,** 427 (1972)
[5] CHAKAROVA, P., BUDEVSKY, O.: Pharmazie, **30,** 524 (1975); J. Electroanal. Chem., **73,** 369 (1976)
[6] BURGER, K., PETHŐ, G., NOSZÁL, B.: Anal. Chim. Acta, **118,** 93 (1980)
[7] FORSLING, W., HIETANEN, S., SILLÉN, L. G.: Acta Chem. Scand., **6,** 905 (1952)

Gábor PETHŐ
Kálmán BURGER
H-1088 Budapest, Múzeum krt. 4/b.

Acta Chimica Academiae Scientiarum Hungaricae, Tomus 108 (2), pp. 167—182 (1981)

PYRIDAZINES CONDENSED WITH A HETERO RING, I

STRUCTURE OF PYRIDO[2,3-*d*]AMINOPYRIDAZINES, I. SEPARATION AND STRUCTURE PROOF OF THE ISOMERIC MONOCHLORO COMPOUNDS PREPARED BY HYDROLYSIS OF 5,8-DICHLOROPYRIDO[2,3-*d*]PYRIDAZINE

K. KÖRMENDY,* T. KOVÁCS,** J. SZULÁGYI,** F. RUFF and I. KÖVESDI

(*Organic Chemical Department, Eötvös Loránd University, Budapest*)

Received August 11, 1980

Accepted for publication December 1, 1980

A new method has been developed for the separation and purification of the isomeric monochloro compounds (**2**, **3**) resulting from the hydrolysis of 5,8-dichloropyrido[2,3-*d*]pyridazine (**1**). The mobility of the chlorine atoms in compound **1** depends on the conditions of the hydrolysis. In alkaline solutions compounds **2** and **3** are formed in nearly identical amounts, whereas in acid hydrolysis the ratio of isomers is shifted towards the formation of **3**. The structural position of the chlorine atom in the isomers has been verified by synthesis; the results (**2**: 8-Cl, and **3**: 5-Cl) are in accordance with the literature data. The formation of compounds such as **24**, **25** in the aminolysis of **2** and **3** substantiates the structures of the aminopyridopyridazinones made from the quinoline acid imide derivatives (*e.g.*, **21** → **24**, **25**).

Bioactivity of some of the aminophthalazinone derivatives prepared in the course of our earlier work prompted us to extend our studies on the relations between physiological action and chemical structure to pyridazine analogues condensed with hetero rings. Pyrido-pyridazine systems of pharmacological interest were examined by several research groups in the sixties [1—7]. From the aspect of our further researches, the results of NITTA and co-workers [1] are particularly important, who prepared the monochloro isomers **2**, **3** by hydrolysis of 5,8-dichloropyrido[2,3-*d*]pyridazine (**1**). Great interest is attached to these compounds not only because they afford the possibility of synthesizing various amino derivatives by aminolysis, but also because they allow rapid identification (Fig. 4) of amino derivatives with uncertain structure, obtained in other synthetic routes [8]; owing to non-selective ring cleavage of quinoline acid imides, a mixture of isomers is always expected. It is thus evident that the definite knowledge of the structures of the reference substances is indispensable for correct determination of the constitution, and this condition is fulfilled only when the structures of **2** and **3** isolated are undoubtedly known.

* To whom correspondence should be addressed.

** Parts of the diploma theses (Budapest, 1977 and 1979) of these authors are included in this paper.

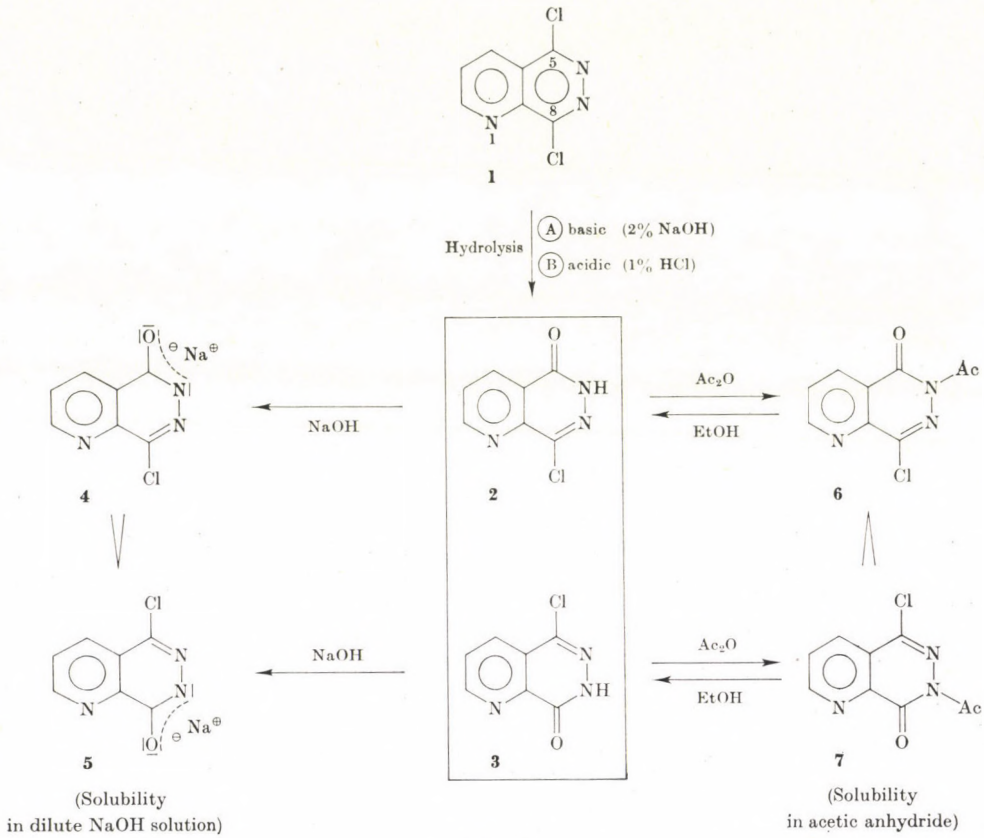

Fig. 1

NITTA *et al.* [1] inferred on the basis of theoretical considerations and quantum chemical calculations that in the hydrolysis of **1** there is a greater possibility for the formation of the C-8 chlorine derivative (**2**) (π-electron density: N-1 1.214, C-5 0.943, C-8 0.955). In alkaline media, the experimental results seemed to support this conclusion (8-Cl 66%, 5-Cl 30%). For the separation of the isomers, NITTA *et al.* utilized the difference in the solubility of the sodium salts of the monochloropyrido[2,3-*d*]pyridazinones. When reproducing their experiments, our results deviated from their data in respect of both the ratio of the isomers and their melting points. It has been found that the original method affords only partial separation (enrichment), since the sodium salt precipitated from the alkaline solution is not homogeneous and both isomers are also contained in the mother liquor.

Our modified procedure was developed on the basis of the literature method. The sodium salt of lower solubility (**5**) can easily be purified by repeated crystallization from dilute sodium hydroxide solution, and the monochloro

compound liberated from the product obtained in this way was found to be chromatographically homogeneous (**3**). For the separation and purification of the other isomer (**2**) enriched in the alkaline mother liquor, the significant difference in the solubilities of the acetylated derivatives (**6** and **7**)* has been utilized.

Under the conditions given in Experimental, only the acetyl derivative **6** separates from the acetic anhydride solution, while **7** remains dissolved. A single recrystallization from acetic anhydride gave a chromatographically homogeneous product. Deacetylation (**6** → **2**) takes place quantitatively on boiling the compound in ethanol solution.

The separation method, described in detail in Experimental (Fig. 5), made possible the isolation of the two isomers as pure substances and in excellent yields. Repeated isolation experiments have shown that in *alkaline hydrolysis* the two isomeric monochloro compounds are formed in nearly identical amounts (**2**: 49%; **3**: 48%), at variance with the literature statement; in *acid hydrolysis* the reaction is shifted towards the formation of **3** (**2**: 40%; **3**: 58%). Our results made dubious the correctness of the earlier structure assignments of the isomers (*i.e.*, that compound **2** obtained in higher amounts in the alkaline hydrolysis was considered to be the 8-Cl derivative), hence a synthetic proof of the structures became necessary.

NOVACEK *et al.* [9] obtained 4-iminopyrido[3,4-*d*]pyridazine-1(2*H*,3*H*)-one from ethyl 3-cyanoisonicotinate by treatment with hydrazine. In analogous reactions, the isomeric amino derivatives (**10** and **14**) were prepared from methyl 2-cyanonicotinate (**8**) and methyl 3-cyanopicolinate (**12**).

FALLAB and ERLENMEYER [10] verified the structures of the esters **8** and **12** by synthesis; our NMR spectroscopic work confirmed the correctness of these assignments, since according to literature data [11] on mono- and multisubstituted pyridine derivatives, the expected chemical shifts of the proton resonances in **12** is significantly higher for all the three protons than in **8**; therefore the amino compounds **10** and **14** derived from these compounds are suitable for the unambiguous determination of the site of attachment of the chlorine atom in the monochloro isomers **2** and **3**.

The hydrazino derivatives (**11**, **15**) were prepared from the two monochloro isomers by refluxing them with hydrazine. These compounds are, similarly to hydrazinophthalazinone, thermally unstable [12]. In melt they decompose with the liberation of ammonia (**11** → **10** and **15** → **14**). The product of the reaction route **2** → **11** → **10** was found to be identical with the

* In the acetylation of the chloro compounds **2** and **3** and chlorophthalazinone, the acetyl group is attached to the amide nitrogen atom, as confirmed unambiguously by the appearance of the two carbonyl bands of the diacylamide in the IR spectrum. The absence of enol ester formation accompanying aromatization indicates that the amide is the more stable tautomeric form.

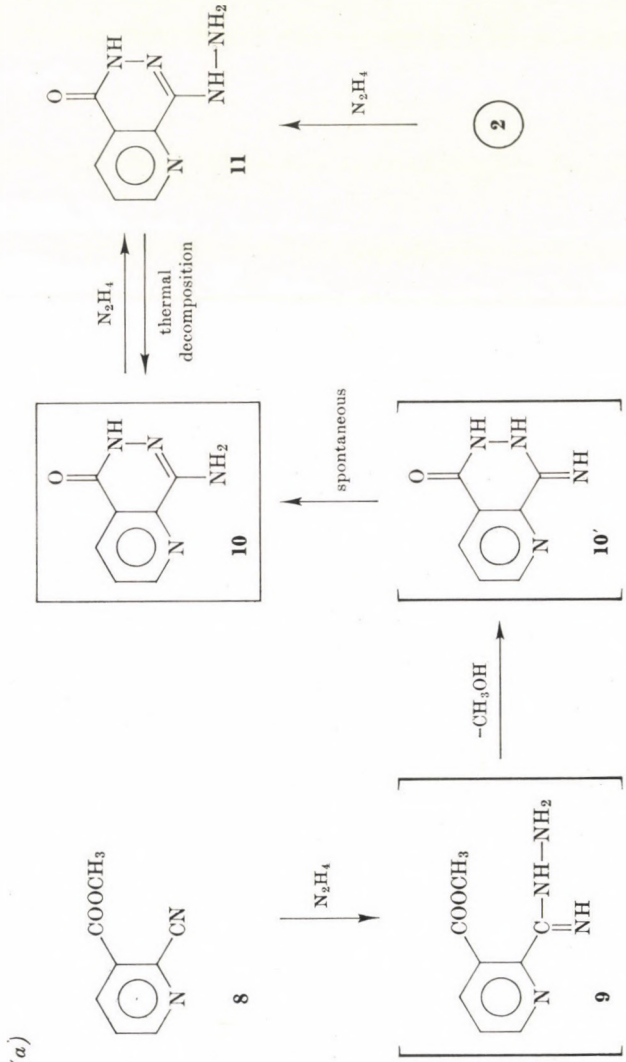
(a)
COOCH3
CN
N
8
N2H4
COOCH3
C—NH—NH2
NH
N
9
-CH3OH
O
NH
NH
N
10'
spontaneous
O
NH
N
NH2
N
10
N2H4
thermal
decomposition
O
NH
N
NH—NH2
N
11
N2H4
2

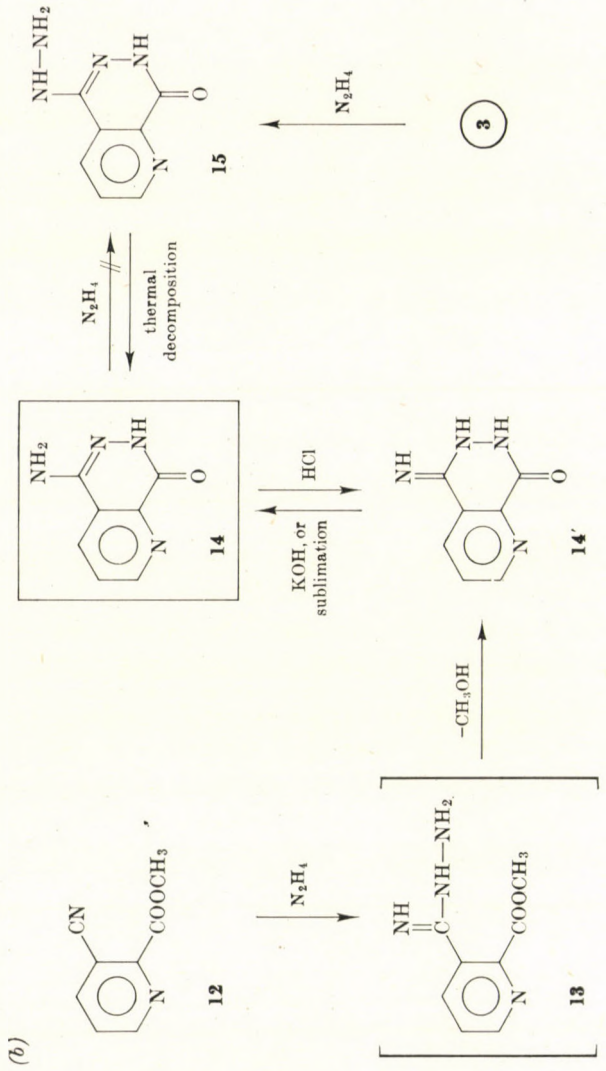
(b)
12
13
14
14'
15
3
N_2H_4
$-CH_3OH$
HCl
KOH, or sublimation
thermal decomposition

Fig. 2

product of the reactions **8** → **9** → **10**, which clearly indicates that in compound **2** the chlorine atom is attached to C-8, and in compound **3** to the C-5 atom. The counter-proof (**12** → **13** → **14** and **3** → **15** → **14**) is necessary to exclude the possibility of isomerisation taking place during the reactions. The two syntheses did not give the same product. In the thermal decomposition of **15** an amino derivative with an endocyclic C=N bond is expected (**14**), however, the product of the synthesis starting from methyl 3-cyanopicolinate (**12**) can also be a desmotropic imino compound (**14'**), as pointed out by NOVACEK [9]. The imino compound can be derived from such a precursor (**13**), in which the position of the C=N bond is given. The conversion **14'** → **14** took place on treatment with alkali or heat, and the IR spectrum of the product obtained in this way became perfectly identical with that of the amino derivative prepared from the chloro compound **3**.

No change was observed in the 8-amino derivative (**10**) on the effect of bases or mineral acids; the 5-amino compound (**14**) can be converted into the imino derivative **14'** in hydrochloric acid medium.

In the case of compound **14** and **14'**, crystal dimorphism is excluded by the observation that on crystallization from water, neither of the compounds transformed into the other. The structure of the imino compound **14'** could not be reliably confirmed by spectroscopy. Although the IR spectra of **14** and **14'** recorded in KBr pellets exhibited significant differences in the range of the NH, C=O and C=N valence vibrations, these data did not afford unambiguous evidence for one or other structure. The NMR spectra of **14** and

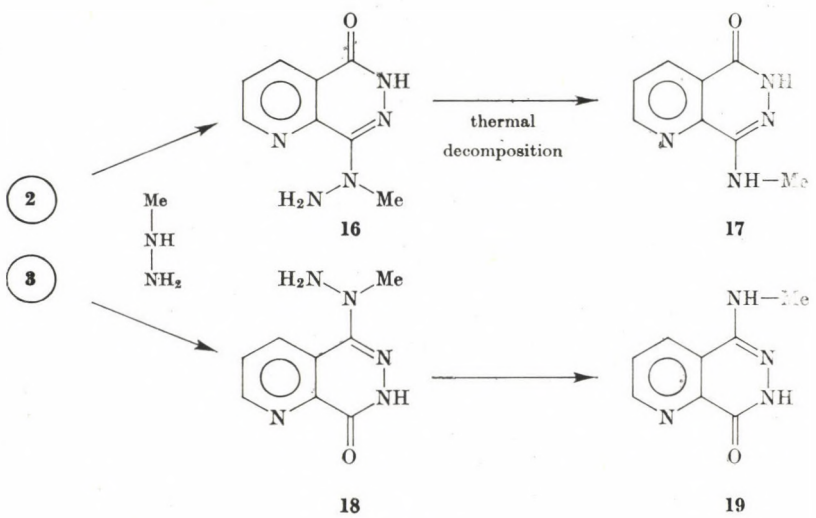

Fig. 3

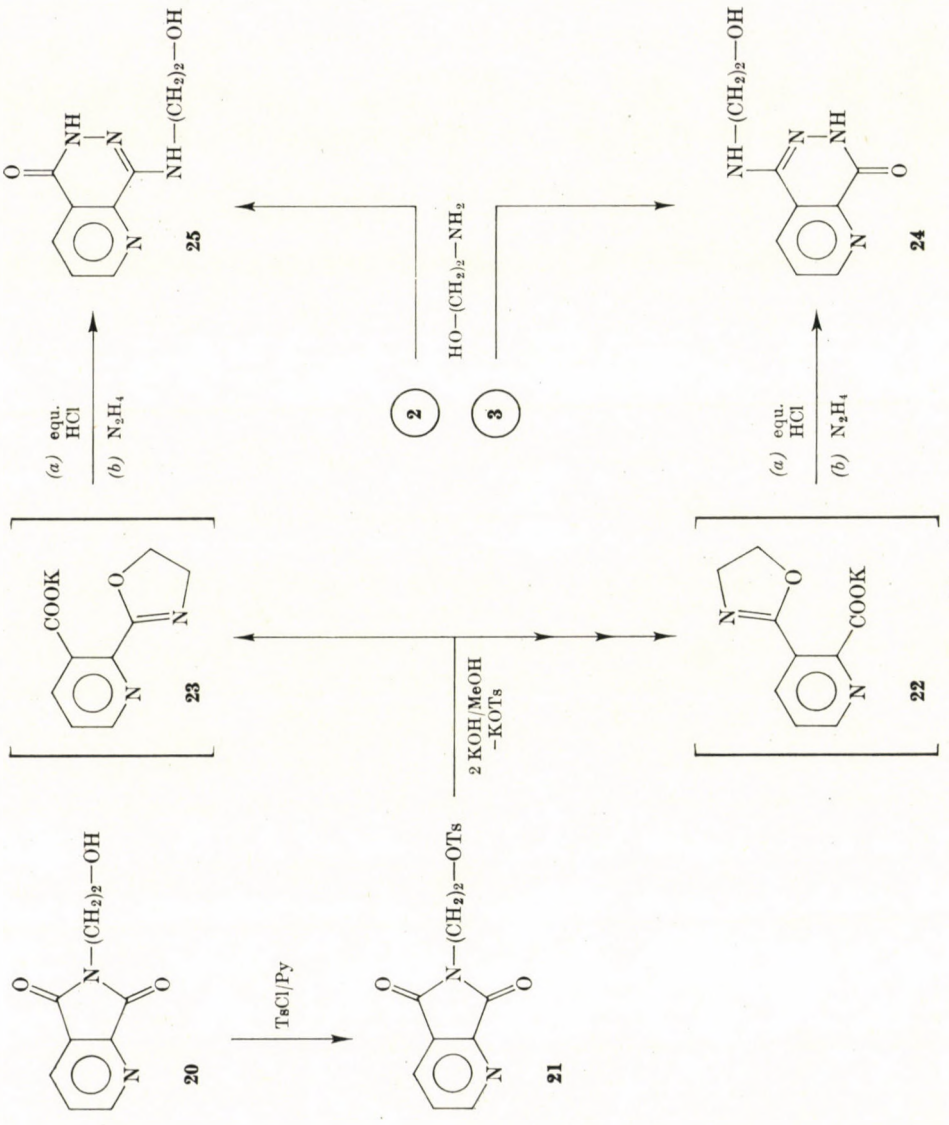
20
TsCl/Py
21
2 KOH/MeOH
–KOTs
23
22
(a) equ. HCl
(b) N_2H_4
25
24
2
3
$HO-(CH_2)_2-NH_2$

Fig. 4

14' in deuterodimethyl sulfoxide were identical confirming the structure containing the amino group. It was also verified under preparative conditions that in the DMSO $-H_2O$ solution, the partial conversion **14'** → **14** took place. In ethanol solution the UV spectra of **14'** and **14** were practically the same, but it is possible that the structural change in the position of the C=N bond causes no significant change in the spectra.

The amino compounds **10** and **14** behave differently with hydrazine. The conversion **10** → **11** takes place readily as expected [12], but refluxing of isomer **14** with hydrazine does not yield the hydrazino derivative **15**; the formation of a mixture of unknown decomposition products of brownish red colour was observed.

The monochloro isomers (**2**, **3**) readily react with methylhydrazine, too. In the products **16** and **18** the methyl group is attached to the nitrogen atom beside the ring, since the NMR signal shows no splitting. Thermal decomposition gives the methylamino derivatives **17** and **19** containing the endocyclic C=N bond. In the NMR spectra recorded in DMSO the methyl group gives rise to a doublet signal while a quartet is assigned to the NH group. The signals of the isomer containing the exocyclic C=N double bond cannot be found in the spectrum. On crystallization from the DMSO $-H_2O$ mixture, compounds **17** and **19** show no change, which indicates that they exist in the endocyclic tautomeric form also in the crystalline state.

One of the possibilities to prepare the hydroxyethylamino derivatives of pyrido[2,3-*d*]pyridazine (**24** and **25**) is the synthesis starting from the readily available tosyloxyethyl imide **21** [8]; however owing to the asymmetric structure of the imide, a mixture of isomers is necessarily formed. The mixture obtained in 93% yield can easily be separated by crystallization from water, since the solubilities of the components are greatly different. Determination of the position of the hydroxyethylamino group in the pure, separated isomers was achieved by comparison with reference substances obtained from the chloro compounds of known structure (**2** → **25** and **3** → **24**). Since the main product was the 5-(2-hydroxyethylamino) derivative (**24**) (the composition of the mixture being 87.1% of **24**, and 12.9% of **25**), the alkaline cleavage of the quinolinic acid imide (**20** and **21**) is due primarily to the rupture of the imide bond in α-position related to the pyridine nitrogen (**20** → **22**); therefore in the non-isolated intermediate* the oxazoline ring must develop at the β-C-atom of the pyridine ring. In the course of the synthesis described above, the isomeric compound **25** can be obtained in low yield only, therefore it is prepared preferably by the aminolysis procedure **2** → **25**.

* Concerning the necessarily postulated formation of the intermediates **22** and **23**, we refer to the mechanism of analogous processes [13].

Experimental

M.p.'s were measured on a Boetius micro melting point apparatus. The IR spectra were recorded in KBr pellets with a UR-10 and an IR-75 (Zeiss, Jena) spectrophotometer. NMR spectra were obtained in DMSO-D_6 solutions with a Varian A-60D instrument, and the UV spectra with a Specord UV-VIS (Zeiss, Jena) apparatus. In the TLC tests Machery—Nagel POLIGRAM^R Sil G/UV_{254} layers (8.5×2.8 cm) were used. The composition of the developing mixture was $CHCl_3$—MeOH—NH_4OH 50 : 20 : 3 *v/v*.

5,8-Dichloropyrido[2,3-*d*]pyridazine (1)

This compound was prepared from quinolinic acid hydrazide [14] according to the procedure described by NITTA *et al.* [1]. Yellow plates were obtained from a mixture of dichloromethane and petroleum ether (b.p. 40—70 °C); m.p. 168—169 °C *(lit.* [15] m.p. 163—164 °C, and [1] 169 °C). M.w. 200.0

IR (KBr): pyridine ring, $\nu C{=}N_{pyridazine}$ 1589, 1556, 1528; γCH_{Py} 793, 675 (1,2,3-trisubst.) cm^{-1}.

Separation of the hydrolysis products (2 and 3) of the dichloro compound 1 (Fig. 5)

Alkaline hydrolysis (A)

The dichloro compound **1** (20.0 g; 0.1 mole) was refluxed with 2% NaOH solution (500 mL) in a flask equipped with a reflux condenser for 30 min. The crude sodium salt (**4** < **5**) separated on cooling from the orange-red solution; for purification it was recrystallized from dilute alkali solution (4 g of Na salt/100 mL of 2% NaOH). Isomer **3** was liberated from the pure salt **5** with acetic acid.

The alkaline mother liquor of the sodium salt was acidified with acetic acid, and the suspension was evaporated to dryness on a rotary evaporator. The air-dry mixture (**2** > **3**) was refluxed with acetic anhydride (2 hrs) to effect acetylation (10 mL of acetic anhydride per 1 g of mixture). The solution was cooled and allowed to stand. The acetyl compound **6** separated after 3—4 hrs, and it was recrystallized from acetic anhydride in order to remove any contamination by the isomer **7**. Deacetylation in ethanol (**6** → **2**) occurred quantitatively to yield the chemically homogeneous isomer. The separation procedure was repeated twice with the mixture obtained from the mother liquors.

Acid hydrolysis (B)

The dichloro compound **1** (20.0 g; 0.1 mole) was refluxed with 1% hydrochloric acid (500 mL) in a flask equipped with a reflux condenser under mechanical stirring for 1 h. The resulting suspension was cooled, the crude mixture of the isomers was filtered off, and the acid mother liquor was evaporated to dryness in vacuum. The combined product was dissolved in 2% NaOH (100 mL of solution per 4 g of mixture) with heating. For the rest, the separation procedure was the same as that given for the alkaline hydrolysis. In the mixture obtained by acid hydrolysis, the isomer **3** is predominating, hence the acetylation of the hydrolysate (**2** < **3**) gives the acetyl derivative strongly contaminated with **7**. Since this makes the separation of isomers more difficult (several recrystallizations from acetic anhydride would be necessary to attain the melting point and chromatographic purity of the compound **6**), it is advisable to start in each case with preparation of the sodium salt.

For the determination of the isomer ratio, recrystallized dichloro compound was used; in other experiments the starting material was the crude product.

5-Chloropyrido[2,3-*d*]pyridazine-8(7*H*)-one (3)

The yields of experiments on the 0.1 mole scale were: 8.79 g (48.4%) (alkaline hydrolysis) and 10.57 g (58.2%) (acid hydrolysis). Colourless, long needles were obtained from water, which sublimed without decomposition at 260—280 °C (*lit.* [1] m.p. 289 °C (d.)). In a sealed Fischer cell, the powdered substance transformed into long needles at about 250 °C, then melted at 310—311 °C. R_f 0.71.

Schematic diagram of the separation of the monochloro isomers **2** and **3**

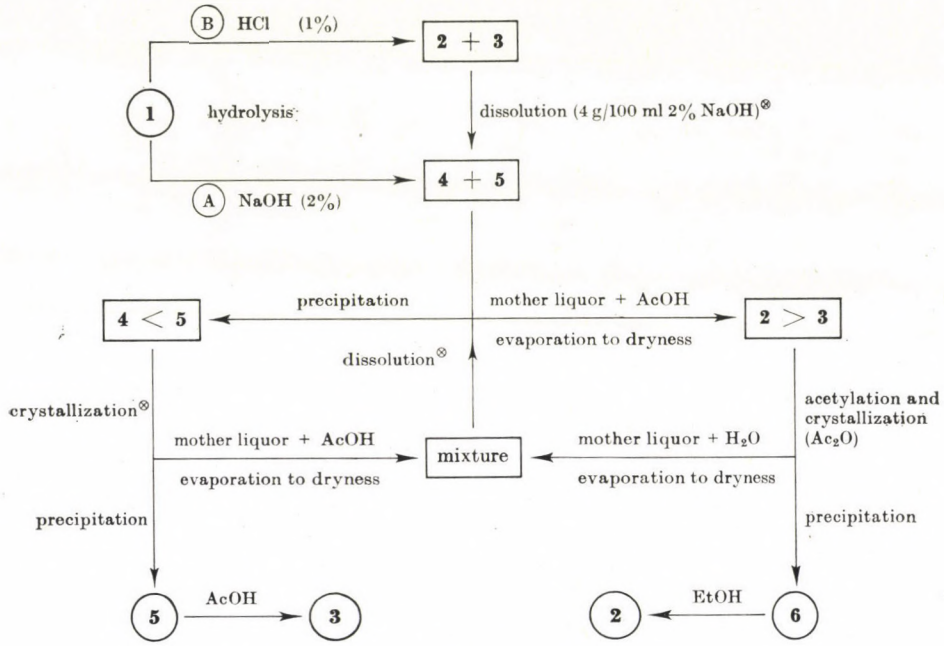

(chromatographically homogeneous isomers)

Fig. 5

$C_7H_4ClN_3O$ (181.6). Calcd. Cl 19.5. Found Cl 19.4%.

IR (KBr): νNH_{amide} 3250—2200; νCO_{amide} 1679; pyridine ring, $\nu C{=}N_{pyridazine}$ 1580, 1542; δNH 1650 (?); γCH_{Py} 802, 681 (1,2,3-trisubst.) cm^{-1}.

8-Chloropyrido[2,3-*d*]pyridazine-5(6*H*)-one (2)

The acetyl compound **6** obtained during the separation procedure (see there) was dissolved in ten parts of ethanol and refluxed with stirring for 1 h. The deacetylated product separated during refluxing in the form of colourless plates (quantitative conversion). In alkaline hydrolysis, 0.1 mole of the dichloro compound yielded 8.93 g (49.2%) of **2**, while in acid hydrolysis, the product was 7.25 g (39.9%). Colourless plates separated from water, ethanol and glacial acetic acid, prisms were obtained from tetrahydrofuran; m.p.: at 250—270 °C partial melting and sublimation without decomposition (*lit.* m.p. 275 °C [1]). In a sealed Fischer cell, the substance transformed at about 230 °C into thick columns with stripes along the longer axis, and melted at 304—305 °C. R_f 0.80.

$C_7H_4ClN_3O$ (181.6). Calcd. Cl 19.5. Found Cl 19.5%.

IR (KBr): νNH_{amide} 3300—2200; νCO_{amide} 1691; δNH 1622 (?); pyridine ring, $\nu C{=}N_{pyridazine}$ 1583, 1565 sh, 1555 sh; γCH_{Py} 786, 707 (1,2,3-trisubst.) cm^{-1}.

5-Chloro-7-acetylpyrido[2,3-*d*]pyridazine-8(7*H*)-one (7)

A mixture of **3** (1.82 g; 0.01 mole) and acetic anhydride (18 mL) was refluxed for 2 hrs. The acetylated product separated from the cold solution in the form of long needles, which transformed into large prisms on standing. The mother liquor was evaporated in vacuum

without filtering off the crystals. The dry residue was dissolved in hot acetic anhydride (5 mL) and the filtered solution was mixed with anhydrous ether (15 mL). Colourless prisms (2.02 g; 90.2%) were obtained, m.p. 158—159 °C. When refluxed in alcohol solution, the substance deacetylated rapidly (**7** → **3**).

$C_9H_6ClN_3O_2$ (223.6). Calcd. Cl 15.9. Found Cl 15.8%.

IR (KBr): νCO_{amide} 1751, 1712; pyridine ring, $\nu C{=}N_{pyridazine}$ 1595, 1575, 1549; γCH_{Py} 831, 712 (1,2,3-trisubst.) cm^{-1}.

6-Acetyl-8-chloropyrido[2,3-*d*]pyridazine-5(6*H*)-one (6)

The isomeric compound **2** (1.82 g; 0.01 mole) was acetylated with acetic anhydride (18 mL) in the manner given for **7**. The product (2.17 g; 97%) crystallized in the form of colourless small needles from a mixture of chloroform and petroleum ether (b.p. 40—70 °C), or from acetic anhydride; m.p. 158—160 °C. When refluxed with alcohol, deacetylation took place rapidly (**6** → **2**).

$C_9H_6ClN_3O_2$ (223.6). Calcd. Cl 15.9. Found Cl 15.7%.

IR (KBr): νCO_{amide} 1752, 1700; pyridine ring, $\nu C{=}N_{pyridazine}$ 1586, 1570, 1557; γCH_{Py} 789, 713 (1,2,3-trisubst.) cm^{-1}.

2-Acetyl-4-chlorophthalazine-1(2*H*)-one

Chlorophthalazinone (0.36 g; 2 mmoles) was refluxed with acetic anhydride (5 mL) for 2 hrs. The mixture which solidified on cooling was decomposed with water. The crude acetyl derivative (0.412 g; 92.5%), m.p. 152—153 °C, crystallized in the form of colourless needles with the same melting point from a mixture of chloroform and petroleum ether (b.p. 40—70 °C). Deacetylation occurred rapidly in alcohol solution.

$C_{10}H_7ClN_2O_2$ (222.7). Calcd. Cl 15.9. Found Cl 15.9%.

IR (KBr): νCO_{amide} 1750, 1690; benzene ring 1600, 1589; $\nu C{=}N_{pyridazine}$ 1561; γCH 768 cm^{-1}.

Methyl 2-cyanonicotinate (8) [10]

Colourless prisms were obtained from a mixture of methanol and petroleum ether (b.p. 40—70 °C); m.p. 89—90 °C (*lit.* [10] m.p. 89—90 °C).

$C_8H_6N_2O_2$ (162.2). Calcd. C 59.2; H 3.7; N 17.3. Found C 59.0; H 3.8; N 17.5%.

IR (KBr): νCN 2236; νCO_{ester} 1726; pyridine ring 1578, 1560; γCH_{Py} 782, 722 (1,2,3-trisubst.) cm^{-1}.

^{1}H-NMR (DMSO): δ 8.80 (H_α), 7.72 (H_β), 8.23 (H_γ), $J_{\alpha,\beta} = 5.0$, $J_{\alpha,\gamma} = 1.5$, $J_{\beta,\gamma} = 8.0$ Hz

Methyl 3-cyanopicolinate (12) [10]

Colourless needles from water m.p. 149.5—150 °C (*lit.* [10] m.p. 150—151 °C).

$C_8H_6N_2O_2$ (162.2). Calcd. C 59.2; H 3.7; N 17.3. Found C 59.1; H 3.6; N 17.4%.

IR (KBr): νCN 2229; νCO_{ester} 1721; pyridine ring 1579, 1556; γCH_{Py} 811, 698 (1,2,3-trisubst.) cm^{-1}.

^{1}H-NMR (DMSO): δ 8.92 (H_α), 7.84 (H_β), 8.47 (H_γ), $J_{\alpha,\beta} = 4.7$, $J_{\alpha,\gamma} = 1.9$, $J_{\beta,\gamma} = 8.0$ Hz.

8-Aminopyrido[2,3-*d*]pyridazine-5(6*H*)-one (10)

(*a*) Methyl 2-cyanonicotinate (0.162 g; 1 mmole) was dissolved in 98% hydrazine hydrate (1.5 mL) and refluxed for 15 min. The reaction mixture was diluted with water (10 mL), allowed to stand a few hours, then the crystals which separated were filtered off. Yellow needles attached to each other in a characteristic way (resembling feather) were obtained from water (0.095 g; 58.6%), m.p. 280—290 °C (subl.). In a sealed Fischer cell, the powdered substance transformed into prisms above 240 °C and melted at 301—302 °C.

(*b*) The 8-hydrazino compound (**11**) (3.54 g; 0.02 mole) was melted carefully over an open flame. After the evolution of gas had ceased, the melt was cooled and recrystallized from water (about 150 mL). The crystalline mixture was dried and the by-products of the pyrolysis were removed by fractional sublimation in the vacuum produced by a water suction

pump, on a bath of 180—190 °C temperature. The residue, whose sublimation temperature is above 200 °C, crystallized from water in the characteristic form described under (*a*) after clarification with carbon. The yield was 1.30 g (40%), m.p. identical with that of the product prepared according to (*a*).

$C_7H_6N_4O$ (162.2). Calcd. N 34.5. Found N 34.7%.

IR (KBr): νNH_2 3380, 3280; νNH_{amide} 3250—2200; νCO_{amide} 1668; $\nu C{=}N$, δNH_2 1626; pyridine ring 1586, 1560; γCH_{Py} 800, 710 (1,2,3-trisubst.) cm^{-1}.

^{1}H-NMR (DMSO): γ 11.83 (s, —CO—NH—), 6.22 (s, $-NH_2$), 9.24 (H_α), 8.03 (H_β), 8.72 (H_γ), $J_{\alpha,\beta} = 4.9$, $J_{\alpha,\gamma} = 1.9$, $J_{\beta,\gamma} = 8.2$ Hz.

UV (EtOH): λ_{max} nm (log ε): 210 (4.29), 217 (4.13), 265 (3.68), 333 (3.58).

The IR spectra of the products obtained according to procedures (*a*) and (*b*) were identical; the substances suffered no change during sublimation, or when treated with 2% KOH solution or hydrochloric acid.

Schiff base: Compound **10** (0.162 g; 1 mmole) was refluxed with benzaldehyde (5 mL) for 2 hrs, whereupon a red solution formed. The excess aldehyde was removed by distillation in vacuum, the residual mass was extracted with hot petroleum ether (b.p. 80—120 °C), the undissolved residue dissolved in chloroform and washed with sodium hydrogen carbonate solution. The evaporation residue of the solution after washing (0.38 g, theoretical yield 0.35 g) was a honey-like material of red colour, which could not be crystallized. It was well soluble in ethyl acetate and insoluble in gasoline fractions. On treatment with dilute hydrochloric acid it decomposed to give benzaldehyde and the 8-amino compound (**10**) with unchanged IR spectrum.

5-Iminopyrido[2,3-*d*]pyridazine-8(6*H*,7*H*)-one (14')

(*a*) Methyl 3-cyanopicolinate (**12**) (0.81 g; 5 mmoles) was refluxed with 98% hydrazine hydrate (5 mL) for 15 min., and diluted with water (10 mL) to obtain the crude product (0.65 g; 80.2%). It crystallized as yellow needles from water, m.p. 330—331 °C.

(*b*) A dilute hydrochloric acid solution of the 5-amino compound (**14**) was refluxed for 30 min, cooled and carefully neutralized with ammonium hydroxide. The substance melted at 330—331 °C after recrystallization from water.

According to the IR spectrum, the substance recrystallized from DMSO was a mixture of **14'** and **14**.

$C_7H_6N_4O$ (162.2). Calcd. N 34.5. Found N 34.7%.

IR (KBr): νNH, νNH_{amide} 3550—2200; νCO_{amide} 1674; $\nu C{=}N$ *(exo)* 1630; pyridine ring 1590, 1553; γCH_{Py} 792, 708 (1,2,3-trisubst.) cm^{-1}.

^{1}H-NMR (DMSO): δ11.82 (s, —CO—NH—), 6.14 (s, $-NH_2$), 9.12 (H_α), 7.97 (H_β), 8.60 (H_γ), $J_{\alpha,\beta} = 4.5$, $J_{\alpha,\gamma} = 1.5$, $J_{\beta,\gamma} = 8.0$ Hz.

UV (EtOH): λ_{max} nm (log ε): 210 (4.34), 217 (4.15), 265 (3.72), 333 (3.57).

5-Aminopyrido[2,3-*d*]pyridazine-8(7*H*)-one (14)

(*a*) The imino compound **14'** underwent tautomeric change when refluxed in 2% potassium hydroxide for 1 h; the product which precipitated on neutralization was recrystallized from water to give yellow needles, m.p. 320—330 °C (subl.). In a sealed Fischer cell it melted at 340 °C.

(*b*) The 5-hydrazino compound (**15**) (0.531 g; 3 mmoles) was melted in a test tube over an open flame till the cessation of gas evolution, then recrystallized from water (30 mL). For further purification, the material was subjected to sublimation in the vacuum produced by a water suction pump (bath temperature 300 °C). The sublimate crystallized from water in the form of yellow needles (0.221 g; 45.5%), the m.p. was the same as that of the product prepared by method (*a*).

(*c*) The imino compound **14'** tautomerized to give the amino compound **14** on repeated sublimations.

The products obtained by tautomerism (procedures (*a*) and (*c*)) and by pyrolysis (*b*) had the same IR spectrum.

$C_7H_6N_4O$ (162.2). Calcd. N 34.5. Found N 34.8%.

IR (KBr): νNH_2 3392, 3298; νNH_{amide} 3250—2400; νCO_{amide} 1675; δNH_2, $\nu C{=}N$ 1625; pyridine ring 1587, 1552; γCH_{Py} 818, 708 (1,2,3-trisubst.) cm^{-1}.

^{1}H-NMR (DMSO): identical with that of compound **14'**.

UV (EtOH): λ_{max} nm (log ε): 210 (4.30), 217 (4.14), 263 (3.71), 333 (3.55).

8-Hydrazinopyrido[2,3-*d*]pyridazine-5(6*H*)-one (11)

(*a*) The 8-Cl compound (**2**) (3.62 g; 0.02 mole) was dissolved in 98% hydrazine hydrate (20 mL) with heating, and the solution was gently refluxed for 1 h. After a few minutes the separation of the reaction product began. Water (200 mL) was added, then the sulfur-yellow needles were filtered off (3.44 g; 97.2%), m.p. 291—293 °C (d). The product can be recrystallized from much water, but the decomposition point remains unchanged.

(*b*) 6-Acetyl-8-chloropyrido[2,3-*d*]pyridazine-5(6*H*)-one (**6**) (2.23 g; 0.01 mole) was added in small portions to 98% hydrazine hydrate (10 mL) stirred mechanically. A yellow suspension was obtained while a strong increase of temperature could be observed; the suspension was then gently refluxed for 1 h. On dilution with water (100 mL) the hydrazino compound (1.74 g; 98.2%) separated, m.p. 290—292 °C (d.).

(*c*) 8-Aminopyrido[2,3-*d*]pyridazine-5(6*H*)-one (**10**) (0.162 g; 1 mmole) or methyl 2-cyanonicotinate (**8**) (0.162 g; 1 mmole) was refluxed for 6 hrs with 98% hydrazine hydrate (1.5 mL). On dilution with water (15 mL) the product separated (0.124 g; 70%). It was filtered off and recrystallized from water; yellow needles, m.p. 290—292 °C (d.). This product was identical with the substances obtained in procedures (*a*) and (*b*).

$C_7H_7N_5O$ (177.2). Calcd. N 39.5. Found N 39.7%.

IR (KBr): νNH_2 3346, 3318 (in intramolecular H-bridge with the N_{Py}); νNH, νNH_{amide} 3280—2200; νCO_{amide} 1658; pyridine ring, $\nu C{=}N_{pyridazine}$ 1602, 1572; δNH 1505; γCH_{Py} 800, 718 (1,2,3-trisubst.) cm^{-1}.

UV (H_2O): λ_{max} nm (log ε): 209 (4.35), 266 (3.73), 325 (3.55).

5-Hydrazinopyrido[2,3-*d*]pyridazine-8(7*H*)-one (15)

A mixture of **3** (1.81 g; 0.01 mole) and hydrazine hydrate (10 mL; 98%) was refluxed for 1 h. The precipitation of **15** started from the orange yellow solution in about 5 min. After dilution with water (100 mL) the product was filtered off (1.60 g; 90.4%). Crystallization from water (about 160 mL) gave pale yellow needles which suffered discolouration in air; m.p. 285—287 °C (d.).

$C_7H_7N_5O$ (177.2). Calcd. N 39.5. Found N 39.6%.

IR (KBr): νNH_2, νNH, νNH_{amide} 3250—2200; νCO_{amide} 1662; pyridine ring, $\nu C{=}N_{pyridazine}$ 1609, 1583, 1553; δNH 1515; γCH_{Py} 782, 718 (1,2,3-trisubst.) cm^{-1}.

UV (H_2O): λ_{max} nm (log ε): 210 (4.37), 264 (3.74), 322 (3.52).

Compound **15** could not be prepared by the hydrazinolysis of **14**; the reaction yielded a dark red reaction product which was not studied further.

8-(1-Methylhydrazino)pyrido[2,3-*d*]pyridazine-5(6*H*)-one (16)

A mixture of the 8-chloro compound (**2**) (3.62 g; 0.02 mole) and methylhydrazine (15 mL) was refluxed for 2 hrs. The product crystallized about the end of refluxing. The excess methylhydrazine was removed by distillation under reduced pressure. The evaporation residue was mixed with some water and filtered off. The halogen-free crude product (3.53 g; 92.4%) was crystallized from water (100 mL) to obtain yellow needles, m.p. 215—217 °C (d.).

$C_8H_9N_5O$ (191.2). Calcd. N 36.6. Found N 36.8%.

IR (KBr): νNH_2 3322, 3205; νNH_{amide} 3200—2500; νCO_{amide} 1674; δNH_2 1597; pyridine ring, $\nu C{=}N_{pyridazine}$ 1578, 1552; γCH_{Py} 801, 748 (1,2,3-trisubst.) cm^{-1}.

^{1}H-NMR (DMSO): δ12.14 (s, —CO—NH—), 5.02 (s, $—NH_2$), 3.05 (s, $N—CH_3$), 9.09 (H_α), 7.83 (H_β), 8.57 (H_γ), $J_{\alpha,\beta} = 4.5$, $J_{\alpha,\gamma} = 2.0$, $J_{\beta,\gamma} = 8.0$ Hz.

5-(1-Methylhydrazino)pyrido[2,3-*d*]pyridazine-8(7*H*)-one (18)

A mixture of methylhydrazine (15 mL) and the 5-chloro compound (**3**) (3.62 g; 0.02 mole) was refluxed for 2 hrs. After removal of the excess methylhydrazine by distillation in the vacuum of a water suction pump, a crude product (3.22 g; 84.3%; halogen-free) was obtained, which crystallized in the form of yellow needles from water, which transformed at 240—250 °C with melting and evolution of gas into needles; these melted then at 345—348 °C with decomposition.

$C_8H_9N_5O$ (191.2). Calcd. N 36.6. Found N 36.9%.

IR (KBr): νNH_2 3307, 3243, 3189; νNH_{amide} 3350—2500; νCO_{amide} 1660; δNH_2 1629; pyridine ring, $\nu C{=}N_{pyridazine}$ 1589, 1548; γCH_{Py} 807, 776, 748 (1,2,3-trisubst.) cm^{-1}.

^{1}H-NMR (DMSO): δ 12.01 (s, —CO—NH—), 4.62 (s, $-NH_2$), 2.98 (s, $N-CH_3$), 9—8.75 (m, H_α, H_γ), 7.85 (H_β), $J_{\alpha,\beta} = 4.2$, $J_{\beta,\gamma} = 8.2$ Hz.

8-Methylaminopyrido[2,3-*d*]pyridazine-5(6*H*)-one (17)

The 8-methylhydrazino derivative (**16**) (0.573 g; 3 mmoles) was fused on a bath heated to 240 °C until no more gas evolved (10—15 min). The product crystallized as yellow needles from water (0.447 g; 84.5%), m.p. 240—241 °C.

$C_8H_8N_4O$ (176.2). Calcd. N 31.8. Found N 31.9%.

IR (KBr): νNH 3428; νNH_{amide} 3330—2400; νCO_{amide} 1683; pyridine ring, $\nu C{=}N_{pyridazine}$ 1608, 1581; δNH 1530; γCH_{Py} 793, 775 (1,2,3-trisubst.) cm^{-1}.

^{1}H-NMR (DMSO): δ 11.79 (s, —CO—NH—), 6.81 (q, $J = 5.0$ Hz, $-NH-CH_3$), 2.88 (d, $J = 5.0$ Hz, $-NH-CH_3$), 9.14 (H_α), 7.87 (H_β), 8.59 (H_γ), $J_{\alpha,\beta} = 4.5$, $J_{\alpha,\beta} = 1.8$, $J_{\beta,\gamma} = 8.2$ Hz.

On recrystallization from a mixture of DMSO and H_2O, the IR spectrum remained unchanged.

5-Methylaminopyrido[2,3-*d*]pyridazine-8(7*H*)-one (19)

The 5-methylhydrazino derivative (**18**) (0.573 g; 3 mmoles) was fused on a bath of 250—260 °C temperature for 20 min. After rapid melting, the substance solidified with strong evolution of gas. The brown crude product was crystallized from water (40 mL) after clarification with carbon, to give yellow needles (0.392 g; 74.1%), m.p. 344—346 °C (d.).

$C_8H_8N_4O$ (176.2). Calcd. N 31.8. Found N 32.0%.

IR (KBr): νNH 3353; νNH_{amide} 3270—2100; νCO_{amide} 1658; pyridine ring, $\nu C{=}N_{pyridazine}$ 1586, 1550; δNH 1540; γCH_{Py} 806, 772 (1,2,3-trisubst.) cm^{-1}.

^{1}H-NMR (DMSO): γ 11.78 (s, —CO—NH—), 6.82 (q, $J = 4.6$ Hz, $-NH-CH_3$), 2.83 (d, $J = 4.6$ Hz, $-NH-CH_3$), 9.00 (H_α), 7.86 (H_β), 8.49 (H_γ), $J_{\alpha,\beta} = 4.2$, $J_{\alpha,\gamma} = 1.5$, $J_{\beta,\gamma} = 8.2$ Hz.

On crystallization from a mixture of DMSO and water the IR spectrum remained unchanged.

2-Hydroxyethylquinolinic acid imide (20)

Quinolinic anhydride [16] (14.9 g; 0.1 mole) was suspended in chloroform (30 mL) in an apparatus equipped with a reflux condenser and a dropping funnel, and a solution of ethanolamine (6.1 g; 0.1 mole) in chloroform (20 mL) was added to the suspension under shaking. After completion of the exothermal reaction, the mixture was refluxed for 30 min, then the solvent was evaporated from the sticky material, and heating was continued in the vacuum produced by a water suction pump; the temperature of the bath was increased gradually to 150—160 °C. The melt was maintained at this temperature until the completion of water release (about 90 min). A yellowish brown viscous honey was obtained, which crystallized in colourless prisms from ethyl acetate; m.p. 106—108 °C. The crude imide was used for preparative purposes.

$C_9H_8N_2O_3$ (192.2). Calcd. C 56.2; H 4.2; N 14.6. Found C 56.3; H 4.1; N 14.7%.

IR (KBr): νOH 3342; νCO_{imide} 1780, 1722; pyridine ring 1602, 1590, 1533; $\nu C{-}O_{alcohol}$ 1022; γCH 811, 730 (1,2-disubst.) cm^{-1}.

2-Tosyloxyethylquinolinic imide (21)

The crude imide (**20**) (0.1 mole) while still warm was shaken with a mixture of anhydrous pyridine (100 mL) and tosyl chloride (28.5 g; 0.15 mole) until the formation of a homogeneous solution (20—30 min). Next day it was diluted to 1 litre with water. The product which separated was allowed to stand for a few hours, filtered off and washed with anhydrous ethanol until it became colourless. The product (20—24 g; 57.7—69.3%) melted at 164—165 °C. Colourless crystals were obtainable from much ethanol, the melting point remained unchanged.

$C_{16}H_{14}N_2O_5S$ (346.4). Calcd. S 9.3. Found S 9.1%.

IR (KBr): νCO_{imide} 1788, 1728; pyridine ring 1598; νSO_2 1362, 1180; δSO_2 579, 554; νCH 814 (1,4-disubst.), 773, 736 (1,2-disubst.) cm^{-1}.

Preparation of the isomeric mixture of (2-hydroxyethylamino)pyrido[2,3-*d*]pyridazinones (21 → 24, 25)

2-Tosyloxyethylquinolinic imide (**21**) (34.64 g; 0.1 mole) was suspended in methanol (300 mL) and potassium hydroxide (13.4 g; 0.24 mole) was dissolved in methanol (300 mL) was added. The mixture was then heated to the boiling point on a water bath. After a short boiling (15 min) the resulting solution was cooled in ice-water and slightly acidified with conc. hydrochloric acid in the presence of a few drops of Methyl Orange indicator. After the addition of hydrazine hydrate (20 mL; 72%) the solution which became rapidly yellow was refluxed for 30 min. The yellow crystals which separated on cooling were filtered off. More product was recovered from the mother liquor by evaporation. The combined yield was 19.13 g (92.8%).

Separation of the isomers was effected by fractional crystallization from water. Compound **24** is significantly less soluble in water than **25**, hence it could be separated from the latter by two recrystallization. Compound **25** enriched in the mother liquor may be isolated as a pure substance after several recrystallizations.

5-(2-Hydroxyethylamino)pyrido[2,3-*d*]pyridazine-8(7*H*)-one (24)

(*a*) The substance obtained by fractional crystallization of the above isomeric mixture was 16.6 g (87.1%; when calculated for the tosyl ester, 80.7%), yellow needles from much water, m.p. 317—318 °C.

(*b*) A mixture of **3** (1.81 g; 0.01 mole) and ethanolamine (5 mL) was refluxed for 15 min (prolonged heating greatly reduced the yield). The solution was diluted with water (50 mL) and neutralized with glacial acetic acid. The isolated crude product was dissolved in 2% NaOH solution then precipitated again with acetic acid. Yellow needles were obtained from water (0.62 g; 30.1%), m.p. 316—318 °C. According to the IR spectrum, the substance was identical with that prepared according to (*a*).

$C_9H_{10}N_4O_2$ (206.2). Calcd. C 52.4; H 4.9; N 27.2. Found C 52.2; H 4.7; N 27.5%.

IR (KBr): νNH, νOH 3326; νNH_{amide} 3250—2200; νCO_{amide} 1644; pyridine ring 1595 sh, 1587; δNH 1548; νC—O 1036; γCH_{Py} 762, 711 (1,2,3-trisubst.) cm^{-1}.

8-(2-Hydroxyethylamino)pyrido[2,3-*d*]pyridazine-5(6*H*)-one (25)

(*a*) Fractional crystallization of the isomeric mixture yielded 2.47 g (12.9%; when calculated for the starting material, 12.0%) of the product. It is significantly more soluble in water than isomer **24**. Yellow needles from water, m.p. 243—244 °C.

(*b*) A mixture of **2** (1.81 g; 0.01 mole) and ethanolamine (5 mL) was refluxed for 30 min. The excess aminoalcohol was evaporated in vacuum. The solidifying evaporation residue was suspended in a little water, the solid product filtered off (1.68 g; 81.5%; halogen-free). Yellow needles from water, m.p. 244—244.5 °C. According to the IR spectrum, it was identical with the product obtained in procedure (*a*).

$C_9H_{10}N_4O_2$ (206.2). Calcd. C 52.4; H 4.9; N 27.2. Found C 52.4; H 5.0; N 27.4%.

IR (KBr): νNH(8) 3427; νOH 3352; νNH_{amide} 3250—2400; νCO_{amide} 1661; pyridine ring, $\nu C{=}N_{pyridazine}$ 1608, 1583, 1550; δNH 1540; νC—O 1068; γCH_{Py} 789, 712 (1,2,3-trisubst.) cm^{-1}.

*

The authors' thanks are due to the Microanalytical Laboratory of the Department (head: Dr. H. MEDZIHRADSZKY) for the elemental analyses; the starting materials were supplied by the BRISTOL Laboratories, Syracuse, N. Y., USA.; this contribution is gratefully acknowledged.

REFERENCES

[1] NITTA, Y., MATSUURA, I., YONEDA, F.: Chem. Pharm. Bull. Tokyo, **13** (5), 586 (1965)
[2] MATSUURA, I., YONEDA, F., NITTA, Y.: Chem. Pharm. Bull. Tokyo, **14** (9), 1010 (1966)
[3] PAUL, D. B., RODDA, H. J.: Aust. J. Chem., **21**, 1291 (1968)
[4] MATSUURA, I., OKUI, K.: Chem. Pharm. Bull. Tokyo, **17** (11), 2266 (1969)

[5] Chugai Pharmaceutical Co. Ltd. (NITTA, Y., YONEDA, F., MATSUURA, I.): Japan Pat. 66 18,831; C. A., **66,** P 46437p (1967)
[6] KAKIMOTO, S., TONOOKA, S.: Bull. Chem. Soc. Japan, **40** (1), 153 (1967)
[7] Chugai Pharmaceutical Co. Ltd. (MATSUURA, I.): Japan Pat. 71 34,718; C.A., **76,** P 145227h (1972)
[8] KÖRMENDY, K.: Acta Chim. Acad. Sci. Hung., **94** (4), 373 (1977)
[9] NOVACEK, L., PALAT, K., BELADNIK, M., MATUSKOVA, E.: Cslká. Farm., **11,** 76 (1962)
[10] FALLAB, S., ERLENMEYER, H.: Helv. Chim. Acta, **34,** 488 (1951)
[11] CLERC, T., PRETSCH, E.: Kernresonanzspektroskopie. Akademische Verlagsgesellschaft. Frankfurt am Main, 1970
[12] KÖRMENDY, K., JUHÁSZ, A., LEMBERKOVICS, É.: Acta Chim. Acad. Sci. Hung., **102** (1), 39 (1979)
[13] KÖRMENDY, K., VOLFORD, J.: Acta Chim. Acad. Sci. Hung., **32,** 115 (1962)
[14] DOMAGALINA, E., KURPIEL, I., MOJEJKO, J.: Roczniki Chem., **38** (4), 571 (1964); C.A., **61,** 10678a (1964)
[15] ARMAREGO, W. L. F.: J. Chem. Soc., **1963,** 6073
[16] PHILIPS, A.: Ann., **288,** 255 (1895)

Károly KÖRMENDY
Teréz KOVÁCS
János SZULÁGYI
Ferenc RUFF
István KÖVESDI

H-1088 Budapest, Múzeum krt. 4/b.

Acta Chimica Academiae Scientiarum Hungaricae, Tomus 108 (2), pp. 183—189 (1981)

SIMULTANEOUS MULTIELEMENT ANALYSIS OF COAL FLY ASH LEACHATES BY D.C. PLASMA-ECHELLE SPECTROMETRY

H. MATUSIEWICZ[1] and D. F. S. NATUSCH[2]

([1]*Institute of General Chemistry, Technical University of Poznań, 60-965 Poznań, Poland,*
[2]*Department of Chemistry, Colorado State University, Fort Collins, CO 80523, U.S.A.*)

Received October 2, 1980

Accepted for publication December 1, 1980

The capabilities and limitations of the multi-elemental technique d.c. plasma atomic emission spectrometry DCP-MAES were evaluated for a complex environmental sample. For the sample investigated, a coal fly ash leachate, the DCP-MAES unit provided selective, sensitive, and rapid analyses. It was found that certain elements are subject to stray light interferences due to the presence of strong Ca signals. However, it is shown that a simple linear correction procedure can often be used to compensate for this problem.

Introduction

With coal becoming an increasingly important world energy source, the major, minor and trace elements present in coal fly ash represent a potentially large, and expanding, contribution to the environmental burden. Of particular importance are those elements which become available by leaching since rainfall water runoff from land fill sites or water within holding ponds all provide means for appreciable amounts of trace metals to enter the environment. Since essentially every element in the periodic table is present at some level in fly ash, all will appear in the process stream. For initial characterization purposes, therefore, an argument can be made for determining as many elements as possible so as to delineate best the behavioral patterns and partitioning among them.

Because of the considerable complexity of environmental samples, a technique capable of analyzing these types of samples must meet a number of criteria: (i) it must ideally provide a simultaneous multielement capability thus minimizing operator time and effort, (ii) it must provide low detection limits for the elements with a high degree of accuracy and precision, (iii) finally, it must be free from interferences and avoid matrix effects as much as possible.

One technique which meets the above criteria is Plasma Emission Spectroscopy [1, 2]. D. C. Plasma-Multi-Atomic-Echelle Spectrometry (DCP-MAES) is a multielement technique for determining both transition and main group elements which provides selectivity, sensitivity, speed and economy. The capabilities are especially important for the analysis of a sample like coal fly

ash leachates since the sample contains a large number of elements which can create interference problems with conventional techniques such as atomic absorption.

The purpose of this paper is to describe the successful application of DCP-MAES to the analysis of water soluble metals in coal fly ash leachates.

Experimental

Reagents, solutions and apparatus

All chemicals were of analytical grade quality or better (J.T. Baker Co. Ltd., U.S.A.). High-purity water from a Mili-Q water purification system Milipore Corporation was used throughout.

Table I

Experimental facilities and operating conditions

Aerosol generation	Pneumatic nebulizer; sample feed rate controlled at 2.1 mL/min by an infusion pump using argon flows of 5.9 L/min for the 3-electrode plasma
Nebulization chamber	Linear polyethylene construction; "inverted flow" configuration used to remove the largest droplets by impingement and gravitational settling. Aerosol delivered to the plasma through a quartz tapered chimney with an exit diameter of 5 mm
D. C. Plasma assembly	Three-electrode unit utilizing graphite electrodes arranged in the "vee" configuration as anodes and a thoriated tungsten electrode approximately 3 cm above the intersection of the "vee" as the cathode. Argon flow rates through ceramic sleeves are maintained at 1.2 L/min for each anode and the cathode
Plasma power supply	Three-electrode system operated at 75 V, 14 A
Plasma observation height	Set at $\sim$1 mm below the intersection of the plasma "vee" by positioning to maximize emission of nickel solution when nebulized. Approximately 1 mm vertical aperature used
Spectrometer	Spectrametrics, Spectraspan III, direct reading polychromator. Echelle-grating with 78 grooves/mm; order wave-length combination selected to maximize blaze efficiency. Entrance slit at 100 μm horizontal and 200 μm vertical. Exit slits at 400 μm vertical; horizontal slit widths and spectral bandpasses given in Table II
Data acquisition system signal amplifiers	As supplied by manufacturers
Photomultipliers	Hamamatsu: R-290 for wave-lengths less than 270 nm; R-268 for wave-lengths in the 270—600 nm range; and R-374 for wave-lengths above 600 nm
Microprocessor	As supplied by manufacturer
Data output	Texas Instruments Silent Writer Model 700

Standard solutions of metals were prepared from Titrisol (Merck), or BDH (England) standards. Acids, bases, and salts were "pro analysi" reagents from Merck, and J.T. Baker.

All glassware was cleaned by leaching with 3 *M* HNO_3 for 48 hrs, then in deionized water for 24 h and finally rinsed with deionized water prior to use.

Spectrometer: Spectraspan III, SMI Spectrametrics, Inc., U.S.A.

Sonicator: Sonicator Cell Disruptor, Model W 200 R, Heat Systems-Ultrasonics Inc., U.S.A.

Sampling

The coal fly ash studied was obtained from the cyclone precipitator in the stack of the Corrette Plant of the Montana Power Corporation (Billings, U.S.A.).

Coal fly ash leaching procedure

22.5 g of fly ash was immersed in 90 mL deionized water and sonically agitated for three hours using a sonic cleaning bath. The solution was then filtered through a 0.45 μm membrane filter. Blank solutions were prepared by these procedure without fly ash. This procedure was chosen as representative of the type of conditions which might occur when fly ash is discharged into a turbulent drain and thence into a river or impoundment pond.

D.C. Plasma-Echelle Spectrometric determination of elements

To assess the extent of elemental leachability from fly ash, leachates were analyzed with a Spectraspan III. The experimental facilities and operating conditions are summarized in Table I.

Table II

Analytical wavelengths and associated data

Element*	Analysis λ (nm)	Order No.	Exit slit width (μm)	Spectral bandpass (nm)
Al	369.153	57	25	0.0029
B	249.678	90	25	0.0018
BaII	455.403	49	25	0.0033
Background	300.61	75	50	0.0044
Be	234.861	96	50	0.0034
CaII	396.847	57	50	0.0058
CdII	214.438	105	50	0.0031
Cr	425.435	53	25	0.0031
Cu	324.754	69	25	0.0024
In	303.936	74	25	0.0022
K	769.898	28	50	0.0117
MgII	279.553	80	25	0.0021
MnII	257.610	88	25	0.0019
Mo	379.825	59	50	0.0056
Na	589.592	38	50	0.0086
Ni	341.476	66	25	0.0025
P	214.911	105	50	0.0031
Pb	405.783	56	25	0.0029
Si	251.611	90	25	0.0018
Sr	460.733	49	25	0.0034

* II indicates ion lines of single charged species

The wave-lengths used were selected on the basis of maximum sensitivity with minimum opportunity for spectral interferences Table II. Indium was selected as the internal standard and a background correction wave-length included. At the initiation of each analysis period, the optimum plasma position and wave-length alignment were checked by using a nickel solution and peaking the signal of the nickel wave-length. The instrument was subsequently calibrated against a multielement standard followed by a blank solution. The standard and sample leachated were run using a common matrix of 0.1 *M* HNO_3, 1000 μg Cs/mL and 20 μg In/mL. Indium provides an internal standard [2]. Under normal operating conditions, following initial calibration, the instrument is automatically calibrated with two calibration points at the operator's discretion. Samples more concentrated than the internal calibration are normally diluted rather than changing the calibration. The internal calibration points are periodically checked using standard solutions. If the results deviated from previous values by more than 5%, recalibration was carried out. All samples and standards were subjected to three or six ten-second integrations during a single nebulization period.

Table III

Concentration of coal fly ash leachates and standard solution,[1] *and comparison of detection limits of DCP-MAES and flame AAS*

Element	Standard (μg/mL)	Concentration		Detection limit	
		(μg/mL)	(μg/g[3])	DCP—MAES (μg/mL)	Flame AAS[5] (μg/mL)
Al[2]	1.000	0.660	264.1	0.010	0.030
B	1.000	0.040	160.1	0.005	6.000
Ba[2]	0.375	0.790	318.1	0.020[4]	0.050
Be	0.500	0	0	0.010	0.002
Ca	15.000	4.9	19.700	0.200[4]	0.001
Cd	0.500	0	0	0.100	0.001
Cr[2]	0.500	0.030	0.14	0.005	0.003
Cu	0.500	0.044	0.22	0.005	0.002
K	10.000	0.21	10.4	0.040[4]	....
Mg	12.500	0	0	0.130	0.0001
Mn[2]	1.000	0.022	0.11	0.010	0.002
Mo[2]	0.500	0.099	4.98	0.010	0.030
Na	12.500	3.5	17.60	0.400[4]	0.002
Ni	0.500	0.024	0.12	0.010	0.005
P	1.000	0	0	0.020	....
Pb[2]	0.800	0.10	4.89	0.010	0.010
Si	1.250	0.021	87.1	0.010	0.100
Sr	7.500	4.5	223.4	0.100[4]	0.010

[1] In added at 20 μg/mL as internal standard and Cs added at 1000 μg/mL as ionization suppressant; solution maintained acidic with 6.5 mL concentrated nitric acid per liter.

[2] Ca stray light correction applied.

[3] Concentration expressed as μg of element extracted per gram of coal fly ash.

[4] Attempts to achieve maximum sensitivity were not made since these elements are normally present at higher concentration in coal fly ash leachates.

[5] From Reference [3].

Results

Samples of coal fly ash leachates were analyzed for 18 elements using the DCP-MAES system. Table III gives the results of the analysis, detection limits [3] and concentrations used in the multielement standard. Analysis time was approximately three minutes per sample.

During the course of the measurements, the standards were observed to change less than $\pm 10\%$ of their original value. Ablation deposits do not appear to accumulate around the graphite anodes and their wear rate is such that readjustment at 6—8 hours intervals appears adequate.

One problem with DCP-MAES is that stray light from some elements, particularly calcium, can create incorrect readings as strong signals affect wavelengths close to the calcium line at 396.8 nm. By adding calcium to the standard solution, a calibration curve can be generated which is then used to correct the analyte concentration. The formula used in this correction is:

$$c_t = c_m - ac_{con.} \tag{1}$$

where c_t and c_m refer to the true and measured concentration of the analyte and $c_{con.}$ refers to that of the concomitant added to the solution. The factor a is obtained from the calibration curve. Table IV gives the calcium stray light correction factors for eight elements [4].

The analysis precision was better than $\pm 10\%$ with few exceptions. The latter were generally observed for those elements subject to stray light interferences and/or those present at concentrations below the detection limits. The precision of the majority of the analyses is $\pm 10\%$; the small fraction of

Table IV

*Data characteristic of Calcium stray light**

Analyte	Correction factor, a	Stray light concentration equivalent (μg/L)
Al	0.905	450
Ba	0.025	13
Cr	0.054	27
Mn	0.031	16
Mo	0.254	125
Ni	0.043	22
Pb	0.546	275
Sr	0.556	280

* For 500 mg/L Ca, see Equation 1

the analyses which exceeded this limit agreed within 20%. In view of the fact that the relative standard deviations of the mean values are typically in the 10—25% range, the agreement observed must be considered very good.

Discussion

Because the use of d.c. plasma coupled to an echelle monochromator is capable of providing measurements on 20 elements simultaneously, it is an excellent technique for the study of complex systems such as coal fly ash leachates. The simplicity of the multielemental operating conditions affords greatly reduced analysis times compared to separate analyses. Even though d.c. plasma is not recognized as a particularly powerful excitation source, the use of a large (f13) aperature coupled with the 3/4 meter echelle monochromator compensates for this problem and provides the high resolution needed for environmental analyses [5]. The DCP-MAES unit used in this study consisted of a d.c. power supply, a three electrode plasma torch, a gas handling and nebulization system, the direct reading echelle monochromator and a microprocessor based data system. Aside from the necesity of the stray light corrections previously discussed (especially for small, 15 μg/mL Ca content leachates), the DCP-MAES does have the disadvantage of being too complex for an unskilled operator. The considerable instrument cost (compared to conventional atomic absorption) is easily compensated for on a cost per sample basis when times for separate analyses are considered.

The complexity of coal fly ash leachates is born out in the results presented in Tables III and I [6]. Not unexpectedly, matrix elements such as calcium, aluminium, barium and strontium show the highest concentrations. The anio-results [6] suggest that these are mainly carbonate and sulfur species, however, the highly alkaline medium makes distinguishing the actual species on the fly ash difficult and no attempt was made to differentiate between the several possibilities.

Aside from the problems listed earlier, no problem was encountered with the complex high salt matrix which characterizes fly ash leachates.

Conclusion

In general, the DCP-MAES system may be considered an economically desirable alternative to analysis by conventional flame absorption. Especially for a system such as a coal fly ash leachate, where a large number of elements are needed with accuracy in a short period of time, and where the system is complex, DCP-MAES offers a considerable advantage. Its primary draw-

backs, aside from the requirements of high initial cost and the need for a skilled operator, are the problem of calcium stray light. In some cases, the detection limits are not quite as low as those obtainable by flame AA.

*

This work was supported in part by the U.S. Environmental Protection Agency under Grants R80395-03 and R806051-01. The authors also wish to thank Dr. David R. TAYLOR for his assistance in preparing the manuscript.

REFERENCES

[1] WINGE, R. K., FASSEL, V. A., KNISELEY, R. N., DEKALB, E., HAAS, W. J.: Spectrochim. Acta, **32B**, 327 (1977)
[2] JOHNSON, G. W., TAYLOR, H. E., SKOGERBOE, R. K.: Appl. Spectrosc., **33**, 451 (1979)
[3] FASSEL, V. A., KNISELEY, E. N.: Anal. Chem., **46**, 1110 A (1974)
[4] JOHNSON, G. W.: Ph. D. Thesis, Colorado State University, Fort Collins, CO, U.S.A., 1979
[5] HARRISON, G. R.: J. Opt. Soc. Chem., **39**, 522 (1949)
[6] MATUSIEWICZ, H., NATUSCH, D. F. S.: Intern. J. Environ. Anal. Chem., **8**, 227 (1980)

H. MATUSIEWICZ 60—956 Poznań, Poland
D. F. S. NATUSCH Fort Collins, CO 80523, U.S.A.

Acta Chimica Academiae Scientiarum Hungaricae, Tomus 108 (2), pp. 191—195 (1981)

INDIRECT POLAROGRAPHIC STUDY OF ACID — BASE EQUILIBRIA OF SOME BENZOIC ACID DERIVATIVES, III*

STRUCTURAL INTERACTIONS

É. GYÁRFÁS,[1] B. TŐKÉS[1] and L. KÉKEDY[2]**

([1]*Laboratory of Physical Chemistry, Medical and Pharmaceutical Institute, Tîrgu Mureş, Romania,* [2]*Department of Inorganic and Analytical Chemistry, "Babeş-Bolyai" University, Cluj—Napoca, Romania*)

Received July 3, 1980

Accepted for publication December 12, 1980

A new structural influence on polarographic activity, manifested in a linear relationship between the half-wave potentials of the mediators and the substituent constant of the benzoic acid derivatives is reported. Theoretical interpretation of the observed correlations is given.

The possibilities of classical polarography to determine rate constants of homogeneous chemical reactions coupled with electrode processes have been used to investigate acid-base equilibria of some benzoic acid derivatives. The direct method [1] is based on the investigation of the kinetic waves of the reduction of H^+-ions formed in the equilibrium:

$$HA \underset{k_r}{\overset{k_d}{\rightleftarrows}} A^- + H^+ \longrightarrow 1/2\ H_2 \tag{1}$$

characterized by the acidity constant:

$$K_a = k_d/k_r, \tag{2}$$

k_d and k_r are the dissociation and the recombination rate constants respectively. The indirect method (drop time, RÜETSCHI [2]) is based on the property of some organic compounds (mediators) to yield double reduction waves in the presence of H^+-ions. Under well-established conditions the first wave is of kinetic nature, allowing the determination of the above mentioned rate constants (k_d and k_r) of the compounds investigated.

Benzoic acid and ten derivatives were investigated in the presence of either azobenzene (A), or *p*-nitraniline (N) as mediators. Experimental conditions were identical with those published earlier [3]. The observed linear

* Part II: Studia Univ. Babeş-Bolyai, Chemia, **25** (1), 71 (1980)

** To whom correspondence should be addressed

relationship between lg $k_{d(A)}$ and/or $k_{d(N)}$ and the substituent constant σ, respectively [3], shows a strong correlation between the rate constant values and the structure of the compounds investigated. In this paper we report on a new structural influence on polarographic activity, manifested in a linear relationship between the half-wave potential of the mediator used (A or N), and the substituent constant of the benzoic acid derivatives investigated (Fig. 1). From the experimental data for the straight lines on Fig. 1 the following equations can be calculated:

$$E_{\frac{1}{2}(A)} = (0.236 \pm 0.015)\sigma - (0.340 \pm 0.03) \qquad (3)$$

$$r = 0.986 \qquad S_0 = \pm 0.009$$

$$E_{\frac{1}{2}(N)} = (0.234 \pm 0.018)\sigma - (0.737 \pm 0.004) \qquad (4)$$

$$r = 0.980 \qquad S_0 = \pm 0.011$$

In principle, such a structural effect could be caused by the change of the pH, the acids investigated being of different strength. If the half-wave potential of the acids would wary due only to the pH-change according to the expression:

$$\mathrm{pH} = -(1.305 \pm 0.038)\sigma + (6.734 \pm 0.011) \qquad (5)$$

than the calculated $E_{\frac{1}{2}} - \sigma$ relationship would coincide with the experimental data (equations (3) and (4), respectively).

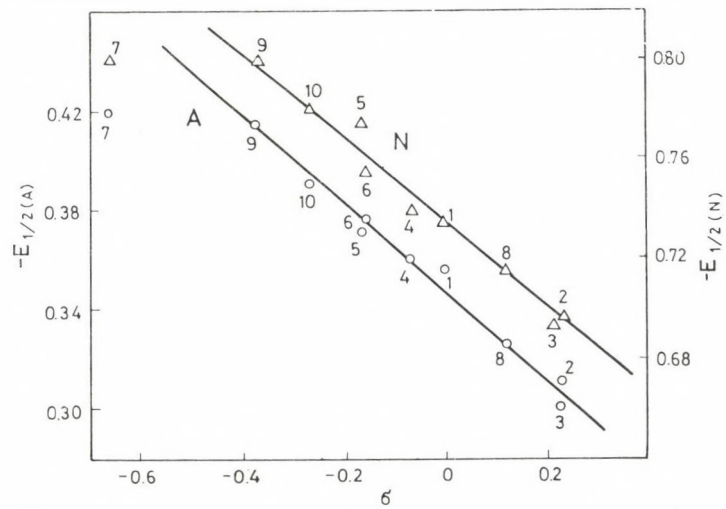

Fig. 1. $E_{\frac{1}{2}} - \sigma$ (substituent constant) dependence. Mediators used: A — azobenzene; N — *p*-nitraniline. The compounds investigated (R in $R-C_6H_4-COOH$): 1 — H; 2 — 4 Cl; 3 — 4 Br; 4 — 3 CH_3; 5 — 4 CH_3; 6 — 3 NH_2; 7 — 4 NH_2; 8 — 30 H; 9 — 40 H; 10 — 40 CH_3

Considering the $E_{\frac{1}{2}}$ — pH relationship, which in the case of azobenzene has the form:

$$E_{\frac{1}{2}(A)} = -(0.131 \pm 0.008)\,\mathrm{pH} + (0.537 \pm 0.057) \qquad (6)$$

$$r = 0.986 \qquad S_0 = \pm 0.0069$$

as well as the pH — σ one, the calculated relationship will be:

$$E_{\frac{1}{2}(A)} = (0.171 \pm 0.015)\sigma - (0.345 \pm 0.001) \qquad (7)$$

The same relationships for *p*-nitraniline are:

$$E_{\frac{1}{2}(N)} = -(0.127 \pm 0.005)\,\mathrm{pH} + (0.122 \pm 0.031) \qquad (8)$$

$$r = 0.995 \qquad S_0 = 0.0038$$

and

$$E_{\frac{1}{2}(N)} = (0.166 \pm 0.007)\sigma - (0.733 \pm 0.006), \qquad (9)$$

respectively. The slopte of equations (7) and (9) differ significantly from those of the experimental ones.

In order to interpret our experimental data we considered the formation of ion-pairs in the solutions, between the anions of the acids investigated and the protonated molecules of the mediators. According to the theory [4, 5, 6] the formation of such associates is the more pronounced the less is the dielectric constant of the medium:

$$\frac{\mathrm{d}\lg K}{\mathrm{d}(1/\varepsilon)} = \frac{N_0 z^2 e^2}{aRT} \qquad (10)$$

K is the stability constant of the ion associate, ε is the dielectric constant and $1/a = 1/a_+ + 1/a_-$; a_+ and a_- being the respective ionic radii. The extent of the ion-pair formation can be affected by the non-uniformity of the electric charge distribution in the ions, a phenomenon frequently encountered by organic ions. This determine an increased potential gradient around the ions and the appearance of increased attraction forces between the cations and anions. The appearance of hydrogen bonds increases the values of the association constants with several order of magnitudes. Allowing for the presence of all these phenomena in our systems, a model has been formulated for the electrochemical process. Accordingly, the following chemical steps preceed the charge-transfer reaction:

$$\mathrm{X{-}C_6H_4COOH} \overset{n\mathrm{M}}{\rightleftarrows} \mathrm{X{-}C_6H_4COOH \cdot M}_n \qquad (11)$$

$$\mathrm{X{-}C_6H_4COOH \cdot M}_n \rightleftarrows \mathrm{X{-}C_6H_4COO^- \cdot M}_m + \mathrm{H^+ \cdot M}_q \qquad (12)$$

$$RN + H^+ \cdot M_q \rightleftarrows RNH^+ + qM \tag{13}$$

$$RNH^+ + X{-}C_6H_4COO^- \cdot M_n \begin{cases} \nearrow\swarrow\ (RNH^+) \cdot ({}^-OCO{-}C_6H_4{-}X) \\ \quad \text{(contacting ion-pair} \\ \nwarrow\searrow\ (RNH^+) \,||\, ({}^-OCO{-}C_6H_4{-}X) \\ \quad \text{(ion-par separated by solvent)} \end{cases} \tag{14}$$

M being a solvent molecule. Equilibrium (14) describes the possibility of formation of either contacting ion-pairs or of ion-pairs separated by solvent shell. The rate determining step is the dissociation of the solvated acid (Eq. 12). This is shown by the linear relationship between lg k_d and σ, as well as by the fact that the dissociation rate constant values (k_d, k_r) determined by either the direct, or the indirect method, are strongly affected by the ionic strength.

Our experimental data are consistent with the fact that the protonation of the mediator (Eq. 13) takes place with a higher rate than the dissociation of the acid, so this latter cannot be the rate determining step [3]. If reaction (13) would be the rate determining, the dissociation rate constants would depend on the basicity of the mediator used. The nearly independence from such a parameter (see [3], Table III) favours our statement. The ion-pairs (mainly contacting ion-pairs) participate in the electrode process as independent chemical entities. In these species the effect of the substituent in the anion can migrate to the reaction centre of the cation, influencing thus the values of the half-wave potentials. This also contributes to the appearence of a linear $E_{\frac{1}{2}} - \sigma$ relationship. This structural interaction can be used for the evaluation of the *ortho*-effect of some substituents. Comparing the $E_{\frac{1}{2}}$ values of the same substituents (with the same inductive and mesomeric effect) but in *ortho* or *para* positions, respectively, we could estimate the so-called "special *ortho*-effect" of the respective substituent (Table I).

Indeed, this effect is a special one, and unexpected, because the $E_{\frac{1}{2}}$ values of the *ortho*-substituted derivatives are less negative than those of the *para*-substituted ones. The easier reduction in this case is in accordance

Table I

$\Delta E_{\frac{1}{2}} = E_{\frac{1}{2}(o)} - E_{\frac{1}{2}(p)}$

Substituent (X)	$\Delta E_{\frac{1}{2}(A)}$, mV	$\Delta E_{\frac{1}{2}(N)}$, mV
CH_3	30	35
Cl	15	10
NH_2	80	80
OH	155	130

with the increased stability of the ion-pairs with *ortho*-substituted anions following the localization of the negative charge on the carboxylic group and the simultaneous hindrance of coplanarity of the carboxylic group with the benzene nucleus

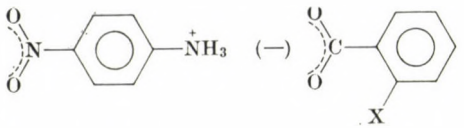

In this way the carboxylate anion exerts a stronger influence on the localization of the positive charge on the amine-nitrogen with a simultaneous decrease of the electron density on the NO_2-group enabling its easier reduction. So we can state that the observed $E_{\frac{1}{2}} - \sigma$ correlation essentially is an effect of the substituent constant of the anion on the stability of the ion-associates.

The anomalous behaviour of the *p*-amino benzoic acid (Fig. 1) (known in the literature too) is due to the more pronounced decrease of acidity (because of internal salt formation) resulting in a smaller σ-value.

REFERENCES

[1] Tőkés, B., Gyárfás, É., Kékedy, L.: Z. Phys. Chem., **260,** 1 (1979)
[2] Rüetschi, P.: Z. Phys. Chem. (Neue Folge), **5,** 323 (1955)
[3] Gyárfás, É., Tőkés, B., Kékedy, L.: Acta Chim. Acad. Sci. Hung., **102,** 143 (1979)
[4] Hammett, L. P.: Osnovi fizitcheskoi organitscheskoi khimii. Mir, Moskva, 1972, pp. 264—266, 286.
[5] Izmailov, N. A.: Elektrokhimiya rastvorov. Khimiya, Moskva, 1976, p. 114
[6] Beletskaya, I. P.: Uspekhi khimii, **44,** 2205 (1975)

Éva Gyárfás
Béla Tőkés } R-4300 Tîrgu Mureș, Str. Gh. Marinescu nr. 38

László Kékedy R-3400 Cluj—Napoca, Str. Arany J., nr. 11, Romania

Acta Chimica Academiae Scientiarum Hungaricae, Tomus 108 (2), pp. 197—214 (1981)

REACTIONS OF MONO- AND DIARYLIDENECYCLOALKANONES WITH THIOUREA AND AMMONIUM THIOCYANATE, V*, **

SYNTHESIS OF 5-ARYL-9-ARYLIDENE-2,3,6,7,8,9-HEXAHYDRO-5*H*-THIAZOLO[2,3-*b*]QUINAZOLINES AND 6-ARYL-10-ARYLIDENE-3,4,7,8,9,10-HEXAHYDRO-2*H*,6*H*-1,3-THIAZINO-[2,3-*b*]QUINAZOLINES

T. LÓRÁND,[1] D. SZABÓ,[1] A. FÖLDESI[2] and A. NESZMÉLYI[3]

([1] *Chemical Institute, Medical University, Pécs,*
[2] *Central Laboratory, Medical University, Pécs, and*
[3] *Central Chemical Research Institute, Hungarian Academy of Sciences, Budapest*)

Received May 14, 1980

In revised form September 16, 1980

Accepted for publication December 17, 1980

4-Aryl-8-arylidene-3,4,5,6,7,8-hexahydro-2(1*H*)-quinazolinethiones (*A*, *M*) react with α,ω-dihalogenoalkanes to yield 5-aryl-9-arylidene-2,3,6,7,8,9-hexahydro-5*H*-thiazolo[2,3-*b*]quinazolines (**Ia**, **IIa**) and 6-aryl-10-arylidene-3,4,7,8,9,10-hexahydro-2*H*,6*H*-1,3-thiazino[2,3-*b*]quinazolines (**IIIa**, **IVa**). Compound *A* undergoes cyclization directly with chloroacetic acid, 2-bromopropionic acid, their ethyl esters, or with chloroacetonitrile, to give **Va**, **VIa** or **Xa**, while **IXa** can only be obtained with 3-bromopropionic acid in a two-step reaction. The structures of the products were verified by chemical and spectroscopical (UV, IR, ^{1}H-NMR, ^{13}C-NMR) methods.

In previous papers [1, 2] we reported the synthesis of some 4-aryl-8-arylidene-3,4,5,6,7,8-hexahydro-2(1*H*)-quinazolinethiones (*A*) and the preparation of their *N*-acyl- (*B*), *S*-alkyl- (*C*) and *N*-acyl-*S*-alkyl- (*D*) derivatives.

In the present paper, cyclic analogues of *B* and *D* are described; these compounds were synthesized with bifunctional reagents. Cyclization reactions with such reagents have been studied by several researchers in the case of *as*-triazine-, pirimidine-, perimidine- and quinazolinethiones [4—13].

In establishing the structures of **Ia**—**VIa**, **IXa**, and **Xa**, the appearance of two isomers should always be considered. In all cases only one isomer was obtained; the structure was determined by spectroscopic and chemical methods.

The fact of cyclization was supported by the IR spectra of the products, by the absence of the νNH band. The UV spectrum of **IIIa** (Table III) was practically identical with the spectrum of the 3-methyl derivative of *C* (R = CH_3) prepared earlier (λ_1: 235 nm, log ε_1: 4.15; λ_2: 279 nm, lg ε_2: 4.45; λ_3: 334 nm, lg ε_3: 3.86 [2]), showing that the chromophore is identical in the two molecules, which also confirms structures **Ia**—**IVa**. The correctness of

* Part IV, see Ref. [3]
** Presented in part as a lecture at the Conference of the Hungarian Chemical Society, Debrecen, 1977

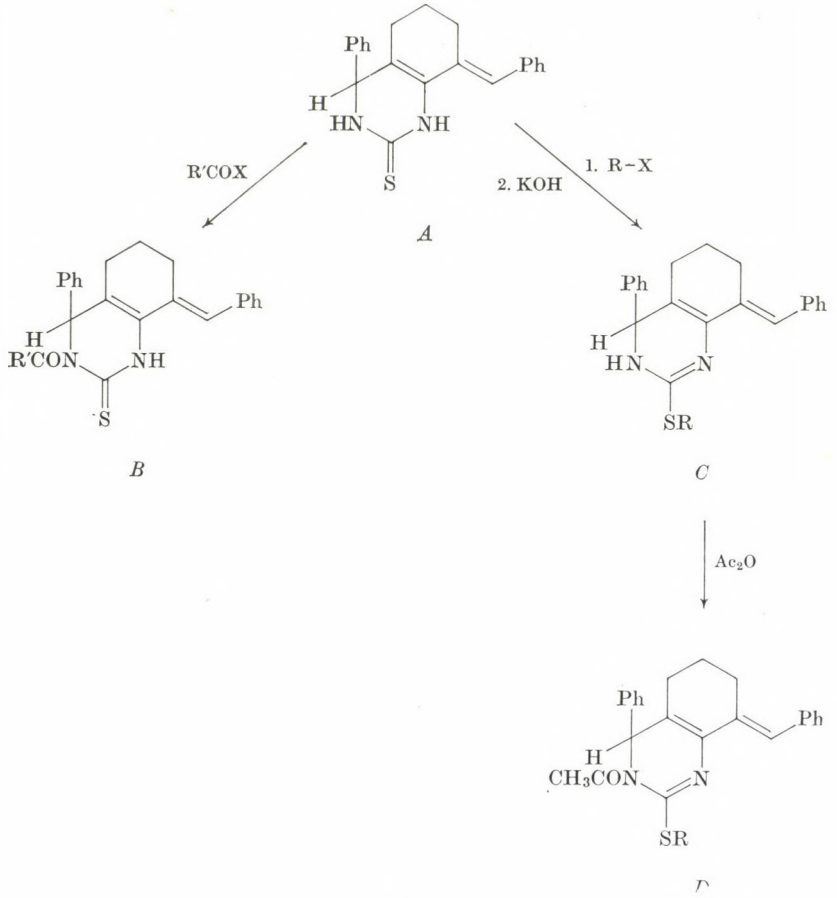

Fig. 1

the structures was also supported by the ^{1}H-NMR and ^{13}C-NMR spectra. In the ^{1}H-NMR spectrum of **Ia**, the multiplet appearing at δ 2.9—3.6 ppm (SCH_2, NCH_2) was new as compared with *A*, and no signal liable to exchange was found. The ^{1}H-NMR spectrum of **Ia** was also recorded in the presence of a shift reagent at various molar ratios (Table I). The largest shift was observed in the case of the methylene groups in the thiazolidine ring, since the sulfur atom has the greatest complexing ability. The change in the chemical shift of the olefinic proton is larger than that of the aliphatic methine proton, *i.e.* Eu^{3+} is closer to the olefinic than to the methine proton, which also supports structure **Ia**.

Table II shows the ^{13}C-NMR spectra of compounds **Ia**—**IIIa** and *A* [1], together with the assignments of the signals. The presence of the closed thiazolo- and 1,3-thiazino rings was indicated by the chemical shift of the No. 2,4

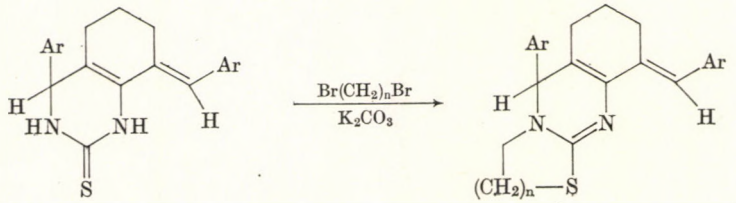

A (Ar = C_6H_5)

M (Ar = 4-CH_3O—C_6H_4)

Ia (n = 1, Ar = C_6H_5)

IIa (n = 1, Ar = 4-CH_3O—C_6H_4)

IIIa (n = 2, Ar = C_6H_5)

IVa (n = 2, Ar = 4-CH_3O—C_6H_4)

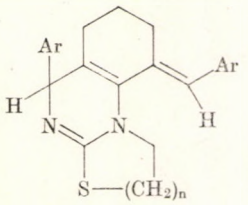

Ib (n = 1, Ar = C_6H_5)

IIb (n = 1, Ar = 4-CH_3O—C_6H_4)

IIIb (n = 2, Ar = C_6H_5)

IVb (n = 2, Ar = 4-CH_3O—C_6H_4)

Fig. 2

Table I

^1H-NMR data of **Ia** *in the presence of the shift reagent* $[Eu(fod)_3\text{-}d_{27}]$

Molar ratio of the complexing agent and **Ia**	CH_2 in cyclohexane ring $\Delta\delta$	SCH_2 NCH_2 $\Delta\delta$	CH $\Delta\delta$	Ar $\Delta\delta$	=CH $\Delta\delta$
1 : 10	0	0.30	0.10	0.05	0.15
1 : 3	0	0.85	0.25	0.10	0.35
1 : 2	0.15	1.10	0.35	0.15	0.50
1 : 1	0.15	1.40	0.45	0.15	0.70

methylene groups, also considering the effect of the hetero atoms [14—15]. The appearance of a new ring is also shown by the β effect of the No. 4 CH carbon atom in compound *A* (downfield shift). On this basis, it can be concluded that the new ring is closed in the direction suggested by us, *i.e.* towards the No. 4 CH (see Fig. 3).

Compound *A* was allowed to react with halogenated carboxylic acids and their esters to obtain quinazolines condensed with 5- or 6-membered lactam rings. (When using chloroacetic acid, 2-bromopropionic acid or their

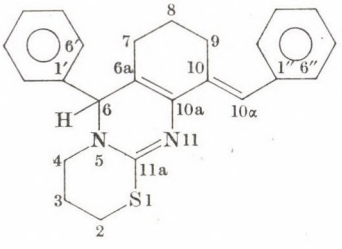

IIIa

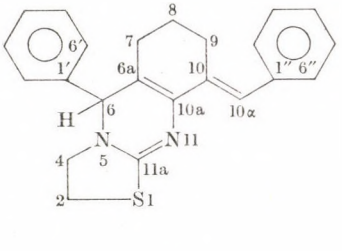

Ia

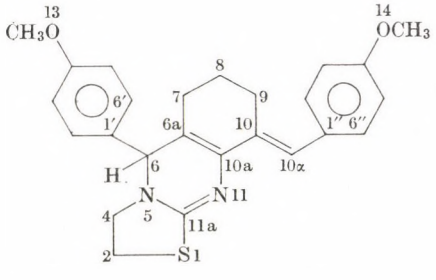

IIa

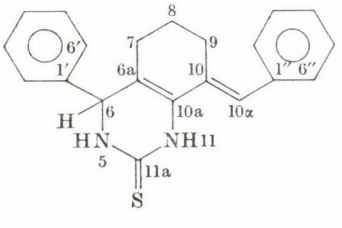

A

Fig. 3

Table II

Chemical shifts, δ ppm

No.	*A*	Ia	IIa	IIIa
2	—	24.7	25.7	24.9
3	—	—	—	27.2
4	—	50.4	51.3	48.0
6	59.0	63.8	64.7	68.9
6a	129.1	135.4[a]	128.6	134.2[a]
7	26.0	26.6	26.1[a]	27.2
8	21.9	21.9	22.0	22.7
9	26.4	26.6	26.9[a]	27.2
10	127.7	134.0[a]	136.1	135.1[a]
10a	114.5	113.6	114.7	114.9
10α	123.0	123.2	123.8	123.8
11a	174.5	159.5	159.9	152.7
1′	137.3	138.1	131.6	138.8
2′	129.4[a]	128.3[b]	130.7	128.7[b]
3′	128.3[a]	128.7[b]	113.6	129.3[b]
4′	126.8	125.5	160.5	126.7
5′	128.3[b]	128.7[c]	113.6	129.3[c]
6′	129.4[b]	128.3[c]	130.7	128.7[c]
1″	142.8	140.5	133.2	141.7
2″	127.0[c]	127.2[d]	129.1	127.4[d]
3″	128.9[c]	127.6[d]	114.4	127.8[d]
4″	128.0	127.8	158.1	128.2
5″	128.9[d]	127.6[e]	114.4	127.8[e]
6″	127.0[d]	127.2[e]	129.1	127.4[e]
13	—	—	55.4[b]	—
14	—	—	55.3[b]	—

[a, b, c, d, e] The assignments of the pair may be interchanged

ethyl esters, the open-chain mercaptocarboxylic acid intermediate could not be isolated, although **Va** and **VIa** have been synthesized by several methods, see Experimental).

In the IR spectra of **Va**—**VIa** (Table IV), no νNH band can be found; the Amide I band appears at 1725 cm^{-1}, which corresponds to the value given for 5-membered lactams (1750—1700 cm^{-1} [16]). The UV spectra are very similar to that of the analogous compound *D* (R = CH_3) prepared earlier [2], and this fact also supports structures **Va**—**VIa**. The ^{1}H-NMR spectra

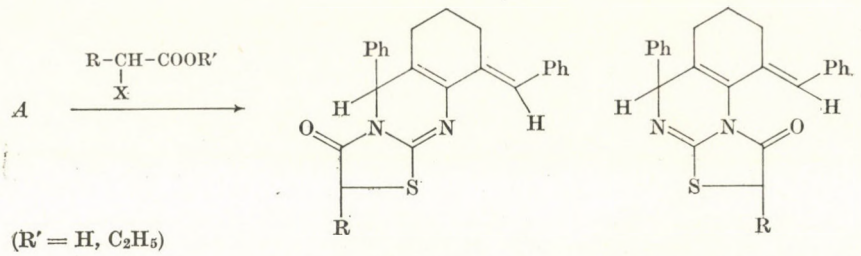

(R′ = H, C_2H_5)
(R = H, CH_3)
(X = Cl, Br)

Va (R = H)
VIa (R = CH_3)

Vb (R = H)
VIb (R = CH_3)

Fig. 4

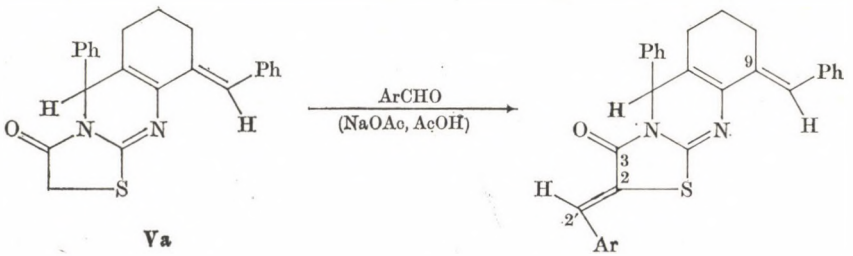

Va

VII a (Ar = C_6H_5)
b (Ar = 2-Cl—C_6H_4)
c (Ar = 2-OH—C_6H_4)
d (Ar = 2-SO_3Na—C_6H_4)
e (Ar = 4-CH_3CONH—C_6H_4)
f (Ar = 4-NH_2—C_6H_4)
g (Ar = 2-thienyl)
h (Ar = 2-furyl)
i (Ar = 2-pyridyl)
j (Ar = 3-pyridyl)
k (Ar = 4-pyridyl)
l (Ar = CH=CH—Ph)
m (Ar = 4-CH_3—C_6H_4)
n (Ar = 4-CH_3O—C_6H_4)
o [Ar = 4-$(CH_3)_2N$—C_6H_4]
p [Ar = 3,4-$(CH_3O)_2$—C_6H_3]
q (Ar = 3-OCH_3—4-OH—C_6H_3)

Fig. 5

Table III

Compound	M.p., °C	Formula M.w.; yield, %	UV (ethanol) λ_{max} (nm)	UV (ethanol) log ε	IR (cm^{-1}) (KBr pellets)	^{1}H-NMR (δ ppm, $CDCl_3$)
Ia	184—194	$C_{23}H_{22}N_2S$ 358.51 42	277 332	4.36 3.86	νC=N: 1620 (sh)	1.2—2.8 m 6H CH_2 2.9—3.6 m 4H SCH_2, NCH_2 4.9 s 1H CH 7.0—7.6 m 10H Ar 7.5 s 1H =CH
IIa	158—160	$C_{25}H_{26}N_2O_2S$ 418.56 34	228 281	4.38 4.34	νC=N: 1610	1.1—3.6 m 10H CH_2, SCH_2, NCH_2 3.8 s 6H OCH_3 4.8 s 1H CH 6.7—7.6 m 9H Ar, =CH
IIIa	159—165	$C_{24}H_{24}N_2S$ 372.53 34	236 280 345	4.11 4.40 3.76	νC=N: 1622	1.2—3.4 m 12H CH_2, SCH_2, NCH_2 4.5 s 1H CH 7.1—7.6 m 11H Ar, =CH
IVa	146—151	$C_{26}H_{28}N_2O_2S$ 432.60 20	288 345	4.71 4.00	νC=N: 1610	1.0—3.5 m 12H CH_2, SCH_2, NCH_2 3.8 s 6H OCH_3 4.4 s 1H CH 6.6—7.0 m 9H Ar, =CH

Table IV

Compound	M.p., °C	Formula M.w., yield, %	UV (ethanol) λ_{max} (nm)	 log ε	IR cm^{-1}) (KBr pellets)	^{1}H-NMR (δ ppm, $CDCl_3$)
Va	195 (d.)	$C_{23}H_{20}N_2OS$ 372.49 54[a] 55[b] 37[c] 77[d]	230 278 322	4.10 4.49 4.01	amide I: 1725	0.9—2.5 m 6H CH_2 3.7 s 2H SCH_2 5.3 s 1H CH 6.5 s 1H =CH 6.7—7.2 m 10H Ar[e]
VIa	200 (d.)	$C_{24}H_{22}N_2OS$ 386.52 55[f] 56[g]	230 278 322	4.13 4.51 4.04	amide I: 1725	1.12 d 3H CH_3[h] J = 6.6 Hz 1.0—2.5 m 6H CH_2 4.06 q 1H SCH 5.3 s 1H CH 6.5 s 1H =CH 6.7—7.2 m 10H Ar[e]
VIIa	217 (d.)	$C_{30}H_{24}N_2OS$ 460.60 49	280 321 388	4.40 4.46 4.13[i]	amide I: 1710	0.9—2.5 m 6H CH_2 5.4 s 1H CH 6.5; 7.7 s 2H =CH 6.8—7.3 m 15H Ar[e]
VIIb	197—199	$C_{30}H_{23}ClN_2OS$ 495.05 34	277 314 384	4.38 4.43 4.00	amide I: 1713	0.9—2.5 m 6H CH_2 5.4 s 1H CH 6.5; 8.1 s 2H =CH 6.6—7.2 m 14H Ar[e]
VIIc	248—251	$C_{30}H_{24}N_2O_2S$ 476.60 54	281 313 370	4.42 4.24 4.08	νOH: 3100—3600 amide I: 1710	1.2—2.9 m 6H CH_2 5.6 s 1H CH 6.7—7.6 m 15H Ar, =CH 7.9 s 1H =CH 10.4 s 1H OH[j]

VIId	263—267	$C_{30}H_{23}N_2NaO_4S_2$ 562.65 48	276 317 384	4.30 4.33 3.00	amide I: 1705	1.0—2.5 m 6H CH_2 5.3 s 1H CH 6.5; 8.5 s 2H =CH 6.6—7.9 m 14H Ar[e]
VIIe	250 (d.)	$C_{32}N_{27}N_3O_2S$ 517.66 74	243 281 376	4.24 4.08 4.40	νNH: 3320 amide I: 1710 1675	1.0—2.6 m 6H CH_2 2.0 s 3H CH_3 5.4 s 1H CH 6.5; 7.7 s 2H =CH 6.7—7.5 m 14H Ar 8.6 s 1H NH[e]
VIIf	223—225	$C_{30}H_{25}N_3OS$ 475.61 57[m]	254 291 406	4.26 4.24 4.54[i]	νNH: 3415 3500[n] amide I: 1700	1.5—2.9 m 6H CH_2 2.9—3.8 s 2H NH_2[k] 5.6 s 1H CH 6.5—7.7 m 16H Ar, =CH
VIIg	216—218	$C_{28}H_{22}N_2OS_2$ 466.63 55	240 281 374	4.05 4.01 4.22[i]	amide I: 1710	1.0—3.0 m 6H CH_2 5.5 s 1H CH 7.0—7.7 m 14H Ar, =CH 7.8 s 1H =CH
VIIh	215—216	$C_{28}H_{22}N_2O_2S$ 450.57 71	241 281 372	4.15 4.11 4.36[i]	amide I: 1715	1.4—2.9 m 6H CH_2 5.5 s 1H CH 6.3—7.7 / 7.0—7.7 m 15H Ar, =CH
VIIi	253—254	$C_{29}H_{23}N_3OS$ 461.59 68	240 272 374	4.22 4.24 4.28[i]	amide I: 1715	1.5—2.9 m 6H CH_2 5.5 s 1H CH 7.0—7.8 / 8.6—8.8 m 16H Ar, =CH
VIIj	221—223	$C_{29}H_{23}N_3OS$ 461.59 83	241 270 353	4.20 4.20 4.06[i]	amide I: 1715	1.4—2.9 m 6H CH_2 **5.6** s 1H CH 7.2—7.9 / 8.4—8.9 m 16H Ar, =CH

Table IV (continued)

Compound	M.p., °C	Formula M.w., yield, %	UV (ethanol) λ_{max} (nm)	UV (ethanol) log ε	IR (cm^{-1}) (KBr pellets)	^{1}H-NMR (δ ppm, $CDCl_3$)
VIIk	248 (d.)	$C_{29}H_{23}N_3OS$ 461.59 62	241 266 342	4.23 4.26 4.11[i]	amide I: 1715	1.5—2.9 m 6H CH_2 5.6 s 1H CH 7.2—7.7, 8.6—8.8 m 16H Ar, =CH
VIIl	193—196	$C_{32}H_{26}N_2OS$ 486.64 51	281 362	4.33 4.46	amide I: 1705 νC=C: 1620 1610[i]	0.9—2.6 m 6H CH_2 5.3 s 1H CH 6.1—7.6 m 19H Ar, =CH[e]
VIIm	225—228	$C_{31}H_{26}N_2OS$ 474.63 32	274 360	4.23 4.51[i]	amide I: 1715	1.0—2.6 m 6H CH_2 2.0 s 3H CH_3 5.4 s 1H CH 6.3—7.4 m 15H Ar, =CH 7.7 s 1H =CH[e]
VIIn	210—215	$C_{31}H_{26}N_2O_2S$ 490.63 56	281 320 391	4.43 4.32 4.34	amide I: 1710	1.0—2.6 m 6H CH_2 3.5 s 3H OCH_3 5.1 s 1H CH 6.3—7.5 m 15H Ar, =CH 7.7 s 1H =CH[e]
VIIo	258—260	$C_{32}H_{29}N_3OS$ 503.67 46	259 299 416	4.58 4.31 4.99[i]	amide I: 1695	1.3—2.9 m 6H CH_2 3.0 s 6H NCH_3 5.5 s 1H CH 6.5—7.8 m 16H Ar, =CH
VIIp	200—205	$C_{32}H_{28}N_2O_3S$ 520.66 64	282 319 390	4.34 4.20 4.29	amide I: 1710	1.0—2.7 m 6H CH_2 3.5 s 6H OCH_3 5.4 s 1H CH 6.3—7.3 m 14H Ar, =CH 7.7 s 1H =CH[e]

VIIq	224—230	$C_{31}H_{26}N_2O_3S$ 506.63 26	258 283 366	4.55 4.52 4.79[i]	amide I: 1710	1.4—3.0 3.9 5.5 6.9—7.8	m s s m	6H CH_2 3H OCH_3 1H CH 16H Ar, =CH

[a] With ethyl chloracetate.
[b] With chloroacetic acid, in DMFA.
[c] With chloroacetic acid, in THF.
[d] With chloroacetic acid, without solvent.
[e] The ^{1}H-NMR spectrum was recorded in TFA.
[f] With ethyl α-bromopropionate.
[g] With α-bromopropionic acid, in DMFA.
[h] The CH_3 signal was superimposed on the signal of CH_2 groups.
[i] The UV spectrum was recorded in THF.
[j] The ^{1}H-NMR spectrum was recorded in DMSO-d_6.
[k] Broad band, exchangeable with D_2O.
[l] Broad band, with two part-maxima.
[m] Yield calculated for the starting **VIIe**.
[n] The IR spectrum was recorded in chloroform.

are also in agreement with this assumption. Even in the 3-acyl derivatives of *A* (compounds *B*), it was observed that the signal of the C-4 CH proton suffered a paramagnetic shift of about 1 ppm as compared with the starting material *A*, owing to the magnetic anisotropy of the C=O group [2]. A similar but smaller (0.4 ppm) effect was found in **Va**—**VIa** which confirms the structure assumed by us.

From the work of Indian authors it is known that the methylene group in thiazolidones condensed with pirimidine or *as*-triazine rings have an acid character, thus they can participate in Perkin condensation under vigorous conditions [6, 13]. When **Va** was allowed to react with aromatic aldehydes, compounds **VIIIa**—**q** were obtained (Table IV).

In the IR spectra of these compounds, the frequency of the Amide I band decreased by about 20 cm^{-1}, owing to the conjugation effect of the C-2 arylidene group. The 2-*Z* configuration of the lactams **VIIa**—**q** is verified by the ^{1}H-NMR spectra in which the signal of the methine proton at C-2' appears at δ 7.7—8.5 ppm, which is in good agreement with the value given for 2-*E*-arylidenecycloalkanones [17—18].

The synthesis of the 1,3-thiazino analogue of **Va** was also attempted by the reaction of 3-bromopropionic acid or its ethyl ester with *A*.

In the latter case no cyclization took place; the mercaptopropionic ester **VIII** was obtained, which was isolated in the form of the picrate (**VIIIa**, Table V).

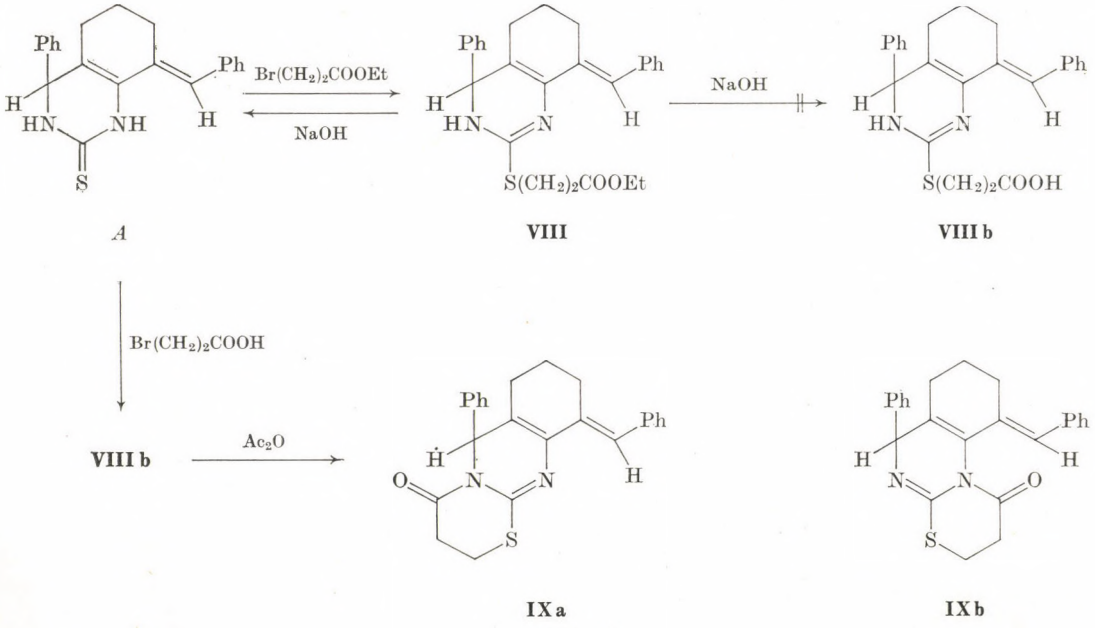

Fig. 6

Table V

Compound	M.p., °C	Formula M.w., yield, %	UV (ethanol) λ_{max} (nm)	UV (ethanol) log ε	IR (cm^{-1}) (KBr pellets)	^{1}H-NMR (δ ppm, $CDCl_3$)
VIIIa	162—166	$C_{32}H_{31}N_5O_9S$	235	4.42	νNH, ν=NH$^+$ 2600—3300	1.1 t 3H CH_3 J = 7.0 Hz
		661.70	276	4.45		1.3—4.2 m 12H CH_2, SCH_2, OCH_2
		69	354	4.24	νC=O: 1740	5.2 s 1H CH
						6.8 s 1H =CH
						7.0—7.5, 8.5 m 13H Ar[a,b]
VIIIb	207—215	$C_{24}H_{24}N_2O_2S$	247	4.22	νNH, νOH 2400—3350	0.9—3.3 m 10H CH_2, SCH_2
		404.53	273	4.35		4.9 s 1H CH
		42			νC=O: 1730	6.5 s 1H =CH
						6.6—7.2 m 10H Ar
						8.4; 9.2 s 2H NH, OH[c]
IXa	128—130	$C_{24}H_{22}N_2OS$	230	4.09	amide I: 1695	1.4—3.4 m 10H CH_2, SCH_2
		386.52	282	4.45		6.0 s 1H CH
		10				7.0—8.0 m 11H Ar, =CH
Xa	191—195	$C_{23}H_{21}N_3S$	278	4.54	ν=NH 3290	1.2—2.9 m 6H CH_2
		371.51	327	3.94	νC=N: 1655	3.7 s 2H SCH_2
		54				5.4 s 1H CH
						6.5—8.0 m 10H Ar
						7.5 s 1H =CH[d]

[a] The NH, =NH$^+$ signals cannot be assigned.
[b] The ^{1}H-NMR spectrum was recorded in DMSO-d_6.
[c] The ^{1}H-NMR spectrum was recorded in TFA.
[d] The signal of the =NH proton cannot be assigned.

The corrseponding acid (**VIIIb**) was to be prepared from **VIII** by alkaline hydrolysis, however, this reaction yielded the starting material *A*; this can be explained by a retro-Michael reaction. The interaction of *A* and 3-bromopropionic acid yielded **VIIIb** (Table V), which was cyclized with acetic anhydride. The product of cyclization (**IXa** or **b**) had neither νOH nor νNH band in the IR spectrum, the Amide I band appeared at 1695 cm^{-1}. In the ^{1}H-NMR spectrum, the methine proton suffered a 1.1 ppm paramagnetic shift as compared with *A* (*A*: δCH 4.9 ppm; **IXa**: δCH 6.0 ppm); this can correspond only to structure **IXa**.

In the reaction of *A* with chloroacetonitrile, the formation of the enamine **Xb** was expected on the basis of the work of DOLESCHALL *et al.* [10].

The spectral data of the product were in contradiction with the enamine structure: in the IR spectrum, only a sharp νNH band of low intensity appeared at 3280 cm^{-1} (in chloroform solution at 3320 cm^{-1}), the νC=N band was found at 1655 cm^{-1}. In the ^{1}H-NMR spectrum, a broad methylene singlet appeared at δ 3.7 ppm (a similar value was observed for the SCH_2 group in the analogous compound **Va**). Hence, according to the spectral data, the product was not the enamine **Xb**, but an imine. Decision between **Xa** and the possible structure **Xc** was made by chemical methods: the substance obtained on hydrochloric

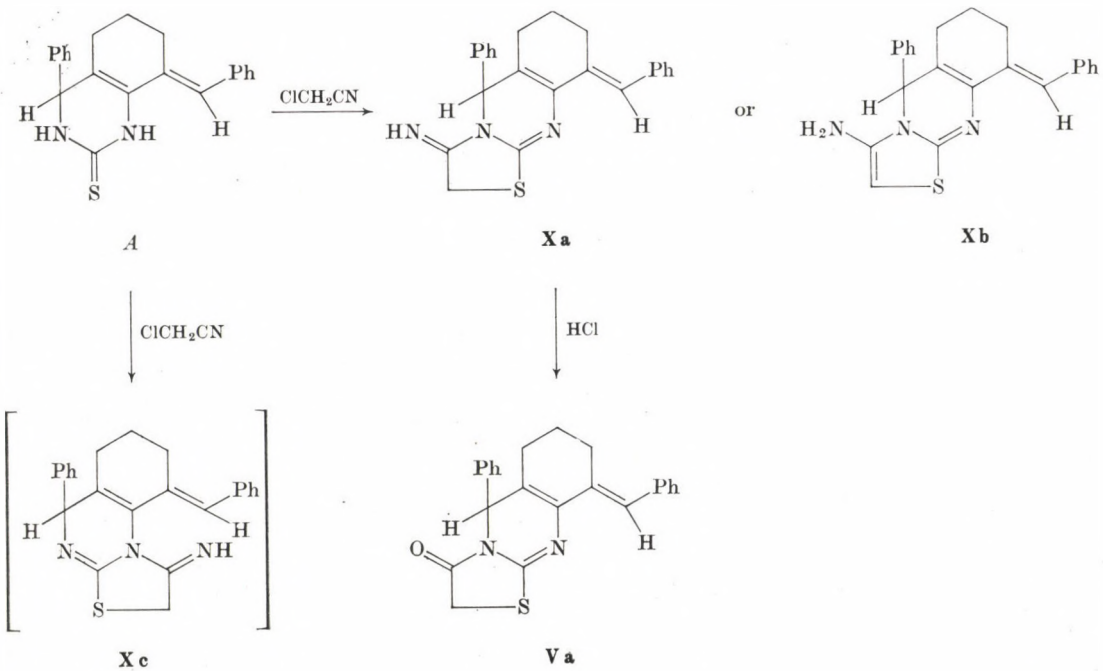

Fig. 7

acid hydrolysis of the imine was identical in all respects with **Va** prepared earlier, which fact substantiates structure **Xa** (Table V).

The cyclization reactions discussed take place probably by a two-step mechanism. The first step is alkylation at the sulfur atom, the second is cyclization through *N*-alkylation or *N*-acylation. This fact is supported by the earlier observation that in the alkylation of *A* only the *S*-alkyl derivative is formed, no *N*-alkylation takes place [2]. This is also verified by the reaction of *A* and 3-bromopropionic acid (see above). Similar results have been obtained by CHAUDHARY *et al.* [7] in the reaction of 2-mercaptoperimidine and chloroacetic acid.

Experimental

The IR spectra were recorded with a Zeiss UR-10 or Specord F5 spectrophotometer; the ^{1}H-NMR spectra were obtained with a Perkin–Elmer R-12 spectrophotometer. A VARIAN XL-100-15 FT instrument was used for recording the ^{13}C-NMR spectra (in $CDCl_3$, room temperature, the internal standard was TMS). The UV spectra were taken with a Perkin–Elmer 402 spectrophotometer. The elemental analysis data of the new compounds were in agreement with the calculated values within the limits of experimental error.

The starting material *A* and *M* were prepared from the appropriate 2,6-diarylidenecyclohexanones with thiourea [1].

Reaction of 4-phenyl-8-benzylidene-3,4,5,6,7,8-hexahydro-2(1*H*)-quinazolinethione (*A*) with α, ω-dibromoalkanes

5-phenyl-9-benzylidene-2,3,6,7,8,9-hexahydro-5*H*-thiazolo-[2,3-*b*]quinazoline (Ia)

Compound *A* (6.64 g; 0.020 mole) was dissolved in anhydrous ethanol (300 mL). 1,2-Dibromoethane (9.40 g; 0.050 mole), anhydrous potassium carbonate (10.35 g; 0.075 mole, in two portions) were added to it, and the reaction mixture was refluxed with the exclusion of moisture for 31 hrs. The solution containing a precipitate was filtered while hot, and the solid was boiled with water to remove inorganic salts. The residue was filtered off and washed with water. The alcoholic mother liquor was concentrated to give a precipitate, which was filtered off and washed with water until free from salts. The combined product was crystallized from methanol.

The syntheses of 6-phenyl-10-benzylidene-3,4,7,8,9,10-hexahydro-2*H*,6*H*-1,3-thiazino [2,3-*b*]quinazoline (**IIIa**) and of the substituted analogues (**IIa**, **IVa**) were effected in the same way.

Compounds **Ia**—**IVa** are colourless crystals; their other properties are summarized in Table III.

Reaction of 4-phenyl-8-benzylidene-3,4,5,6,7,8-hexahydro-2(1*H*)-quinazolinethione (*A*) with halogenated carboxylic acids and their esters

5-Phenyl-9-benzylidene-2,3,6,7,8,9-hexahydro-5*H*-thiazolo-[2,3-*b*]quinazolin-3-one (Va)

Method A

Compound *A* (6.64 g; 0.020 mole) was dissolved in anhydrous ethanol (250 mL). Ethyl chloroacetate (2.45 g; 0.020 mole) was added, and the reaction mixture was refluxed for 14.5 hrs with the exclusion of moisture. The crystals which separated on cooling were filtered off and washed with ethanol. The product was recrystallized from methanol.

Method B

Compound *A* (6.64 g; 0.020 mole) and sodium hydroxide (2.40 g; 0.060 mole) were dissolved in a mixture of water (15 mL) and dimethylformamide (70 mL). Chloroacetic acid (5.67 g; 0.060 mole) and a solution of $Na_2CO_3 \cdot 10\ H_2O$ (5.73 g; 0.020 mole) in a mixture of

water and dimethylformamide (35 mL each) were added, and the reaction mixture was refluxed on a water bath for 4.5 hrs. Water and concentrated hydrochloric acid were then added, the crystals which separated on cooling were filtered off and washed with water until neutral reaction. The product was recrystallized from glacial acetic acid.

Method C

Compound *A* (6.64 g; 0.020 mole) was dissolved in tetrahydrofuran (60 mL) and an aqueous solution (15 mL) of chloroacetic acid (2.08 g; 0.022 mole) and sodium hydroxide (1.20 g; 0.030 mole) was added to it. The reaction mixture was refluxed on a water bath for 15 hrs. The brown solution was clarified with carbon, filtered and concentrated. The solution was acidified with *conc.* HCl to obtain a deposit of crystals; these were filtered off and washed with water until neutral reaction. The product was crystallized from methanol.

Method D

Chloroacetic acid (3.00 g; 0.032 mole) was melted on a water bath and compound *A* (1.00 g; 0.003 mole) was added to it in small portions. The homogeneous melt was heated on a water bath for 30 min. On cooling a mass of crystals was obtained. After standing for 24 hrs, the crystals were rubbed with water, filtered off and washed with water until neutral. The product was recrystallized from acetone.

The preparation of 2-methyl-5-phenyl-9-benzylidene-2,3,6,7,8,9-hexahydro-5*H*-thiazolo-[2,3-*b*]quinazolin-3-one (**VIa**) was effected similarly, according to methods A and B. The product was crystallized from methanol or galcial acetic acid.

Compounds **Va**, **VIa** are colourless crystals; for other data, see Table IV.

Reaction of 5-phenyl-9-benzylidene-2,3,6,7,8,9-hexahydro-5*H*-thiazolo[2,3-*b*]quinazolin-3-one (Va) with aromatic aldehydes

2,9-Dibenzylidene-5-phenyl-2,3,6,7,8,9-hexahydro-5*H*-thiazolo[2,3-*b*]quinazolin-3-one (VIIa)

Compound **Va** (5.48 g; 0.015 mole) was dissolved in glacial acetic acid (120 mL) and benzaldehyde (1.59 g; 0.015 mole) and anhydrous sodium acetate (1.23 g) were added. The reaction mixture was refluxed for 4 hrs. The crystals which separated on cooling were filtered off, washed with glacial acetic acid then with water until neutral reaction. The product was recrystallized from benzene.

The synthesis of **VIIIb—e** and **VIIg—q** was effected in a similar manner by the reaction of **Va** and the appropriate aromatic aldehyde. The colour of the products varied from pale yellow to orange red. Compounds **VIIb**, **e**, **h**, **i—m**, **o**, **q** were crystallized from benzene, **VIId**, **g**, **n**, **p** from acetone, and methanol was used for **VIIc**. Compound **VIIf** was obtained from **VIIe** by hydrolysis with sulfuric acid and making the reaction mixture alkaline. Compound **VIIf** was a yellow crystalline substance which was recrystallized from benzene.

Other data of **VIIa—q** are shown in Table IV.

Reaction of 4-phenyl-8-benzylidene-3,4,5,6,7,8-hexahydro-2(1*H*)-quinazolinethione (*A*) with ethyl 3-bromopropionate

Ethyl (4-phenyl-8-benzylidene-3,4,5,6,7,8-hexahydro-quinazoline-2-mercaptopropionate) (VIII)

Compound *A* (6.64 g; 0.020 mole) was dissolved in anhydrous ethanol (250 mL). Ethyl 3-bromopropionate (5.43 g; 0.030 mole) was added, and the reaction mixture was refluxed for 32 hrs with the exclusion of moisture. The solvent was evaporated to leave a yellow oil which could not be crystallized; the substance was therefore isolated as the picrate (**VIIIa**). The yellow oil was dissolved in some ethanol and an ethanolic solution of picric acid (4.58 g; 0.020 mole) was added to it. The yellow crystals were recrystallized from ethanol.

Alkaline hydrolysis of VIII

The ester (**VIII**) prepared as described above was dissolved in ethanol (50 mL), mixed with 1*N* NaOH (10 mL), and the solution was refluxed for 8.5 hrs; then 18% hydrochloric acid (20 mL) was added. The crystals which separated on cooling were filtered off and recrystallized from acetone. The product (6.37 g; 96%) was identical with *A* in all respects.

Reaction of 4-phenyl-8-benzylidene-3,4,5,6,7,8-hexahydro-2(1*H*)-quinazolinethione (*A*) with 3-bromopropionic acid

4-Phenyl-8-benzylidene-3,4,5,6,7,8-hexahydroquinazoline-2-mercaptopropionic acid (VIIIb)

3-Bromopropionic acid (6.89 g; 0.045 mole) was melted on a water bath and compound *A* (3.32 g; 0.010 mole) was added to it in small portions. The homogeneous melt was heated on a water bath for 5 hrs. The oil was then dissolved in some methanol and poured into water. The oil which separated was allowed to stand for 1 day, whereupon it crystallized. The crystals were filtered off, washed with water until neutral and recrystallized from a mixture of acetone and methanol.

Reaction of VIIIb with acetic anhydride

6-Phenyl-10-benzylidene-3,4,7,8,9,10-hexahydro-2*H*, 6*H*-1,3-thiazino[2,3-*b*]quinazolin-4-one (IXa)

Compound **VIIIb** (1.09 g; 0.03 mole) was dissolved in acetic anhydride (30 mL) and the reaction mixture was refluxed for 4 hrs with the exclusion of moisture. The solution was then poured into water; the yellow oil which separated became crystalline on standing for 1 day. The crystals were filtered off and washed with water until neutral; the product was recrystallized from a mixture of methanol and acetone.

VIIIb and **IXa** are colourless crystals; other data of **VIIIa—b** and **IXa** are given in Table V.

Reaction of 4-phenyl-8-benzylidene-3,4,5,6,7,8-hexahydro-2(1*H*)-quinazolinethione (*A*) with chloroacetonitrile

3-Imino-5-phenyl-9-benzylidene-2,3,6,7,8,9-hexahydro-5*H*-thiazolo[2,3-*b*]quinazoline (Xa)

Compound *A* (13.28 g; 0.040 mole) was dissolved in ethanol (350 mL) and anhydrous potassium carbonate (6.90 g; 0.050 mole) and chloroacetonitrile (2.53 g; 0.040 mole) were added to the solution, which was then refluxed for 6.5 h. A colourless precipitate separated on cooling. This was filtered off, rinsed with ethanol and washed with water until neutral. The product was recrystallized from methanol. Data of **Xa** are given in Table V.

Hydrolysis of Xa with hydrochloric acid

Compound **Xa** (0.20 g; 0.0005 mole) was dissolved in a mixture of methanol (50 mL) and *conc.* HCl (30 mL), and the reaction mixture was refluxed for 12 hrs. The solution was poured into water, and the colourless precipitate which separated was filtered off and washed with water until neutral. The product (0.15 g; 74%), crystallized from methanol, was identical with **Va** in all respects.

*

The authors' thanks are due to Dr. R. OHMACHT, and Mrs. M. OTT for the analyses, to Dr. P. MOLNÁR and Mrs. Gy. HALÁSZ for the UV spectra, as well as to Miss Cs. SZEGVÁRI, Miss E. MÁTRAI, Miss H. TENCZ and Mrs. E. BLESZITY for technical assistance.

REFERENCES

[1] LÓRÁND, T., SZABÓ, D., FÖLDESI, A., NESZMÉLYI, A.: Acta Chim. Acad. Sci. Hung., **94**, 51 (1977)
[2] LÓRÁND, T., SZABÓ, D., FÖLDESI, A.: Acta Chim. Acad. Sci. Hung., **104**, 147 (1980)
[3] LÓRÁND, T., SZABÓ, D., FÖLDESI, A., NESZMÉLYI, A.: Acta Chim. Acad. Sci. Hung. (In the press)
[4] CADHA, V. K., PUJARI, H. K.: Can. J. Chem., **47**, 2841 (1969)
[5] DHAKA, K. S., CADHA, V. K., PUJARI, H. K.: Indian J. Chem., **11**, 554 (1973)
[6] SINGH, B. D., CHAUDHURRY, D. N.: Indian Chem. Soc., **47**, 759 (1970)
[7] CHAUDHARY, H. S., PUJARI, H. K.: Indian J. Chem., **7**, 767 (1969)

[8] JAENECKE, G., MALLON, H. J. RAEPKE, H.: Z. f. Chem., **8,** 462 (1968)
[9] NYITRAI, J., BÉKÁSSY, S., LEMPERT, K.: Acta Chim. Acad. Sci. Hung., **53,** 311 (1967)
[10] DOLESCHALL, G., HORNYÁK, GY., HORNYÁK-HÁMORI, M., LEMPERT, K., WOLFNER, A.: Acta Chim. Acad. Sci. Hung., **53,** 385 (1967)
[11] HORNYÁK, GY., ÁGAI, B., SZÖCS, L., LEMPERT, K.: Acta Chim. Acad. Sci. Hung., **88,** 413 (1976)
[12] TREPANIER, D. L., KRIEGER, P. E.: J. Heterocyclic Chem., **7,** 1231 (1970)
[13] ALI, M. I., ABD-ELFATTAH, A. M., HAMMONDA, H. A., HUSSEIN, S. M.: Indian J. Chem., **13,** 109 (1975)
[14] BREITMAYER, E., VOELTER, W.: ^{13}C-NMR Spectroscopy, Verlag Chemie, Berlin, 1974
[15] ELIEL, E. L., PIETRUSIEWICZ, K. M.: Topics in Carbon-13 NMR Spectroscopy Vol. **3,** p. 172. Ed. G. C. LEVY. Wiley and Sons, New York, 1979
[16] BELLAMY, L. J.: The Infra-red Spectra of Complex Molecules, p. 214. Methuen, London — Wiley, New York, 1966
[17] HASSNER, A., MEAD, T. C.: Tetrahedron, **20,** 2201 (1964)
[18] KEVILL, D. N., WEILER, E. D., CROMWELL, N. H.: J. Org. Chem., **29,** 1276 (1964)

Tamás LÓRÁND
Dezső SZABÓ
András FÖLDESI
H-7643 Pécs, Szigeti út 12.

András NESZMÉLYI H-1025 Budapest, Pusztaszeri út 57—59.

INDEX

PHYSICAL AND INORGANIC CHEMISTRY

ORGANIC CHEMISTRY

ANALYTICAL CHEMISTRY

Printed in Hungary

A kiadásért felel az Akadémiai Kiadó igazgatója. Műszaki szerkesztő: Rózsa Katalin

A kézirat nyomdába érkezett: 1981. III. 16. — Terjedelem: 10 (A/5) ív, 39 ábra

81.9452 Akadémiai Nyomda, Budapest — Felelős vezető: Bernát György

Les Acta Chimica paraissent en français, allemand, anglais et russe et publient des mémoires du domaine des sciences chimiques.

Les Acta Chimica sont publiés sous forme de fascicules. Quatre fascicules seront réunis en un volume (3 volumes par an).

On est prié d'envoyer les manuscrits destinés à la rédaction à l'adresse suivante:

Acta Chimica
Budapest, P.O.B. 67, H-1450, Hongrie

Toute correspondance doit être envoyée à cette même adresse.

La rédaction ne rend pas de manuscript.

Abonnement en Hongrie à l'Akadémiai Kiadó (1363 Budapest, P.O.B. 24, C. C. B. 215 11488) à l'étranger à l'Entreprise du Commerce Extérieur « Kultura » (H-1389 Budapest 62, P.O.B. 149 Compte-courant No. 218 10990) ou chez représentants à l'étranger.

Die Acta Chimica veröffentlichen Abhandlungen aus dem Bereich der chemischen Wissenschaften in deutscher, englischer, französischer und russischer Sprache.

Die Acta Chimica erscheinen in Heften wechselnden Umfanges. Vier Hefte bilden einen Band. Jährlich erscheinen 3 Bände.

Die zur Veröffentlichung bestimmten Manuskripte sind an folgende Adresse zu senden

Acta Chimica
Budapest, Postfach 67, H-1450, Ungarn

An die gleiche Anschrift ist jede für die Redaktion bestimmte Korrespondenz zu richten.

Manuskripte werden nicht zurückerstattet.

Bestellbar für das Inland bei Akadémiai Kiadó (1363 Budapest, Postfach 24, Bankkonto Nr. 215 11488), für das Ausland bei »Kultura« Außenhandelsunternehmen (H-1389 Budapest 62, P.O.B. 149. Bankkonto Nr. 218 10990) oder seinen Auslandsvertretungen.

«Acta Chimica» издают статы по химии на русском, английском, французском и немецком языках.

«Acta Chimica» выходит отдельными выпусками разного объема, 4 выпуска составляют один том и за год выходят 3 тома.

Предназначенные для публикации рукописи следует направлять по адресу:

Acta Chimica
Budapest, P.O.B. 67, H-1450, ВНР

Всякую корреспонденцию в редакцию направляйте по этому же адресу.

Редакция рукописей не возвращает.

Отечественные подписчики направляйте свои заявки по адресу Издательства Академии Наук (1363 Budapest, P.O.B. 24. Текущий счет 215 11488), а иностранные подписчики через организацию по внешней торговле «Kultura» (H-1389 Budapest 62, P O.B. 149. Текущий счет 218 10990) или через ее заграничные представительства и уполномоченных.

Reviews of the Hungarian Academy of Sciences are obtainable at the following addresses:

AUSTRALIA
C.B.D LIBRARY AND SUBSCRIPTION SERVICE, Box 4886, G.P.O., *Sydney N.S.W. 2001*
COSMOS BOOKSHOP 145 Ackland Street, *St. Kilda (Melbourne), Victoria 3182*

AUSTRIA
GLOBUS Höchstädtplatz 4, *1200 Wien XX*

BELGIUM
OFFICE INTERNATIONAL DE LIBRAIRIE, 30 Avenue Marnix, *1050 Bruxelles*
LIBRAIRIE DU MONDE ENTIER, 162 Rue du Midi, *1000 Bruxelles*

BULGARIA
HEMUS Bulvar Ruszki 6, *Sofia*

CANADA
PANNONIA BOOKS, P.O. Box 1017, Postal Station "B", *Toronto, Ontario M5T 2T8*

CHINA
CNPICOR, Periodical Department, P.O. Box 50, *Peking*

CZECHOSLOVAKIA
MAD'ARSKÁ KULTURA, Národní třida 22, *115 66 Praha*
PNS DOVOZ TISKU, Vinohradská 46, *Praha 2*
PNS DOVOZ TLAČE, *Bratislava 2*

DENMARK
EJNAR MUNKSGAARD Norregade 6, *1165 Copenhagen*

FINLAND
AKATEEMINEN KIRJAKAUPPA, P.O. Box 128, *SF-00101 Helsinki 10*

FRANCE
EUROPERIODIQUES S. A., 31 Avenue de Versailles, *78170 La Celle St.-Cloud*
LIBRAIRIE LAVOISIER, 11 rue Lavoisier, *75008 Paris*
OFFICE INTERNATIONAL DE DOCUMENTATION ET LIBRAIRIE, 48 rue Gay-Lussac, *75240 Paris Cedex 05*

GERMAN DEMOCRATIC REPUBLIC
HAUS DER UNGARISCHEN KULTUR, Karl-Liebknecht-Strasse 9, *DDR-102 Berlin*
DEUTSCHE POST ZEITUNGSVERTRIEBSAMT, Strasse der Pariser Kommüne 3—4, *DDR-104 Berlin*

GERMAN FEDERAL REPUBLIC
KUNST UND WISSEN ERICH BIEBER, Postfach 46, *7000 Stuttgart 1*

GREAT BRITAIN
BLACKWELL'S PERIODICALS DIVISION, Hythe Bridge Street, *Oxford OX1 2ET*
BUMPUS, HALDANE AND MAXWELL LTD., Cowper Works, *Olney, Bucks MK46 4BN*
COLLET'S HOLDINGS LTD., Denington Estate, *Wellingborough, Northants NN8 2QT*
W.M. DAWSON AND SONS LTD., Cannon House, *Folkestone, Kent CT19 5EE*
H. K LEWIS AND CO., 136 Gower Street, *London WC1E 6BS*

GREECE
KOSTARAKIS BROTHERS, International Booksellers, 2 Hippokratous Street, *Athens-143*

HOLLAND
MEULENHOFF-BRUNA B.V., Beulingstraat 2, *Amsterdam*
MARTINUS NIJHOFF B.V., Lange Voorhout 9—11, *Den Haag*
SWETS SUBSCRIPTION SERVICE, 347b Heereweg, *Lisse*

INDIA
ALLIED PUBLISHING PRIVATE LTD., 13/14 Asat Ali Road, *New Delhi 110001*
150 B-6 Mount Road, *Madras 600002*
INTERNATIONAL BOOK HOUSE PVT. LTD., Madame Cama Road, *Bombay 400039*
THE STATE TRADING CORPORATION OF INDIA LTD., Books Import Division, Chandralok, 36 Janpath, *New Delhi 110001*

ITALY
EUGENIO CARLUCCI, P.O. Box 252, *70100 Bari*
INTERSCIENTIA, Via Mazzé 28, *10149 Torino*
LIBRERIA COMMISSIONARIA SANSONI, Via Lamarmora 45, *50121 Firenze*
SANTO VANASIA, Via M. Macchi 58, *20124 Milano*
D. E. A., Via Lima 28, *00198 Roma*

JAPAN
KINOKUNIYA BOOK-STORE CO. LTD., 17-7, Shinjuku-ku 3 chome, Shinjuku-ku, *Tokyo 160-91*
MARUZEN COMPANY LTD., Book Department P.O. Box 5056 Tokyo International, *Tokyo 100-31*
NAUKA LTD., IMPORT DEPARTMENT, 2-30-19 Minami Ikebukuro, Toshima-ku, *Tokyo 171*

KOREA
CHULPANMUL, *Phenjan*

NORWAY
TANUM-CAMMERMEYER, Karl Johansgatan 41—43, *1000 Oslo*

POLAND
WĘGIERSKI INSTYTUT KULTURY, Marszałkowska 80, *Warszawa*
CKP I W ul. Towarowa 28 *00-958 Warsawa*

ROMANIA
D. E. P., *Bucureşti*
ROMLIBRI, Str. Biserica Amzei 7, *Bucureştt*

SOVIET UNION
SOJUZPETCHATJ — IMPORT, *Moscow*
and the post offices in each town
MEZHDUNARODNAYA KNIGA, *Moscow G-200*

SPAIN
DIAZ DE SANTOS, Lagasca 95, *Madrid 6*

SWEDEN
ALMQVIST AND WIKSELL, Gamla Brogatan 26, *101 20 Stockholm*
GUMPERTS UNIVERSITETSBOKHANDEL AB, Box 346, *401 25 Göteborg 1*

SWITZERLAND
KARGER LIBRI AG, Petersgraben 31, *4011 Base*

USA
EBSCO SUBSCRIPTION SERVICES, P.O. Box 1943, *Birmingham, Alabama 35201*
F. W. FAXON COMPANY, INC., 15 Southwest Park, *Westwood, Mass, 02090*
THE MOORE-COTTRELL SUBSCRIPTION AGENCIES, *North Cohocton, N. Y. 14868*
READ-MORE PUBLICATIONS, INC., 140 Cedar Street, *New York, N. Y. 10006*
STECHERT-MACMILLAN INC., 7250 Westfield Avenue, *Pennsauken N. J. 08110*

VIETNAM
XUNHASABA, 32, Hai Ba Trung, *Hanoi*

YUGOSLAVIA
JUGOSLAVENSKA KNJIGA, Terazije 27, *Beograd*
FORUM, Vojvode Mišića 1, *21000 Novi Sad*

16. XI. 1981 HU ISSN 0001—5407 Index: 26.007

ACTA CHIMICA

ACADEMIAE SCIENTIARUM HUNGARICAE

TOMUS 108 FASCICULUS 3

AKADÉMIAI KIADÓ, BUDAPEST

1981

ACTA CHIM. ACAD. SCI. HUNG. ACASA2 108 (3) 215–324 (1981)

ACTA CHIMICA

A MAGYAR TUDOMÁNYOS AKADÉMIA KÉMIAI TUDOMÁNYOK OSZTÁLYÁNAK IDEGEN NYELVŰ KÖZLEMÉNYEI

Acta Chimica is a journal for the publication of papers on all aspects of chemistry in English, German, French and Russian.

Acta Chimica is published in 3 volumes per year. Each volume consists of 4 issues of varying size

Manuscripts should be sent to

Acta Chimica
Budapest, P.O. Box 67, H-1450, Hungary

Correspondence with the editors should be sent to the same address. Manuscripts are not returned to the authors.

Hungarian subscribers should order from Akadémiai Kiadó, 1363 Budapest, P.O.B. 24. Account No. 215 11488.

Orders from other countries are to be sent to "Kultura" Foreign Trading Company (H-1389 Budapest 62, P.O.B. 149. Account No. 218 10990) or its representatives abroad.

Acta Chimica Academiae Scientiarum Hungaricae, Tomus 108 (3), pp. 215—217 (1981)

A FAVORSKII REARRANGEMENT INVOLVING A CARBANION AS A NUCLEOPHILE

M. I. QURESHI

(Department of Chemistry, Faculty of Science, Garyounis University, Benghazi, Libya)

Received May 22, 1980

Accepted for publication August 21, 1980*

Treatment of 2-bromo-methylcycloheptanone **3** with acetoacetic ester in the presence of sodium ethoxide furnished ethyl 1'-methylcyclohexylcarbonylacetate **6** in 34.9% yield. A mechanism leading to the formation of the β-keto ester **6** *via* Favorskii rearrangement involving nucleophilic attack of a carbanion (sodioacetoacetic ester) on the cyclopropanone intermediate **4** is suggested.

The Favorskii rearrangement [1] is a useful synthetic tool for ring contraction and for the preparation of acids, ester and amides by the reaction of α-haloketones with hydroxides, alkoxides or amines. The currently accepted mechanism [1] of this reaction, involving the attack of a nucleophile ($\overline{O}H$, $\overline{O}R$ or $:NR_3$) on the cyclopropanone intermediate **1**, suggested that it might be possible to carry out the reaction under conditions that would permit the nucleophilic attack of a carbanion on **1**, so as to form ketonic products **2.**

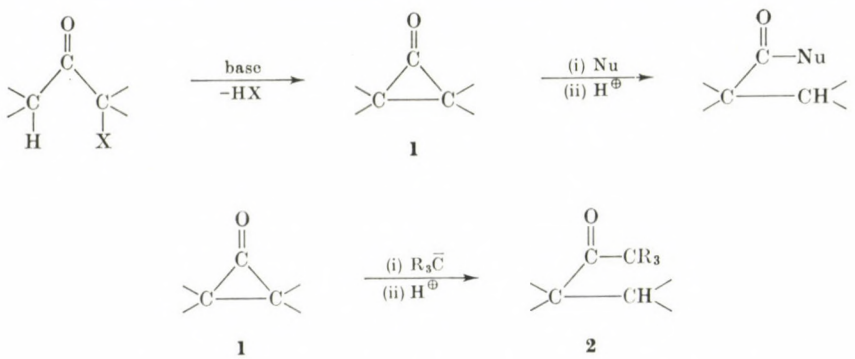

1 **2**

The present paper reports the successful application of this method using sodioacetoacetic ester as the carbanion and 2-bromo-2-methylcycloheptanone **3** as the α-haloketone.

The α-bromoketone **3** was prepared by *N*-bromosuccinimide bromination of 2-methylcycloheptanone. Treatment of **3** with acetoacetic ester in the presence of sodium ethoxide in boiling ethanol furnished the β-keto ester **6**

* In final form accepted March 25, 1981

as the chief product, which was isolated by a combination of fractional distillation and preparative thin-layer chromatography.

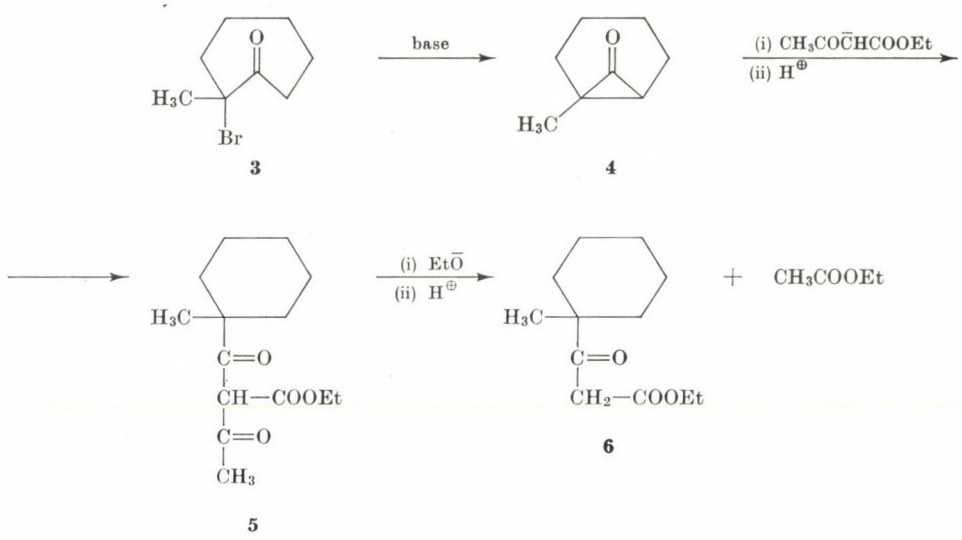

3 4 5 6

Formation of the β-keto ester **6** might reasonably be explained as follow the cyclopropanone intermediate **4**, obtained by attack of a base ($Et\bar{O}$ or $CH_3C\bar{O}CHCOOEt$) on the α-bromoketone **3**, reacts with $CH_3C\bar{O}CHCOOEt$ to form the β,β'-diketo ester **5**. Subsequent cleavage of **5** by attack of $Et\bar{O}$ leads to the β-keto ester **6**.

Structural assignment was made on the basis of elementary analysis and spectra, and by the conversion of **6** into the known compound, 1-methyl-1--acetylcyclohexane **7**.

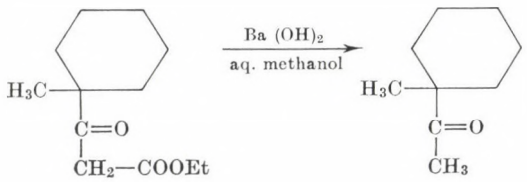

6 7

Experimental

IR spectra were recorded on a Unicam SP1000 spectrophotometer and refer to thin films on NaCl discs unless stated otherwise. UV spectra were obtained on a Unicam SP 1800 spectrophotometer, using 95% ethanol as solvent. NMR spectra were measured on a 60 MHz instrument using $CDCl_3$ as solvent. Chemical shifts are given in τ units using TMS as internal reference.

Thin- (0.25 mm) and thick- (1.0 mm) layer chromatography plates were prepared from Kieselgel DF (Riedel-De Haen). All organic extracts were dried over anhydrous magnesium sulphate.

2-Bromo-2-methylcycloheptanone (3)

2-Methylcycloheptanone (1.26 g), benzoyl peroxide (20 mg) and CCl_4 (20 mL) were heated under reflux until all the solid materials came to the top of the liquid surface (1.5 h). Work-up by washing with water, drying and concentration gave 2.05 g (quantitative yield) of the bromoketone as an oil, b.p. 64—68 °C (air bath temperature) at 0.37 mbar.

IR: ν_{max} 1705 cm^{-1}.

NMR: 8.23 (3H, s, methyl group).

$C_8H_{13}OBr$. Calcd. C 46.84; H 6.39; Br 38.87. Found C 47.06; H 6.20; Br. 39.10%.

Ethyl 1'-methylcyclohexylcarbonylacetate (6)

Ethyl acetoacetate (2.60 g) was added to a sodium ethoxide solution prepared by dissolving sodium (0.46 g) in ethanol (20 mL). After stirring at room temperature for 5 min, 2-bromo-2-methylcycloheptanone (2.05 g) was added. The mixture was heated under reflux for 3 hrs. The ethanol was then removed by distillation and water (30 mL) was added. Extraction with ether, drying and concentration gave an oil (2.91 g). Purification by fractional distillation followed by preparative TLC furnished ethyl 1'-methylcyclohexylcarbonylacetate **6** (0.74 g; 34.9%) as a colourless oil, b.p. 100 °C (air bath temperature) at 0.8 mbar.

IR: ν_{max} 1745, 1703, 1642 and 1610 cm^{-1}.

UV: λ_{max} 250 nm (3380).

NMR: 5.85 (2H, q, $COOCH_2CH_3$); 6.51 (2H, s, $COCH_2COOEt$); 8.78 (3H, t, $COOCH_2CH_3$) 8.9 (3H, s, quaternary methyl).

$C_{12}H_{20}O_3$. Calcd. C 67.89; H 9.50. Found C 67.85; H 9.21%.

1-Methyl-1-acetylcyclohexane (7)

Ethyl 1'-methylcyclohexylcarbonylacetate **6** (63 mg) was heated under reflux with $Ba(OH)_2$. 8 H_2O (120 mg), methanol (1 mL) and water (1.5 mL) for 16 h. Work-up by the addition of water and extraction with ether, followed by drying and concentration of the ethereal extract gave 31 mg of 1-methyl-1-acetylcyclohexane as a colourless oil, b.p. 60—62 °C (air bath temperature) at 1.33 mbar.

IR: ν_{max} 1700 cm^{-1}.

NMR: 7.9 (3H, s, $COCH_3$); 8.92 (3H, s, quaternary methyl group).

$C_9H_{16}O$. Calcd. C 77.08; H 11.50. Found C 77.32; H 11.29%.

The 2,4-dinitrophenylhydrazone derivative had m.p. 130—132 °C (*lit.* [2] m.p. 134 °C).

REFERENCES

[1] March, J.: Advanced Organic Chemistry', p. 991, McGraw-Hill Inc., New York, 1977, and references cited therein

[2] Rouzaud, J., Cauquil, G., Giral, L.: Bull. Soc. Chim. France, **1965** (7), 2030

Mohammad Ismail Qureshi

Department of Chemistry, Faculty of Science, Garyounis University, P.O. Box 9480, Benghazi, Libya

Acta Chimica Academiae Scientiarum Hungaricae, Tomus 108 (3), pp. 219—227 (1981)

TRANSITION METAL CHEMISTRY OF OXIME CONTAINING LIGANDS, XIII

COBALT(II) COMPLEXES OF *SYN*-PHENYL-2-PYRIDYLKETOXIME AND *SYN*-METHYL-2-PYRIDYLKETOXIME

M. MOHAN and B. D. PARAMHANS

(*Department of Chemistry, N.R.E.C. College, Khurja, U.P.*, 203131, *India*)

Received March 4, 1980

In revised form August 21, 1980

Accepted for publication September 30, 1980*

Cobalt(II) complexes of the types $[Co(HL)_2(X)_2]$ (where HL = *syn*-phenyl-2-pyridylketoxime (Hppk) or *syn*-methyl-2-pyridylketoxime (Hmpk) and X = Cl, Br, I, NCS, NCSe, $1/2SO_4$ or OAc) and $[Co(HL)_2(NO_3)]NO_3$ (where HL = Hppk or Hmpk) were synthesized and characterized by elemental analysis, molar conductance in solution, molecular weight determination, X-ray powder diffraction, magnetic moments (300—78 K), diffuse reflectance and infrared (4000—200 cm^{-1}) spectral measurements. These studies suggest a dimeric halo-bridged *cis*-distorted octahedral structure for $[Co(HL)_2(X)_2]$ (where HL = Hppk or Hmpk and X = Cl, Br or I) and a monomeric *cis*-pseudo-octahedral structure for the remaining cobalt(II) complexes.

Introduction

syn-Phenyl-2-pyridylketoxime (Hppk) and *syn*-methyl-2-pyridylketoxime (Hmpk) have features in common with ligands of both the 2,2'-bipyridyl and dimethylglyoxime types. In spite of the obvious interest associated with these ligands, very little work has been reported. Formation constants of nickel(II) complexes of Hmpk and a number of complexes formed by Hppk have been reported [1, 2]. WARD, MEEK and CHENEY [2] have isolated and characterized a series of nickel(II) complexes with Hppk. SEN and MALONE [4] have described manganese(II), cobalt(II), nickel(II) and palladium(II) complexes with Hppk of the compositions $[Mn(Hppk)_2(Cl)_2]$; $[Co(Hppk)_2(NO_3)_2]$: $[Ni(Hppk)_2(NO_3)_2]$; [Pd(Hppk)(ppk)Cl] and $[Pd(ppk)_2]$ (where ppk = anion of Hppk). Aside from this work, no other studies dealing with the complexes of Hppk and Hmpk have appeared in the literature. In this paper, we report the synthesis and characterization of some cobalt(II) complexes with Hppk and Hmpk. The complexes have been characterized by elemental analysis, molar conductance, molecular weight, X-ray powder diffraction, magnetic susceptibility, diffuse reflectance and infrared spectral measurements.

* In final form accepted March 11, 1981

Experimental

syn-Phenyl-2-pyridylketoxime (Hppk) and *syn*-methyl-2-pyridylketoxime (Hmpk) have been prepared from 2-benzoylpyridine and 2-acetylpyridine (K & K Laboratory, New York) according to the method of DRAGO and BAUCOM [3] and their authenticity was established by elemental analysis and I.R. spectra. M.p. 163—164 °C (Hppk); 121—122 °C (Hmpk). The hydrated cobalt(II) salts, 2,2-dimethoxypropane (K & K Laboratories, New York) and other solvents were of reagent grade.

Isolation of the Complexes

The following general procedure was used for the isolation of the cobalt(II) complexes. Cobalt(II) salt hexahydrate (0.04 mol) was dissolved in a mixture of EtOH (25 cm^3) and 2,2'-dimethoxypropane (20 cm^3) or in a minimum amount of H_2O (in case of sulphate and acetate salt) and was heated for 2—4 hrs under reflux. Hppk or Hmpk (0.08 mol) was dissolved in the same solvent mixture and was heated to boil. Ligand and metal salt solutions were then mixed and the pink solution mixture was heated for 2—6 hrs under reflux. On cooling the solution mixture at room temperature the polycrystalline solid was obtained. The solid was filtered, washed with water (in case of sulfato and acetato complexes), EtOH and Et_2O and dried over P_4O_{10} in vacuum.

Physicochemical Studies

Conductance measurements were carried out on a type CL01/01 Toshniwal conductivity bridge. Molecular weights were determined cryoscopically. The molecular weights of the complexes are given in Table I. Magnetic measurements from room temperature to 78 K were made on a standard GOUY's balance using $HgCo(NCS)_4$ as a calibrant; diamagnetic corrections were estimated by using PASCAL's constants. X-ray powder diffraction patterns were obtained on a Siemens Powder diffractometer using nickel filtered CuK_α radiation.

Diffuse reflectance spectra of all the complexes at room temperature were measured on a Cary-14 spectrophotometer equipped with a reflectance accessory using MgO as a reference. The infrared spectra in the region 400—200 cm^{-1} of Hppk and Hmpk and their complexes were measured on a Perkin–Elmer 337 spectrophotometer in CsI.

The cobalt content of the complexes was estimated by EDTA titration using Eriochrome Black T as an indicator, after destroying the organic portion first with aqua regia and then with *conc.* H_2SO_4. Halides were estimated by VOLHARD's method and nitrate was determined as its nitrone salt. C, H and N analyses were obtained through the kind courtesy of Microanalytical Laboratory C.D.R.I., Lucknow. The analytical data are presented in Table I.

Results and Discussion

On interaction with Hppk and Hmpk the cobalt(II) ion yields complexes corresponding to the general formula $[Co(HL)_2(X)_2]$ (where HL = Hppk or Hmpk and X = Cl, Br, I, NCS, NCSe, OAc or $1/2SO_4$) and $[Cu(HL)_3(NO_3)](NO_3)$ (where HL = Hppk or Hmpk). All the complexes are quite stable at room temperature and do not exhibit any decomposition even after prolonged standing. All the complexes are insoluble in water and non-polar solvents and, except for the cobalt(II) halo complexes, partially soluble in moderately polar solvents and soluble in polar solvents. The molar conductance of $[Co(HL)_2(X)_2]$ (where HL = Hppk or Hmpk and X = NCS, NCSe, OAc or $1/2SO_4$) and $[Co(HL)_2(NO_3)](NO_3)$ (where HL = Hppk or Hmpk) complexes in MeOH at the concentration level of 10^{-3} *M* lie in the range 0.38—1.02 and 90.5—98.7 mhos cm^{-2} mol^{-1} suggesting the presence of non-ionic and uni-univalent electrolytes [4] in the solvent, respectively. Molecular weights of $[Co(HL)_2(X)_2]$ (where HL = Hppk or Hmpk and X = NCS, NCSe, OAc

Table I

Analytical data of cobalt(II) complexes

Compound	M.W.[a]	Found (Calc.) %				
		C	H	N	X	M
$[Co(Hppk)_2(Cl)_2]_2$	—	54.80 (54.76)	3.77 (3.80)	10.70 (10.64)	13.60 (13.50)	11.24 (11.19)
$[Co(Hppk)_2(Br)_2]_2$	—	40.85 (40.88)	3.20 (3.25)	9.14 (9.10)	26.14 (26.02)	9.63 (9.57)
$[Co(Hppk)_2(I)_2]_2$	—	40.60 (40.62)	2.88 (2.82)	7.93 (7.89)	35.90 (35.83)	8.40 (8.30)
$[Co(Hppk)_2(NO_3)](NO_3)$	585.7 (578.9)	49.78 (49.75)	3.48 (3.45)	9.72 (9.67)	21.52 (21.41)	10.26 (10.17)
$[Co(Hppk)_2(NCS)_2]$	576.2 (570.9)	50.40 (50.44)	3.54 (3.50)	9.76 (9.80)	20.40 (20.32)	10.42 (10.31)
$[Co(Hppk)_2(NCSe)_2]$	670.4 (664.9)	46.97 (46.92)	3.10 (3.10)	12.70 (12.63)	23.82 (23.76)[b]	8.98 (8.85)
$[Co(Hppk)_2(OAc)_2]$	575.8 (572.9)	58.70 (58.64)	4.56 (4.53)	9.80 (9.77)	—	10.36 (10.28)
$[Co(Hppk)_2(SO_4)]$	554.6 (550.9)	52.22 (52.27)	3.71 (3.63)	10.20 (10.16)	—	10.77 (10.69)
$[Co(Hmpk)_2(Cl)_2]_2$	—	41.84 (41.80)	3.92 (3.98)	13.90 (13.93)	17.73 (17.66)	14.72 (14.64)
$[Co(Hmpk)_2(Br)_2]_2$	—	34.30 (34.22)	3.20 (3.26)	11.52 (11.40)	32.68 (32.59)	12.10 (11.99)
$[Co(Hmpk)_2(I)_2]_2$	—	28.78 (28.72)	2.70 (2.73)	9.60 (9.57)	43.50 (43.42)	10.17 (10.07)
$[Co(Hmpk)_2(NO_3)](NO_3)$	462.8 (454.9)	36.98 (36.98)	3.60 (3.51)	12.40 (12.31)	27.34 (27.25)	12.99 (12.94)
$[Co(Hmpk)_2(NCS)_2]$	452.5 (446.9)	37.62 (37.59)	3.50 (3.58)	12.60 (12.53)	25.80 (25.95)	13.26 (13.17)
$[Co(Hmpk)_2(NCSe)_2]$	546.2 (540.9)	35.54 (35.49)	2.90 (2.95)	15.60 (15.90)	29.28 (29.21)[b]	10.97 (10.88)
$[Co(Hmpk)_2(OAc)_2]$	456.4 (448.9)	48.16 (48.11)	4.94 (4.90)	12.50 (12.48)	—	13.04 (13.12)
$[Co(Hmpk)_2(SO)_4]$	438.7 (426.9)	39.42 (39.35)	3.79 (3.74)	13.15 (13.11)	—	13.86 (13.79)

[a] Found (Calc.) [b] Se

or $1/2SO_4$) and $[Co(HL)_2(X)_2(NO_3)](NO_3)$ where HL = Hppk or Hmpk) in formamide show that they are monomeric complexes.

The X-ray powder diffraction patterns* for each of the cobalt(II) complexes under study have been measured and compared for any indication of isomorphism. The results indicate that $[Co(HL)_2(X)_2]$ (where HL = Hppk or Hmpk and X = NCS, NCSe or OAc) are X-ray isomorphous and are isostructural. The patterns of $[Co(HL)_2(SO_4)]$ and $[Co(HL)_2(NO_3)](NO_3)$ complexes have many lines in common with the above complexes and they are probably isostructural. The patterns of cobalt(II) halo complexes are not isomorphous with any set of the complexes mentioned above and hence, are structurally different.

Infrared Spectra

Hppk and Hmpk exhibit multiple bands over the range 3300—2800 cm^{-1} which are assigned [2] to intermolecular hydrogen-bonded OH of the NOH groups. The νC—H stretching vibrations, which could be present in this region, are obscured by νOH absorption bands. The spectra of all cobalt(II) complexes exhibit strong broad bands in the 3480—3400 and 3060—3050 cm^{-1} range which are assigned [2] to free OH of NOH groups and νC—H stretching vibrations of the ligand molecule, respectively. The νC=N (acyclic) and νN—O stretching vibrations in free Hppk and Hmpk are observed at *ca.* 1612 and 980 cm^{-1} respectively. These stretching vibrations are shifted to *ca.* 1650 and 1070 cm^{-1} in their cobalt(II) complexes an indication of coordination of neutral oxime nitrogen atom to the cobalt(II) ion [5]. The coordination of the pyridine nitrogen atom is indicated by shifting and splitting of the ring vibrations as is usually observed [6] for other metal(II) pyridine complexes.

In the 400—200 cm^{-1} region Hppk and Hmpk exhibit bands at 400 (s), *ca.* 335 (s), *ca.* 290 (m), *ca.* 275 (w), *ca.* 250 (vs) and *ca.* 220 (s) cm^{-1}, whereas cobalt(II) complexes have absorption bands of varying intensity at *ca.* 390; *ca.* 335; *ca.* 305, 295; *ca.* 250 and *ca.* 200 cm^{-1} assigned to ligand absorption bands. In chloro complexes two bands are observed at 230 (m) and *ca.* 216 (w) cm^{-1} assigned to νCo—Cl stretching vibrations. No νCo—Br and νCo—I bands are observed in this region. The relatively low frequency assigned to these νCo–halo vibrations [7] are consistent with a *cis*-halogen bridge structure, although νCo–halo vibrations are expected over a wide range and some terminal νCo–halo frequencies are also reported in this region. The low symmetry of these complexes should lead to the observation of up to four νCo—N (ligand) stretching vibrations [8]. In these complexes four stretching vibrations of varying intensity are observed at *ca.* 370; *ca.* 355, 315 and *ca.* 280 cm^{-1}. These are assigned to νCo—N (ligand) vibrations, though in case of nitrato,

* The details of X-ray powder diffraction results can be obtained from the authors on request.

acetato and sulfato complexes a νCo—O stretching band is also observed in this region. The similarity of νCo—N (ligand) vibrations suggests that in all these complexes the two ligand molecules have the same configuration in relation to each other.

In nitrato complexes additional bands are observed at *ca.* 990 (s), 810 (w), *ca.* 1250 (s), *ca.* 780 (sh) and 655 (s) cm^{-1} assigned to NO_2 symmetric stretch, NO_2 symmetric band, NO_2 asymmetric stretch, NO_2 asymmetric band and out-of-plane vibrations of bidentate coordinated (C_{2v}) nitrate group [9]. This is further confirmed by the presence of the ($\nu_1 + \nu_2$) combination mode of vibrations [10] at *ca.* 1810 (m) and 1760 (m) cm^{-1}. The sharp intensive band at 830 cm^{-1} and a very sharp broad band at 1350 cm^{-1} indicate the presence of ionic (D_{3h}) nitrate group [9].

In isothiocyanato and isoselenocyanato complexes, very strong bands are observed at 2070 and 2020 cm^{-1} assigned to ν_1[(C—N) stretching] vibration of N-bonded thiocyanato or selenocyanato groups [11]. The observed splitting of ν_1 vibration is an indication of *cis*-configuration [11]. The ν_2 [(N—C—S) or N—C—Se)] and ν_3 [C—S or C—Se)] stretching vibrations are obscured by ligand absorption bands.

In sulfato complexes the presence of ν_1 at 1020 (m); ν_2 at 450 (m, b); ν_3 at 1075 (w), *ca.* 1102 (s) and *ca.* 1175 (m) and ν_4 at 610 (s) cm^{-1} suggest a bidentate sulfato group [12], whereas the presence of a unidentate acetate group [13] is confirmed by the appearance of ν COO symmetric and ν COO asymmetric stretching vibrations at 1700 (m, b) and 1425 (s) cm^{-1} in $[Co(HL)_2(OAc)_2]$ complexes.

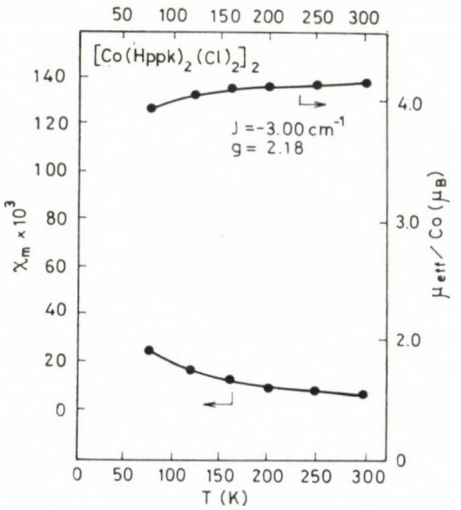

Fig. 1. Molar susceptibility (cm^3) and effective magnetic moment (μ_{eff} in μ_B) *vs.* temperature curves for $[Co(Hppk)_2(Cl)_2]_2$. The solid lines are least-squares theoretical fis using an $S_1 = S_2 = 3/2$ isotropic dimer expression where single-ion zero-field interaction are ignored

Magnetic Susceptibility

The temperature dependent magnetic susceptibility data for $[Co(Hppk)_2(Cl)_2]$ complex is illustrated in Fig. 1 and the μ_{eff} values of the other complexes at room temperature and 78 K are presented in Table II. Some

Table II

Magnetic susceptibility data of cobalt(II) complexes

Compound	T(K)	χ_m(cm^3)	$\mu_{eff}(\mu_B)$	J (Cm^{-1})	g
$[Co(Hppk)_2(Cl)_2]_2$	300.0	7 220	4.18	−3.00	2.18
	78.0	24 425	3.92		
$[Co(Hppk)_2(Br)_2]_2$	297.5	7 280	4.18	−2.50	2.17
	78.0	25 180	3.98		
$[Co(Hppk)_2(I)_2]_2$	298.0	7 340	4.20	−2.0	2.17
	78.0	25 430	4.00		
$[Co(Hppk)_2(NO_3)](NO_3)$	299.2	8 400	4.50		
	78.0	31 060	4.42		
$[Co(Hppk)_2(NCS)_2]$	295.7	8 720	4.56		
	78.0	32 050	4.49		
$[Co(Hppk)_2(NCSe)_2]$	296.2	8 440	4.60		
	78.0	31 900	4.48		
$[Co(Hppk)_2(OAc)_2]$	297.2	8 600	4.54		
	78.0	31 480	4.45		
$[Co(Hppk)_2(SO_4)]$	298.7	8 480	4.52		
	78.0	31 620	4.46		
$[Co(Hmpk)_2(Cl)_2]_2$	300.0	7 150	4.16	−2.98	2.18
	78.0	25 180	3.98		
$[Co(Hmpk)_2(Br)_2]_2$	299.8	7 190	4.17	−2.50	2.17
	78.0	25 300	3.99		
$[Co(Hmpk)_2(I)_2]_2$	300.0	7 220	4.18	−1.98	2.16
	78.0	25 690	4.02		
$[Co(Hmpk)_2(NO_3)](NO_3)$	297.6	8 625	4.55		
	78.0	31 760	4.47		
$[Co(Hmpk)_2(NCS)_2]$	300.0	8 635	4.57		
	78.0	31 900	4.48		
$[Co(Hmpk)_2(NCSe)_2]$	296.4	9 006	4.64		
	78.0	32 475	4.52		
$[Co(Hmpk)_2(OAc)_2]$	299.2	8 470	4.52		
	78.0	31 760	4.47		
$[Co(Hmpk)_2(SO_4)]$	297.4	8 590	4.54		
	78.0	32 045	4.49		

support for the presence of a dimer in these cobalt(II) halo complexes is visible in μ_{eff}/Co at low temperature, indicating a weak antiferromagnetic interaction. The susceptibility data for these cobalt(II) halo complexes were fitted to the BALL—BLAKE [14] equation for isotropic exchange in a cobalt(II) dimer

$$\chi_m = \frac{2N\beta^2 g^2}{kT}\left[\frac{e^{-10X} + 5e^{-6X} + 14}{e^{-12X} + 3e^{-10X} + 5e^{-6X} + 7}\right]$$

where $X = J/kT$.

This is an admittedly simple model wherein the temperature dependence of the magnetic susceptibility for a cobalt(II) dimer is assumed to be due to entirely to exchange interaction with an assumed isotropic g, and intermolecular exchange interactions accounted for by a WEISS constant. Fitting of magnetic data to the above model, which uses the spin-only equations, yields $J = -ca.$ 3.00 cm^{-1} (Cl); $-ca.$ 2.50 (Br) and $-ca.$ 2.00 (I) and $g = ca.$ 2.18 and $\Theta = ca.$ $-1.3°$. It is difficult to obtain an accurate value of J for such antiferromagnetic interaction, however, it is clear that in these dimeric halo complexes, the exchange coupling is slightly antiferromagnetic.

In contrast, cobalt (II) complexes of the types $[Co(HL)_2(X)_2]$ (where HL = Hppk or Hmpk and X = NCS, NCSe, OAc or $1/2SO_4$) and $[Co(HL)_2(NO_3)](NO_3)$ (where HL = Hppk or Hmpk) exhibit μ_{eff} values at room temperature in the 4.70—4.85 μ_B range. These are higher than the spin-only value of 3.87 μ_B expected for three unpaired electrons but lower than the value of 5.0 μ_B which is usually observed for regular octahedral cobalt(II) complexes. The mechanism which best accounts for the low values of μ_{eff} involves a partial quenching of the orbital angular moment by a low-symmetry ligand field component. As the temperature is lowered to 78 K, the μ_{eff} values decrease to *ca.* 96% of their room temperature value as observed for other distorted monomeric octahedral cobalt(II) complexes.

Reflectance Spectra

The diffuse reflectance spectra of free ligands Hppk and Hmpk and their cobalt(II) complexes have been measured at room temperature and are detailed in Table III. The ultraviolet spectra of free ligands exhibit three intense transition bands at *ca.* 34,500, *ca.* 37,900 and *ca.* 41,500 cm^{-1} which are assigned [15] to $\pi \rightarrow \pi^*$ transitions. The position of the bands and the assignment follow those for 1,10-phenanthroline, confirming [15] the *cis*- form of Hppk and Hmpk in the solid state. The spectra of all cobalt(II) complexes in the ultraviolet region show three bands in the 30,770—32,800; 35,715—39,840 and 40,160—41, 645 cm^{-1} region. These spectral bands almost lie at the same region as in the *cis*-form of the ligands, suggesting that in all the complexes the ligands have a *cis*-configuration in the solid state. The splitting of the first band of the order of *ca.* 1000 cm^{-1} suggest that it is vibrational in origin.

In the visible region, the absorption bands observed in the 7,690—8,095 and 7,930—8,900 cm^{-1} range can be assigned to $^4A_2 \rightarrow {}^4A_1$, $^4B_1$ and $^4A_2 \rightarrow {}^4B_2$ transitions, both of which arise from the splitting of the ν_1 band (O_h symmetry) when the symmetry is lowered to C_{2v}. The medium intensity band in the 15,625—16,537 cm^{-1} range can be assigned to a $^4A_2 \rightarrow {}^4A_2$ transition which arises from the ν_2 band (O_h symmetry) in C_{2v}. The band system at *ca.* 20,000

Acta Chim. Acad. Sci. Hung. 108, 1981

Table III

Reflectance spectral data and ligand field parameters for cobalt(II) complexes
(All value except β are in cm^{-1} units: $B_0 = 971\ cm^{-1}$)

Assignment/ Parameter	$[Co(Hppk)_2(X)_2]$			$[Co(Hppk)_2(NO_3)](NO_3)$	$[Co(Hppk)_2(X)_2]$			
	X = Cl	X = Br	X = I		X = NCS	X = NCSe	X = OAc	X = 1/2SO$_4$
$^4A_2^a \rightarrow {}^4A_1, {}^4B_1$	7 690	7 745	7 738	8 090				
$\rightarrow {}^4B_2$	7 930	7 970	7 978	8 250	8 270	8 200	7 915	7 940
$\rightarrow {}^4A_1, {}^4A_2$	15 625	15 680	15 665	16 340	16 395	16 400	15 610	15 625
$\rightarrow {}^4B_1, {}^4B_2$	18 520	18 580	18 550	18 995	19 050	19 060	18 510	18 535
$\rightarrow {}^4A_2$	20 835	20 900	20 860	21 860	22 124	22 135	20 830	20 850
Spin-forbidden	14 285	14 200	14 150	15 000	15 150	15 140	14 280	14 280
$^4T_1(F) \rightarrow {}^2T_1({}^2G)$								
Dq	770	770	770	800	810	820	770	770
B	785	780	775	840	865	865	784	788
β	0.80	0.80	0.79	0.86	0.88	0.88	0.80	0.81
$^4A_2^a \rightarrow {}^4A_1, {}^4B_1$	8 070	8098	8 095					
$\rightarrow {}^4B_2$	8 350	8 400	8 400	8 710	8 725	8 650	8 340	8 360
$\rightarrow {}^4B_1, {}^4A_2$	16 500	16 560	16 537	17 240	17 292	17 300	16 440	16 468
$\rightarrow {}^4B_1, {}^4B_2$	18 660	18 725	18 700	19 150	19 200	19 218	18 650	18 660
$\rightarrow {}^4A_2$	22 300	22 368	22 328	22 330	23 610	23 625	22 280	22 300
Spin-forbidden	14 350	14 360	14 350	14 670	14 990	15 010	14 280	14 360
$^4T_1 \rightarrow {}^2T_1({}^2G)$								
Dq	815	816	814	853	857	865	810	811
B	815	814	810	844	858	877	810	810
β	0.84	0.84	0.83	0.87	0.88	0.90	0.83	0.83

cm^{-1} can be assigned to $^4A_2 \rightarrow {}^4A_2$, $^4B_1$, $^4B_2$ transitions, which arise from the ν_3 band (O_h symmetry). The weak band at *ca.* 14,000 cm^{-1} can be assigned to spin-forbidden transition.

The remaining cobalt(II) complexes also exhibit spectra typical of *cis*--octahedral complexes except that the splitting of the band system is much less than that of halo complexes. This may be due to the adjacent position of N and O in the spectrochemical series which reduces the asymmetry of the ligand field.

The various crystal field parameters for the present cobalt(II) complexes are calculated from these spectral transition bands with the expressions of KONIG [16] and are given in Table III.

*

The authors are grateful to Dr. S. SINGH for providing the necessary facilities and to U.G.C., New Delhi for financial support to one of us (B.D.P.). The authors thank the authorities of T.I.F.R., Bombay and Delhi University, Delhi for magnetic measurements. Thanks are also due to the authorities of R.S.I.C., I.I.T. Madras and Guru Nanak Dev University, Amritsar for recording reflectance and infrared spectra.

REFERENCES

[1] EMMERT, B., DIEHL, K.: Chem. Ber., **62,** 1788 (1929); SEN, B.: Chem. Ind., **1958,** 562; SEN, B., MALONE, D. B. V. M.: J. Inorg. Nucl. Chem., **34,** 3509 (1972)
[2] WARD, L. G., MEEK, T. L., CHENEY, G. E.: Inorg. Chim. Acta, **4,** 43 (1970)
[3] DRAGO, R. S., BAUCOM, E. I.: Inorg. Chem., **11,** 2064 (1972)
[4] GEARY, W. J.: Coord. Chem. Rev., **7,** 81 (1971)
[5] KRAUSE, R. A., COLTHUP, N. B., BUSCH, D. H.: J. Phys. Chem., **65,** 2216 (1961)
[6] GILL, N. S., NUTTALL, R. H., SCAIFE, D. E., SHARP, D. W. A.: J. Inorg. Nucl. Chem., **18,** 79 (1961); FIGGINS, P. E., BUSCH, D. H.: J. Phys. Chem., **65,** 2236 (1961); ZERBI, G., OVEREND, J., CRAWFORD, B.: J. Chem. Phys., **38,** 122 (1963); GREEN, J. H. S., KYNASTON, W., PAISLEY, H. M.: Spectrochim. Acta, **20,** 879 (1964); GILL, N. S., KINGDON, H. J.: Aust. J. Chem., **19,** 2197 (1966)
[7] POSTMUS, C., FERRARO, J. R., QAUTTROCHI, A., SHOBATAKE, K., NAKAMATO, K.: Inorg. Chem., **8,** 1851 (1969); DOSSER, R. J., UNDERHILL, A E.: J. Inorg. Nucl. Chem., **36,** 1239 (1974) and references therein
[8] FERRARO, J. R.: Low-Frequency Vibrations of Inorganic and Coordination Compounds, p. 205 Plenum Press, New York, 1971
[9] CURTIS, N. F., CURTIS, Y. M.: Inorg. Chem., **4,** 804 (1965)
[10] LEVER, A. B. P., MANTOVANI, E., RAMASWAMY, B. S.: Can. J. Chem., **44,** 1957 (1971)
[11] KONIG, E., MADEJA, K.: Inorg. Chem., **6,** 48 (1967) and references therein
[12] HEZEL, A., ROSS, S. D.: Spectrochim. Acta, **24A,** 985 (1968)
[13] LEVER, A. B. P., LEWIS, J., NYHOLM, R. S.: J. Chem. Soc., **1962,** 5262; GRIFFITH, W. L.: J. Chem. Soc. (A), **1969,** 2270
[14] BALL, P. W., BLAKE, A. B.: J. Chem. Soc. (A), **1969,** 1414
[15] MCWHINNIE, W. R., MILLER, J. D.: Advan. Inorg. Chem. Radiochem., **12,** 135 (1969); KRUMHOLZ, P.: Structure and Bonding, **9,** 139 (1971)
[16] KONIG, E.: Structure and Bonding, **9,** 175 (1975)

Madan MOHAN
Bhikari D. PARAMHANS } Shiv Niwas KOT Khurja—203131, U.P., India

Acta Chimica Academiae Scientiarum Hungaricae, Tomus 108 (3), pp. 229—234 (1981)

PREPARATION, INFRARED ABSORPTION SPECTRA AND X-RAY POWDER DIFFRACTION PATTERNS OF MIXED (Ca + Sr + Mg) HYDROXYLAPATITES

H. Ch. PANDEY,[1] S. PANDEY[2] and P. N. PATEL[1]*

([1]*P.G. Department of Chemistry, G. M. College, Sambalpur*
[2]*Department of Zoology, Women's College, Sambalpur, India,*)

Received September 12, 1980

Accepted for publication November 1, 1980**

Homogeneous solid solutions of calcium, strontium and magnesium hydroxylapatite have been prepared over the entire compositional range by the method of co-precipitation in aqueous media. Frequencies (cm^{-1}) and assignments for the infrared absorption and the lattice constants of the solid solutions have been measured and found to vary linearly with composition.

Introduction

Calcium hydroxylapatite (CaHA), $Ca_{10}(PO_4)_6(OH)_2$, the principal inorganic constituent of human bones and teeth [1, 2] belongs to an isomorphous series of compounds known as apatites. Calcium hydroxylapatite (CaHA) also exists in nature as the mineral hydroxylapatite, which is similar if not identical to that in bone material, it can be prepared from aqueous media [3,4]. The ionic radii [5] of calcium (0.99 Å), strontium (1.13 Å) and magnesium (0.65 Å) are close enough to enable the formation of solid solutions between isomorphous substances containing these ions. Apatite undergoes a series of cationic and anionic replacement reactions [6]. The $Ca^{2+} \rightarrow Sr^{2+}$ and/or Mg^{2+} replacement reactions in CaHA are of extreme biological significance and in view of its action on calcified tissue is interesting. They form the basis of incorporation of Sr^{2+} and Mg^{2+} into human skeletal system according to the following equation:

$$Ca_{10}(PO_4)_6(OH)_2 + nSr^{2+} + mMg^{2+} \rightarrow$$
$$Ca_{10-(n+m)}Sr_nMg_m(PO_4)_6(OH)_2 + (n + m)Ca^{2+}$$

Solid solutions of calcium, strontium and magnesium hydroxylapatites were prepared separately earlier [7] by firing mixtures containing various propor-

* To whom correspondence should be addressed
** In final form accepted April 2, 1981

tions of calcium, strontium and magnesium hydroxylapatite at about 1300 °C. These samples prepared by the solid state reaction were, however, found to be discontinuous and non-homogeneous.

Now an attempt has been made at a new method of preparation of the homogeneous solid solutions of mixed (Ca + Sr + Mg) hydroxylapatite over the entire compositional range by the method of co-precipitation [8—10].

Experimental

Materials

All chemicals used for the preparation of these samples were either AR (BDH) or E. MERCK EXTRA Pure grade. Water used in the preparation and in washing was boiled to remove CO_2 and then used immediately.

Preparation

Stoichiometric quantities of ammonium dihydrogen phosphate (Solution A) and a solution containing Ca^{2+}, Sr^{2+} and Mg^{2+} ions in the proportion desired for the solid solutions (Solution B) were prepared separately in carbondioxide free doubly distilled water. The pH of these solutions were maintained above 11 by the addition of excess of liquor ammonia. Then a part of the solution B was transferred into a flask (2 dm^3) fitted with two separating funnels and a delivery tube. Solution A and Solution B were poured individually into the separating funnels and added dropwise to the flask simultaneously. Precipitation was carried out in carbondioxide-free atmosphere and the precipitation medium was well stirred by bubbling CO_2 free air to prevent the formation of carbonato-apatites.

The precipitate and mother liquor were aged by boiling under reflux for 30 min to improve the homogeneity and crystallinity of the precipitate and maintenance of the desired pH during precipitation was ensured by testing the filtrate after separation of the precipitate, since any alteration of pH of the medium during precipitation leads to the formation of calcium deficient apatites [11]. The precipitate was washed thoroughly with doubly distilled water to free it from ammonium salts. Samples dried at 100 °C for few hours were analyzed colorimetrically [12] and their molar volumes were determined by density method using toluene [13] as a solvent.

Infrared absorption techniques

Samples used for infrared studies were washed with acetone and air dried. All the bands were recorded on a Grating Infrared Spectrophotometer Model 577 (Perkin–Elmer) in KBr medium. A few milligrams of the sample was ground with two drops of Nujol in an agate mortar. About 50 mg of a fine polyethylene powder (VESTOLENA 6016 Chem. Weka Huels, Germany) was added. The resulting paste was melted rapidly at about 140° and pressed between glass plates to a slightly wedge-shaped film of an average thickness of 0.1 mm.

X-Ray diffraction techniques

Samples dried at 110° for few hours were used for X-ray diffraction. The X-ray diffraction patterns of the samples were obtained with Siemens Powder diffractometer with NaCl(Tl) counter employing CuK_α (Nickel filtered) radiation with a scanning speed of 1 degree (2Θ) per min (using tube voltage of 30 kV and 24 mA, respectively).

Lattice p constant measurements

CaHA, SrHA and MgHA are hexagonal with two lattice constants a_0 and c_0. These were determined [14, 15] for all the samples by measuring the diffraction angle 2Θ of the three planes: (312), (213) and (321). Each sample was thoroughly mixed with 25% NaCl (recrystallized from HCl) which served as a standard. So that the observed values of sin Θ for the solid solution lines could be corrected directly for absorption and instrumental errors.

Table I

Chemical analyses of calcium, strontium and magnesium hydroxylapatites and their solid solutions

Sample No.	Wt %				Molecular Formula	Mol. Vol	G. atom ratio $\frac{Ca+Sr+Mg}{P}$	Lattice paramater (A_0)		Unit cell volume $\frac{\sqrt{3}}{2}a^2c$	Frequency (cm^{-1})		
	Ca	Sr	Mg	P				a	c		PO_4^{3-} ν_4	PO_4^{3-} ν_3	OH^- ν_3
1	39.88	—	—	18.51	$Ca_{10}(PO_4)_6(OH)_2$	338.32	1.665	9.37	6.86	523.12	570 sh	1075 br	3450 sh
2	31.03	8.06	2.47	17.99	$Ca_8Sr_{0.95}Mg_{1.05}(PO_4)_6(OH)_2$	337.72	1.656	9.41	6.90	529.13	565 sh	1065 br	3445 sh
3	28.01	7.76	4.79	18.31	$Ca_{7.1}Sr_{0.90}Mg_{2.0}(PO_4)_6(OH)_2$	337.57	1.655						
4	26.18	14.72	2.72	17.36	$Ca_{7.0}Sr_{1.8}Mg_{1.2}(PO_4)_6(OH)_2$	334.83	1.655						
5	23.40	15.27	4.45	17.51	$Ca_{6.2}Sr_{1.85}Mg_{1.95}(PO_4)_6(OH)_2$	333.98	1.666	9.46	6.98	540.96	555 sh	1055 br	3415 sh
6	18.45	17.38	6.66	17.56	$Ca_5Br_{2.1}Mg_{2.9}(PO_4)_6(OH)_2$	336.18	1.646						
7	18	22.29	4.62	16.84	$Ca_{5.1}Sr_{2.8}Mg_{2.1}(PO_4)_6(OH)_2$	336.84	1.656						
8	14.57	22.58	7.27	17.12	$Ca_{3.95}Sr_{2.8}Mg_{3.25}(PO_4)_6(OH)_2$	338.54	1.644	9.58	7.04	559.54	552 sh	1050 br	3400 sh
9	11.22	22.89	9.53	17.36	$Ca_{3.0}Sr_{2.8}Mg_{4.2}(PO_4)_6(OH)_2$	339.16	1.656						
10	10.73	29.62	6.62	16.33	$Ca_{3.05}Sr_{3.85}Mg_{3.1}(PO_4)_6(OH)_2$	333.14	1.654						
11	7.18	29.44	9.26	16.66	$Ca_2Sr_{3.75}Mg_{4.25}(PO_4)_6(OH)_2$	336.18	1.666	9.60	7.10	566.67	548 sh	1048 br	3855 sh
12	3.75	31.98	10.5	16.56	$Ca_{1.05}Sr_{4.1}Mg_{4.25}(PO_4)_6(OH)_2$	334.32	1.665						
13	3.40	37.15	8.25	15.77	$Ca_1Sr_5Mg_4(PO_4)_6(OH)_2$	331.12	1.666						
14		36.26	11.12	16.20	$Sr_{4.75}Mg_{5.25}(PO_4)_6(OH)_2$	329.88	1.666	9.68	7.24	587.52	540 sh	1035 br	3300 sh
15		59.20	—	12.57	$Sr_{10}(PO_4)_6(OH)_2$	364.61	1.665	9.74	7.26	596.57	530 sh	1030 br	3325 sh
16		—	28.71	21.95	$Mg_{10}(PO_4)_6(OH)_2$	350.08	1.665	8.72	6.42	422.77	530 sh	1025 br	3275 sh

br = broad, sh = sharp

The lattice constant of NaCl at 26° was taken to be 5.6403 Å [16]. A least squares calculation on the corrected values of $\sin\Theta$ for the three reflections then gave the two parameters, a_0 and c_0, for each sample. The diffraction lines were quite sharp and the diffraction angle read by counting over the top of the peak with the scaling unit and estimating the position of maximum intensity from a plot of intensity against 2Θ. The average probable error in unit cell parameters is less than ± 0.005 Å.

Results and Discussion

The results of chemical analysis of the samples were given in Table I. Based on the fact that one mole of each sample has a total 10 g-atoms of calcium and/or strontium and/or magnesium the molecular formulas of the samples were calculated from the results of the columns 2—4 and included in column 6 of Table I. The g-atom ratio (Ca + Sr + Mg)/P in one mole of each sample was calculated from the results of columns 2—5 and given in column 8 of the table. The fact that the observed value of molar g-atom ratios of Ca/P, Sr/P, Mg/P for the end members and (Ca + Sr + Mg)/P were found to be equal to 1.65 (theoretical 1.67) is consistent with the formation of homogeneous solid solution [13]. This was further supported by the closeness of the values of molar volumes of the end members and those of the intermediate samples which lie within the range of end members.

The formation of solid solutions can be further confirmed by the X-ray diffraction analysis. It is well established that all the members of the apatite series belong to the hexagonal-dipyramidal class — $6/_m$ (space group $P6_{3/m}$) [17, 18] lattice parameters showed unit cell dilation and contraction consequent upon the introduction of larger ion Sr^{2+} (1.13 Å) and smaller ion Mg^{2+} (0.65 Å) respectively, in place of Ca^{2+} (0.99 Å) ion in the apatite lattice. Such dilation and contraction with the proportion of Ca—Sr—MgHA was evident that the unit cell volume of the samples calculated on the basis of the experimentally determined lattice constant increased with the proportion of strontium content and decreased with the proportion of magnesium content in Ca—Sr—MgHA.

The lattice constants are plotted in Fig. 1 against atom % strontium and magnesium are seen to lie on a straight line joining the two end members to within the probable errors of the lattice constants. This, of course is the real evidence for solid solution in this series and clearly shows that these preparations are not mixtures of two components or one component with absorbed material.

The CaHA and its solid solutions with strontium and magnesium have hexagonal crystalline structure and are interesting examples of solid state of fairly simple molecules of tetrahedral symmetry where bands become allowed due to relaxation of the molecular symmetry [19] selection rules due to the influence of site symmetry. The ideal symmetry of tribasic phosphate ion in the free or undistorted state is tetrahedral — a member of T_d point group.

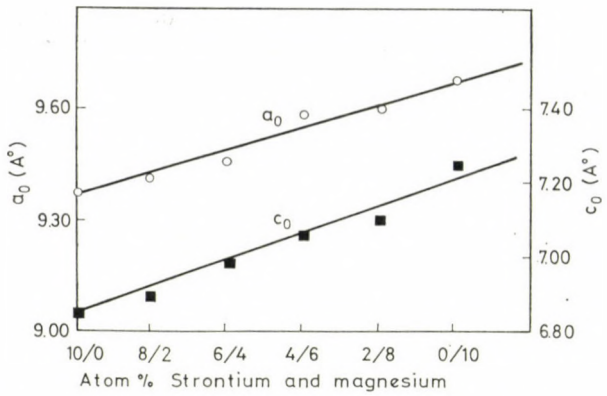

Fig. 1. Lattice constants of solid solutions *vs.* atom % strontium and magnesium

In this ideal symmetry condition only a few absorption bands corresponding to ν_4 (570 cm^{-1}) and ν_3 (1075 cm^{-1}) of PO_4^{3-} and ν_1 (630 cm^{-1}) and ν_3 (3450 cm^{-1}) of OH^- were clearly observed. From the spectra of the samples it could be seen that the ν_3 and ν_4 frequencies corresponding to PO_4^{3-} ion and ν_1 and ν_3 corresponding to OH^- ion are shifted to lower frequencies and the shape of the peaks was affected by the introduction of strontium and magnesium ion into the samples. The shift of the ν_3 and ν_4 of PO_4^{3-} vibrations to lower frequencies may be due to the effect of binding energy and atomic mass. The lowering of frequency of ν_3 of OH^- indicates the presence of hydroxyl group in the apatite [20]. This hydroxyl group in hydroxylapatite lies in the internuclear axis coincident with six fold screw axis. In BARNES expression [21]

$$\nu = \frac{1}{2\pi c}\sqrt{\frac{K}{\mu}}$$

which gives a relationship between frequency, atomic mass and force constant. The vibrational frequencies are dependent on the reduced mass μ of the participating atoms and restoring forces K between atoms, all other terms remaining constant. When the equilibrium distance between the positive and the negative atoms of the molecule is decreased K generally increases in the above equation. This equilibrium distance depends on the ionic radii of the participating atoms in the molecule. Substitution of Ca^{2+} with a nucleus like Sr^{2+} and/or Mg^{2+} gives rise to stronger co-ordination of the PO_4^{3-} group through oxygen. This in turn weakens the P—O bond, lowering K (increasing P—O bond length) and the frequency is lowered. The PO_4^{3-} bonding is normally around 520 cm^{-1} and bending modes do not shift very much under these conditions. But here the substitution is more complex, presumably because of

the splitting of the triply degenerate mode at 600 cm^{-1} and thus there is an increase in the frequency from 520 cm^{-1} to 570 cm^{-1}. This theoretical explanation agrees well with the experimental data.

*

The author is highly grateful to Prof. G. FERRARIS of University of Torino (Italy) for X-ray data and Dr. M. M. DHAR, F.N.A., C.D.R.I., Lucknow for infrared spectra. The financial support to the author by University Grants Commision is gratefully acknowledged.

REFERENCES

[1] NEUMAN, W. F., NEUMAN, M. W.: Chem. Rev., **53,** 1 (1953)
[2] ROBINSON, R. A.: J. Bone and Joint Surg., **34,** 389 (1962)
[3] WALLACYS, R., CHOUDRON, G.: Compt. rend., **231,** 355 (1950)
[4] HAYEK, E., STANDLMANN, W.: Angew. Chem., **67,** 327 (1955)
[5] WELLS, A. F.: "Structural Inorganic Chemistry", Oxford University Press, London, 1959, pp. 70
[6] VAN WAZER, J. R.: "Phosphorus and Its Compounds", Vol. **1,** p. 530, New York, Interscience Publishers, Inc.
[7] VAN WAZER, J. R.: "Phosphorus and Its Compounds", Vol. **2,** p. 1429, New York, Interscience Publishers, Inc. 1966
[8] PATEL, P. N.: J. Chem. Ind. (London), **20,** 804 (1978)
[9] PATEL, P. N.: J. Ind. Chem. Soc., **56,** 4, 410 (1979)
[10] PATEL, P. N.: J. Inorg. Nucl. Chem., **42,** 1129 (1980)
[11] BERRY, E. E.: J. Inorg. Nucl. Chem., **29,** 1585 (1967)
[12] PATEL, P. N.: Z. Anal. Chem. (In press)
[13] PARTINGTON, J. R.: "An Advanced Treaties on Physical Chemistry", Vol. **3,** p. 121, Longman Green and Co.
[14] AZAROFF, L. V.: "Elements of X-ray Crystallography" Chapter *18*, London, McGraw-Hill Book Co., 1968
[15] CULLITY: "Elements of X-ray Diffraction", pp. 309—313
[16] STRAUMANIS, M., LEVINS, A.: Z. Phys., **109,** 728 (1938)
[17] MEHMEL, M.: Z. Krist., **75,** 323 (1930); NÁRAY-SZABÓ, G.: *ibid.*, **75,** 387 (1930)
[18] HENTSCHEL, H.: Mineral Geol., **1923,** 609
[19] NAKAMOTO, K.: "Infrared Spectra of Inorganic and Coordination Compounds", p. 103, New York, John Wiley & Sons. Inc., 1966
[20] ENGEL, G., KLEE, W. E.: J. Solid State Chem., **6,** 28 (1972)
[21] BARNES, R. B., CORE, R. C., LIDDEL, V., WILLIAMS, V. Z.: in "Infrared Spectroscopy" Reinhold, New York 1944

Himadri Ch. PANDEY, Prema N. PATEL — P.G. Department of Chemistry, G.M. College, Sambalpur, India

Shanti PANDEY — Department of Zoology, Women's College, Sambalpur, India

Acta Chimica Academiae Scientiarum Hungaricae, Tomus 108 (3), pp. 235—248 (1981)

DECOMPOSITION OF PROPIONALDEHYDE INITIATED BY THE THERMAL DECOMPOSITION OF AZOETHANE*

A. PÉTER, G. ÁCS, I. HORVÁTH and P. HUHN**

(Department of Inorganic and Analytical Chemistry, József Attila University of Sciences, Reaction Kinetics Research Group, Hungarian Academy of Sciences, Szeged)

Received March 28, 1980

In revised form June 2, 1980

Accepted for publication December 12, 1980

Hydrogen atom abstraction by ethyl radicals from various positions of propionaldehyde was studied in the temperature range of 538—596 K. The ethyl radicals were produced by thermal decomposition of azoethane. With the rate constant of 10^{10} ($dm^3\ mol^{-1}\ s^{-1}$) accepted for ethyl radical recombination, the expressions

$$\log k_{23} = (7.7 \pm 0.1) - (26.3 \pm 0.8)/2.303 \cdot RT,$$

$$\log k_{24} = (8.1 \pm 0.3) - (53.3 \pm 3.1)/2.303 \cdot RT \text{ and}$$

$$\log k_{25} = (8.0 \pm 0.1) = (34.8 \pm 1.2)/2.303 \cdot RT \text{ for the reactions}$$

(23) $C_2H_5 + C_2H_5CHO \rightarrow C_2H_6 + C_2H_5\dot{C}O$

(24) $C_2H_5 + C_2H_5CHO \rightarrow C_2H_6 + \dot{C}H_2-CH_2-CHO$

(25) $C_2H_5 + C_2H_5CHO \rightarrow C_2H_6 + CH_3-\dot{C}H-CHO$

were obtained (dm^3, s, kJ, mol units).

Based on the experimental results and literature data, a mechanism has been proposed to account for the initial stage of reaction. The set of differential equations of the mechanism was numerically integrated and the product-time functions obtained were compared with the measured data.

Introduction

According to the experimental results of our previous studies on the thermal decomposition of propionaldehyde [1] it is probable that in the reaction between ethyl radicals and propionaldehyde the abstraction of formyl hydrogen atom dominates, hydrogen abstraction from the methyl and methylene groups, however, also takes place. Although it is very important to know the presence, contribution and rate coefficients of the latter two reactions for the further elucidation of the kinetics of decomposition, this task could not be solved under the conditions of the pure decomposition of aldehyde.

* Also submitted to Magyar Kémiai Folyóirat

** To whom correspondence should be addressed

Two, slightly different rate coefficients characterizing the abstraction of the formyl hydrogen atom of propionaldehyde can be found in the literature [2, 3], but the problem of the abstraction of hydrogens in α and β positions has not been studied so far. It is true in general that the abstraction reactions of one radical with hydrogens in different positions have been investigated on a relatively few compounds only.

This work deals with the decomposition of propionaldehyde initiated by the thermal decomposition of azoethane. Our primary concern is the investigation of the possibilities of the three conceivable hydrogen abstraction reactions and the determination of the corresponding rate coefficients. On the basis of the data obtained a computer simulation of the possible mechanism of initiated decomposition was also performed.

Experimental

The measurements were carried out in a simple high vacuum system. The reaction vessel, 400 cm^3 in volume and made of supremax glass, was thermostated to an accuracy of ± 0.5 K in a brass-lined oven. In the apparatus teflon valves were applied in order to avoid the dissolution of substances in tap lubricant.

The reaction was monitored by gas chromatographic analysis. The various substances were determined on the following columns and under the following experimental conditions:

Nitrogen, carbon monoxide: molecular sieve column 5A, 1.2 m in length and 4 mm in internal diameter; flow rate of hydrogen 30 cm^3/min, temperature of thermostat 333 K.

Azoethane: 2 m column, 4 mm in internal diameter, filled with 20% ethyleneglycol-bis(propionitrile) dimethyl ether on Chromosorb W support; flow rate of hydrogen 35 cm^3/min, temperature of thermostat 333 K.

C_1-C_4 hydrocarbons: 3.6 m column, 3 mm in internal diameter, filled with Spherosil XOB 075; flow rate of nitrogen 30 cm^3/min, temperature of thermostat 323 K.

In the latter case flame ionization, in the former two cases thermal conductivity detector was applied.

Propionaldehyde was a product of BDH, distilled on a column with high number of theoretical plates and then purified by low temperature distillation. Azoethane was prepared by the method of RENAUD and LEITCH [4] and purified with a Carlo Erba Fractovap 2400 V preparative gas chromatograph. The gas chromatographically pure substance was stored in a dark vessel.

Measurements and Discussion

The measurements were carried out in the temperature range of 538—596 K, at an initial pressure of 13.33 kPa. The partial pressure of azoethane was either 0.67 or 1.33 kPa, and that of propionaldehyde 12.67 or 12.00 kPa respectively. In the initial stage of thermal decomposition nitrogen, carbon monoxide, ethane, ethylene and butane and in some cases very small amounts of methane, propane and hydrogen were determined. The formation of the products was generally followed up to high conversions; the initial rates determined from the product curves are given in Tables I and II.

On the basis of previous experience [1, 5] and the results of present measurements, the mechanism shown in Table III is suggested for the initial

Table I

The initial rates of product formation
$P_0 = 1.33$ kPa azoethane + 12.00 kPa propionaldehyde

Products	$10^4 \cdot R_0$ (kPa · s^{-1})					
	538 K	558 K	573 K	576 K	593 K	598 K
N_2	1.03	5.72	18.33	21.33	73.62	105.32
CO	7.23	27.20	64.39	66.66	186.65	229.31
C_2H_6	9.55	36.80	89.06	92.12	257.31	321.30
C_2H_4	0.06	0.31	1.05	1.31	4.81	5.60
C_4H_{10}	0.08	0.80	3.67	3.80	20.66	29.33
CH_4	0.04	0.20	0.52	—	1.73	—
C_3H_8	—	—	0.15	—	0.69	—

Table II

The initial rates of product formation
$P_0 = 0.67$ kPa azoethane + 12.67 kPa propionaldehyde

Products	$10^4 \cdot R_0$ (kPa · s^{-1})			
	538 K	558 K	573 K	593 K
N_2	0.48	2.85	9.08	36.44
CO	3.81	17.73	41.86	118.65
C_2H_6	5.11	23.20	55.73	161.32
C_2H_4	0.03	0.17	0.53	2.25
C_4H_{10}	0.02	0.31	1.24	7.56
CH_4	0.02	0.08	0.25	0.92
C_3H_8	—	—	0.04	0.27

stage of the thermal decomposition of propionaldehyde initiated by azoethane. The first 22 steps of the mechanism describe the complete decomposition of azoethane, which was discussed in a previous paper [5]. According to the suggested mechanism, the ethyl radical may abstract three hydrogen atoms, bonded in different places from the aldehyde molecule. Of the three hydrogen atoms, the bond of the formyl hydrogen is the weakest, *ca.* 360 kJ/mol [6], and thus the appropriateness of reaction (23) needs not be particularly justified. Should only the abstraction reaction (23) take place, the ethyl and propionyl radicals would carry the chain, and in the break-down reaction only the ethyl radical would dominate. A conseuqence of this mechanism would be that the formation rates of butane arising from the recombination of the ethyl radical (with correction $k_2 : k_3$) and of nitrogen arising from initiation would be the same. However, it can be seen from Tables I and II that the

Table III

Mechanism and Arrhenius parameters

	Elementary reactions	$\log_{10} A$ s^{-1}, $dm^3 \cdot mol^{-1} \cdot s^{-1}$	E kJ mol^{-1}	References
(1)	AE → $N_2 + 2\ C_2H_5$	15.8	205.1	[9]
(2)	$2\ C_2H_5$ → $C_2H_6 + C_2H_4$	9.1	0.0	(a)
(3)	$2\ C_2H_5$ → C_4H_{10}	10.0	0.0	[8]
(4)	$C_2H_5 + AE$ → $C_2H_6 + \mu_1$	8.3	52.3	(b)
(5)	$C_2H_5 + AE$ → $C_2H_6 + \mu_2$	8.1	33.5	(b)
(6)	$CH_3 + AE$ → $CH_4 + \mu_2$	8.4	33.5	(b)
(7)	μ_1 → $C_2H_4 + N_2 + C_2H_5$	14.0	117.2	(b)
(8)	μ_2 → $CH_3CH{=}N{-}N{=}CH_2 + CH_3$	13.2	136.0	(b)
(9)	μ_2 → $C_2H_4N_2 + C_2H_5$	13.0	150.6	(b)
(10)	$C_2H_5 + \mu_2$ → $2\text{-}C_4H_9N_2C_2H_5$	9.9	0.0	(b)
(11)	$C_2H_5 + \mu_2$ → $CH_3CH{=}N{-}N{=}(C_2H_5)_2$	9.5	0.0	(b)
(12)	$2\text{-}C_4H_9N_2C_2H_5$ → $2\text{-}C_4H_9 + N_2 + C_2H_5$	17.5	217.4	(b)
(13)	$2\text{-}C_4H_9$ → $CH_3 + C_3H_6$	14.2	141.8	[12]
(14)	$CH_3 + C_2H_5$ → $CH_4 + C_2H_4$	8.9	0.0	[13]
(15)	$CH_3 + C_2H_5$ → C_3H_8	10.5	0.0	[13]
(16)	$CH_3 + CH_3$ → C_2H_6	10.4	0.0	[14]
(17)	$C_2H_5 + 2\text{-}C_4H_9$ → $C_2H_6 + C_4H_8$	9.3	0.0	(c) [13]
(18)	$C_2H_5 + 2\text{-}C_4H_9$ → $C_4H_{10} + C_2H_4$	9.1	0.0	(c) [13]
(19)	$C_2H_5 + 2\text{-}C_4H_9$ → $i\text{-}C_6H_{14}$	10.0	0.0	(c) [13]
(20)	$2\ 2\text{-}C_4H_9$ → $C_4H_{10} + C_4H_8$	9.3	0.0	(c) [13]
(21)	$2\ 2\text{-}C_4H_9$ → $i\text{-}C_8H_{18}$	9.5	0.0	(c) [13]
(22)	$2\ \mu_2$ → product	9.0	0.0	(b)
(23)	$C_2H_5 + A$ → $C_2H_6 + CH_3{-}CH_2{-}CO$	7.7	26.0	see text
(24)	$C_2H_5 + A$ → $C_2H_6 + CH_2{-}CH_2{-}CHO$	8.1	53.6	see text
(25)	$C_2H_5 + A$ → $C_2H_6 + CH_3{-}CH{-}CHO$	7.9	35.6	see text
(26)	$CH_3{-}CH_2{-}CO$ → $C_2H_5 + CO$	13.3	61.5	[11]
(27)	$CH_3{-}CH_2{-}CO$ → $CH_3 + CH_2CO$	15.5	125.6	[7]
(28)	$CH_2{-}CH_2{-}CHO$ → $C_2H_4 + CO + H$	14.0	117.2	(b)
(29)	C_2H_5 (or R) + $CH_3{-}CH{-}CHO$ → product	9.8	0.0	(b)
(30)	$2\ CH_3{-}CH{-}CHO$ → product	9.7	0.0	(b)
(31)	$CH_3 + A$ → $CH_4 + CH_3{-}CH_2CO$	8.3	26.0	(b)
(32)	$H + A$ → $H_2 + CH_3{-}CH_2{-}CO$	8.4	20.9	(b)

AE = $C_2H_5N_2C_2H_5$; $\mu_1 = \dot{C}H_2CH_2N_2C_2H_5$; $\mu_2 = CH_3CH\cdots N\cdots N{-}C_2H_5$; A = C_2H_5CHO

(a) accepted $k_2/k_3 = 0.14$; (b) on the basis of analogies and optimized; (c) assumed $k(2-C_3H_7) \simeq k(2-C_2H_5)$.

formation rate of butane is much lower than that of nitrogen. This fact supports the presence of reactions (24) and (25), because they yield radicals which may take part in further break-down reactions in addition to the ethyl radical. Since, however, the bond strength of hydrogen atom is *ca.* 360 kJ/mol in the reaction (23) and by about 33—38 kJ/mol greater in the reactions (24), (25) [6], it is clear that their contribution is much smaller than that of reaction (23).

For the determination of the rate coefficient of reaction (23) the reactions of the propionyl radical must be accounted for. This radical decomposes very rapidly into ethyl radical and carbon monoxide. Therefore, abstraction reaction (23) can be followed by measuring the amount of carbon monoxide. The other decomposition possibility of propionyl radical, into ketene and methyl radical, is insignificant; the k_{26}/k_{27} ratio is 4.5×10^3 at 573 K [7].

However, carbon monoxide arises not only from the decomposition of the propionyl radical; the cleavage of the radical formed in reaction (24) also produces carbon monoxide (most certainly in two steps) and an equivalent amount of ethylene. On the basis of the mechanism shown in Table III, the rate of carbon monoxide formation can be given as

$$R_{CO} = R_{26} + R_{28} = R_{23} + R_{24} + R_{31} + R_{32}.$$

Since R_{31} and R_{32} are negligible in comparison with the other two terms (two orders less methane is formed than carbon monoxide, and the amount of hydrogen is even less than that of methane),

$$R_{CO} = k_{23}[C_2H_5]\,[A] + R_{C_2H_4} - k_2/k_3 \cdot R_{C_4H_{10}} - k_4[C_2H_5]\,[AE],$$

where A is propionaldehyde and AE is azoethane.

In the rate of ethylene formation the amount of ethylene obtained in the decomposition of azoethane is negligible owing to its small contribution (explained below). Expressing the concentration of ethyl radicals from the rate of butane formation, $R_{C_4H_{10}} = k_3[C_2H_5]^2$, one obtains

$$k_{23} = \frac{R_{CO} - R_{C_2H_4} + k_2/k_3 \cdot R_{C_4H_{10}}}{R_{C_4H_{10}}^{1/2}} \cdot \frac{k_3^{1/2}}{[A]}.$$

For the rate coefficient of the recombination of ethyl radicals the values of $\log_{10} k_3 = \log_{10} A_3\ (dm^3 \cdot mol^{-1} \cdot s^{-1}) = 10.0$ was accepted from the literature data [8], and thus the logarithm of the rate coefficient of the abstraction reaction is, according to our measurements,

$$\log_{10} k_{23}\ (dm^3 \cdot mol^{-1} \cdot s^{-1}) = (7.7 \pm 0.1) - (26.3 \pm 0.8)\ kJ\ mol^{-1}/2.3\,RT$$

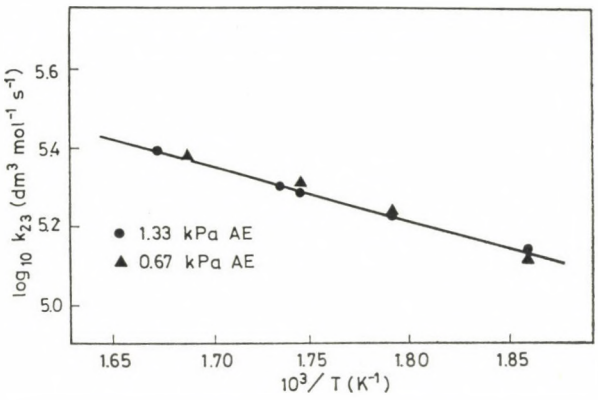

Fig. 1. Arrhenius plot of rate constant k_{23}

(with a correlation coefficient of 0.9968). The Arrhenius plot of k_{23} can be seen in Fig. 1.

Hydrogen abstraction from the methyl group of the aldehyde molecule yields the radical $\dot{C}H_2—CH_2—CHO$, which produces ethylene by decomposition. The presence of reactions (24) and (28) is supported by the experimental fact that the ethylene : butane ratio is higher than k_2/k_3 (disproportionation of ethyl radical *vs.* its recombination) for all composition and temperatures.

For the expression of rate coefficient k_{24} the ethylene balance should be taken into account:

$$R_{C_2H_4} = R_2 + R_4 + R_{24},$$

$$R_{C_2H_4} = k_2/k_3 \cdot R_{C_4H_{10}} + k_4[C_2H_5]\,[AE] + k_{24}[C_2H_5]\,[A],$$

$$k_{24} = \frac{R_{C_2H_4} - k_2/k_3 \cdot R_{C_4H_{10}} - k_4/k_3^{1/2} \cdot R_{C_4H_{10}}^{1/2}\,[AE]}{R_{C_4H_{10}}^{1/2}} \cdot \frac{k_3^{1/2}}{[A]}.$$

The value of k_4 was determined in our previous work [5] dealing with the pure decomposition of azoethane (Table III). Using this value, the logarithm of the rate coefficient of abstraction reaction (24) is, according to our measurements,

$$\log_{10} k_{24}(\mathrm{dm^3\,mol^{-1}\,s^{-1}}) = (8.1 \pm 0.3) - (53.3 \pm 3.1)\,\mathrm{kJ \cdot mol^{-1}}/2.3\,RT$$

(with a correlation coefficient of 0.9900). The Arrhenius plot is shown in Fig. 2.

Hydrogen abstraction from the methylene group gives, in addition to ethane, the radical $CH_3—\dot{C}H—CHO$ (25). This radical is less reactive, from the aspect of chain propagation it is a "wrong radical", due probably to a

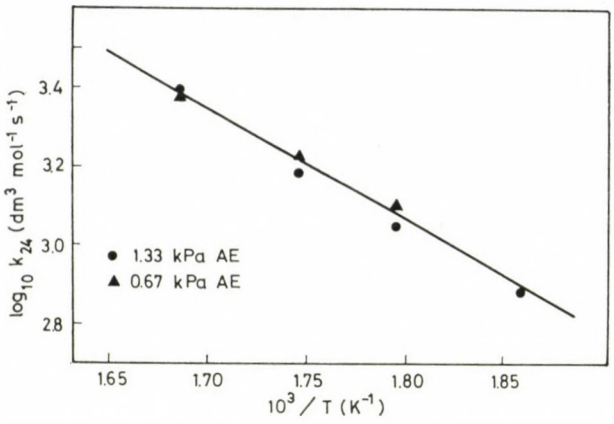

Fig. 2. Arrhenius plot of rate constant k_{24}

resonance stabilization. Under our experimental conditions it takes part mainly in break-down reactions (29) and (30).

The recombination products of $CH_3—\dot{C}H—CHO$ radical were not measured; the rate coefficient of abstraction reaction, however, may be determined indirectly through measuring ethane formation:

$$R_{C_2H_6} = R_{23} + R_{24} + R_{25} + R_2 + R_4 + R_5,$$

$$R_{C_2H_6} = R_{CO} + k_{25}[C_2H_5]\,[A] + k_2/k_3 \cdot R_{C_4H_{10}} + (k_4 + k_5)[C_2H_5]\,[AE],$$

$$k_{25} = \frac{R_{C_2H_6} - R_{CO} - k_2/k_3 \cdot R_{C_4H_{10}}}{R_{C_4H_{10}}^{1/2}} \cdot \frac{k_3^{1/2}}{[A]} - \frac{(k_4 + k_5)\,[AE]}{[A]}.$$

Using the value for k_5 given in Table III, one obtains the logarithm of the rate coefficient of abstraction reaction (25)

$$\log_{10} k_{25}(\mathrm{dm^3\ mol^{-1}\ s^{-1}}) = (8.0 \pm 0.1) - (34.8 \pm 1.2)\,\mathrm{kJ \cdot mol^{-1}}/2.3 \cdot RT$$

(with a correlation coefficient of 0.9956). The Arrhenius plot of k_{25} is shown in Fig. 3.

It is noted that if in the expressions for k_{24} and k_{25} reactions (4) and (5) are not taken into account (*i.e.* ethylene and ethane arising from azoethane is neglected), the results obtained differ from the above data well within the experimental error. This indicates that the own chain decomposition of azoethane is slow and practically negligible.

The values of rate constants k_{24} and k_{25} are in good agreement with the reactivity conditions one can meet in connection with analogous hydrogen abstraction reactions from the methyl and methylene groups of hydrocarbons.

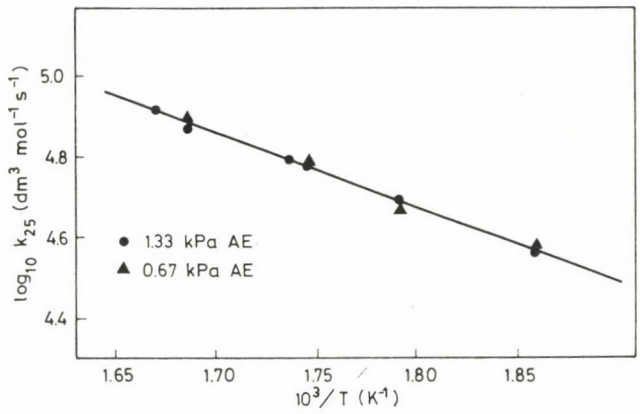

Fig. 3. Arrhenius plot of rate constant k_{25}

We also attempted to determine the chain length of the decomposition of propionaldehyde initiated by azoethane. The rate of initiation reaction can be measured through the rate of nitrogen formation. The consumption of aldehyde was not followed, we approximated it with the formation of ethane in the following manner:

$$R_A = R_{C_2H_6} - (R_2 + R_4 + R_5)$$

and chain length was expressed as

$$\lambda = \frac{R_{C_2H_6} - k_2/k_3 \cdot R_{C_4H_{10}} - (k_4 + k_5)\, k_3^{-1/2} R_{C_4H_{10}}^{1/2} [AE]}{2 \cdot R_{N_2}} .$$

The chain lengths calculated in this way from the initial rates are given in Table IV. The results show that the initiated decomposition of propionaldehyde is a short-chained process. The inclusion of R_4 and R_5 is, at present, of theoretical importance only.

Table IV

Variation of chain length with temperature

T, K	P_0 = 1.33 kPa azoethane + 12.00 kPa aldehyde	P_0 = 0.67 kPa azoethane + 12.67 kPa aldehyde
538	4.4	5.0
558	3.1	4.0
573	2.3	3.0
593	1.8	2.2

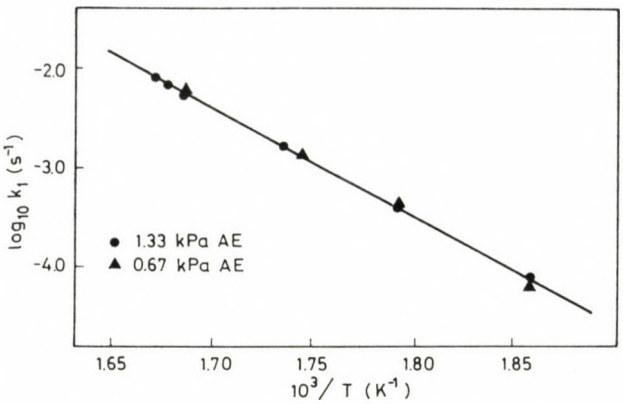

Fig. 4. Arrhenius plot of rate constant k_1

In some experiments we determined the rate of azoethane consumption; it was the same, within the experimental error, as the rate of nitrogen formation. This result induced us to calculate a first-order rate coefficient on the basis of nitrogen formation, according to the simple relationship

$$R_{AE} = R_{N_2} = k_1 [AE]; \quad k_1 = \frac{R_{N_2}}{[AE]}.$$

Performing the calculations and constructing the Arrhenius plot (see Fig. 4) we obtained the following value for the logarithm of rate coefficient:

$$\log_{10} k_1(s^{-1}) = (15.9 \pm 0.2) - (206.0 \pm 2.2)\,kJ \cdot mol^{-1}/2.3 \cdot RT$$

(correlation coefficient: 0.9996).

The coefficient is denoted by k_1 since the numerical value is in very good agreement with the rate coefficient of the primary decomposition of azoethane

$$(C_2H_5)_2N_2 \rightarrow N_2 + 2\ C_2H_5 \qquad (1)$$

obtained in our previous investigations [9]:

$$\log_{10} k_1(s^{-1}) = (15.8 \pm 0.1) - (205.1 \pm 1.5)\,kJ \cdot mol^{-1}/2.3 \cdot RT$$

In the investigations cited the decomposition of azoethane was measured in the presence of large excess of ethylene. Together with the recent result it can be concluded that in the suppression of the chain-decomposition of azoethane large excesses of either ethylene or propionaldehyde give the same

final result. With the development of the chain reaction (C_2H_5 + AE abstraction) the addition onto ethylene competes successfully in the former case, and in the latter one hydrogen abstraction from the formyl group of the aldehyde is energetically more favourable than the other abstraction reaction(s): $E_{23} = 26.3$ kJ/mol $< E_5 = 34.8$ kJ/mol. Therefore, in both cases azoethane is consumed almost exclusively in the primary reaction, and nitrogen is formed only in this reaction.

The aim of our investigations was the determination of hydrogen abstraction recations. In this respect we modelled by a computer program the mechanism conceivable on the basis of the results obtained on the initiated decomposition of aldehyde. Elementary steps (1)—(22) of Table III have already been modelled [5], the Arrhenius parameters shown are the result of this approximation. Reactions (23)—(32) represent the elementary reactions proceeding in the initial stage of the initiated decomposition of aldehyde. The system of differential equations derivable from the reaction mechanism was integrated numerically by the method of GEAR [10].

For the numerical integration the rate coefficients were selected as follows. For reactions (26) and (27) the values found in the literature [11, 7] were accepted and not changed later. The rate coefficients of the other, not mentioned reactions were changed during the calculation, and the starting values of these coefficients were estimated on the basis of analogies or, in

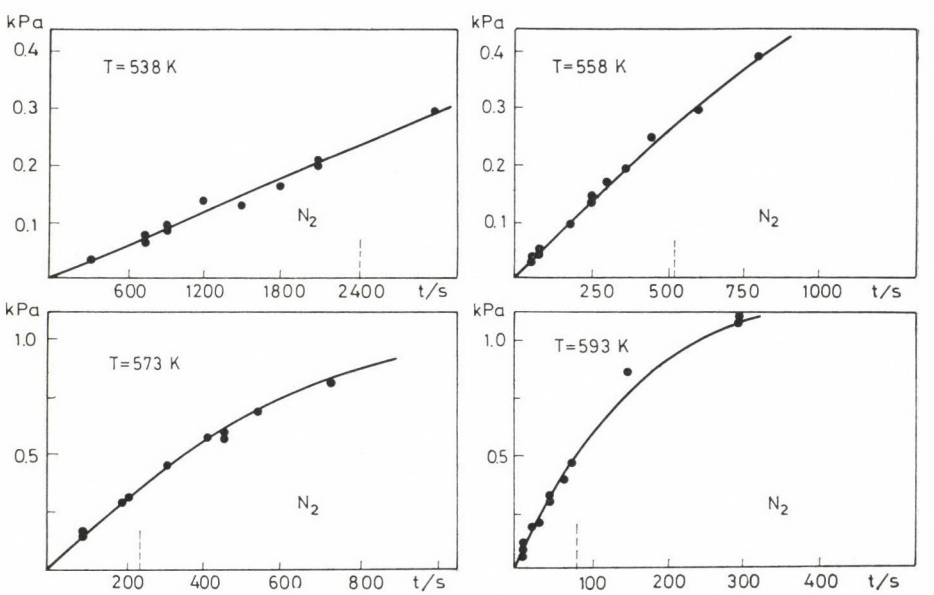

Fig. 5. The variation of calculated and measured amounts of nitrogen as a function of reaction time at four temperatures; $P_0 = 1.33$ kPa azoethane + 12.00 kPa propionaldehyde

the case of reactions (23), (24) and (25) from the results of calculations discussed above. The directions of changes were derived from the results obtained by changing only one parameter. Table III shows the Arrhenius parameters giving the best agreement. The Arrhenius parameters of reactions (23), (24) and (25) had to be changed so little that the change was within the experimental error of their determination.

The results of calculations for four temperatures, for the 1.33 azoethane — 12.00 kPa propionaldehyde mixture, are given in Figs 5—10. The other

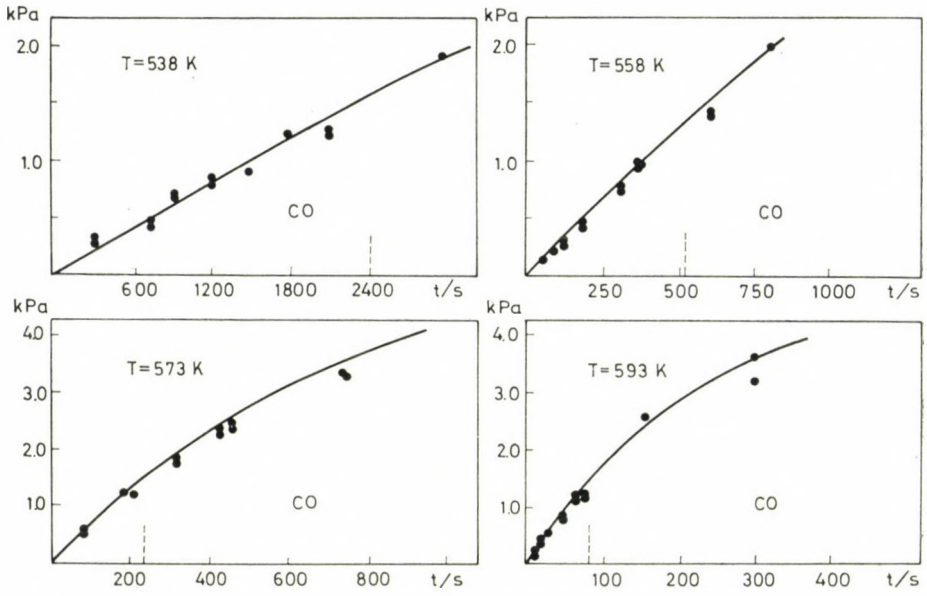

Fig. 6. The variation of the calculated and measured amounts of carbon monoxide as a function of reaction time at four temperatures; $P_0 = 1.33$ kPa azoethane + 12.00 kPa propionaldehyde

mixture led to similar results. The points in the figures represent measured data, the solid lines show the calculated curves. The reaction time belonging to 15% conversion is indicated by a vertical broken line.

Although our mechanism pertains to the initial stage of initiated decomposition, it can be seen that the agreement is satisfactory up to high conversions. Deviations can be observed in two cases. First, ethylene is consumed in an oligomerization reaction not taken into account in the mechanism. Second, in the case of methane at higher temperatures a further source of methyl radical must probably be taken into account.

It is noted that the calculated propionaldehyde and azoethane consumptions gave rise to the same chain length values than the experimental data.

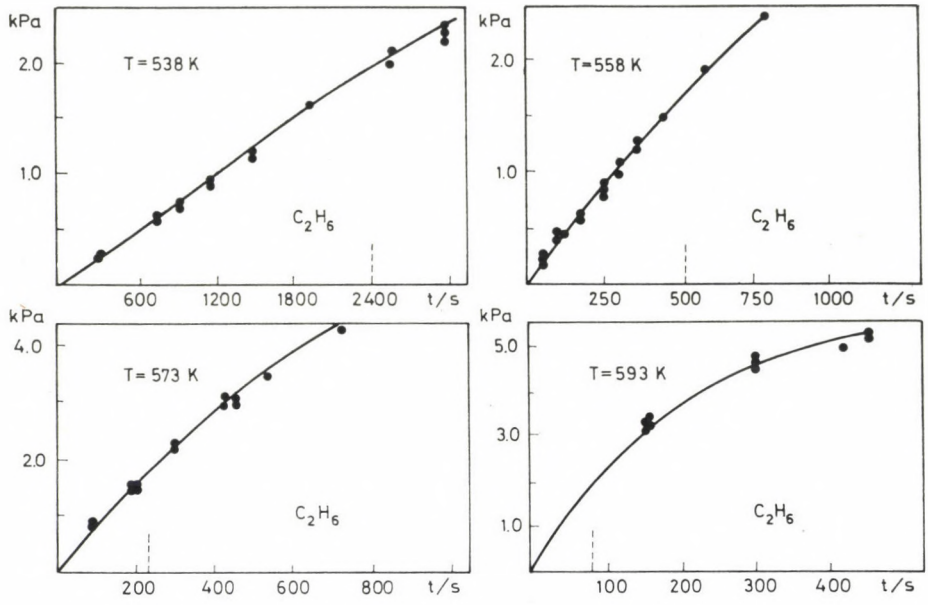

Fig. 7. The variation of the calculated and measured amounts of ethane as a function of reaction time at four temperatures; $P_0 = 1.33$ kPa azoethane + 12.00 kPa propionaldehyde

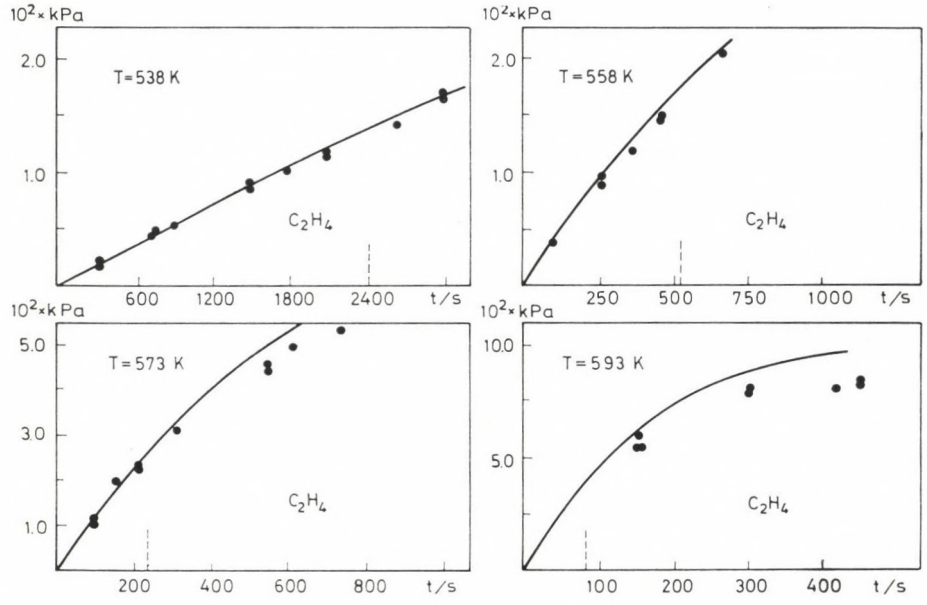

Fig. 8. The variation of the calculated and measured amounts of ethylene as a function of reaction time at four temperatures; $P_0 = 1.33$ kPa azoethane + 12.00 kPa propionaldehyde

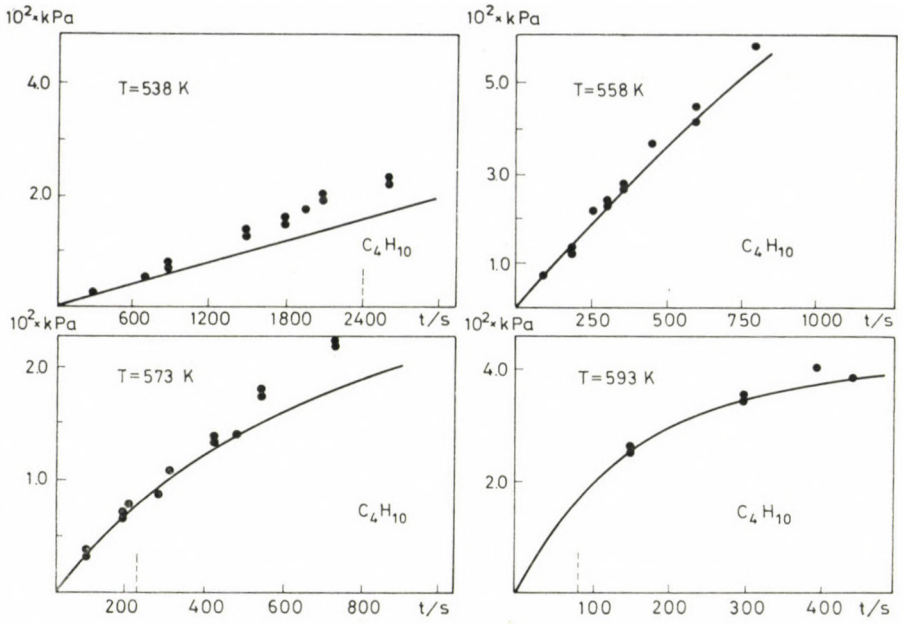

Fig. 9. The variation of the calculated and measured amounts of butane as a function of reaction time at four temperatures; $P_0 = 1.33$ kPa azoethane + 12.00 kPa propionaldehyde

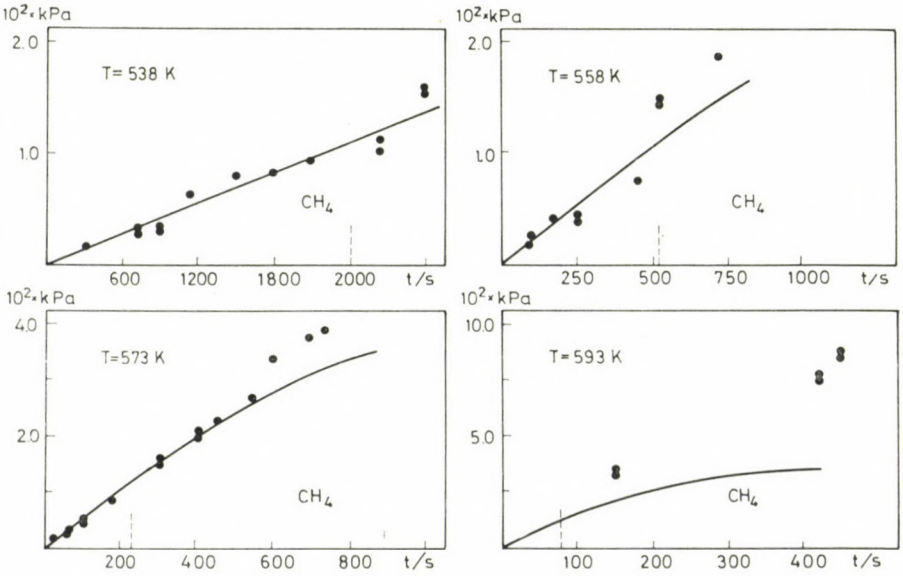

Fig. 10. The variation of the calculated and measured amounts of methane as a function of reaction time at four temperatures; $P_0 = 1.33$ kPa azoethane + 12.00 kPa propionaldehyde

REFERENCES

[1] ÁCS, G., TÓTH, G., HUHN, P.: Acta Chim. Acad. Sci. Hung., **82,** 317 (1974)
[2] VOLMAN, D. H., BRINTON, R. K.: J. Chem. Phys., **20,** 1964 (1952)
[3] KERR, J. A., TROTMAN-DICKENSON, A. F.: J. Chem. Soc., **1960,** 1611
[4] RENAUD, R., LEITCH, L. C.: Canad. J. Chem., **32,** 545 (1954)
[5] HUHN, P., ÁCS, G., PÉTER, A., HORVÁTH, I.: Magyar Kémiai Folyóirat, **85,** 446 (1979)
[6] FÖRGETEG, S., BÉRCES, T., MÁRTA, F., DÓBÉ, S.: Acta Chim. Acad. Sci. Hung., **100,** 111 (1979)
[7] ÁCS, G., TÓTH, G., HUHN, P.: Acta Chim. Acad. Sci. Hung., **82,** 425 (1974)
[8] GOLDEN, D. M., CHOO, K. Y., PERONA, M. J., PISZKIEVICZ, L. W.: Int. J. Chem. Kinetics, **8,** 381 (1976)
[9] ÁCS, G., PÉTER, A., HUHN, P.: Magyar Kémiai Folyóirat, **86,** 529 (1980)
[10] GEAR, G. W.: Numerical Initial Value Problems in Ordinary Differential Equations. Prentice-Hall, Inc. Englewood Cliffs, New Jersey, 1971
[11] KERR, J. A., LLOYD, A. C.: Trans. Faraday Soc., **63,** 2480 (1967)
[12] BENSON, S. W., O'NEAL, H. E.: Kinetic Data on Unimolecular Reactions, NSRDS-NBS 21. (1970)
[13] Radical-Radical Reactions. Dispr. *vs.* Combination, Chemical Reviews, **73,** 441 (1973)
[14] WALKER, R. W.: Gas Kinet. Energy Transfer, **2,** 296 (1977)

Antal PÉTER
Gábor ÁCS
István HORVÁTH
Péter HUHN

H-6720 Szeged, Dóm tér 7.

Acta Chimica Academiae Scientiarum Hungaricae, Tomus 108 (3), pp. 249—253 (1981)

STUDIES ON REDUCTION OF SOME ACTINIDES AND LANTHANIDES IN CHLORIDE MELTS

N. B. MIKHEEV, R. A. DYACHKOVA and L. N. AUERMAN

(Institute of Physical Chemistry of the Academy of Sciences of the USSR, Moscow, USSR)

Received July 31, 1980

Accepted for publication December 12, 1980

The study of the distribution of microquantities of actinides and lanthanides in $(LnOCl)_{solid\ phase}-(LnCl_3-LnCl_2-SrCl_2)_{melt}$ systems showed that Am^{3+}, Bk^{3+} and Pm^{3+} are reduced with neodymium dichloride. The number of electrons participating in the reduction reactions was determined and a conclusion was drawn on the reduction of these elements to the 2+ oxidation state. The oxidation potential of the Am^{3+}/Am^{2+}, Bk^{3+}/Bk^{2+}, Pm^{3+}/Pm^{2+} couples referred to the Nd^{3+}/Nd^{2+} potential in the melts at 900 °C was established.

Introduction

Melted alkali and alkali earth metals halogenide systems are able to stand low oxidation potentials and thus they can be used in the investigation of the reduction of actinides and lanthanides to lower oxidation states. MULLINS *et al.* [1] studied the distribution of americium between metallic plutonium melt and that of an equimolar KCl and NaCl mixture and found that americium was reduced by metallic plutonium to its +2 oxidation state. MAILEN and FERRIS [2] reported on the oxidation state of plutonium, americium, curium and californium based on the distribution of microquantities of these elements between the melt of lithium chloride and that of metallic bismuth containing metallic lithium. They established that the oxidation state of californium in the given system is +2 and that of plutonium, americium and curium is +3. FERRIS, MAILEN and SMITH [3] made a conclusion that in a system where the melt of lithium fluoride and berillium fluoride mixture is the salt phase and the melt of metallic bismuth, containing lithium, is the metallic phase, americium is present in the salt phase both in +3 and +2 oxidation states and its mean valency varies from 2.7 to 2.1, depending on the lithium concentration in the melted bismuth phase, while californium is present in this system in the +3 oxidation state. Such a conclusion is difficult to account for since the standard oxidation potential of the Am^{3+}/Am^{2+} couple is much more negative than that of Cf^{3+}/Cf^{2+}.

It is doubtless that using "salt melt-metal melt"systems for the identification of lower valence states interactions in the metal phase influence the behaviour of the elements studied, and thus, make the interpretation of their valency more difficult.

Experimental

When studying lower valence states of some actinides and lanthanides, present in microquantities, we used a different approach based on the distribution of microcomponents between the salt melt and the solid crystal phase, *i.e.* the method of cocrystallization in melted salts. A lanthanide oxychloride was used as the solid phase and the melt of tri- and dihalogenides of the same lanthanide element and strontium chloride was used as the liquid phase. Strontium chloride was introduced to maintain constant molarity ratio $LnOCl : LnCl_3 : (LnCl_2 + SrCl_2)$ in the melt. In such a system actinides and lanthanides isomorphically cocrystallize with oxychloride present in the +3 oxidation state and are not captured by the solid phase in a lower oxidation state.

The equilibrium distribution of the microcomponent in the +3 oxidation state in a system without a reducing agent, assuming that the activity coefficient M^{3+} in the solid phase is equal to 1, and activity coefficient m^{3+} in the liquid phase are constant, can be given by the following equation:

$$D = \left(\frac{m^{3+}}{M^{3+}}\right)_{\text{solid phase}} \times \left(\frac{M^{3+}}{m^{3+}}\right)_{\text{melt}} \tag{1}$$

where M^{3+} and m^{3+} are the equilibrium quantities of the macro- and microcomponents and D is the cocrystallization coefficient of the microcomponent (no reducing agent).

In the case when lanthanide dichloride, which is a reducing agent with respect to the studied microcomponent, is present in the system and in the case of partial reduction of the microcomponent the cocrystallization coefficient of the microcomponent (D') which is estimated experimentally is described by the following equation:

$$D' = \left(\frac{m^{3+}}{M^{3+}}\right)_{\text{solid phase}} \times \left(\frac{M^{3+} + M^{2+}}{m^{3+} + m^{(3-n)+}}\right)_{\text{melt}} \tag{2}$$

where M^{2+} and $m^{(3-n)}$ are the equilibrium quantities of the macro- and microcomponents in the reduced state.

The cocrystallization coefficient of the microcomponent in the presence of a reducing agent is connected with the cocrystallization coefficient in a system without reducer by the following equation:

$$D' = D \frac{\left(\frac{M^{2+}}{M^{3+}} + 1\right)_{\text{melt}}}{\left(\frac{m^{(3-n)+}}{m^{3+}} + 1\right)_{\text{melt}}} . \tag{3}$$

It follows from equation 3 that in case of equal ratios of the reduced and oxidized forms of both components in the melt, $D = D'$. If the microcomponent reduces easier than the macrocomponent, then $\frac{m^{(3-n)+}}{m^{3+}} > \frac{M^{2+}}{M^{3+}}$ and $D' < D$. In the opposite case $D' > D$. Thus when studying the dependence of the distribution coefficient of a lanthanide or actinide microquantity upon the ratio of the reduced and oxidized forms of the macrocomponent in the systems mentioned above it is possible to establish whether reduction of the microelement takes place and, if it does, to determine relative stability of the reduced form in comparison with divalent form of the macrocomponent of the system. The oxidation state after reduction can be established by the determination of the number of electrons (n) praticipating in the reduction reaction of a trivalent actinide or lanthanide. Obviously, the following equation is true for the equilibrium:

$$E_m^0 - \frac{RT}{nF} \ln \frac{m^{(3-n)+}}{m^{3+}} = E_M^0 - \frac{RT}{F} \ln \frac{M^{2+}}{M^{3+}} . \tag{4}$$

Then deriving from Eqs 2, 3 and 4 it follows that

$$\lg \left[\frac{D}{D'}\left(1 + \frac{M^{2+}}{M^{3+}}\right) - 1\right] = a + n \lg \frac{M^{2+}}{M^{3+}} \tag{5}$$

where $a = \frac{E_m^0 - E_M^0}{2.3\, RT/nF}$.

Therefore, if the D/D' and M^{2+}/M^{3+} ratios are known, then the value of "n" can be found.

Experiments on the distribution of the microcomponent in $(LnOCl)_{solid\ phase}-(LnCl_3-LnCl_2-SrCl_2)_{melt}$ systems were performed at 900 °C in hermetically sealed crucibles made of molybdenum or tantalum in argon atmosphere. Melting was carried on for a time sufficient for the thermodynamical equilibrium to set in the system then the melt was cooled, and 0.1 M HCl added. Then the melt phase consisting of lanthanide tri- and dihalogenides and strontium chloride, completely dissolved while the oxychloride phase remained unchanged. The phases were separated by centrifugation and the distribution of micro- and macrocomponents of the system between the phases was determined.

The divalent form content of the macrocomponent in the melt was determined by the volume of hydrogen evolved when the melt was dissolved in acid, while the total macrocomponent quantity was determined by complexometric titration. On the basis of the obtained data we calculated the cocrystallization coefficients of D and D' microcomponents.

Results

The studies on the distribution of promethium, berkelium and cerium between the solid phase and the melt in $(SmOCl)_{solid\ phase}-(SmCl_3-SmCl_2-SrCl_2)_{melt}$ system showed that the cocrystallization coefficients of all the three elements increase with an increase in the Sm^{2+}/Sm^{3+} ratio, and therefore these elements are not reduced in melts containing $SmCl_2$.

The use of $(NdOCl)_{solid\ phase}-(NdCl_3-NdCl_2-SrCl_2)_{melt}$ system enables us to reach far lower oxidation potentials. We studied the behaviour of americium, berkelium and cerium in the system. The results are shown in Fig. 1. The samarium cocrystallization coefficients rapidly decrease when even small

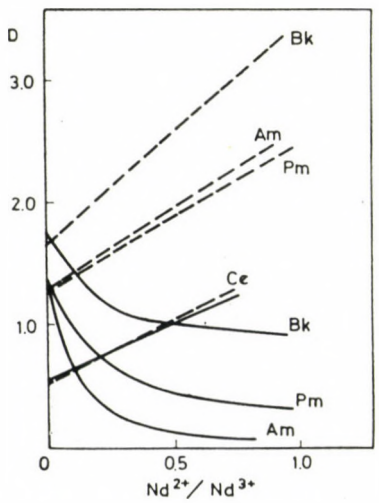

Fig. 1. Dependence of the cocrystallization coefficients of Am, Bk, Pm, Ce on the Nd^{2+}/Nd^{3+} ratio. Continuous line–experimental values, Dotted lines–values calculated using Eq. 3, assuming that Am, Bk, Pm, Ce are present in the +3 oxidation state

quantities of divalent neodymium are introduced, and they reach values $<10^{-2}$ so that their exact determination by experimental methods becomes difficult. The distribution coefficients of americium, berkelium, promethium also decrease with an increase in the Nd^{2+}/Nd^{3+} ratio in the melt, and this decrease is most expressed in the case of americium, less in that of promethium, and least in that of berkelium. In the same figure there are dependences of the cocrystallization coefficients of americium, berkelium and promethium upon the Nd^{2+}/Nd^{3+} ratio. The dependences are obtained by calculations with the assumption that these elements are present in the melt in the trivalent state. As it is seen from Fig. 1 theoretically calculated and experimentally observed dependences of cocrystallization coefficients of microcomponents upon the Nd^{2+}/Nd^{3+} ratio are greatly different. This fact allows us to make a conclusion about the reduction of the three microelements.

In Fig. 1 there are also data on cerium distribution in the same system. Being different from americium, berkelium and promethium, the cerium cocrystallization coefficients increase with an increase in the Nd^{2+}/Nd^{3+} ratio in the melt, and the experimentally found dependence of the cocrystallization coefficients upon the Nd^{2+}/Nd^{3+} ratio in the melt coincides, within experimental error, with the dependence calculated using equation 3, if it is assumed that the total cerium is present in the oxidation state of $+3$. Therefore, Ce^{3+} is practically not reduced by neodymium dichloride within the Nd^{2+}/Nd^{3+} concentration ratio range less than or equal to 1.2.

In Fig. 2 there is the following dependence:

$$\lg\left[\frac{D}{D'}\left(1+\frac{M^{2+}}{M^{3+}}\right)-1\right] \quad \text{upon} \quad \lg\frac{M^{2+}}{M^{3+}}.$$

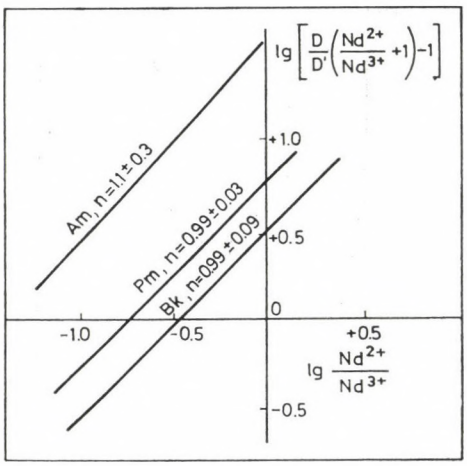

Fig. 2. Dependence $\lg\left[\frac{D}{D'}\left(1+\frac{Nd^{2+}}{Nd^{3+}}\right)-1\right]=f\lg\frac{Nd^{2+}}{Nd^{3+}}$ for Am, Bk, Pm

Deriving from this dependence and using the method of least squares the value of "n" (see equation 5), the number of electrons taking part in the reduction of a lanthanide or actinide microcomponent, was determined. Thus all these elements are reduced by divalent neodymium to the $+2$ oxidation state. Equation 5 enables us to determine the difference in the oxidation potentials m^{3+}/m^{2+} couple of the microelement and that neodymium at 900 °C in the melt containing $NdCl_2$, $NdCl_3$, and $SrCl_2$. It turned out that ΔE^0_{Am-Nd} is equal to 0.3 ± 0.1; $\triangle E^0_{Pm-Nd} = 0.18 \pm 0.05$ v and $\Delta E^0_{Bk-Nd} = 0.12 \pm 0.02$ v.

Thus studies on the distribution of actinide and lanthanide microquantities in $(LnOCl)_{solid\ phase}-(LnCl_3-LnCl_2-SrCl)_{melt\ system}$ make it possible not only to establish the fact of reduction of an actinide or lanthanide but also to determine the degree of its reduction as well as to find the difference in the oxidation potentials of the micro- and macroelements, which take part in oxidation-reduction reactions.

REFERENCES

[1] MULLINS, L. J., BEAMONT, A. J., LEARY, A. J.: J. Inorg. Nucl. Chem., **30,** 147 (1968)
[2] MAILEN, J. C., FERRIS, L. M.: Inorg. Nucl. Chem. Lett., **7,** 431 (1971)
[3] FERRIS, L. M., MAILEN, J. C., SMITH, F. J.: J. Inorg. Nucl. Chem., **33,** 1325 (1971)

N. B MIKHEEV
R. A. DYACHKOVA
L. N. AUERMAN
Institute of Physical Chemistry of Academy of Sciences of the USSR
Leninsky prospect, 31 Moscow, USSR

Acta Chimica Academiae Scientiarum Hungaricae, Tomus 108 (3), pp. 255–263 (1981)

SYNTHESIS AND TESTING OF 1-ARYL-1,4--DIHYDRO-3(2*H*)-BENZOISOQUINOLINONES OF POTENTIAL ANTICONVULSANT ACTION

L. Hazai, Gy. Deák* and M. Dóda

(*Institute of Experimental Medicine, Hungarian Academy of Sciences, Budapest*)

Received October 17, 1980

Accepted for publication December 17, 1980

The method developed for the synthesis of 1-aryl-1,4-dihydro-3(2*H*)-isoquinolinones has been extended to the preparation of derivatives containing an additional fused benzene ring. The benzo[*f*] and benzo[*h*] derivatives were prepared from the appropriate naphthylacetonitriles. The benzo[*g*] isomer was synthesized from 1-chloro--2-naphthylacetonitrile; hydrogenolysis was used to remove the chlorine from 5-chloroisoquinolinone obtained as the primary product. For the purpose of biological tests, the 1-(4'-aminophenyl) and 1-[4'-(ethylaminoacetyl)-aminophenyl] derivatives of benzoisoquinolinones have been prepared; one of them had significant anticonvulsant action.

In an earlier paper [1], the synthesis and pharmacology of 1-aryl-1,4--dihydro-3(2*H*)-isoquinolinones (**I**), members of a new group of anticonvulsants were discussed.

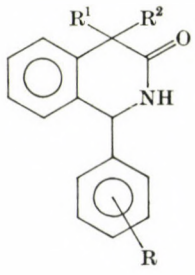

R = H, NH_2;

R^1, R^2 = H, alkyl

I

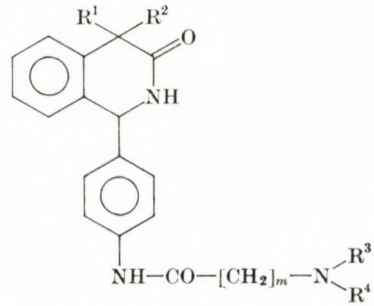

m = 0—3; R^1, R^2 = H, CH_3;

R^3, R^4 = H or alkyl

II

Scheme 1

As reported, particularly good activity was found in the derivatives where R = alkylaminoacylamino (**II**), the best being the ethylaminoacetylamino group (Scheme 1).

* To whom correspondence should be addressed

In continuation of this work, the effect of the presence of a benzene ring fused with the homoaromatic ring of the isoquinolinone skeleton on biological activity was to be established. The synthesis of 1,4-dihydro-3(2*H*)-isoquinolinones [2] effected in 1 : 1 polyphosphoric acid from arylacetonitriles and aromatic aldehydes has been therefore extended to naphthylacetonitriles.

The reaction of 1-naphthylacetonitrile and an aromatic aldehyde in PPA gave the corresponding 1-phenyl-1,4-dihydro-3(2*H*)-benzo[*f*]isoquinolinone derivative in satisfactory yields (Scheme 2). In the case of R = NO_2,

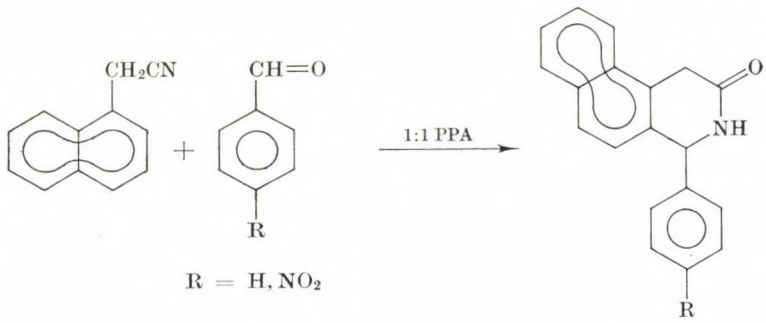

1 R = H
2 R = NO_2
3 R = NH_2

Scheme 2

reduction in the presence of palladium on carbon catalyst yielded the R=NH_2 derivetive (**3**).

In the reaction of 2-naphthylacetonitrile and benzaldehyde, two possibilities of ring closure had to be considered; the reaction mixture could be processed only by the column chromatographic technique, owing to heavy contamination; benzo[*h*]isoquinolinone (**4**) was isolated in 64% yield, the benzo[*g*]isomer could not be detected.

In the NMR spectrum of the compound obtained, the 6.30d shift of H-1 is very great, showing that the C-1 phenyl group cannot be in *equatorial* position because of steric hindrance; hence the probable structure of the compound is the following.

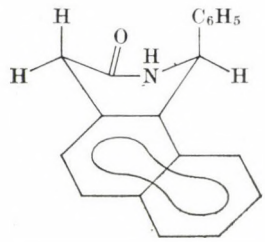

The reaction was also effected with *p*-nitrobenzaldehyde, and the R = $= NH_2$ derivative (**6**) was prepared by catalytic hydrogenation of the R $= NO_2$ compound (**5**).

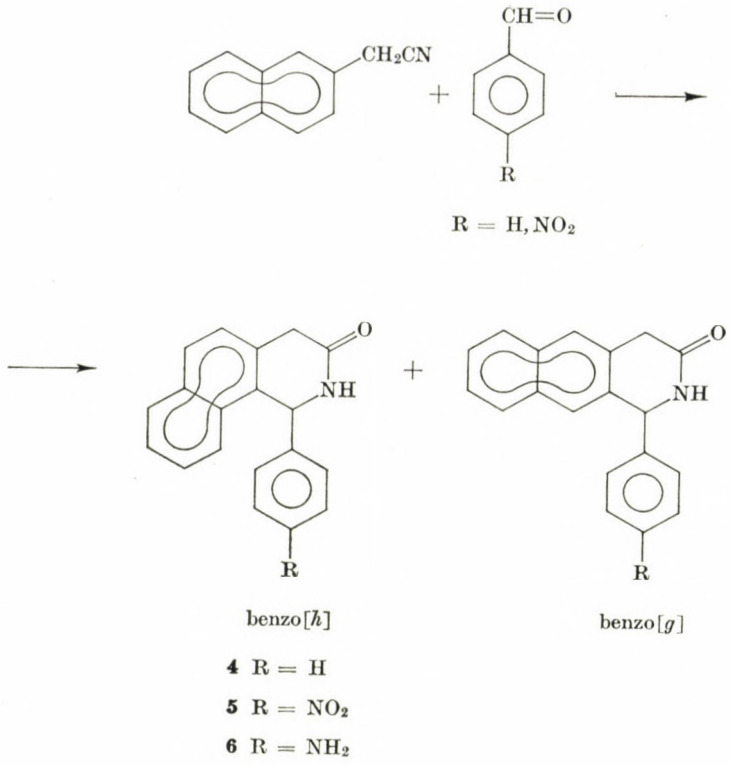

benzo[*h*] benzo[*g*]

4 R = H
5 R = NO_2
6 R = NH_2

For the synthesis of the benzo[*g*] derivative it seemed promising to start from a 2-naphthylacetonitrile carrying a substituent at C-1 which can easily be removed at a later stage of the synthesis. The chloro derivative appeared suitable for this purpose. This compound was prepared as follows: 2-methyl--naphthalene was chlorinated with sulfuryl chloride to yield 1-chloro-2-methyl--naphthalene [5], and this was converted into 2-bromomethyl-1-chloronaphthalene [6] by means of *N*-bromosuccinimide. The nitrile was prepared by reaction with alkali cyanide, and this was then allowed to react with benzaldehyde in PPA to yield compound **7** (Scheme 3).

This chlorine derivative was then hydrogenated in the presence of a base to convert it in a hydrogenolysis reaction into 1-phenyl-1,4-dihydro-3(2*H*)-benzo[*g*]isoquinolinone (**9**). Thus the isoquinolinones containing a fused benzene ring in all the three possible ways have been successfully prepared.

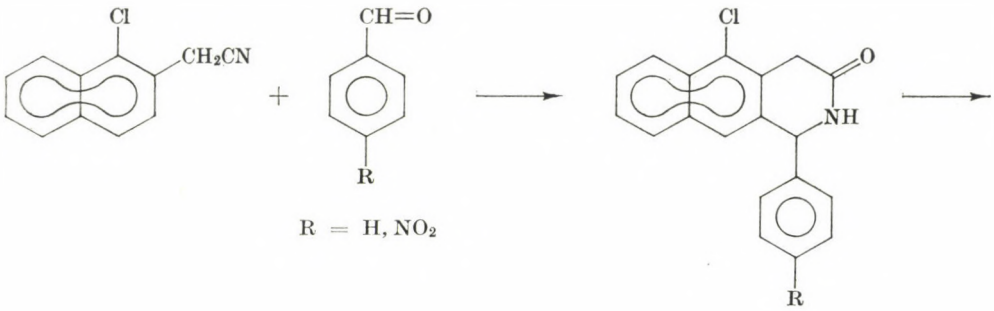

7 R = H

8 R = NO_2

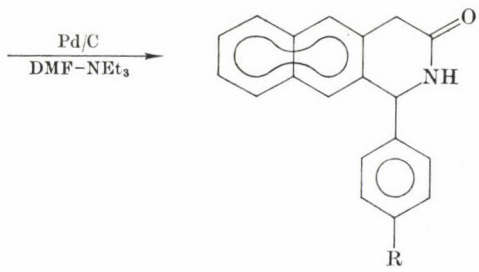

9 R = H

10 R = NH_2

Scheme 3

The fundamental difference between the NMR spectra of the compound containing the chlorine substituent and the product of hydrogenolysis is the shift of the C-6 proton due to the vicinity of the chlorine atom.

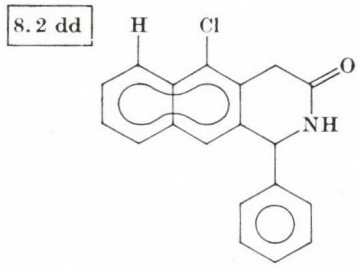

Catalytic hydrogenation of the 4'-nitro-5-chloro derivative (**8**) in the presence of a base yielded **10**; in the course of attempted Bechamp reduction only decomposition products could be isolated from the reaction mixture.

The next task was the introduction of the alkylaminoacylamino side chain. On the basis of earlier experience [1], the ethylaminoacetylamino group was chosen and the syntheses were carried out in the following manner: the 4'-amino derivatives described above were allowed to react with chloroacetyl chloride in the presence of triethylamine to yield the Y : CO—CH_2—Cl derivatives. This was followed by a reaction with ethylamine in a bomb tube to obtain the benzo[*f*], benzo[*h*] and benzo[*g*] derivatives with the side chain Y : CO—CH_2—NH—C_2H_5 (Scheme 4).

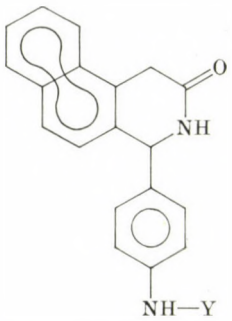

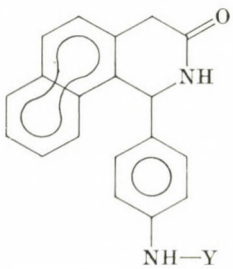

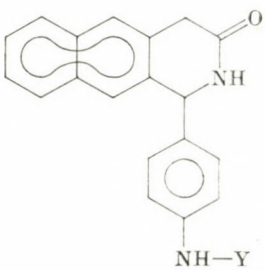

Y = $COCH_2Cl$,	**11**	**13**	**15**
Y = $COCH_2NHC_2H_5$	**12**	**14**	**16**

Scheme 4

In the pharmacological examination of the new compounds discussed above, their potential anticonvulsant action was tested in mice and the MES (Maximal Electroshock Seizures), the PTZ (Antypentylenetetrazole) and LD_{50} (acute toxicity) values, as well as the neurotoxicity of the compounds were determined. In order to compare the effectivity of compounds producing a certain protective action against electroshock, the protective index PI was used, which is the quotient of the values $ED_{50\,rotarod}$ referring to the neurotoxicity and ED_{50}MES. The PI value of 5,5-diphenylhydantoin, used as standard, is 15; one of the compounds prepared by us earlier [1] has a PI value of about 59. Most of the benzoisoquinolinone derivatives were found to be almost ineffective; two of them produced a small hindering action, these were compounds **10** and **12** {1-(4'-aminophenyl)-1,4-dihydro-3(2*H*)-benzo[*g*]-isoquinolinone and 1-[4'-(ethylaminoacetyl)aminophenyl]-1,4-dihydro-3(2*H*)-benzo[*f*]isoquinolinone, respectively} (PI < 20). However, compound **3** {1-(4'-aminophenyl)--1,4-dihydro-3(2*H*)-benzo[*f*]isoquinolinone} showed a significant activity (PI > 53).

Experimental

Preparation of benzoisoquinolinone derivatives

1-Phenyl-1,4-dihydro-3(2*H*)-benzo[*f*]isoquinolinone (1)

1-Naphthylacetonitrile [3] (19.9 g; 0.119 mole) was added to 1 : 1 PPA (200 g), then the mixture was stirred at 90 °C for 30 min. Benzaldehyde (12.6 g; 0.119 mole) was added dropwise, the reaction mixture was stirred at 120 °C for 3 hrs, it was allowed to cool to 80 °C, poured into water (1500 cm^3), made alkaline with *conc.* ammonium hydroxide, brought to boil, the solid product was filtered off while hot, washed with hot water then dried under an infrared heat lamp. M.p. 223—224 °C (butanol). Yield: 68.9%.

$C_{19}H_{15}NO$. Calcd. C 83.50; H 5.53; N 5.12. Found C 83.43; H 5.74; N 5.08%.

UV (95% ethanol) $\lambda_{max}(\varepsilon)$: 261 (4360), 269 (5000), 278 (5280), 288 nm (4140).

^{1}H-NMR ($CDCl_3$): δ (ppm) 4.10 (2H, d, C4—CH_2); 5.80 (1H, q, C1—H; $J_{NHCH} = 2.5$ Hz); 7.05 (1H, overlapping, NH); 7.06 (1H, d; $J_0 = 9$ Hz); 7.28 (5H, s); 7.5—8.0 (5H, m).

IR (KBr): νCO 1670 cm^{-1}.

1-(4'-Nitrophenyl)-1,4-dihydro-3(2*H*)-benzo[*f*]isoquinolinone (2)

1-Naphthylacetonitrile (8.6 g; 0.0514 mole) and 4-nitrobenzaldehyde (7.78 g; 0.0514 mole) were allowed to react in 1 : 1 PPA (120 g) in accordance with the previous procedure. M.p. 231—232 °C (from chloroform); yield: 55.7%.

$C_{19}H_{14}N_2O_3$. Calcd. C 71.70; H 4.43; N 8.80. Found C 71.59; H 4.58; N 8.51%.

IR (KBr): νCO 1680, νNO_2 1355, 1530 cm^{-1}.

1-(4'-Aminophenyl)-1,4-dihydro-3(2*H*)-benzo[*f*]isoquinolinone (3)

1-(4'-Nitrophenyl)-1,4-dihydro-3(2*H*)-benzo[*f*]-isoquinolinone (8.5 g; 0.0267 mole) was subjected to hydrogenation in 99.5% acetic acid (600 cm^3) in the presence of 10% Engelhardt Pd/C catalyst (2 g), prehydrogenated in 99.5% acetic acid (100 cm^3), at room temperature and atmospheric pressure. After the absorption of hydrogen had ceased, the catalyst was filtered off, the filtrate was evaporated and the remaining oil rubbed with 1 : 1 diluted NH_4OH. The solid product was filtered off, washed with water and dried under an infrared heat lamp. M.p. 262—264 °C (d.) (from butanol). Yield: 65.6%.

$C_{19}H_{16}N_2O$. Calcd. C 79.13; H 5.59; N 9.72. Found C 79.15; H 5.82; N 9.88%.

IR (KBr): νCO 1665, νNH_2 3340, 3460 cm^{-1}.

1-Phenyl-1,4-dihydro-3(2*H*)-benzo[*h*]isoquinolinone (4)

2-Naphthylacetonitrile [4] (5.5 g; 0.0329 mole) was allowed to react with benzaldehyde (3.49 g; 0.0329 mole) in 1 : 1 PPA (100 g) in the manner given for the benzo[*f*] derivative. The crude product was subjected to chromatographic separation on an Al_2O_3 column (eluting agent: chloroform), the fractions were evaporated to dryness and rubbed with ether. M.p. 269—270 °C (butanol). Yield 64%.

$C_{19}H_{15}NO$. Calcd. C 83.50; H 5.53; N 5.12. Found C 83.59; H 5.74; N 5.13%.

IR (KBr): νCO 1675 cm^{-1}.

UV (95% ethanol) λ_{max} (ε): 269 (4000), 278 (4360), 286 nm (3480).

^{1}H-NMR ($CDCl_3$): δ (ppm) 3.85 (2H, s, C4—CH_2); 6.30 (1H, d, C1—H; $J_{NHCH} = 3.7$ Hz); 7.05—7.7 (7 + 1H, ArH + NH); 7.7—8.0 (4H, m).

1-(4'-Nitrophenyl)-1,4-dihydro-3(2*H*)-benzo[*h*]isoquinolinone (5)

2-Naphthylacetonitrile (1.67 g; 0.01 mole) was added to 1 : 1 PPA (30 g) and the reaction mixture was stirred at 90 °C for 30 min. *p*-Nitrobenzaldehyde (1.51 g; 0.01 mole) was then added at 120 °C during 1 h. After stirring for 3 hrs the mixture was poured into water (300 cm^3), the pH was adjusted to 8 with *conc.* NH_4OH, the mixture was boiled, the substance which

separated was filtered off while hot, washed with hot water and dried. M.p. 208—210 °C (butanol). Yield: 81.8%

$C_{19}H_{14}N_2O_3$. Calcd. 71.69; H 4.43; N 8.80. Found C 71.66; H 4.30; N 8.80%.

IR (KBr): νCO 1670, νNO_2 1345, 1520 cm^{-1}.

1-(4'-Aminophenyl)-1,4-dihydro-3(2*H*)-benzo[*h*]isoquinolinone (6)

The previous nitro derivative (**5**) (7.8 g; 0.0242 mole) was dissolved in DMF (50 cm^3) and hydrogenated in the presence of 10% Engelhardt catalyst (2 g), which had been prehydrogenated in DMF (100 cm^3), at room temperature, under atmospheric pressure until the absorption of hydrogen ceased. The filtered solution was evaporated to dryness and the residual oil mixed with distilled water whereupon it solidified. The substance was filtered off, dissolved in dimethylformamide and passed through a column packed with Al_2O_3; the product was eluted with DMF. The DMF fractions were combined, the solvent was evaporated and the remaining oil was rubbed with distilled water to give a solid product, m.p. 257—259 °C (butanol); yield: 57.3%.

$C_{19}H_{16}N_2O$. Calcd. C 79.14; H 5.59; N 9.71. Found C 79.37; H 5.77; N 9.85%.

IR (KBr): νCO 1650, νNH_2 3335, 3445 cm^{-1}.

1-Chloro-2-naphthylacetonitrile

2-Bromomethyl-1-chloronaphthalene [6] (11.7 g; 0.046 mole) was dissolved in ethanol (100 cm^3), and an aqueous solution (20 cm^3) of KCN (6 g; 0.092 mole) was added, with stirring. After refluxing for 3 hrs, the reation mixture was poured into water (500 cm^3), the solid product was filtered off, washed with water and dried. M.p. 104—105 °C (ethanol). Yield: 84.7%.

$C_{12}H_8ClN$. Calcd. C 71.47; H 4.0; N 6.95; Cl 17.58. Found C 71.57; H 4.15; N 7.02; Cl 17.63%.

IR (KBr): νCN 2250 cm^{-1}

1-Phenyl-5-chloro-1,4-dihydro-3(2*H*)-benzo[*g*]isoquinolinone (7)

1-Chloro-2-naphthylacetonitrile (3.2 g; 0.016 mole) and benzaldehyde (1.7 g; 0.016 mole) were allowed to react in 1 : 1 PPA (60 g) in the manner given above. M.p. 222—224 °C (benzene). Yield: 51%.

$C_{19}H_{14}ClNO$. Calcd. C 74.15; H 4.58; N 4.55; Cl 11.52. Found C 74.40; H 4.80; N 4.56; Cl 11.46%.

IR (KBr): νCO 1675 cm^{-1}.

UV (95% ethanol) λ_{max} (ε): 321 (472), 283 (10771), 274 nm (9327).

^{1}H-NMR ($CDCl_3$): δ (ppm) 4.05 (2H, s, C4—CH_2); 5.85 (1H, d, C1—H; J_{NHCH} = 2 Hz); 7.25—7.75 (9H, m, ArH); 8.20 (dd, J = 1.9 Hz, 1.5 Hz).

1-Phenyl-1,4-dihydro-3(2*H*)-benzo[*g*]isoquinolinone (9)

A mixture of the above halogen derivative (1 g; 0.00326 mole) and triethylamine (1.8 cm^3; 1.32 g; 0.013 mole) in DMF (50 cm^3) was added to 10% Pd/C catalyst (0.3 g) which had been prehydrogenated in DMF (30 cm^3). Hydrogenation under atmospheric pressure was continued until the absorption of hydrogen had stopped, the catalyst was filtered off, the solvent evaporated, the residue rubbed with water, the solid filtered off and dried. M.p. 245—246 °C (butanol). Yield: 55%.

$C_{19}H_{15}NO$. Calcd. C 83.49; H 5.53; N 5.12. Found C 83.28; H 5.37; N 5.25%.

IR (KBr): νCO 1665, 1630 cm^{-1}.

UV (95% ethanol) λ_{max} (ε): 318 (384), 288 (4846), 276 (7940), 267 nm (7762).

^{1}H-NMR ($CDCl_3$): δ (ppm) 3.87 (2H, C4—CH_2); 5.81 (1H, d, C1—H; J_{NHCH} = 2.5 Hz); 6.93 (1H, d); 7.2—7.5 (8H, m, ArH); 7.6—7.8 (3H, m).

5-Chloro-1-(4'-nitrophenyl)-1,4-dihydro-3(2*H*)-benzo[*g*]isoquinolinone (8)

1-Chloro-2-naphthylacetonitrile (4.03 g; 0.02 mole) was added to 1 : 1 PPA (60 g) and the mixture was stirred at 90 °C for 30 min. *p*-Nitrobenzaldehyde (3.02 g; 0.02 mole) was added during 1 h at 120 °C, and the reaction mixture was stirred at this temperature

for 3 hrs After cooling, the reaction mixture was poured into water (600 cm^3) and made alkaline with *conc.* NH_4OH. The substance which separated was extracted with chloroform, the organic phase was washed with water, dried over Na_2SO_4 and evaporated to dryness. The product was purified in chloroform solution on an Al_2O_3 column. The fractions containing the product were combined, the solvent was removed and the residue rubbed with ether. Crystallization from butanol gave 1.8 g (25.5%) of **8**, m.p. 243—246 °C (d.).

$C_{19}H_{13}ClN_2O_3$. Calcd. C 64.69; H 3.71; N 7.94; Cl 10.05. Found C 64.79; H 3.75; N 8.11; Cl 10.05%.

IR (KBr): νCO 1680, νNO_2 1350, 1520 cm^{-1}.

1-(4'-Aminophenyl)-1,4-dihydro-3(2*H*)-benzo[*g*]isoquinolinone (10)

The above compound (**8**) (6.4 g; 0.0181 mole) was hydrogenated in DMF (200 cm^3) containing triethylamine (10.05 cm^3; 7.33 g; 0.0724 mole) in the presence of Pd/C catalyst (1.8 g) at room temperature, under atmospheric pressure. When no more hydrogen was absorbed, the catalyst was filtered off, the filtrate evaporated to dryness, the residue rubbed with water and dried. M. p. 261 °C (d.) (dioxan). Yield: 67.3%.

$C_{19}H_{16}N_2O$. Calcd. C 79.14; H 5.59; N 9.71. Found C 78.89; H 5.98; N 9.76%.

IR (KBr): νCO 1650, νNH_2 3340, 3440 cm^{-1}.

^{1}H-NMR (DMSO-d_6): δ (ppm) 5.60 (1H, d, Cl—H; $J_{NHCH} = 3$ Hz); 8.47 (1H, d, NH); 6.51 (2H, d, ArH-1); 6.95 (2H, d); 7.4—7.55 (2H, m, ArH); 7.7—7.9 (4H, m).

Preparation of benzoisoquinolinones carrying an alkylaminoacetylamino side chain

1-(4'-Chloroacetylamino)phenyl-1,4-dihydro-3(2*H*)-benzo[*f*]isoquinolinone (11)

The amino derivative **3** (5.65 g; 0.02 mole) was dissolved in 99.5% acetic acid (50 cm^3) and triethylamine (2.22 g; 0.022 mole) and chloroacetyl chloride (2.48 g; 0.022 mole) were added dropwise, with stirring. The reaction mixture was then stirred at 55 °C for 6 hrs The product which separated was filtered off, washed with water until neutral and dried. M.p. 260 °C (d.) (butanol). Yield: 71.2%.

$C_{21}H_{17}N_2O_2Cl$. Calcd. C 69.14; H 4.70; N 7.68; Cl 9.72. Found C 69.27; H 4.97; N 7.65; Cl 9.86%.

IR (KBr): νCO 1670, 1710 cm^{-1}.

1-(4'-Chloroacetylamino)phenyl-1,4-dihydro-3(2*H*)-benzo[*h*]isoquinolinone (13)

The amino derivative **6** (2.0 g; 0.00694 mole) was allowed to react with chloroacetyl chloride (0.78 g; 0.006944 mole) in acetic acid (20 cm^3) in the presence of triethylamine (0.7 g; 0.006944 mole), as described above. In this case, the product did not separate from the reaction mixture, thus it was poured into water (200 cm^3); the solid which separated was filtered off, washed with water and dried. M.p. > 270 °C (butanol). Yield: 69.9%.

$C_{21}H_{17}N_2O_2Cl$. Calcd. C 69.14; H 4.70; N 7.68; Cl 9.72. Found C 69.27; H 4.69; N 7.93; Cl 9.72%.

IR (KBr): νCO 1660, 1730 cm^{-1}.

1-(4'-Chloroacetylamino)phenyl-1,4-dihydro-3(2*H*)-benzo[*g*]isoquinolinone (15)

The 4'-amino derivative **10** (3.5 g; 0.012 mole) was dissolved in 99.5% acetic acid (47 cm^3); triethylamine (1.22 g; 0.0121 mole) then chloroacetyl chloride (1.36 g; 0.0121 mole) were added dropwise, with stirring, at 50—55 °C. The reaction mixture was stirred further at 50—55 °C for 6 hrs and poured into water (500 cm^3). The product which separated was filtered off, washed thoroughly with water and dried. M.p. 243—246 °C (d.) (methanol). Yield: 59%.

$C_{21}H_{17}ClN_2O_2$. Calcd. C 69.14; H 4.70; N 7.68; Cl 9.72. Found C 69.12; H 4.71; N 7.48; Cl 10.03%.

IR (KBr): νCO 1640, 1690 cm^{-3}.

1-[4'-(Ethylaminoacetyl)aminophenyl]-1,4-dihydro-3(2*H*)-benzo[*f*]-isoquinolinone (12)

The chloroacetyl derivative **11** (2.4 g; 0.0066 mole) was mixed ethylamine (60 cm^3) and heated at 70 °C in a bomb tube for 10 h. After cooling, the content of the tube was poured into ice-water (600 cm^3), the product was filtered off and washed with water until neutral. M.p. 230—232 °C (butanol). Yield: 48.9%.

$C_{23}H_{23}N_3O_2$. Calcd. C 73.97; H 6.21; N 11. 25. Found C 73.94; H 6.29; N 11.23%.

IR (KBr): νCO 1640, 1680 cm^{-1}.

1-[4'-(Ethylaminoacetyl)aminophenyl]-1,4-dihydro-3(2*H*)-benzo[*h*]isoquinolinone (14)

The chloroacetyl derivative **13** (1.3 g; 0.00353 mole) was allowed to react with ethylamine (50 cm^3) according to the above procedure. The ethylamine mixture was poured into ice-water (500 cm^3), the product was filtered off, washed with water and dried. M.p. 209—211 °C (butanol). Yield: 41.6%.

$C_{23}H_{23}N_3O_2$. Calcd. C 73.97; H 6.21; N 11.25. Found C 73.70; H 6.10; N 11.28%.

IR (KBr): νCO 1660, 1700 cm^{-1}.

1-[4'-(Ethylaminoacetyl)aminophenyl]-1,4-dihydro-3(2*H*)-benzo[*g*]isoquinolinone (16)

The chloroacetyl derivative **15** (2.4 g; 0.066 mole) was allowed to react with ethylamine (60 cm^3) according to the above procedure. After cooling the bomb tube, the product was filtered off from the ethylamine solution, washed with water thoroughly, and dried. The crude product was then purified by refluxing with ethanol. M.p. 219—221 °C. Yield: 81.5%.

$C_{23}H_{23}N_3O_2$. Calcd. C 73.97; H 6.21; N 11.25. Found C 73.78; H 6.23; N 11.31%.

IR (KBr): νCO 1640, 1675 cm^{-1}.

*

The authors express their thanks to Dr. J. Haskó—Breuer and to Dr. G. Tóth for recording the IR and NMR spectra, respectively, and to Miss M. Fodor and Mrs. G. Kalász for the microanalyses. Excellent technical assistance of Mrs. I. Bozsóky—Téglás is gratefully acknowledged.

REFERENCES

[1] Deák, Gy., Dóda, M., György, L., Hazai, L., Sterk, L.: J. Med. Chem., **20,** 1384 (1977)
[2] Deák, Gy., Gáll-Istók, K., Hazai, L., Sterk, L.: Synthesis, **1975,** 393
[3] Shirley, D. A.: Preparation of Organic Intermediates, pp. 210. New York, Wiley, 1951
[4] Mayer, F., Oppenheimer, T.: Chem. Ber., **49,** 2140 (1916)
[5] Houben—Weyl—Müller: Methoden der Organischen Chemie, Vol. **5**/3, p. 881., G. Thieme Verlag, Stuttgart, 1962
[6] Shoesmith, J. B., Mackie, A.: J. Chem. Soc., **1930,** 1584

László Hazai
Gyula Deák
Margit Dóda
H-1450 Budapest, P.O.B. 67.

Acta Chimica Academiae Scientiarum Hungaricae, Tomus 108 (3), pp. 265—285 (1981)

SEMIEMPIRICAL FORCE METHOD TREATMENT OF THE VIBRATIONAL SPECTRA OF AMIDES, I

IN-PLANE VIBRATIONS OF SOME SIMPLE AMIDES

A. BALÁZS

(Eötvös Loránd University, Department of General and Inorganic Chemistry, Budapest)

Received March 5, 1980

In revised form September 29, 1980

Accepted for publication January 6, 1981

A CNDO/2 force method calculation has been carried out on the in-plane force field of formamide, acetamide, *N*-methylformamide, and *N*-methylacetamide. After a least-squares fitting for the spectra with a few empirical scaling parameters, the force constant matrices are reasonably good even to permit critical judgement of the vibrational assignments of all the four molecules including *N*-deuterated derivatives. The ^{15}N isotope shifts of formamide and acetamide are also correctly reproduced. The scaling factors are proven to be transferable and are shown to permit calculation of fundamental frequencies of related molecules within a mean deviation of 30 cm^{-1}.

Introduction

In the past two decades a number of studies have dealt with the vibrational spectra of proteins and polyamino acids in relation to their structure [1]. According to stereochemical studies, the peptide unit is nearly planar *trans* [2], due to the partial double bond character of the central C—N bond. The biological significance of proteins explains that smaller amides which serve as models for the peptide link in polypeptides became of high importance.

Several papers have been published on the vibrational spectra and force field of formamide [3—9], acetamide [10—16], *N*-methylformamide [14, 17—27], and *N*-methylacetamide [14, 17, 18, 24, 25, 28—38]. The common feature of the calculations is that they use empirical potential functions based on simplified models. Only a few quantum-chemical calculations have been concerned with the force field of these molecules [39—42]. A more advanced theoretical investigation of the complete force field is in progress in our laboratory.

In this study we will be concerned with the in-plane vibrations of formamide (FA), acetamide (AA), *N*-methylformamide (NMFA) and *N*-methylacetamide (NMAA). Besides the parent compounds, the vibrational spectra of *N*-deuterated derivatives and some ^{15}N isotope shifts (FA, AA) are also discussed. Our purpose was the further investigation of the competence of the CNDO/2 method (which is much cheaper than an *ab initio* study) in the nor-

mal coordinate analysis of medium-size molecules such as amides, and a critical analysis of the assignments.

Also, this study was done as a first step towards a similar investigation of larger diamides.

Details of computation

The computational method was the force method [43, 44] in its semi-empirical CNDO/2 version [45]. In this, the first derivatives of the energy with respect to the nuclear coordinates are calculated in an exact analytical way. They are determined for appropriate nuclear configurations, corresponding to the distortion of the vibrational coordinates in negative and positive directions from a reference geometry. The second derivatives (force constants) are then obtained by numerical derivation from the first derivatives. Distortions of ± 1.5 pm and ± 0.02 rad were used for stretching and bending type coordinates, respectively. The vibrational coordinates were chosen as local symmetry coordinates according to the recommendations of ref. [46]. They are listed in Table I (See also Fig. 1).

It was shown in previous studies from this laboratory [45, 47—49] that the CNDO/2 force method yields reliable force constants after appropriate scaling on the experimental frequencies with a few empirical scaling factors. In this procedure, the diagonal $F_{i,i}$ force constants are multiplied by an empirical factor ϱ_i, while $\sqrt{\varrho_i \varrho_j}$ is used for a coupling term $F_{i,j}$. The optimum

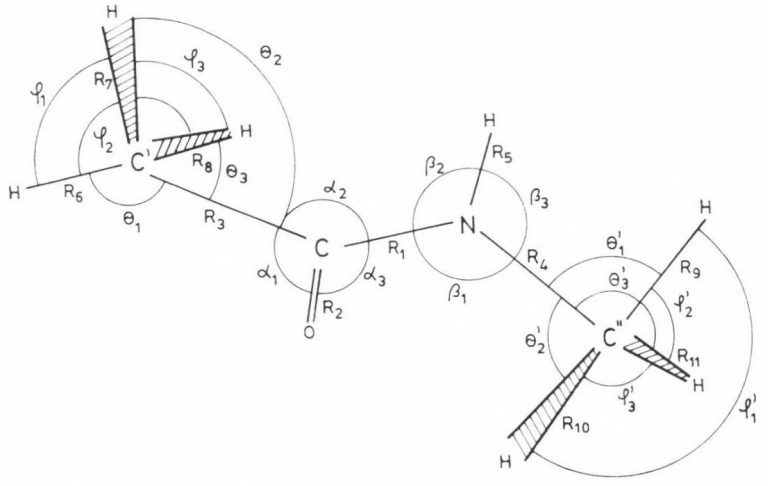

Fig. 1. Internal coordinates used in the most general case of *N*-methylacetamide. A H atom stands for C′ in the case of FA and NMFA, and for C′′ in FA and AA. For the construction of local symmetry coordinates, see Table I

Table I

Symmetry coordinates

		Symbol
S_1	ΔR_3	νCH(FA,NMFA),νCC′(AA,NMAA)
S_2	ΔR_2	νCO
S_3	ΔR_1	νCN
S_4	ΔR_4	νNH_c(FA,AA),νNC′′(NMFA,NMAA)
S_5	ΔR_5	νNH_t
S_6	$\Delta\alpha_3$	δNCO
S_7	$\frac{1}{\sqrt{2}}(\Delta\alpha_2 - \Delta\alpha_1)$	δCH(FA,NMFA),δC′(AA,NMAA)
$S_{8/1}$	$\frac{1}{\sqrt{6}}(2\Delta\beta_3 - \Delta\beta_1 - \Delta\beta_2)$	δNH_2(FA,AA)
$S_{8/2}$	$\Delta\beta_1$	δCNC′′(NMFA,NMAA)
$S_{9/1}$	$\frac{1}{\sqrt{2}}(\Delta\beta_2 - \Delta\beta_1)$	rNH_2(FA,AA)
$S_{9/2}$	$\frac{1}{\sqrt{2}}(\Delta\beta_2 - \Delta\beta_3)$	δNH(NMFA,NMAA)
S_{10}	$\frac{1}{\sqrt{3}}(\Delta R_6 + \Delta R_7 + \Delta R_8)$	$\nu_s C'H_3$(AA,NMAA)
S_{11}	$\frac{1}{\sqrt{6}}(2\Delta R_6 - \Delta R_7 - \Delta R_8)$	$\nu_a C'H_3$(AA,NMAA)
S_{12}	$\frac{1}{\sqrt{6}}(\Delta\theta_1 + \Delta\theta_2 + \Delta\theta_3 - \Delta\varphi_1 - \Delta\varphi_2 - \Delta\varphi_3)$	$\delta_s C'H_3$(AA,NMAA)
S_{13}	$\frac{1}{\sqrt{6}}(2\Delta\theta_1 - \Delta\theta_2 - \Delta\theta_3)$	r$C'H_3$(AA,NMAA)
S_{14}	$\frac{1}{\sqrt{6}}(2\Delta\varphi_3 - \Delta\varphi_2 - \Delta\varphi_1)$	$\delta_a C'H_3$(AA,NMAA)
S_{15}	$\frac{1}{\sqrt{6}}(\Delta R_9 + \Delta R_{10} + \Delta R_{11})$	$\nu_s C''H_3$(NMFA,NMAA)
S_{16}	$\frac{1}{\sqrt{6}}(2\Delta R_9 - \Delta R_{10} - \Delta R_{11})$	$\nu_a C''H_3$(NMFA,NMAA)
S_{17}	$\frac{1}{\sqrt{6}}(\Delta\theta'_1 + \Delta\theta'_2 + \Delta\theta'_3 - \Delta\varphi'_1 - \Delta\varphi'_2 - \Delta\varphi'_3)$	$\delta_s C''H_3$(NMFA,NMAA)
S_{18}	$\frac{1}{\sqrt{6}}(2\Delta\theta'_1 - \Delta\theta'_2 - \Delta\theta'_3)$	r$C''H_3$(NMFA,NMAA)
S_{19}	$\frac{1}{\sqrt{6}}(2\Delta\varphi'_3 - \Delta\varphi'_2 - \Delta\varphi'_1)$	$\delta_a C''H_3$(NMFA,NMAA)

Table II

Scaling factors

Coordinate type	ϱ	Molecule
a) stretching		
1) νCH, νNH	0.3500 (fixed)	FA,AA,NMFA,NMAA
2) νCO	0.2713	FA,AA,NMFA,NMAA
3) νCN	0.3075	FA,AA,NMFA,NMAA
4) νCC′, νNC″	0.3475	AA,NMFA,NMAA
b) bending		
5) δCH	0.8577	FA,NMFA
6) δNH_2	0.8526	FA,AA
7) rNH_2	1.0370	FA,AA
8) $\delta_s CH_3$, $\delta_a CH_3$, rCH_3	0.7218	AA,NMFA,NMAA
9) δNH	0.9614	NMFA,NMAA
10) δC′	1.2101	AA,NMAA
11) δCNC″	1.6825	NMFA,NMAA
12) δNCO	0.9646	FA,AA,NMFA,NMAA

values of the scaling factors are determined by fitting them to the experimental frequencies in a least-squares procedure.

The requirements of the scaling were based on natural physical considerations: using the same scaling factor for physically similar coordinates, thus keeping the number of factors low, and scaling several molecules together. The procedure was as follows. The 45 in-plane force constants of FA were scaled with 7 factors and, as a first approximation, 6 corresponding factors were transferred and kept fixed in AA with 3 new variable factors added: $\varrho\nu$CC′, $\varrho\delta$C′, $\varrho(\delta_s C'H_3$, $rC'H_3$, $\delta_a C'H_3)$. In the second approximation the scaling factors were further refined by scaling the two molecules together. The deuterated compounds were unusable because of the lack of reliable vapour or matrix data. Similar was the case with the ^{15}N isotope shifts. These experimental data served only for retrospective checking of the force fields. Though in order to obtain good "average" "amide" scaling factors it would have been desirable to include in the procedure NMFA and NMAA (and their *N*-deuterated derivatives), this was impossible because of the lack of fully assigned, consistent vapour or matrix spectra. Therefore, in the case of NMFA we transferred and kept fixed the analogous FA—AA scaling factors and only the factors

corresponding to the δCNC'', δNH coordinates were fitted. In the case of NMAA, where only condensed phase data are available, all the scaling factors were transferred from the other molecules and kept fixed for the analogous coordinates. Thus a gradual transfer of the empirical factors was applied. In this way 12 factors were adjusted to fit 149 frequencies (445 force constants). We did not pay attention to frequencies above 2000 cm^{-1}. NH and CH stretching coordinates were scaled with a single, fixed factor from the beginning. The results of this more sophisticated procedure are is accordance with earlier results concerning stretching type coordinates, and contribute to the experience that heavy atom bending coordinates are best fitted by a scaling factor of 1.2 or greater, while bending coordinates involving H atom(s) are fitted by 0.85 or smaller [47—49]. The scaling factors ϱ_i are listed in Table II.

Selection of experimental data

In order to obtain reliable force fields, we used vapour phase or matrix data in the analysis. This is rather important in the case of amides because of the well known effects of hydrogen bonding in condensed phases. In several studies, only parts of the spectrum were investigated in gaseous state, or bands occurring in condensed phase were not detected in the vapour. For this reason, in several cases the experimental data used were taken from different authors. Where this is also connected with uncertainties in the assignments, a separate discussion is given on these frequencies.

The vapour phase data of KING [5] were used in the case of FA, except for one frequency (where KING gives evidently wrong assignments in the 1050—1150 cm^{-1} region and measures only a combination band), which was taken from TANAKA and MACHIDA [8] in solution. For the *N*-deuterated compound the experimental spectrum of the latter authors was taken for comparison [8], except for one frequency, which is from the liquid state Raman study of SMITH and THOMPSON [7]. ^{15}N isotope shift values are those of PARELLADA and ARENAS [9].

Similar selection of data was carried out in the case of the other eight molecular species (See Table IV).

Despite some debate, particularly concerning NMFA [17, 20, 21, 22, 24, 26], it is now generally accepted that the molecular structure of these compounds is predominantly planar and *trans* (NMFA, NMAA) both in the condensed and in the vapour phase. The reference geometry used in this study was an experimental one in the case of FA [50]. For the other three molecules, theoretical *ab initio* geometries [51] with a subsequent adjustment of C–H bond lengths (+1.1 pm) and N—H bond lengths (+0.6 pm) were used.

Acta Chim. Acad. Sci. Hung. 108, 1981

Table III

*Scaled in-plane force constant matrices**

a) Formamide

S_1	S_2	S_3	S_4	S_5	S_6	S_7	S_8	S_9
4.42								
0.25	10.46							
0.19	0.75	6.84						
0.00	−0.01	0.18	6.90					
0.00	0.00	0.17	0.07	6.91				
−0.26	0.27	0.27	−0.02	0.04	1.43			
0.01	−0.17	0.15	0.02	0.00	0.01	0.68		
−0.01	−0.02	−0.19	0.06	0.06	−0.01	−0.02	0.45	
0.03	−0.02	−0.02	0.14	0.12	−0.12	0.03	0.00	0.60

b) Acetamide

S_1	S_2	S_3	S_4	S_5	S_6	S_7	S_8	S_9	S_{10}	S_{11}	S_{12}	S_{13}	S_{14}
4.28													
0.39	10.64												
0.28	0.73	6.58											
0.01	0.00	0.18	6.96										
0.00	0.00	0.16	0.08	7.02									
−0.34	0.21	0.24	−0.04	0.05	1.51								
−0.02	−0.26	0.22	0.04	0.00	0.03	1.03							
−0.02	−0.03	−0.18	0.07	0.07	0.00	−0.04	0.47						
0.02	−0.02	−0.03	0.13	−0.13	−0.12	0.04	0.00	0.61					
0.17	0.00	0.00	0.00	0.00	−0.02	0.00	0.00	0.00	4.79				
0.00	0.00	0.00	0.00	0.00	0.00	0.05	0.00	0.00	0.06	4.65			
0.20	0.03	0.03	0.00	0.00	−0.05	0.01	0.00	0.00	−0.10	0.00	0.56		
0.04	−0.04	0.02	0.01	0.00	−0.01	0.11	−0.01	0.02	0.00	0.13	0.02	0.57	
0.00	0.00	0.01	0.00	0.00	−0.01	0.03	0.00	0.00	0.00	−0.13	0.01	−0.05	0.54

c) *N*-methylformamide

S_1	S_2	S_3	S_4	S_5	S_6	S_7	S_8	S_9	S_{10}	S_{11}	S_{12}	S_{13}	S_{14}
4.47													
0.25	10.45												

0.20	0.78	6.84																
0.00	−0.03	0.22	5.18															
0.00	0.00	0.17	0.11	6.96														
−0.30	0.32	0.31	−0.03	0.05	1.82													
0.00	−0.17	0.16	0.02	0.00	0.00	0.69												
0.06	0.00	0.08	0.13	−0.23	−0.08	0.07	1.19											
0.00	0.04	0.18	−0.15	0.02	0.07	0.01	0.00	0.54										
0.00	0.01	−0.01	0.24	0.00	0.00	0.00	0.03	0.00	4.79									
0.00	−0.01	0.01	−0.02	0.00	0.00	0.00	0.03	0.01	0.03	4.62								
0.00	0.01	−0.01	0.31	0.01	−0.01	0.00	0.03	−0.02	−0.10	0.00	0.63							
0.01	0.00	0.03	−0.02	−0.02	−0.02	0.01	0.05	0.03	0.00	0.13	0.00	0.73						
0.00	0.00	0.01	0.00	0.00	0.00	0.00	0.02	0.00	0.00	−0.14	0.00	−0.06	0.55					

d) N-methylacetamide

S_1	S_2	S_3	S_4	S_5	S_6	S_7	S_8	S_9	S_{10}	S_{11}	S_{12}	S_{13}	S_{14}	S_{15}	S_{16}	S_{17}	S_{18}	S_{19}
4.28																		
0.38	10.46																	
0.29	0.76	6.74																
0.01	−0.02	0.22	5.21															
0.01	0.00	0.17	0.11	6.97														
−0.39	0.26	0.27	−0.04	0.05	1.93													
−0.02	−0.26	0.24	0.04	0.01	0.02	1.05												
0.05	0.01	0.08	0.13	−0.24	−0.10	0.08	1.28											
0.01	0.04	0.19	−0.16	0.02	0.06	0.02	−0.01	0.55										
0.17	0.00	0.01	0.00	0.00	−0.03	0.00	0.00	0.00	4.79									
0.01	0.00	0.00	0.00	0.00	0.00	0.05	0.01	0.00	0.06	4.64								
0.20	0.02	0.03	0.00	0.00	−0.06	0.01	0.00	0.00	0.11	0.00	0.56							
0.04	−0.03	0.02	0.00	0.00	−0.01	0.11	0.03	0.00	0.00	0.13	0.02	0.57						
0.00	0.00	0.01	0.00	0.00	−0.01	0.03	0.00	0.00	0.00	−0.13	0.01	−0.05	0.54					
0.00	0.01	−0.01	0.25	0.00	0.00	0.00	0.03	−0.01	0.00	0.00	0.00	0.00	0.00	4.79				
0.00	−0.01	0.01	−0.02	0.00	0.00	0.00	0.04	0.01	0.00	0.00	0.00	0.00	0.00	0.02	4.61			
0.00	0.01	−0.01	0.31	0.01	−0.01	0.01	0.03	−0.02	0.00	0.00	0.00	0.00	0.00	−0.10	0.00	0.63		
0.01	0.00	0.02	−0.02	−0.02	−0.03	0.01	0.06	0.02	0.00	0.00	0.00	0.00	0.00	0.00	0.13	0.00	0.73	
0.00	0.00	0.01	0.00	0.00	0.00	0.00	0.03	0.00	0.00	0.00	0.00	0.00	0.00	0.00	−0.14	0.00	−0.06	0.56

* Units are 10^{-18} Nm, 10^{-8} N and 10^{2} Nm^{-1} for bending-bending, bending-stretching, and stretching-stretching type force constants, respectively

Results and Discussion

Formamide

The experimental and calculated frequencies of FA, its *N*-deuterated derivative and the ^{15}N isotope shifts are presented in Table IV/a, b, c together with the experimental assignments and the computed T.E.D. values.* As can be seen from Table IV/a, the agreement between observed and calculated frequencies of the parent compound below 2000 cm^{-1} is very good (mean deviation including higher frequencies is 16 cm^{-1}), while for the *N*-deuterated derivative it is reasonable (experimental frequencies measured in solution).

The infrared and Raman spectra of FA (and its deuterated derivatives) was recorded and assigned by EVANS (vapour phase) [3], SUZUKI (also of the deuterated derivatives, liquid state; normal coordinate analysis) [4]. Later KING [5], SMITH and THOMPSON [7] modified the assignments at some points.

Concerning assignments, the most important point is the position of the rNH_2 mode. SUZUKI [4] assigned the 1090 cm^{-1} band (liquid state) to rNH_2. Essentially the same assignment was accepted by TANAKA and MACHIDA [8] (1084 cm^{-1}, chloroform solution), as well as by SMITH and THOMPSON [7] (1095 cm^{-1}, Raman, liquid). EVANS [3] considers 3 bands in this region and assigns the 1160 cm^{-1} band to rNH_2 (interpreting the bands at 1030 and 1060 cm^{-1} as the out-of-plane modes γCH and wNH_2). A strikingly different assignment is given by KING [5]: he assigns the vapour band at 600 cm^{-1} to rNH_2 (with the 1160 cm^{-1} band not observed and γCH put to 1050 cm^{-1}).

Our results evidently confirm the SUZUKI type assignments both for the parent and the *N*-deuterated molecule (See Table IV/a, b).

As to the qualitative description of the fundamental modes, SMITH and THOMPSON [7] interchange the assignments of the liquid state bands at 1390 cm^{-1} and 1315 cm^{-1} (1390 cm^{-1} and 1255 cm^{-1} in the vapour [5]) mainly on Raman intensity arguments. They assign the former to ν_sOCN ($\nu C{=}O + \nu C{-}N$ coupled symmetric stretching) and the latter to δCH, contrary to all previous assignments (*e.g.* [3, 4, 5]). Our results do not support such an interchange. Note also that in the *N*-deuterated species SMITH and THOMPSON [7] use individual δND_{cis} and δND_{trans} motions for the characterization of the modes observed at 1099 and 897 cm^{-1} (Raman bands at 1123 and 922 cm^{-1} in the liquid). We did not find such a decoupling of the *cis* and *trans* δND motions.

In other cases our calculations confirm experimental assignments [3, 4, 5, 7, 8]. However, there are a few points worth mentioning. According to our results, the two frequencies at 1084 cm^{-1} (solution) [8] and 1255 cm^{-1} (vapour) [5] of the parent molecule arise from a strong interaction between the rNH_2 and νCN modes. Contrary to some previous interpretations (*e.g.* [4]),

* For definition, see Table IV

the normal mode corresponding to the 1390 cm^{-1} vapour band of the parent molecule (assigned mainly to δCH) does not show a larger νCN component.

In the normal mode corresponding to the 1755 cm^{-1} vapour band (1690 cm^{-1} in the liquid state [4]) we find only about 14% νCN motion according to the energy distribution. The amplitude ratio is, however, near -1, thus it is possibly reasonable to assign this band as ν_{as}OCN instead of νCO [4, 7]. It seems less justified to assign any band as the corresponding ν_sOCN mode as was done by SMITH and THOMPSON [7]. The coupling of νCN and νCO is in accordance with a large positive interaction force constant (0.75×10^2 Nm^{-1}). There is also considerable mixing of the νCO and δCH vibrational modes in the normal modes observed at 1390 cm^{-1} (generally assigned as δCH) and that at 1755 cm^{-1}. However, the relative weights are rather sensitive to small changes in the force field (See Table IV/a, b; Table III/a).

As can be seen in Table IV/c, the ^{15}N isotope shifts [9] are correctly reproduced by the calculation.

The in-plane force constant matrix of FA is presented in Table III/a.

Acetamide

The experimental assignments and computed energy distributions are given in Table IV/d, e, f. The in-plane *F*-matrix is shown in Table III/b. The vapour, solution, liquid state, and matrix spectra of AA were studied and assigned by KUTZELNIGG and MECKE [10], KING [13], SUZUKI (also the deuterated derivatives) [11], UNO *et al.* [12]; calculations of the spectra were done by SUZUKI [11], GARRIGOU—LAGRANGE [15] and WARSHEL et *al.* [14]. As can be seen in Table III/d, our calculated spectrum of the parent molecule is in good agreement again with the experimental values, particularly below 2000 cm^{-1} (mean deviation 17 cm^{-1}) and thus seems to permit critical judgement of experimental assignments at some dubious points.

In the vapour spectrum KUTZELNIGG and MECKE observed a band at 1385 cm^{-1} and assigned it to $\delta_a CH_3$ [10]. The corresponding band (at 1370 cm^{-1}) in Ar matrix was assigned to $\delta_s CH_3$ by KING [13]. Our results support KING's assignment. On the other hand, the band in matrix at 1432 cm^{-1} (assigned to $\delta_a CH_3$ [13]) was not observed in the vapour by the early authors [10]. Our calculations support the assigment of $\delta_a CH_3$ to a band of the isolated molecule at this frequency. The 1160 cm^{-1} band, assigned to rNH_2 of the self-associated molecules in solid film was not found by KING in the matrix [13] and he assigns rNH_2 of the isolated molecular species to a band at 790 cm^{-1}. Our results, as in the case of FA, exclude the possibility of rNH_2 occurring at such a low frequency and the assignment of Kutzelnigg and Mecke to the 1134 cm^{-1} frequency (vapour) [10] is confirmed.

The vapour band at 500 cm^{-1} (assigned to an asymmetric skeletal bending in ref. 10.) is assigned to an out-of-plane vibration γNH_2 at 508 cm^{-1} in the matrix by KING [13]. The 430 cm^{-1} (in solution) band of KUTZELNIGG and MECKE (assigned to γNH_2) [10] is found at 427 cm^{-1} in the matrix by KING and is assigned to δCCN [13]. Finally, KING assigns the wagging mode of NH_2 to a band at 268 cm^{-1} [13]. Since the lowest frequency in-plane band assigned mainly to δCCN is expected in the 500—400 cm^{-1} region [11, 12], only a study including also the out-of-plane modes could definitely decide between the assignments. The CNDO/2 method is inappropriate for this purpose. A preliminary *ab initio* study suggests [53] that either the 427 cm^{-1} (430 cm^{-1}) band is the lowest frequency in-plane band, or this lies at a somewhat lower wavenumber and the band around 430 cm^{-1} of the isolated molecule corresponds to an out-of-plane mode. During the scaling procedure we accepted KING's assignment.

The general structure of the normal modes is similar to those obtained by other authors for the parent molecule and for the *N*-deuterated derivatives [11, 12, 14, 15] [See Table IV/d, e, f).

It is noteworthy that the calculations yield an almost pure νCO vibrational mode for the 1728 cm^{-1} frequency ("amide I" band) of the parent molecule and for the corresponding bands of the *N*-deuterated derivatives; the νCN contribution is negligible and even the amplitude ratios are greatly decreased (~ -0.5) as compared with FA. We refer for further details to Table IV/d, e, f. Large differences occur in the region above 2000 cm^{-1} between the experimental and calculated frequencies of the *N*-deuterated molecules, and the agreement is generally less satisfactory than for the parent compound. However, the difference, for example, between the observed and calculated νNH, νND frequencies corresponds to what is expected for the isolated and associated compounds. Furthermore, we believe the experimental values of ref. [12] to be too high, as the lowest frequency in-plane (skeletal) modes are localized to rather high wavenumbers even for the parent compound, whereas these are known to be relatively stable for a change of phase. The ^{15}N isotope shifts [16] are well reproduced as can be seen in Table IV/g.

N-methylformamide

The experimental and calculated frequencies, experimental assignments and computed T.E.D. values are listed in Table IV/h, i, while the in-plane force constant matrix is given in Table III/d.

The vapour, solution, and liquid state infrared and Raman spectra of NMFA and its *N*-deuterated derivative were measured and assigned by MIYAZAWA *et al.* (in the vapour, in a limited region, 1800—800 cm^{-1}) [18],

DE GRAAF and SUTHERLAND (liquid state) [19], JONES [20], HALLAM and JONES (vapour spectra at room temperature with a 40 m pathlength cell) [26], SUZUKI (also the *C*-deuterated derivatives, liquid state) [23], ITOH and SHIMANOUCHI (far infrared region, liquid state) [25]. Calculations of the spectra were made by SUZUKI [23], WARSHEL *et al.* [14], DALCHIS *et al.* [27] and others. The main problem concerning NMFA since the early studies was the interpretation of vibrational spectra in terms of the *cis-trans* isomerism around the central C—N bond, particularly in the vapour state [17, 20, 21, 22, 24, 26]. We have made no calculations on the *cis* isomer because CNDO/2 does not seem to be reliable enough for this purpose. (The confusion of experimental results prohibits any scaling or checking.) However, there are some questions of importance in the experimental assignments of the spectra even in the case of the *trans* isomer.

For the lowest frequency in-plane band (δCNC) the following experimental values were found: 297 cm^{-1} (in liquid) in ref. [23]; 302 cm^{-1} (Raman, liquid) in ref. [19]. (The latter authors also reported a Raman band at 242 cm^{-1} and assigned it to τCH_3; this was not definitely confirmed by ref. [25].) A preliminary *ab initio* study yielded 260 cm^{-1} [53]. For the δNCO mode: 624 cm^{-1} (in liquid) in ref. [19] and ref. [20] (in solution); 771 cm^{-1} (in liquid, 762 cm^{-1} for the *N*-deuterated derivative) in ref. [23]; 772 cm^{-1} (in vapour) in ref. [26]. This latter high value is explained by the interaction of the δCNC, δNCO modes splitting far apart the two frequencies (ref. [23]). (The δNCO mode is around 550 cm^{-1} in FA and AA). At the same time, the 785 cm^{-1} (in vapour) band was assigned to γCH in ref. [20].

To investigate the above problem, the two added variable factors ($\varrho\delta$CNC, $\varrho\delta$NH) were optimized first in such a way that these two questionable frequencies were omitted. The results showed that the mode corresponding mainly to the δNCO vibration lies above 700 cm^{-1}. Then the corresponding value taken from the vapour spectrum [26] was included in accordance with the assignment of SUZUKI [23] and HALLAM and JONES [26]. The results indicated that the lowest-lying in-plane frequency should be in range of 250 cm^{-1} to 300 cm^{-1}. Thus the 297 cm^{-1} value was accepted and the scaling factor for the δCNC'' coordinate was obtained. The anomalously large value (1.6825) corresponds to a much too low diagonal force constant which is presumably a deficiency of the CNDO/2 parametrization in describing the heavy atom in-plane bending motions around the nitrogen atom. As a whole, however, our results are in accordance with SUZUKI's early assignment concerning the band around 770 cm^{-1}, and exclude the possibility of assigning this mode as low as 624 cm^{-1}. The assignment of the band around 300 cm^{-1} is also confirmed (See Table IV/h). It should be noted that our calculations, containing only the in-plane modes, do not exclude the possibility of assigning δNCO to the 715 cm^{-1} vapour band [20] (720 cm^{-1} in the liquid state [23]), which

is assigned as 2γCO [20] or γCH + γNH [23]. Similarly, the origin of the 242 cm^{-1} Raman band in liquid is not yet clear.

The structure of the modes corresponding to the "amide I,I'" bands (see Table IV/h, i) is similar to the case of FA. In one case (1450, 1411 cm^{-1} experimental frequencies) the calculated characterization is evidently reversed; these are calculated as only 14 cm^{-1} apart and are very mixed vibrations.

At some points our results do not agree with the SUZUKI-type characterizations. For details see Table IV/h, i and ref. [23]. We find justifiable to call the mode corresponding to the "amide II" band a ν_aCNC'' vibration; the ν_sCNC'' vibration lies at 948 cm^{-1} (see Table IV/h). The analysis of the amplitudes shows also the importance of interaction of the νNC'', rC'' H_3 vibrations. In the normal mode at 981 cm^{-1} ("amide III'" band) the decoupling of the δND and νCN vibrations is smaller than is generally assumed for the *N*-deuterated derivative [18, 23]. These results are also confirmed by ref. [53]. For further details see Table IV/h, i.

N-methylacetamide

The experimental and calculated frequencies, experimental assignments and theoretical T.E.D. values are shown in Table IV/j, k, whereas the in-plane force constant matrix is given in Table III/d.

Infrared and Raman spectra of NMAA and its *N*-deuterated derivative were first measured and assigned by MIYAZAWA *et al.* in the liquid state [18]; similar studies were made by JONES [24], and by BRADBURRY and ELLIOT (solid state) [28]. The first systematic study in the liquid and solid state was carried out by SCHNEIDER *et al.* giving detailed assignment of the spectra of the parent molecule and many deuterated derivatives [30]. ITOH and SHIMANOUCHI investigated the far infrared spectra in the liquid state [25]. Further studies were made by HARADA *et al.* (solution) [37], FILLAUX and DE LOZÉ (argon and nitrogen matrix) [35]. Calculations of the spectra were made by MIYAZAWA *et al.* [28], JAKES and SCHNEIDER [31], WARSHEL *et al.* [14], JAKES and KRIM [32], REY—LAFON *et al.* [34], POPOV *et al.* [33], SHIMANOUCHI *et al.* [36].

In the case of NMAA we worked with fixed scaling factors obtained for the corresponding symmetry coordinates in FA, AA and NMFA, thus the spectra of NMAA and the deuterated species serve as a first real test for the transferability of these scaling factors.

Below 2000 cm^{-1} the agreement with the experimental values, despite condensed phase effects, is satisfactory, the mean deviation being below 30 cm^{-1}. The largest deviation occurs for νCO at 1660 (1647) cm^{-1} where the calculated values are 1723 (1717) cm^{-1} respectively; the calculated values,

however, agree with a vapour phase value of about 1730 cm^{-1} for the parent molecule [26].

Concerning the characterization of the normal modes, our results are generally in agreement with the experimental work of SCHNEIDER *et al.* [30], which formed the basis of the analysis.

The "amide I and I'" bands turn out to be quite pure νCO, vibrations again like in the case of AA.

In the normal modes of the parent molecule, the structure of the vibrations corresponding to the "amide II, III, IV" bands is in agreement with what is generally supposed about these modes (*e.g.* [18, 28, 37]): chiefly δNH + νCN in amide II and III, δNCO in amide IV. It is also confirmed that the skeletal stretching modes νNC'', νCC' interact with the *N*-methyl (*C*-methyl) in-plane rocking modes (see Table IV/j, k). However, no strong coupling of νCN and νNC'' is shown, contrary to the case of NMFA. Our results also confirm early suggestions [28] that the significant lowering in frequency of the "amide IV" band (628 cm^{-1}) as compared with NMFA (772 cm^{-1}) is due to an interaction of δNCO with the νCC' mode. The energy distribution also supports the assignment of SCHNEIDER *et al.* against those of JONES at several points (see Table IV/j, and ref. [30, 24]). The usual "amide III'" assignment (decoupled

Table IV

Experimental and calculated frequencies and assignments[1]

Frequencies (cm^{-1})			Assignment	
a) $HCONH_2$				
Exp. [5]	Calcd.		Exp. [5]	T.E.D.
	Description after ref. [18]			
565	566	Amide IV	δNCO	85 δNCO + 10 rNH_2
1084*	1074		rNH_2^+	45 rNH_2 + 38 νCN + 13 νCO
1255	1254	Amide III	νCN	43 νCN + 39 rNH_2 + 13 δNCO
1390	1389		δCH	67 δCH + 28 νCO
1580	1577	Amide II	δNH_2	91 δNH_2
1755	1751	Amide I	νCO	51 νCO + 27 δCH + 14 νCN
2855	2824		νCH	100 νCH
3448	3481		$\nu_s NH_2$	52 νNH_c + 48 νNH_t(100 $\nu_s NH_2$)
3570	3564		$\nu_a NH_2$	48 νNH_c + 52 νNH_t(100 $\nu_a NH_2$)

* From ref. [8]

Table IV (contd.)

b) $HCOND_2$

Exp. [5]	Calcd.	Exp. [8]**	T.E.D.
531*	507	δNCO	72 δNCO + 24 rND_2
897	901	rND_2	58 rND_2 + 17 νCN
1099	1086	δND_2	58 δND_2 + 19 νCN + 12 δNCO + 11 γND_2
1316	1273	νCN	45 νCN + 35 δND_2 + 11 δCH
1391	1396	δCH	61 δCH + 34 νCO
1708	1739	νCO	55 νCO + 27 δCH + 14 νCN
2481	2514	$\nu_s ND_2$	51 νND_c + 48 νND_t(99 $\nu_s ND_2$)
2650	2650	$\nu_a ND_2$	51 νND_t + 49 νND_c(100 $\nu_a ND_2$)
2874	2825	νCH	100 νCH

* From ref. [7]
** In fact based on a normal coordinate analysis

c) $HCO^{15}NH_2$ isotope shifts

Exp. frequency of the parent molecule [5] (cm^{-1})	Exp. [9]	Calcd.
($\Delta\nu = \nu HCO^{15}NH_2 - \nu CHO^{14}NH_2$)		
565	−3	− 3.42
1084	—	−10.79
1255	−7	−10.44
1390	0	− 0.15
1580	−6.7	− 5.57
1755	−3	− 3.13
2855	—	0.00
3448	−5	− 3.71
3570	−10	−11.31

δND) is, however, interchanged with the next higher frequency rCH_3 (*C*-methyl) assignment at 965 and 1000 cm^{-1} as compared with the experimental assignment. (Neighbouring frequencies with only 14 cm^{-1} calculated difference.) The large coupling of the νNC'' mode with the δND vibration at 1000 cm^{-1} (though the assignment is interchanged) and the fact that δND has a large amplitude in the normal mode corresponding to the 1123 cm^{-1} frequency mainly due to νNC'', (though its contribution to total energy is negligible) shows similarities with the case of NMFA, where this interaction is also present.

Table IV (contd.)

d) CH_3CONH_2

Exp. [13]	Calcd.	Description after ref. [18]	Exp. [13]	T.E.D.
427	421		δCCN	68 δC′ + 18 δNCO
547	539	Amide IV	δCO	65 δNCO + 17 δC′
840	837		νCC	64 νCC′ + 18 νCN
970	955		rCH_3	77 r$C'H_3$ + 14 νCN
1134*	1132		rNH_2^+	64 rNH_2 + 17 νCO
1316	1329	Amide III	νCN	33 $\delta_s C'H_3$ + 30 νCN + 13 rNH_2
1370	1402		$\delta_s CH_3$	48 $\delta_s C'H_3$ + 15 $\delta_a C'H_3$ + 13 νCC′ + 13 νCN
1432	1434		$\delta_a CH_3$	82 $\delta_a C'H_3$ + 14 $\delta_s C'H_3$
1586	1612	Amide II	δNH_2	92 δNH_2
1728	1736	Amide I	νCO	69 νCO
2860*	2869		$\nu_s C'H_3$	94 $\nu_s C'H_3$
2930*	2941		$\nu_a C'H_3$	94 $\nu_a C'H_3$
3436	3505		$\nu_s NH_2$	61 νNH_c + 39 νNH_t(100 $\nu_s NH_2$)
3557	3581		$\nu_a NH_2$	61 νNH_t + 39 νNH_c(100 $\nu_a NH_2$)

* From ref. [10]

e) CH_3CONHD_t

Exp. [12]	Calcd.	Exp. [12]	T.E.D.
455	400	δCCN	62 δC′ + 21 δNCO
568	534	δNCO	60 δNCO + 22 δC′
871	834	νCC	66 νCC′ + 14 νCN
933	900	δND_t	33 rNHD_t + 32 r$C'H_3$ + 21 νCN
1045	1007	rCH_3	50 r$C'H_3$ + 25 rNHD_t
1359	1328	$\delta_s CH_3$	34 $_sC'H_3$ + 32 νCN
1398	1402	νCN	48 $\delta_s C'H_3$ + 15 $\delta_a C'H_3$ + 13 νCC′ + 12 νCN
1453	1433	$\delta_a CH_3$	82 $\delta_a C'H_3$ + 13 $\delta_s C'H_3$
1475	1451	δNH_c	77 δNHD_t
1652	1734	νCO	70 νCO
2417	2602	νND_t	99 νND_t
2926	2869	$\nu_s CH_3$	94 $\nu_s C'H_3$
3000	2941	$\nu_a CH_3$	94 $\nu_a C'H_3$
3270	3536	νNH_c	100 νNH_c

Table IV (contd.)

f) CH_3COND_2

Exp. [12]	Calcd.	Exp. [12]	T.E.D.
442	389	δCCN	55 δC′ + 26 δNCO
548	519	δNCO	51 δNCO + 29 δC′
817	796	νCC	62 νCC′ + 20 rND_2 + 11 νCN
933	898	rND_2	33 rND_2 + 27 rC′H_3 + 25 νCN
1036	991	rCH_3	53 rC′H_3 + 22 rND_2 + 12 νCO
1185	1163	δND_2	75 δND_2
1359	1345	$\delta_s CH_3$	47 δ_sC′H_3 + 27 νCN + 12 δND_2
1411	1407	νCN	37 δ_sC′H_3 + 19 νCN + 18 δ_aC′H_3 + 15 νCC′
1453	1434	$\delta_a CH_3$	79 δ_aC′H_3 + 16 δ_sC′H_3
1644	1724	νCO	74 νCO
2316	2534	$\nu_s ND_2$	56 νND_c + 44 νND_t(100 $\nu_s ND_2$)
2530	2660	$\nu_a ND_2$	56 νND_t + 44 νND_c(100 $\nu_a ND_2$)
2926	2869	$\nu_s CH_3$	94 ν_sC′H_3
3000	2941	$\nu_a CH_3$	94 ν_aC′H

g) $CH_3CO^{15}NH_2$ isotope shifts

Frequency of the parent molecule [13] (cm^{-1})	Exp. [16]	Calcd.
($\Delta\nu = \nu CH_3CO^{15}NH_2 - \nu CH_3CO^{14}NH_2$)		
427	−4.0	−3.31
547	−2.4	−2.75
840	−5.1	−5.44
970	−2.8	−3.15
1134	−6.2	−7.16
1316	0.0	−4.44
1370	−4.8	−2.43
1432	0.0	−0.1
1586	−4.0	−6.33
1728	−4.0	−2.34
2860	0.0	0.0
2930	0.0	0.0
3436	−7.6	−4.02
3557	−13.5	−11.06

Table IV (contd.)

h) $HCONHCH_3$

Exp. [20]	Calcd.		Exp. [20]	T.E.D.
	Description after ref. [18]			
297*	275		δCNC*	64 δCNC'' + 32 δNCO
772**	722	Amide IV	δNCO**	55 δNCO + 24 δCNC''
948**	947		νNC**	53 νNC'' + 26 νCN + 14 r$C''H_3$
1149***	1138		rCH_3	68 r$C''H_3$
1200	1208	Amide III	νCN + δNH	35 νCN + 25 νNC'' + 22 δNH
1387***	1396		δCH	66 δCH + 28 νCO
1411	1443		$\delta_s CH_3$	76 $\delta_a C''H_3$ + 16 $\delta_s C''H_3$
1450****	1457		$\delta_a CH_3$****	68 $\delta_s C''H_3$ + 21 $\delta_a C''H_3$
1498	1520	Amide II	δNH + νCN	62 δNH + 12 νCN + 11 $\delta_s C''H_3$
1724	1746	Amide I	νCO	54 νCO + 28 δCH + 14 νCN
2732	2841		$\nu_s CH_3$	100 νCH
2934	2872		$\nu_a CH_3$	99 $\nu_s C''H_3$
3052	2929		νCH	99 $\nu_a C''H_3$
3480	3535		νNH	100 νNH

* From ref. [23]
** From ref. [26]
*** Solution
**** From ref. [19]

i) $HCONDCH_3$

Exp. [23]	Calcd.		Exp. [23]	T.E.D.
	Description after ref. [18]			
297	273		δCNC + δOCN	64 δCNC'' + 32 δNCO
762	716	Amide IV′	δOCN	55 δNCO + 24 δCNC''
943	930		νNC + δND	55 νNC'' + 23 δND + 13 rCH_3
981	963	Amide III′	δND	52 δND + 35 νCN
1155	1142		rCH_3	70 r$C''H_3$ + 11 νNC''
1383	1368		δCH	36 νCN + 20 δND + 16 νNC''
1405	1400		$\delta_s CH_3$	59 δCH + 35 νCO
1436	1446	Amide II′	νCN + $\delta_a CH_3$	95 $\delta_a C''H_3$
1467*	1470		$\delta_a CH_3$*	85 $\delta_s C''H_3$
1662	1742	Amide I′	νCO	54 νCO + 29 δCH + 14 νCN
2474*	2587		νND*	99 νND
2743*	2842		$\nu_s CH_3$*	100 νCH
2879*	2872		νCH*	99 $\nu_s C''H_3$
2943*	2929		$\nu_a CH_3$*	99 $\nu_a C''H_3$

* From ref. [19]
** In fact based on a normal coordinate analysis

Table IV (contd.)

j) $CH_3CONHCH_3$

Exp. [30]	Calcd.		Exp. [30]	T.E.D.
	Description after ref. [18]			
279*	254		δCNC	53 δCNC'' + 32 δNCO + 12 δC'
431*	434		δCCN	67 δC'
628	608	Amide IV	Amide IV	44 δNCO + 27 νCC' + 15 δCNC''
883	856		νCC	24 νCN + 24 νCC' + 17 rC''H_3 + 10 νCO
991	942		rCH_3(C)	63 rC'H_3 + 13 νCC'
1114	1072		νNC	45 νNC'' + 17 rC''H_3 + 14 rC'H_3
1161	1157		rCH_3(N)	55 rC''H_3 + 18 νNC''
1265*	1277	Amide III	Amide III*	29 νCN + 27 δNH + 11 δ_sC'H_3 + 10 νCC
1374	1389		$\delta_s CH_3$(C)	73 δ_sC'H_3 + 13 δ_aC'H_3
1414	1434		$\delta_s CH_3$(N)	86 δ_aC'H_3 + 11 δ_sC'H_3
1458	1446		$\delta_a CH_3$(C)	81 δ_aC''H_3 + 14 δ_sC''H_3
1471	1462		$\delta_a CH_3$(N)	77 δ_sC''H_3 + 16 δ_aC''H_3
1511*	1542	Amide II	Amide II*	56 δNH + 22 νCN
1660	1723	Amide I	Amide I	71 νCO
2935	2868		$\nu_s CH_3$	94 ν_sC'H_3
2935	2872		$\nu_s CH_3$	99 ν_sC''H_3
2994	2926		$\nu_a CH_3$	99 ν_aC''H_3
2994	2940		$\nu_a CH_3$	95 ν_aC'H_3
3495*	3539		νNH	100 νNH

* From ref. [35]

Conclusion

The calculations show that the force method within the CNDO/2 framework correctly reproduces the vibrational spectra of medium-size organic molecules like amides and helps the assignment of the spectra if the force field is appropriately scaled. The scaling procedure is physically consistent: a single scaling factor is used for a set of similar vibrational coordinates.

We believe that the calculated diagonal force constants are precise within 10% and a similar order of precision is expected for the larger coupling terms (corresponding to at most 5% error in the frequencies in general). The precision is presumably decreased in parallel to the absolute values.

The scaling factors are transferable, which is indicated by the fact that in the case of NMAA and its deuterated derivative fixed, transferred factors were used and the numerical agreement with experimental frequencies is

Table IV (contd.)

k) $CH_3CONDCH_3$

Exp. [30]	Calcd.		Exp. [30]	T.E.D.
	Description after ref. [18]			
277*	253		δCNC	53 δCNC'' + 32 δNCO + 12 δC'
429*	431		δCCN	66 δC' + 11 δCNC''
628	605	Amide IV'	Amide IV'	45 δNCO + 26 νCC' + 15 δCNC''
872	849		νCC	25 νCN + 24 νCC' + 15 rC''H_3
965	939	Amide III'	Amide III'	61 rC'H_3 + 14 δND
1000	953		rCH_3(C)	47 δND + 31 νNC''
1123	1126		νNC	34 νNC'' + 16 rC'H_3 + 13 νCC'
1185	1154		rCH_3(N)	68 rC''H_3
1372	1370		$\delta_s CH_3$(C)	74 δ_sC'H_3
1406	1428		$\delta_s CH_3$(N)	71 δ_aC'H_3
1446	1441		$\delta_a CH_3$(C)	22 δ_sC''H_3 + 20 δ_aC'H_3 + 16 δ_sC'H_3 + + 14 νCN + 12 δ_aC''H_3
1471	1450		$\delta_a CH_3$(N)	83 δ_aC''H_3
1485	1475	Amide II'	Amide II'	65 δ_sC''H_3 + 11 νNC'' + 10 νCN
1647	1717	Amide I'	Amide I'	73 νCO
—	2598		—	99 νND
2938	2868		$\nu_s CH_3$	94 ν_sC'H_3
2938	2872		$\nu_s CH_3$	99 ν_sC''H_3
2994	2926		$\nu_a CH_3$	99 ν_aC'H_3
2994	2940		$\nu_a CH_3$	94 ν_aC'H_3

* From ref. [35]

[1] The T.E.D. criterion [52] was used throughout this study: Total energy contribution of the jth internal coordinate in the ith normal mode is calculated as

$$M_{ij} = L_{ij}^{-1} \; L_{ji},$$

where L is the matrix of vibrational eigenvectors

The calculated values have been multiplied by 100 and only those above 10 are listed in Table IV.

satisfactory; the mean deviation is below 30 cm^{-1}. For this reason, the force method in this CNDO/2 version can be expected to be adequate for theoretical calculation of the spectra of larger molecules where at present no reliable experimental data are available and in which cases the *ab initio* approach is too expensive .On the basis of the present results we hope to calculate the force fields of diamides which can be regarded as segments of the polypeptide chain such as *N*-acetyl-*N*'-methylalanilamide.

*

The author wishes to express his thanks to Dr. Géza Fogarasi for many help ful dis cussions and for making available the preliminary results of his *ab initio* study.

REFERENCES

[1] Sutherland, G. B. B. M.: in Adv. Prot. Chem. **VII.** Acad. Press, New York 1952; Miyazawa, T. M.: in Fashman, G. D. (ed.) Poly-α-Amino Acids, p. 69. Dekker, New York, 1967; Lord, R. C.: Proc. Int. Congr. Pure Appl. Chem. Suppl. 23, **7,** 179 (1971), Yu, N. T., Liu, C. S.: J. Amer. Chem. Soc., **94,** 7572 (1972); Koenig, J. L., Sutton; P. L.: Biopolymers, **8** 167 (1969); **9,** 2229 (1970); **10,** 89 (1971)
[2] Fasman, G. D. (ed.): Poly-α-Amino Acids. Dekker, New York 1967; Timasheff, S. N., Fasman, G. D. (eds): Structure and Stability of Biological Macromolecules, Dekker, New York 1969
[5] Evans, J. C.: J. Chem. Phys., **22,** 1228 (1954); **31,** 1453 (1959)
[4] Suzuki, I.: Bull. Chem. Soc. Japan, **33,** 1359 (1960)
[5] King, S. T.: J. Phys. Chem., **75,** 405 (1971)
[6] Shimanouchi, T. *et al.*: J. Mol. Spectry, **42,** 86 (1972)
[7] Smith, C. H., Thompson, R. H.: J. Mol. Spectry., **42,** 227 (1972)
[8] Tanaka, Y., Machida, K.: J. Mol. Spectry., **63,** 306 (1976)
[9] Parellada, R., Arenas, J.: An. R. Soc. Esp. Fis. Quim. ser. B, **66,** 653 (1970)
[10] Kutzelnigg, W., Mecke, R.: Spectrochim. Acta, **18,** 549 (1962)
[11] Suzuki, I.: Bull. Chem. Soc. Japan, **35,** 1279 (1962)
[12] Uno, T., Machida, K., Saito, Y.: Bull. Chem. Soc. Japan, **42,** 897 (1969)
[13] King, S. T.: Spectrochim. Acta, **28 (1) A,** 165 (1972)
[14] Warshel, A., Levitt, M., Lifson, S.: J. Mol. Spectry., **33,** 84 (1970)
[15] Garrigou-Lagrange, C.: J. Chim. Phys., **71,** 149 (1974)
[16] Parellada, R., Arenas, J.: An. R. Soc. Esp. Fis. Quim. Ser. B, **66,** 283 (1970)
[17] Russel, R. A., Thompson, H. W.: Spectrochim. Acta, **8,** 138 (1958)
[18] Miyazawa, T., Shimanouchi, T., Mizushima, S. I.: J. Chem. Phys., **24,** 408 (1956)
[19] De Graaf, D. E., Sutherland, G. B. B. M.: J. Chem. Phys., **26,** 716 (1957)
[20] Jones, R. L.: J. Mol. Spectry., **2,** 581 (1958)
[21] Jones, R. L.: J. Mol. Spectry., **7,** 460 (1961)
[22] Miyazawa, T.: J. Mol. Spectry., **4,** 155 (1960)
[23] Suzuki, I.: Bull. Chem. Soc. Japan, **35,** 540 (1962)
[24] Jones, R. L.: Mol. Spectry., **11,** 411 (1963)
[25] Itoh, K., Shimanouchi, T.: Biopolymers, **5,** 921 (1967)
[26] Hallam, H. E., Jones, C. M.: Trans. Farad. Soc., **65,** 260 (1969)
[27] Dalchis, M. I., Dashevskii, N. G., Kitaigorodskii, A. I.: Biopolymers, **12(S)** 1763 (1973)
[28] Miyazawa, T., Shimanouchi, T., Mizushima, S. I.: J. Chem. Phys., **29,** 611 (1958)
[29] Bradbury, E., Elliot, M.: Spectrochim. Acta, **19,** 995 (1963)
[30] Schneider, B., Horeni, A., Pivcova, H., Honzl, J.: Coll. Czech. Chem. Commun., **30,** 2196 (1965); Pivcova, H., Schneider, B., Stokr, J.: Coll. Czech. Chem., Commun, **30,** 2215 (1965)
[31] Jakes, J., Schneider, B.: Coll. Czech. Chem. Commun, **33,** 643 (1968)
[32] Jakes, J., Krim, S.: Spectrochim. Acta, **27/A,** 19 (1971)
[33] Popov, E. M., Zhetova, V. N., Kogan, G. A.: Zh. Strukt. Khim., **11,** 1053 (1970)
[34] Rey-Lafon, M., Forel, M. T., Garrigou-Lagrange, C.: Spectrochim. Acta, **29 A,** 471 (1973)
[35] Fillaux, F., de Lozé, C.: Chem. Phys. Lett., **39,** 547 (1976)
[36] Shimanouchi, T., Koyama, Y., Itch, K.: Progr. Polym. Sci, Japan, **7,** 276 (1974)
[37] Harada, I., Sugawara, Y., Matsura, H., Shimanouchi, T.: J. Raman Spectroscopy **4,** 91 (1975)
[38] Fillaux, F., de Lozé, C.: J. Chim. Phys.—Phys. Chim. Biol., **73,** 1004, 1010 (1976)
[39] Ottersen, T., Jensen, H. H.: J. Mol. Struct., **26,** 355 (1975)
[40] Janoschek, R.: Theoret. Chim. Acta, **32,** 49 (1973)
[41] Ottersen, T.: Acta Chem. Scand., **A29,** 939 (1975)
[42] Sarathy, K. P.: Indian J. Biochem. Biophys., **12,** 172 (1975)
[43] Pulay, P.: Mol. Phys., **17,** 197 (1969)

[44] PULAY, P.: in SCHÄFER, H. F. (ed.): Modern Theoretical Chemistry, vol. **IV.** Plenum, New York 1977
[45] PULAY, P., TÖRÖK, F.: Mol. Phys., **25,** 1153 (1973)
[46] PULAY, P., FOGARASI, G., PANG, F., BOGGS, J. E.: J. Amer. Chem. Soc., **101,** 2550 (1979)
[47] TÖRÖK, F., HEGEDÜS, Á., KÓSA, K., PULAY, P.: J. Mol. Struct., **32,** 93 (1976)
[48] PANCHENKO, YU. N., PULAY, P., TÖRÖK, F.: J. Mol. Struct. **34,** 283 (1976)
[49] FOGARASI, G., PULAY, P.: J. Mol. Struct., **39,** 275 (1977)
[50] HIROTA, S.: J. Mol. Spectry., **49,** 251 (1974)
[51] FOGARASI, G., PULAY, P., TÖRÖK, F., BOGGS, J. E.: J. Mol. Struct., **57,** 259 (1979)
[52] PULAY, P., TÖRÖK, F.: Acta Chim. Acad. Sci. Hung., **47,** 273 (1966)
[53] FOGARASI, G.: to be published

András BALÁZS H-1088 Budapest, Múzeum krt. 6—8.

Acta Chimica Academiae Scientiarum Hungaricae, Tomus 108 (3), pp. 287—303 (1981)

MECHANICAL-RHEOLOGICAL STUDIES ON POLYMER NETWORKS, III

EFFECT OF THE POLYMER—ANALOGOUS TRANSFORMATION ON THE MOLECULAR PARAMETERS

F. HORKAY,[1] M. NAGY[2] and M. ZRINYI[2]

([1] *National Institute of Occupational Health, Budapest,*
[2] *Department of Colloid Science, Eötvös Loránd University, Budapest*)

Received May 20, 1980

Accepted for publication January 6, 1981

Investigations were carried out for the determination of the mechanical properties of poly(vinyl acetate) (PVAc) gels, prepared from chemically cross-linked polyvinyl alcohol (PVA) gels by topo-analogous transformation in the gel phase at unchanged steric structure.

It has been found, in conformity with theory, that for PVAc gels the product $K_1 \nu_{el}^* q_0^{-2/3}$ is independent of the swelling ratio and that presumably permanent entanglements do not contribute considerably in these systems to the change in HELMHOLTZ energy in conjunction with deformation.

Approximating the chain size in the reference state with relationships valid for dilute polymer solutions, a value was obtained for the ratio of the $K_1 \nu_{el}^* q_0^{-2/3}$ products pertinent to PVAc — acetone and PVA — water systems, which agreed well with experimental results.

Using a scaling law, it has been shown that the concentration dependence of the correlation length and of the modulus is primarily determined by the structure of the gel.

Introduction

In the first two parts of this series results of mechanical investigations on chemically cross-linked polyvinyl alcohol (PVA) hydrogels have been reported.

It has been established that the behaviour of these systems considerably differs from that of the ideal models, serving as basis for the statistical thermodynamical calculations. It has been found among others, that the value of the product $K_1 \nu_{el}^* q_0^{-2/3}$ which, according to the theory, is independent of the swelling ratio, substantially increases with increasing volume fraction of the polymer. On substituting for the single factors of the product $K_1 \nu_{el}^* q_0^{-2/3}$ theoretical data generally accepted today, unrealistic values are obtained.

One part of the anomalies reflected by the experimental results has been qualitatively interpreted by the change in structure of the PVA gels with decreasing the swelling degree. X–ray diffraction investigations unequivocally showed that with diminishing swelling ratio supramolecular associations are formed in the gel, the crystalline character of which becomes more and more distinct with increasing volume fraction of the polymer.

To establish whether characteristics in the mechanical and swelling properties of the gels are to be attributed to ordering of the polymer chains, or they arise from the structure of the network, the topo-analogous transformation method [1] has been used.

The essence of this method is the conversion of a cross-linked polymer network by polymer-analogous transformation carried out in the gel phase into another polymer, without changing the steric structure of the gel, *i.e.* the number of the chemical junction points, or the number of the monomer units between these points. Topo-analogous transformation offers, among others, a possibility to prepare from a gel swelling in water another system of identical steric structure, swelling in a non-polar medium. Thus, by comparing the characteristics of the two or possibly several kinds of such systems, properties in conjunction with the structure of the gel or with other factors (*e.g.* the interactions between the polymer chains and the medium or the network chains with one another) can be separated.

It should be mentioned that theoretical possibilities involved in topo-analogous transformations and the information obtainable by their application are mentioned only briefly in the present communication; they will be discussed in the near future in a separate paper.

Theoretical survey

As is well known, the relationship between the force induced by unidirectional deformation in homogeneous and isotropic networks at constant volume, and the macroscopic deformation ratios can be described by the following equation [2]:

$$f = \frac{RT\, K_1 \nu_{el}^* q_0^{-2/3} q_i^{2/3} V_d}{L_{Vx}} (\Lambda_x - \Lambda_x^{-2}) \qquad (1)$$

where K_1 is a constant depending on the steric structure of the given gel, ν_{el}^* is the quantity in mol of the elastically active network chains in unit volume of the unswollen network, q_i is the swelling ratio of the network, q_0 the so-called memory parameter, and V_d the volume of the dry gel. Λ_x is the deformation ratio determined in the direction of the force (in unidirectional stretching or compression $\Lambda_x = \frac{L_x}{L_{Vx}}$, where L_x is the length of the deformed, while L_{Vx} that of the undeformed sample of volume V, measured in the direction of the x-axis), R the gas constant and T the temperature.

It can be seen from Eq. (1) that the value of the product $K_1 \nu_{el}^* q_0^{-2/3}$, containing the molecular parameters characteristic of the gel, can be determined

experimentally. To obtain further information about the individual factors other considerations are needed in connection with the model system.

According to the theory, the value of K_1 is determined primarily by the steric structure of the gel; its magnitude is constant for a given system, it does not depend either on the actual swelling ratio of the gel, or on the interactions of the polymer — solvent system.

If the gel is prepared by cross-linking of the polymer in solution, ν^*_{el} can be calculated on the basis of the relationship

$$\nu^*_{el} = \nu^* \left(1 - \frac{2d_2}{\overline{M}_n}\right) = \nu^* \left(1 - \frac{2\overline{M}_c}{\overline{M}_n}\right) \tag{2}$$

where ν^* is the concentration of all the network chains in the system, d_2 the density of the polymer, $\overline{M}_c$ is the number average relative molecular mass of the network chains, and $\overline{M}_n$ that of the polymer molecules in the initial solution [3]. Among the network defects Eq. (2) takes into consideration only the so-called pendent chains, which are linked only by one of their ends to the junction points. The theoretical calculation of other network defects (unreacted functional groups, cycles, entanglements, *etc.*). is not yet solved. The clearing of the role of permanent entanglements causes particular problems. The contribution of these to the change in HELMHOLTZ energy, accompanied by the deformation of the network, may depend considerably on the swelling ratio of the gel (Fig. 1). As shown schematically in Fig. 1, on increasing the swelling ratio (*e.g.* by exchanging the medium for a thermodynamically better solvent), entanglements act as if they were permanent cross-links, increasing thereby the quantity of the elastically active network chains, or the elastic work needed for the production of a given deformation.

A further theoretical difficulty is raised by the calculation of the value of parameter q_0. The appearance of q_0 in the fundamental equations is due to the fact that in the calculation of the change in HELMHOLTZ energy, accompanied by the deformation of the network, the reference state is the unperturped, force-free state of the network chains. If no change in volume occurs during

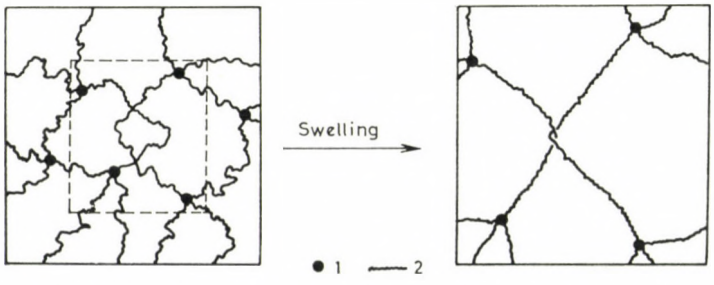

Fig. 1. Effect of swelling on permanent entanglements. (1) junction point, (2) network chain

deformation, then the change in HELMHOLTZ energy can be expressed in the following form:

$$\Delta A_{el} = \frac{RT K_1 \nu_{el}^* V_d}{2} (\lambda_x^2 + \lambda_y^2 + \lambda_z^2 - 3) \tag{3}$$

where λ_x, λ_y and λ_z are deformation ratios in the various directions of space, referred to the reference state. If the mean end-to-end distance of the network chains in the reference state is denoted by $\langle r \rangle_{os}$, and in the isotropic swollen gel by $\langle r \rangle_i$, then the following relationship can be written for the macroscopic deformation ratio Λ_x defined earlier and for λ_x:

$$\Lambda_x = \lambda_x \frac{\langle r \rangle_{os}}{\langle r \rangle_i} . \tag{4}$$

Introducing the swelling ratio instead of the chain size,

$$q_0 = \left(\frac{\langle r^2 \rangle_{os}}{\langle r^2 \rangle_d} \right)^{3/2}, \quad \text{and} \quad q_i = \left(\frac{\langle r^2 \rangle_i}{\langle r^2 \rangle_d} \right)^{3/2}$$

where $\langle r^2 \rangle_d$ is the mean square end-to-end distance of the network chains at a swelling ratio of $q_i = 1$, the following equation is obtained from Eq. (4):

$$\Lambda_x = \lambda_x \left(\frac{q_i}{q_o} \right)^{-1/3} . \tag{5}$$

Expressing λ_x and introducing it into Eq. (3), the following equation is obtained for the force in the case of unidirectional deformation at constant volume:

$$f = \left(\frac{\partial \Delta A_{el}}{\partial L_x} \right)_{T,V} = \frac{RT K_1 \nu_{el}^* V_d}{L_{Vx}} \left(\frac{q_i}{q_o} \right)^{2/3} (\Lambda_x - \Lambda_x^{-2}) \tag{6}$$

which is identical to Eq. (1).

It is evident from the aforesaid that q_0 is unequivocally related to the conformation belonging to the unperturbed state of the network chains as it is indicated also by the name "memory-parameter".

The approximation $q_0 = q_c$, $\left[q_c = \left(\frac{\langle r^2 \rangle_c}{\langle r^2 \rangle_d} \right)^{3/2} \right.$ where $\langle r^2 \rangle_c$ is the mean square end-to-end distance of the network chains at the volume of gel preparation $\left. \right]$, often used in the interpretation of experimental results, is based on the approximation

$$q_o^{2/3} = \frac{\langle r^2 \rangle_{os}}{\langle r^2 \rangle_d} = \frac{\langle r^2 \rangle_{os}}{\langle r^2 \rangle_d} \frac{\langle r^2 \rangle_c}{\langle r^2 \rangle_c} = \frac{\langle r^2 \rangle_{os}}{\langle r^2 \rangle_c} q_c^{2/3} \tag{7}$$

and on the assumptions that before cross-linking, the polymer molecules are in a near unperturbed state in the solution, and that the cross-linking process does not change considerably the conformation of the chains, *i.e.* $\langle r^2 \rangle_{os} = \langle r^2 \rangle_c$. The latter assumption implicitely means also that the interaction parameter of the polymer — solvent system is not considerably changed by cross-linking, but only the coordination number of the monomer units varies in the environment of the cross-links. This is fulfilled with good approximation only if cross-linking is produced without the introduction of chemical reagents (*e.g.* by electromagnetic or neutron irradiation).

In all the other cases it should be taken into consideration that the physical and chemical properties of the low molecular bi- or polyfunctional compounds, used for the cross-linking of dissolved polymer molecules, generally differ from those of the macromolecules, so that on reacting with the functional groups of the macromolecules they can change considerably important properties of the polymer molecules, thus *e.g.* their equilibrium conformation and the interaction parameter of the polymer — solvent system. Moreover, the effect of the cross-links already formed on the further course of cross-linking reaction is not yet known. Probably the q_0 value characteristic of the system also changes continuously with cross-linking, and the equilibrium conformation of the network chains depends substantially on the section of gel formation in which they were incordorated into the network, and on the number of junction points and unreacted functional groups located on the network chains.

The exact theoretical calculation of the memory-parameter would be possible only if the prevailing characteristic thermodynamic and kinetic parameters of the systems were known. However, with the present theoretical approaches, and without the knowledge of the physical quantities needed (*e.g.* the reactivity of macromolecules of different substitution incorporated into the network, the relationship between reactivity and the conformation of the molecules), this problem cannot be considered as solved.

Experimental

Our investigations were carried out on poly(vinyl acetate) (PVAc) gels. The PVAc gels were prepared from polyvinyl alcohol (PVA) gels by topo-analogous transformation, by total reacetylation in the gel phase. (The preparation of the PVA gels has been described in detail in an earlier communication [4]).

Topo-analogous transformation was carried out by gradually exchanging in a few days, at room temperature, the medium of the water swollen PVA gels with a 50 vol% pyridine: : 40 vol% acetic anhydride : 10 vol% glacial acetic acid mixture. It was found that the presence of about 10 vol% of glacial acetic acid affects favourably the kinetics of the process, particularly in the initial section of reacetylation, and gels swell better in this medium than in pyridine — acetic acid mixture, generally used for acetylation. Next, at a ratio of 100 volume of acetylating mixture and 1 volume of swollen gel, the systems were boiled under reflux in a spherical flask, for 8 hours at 363 K. The acetylating mixture was replaced in each hour with

a fresh mixture, and in the last three hours, when reacetylation was already advanced, the glacial acetic acid was omitted from the fresh mixture, to shift the equilibrium as far as possible in the direction of acetate formation.

After the termination of the process the systems were allowed to cool, and the medium of the gels was exchanged with acetone or toluene. This exchange of solvent was continued until foreign substances could not be detected even by interferometry in the equilibrium liquid.

Chemicals of analytical grade, produced by REANAL, were used for reacetylation. Some characteristics of PVA gels subjected to topo-analogous transformation are summarized in Table I. (Mechanical investigations relevant to these gels have been reported in two earlier communications [5, 6].)

Table I

Main characteristics of PVA gels before reacetylation

1. Characteristics of gels prepared from a polymer of relative molecular mass $\overline{M}_w = 100\,000$:
   Polymer concentration at cross-linking: 3, 6, 9, 12 wt.%
   Medium of cross-linking: water, 90 wt.% dimethyl-sulfoxide — 10 wt.% water mixture (DMSO)
   Cross-linking agent: glutaric aldehyde (GDA); succinic dialdehyde (SDA)

   * Degree of cross-linking: 50, 100, 200, 400

2. Characteristics of gels prepared from PVA fractions
   a) Average relative molecular mass of the fractions:
      I. 22 300, II. 52 600, III. 102 700, IV. 139 600, V. 345 500
   b) Symbols of gels prepared from the polydisperse polymer:
      Gels prepared by mixing different amount of fractions I and V: PD I, PD II, PD III
      Gels prepared by mixing different amount of fractions II and V: PD 1, PD 2, PD 3
   Polymer concentration at cross-linking: 9 wt.%
   Medium of cross-linking: water
   Cross-linking agent: GDA
   Degree of cross-linking: 50, 100, 200, 400

* The degree of cross-linking is the ratio of the moles of the monomer of the polymer and that of the cross-linking agent.

For the determination of the mechanical properties of PVAc gels, the apparatus designed by us and described earlier in detail has been used, which is suitable for the accurate determination of the force *vs.* deformation function in the case of unidirectional compression [4]. In the investigation of the dependence of the mechanical characteristics on the swelling ratio, the latter has been changed by the equilibrium swelling-degree decreasing method developed by us [7].

All the investigations were carried out at 298 $\pm$ 0.1 K. In all cases the arithmetic mean of three parallel measurements was used for evaluation. The reproducibility of mechanical measurements was generally found to be within 5%.

Results and Discussion

Since the complete proceeding of the chemical conversion of the polymer forming the gel skeleton is the fundamental precondition of the validity of the conclusions to be drawn from our investigations, increased attention was paid to its checking in the elaboration of the technical details of the topo-analogous transformation. The proceeding of the process has been studied on a large number of gels of different degrees of cross-linking, prepared in

various media with different cross-linking agents. Information on the extent of conversion was obtained on one hand by mass measurements. PVA gels of known mass were reacetylated, and the mass of the PVAc gels prepared in this way was compared with theoretical values calculated on the basis of the chemical reaction. The mass of the PVA and PVAc gels and the deviation of calculated and experimentally determined values are listed for a few gels in Table II. It can be seen that generally this difference does not exceed 1—2%.

Table II

Solids content of PVA gels and of PVAc gels prepared from them by topo-analogous transformation

*Symbol of the gel	Solids content of the PVA gel (g)	Solids content of the PVAc gels	
		Experimental value (g)	Calculated value (g)
12/50/GDA/water	0.0943	0.1812	0.1843
6/400/GDA/water	0.0450	0.0863	0.0879
9/50/GDA/DMSO	0.0705	0.1328	0.1378
3/100/GDA/DMSO	0.0210	0.0401	0.0410
12/200/SDA/water	0.0928	0.1791	0.1814
6/200/SDA/DMSO	0.0435	0.0832	0.0850

* Symbol of the gels: polymer concentration at cross-linking/degree of cross-linking/cross-linking agent/medium of cross-linking

The saponification number supported our earlier results, according to which, the acetate content of the gels is about 98—99 mol%.

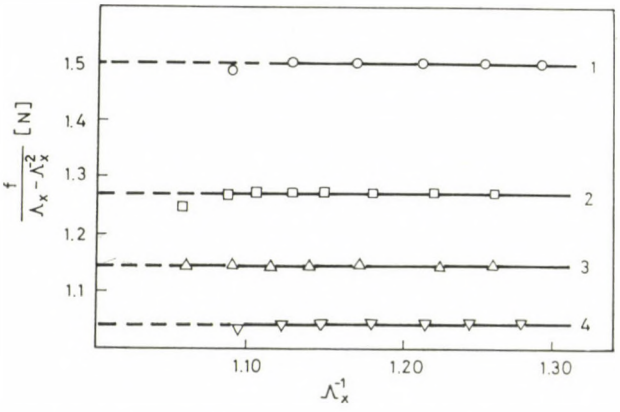

Fig. 2. Application of the MOONEY—RIVLIN equation for PVAc gels. (Symbol of the system: 6/50/GDA/DMSO.) v_2: (1) 0.163; (2) 0.221; (3) 0.286; (4) 0.366

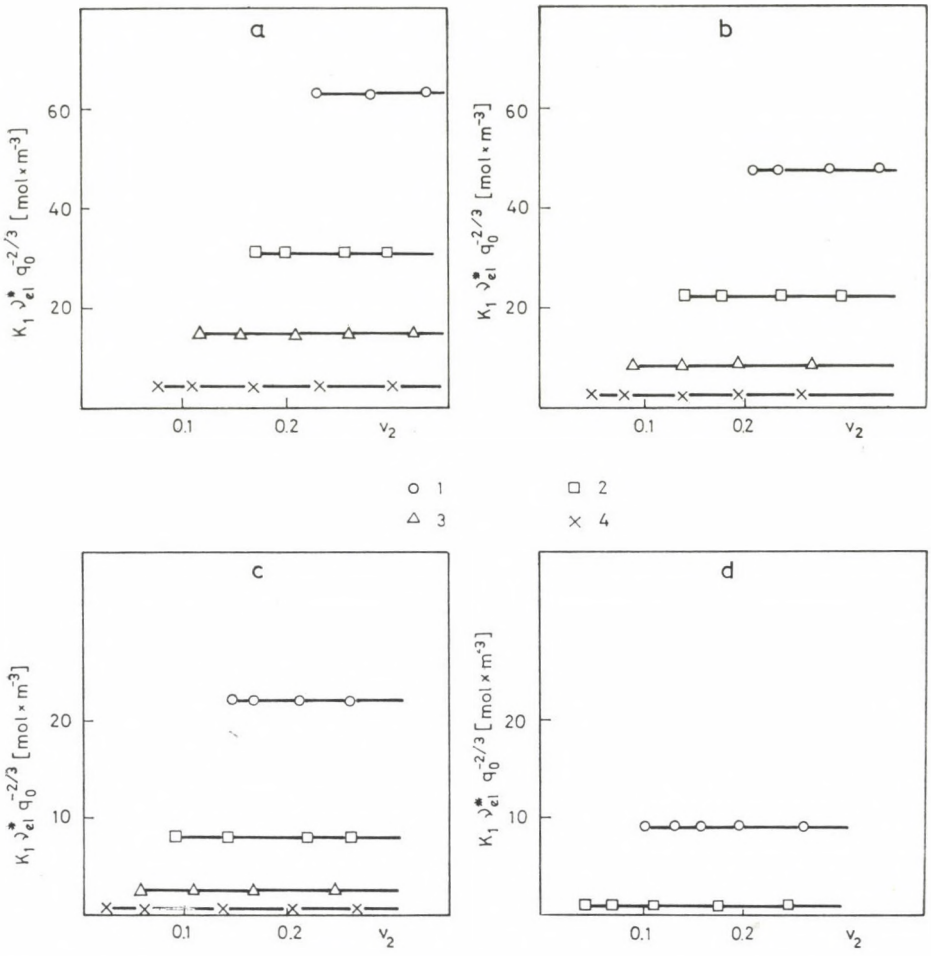

Fig. 3. Dependence of $K_1 v^*_{el} q_0^{-2/3}$ on the volume fraction of the polymer for PVAc gels (cross-linking agent: GDA, medium of cross-linking: water, polymer concentration at cross-linking: a. 12 wt.%, b. 9 wt.%, c. 6 wt.%, d. 3 wt.%). Degree of cross-linking: (1) 50; (2) 100; (3) 200; (4) 400; swelling agent: toluene

Mechanical measurements were evaluated on the basis of the relationship

$$f = 2C_1(\Lambda_x - \Lambda_x^{-2}) + 2C_2(\Lambda_x - \Lambda_x^{-2})\Lambda_x^{-1} \tag{8}$$

deducible for force from MOONEY—RIVLIN's equation [8, 9]. For ideal networks $2C_1$ is equal to the product

$$\frac{RT\, K_1 v^*_{el} q_0^{-2/3} q_i^{2/3} V_d}{L_{Vx}}$$

and $C_2 = 0$.

Similarly as in the case of PVA gels, it was found for all the PVAc gels that, independently of the swelling ratio, C_2 is zero within the limits of experimental error (Fig. 2).

In knowledge of the $2C_1$ values the product $K_1 \nu_{el}^* q_0^{-2/3}$, characteristic of the gels, has been calculated; it was strongly dependent on the swelling ratio in PVA — water systems, considerably increasing with increasing volume fraction of the polymer [5]. As it can be seen on Fig. 3, the value of $K_1 \nu_{el}^* q_0^{-2/3}$ for the different PVAc gels are independent of the swelling ratio in accordance with the theory. This supports our earlier finding that in PVA — water systems $K_1 \nu_{el}^* q_0^{-2/3}$ increases with diminishing swelling ratio because of gradually increasing orientation, and crystallization. The interaction between the PVAc chains is considerably weaker than in the case of PVA, which does not promote the formation of associations.

Table III contains $K_1 \nu_{el}^* q_0^{-2/3}$ values and equilibrium volume swelling ratios determined for a few PVAc gels in swelling equilibrium with toluene

Table III

$K_1 \nu_{el}^* q_0^{-2/3}$ values and equilibrium swelling ratios of PVAc gels in various diluents ($T = 298$ K)

Symbol of the system	Swelling agent			
	toluene		acetone	
	$K_1 \nu_{el}^* q_0^{-2/3}$ mol m^{-3}	q_i	$K_1 \nu_{el}^* q_0^{-2/3}$ mol m^{-3}	q_i
9/100/GDA/water	22.2	7.25	21.8	10.31
9/200/GDA/water	8.0	11.24	7.3	18.52
9/400/GDA/water	2.4	21.28	2.2	35.71
9/100/GDA/DMSO	24.5	7.14	23.4	10.20
9/200/GDA/DMSO	11.2	10.99	9.5	17.24
9/400/GDA/DMSO	3.3	18.52	2.8	31.25
9/100/SDA/water	23.0	7.25	23.9	10.53
9/200/SDA/water	13.6	9.71	11.2	16.67
9/400/SDA/water	4.8	15.38	4.8	27.03
9/100/SDA/DMSO	26.2	6.29	28.1	9.71
9/200/SDA/DMSO	15.1	8.77	14.2	14.08
9/400/SDA/DMSO	7.7	14.08	6.7	23.81

or acetone. It will be noted that the swelling ratio of the gels is substantially higher in acetone than in toluene, but the corresponding $K_1 \nu_{el}^* q_0^{-2/3}$ values differ only slightly from one another. These experimental results show, in conformity with Fig. 3, that permanent entanglements do not play considerably role in the gels investigated. The contribution of entanglements to the

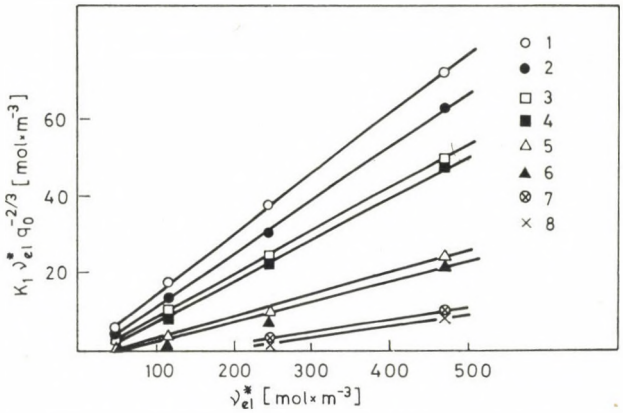

Fig. 4. Determination of the value $K_1 q_0^{-2/3}$ (topological factor). (1) 12 wt.% GDA/DMSO, (2) 12 wt.% GDA/water, (3) 9 wt.% GDA/DMSO, (4) 9 wt.% GDA/water, (5) 6 wt.% GDA/DMSO, (6) 6 wt.% GDA/water, (7) 3 wt.% GDA/DMSO, (8) 3 wt.% GDA/water, swelling agent: toluene

work needed for the production of deformation should change with the change of the swelling ratio (see Fig. 1), and this would diminish the product $K_1 \nu^*_{el} q_0^{-2/3}$ with increasing volume fraction of the polymer. It becomes apparent from Table III that an increase in the value of $K_1 \nu^*_{el} q_0^{-2/3}$ cannot be detected even in the case of gels with a comparatively high swelling ratio.

In Fig. 4 the $K_1 \nu^*_{el} q_0^{-2/3}$ values of PVAc gels are plotted as a function of ν^*_{el} calculated on the basis of Eq. (2). It can be esatablished that straight lines are obtained for all the systems, similarly as in the case of PVA gels. The topological factors $K_1 q_0^{-2/3}$, calculated from the slope of the straight lines and

Table IV

q_0 values of PVAc gels
(swelling agent: toluene, $T = 298$ K)

*Symbol of the system	$K_1 q_0^{-2/3}$	q_0 ($K_1 = 1$)	q_0 ($K_1 = 0.5$)
12/GDA/DMSO	0.150	17.2	6.1
12/GDA/water	0.125	22.6	8.0
9/GDA/DMSO	0.100	31.6	11.2
9/GDA/water	0.088	38.3	13.5
6/GDA/DMSO	0.050	89.4	31.6
6/GDA/water	0.040	125.0	44.2
3/GDA/DMSO	0.022	306.5	108.3
3/GDA/water	0.015	544.3	192.5

* Polymer concentration at cross-linking/cross-linking agent/medium of cross-linking

the q_0 values calculated for $K_1 = 1$ and $K_1 = 0.5$ are summarized in Table IV. Data in the table show that q_0 differs substantially from q_c adjusted experimentally, or from the value expected on the basis of the same.

Since q_0 calculated under fixed conditions is generally very high (the reference state falls into the region of dilute solutions), the dependence of the product $K_1 \nu_{el}^* q_0^{-2/3}$ on the average molecular mass of the network chains is approximated, similarly to the calculations of other authors [10, 11], with the relationship

$$K_1 \nu_{el}^* q_0^{-2/3} = C \overline{M}_c^{-1.16} \tag{9}$$

obtained from the FLORY—FOX and the KUHN—MARK—HOUWINK equations for the system PVAc — toluene. (Constants of the KUHN—MARK—HOUWINK equation at 298 K: $K = 108 \times 10^{-5} \frac{100 \text{ cm}^3}{\text{g}}$, $a = 0.53$ [12]). In the derivation of Eq. (9) it has been assumed that the conformation of the network chains is the same in the polymer solution of infinite dilution and in the reference state of the gel, further that the quantity of the elastically active network chains can be calculated on the basis of Eq. (2).

In Fig. 5 the log $K_1 \nu_{el}^* q_0^{-2/3}$ values determined for PVAc — toluene gels are plotted as a function of log $\overline{M}_c$. It can be seen that the points are located

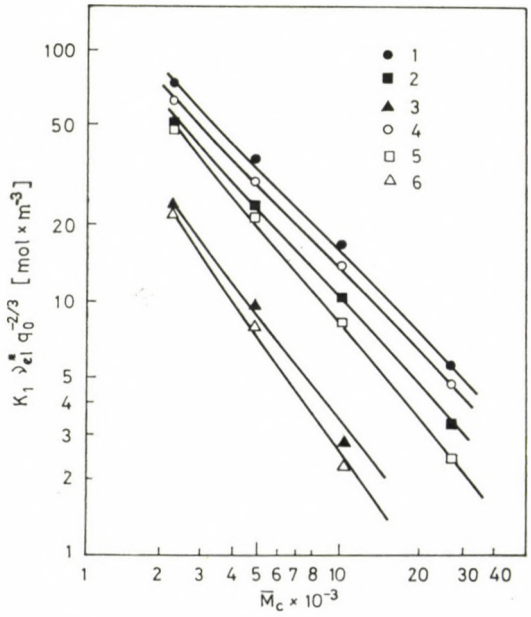

Fig. 5. log $K_1 \nu_{el}^* q_0^{-2/3}$ *vs.* lg $\overline{M}_c$ for PVAc — toluene gels. (1) 12/GDA/DMSO, (2) 9/GDA/DMSO, (3) 6/GDA/DMSO, (4) 12/GDA/water, (5) 9/GDA/water, (6) 6/GDA/water

with good approximation along straight lines, the slopes of which vary between -1.0 and -1.1. This agrees fairly well with the exponent calculated theoretically, indicating that in the reference state of the gel the mean square end-to-end distances of the network chains change with the molecular mass according to a similar function as in the dilute polymer solutions.

Topo-analogous transformation offers a possibility to investigate how far the molecular parameters characteristic of the gels are affected by a change in the chemical nature of the polymer chains. Thus, the validity of theoretical relationships can be studied by an approach differing in principle from those used earlier.

If the $K_1 \nu_{el}^* q_0^{-2/3}$ values of PVAc gels are plotted as a function of the $K_1 \nu_{el}^* q_0^{-2/3}$ values of the respective PVA gels extrapolated to infinite dilution (Fig. 6), a straight line is obtained, the slope of which is ≈ 1.3.

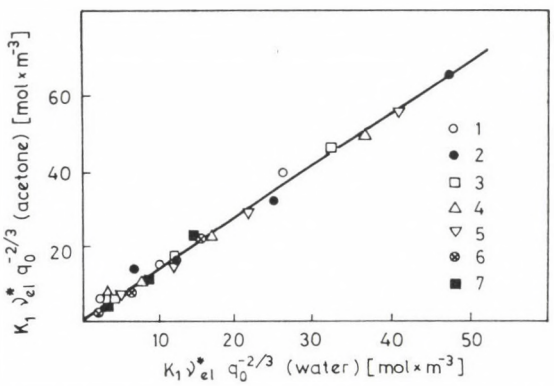

Fig. 6. The effect of the topo-analogous transformation on $K_1 \nu_{el}^* q_0^{-2/3}$. (1) fraction I, (2) fraction V (3) PD I, (4) PD II, (5) PD III, (6) 9/GDA/water, (7) 9/SDA/water

Let us investigate the effect of the topo-analogous transformation on the individual factors of the product $K_1 \nu_{el}^* q_0^{-2/3}$.

K_1, which is a model constant in conjunction with the steric structure of the gel, cannot be substantially changed by the topo-analogous transformation carried out at unchanged steric structure.

The change of ν_{el}^* can be calculated when the relative molecular mass of the monomer units and the densities of the polymers are known (M_0^{PVA}: 44; M_0^{PVAc}: 86; d_0^{PVA}: 1.27 gcm^{-3}; d_0^{PVAc}: 1.17 gcm^{-3}).

The effect of the topo-analogous transformation on q_0 can be estimated on the basis of the constants of the KUHN—MARK—HOUWINK equation, because q_0 values of both PVA and PVAc gels fall into the region of the dilute solution.

Under consideration of the aforesaid

$$\frac{K_1 \nu_{el}^* q_0^{-2/3}(\mathrm{PVAc})}{K_1 \nu_{el}^* q_0^{-2/3}(\mathrm{PVA})} = \frac{d_2^{\mathrm{PVAc}}}{d_2^{\mathrm{PVA}}} \frac{\overline{M}_{c(\mathrm{PVA})}}{\overline{M}_{c(\mathrm{PVAc})}} \frac{\langle r^2 \rangle_d^{\mathrm{PVAc}}}{\langle r^2 \rangle_d^{\mathrm{PVA}}} \frac{\langle r^2 \rangle_{os}^{\mathrm{PVA}}}{\langle r^2 \rangle_{os}^{\mathrm{PVAc}}}. \tag{10}$$

In Eq. (10) the ratio $\overline{M}_{c(\mathrm{PVA})}/\overline{M}_{c(\mathrm{PVAc})}$ can be substituted by the relative molecular mass of the monomers. The ratio of the $\langle r^2 \rangle_d$ values can be calculated on the basis of geometrical considerations with the relationship

$$\frac{\langle r^2 \rangle_d^{\mathrm{PVAc}}}{\langle r^2 \rangle_d^{\mathrm{PVA}}} = \left(\frac{2\overline{M}_{c(\mathrm{PVAc})} N_A d_2^{\mathrm{PVA}}}{2\overline{M}_{c(\mathrm{PVA})} N_A d_2^{\mathrm{PVAc}}} \right)^{2/3}. \tag{11}$$

From the FLORY—FOX and the KUHN—MARK—HOUWINK equations we get

$$\frac{\langle r^2 \rangle_{os}^{\mathrm{PVA}}}{\langle r^2 \rangle_{os}^{\mathrm{PVAc}}} = \left(\frac{\Phi \alpha_{\mathrm{PVAc}}^3 K^{\mathrm{PVA}} \overline{M}_{c(\mathrm{PVA})}^{a^{\mathrm{PVA}}}}{\Phi \alpha_{\mathrm{PVA}}^3 K^{\mathrm{PVAc}} \overline{M}_{c(\mathrm{PVAc})}^{a^{\mathrm{PVAc}}}} \right)^{2/3} \tag{12}$$

where K^{PVA} and a^{PVA}, and K^{PVAc} and a^{PVAc} are the constants of the KUHN—MARK—HOUWINK equations of the respective polymer-solvent systems, α is the expansion factor and Φ the so-called FLORY constant.

If we disregard in first approximation that Φ and α are different in PVA and PVAc solutions, performing the numerical substitutions, the following relationship is obtained:

$$\frac{K_1 \nu_{el}^* q_0^{-2/3}(\mathrm{PVAc})}{K_1 \nu_{el}^* q_0^{-2/3}(\mathrm{PVA})} = 0.778 \left(\frac{K^{\mathrm{PVA}}}{K^{\mathrm{PVAc}}} \frac{\overline{M}_{c(\mathrm{PVA})}^{a^{\mathrm{PVA}}}}{\overline{M}_{c(\mathrm{PVAc})}^{a^{\mathrm{PVAc}}}} \right)^{2/3}. \tag{13}$$

Taking into account Eq. (13) we can write *e.g.* for PVA — water [13] and PVAc — acetone [14] systems:

$$\frac{K_1 \nu_{el}^* q_0^{-2/3}(\mathrm{PVAc})}{K_1 \nu_{el}^* q_0^{-2/3}(\mathrm{PVA})} = 0.778 \left(\frac{4.28 \times 10^{-4}}{0.86 \times 10^{-4}} \frac{\overline{M}_{c(\mathrm{PVA})}^{0.64}}{\overline{M}_{c(\mathrm{PVAc})}^{0.72}} \right)^{2/3} = 2.27 \left(\frac{\overline{M}_{c(\mathrm{PVA})}^{0.64}}{\overline{M}_{c(\mathrm{PVAc})}^{0.72}} \right)^{2/3} \tag{14}$$

Since for the gels studied $1000 < \overline{M}_{c(\mathrm{PVA})} < 20\,000$ $\left(\text{i.e.} \left(\frac{\overline{M}_{c(\mathrm{PVA})}^{0,64}}{\overline{M}_{c(\mathrm{PVAc})}^{0.72}} \right)^{2/3} = 0.4—0.6 \right)$, the ratio according to Eq. (14) scarcely differs from that found experimentally.

This finding supports our results discussed earlier, that chain size in the reference state can be well approximated with relationships valid for dilute solutions, at least in the case of gels with high q_0 values.

Theoretical and experimental investigations aimed at the elucidation of the universal features of second order phase transitions and other critical phenomena resulted in the recognation of several analogies between the phase transition of ferromagnetic systems and the conformation-dependent properties

of polymer chains. By the application of scaling laws the elaboration of a novel theory of polymers, differing also in principle from earlier theories, became possible [15, 16].

It can be shown that in a thermodynamically good solvent there is a relationship between the polymer concentration (c^*) falling into the transiton region of the dilute and moderately concentrated solutions and the number of monomer units (N), building up the molecule [17]:

$$c^* \propto N^{-4/5}. \tag{15}$$

In a polymer solution of concentration, c^*, the available volume is filled up by the macromolecules, so that their segment clouds just do not interpenetrate, and thus

$$c^* \propto \frac{N}{R^3} \tag{16}$$

where R is the radius of gyration, depending on N [18] according to

$$R \propto N^{3/5}. \tag{17}$$

The proportionality (15) can be obtained from Eqs (16) and (17) by substitution.

According to the theory, in a polymer solution of concentration $c = c^*$ a change produced in any part of the macromolecule extends over the whole chain (the correlation length ξ is the same as the radius of the molecule). In the semi-dilute regime ($c^* < c \ll 1$), where the chains already overlap considerably, the correlation length is equal to the distance between the adjacent contact points ($\xi < \mathrm{R}$). As the number of contact points in unit volume is independent of N and depends at a given temperature only on the concentration of the polymer, the following relationship can be given for the correlation length:

$$\xi(c) = R\left(\frac{c^*}{c}\right)^x. \tag{18}$$

where the value of the exponent, x, is still unknown. Under consideration of Eqs (15) and (17), from Eq. (18) we get

$$\xi(c) \propto c^{-3/4}. \tag{19}$$

In accordance with the aforesaid, in the case of networks the correlation length can be identified with the length of the chain sections between the junction points. As the value of the modulus ($E = RTK_1\nu_{\mathrm{el}}^* q_0^{-2/3} q_i^{-1/3}$) is directly proportional to the density of cross-links (n), *i.e.*

$$E \propto n \tag{20}$$

using the relationship

$$n \propto \xi^{-3}(c_e) \tag{21}$$

the proportionality

$$E \propto c_e^{9/4} \tag{22}$$

is obtained, where c_e is the concentration of the polymer in the gel in swelling equilibrium [17, 19].

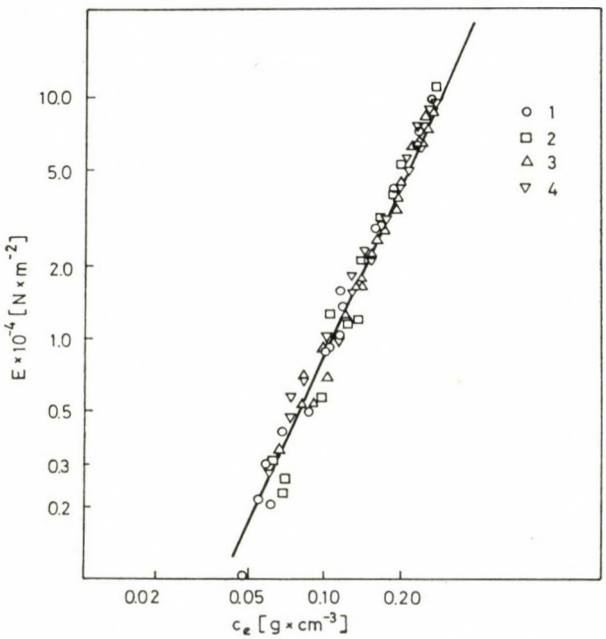

Fig. 7. log E *vs.* log c_e for PVAc — toluene gels. (1) GDA/water, (2) GDA/DMSO, (3) systems marked with PD, (4) systems marked with I, II, III, IV, V

In Figs 7 and 8, E and c_e values belonging together are plotted double logarithmically for the gels PVAc — toluene and PVAc — acetone. As can be seen the points lie along straight lines within the experimental error for both types of systems, and the slopes of these lines are also virtually identical. The exponent is about 2.1—2.3, which is close to both the theoretical value and the value found earlier for the system PVA — water [6]. The fact that the exponent is not considerably influenced either by the polymer-analogous transformation of the gels at unchanged steric structure, or by the chemical nature of the swelling agents, indicates that the correlation length and the concentration dependence of the modulus derivable from it are primarily determined by the steric structure of the gels.

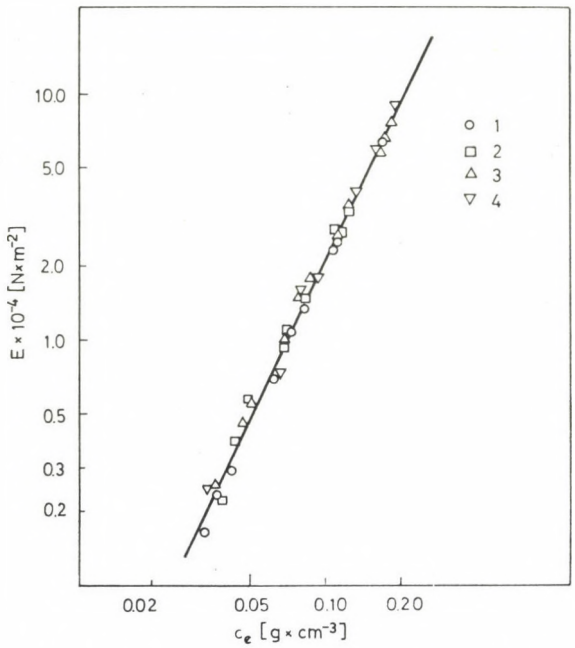

Fig. 8. log E *vs.* log c_e for PVAc — acetone gels. (1) GDA/water, (2) GDA/DMSO, (3) systems marked with PD, (4) systems marked with I, II, III, IV, V

It can be established in summary that topo-analogous transformation is a new experimental possibility, which may contribute to the better understanding of the mechanical and swelling behaviour of gels. As became evident also from the present investigations, the role of the parameter q_0 is the least known. As the topo-analogous transformation does not affect the value of K_1, and if the chemical reaction proceeds completely, the change of v_{el}^* can be calculated in knowledge of the relative molecular mass of the monomer units and of the density of the polymers, it is to be hoped that topo-analogous transformation will be utilized first of all for the elucidation of problems in conjuction with q_0.

*

We wish to thank Dr. János KABAI for supporting this work. Thanks are due to Mrs. Miklós HERCZEG for her careful experimental work.

REFERENCES

[1] NAGY, M., HORKAY, F., ZRINYI, M., WOLFRAM, E.: 8th Europhys. Conf. Macromol. Phys. Bristol, **3A,** 55 (1978)
[2] DUŠEK, K., PRINS, W.: Fortschr. Hochpolym. Forschung, **6,** 1 (1969)
[3] FLORY, P. J.: J. Chem. Phys., **18,** 108 (1950)
[4] HORKAY, F., NAGY, M., ZRINYI, M.: Acta Chim. Acad. Sci. Hung., **103,** 387 (1980)
[5] HORKAY, F., NAGY, M.: Magy. Kém. Folyóirat, **86,** 535 (1980)

[6] HORKAY, F., NAGY, M.: Acta Chim. Acad. Sci. Hung. (In press)
[7] NAGY, M., HORKAY, F.: Acta Chim. Acad. Sci. Hung. **104,** 49 (1980)
[8] MOONEY, M.: J. Appl. Phys., **11,** 582 (1940)
[9] TRELOAR, L. R. G.: The Physics of Rubber Elasticity. Clarendon Press, Oxford 1975
[10] BELKEBIR-MRANI, A., HERZ, J. E., REMPP, P.: Makromol. Chem., **178,** 485 (1977)
[11] BELKEBIR-MRANI, A., BEINERT, G., HERZ, J., REMPP, P.: Europ. Polym. J., **13,** 277 (1977)
[12] BRANDRUP, J., IMMERGUT, E. H.: Polymer Handbook. Wiley, New York 1974
[13] MATSUMOTO, M., OHYANAGI, Y.: Kobunshi Kagaku, **17,** 17 (1960)
[14] CHINAI, S. N., SCHERER, P. L., LEVI, D. W.: J. Polym. Sci., **17,** 117 (1955)
[15] DES CLOISEAUX, J.: J. Phys. (Paris), **36,** 281 (1975)
[16] DE GENNES, P. G.: Phys. Lett., **A 38,** 339 (1972)
[17] DAOUD, M., COTTON, J. P., FARNOUX, B., JANNINK, G., SARMA, G., BENOIT, H., DUPLESSIX, R., PICOT, C., DE GENNES, P. G.: Macromolecules, **8,** 804 (1975)
[18] FLORY, P. J.: Principles of Polymer Chemistry. Cornell University Press, Ithaca, New York 1967
[19] DE GENNES, P. G.: Macromolecules, **9,** 587 (1976)

Ferenc HORKAY H-1096 Budapest, Nagyvárad tér 2.

Miklós NAGY
Miklós ZRINYI } H-1088 Budapest, Puskin u. 11—13.

Acta Chimica Academiae Scientiarum Hungaricae, Tomus 108 (3), pp. 305—315 (1981)

STUDY OF THE MOLECULAR COMPONENT OF DIETHYL ETHER DECOMPOSITION

I. SERES and G. SZABÓ

(Reaction Kinetics Research Group of the Hungarian Academy of Sciences, Szeged, Institute of Inorganic and Analytical Chemistry, A. József University Szeged)

Received November 1, 1980

Accepted for publication January 6, 1981

The thermal decomposition of 6.7 kPa diethyl ether was examined at 824 K, and that of 26.7 kPa diethyl ether at 783, 803 and 824 K in the presence of 1.3 kPa NO, product analysis being performed with a gas chromatograph. Under the assumption that the radical-induced decomposition of the ethanol intermediate is minimal under such conditions, the rate constant of the molecular component of diethyl ether decomposition has been determined:

$$k_m = 10^{(12.7\pm0.8)} \exp\left[-(256\pm12)\ \text{kJ mol}^{-1}/RT\right]\text{s}^{-1}$$

Introduction

In earlier publications [1—3] we have demonstrated that the decomposition of diethyl ether involves the participation of molecular and radical processes. In the presence of acetaldehyde an increase was observed in the role of the radical component of the decomposition, with an accompanying decrease in the relative importance of the molecular pathway. It was found that ethanol formed in the molecular reaction undergoes radical-induced decomposition. Since this induced decomposition is already relatively more important at the beginning of the process, the data obtained for the rate constant of the molecular component of diethyl ether decomposition, calculated on the basis of the initial rate of the accumulation of ethanol, are smaller than the actual values.

In the presence of nitrogen monoxide the decomposition of diethyl ether is slowed down considerably [4] as a consequence of the inhibition of the radical processes; nitrogen monoxide has no effect on the molecular processes. The aim of the present work is to obtain more accurate data on the rate of the molecular decomposition, by using nitrogen monoxide to decrease the role of the radical processes to a minimum in the thermal decomposition of diethyl ether, the error caused by the induced decomposition of ethanol thereby being diminished.

Experimental

The experiments were performed in a vacuum apparatus described earlier [1]. Gas-chromatographic product analysis was carried out similarly as for non-inhibited decompositions [5].

Materials used:

(i) Nitrogen monoxide was prepared by the method of WINKLER [6]. It was washed with 90% sulfuric acid and with 50% potassium hydroxide in intensive strubbers, and frozen out with liquid air after drying with anhydrous calcium chloride and phosphorus pentoxide. It was next sublimed four times in high vacuum from a temperature of 153 K, the receiver being cooled with liquid air. In every case, only the middle fraction was collected. The storage flask was flushed out several times with nitrogen monoxide, and was evacuated before the storage of nitrogen monoxide.

(ii) Diethyl ether was a Chinoin product of the highest analytical purity. After drying over calcium chloride and metallic sodium, it was distilled repeatedly in high vacuum. It did not contain impurities detectable gas-chromatographically.

Results and Discussion

The literature data [7] indicate that the decomposition of diethyl ether is inhibited maximally by less than 1 kPa nitrogen monoxide. Accordingly, the experiments were carried out in the presence of 1.3 kPa nitrogen monoxide. The decomposition of 26.7 kPa diethyl ether was investigated at 783, 804 and 824 K, and that of 6.7 kPa diethyl ether at 824 K, in the presence of 1.3 kPa nitrogen monoxide. As an illustration of the results obtained in the case of the decomposition of 26.7 kPa diethyl ether in the presence of 1.3 kPa nitrogen monoxide, Fig. 1 presents the product *vs.* time curves obtained at 824 K. Curves similar in nature were obtained at other temperatures. In order that a suitable comparison may be achieved with the reaction in the absence of nitrogen monoxide, Fig. 2 presents the partial pressure of the products of 26.7 kPa diethyl ether decomposing at 823 K, as a function of the reaction time.

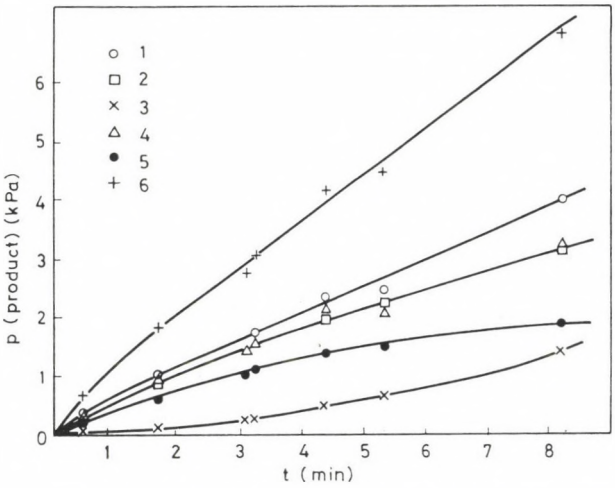

Fig. 1. Decomposition products of 26.7 kPa diethyl ether at 824 K in the presence of 1.3 kPa NO as a function of the reaction time. Notation: (1) ethane; (2) acetaldehyde; (3) carbon monoxide and methane; (4) ethylene; (5) ethanol; (6) measured pressure increase

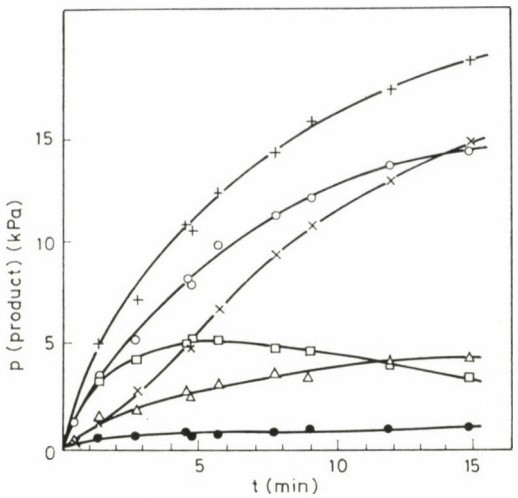

Fig. 2. Decomposition products of 26.7 kPa diethyl ether at 823 K as a function of the reaction time. Notation as in Fig. 1

From a comparison of Figs 1 and 2 it may be seen that the overall rate of decomposition decreases strongly in the presence of nitrogen monoxide, 2 and 7.5 min, respectively, being necessary for the attainment of 25% conversion. It is also very striking that in the inhibited reaction the amounts of ethylene and ethanol are increased considerably compared to those of ethane and acetaldehyde. The induced decomposition of acetaldehyde is strongly suppressed in the presence of nitrogen monoxide, as indicated by the accumulation of carbon monoxide. The situation is probably the same with the induced decomposition of ethanol, for it can be seen from Fig. 1 that in the presence

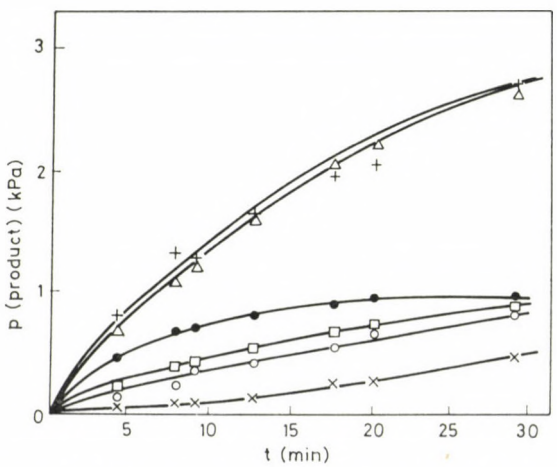

Fig. 3. Decomposition products of 6.7 kPa diethyl ether at 824 K in the presence of 1.3 kPa NO as a function of the reaction time. Notation as in Fig. 1

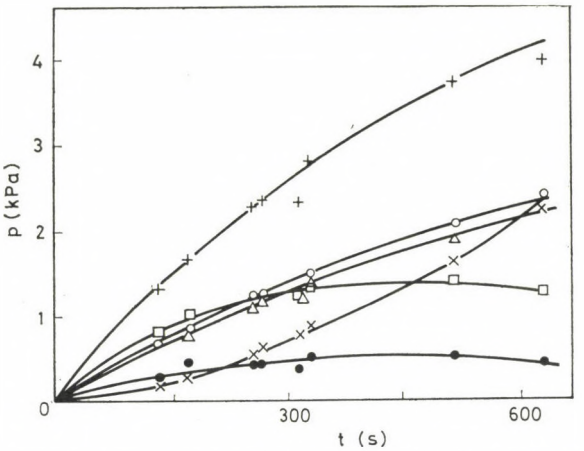

Fig. 4. Decomposition products of 6.7 kPa diethyl ether at 824 K as a function of the reaction time. Notation as in Fig. 1

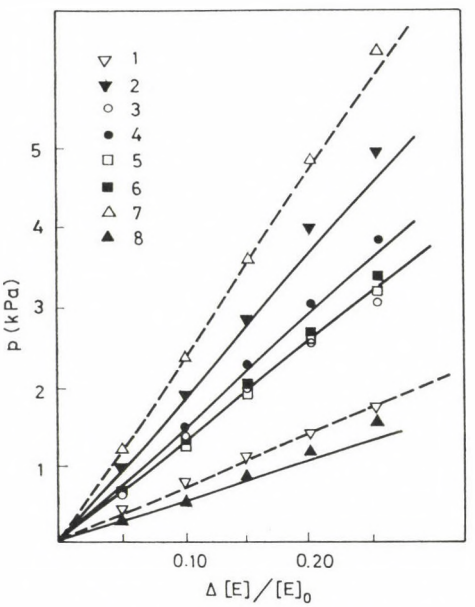

Fig. 5. Partial pressures of ethylene and ethane as functions of the conversion. Notation: 823 K, 26.7 kPa ether: (1) ethylene, (2) ethane; 824 K, 26.7 kPa ether + 1.3 kPa NO: (3) ethylene, (4) ethane; 824 K, 6.7 kPa ether: (5) ethylene, (6) ethane; 824 K, 6.7 kPa ether + 1.3 kPa NO: (7) ethylene, (8) ethane

of nitrogen monoxide the quantity of carbon monoxide does not attain the quantity of ethanol, even at 25% conversion.

The share of the decomposition route into ethanol and ethylene is strikingly increased when 6.7 kPa diethyl ether is decomposed in the presence of 1.3 kPa nitrogen monoxide, as can be assessed from a comparison of Figs

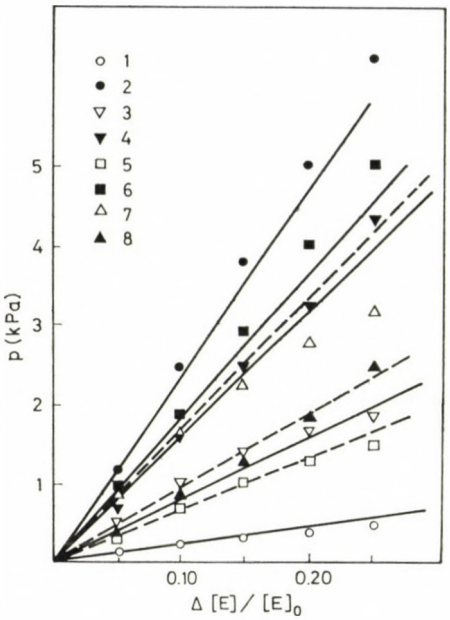

Fig. 6. Partial pressure of ethanol and sum of partial pressures of carbon monoxide and acetaldehyde as functions of the conversion. Notations: 823 K, 26.7 kPa ether: (1) ethanol, (2) (CO + CH_3CHO); 824 K, 26.7 kPa ether + 1.3 kPa NO: (3) ethanol, (4) (CO + CH_3CHO); 824 K, 6.7 kPa ether: (5) ethanol, (6) (CO + CH_3CHO); 824 K, 6.7 kPa ether + 1.3 kPa NO: (7) ethanol, (8) (CO + CH_3CHO)

1—2 and 3—4. In Figs 3 and 4 the decomposition products of 6.7 kPa diethyl ether in the presence and absence, respectively, of 1.3 kPa nitrogen monoxide are presented as a function of the reaction time.

Additional information is obtained on the processes occurring in the thermal decomposition of diethyl ether if the amounts of the individual products are investigated as a function of the conversion. Figure 5 presents the partial pressures of ethylene and ethane, and Fig. 6 those of ethanol and acetaldehyde (increased by the partial pressure of carbon monoxide), as functions of the conversion. For better comparison, the values obtained in the experiments performed at an initial pressure of 6.7 kPa have been multiplied by 4. It may be stated quite definitely that the partial pressures of the products of the chain process characterized by the stoichiometry

$$(C_2H_5)_2O \rightarrow C_2H_6 + CH_3CHO \qquad (I)$$

show an upward curvature in all cases with the conversion. In contrast, the partial pressures of the products of the molecular process

$$(C_2H_5)_2O \rightarrow C_2H_4 + C_2H_5OH \qquad (II)$$

exhibit an opposite trend.

Thus reaction (I) becomes more favoured than reaction (II) with the increase of the conversion. This appears contradictory if it is considered that reaction (I) is of order 3/2 and reaction (II) is of order 1, and that the importance of the latter reaction compared to that of the former one increases to a slight extent as the conversion rises. The contradiction can be resolved if it is assumed that the transformation of the products of process (II) into the products of process (I) by means of secondary reactions is significant, overcompensating the effect arising as a consequence of the decrease in ether concentration.

The above conclusion is supported by Fig. 7, where the ratios of the ethylene and ethane concentrations and the ethanol and acetaldehyde + carbon monoxide concentrations have been plotted as functions of the conversion. The ratio of the corresponding products of the molecular and of the radical decomposition of diethyl ether decreases with increasing conversion; the decrease is particularly marked in the presence of nitrogen monoxide. It is also clear that the ratio of the concentrations of the hydrocarbons is substantially larger than that of the oxygen-containing compounds, whereas these ratios should agree if there were no secondary processes.

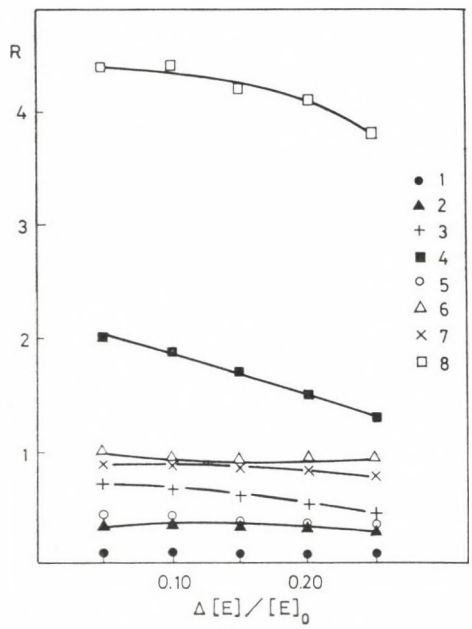

Fig. 7. Ratios ethylene: ethane and ethanol: (carbon monoxide + acetaldehyde) as functions of the conversion at 824 K. Notation: $[C_2H_5OH]/([CO] + [CH_3CHO])$: (1) 26.7 kPa ether, (2) 6.7 kPa ether, (3) 26.7 kPa ether + 1.3 kPa NO, (4) 50 Torr ether + 10 Torr NO; $[C_2H_4]/[C_2H_6]$: (5) 26.7 kPa ether, (6) 6.7 kPa ether, (7) 26.7 kPa ether + 1.3 kPa NO, (8) 6.7 kPa ether + 1.3 kPa NO

On the basis of our experimental results, the following statements can be made.

1. In the presence of nitrogen monoxide the chain component of the decomposition of diethyl ether is suppressed and the molecular pathway becomes more important.

2. The effects of 1.3 kPa nitrogen monoxide on the distributions of the decomposition products of 26.7 and 6.7 kPa diethyl ether are of similar extents qualitatively.

3. There is a significant difference between the ratios of the oxygen-containing and the hydrocarbon products, which is indicative of secondary processes.

4. Since the same radicals are responsible for the chain decompositions of diethyl ether, acetaldehyde and ethanol, and also for the formation of acetaldehyde from diethyl ether and ethanol in the presence of nitrogen monoxide too, and since their concentration is substantially lower then in the non-inhibited decomposition, as shown by the rate of carbon monoxide formation, our experimental results can be explained on the assumption of the molecular decomposition of the product ethanol, in accordance with the earlier observations by FREEMAN [8].

5. On the appreciable suppression of the chain decomposition of diethyl ether with nitrogen monoxide it was not possible to find a characteristic product, the quantity of which is a clear-cut measure of the molecular reaction pathway at any conversion. However, our experimental data do permit the rate of the molecular reaction to be determined considerably more accurately than previously.

In order to estimate the quantity of diethyl ether decomposed by the molecular pathway, we set out from the point that the decomposition mechanism in the presence of nitrogen monoxide is quite similar to that of the uninhibited process [1], but the concentration of the β radicals decreases in the presence of nitrogen monoxide, and hence the role of the molecular decomposition is increased.

Our experimental data indicate that a radical pathway is followed in the formation of a smaller proportion of ethylene, which is a consequence of primary hydrogen abstraction from diethyl ether. The same applies the formation of ethane. We assumed earlier that the ratio of the rate constants of abstraction of methylene and methyl hydrogens is 10. This assumption is supported by the more recent measurements of PRYOR *et al.* [9] and FOUCAULT and MARTIN [10].

On the above basis, very little ethylene is to be expected to from *via* a radical pathway in the decomposition of diethyl ether as compared to the formation of ethane, and even to the formation of ethylene by a molecular route. However, its quantity is still negligible compared to that of the ethylene

formed molecularly in the presence of nitrogen monoxide. Thus, the pressure of diethyl ether decomposed *via* the radical and molecular pathways, respectively, are

$$-\Delta p(\mathrm{E})_{\mathrm{R}} = p(\mathrm{C_2H_6}), \text{ and} \tag{a}$$

$$-\Delta p(\mathrm{E})_{\mathrm{M}} = -p(\mathrm{E}) - p(\mathrm{C_2H_6}) \tag{b}$$

In the presence of nitrogen monoxide, ethanol undergoes mainly dehydration, its dehydrogenation being of lesser importance [8]. Hence the quantity of diethyl ether decomposed *via* the molecular route may be given also by the expression

$$-\Delta p(\mathrm{E})_{\mathrm{M}} = p(\mathrm{C_2H_5OH}) + \frac{p(\mathrm{C_2H_4}) - p(\mathrm{C_2H_5OH})}{2}. \tag{c}$$

Table I

Calculated values of $\Delta p(E)_{\mathrm{M}}$ and $\Delta p(E)_{\mathrm{R}}$, the ether consumed in the molecular and radical decomposition

	Measured		Calculated		
t (min)	$-\Delta p(\mathrm{E})$ (kPa)	$p(\mathrm{C_2H_6})$ (kPa)	$-\Delta p(\mathrm{E})_{\mathrm{M}}$ (kPa) from (b)	$-\Delta p(\mathrm{E})_{\mathrm{M}}$ (kPa) from (c)	$-\Delta p(\mathrm{E})_{\mathrm{R}}$ (kPa) from (d)
783 K, 26.7 kPa ether + 1.3 kPa NO					
10	2.07	1.07	1.00	0.80	1.07
20	3.60	2.13	1.47	1.27	2.20
30	5.06	3.07	2.00	1.87	3.27
40	6.27	4.00	2.27	2.13	4.13
50	7.13	4.87	2.53	2.73	5.13
60	8.46	5.60	2.87	2.87	5.67
70	9.60	6.40	3.20	3.13	6.40
80	10.7	7.06	3.60	3.40	6.93
803 K, 26.7 kPa ether + 1.3 kPa NO					
5	1.60	0.80	0.80	0.67	0.93
10	3.13	1.60	1.53	1.20	1.87
15	4.67	2.53	2.13	1.73	3.13
20	6.13	3.53	2.53	2.13	4.27
25	7.53	4.60	2.93	2.73	5.33
30	8.73	5.47	3.27	2.93	6.40
35	10.00	6.40	3.60	3.33	7.33
40	11.20	7.20	4.00	3.47	8.13

Thus, the quantity of ether decomposed *via* radical pathway can also be expressed as

$$-\Delta p(\mathrm{E})_{\mathrm{R}} = p(\mathrm{CH_3CHO}) + p(\mathrm{CO}). \qquad \text{(d)}$$

The correctness of our reasoning is confirmed by the data in Table I, which gives data calculated from the expressions (b), (c) and (d).

The data calculated from relations (b) and (c) agree satisfactorily, as do $p(\mathrm{C_2H_6})$ and $\Delta p(\mathrm{E})_{\mathrm{R}}$ calculated from (d), though the values obtained from (c) are smaller and those obtained from (d) a little larger than the expected values. The cause of this may be the slight dehydrogenation of the alcohol and the consumption of ethylene in secondary reactions.

On the above basis, a possibility arises for calculation of the rate of the molecular component in the decomposition of diethyl ether. The results obtained are to be found in Table II.

The data calculated from experiments performed in the absence of nitrogen monoxide are given in Table III, together with the data of LAIDLER and MCKENNEY [11] and FOUCAULT and MARTIN [10].

Tables II and III reveal that the highest rate is obtained for the molecular decomposition when the initial rate for the alcohol accumulated in the presence of nitrogen monoxide is corrected in accordance with expression (c) (Table II,

Table II

Rate constant at 800 K *and Arrhenius parameters of the molecular decomposition, calculated from the inhibited reactions*

	Basis of calculation			
	$v_0(\mathrm{C_2H_5OH}) + \frac{v_0(\mathrm{C_2H_4}) - v_0(\mathrm{C_2H_5OH})}{2}$	Expressions		$v_0(\mathrm{C_2H_5OH})$
		(b)	(c)	
$\log (k_{800}/\mathrm{s}^{-1})$	−3.90	−4.05	−4.10	−4.0
E(kJ mol^{-1})	239	260	268	251
$\log (A/\mathrm{s}^{-1})$	11.70	12.8	13.35	12.38

Table III

Rate constant at 800 K *and Arrhenius parameters of the molecular decomposition. calculated from reactions in the absence of* NO, *together with the data of* LAIDLER *and* MCKENNEY [11] *and* FOUCAULT *and* MARTIN [10]

	Basis of calculation							
	$v_0(\mathrm{E}) - v_0(\mathrm{C_2H_6})$			$v_0(\mathrm{C_2H_5OH})$			ref. [11]	ref. [10]
$\log (k_{800}/\mathrm{s}^{-1})$	−3.94	−3.98	−3.96	−4.22	−4.26	−4.23	−4.96	−3.95
E(kJ mol^{-1})	263	285	268	277	272	280	352	261
$\log (A/\mathrm{s}^{-1})$	13.2	14.6	13.5	13.8	13.5	14.0	18.4	13

column 1). Nearly the same rate is obtained if the rate data resulting from the $\Delta p(\mathrm{E})_{\mathrm{M}}$ values calculated *via* (b) and (c) within each reaction are taken as basis (Table II, column 2). The agreement with the preceding data is surprisingly good if the rate constant of the molecular decomposition is calculated from the initial rate of $\Delta p(\mathrm{E})_{\mathrm{M}}$ on the basis of expression (b) in the reactions in the absence of nitrogen monoxide. The rate constant of the molecular component in the decomposition of diethyl ether can be given in the form

$$k_{1\mathrm{m}} = 10^{(12.7 \pm 0.8)} \exp\left[-(256 \pm 12)\ \mathrm{kJ\ mol^{-1}}/RT\right] \mathrm{s^{-1}}.$$

On the above basis, it may be stated that the molecular decomposition of diethyl ether proceeds at a substantially higher rate than would be expected from the pressure measurements of LAIDLER and MCKENNEY [11] (Table III, column 7); the data are only slightly different from those derived by FOUCAULT and MARTIN [10] from initial rates measured at a low conversion (Table III, last column).

Table IV

Data relating to molecular decomposition of certain ethers

	$(CH_3)_3COCH_3$		$(CH_3)_3COC_2H_5$	$(CH_3)_2CHOCH(CH_3)_2$
	[12]	[13]	[14]	[15]
$\log (k_{800}/\mathrm{s^{-1}})$	−2.3	−2.3	−2.1	−2.6
E(kJ mol^{-1})	257 ± 2	247	250 ± 2	266
$\log (A/\mathrm{s^{-1}})$	14.4 ± 0.2	13.9	14.1 ± 0.1	14.6

The occurrence of molecular decomposition has also been assumed for other ethers. Data relating to the molecular component of the decomposition in the case of some short-chain aliphatic ethers are given in Table IV.

*

The authors are indebted to Professor Z. G. SZABÓ for initiation of the investigation and to Professor P. HUHN for helpful discussions.

REFERENCES

[1] SERES, I., HUHN, P.: Magy. Kém. Folyóirat, **81,** 120 (1975)
[2] SERES, I., LABÁDI, I., HUHN, P.: Magy. Kém. Folyóirat, **83,** 131 (1977)
[3] SERES, I., HUHN, P.: Magy. Kém. Folyóirat, **83,** 138 (1977)
[4] FREEMAN, G. R.: Proc. Roy. Soc., **245A,** 49 (1958)
[5] SERES, I.: Magy. Kém. Folyóirat, **78,** 173 (1972)
[6] WINKLER, L. W.: Ber. dtsch. Ges., **34,** 1408 (1901)

[7] HOBBS, J. E.: Proc. Roy. Soc., **A167,** 455 (1938)
[8] FREEMAN, G. R.: Proc. Roy. Soc., **245A,** 78 (1968)
[9] PRYOR, W. A., FULLER, D. L., TANLEY, J. P.: J. Amer. Chem. Soc., **94,** 1634 (1972)
[10] FOUCAULT, J. F., MARTIN, R.: J. Chim. Phys., **75,** 132 (1978)
[11] LAIDLER, K. J., MCKENNEY, D. J.: Proc. Roy. Soc., **A278,** 523 (1964)
[12] DALY, J., WENTRUP, C.: Austral. J. Chem., **21,** 2711 (1968)
[13] CHOO, K. Y., GOLDEN, D. M., BENSON, S. W.: Int. J. Chem. Kinet., **6,** 631 (1974)
[14] DALY, J., WENTRUP, C.: Austral. J. Chem., **21,** 1535 (1968)
[15] DALY, H. J., STIMSON, V. R.: Austral. J. Chem., **19,** 239 (1966)

István SERES
Gábor SZABÓ
H-6720 Szeged, Dóm tér 7.

RECENSIONES

CAMMAN, K.: *Working with Ion-Selective Electrodes Chemical Laboratory Practice*

Springer-Verlag Berlin, Heidelberg, New York, 1979. XII. p. 226.

This up to date monograph written in English is an enlarged and revised version of the second German edition of the author's book "Das Arbeiten mit ionenselectiven Electroden" (Springer-Verlag 1977).

The monograph provides a good survey of the theoretical and practical aspects of ion-selective electrodes, giving a good proportion between theory and practice. The theoretical as well practical problems are treated from a modern electrochemical aspect, which was not common in books appeared earlier on this subject. The main topics dealt with are as follows: fundamentals of potentiometry, electrode potential measurements, ion-selective electrodes, measuring techniques with ion-selective electrodes, analysis techniques with ion-selective electrodes, applications of ion-selective electrodes. A special merit of the book is a critical treatment of the specific analytical techniques, with regard to the accuracy of the methods. The potentialities of the various techniques are demonstrated by practical examples, which gives a valuable aid to practising analysts for the selection of a method best suited to a certain analytical task.

Based on the literature, a survey is given on the application of ion-selective electrodes in different fields of analytical chemistry in a tabulated form. Problems and techniques connected with applications in physiology, biology, medicine and environmental protection are treated separately in greater detail.

The terminology used in the book is in line with IUPAC recommendations.

The book will be of interest to researchers, practising analytical chemists and university students who want to get high level and at the same time practical knowledge of the basic characteristics and applications of ion-selective electrodes.

This new, English edition covers practically completely the relevant literature and gives a list of manufacturers of ion-selective electrodes. The appendix contains tables useful in the evaluation of analytical methods using ion-selective electrodes.

K. TÓTH

Electric Phenomena in Polymer Science

Advances in Polymer Science, Vol. 33

Springer-Verlag, Berlin, Heidelberg, New York, 1979, p. 174.

The book contains four surveys about electric phenomena in the field of polymer science.

Giuliano MENGOLI's paper, "*Feasibility of Polymer film Coatings Throughs Electro-initiated Polymerization in Aqueous Medium*" deals with the feasibility of preparing polymeric coatings on the surface of conductive substrates (metals). For the electrophoretic coating technique used so far a high potential difference (100—150 V) was necessary and the adhesion of the deposited polymer particles was rather poor. Coating by "*in situ*" electropolymerization is very promising both for technology and practice, particularly of the procedure can be carried out in non-polluting aqueous medium. A survey is given about the experimental realization, and how the active species formed on the electrodes in water medium are able to initiate

polymerization chains, *i.e.* the different ways of radical generation. The methods and monomers for this purpose known up to the present are described, such as the parameters influencing the electroinitiated polymerization of diacetone acrylamide, experiences obtained in the case of methyl vinyl ketone and acrylamide. A view is given about the limiting factors of "*in situ*" electropolymerization, together with a survey of possible routes for the methodical development and the most promising further investigations.

R. V. SUBRAMANIAN: "*Electroinitiated Polymerization on Electrodes*". The first part of this study discusses the electroinitiated copolymerization of acrylonitrile, benzonitrile, phenols, acrolein, that of monomer pairs containing double bonds of opposite polarities, and the conditions of polyimide formation by electroinitiation. In the second part the electroinitiated polymer coating of, and polymer grafting to, graphite fibers are dealt with, together with the stereoregularity of the polymer formed in this manner. Such polymer-coated graphite fibers make possible the production of composite materials with unique properties where interactions on the surface are essentially more effective. This aspect is also of great interest for practical application.

Graham WILLIAMS: "*Molecular Aspects of Multiple Dielectric Relaxation Processes in Solid Polymers*". This survey outlines first the α,- β-relaxations of amorphous polymers, the molecular theory of dipole relaxation, and the various general and specific models for molecular motion. Further, the dielectric relaxation processes that can be observed in crystalline polymers are discussed in subdivisions of polymers of medium and high degree of crystallinity. Finally, an evaluation is presented about the methods of investigation dielectric and mechanical relaxation, ^{1}H-NMR and ^{13}C-NMR techniques which complete each other, and about the still unsolved problems that are expected to be solved in the near future making possible an even more successful physical explanation of motions in solid polymers.

H. BLOCK: "*The Nature and Application of Electrical Phenomena in Polymers*". While some years ago almost merely the electric insulating ability of synthetic polymers was utilized for technical applications, nowadays considerable valuable information may be obtained by dielectric measurements about the structures of polymers and their changes in the liquid and solid states. Beyond these, novel, significant fields of application have been opened for piezo- and pyro-electric polymers, conductive polymers and photoconductive polymers. These latter have found rapidly developing practical applications in the field of electroimaging. It is enough to refer here to the Xerox-process, or to the possibilities of silver-free photography and photocopying, and to reprography. The aforementioned polymer behaviours are covered in the last survey of the book with clear-cut explanations.

It has to be observed that it is regrettable that in spite of its significance in technics and particularly in safety regulations, a survey regarding electrostatic phenomena on polymers, including the essence of electrostatic charging, the nature of the charged species, and the possibilities of eliminating electrostatic charging, cannot be found in this volume.

Otherwise, the book may be used to advantage by technical specialists and scientists interested in the electrical behaviour of polymers.

Gy. HARDY

S. BAJUSZ: *Peptide Synthesis*

Recent Results in Chemistry, Vol. 48

Akadémiai Kiadó, Budapest, 1980. p. 231, 53 figures, 11 tables (In Hungarian)

The years of rapid development in research on peptide chemistry are covered by this volume, *i.e.* the time between 1970 and 1977; the book is a direct continuation of the comprehensive survey published on peptide chemistry in Vol. 3 of the present series (K. MEDZIHRADSZKY: *Synthesis of natural peptides*).

The contents of the book can be divided into two parts. In the first, the author discusses the problems of peptide synthesis in 156 pages; the second part ("Synthetic peptides in the research of structure-activity relationships", 44 pages) presents examples for the biological role and mechanism of action of peptides. The book provides thus much more information than expected on the basis of the short title "Peptide synthesis".

The author makes an original approach to the problems of peptide synthesis. In the first part of the work, synthetic problems following from the nature of certain amino acids are discussed in such a way that even readers not quite familiar with peptide chemistry can

realize that almost each amino acid is an "individual" entity, hence the design and accomplishment of synthesis of a polypeptide is far from being a simple routine task. The author treats, according to his own words "without claim to completeness", the methods of protecting the amino and carboxyl groups and the establishment of the peptide bond, discussing however, all important new methods and protective groups and also including the new ways of introducing the old, well-proved protective groups. He deals with racemization, an extremely important process in peptide synthesis, over almost 20 pages; here, after presenting the newest results, the author summarizes in some fundamental statements the recent knowledge how racemization can be reduced to minimum. In the chapter entitled "Construction of the peptide chain", the method of minimum side-chain protection and the methods of "rapid" peptide synthesis are described in detail, with special attention to solid-phase synthesis. (The latter topic takes 47 of a total of 56 pages constituting this chapter, indicating the wide-spread application and importance of solid-state synthetic methods.) In the second part of the book, the role of peptides in the regulation of life-processes are demonstrated on excellently selected examples (ribonuclease, angiotensins, releasing and release-inhibiting hormones, other biologically active peptides, such as enkephalins and endorphins), and the importance of synthetic peptide chemistry is shown in promoting biochemical, biological, and pharmacological research. The author gives a very concise treatment of the extraordinarily rich material, compressing it into about 200 pages. The difficulties, troubles in peptide research are presented, even undecided issues are mentioned. The very enjoyable, readable book with its vivid style presents several new statements; in this way it will be of interest not only to beginners but also to experts of the field. The book can also be recommended to researchers working in fields other than peptide chemistry, if they learn and accept the special language.

The 438 literature references present a good selection from among the most important peptide chemical papers and other publications which appeared between 1970 and 1977. A continuation of this long-needed book within a few years would be desirable describing the recent rapid development since 1977.

B. PENKE

DUFFY, J. I.: *Chemicals by Enzymatic and Microbial Processes* (Recent Advances)

Chemical Technology Review No. 161. Noyes Data Corporation,

Park Ridge, New Jersey, USA, 1980, p. 385.

The book offers detailed technological information based on patents filed in the USA since 1975, and at the same time serves as a guide to the patent literature in this field. The volume gives a detailed description of microbiological and enzymatic processes (strains, culture media, conditions of production, *etc.*) and also deals with technological aspects of the problem (reactors, product isolation, *etc.*). Thus the volume may be of interest not only to microbiologists and organic chemists, but also to experts (researchers and technologists) of the industry, governing the research and development of industrial enterprises.

Owing to the economic efficiency of these biochemical methods, a growing trend in the chemical industry to apply microorganisms and enzymes for the production of chemicals and considerable progress in this field (development of genetic methods, determination of regulatory and metabolic pathways) have been observed over the past decade. This development has been utilized mainly by the food industry: considerable research capacity has been concentrated on the production of amino acids and proteins (SCP). Other topics receiving increasing interest are the production of microbial polysaccharides, or the isomerization of saccharides and enzymatic decomposition of polysaccharides. The volume covers a wide range of microbiological procedures, giving information and detailed description on organic acids, amino acids, peptides, proteins, nucleic acids and derivatives, as well as alcohols, carbohydrates, vitamins and other organic compounds (methane, ergot alkaloids, *etc.*).

Microbes and their enzymes have now become an integral part of the chemical industry and the technology is further improving at a rapid rate.

Applicability of the volume is greatly facilitated by the US Patent Number Index (244 patents), Inventor Index and Company Index.

L. NYESTE

NOWACKI, P.: *Health Hazards and Pollution Control in Synthetic Liquid Fuel Conversion*

Noyes Data Corp., Park Ridge, New Jersey, USA, 1980, p. 511

This new book of the Noyes Data Corp. describes and discusses the environmental aspects of coal liquefaction, oil shale processing and tar sands conversion. The intention of the author is to provide fast access to the most advanced pollution research data now available and to sketch the limitations of such data.

The book consists of 15 chapters. In the first chapter, a preliminary discussion of composition and structural features peculiar to coal, oil shale and tar sands is given. The second chapter reviews the liquid fuel production processes, the third and fourth chapters deal with pollution sources and health effects associated with coal liquefaction. The toxicity, carcinogecity, synergetics, interactions and residual effects of each element, trace element, particulate or compound are treated at length.

The next — and longest — chapter of the book reviews the pollution control methods and possibilities for coal liquefaction in general. In this chapter, a very good tabulation of potential pollutants and processes of their treatment helps easy orientation. The flow diagrams of the more important pollution control processes are also given.

In the following two chapters environmental aspects of three US coal liquefaction processes (Solvent Refined Coal, H-Coal and Exxon Donor Solvent) are reviewed in detail. These three processes are in the most advanced stage of development and seem to be quite promising.

The Solvent Refined Coal (SRC) system utilizes a noncatalytic direct hydrogenation process. There are two basic system variations, this study has been aimed primarily at the SRC-II system, which produces low sulphur fuel-oil and naphta. A pilot plant, processing 30 tons/day of coal has been working on the basis of the SRC-II process in Fort Lewis, Washington since 1977. The study contained in the book is based on the design of a 8000 m^3 products/day commercial facility, which is planned to be built in Morgantown for start-up in 1984.

The H-Coal and Exxon Donor Solvent (EDS) process have similar products and wastes within the estimation accuracy allowed by available information. Since 1980, a pilot plant is working on the basis of each of the two processes enabling the study of the processes on a quite large scale. The descriptions in the book are based on hypothetical plants designed to produce 8000—8000 m^3/day of products according to each of the two processes (in case of the H-Coal process the description is based on the fuel-oil mode of operation).

The 8th chapter gives a short description of the environmental aspects of the Fischer—Tropsch synthesis. In this chapter, experiences with the commercial Fischer—Tropsch facility in South Africa (SASOL) are utilized, but the concept serving the basis of the estimation of pollutants is not identical with the SASOL technology. It is a hypothetical plant somewhere in the Eastern Coal Region of the US, processing 27 000 tons/day of cleaned bituminous coal. The design of this plant incorporates advanced technology solutions, such as a high temperature-high pressure gasifier based on Bi-Gas principles and a flame-sprayed catalytic reactor for Fischer—Tropsch conversion.

The next two chapters are devoted to the pollutants and health effects associated with oil shale processing, followed by a very important chapter, which discusses the possibilities and different methods of environmental control in oil shale processing in general. The general possibilities and discussions are followed by the assessment of emissions and effluent characteristics involved in several particular oil shale conversion processes; namely the TOSCO-II, Paraho, Union Oil and the *in-situ* conversion processes are considered.

Chapter 13 describes the environmental impacts of surface tar sand mining, in situ production of tar sand, and tar sand processing. Tar sands, are a potential source of synthetic fuel, but their utilization in the future is greatly dependent upon the environmental effects of their production and processing.

A separate chapter deals with the well-known carbon-dioxide problem (greenhouse-effect). As a result of burning and processing fossil fuels, the CO_2 concentration in the atmosphere has increased from about 295 ppm by volume in 1860 to the current level of 331 ppm. As the author notes: "At present, with no CO_2 emission controls, about 5×10^9 metric tons of carbon per year as CO_2 are emitted to the atmosphere . . . About 50% of this carbon can be accounted for by the increase in the CO_2 concentration of the atmosphere." After the short description of the problem, possibilities for the solution are given, options of the removal, reuse and disposal of carbon dioxide are listed.

The final chapter of the book lists and explains those US laws and regulations which have impacts on synthetic fuel technology and on the siting of such plants. A short hypothetical case-study is also given, in this chapter.

The book edited by Perry NOWACKI gives a very thorough, well proportioned overview and often detailed discussion of the environmental and health hazards in synfuel conversion and of the possibilities to control them. It is not easy to give exact characteristics and amounts of wastes from synfuel plants, because very few commercial facilities and even pilot plants exist. In spite of this difficulty the book gives many valuable informations on a broad field. It is hoped that this book will greatly contribute to the easy recognition of many environmental and health problems connected with syntetic liquid fuel conversion and will give practical help in solving them.

The editor of the book utilized 29 reports made by different laboratories and companies for the Environmental Protection Agency, for the US Dept. of Energy and the U.S. authorities. These are listed at the end of the book. In addition, reference lists can be found at the end of each chapter.

G. SZÉCHY

Electroless and Other Nonelectrolytic Plating Technique Recent Developments

Chemical Technology Review No. 171

Edited by J. I. DUFFY

Noyes Data Corp., Park Ridge, New Jersey, USA, 1980

The theme of this recent publication of NDC is a very important, rapidly developing kind of plating, the so called electroless or nonelectrolytic plating.

The title is not completely correct, because the platings discussed are produced partly as a result of electrochemical reactions, and thus, cannot be called either electroless of non-electrolytic. These coatings are produced from the solution of metal ions, without external current source, mostly with the aid of some reducing agent. These coatings, or rather this plating technique steadily gains ground, mainly in electronics. The book also treats some thermal coatings.

The book covers a very large material, 225 patents, which have been published in the United States since 1978, *i.e.* in the last two years.

The first chapter deals with noble metals, with gold, silver and platinum plating. In the field of gilding, the cyanide-free process is of importance. Even such an ancient process as silver mirror preparation is capable of revival, as shown by the process described in this chapter. The process suitable for the platina plating of titanium is also of importance.

The second chapter discusses some base or intermediate coatings. In addition to a few modifications of the chemical copper bath already known, some thermic copper plating processes are also described. Chemical iron- and tin plating are also included in this chapter.

In the chapter on protective coatings the deposition of aluminium, zinc, chromium and superalloys are described. This too involves thermal processes besides chemical methods. In eddition to problems of the deposition of the coating, the chapter discusses also the effect of the base metals on the deposition process itself. It is very interesting that even technical problems of application are taken into consideration, as *e.g.* the coatings suitable for the prevention of stress corrosion cracking.

NBC covered the problem of the plating of plastics in two previous volumes. The fact that a chapter is devoted also in this book to the discussion of these problems shows that the subject is evergreen.

Essentially, this chapter covers almost all the aspects of plastics plating, from the basic substances through sensibilization to the applicable coatings.

A relatively brief chapter deals with the plating methods of glass and ceramics.

In accordance with its importance, the methods and possibilities of the application of metal coatings in electronics are discussed on more than 100 pages. Methods in conjunction with printed circuits, integrated circuits, superconductors and thick-layer circuits are discussed. Separate chapters deal with the individual types of components, as *e.g.* electrodes, resistors,

capacitors. A separate part is devoted to solar collectors, proving their steadily growing importance. The growing importance of environmental protection and energy management is reflected in the discussion of oxygen sensors, indispensable in the operation of furnaces.

A separate chapter deals with the important theme of magnetic coatings. The chemical method is particularly suitable for the preparation of magnetic memory discs, because it provides for an extraordinary uniform layer thickness. Bubble circuits are an interesting part of this chapter.

Phototechniques play an important role in the preparation of printed and integrated circuits, because the very high-precision of microminiaturized circuits can only be prepared with his technique. According to their importance, masks, photomaterials, printing technique and optical mirror layers are separately discussed.

In the last chapter, thermal coatings, screening masks needed for selective metal plating, and some methods, which cannot be classed into the aforegoing chapters, are discussed.

In the book, the description of the single patents begins with the title of the patent, the names of the inventors, the name of the company, the number of the patent and the date of filing. This is followed by a clear, easily understandable description of the content.

The indexes of the companies, inventors and patent numbers are at the end of the book. Since NBC publications summarize the most recent results of patent literature, they are of great value to *R* and *D*.

F. Haskó

Metal Ions in Biological Systems edited by Helmut Siegel, Vol. 10: *Carcinogenicity and Metal Ions*

Marcel Dekker, Inc., New York and Basel, 1980. XXII and 381 pages

The book consists of 10 chapters and is the work of 18 authors. The aim of the first chapter is to show on the basis of present knowledge the role of metal ions in genetic regulation, how they damage regulation by interfering with the synthesis processes of DNA, RNA and protein. The reader obtains a survey on the connection between the influence of various metal compounds on the fidelity of DNA synthesis and their mutagenic/carcinogenic effect. Chapter 2 discusses the carcinogenic metals and compares them. For detecting mutagenic and carcinogenic effects different *in vivo* and *in vitro* models are available. According to experiences up to the present, Cr, Ni, Cd, As and Be compounds are most likely to be responsible for human cancer: in several test-systems they show genetic toxicity as well. This suggests that the mutagenic effect may play a role in the carcinogenicity of metal ions.

In Chapter 3 data are presented concerning the amounts of metal ions in blood and other tissues of healthy people and cancer patients. It has been shown that a connection can be found between the metal ion level of the blood serum and the growth or regression of carcinomas. Metal ion traces are necessary for the function of numerous enzymes, but, at the same time, they may act as enzyme inhibitors. Certain trace metals promote or inhibit the activity of such enzymes which transform carcinogenic compounds into effective substances, *e.g.* Cu, Mg, Fe, Zn, Ni, Co, *etc.*

Chapter 4 makes the reader acquainted with the importance of paramagnetic metal ions in the growth of malignant tumours. In tissues of animals suffering in leukaemia or solid tumours no proof has been obtained with ESR method for deviation characteristic for malignancy, though the concentration of several paramagnetic ions shows unambiguous variation. Some of these variations may reflect a disturbance in normal metabolism, which, in turn, is frequently caused by infiltrations of malignant cells.

Chapter 5 treats the coeruloplasmin and Cu level in blood, as well as its transferrin and Fe level, and their variations in a malignant state. The authors discuss separately data obtained by the study of solid tumours, malignant lymphomas and various types of leukaemia.

Chapter 6 deals with relationships between trace elements and human leukaemia. In the majority of malignant processes significant changes can be observed in the trace amounts of heavy metals; in different organs or tissues of the same organism antiparallel changes can also occur. These studies are made as deep as the molecular level. They have significance in both the diagnosis and the evaluation of therapeutic effect.

A separate chapter (Chapter 7) is devoted to the role of Zn in the formation and growth of malignant tumours. Epidemiologic studies have not proven the carcinogenic effect of Zn

deficiency or Zn excess on humans. The variations of the Zn content in the blood serum of cancer patients are rather difficult to explain. No conclusions can be drawn from the variations of the Zn level observed in carcinomas concerning its special role in tumour growth. The authors discuss in details the importance of Zn in therapy.

Chapter 8 discusses the connection between malignant growth and cyanocobalamin. The authors present mostly their own results: the special properties of $CN-B_{12}$ and cobamide coenzymes during the process of tumour growth. They have established that the properties of $CN-B_{12}$ and $ADO-B_{12}$ are different, but it is not yet clear how generally this is valid.

Chapter 9 is devoted to the occurrence, absorption, distribution, excretion and place in the food chain of selenium (Se). No carcinogenic effect of it has been found, on the contrary, it excels with its anti-carcinogenic effect, which is due to its antioxidant properties.

The last chapter (Chapter 10) of the book treats the application of radioactive metal ions and their complexes in the diagnosis of tumours. Radionuclides most frequently used are ^{67}Ga, ^{99m}Tc, ^{111}In, ^{113m}In, ^{123}I, ^{169}Yb, ^{197}Hg and ^{201}Tl. The anticancer drug bleomycin forms chelates with numerous metals, but the ^{99}Te-bleomycin complex can be applied in the diagnosis of carcinomas.

The book gives a very good and valuable survey on the importance of metal ions in the process of malignization for researchers dealing with carcinogenesis, but pharmacologists, toxicologists, biochemists, enzymatologists and other experts of similar fields can also benefit from this book.

I. PÁLYI

Metal Ions in Biological Systems edited by Helmut SIGEL, Vol. 11: *Metal Complexes as Anticancer Agents*

Marcell Dekker, Inc., New York and Basel, 1980. XX and 427 pages

This book consists of 8 chapters and is the work of 13 authors.

Chapter 1 discusses the anticancer properties of various metal complexes. Pt-complexes are especially efficient. The authors present earlier studies on metals, and the history of the discovery and application of the anticancer Pt-complexes. Such a Pt-complex was marketed in 1978—1979 under the name Platinol in USA and Neoplatin in U.K., respectively. Among the other metals (Rh, Pd, Ru, Ir, Cu, Co, Fe, Zn, Ni) several derivatives of Rh show some activity; the derivatives of the other elements—though they have some biological effect—cannot be considered as anticancer agents.

Chapter 2 introduces the chemical properties and binding of Pt(II) to biological macromolecules.

Chapter 3 surveys the clinical aspects of Pt-containing anticancer agents by reviewing results in animal tests, its toxic side-effects in the test animals, its distribution in the organism and studies on drug combinations. A good survey is given on the mechanism of action of Pt-complexes, and on experiments concerning their mutagenic and carcinogenic effect. Finally, clinical experiments are described, which began in 1971, and results achieved in combination therapy.

Chapters 4 and 5 include experiments with Cu- and Ru-complexes as anticancer agents. The bleomycin-Cu complex was found to be efficient against certain animal tumours. The isotope of Ru can be considered rather as a tumour-specific radiodiagnostic agent.

The first part of Chapter 6 provides a useful survey on alkylating agents, while in the second part their metal complexes are described. The application of some Mg-and Ca-complexes of aziridinyl derivatives resulted in a significant survival of L1210 and P388 leukaemic mice. On the contrary, the Rh-complex of cyclophosphamide was not efficient. Nevertheless, the authors see some prospect in the synthesis and testing of new metal complexes of alkylating agents, which may possess more favourable properties.

Numerous anticancer antibiotics could be isolated, *e.g.* bleomycin, tallisomycin, phleomycin, streptonigrin, daunomycin, adriamycin. Their mechanism of action and their metal-binding properties are described comprehensively in Chapter 7. Mostly Fe, Co, Ni, Cu, and Zn are involved in the bonds. Enzymes are frequently primary points of attack for chemotherapeutics.

In Chapter 8 the interactions between enzymes, metals and anticancer agents are described. One field treated is the interaction between enzymes and metal-containing compo-

nents, the enzyme-inhibiting effect of Pt-complexes, though other metals are also shortly mentioned.

The other represented field is the metallo-enzymes and enzymes activated by metal ions which are either inhibited by the anticancer agents, or the enzymes take part in the metabolism of the agents.

The book provides an excellent survey mainly for those experts dealing with both theory and practice, who are interested in the chemotherapy of cancer, but researchers in the field of toxicology, pharmacology, biochemistry, biophysics, enzymology can also benefit from it.

I. PÁLYI

V. N. KONDRATIEV, E. E. NIKITIN: *Gas-Phase Reactions Kinetics and Mechanisms*

Springer-Verlag Berlin, Heidelberg, New York 1981 XIV + 241 pp

The kinetic investigations of the gas reactions, initiated by the doctoral thesis of BODENSTEIN nearly hundred years ago, are now in their third period. While during the first period the aim was to determine the kinetic parameters macroscopically, in the second one, by the discovery of the reaction chains, it became a task to establish elementary steps constituting the complex processes, and together with it to determine the kinetic parameters of these steps. The present, third period actually started with the paper of EYRING and POLÁNYI 50 years ago, which placed the transition state concept in the centre of the investigations. Here not only the spatial location of the atoms of the reacting molecules related to one another and their migration were considered, but also the energy relations of the reacting particles. This aim, however, demanded not only to develop a new theoretical conception on the chemical events, but also to explore new microphysical processes. The most interesting form among these, being the most important, is the transfer of energy between molecules. At present, however, the concept of reacting molecules encompasses also the excited, and electrically charged particles, *i.e.* ions. While a quarter of a century ago it was the flash photolysis that widened the boundaries of the photochemical investigations, to-day, beside the effect induced by the laser, reaction systems brought about by other electromagnetic and particle radiations, are the subjects of investigations. Considering that in complex processes it is the first step, the primary act, that initiates the events, from the point of view of the conversion also the secondary reactions, the chain propagation and the destruction of the carriers are of decisive significance, thus also the preconditions of these are to be known and examined. The chapters of the book deal with these problems and topics in a marvellously logical and concise manner. The reader does not find detailed discussions on individual reactions, but illustrations of the just discussed laws, and theories.

From practical point of view from among all gas reactions the combustion processes are of greatest importance, but they are also the most intricate at the same time. The introductory theoretical chapters of the monography and those on the relatively simpler processes as well, quasi as a matter of course, are closed by the treatment of the combustion and the flame, explosions and detonations.

The English-speaking readers find references mostly to previous monographs and reviews of the Western literature whereas they can enjoy a lot of citations to Russian papers.

The first authors of the monography Professor V. N. KONDRATIEV, beside N. N. SEMENOV, has been the greatest personality of the Soviet reaction kinetics, who not only contributed to the development by his fundamental discoveries, but also undertook the devoted work to select the correct values from among the data published in the literature with insufficient criticism. He not only specified the problems, methods and results again and again, but together with his young colleagues, grown up by his side, as for instance the second author of the monography E. E. NIKITIN and the coauthor of one of the chapters V. L. TAL'ROSE, always showed a newer and clearer picture on the state of gas reaction kinetics. His decease, just two years ago (22. 2. 1979), is deeply sorrowful, but it can be hoped that his life-work will not only live on at his colleagues, but will even be further developed.

On the get-up of the work it is only enough to remark that it was published by Springer-Verlag, and what is more, in the highest execution.

Z. G. SZABÓ

INDEX

PHYSICAL AND INORGANIC CHEMISTRY

ORGANIC CHEMISTRY

Printed in Hungary

A kiadásért felel az Akadémiai Kiadó igazgatója — Műszaki szerkesztő: Rózsa Katalin

A kézirat nyomdába érkezett: 1981. IV. 16. — Terjedelem: 9,75 (A/5) ív, 40 ábra

81.9556 Akadémiai Nyomda, Budapest — Felelős vezető: Bernát György

Les Acta Chimica paraissent en français, allemand, anglais et russe et publient des mémoires du domaine des sciences chimiques.

Les Acta Chimica sont publiés sous forme de fascicules. Quatre fascicules seront réunis en un volume (3 volumes par an).

On est prié d'envoyer les manuscrits destinés à la rédaction à l'adresse suivante:

Acta Chimica
Budapest, P.O.B. 67, H-1450, Hongrie

Toute correspondance doit être envoyée à cette même adresse.

La rédaction ne rend pas de manuscript.

Abonnement en Hongrie à l'Akadémiai Kiadó (1363 Budapest, P.O.B. 24, C. C. B. 215 11488) à l'étranger à l'Entreprise du Commerce Extérieur « Kultura » (H-1389 Budapest 62, P.O.B. 149 Compte-courant No. 218 10990) ou chez représentants à l'étranger.

Die Acta Chimica veröffentlichen Abhandlungen aus dem Bereich der chemischen Wissenschaften in deutscher, englischer, französischer und russischer Sprache.

Die Acta Chimica erscheinen in Heften wechselnden Umfanges. Vier Hefte bilden einen Band. Jährlich erscheinen 3 Bände.

Die zur Veröffentlichung bestimmten Manuskripte sind an folgende Adresse zu senden

Acta Chimica
Budapest, Postfach 67, H-1450, Ungarn

An die gleiche Anschrift ist jede für die Redaktion bestimmte Korrespondenz zu richten.

Manuskripte werden nicht zurückerstattet.

Bestellbar für das Inland bei Akadémiai Kiadó (1363 Budapest, Postfach 24, Bankkonto Nr. 215 11488), für das Ausland bei »Kultura« Außenhandelsunternehmen (H-1389 Budapest 62, P.O.B. 149. Bankkonto Nr. 218 10990) oder seinen Auslandsvertretungen.

«Acta Chimica» издают статы по химии на русском, английском, французском и немецком языках.

«Acta Chimica» выходит отдельными выпусками разного объема, 4 выпуска составляют один том и за год выходят 3 тома.

Предназначенные для публикации рукописи следует направлять по адресу:

Acta Chimica
Budapest, P.O.B. 67, H-1450, ВНР

Всякую корреспонденцию в редакцию направляйте по этому же адресу.

Редакция рукописей не возвращает.

Отечественные подписчики направляйте свои заявки по адресу Издательства Академии Наук (1363 Budapest, P.O.B. 24. Текущий счет 215 11488), а иностранные подписчики через организацию по внешней торговле «Kultura» (H-1389 Budapest 62, P.O.B. 149. Текущий счет 218 10990) или через ее заграничные представительства и уполномоченных.

Reviews of the Hungarian Academy of Sciences are obtainable at the following addresses:

AUSTRALIA
C.B.D LIBRARY AND SUBSCRIPTION SERVICE, Box 4886, G.P.O., *Sydney N.S.W. 2001*
COSMOS BOOKSHOP, 145 Ackland Street, *St. Kilda (Melbourne), Victoria 3182*

AUSTRIA
GLOBUS, Höchstädtplatz 4, *1200 Wien XX*

BELGIUM
OFFICE INTERNATIONAL DE LIBRAIRIE, 30 Avenue Marnix, *1050 Bruxelles*
LIBRAIRIE DU MONDE ENTIER, 162 Rue du Midi *1000 Bruxelles*

BULGARIA
HEMUS Bulvar Ruszki 6, *Sofia*

CANADA
PANNONIA BOOKS, P.O. Box 1017, Postal Station "B", *Toronto, Ontario M5T 2T8*

CHINA
CNPICOR, Periodical Department, P.O. Box 50, *Peking*

CZECHOSLOVAKIA
MAD'ARSKÁ KULTURA, Národní třida 22, *115 66 Praha*
PNS DOVOZ TISKU, Vinohradská 46, *Praha 2*
PNS DOVOZ TLAČE, *Bratislava 2*

DENMARK
EJNAR MUNKSGAARD Norregade 6, *1165 Copenhagen*

FINLAND
AKATEEMINEN KIRJAKAUPPA, P.O. Box 128, *SF-00101 Helsinki 10*

FRANCE
EUROPERIODIQUES S. A., 31 Avenue de Versailles, *78170 La Celle St.-Cloud*
LIBRAIRIE LAVOISIER, 11 rue Lavoisier, *75008 Paris*
OFFICE INTERNATIONAL DE DOCUMENTATION ET LIBRAIRIE, 48 rue Gay-Lussac, *75240 Paris Cedex 05*

GERMAN DEMOCRATIC REPUBLIC
HAUS DER UNGARISCHEN KULTUR, Karl-Liebknecht-Strasse 9, *DDR-102 Berlin*
DEUTSCHE POST ZEITUNGSVERTRIEBSAMT, Strasse der Pariser Kommüne 3—4, *DDR-104 Berlin*

GERMAN FEDERAL REPUBLIC
KUNST UND WISSEN ERICH BIEBER, Postfach 46, *7000 Stuttgart 1*

GREAT BRITAIN
BLACKWELL'S PERIODICALS DIVISION, Hythe Bridge Street, *Oxford OX1 2ET*
BUMPUS, HALDANE AND MAXWELL LTD., Cowper Works, *Olney, Bucks MK46 4BN*
COLLET'S HOLDINGS LTD., Denington Estate, *Wellingborough, Northants NN8 2QT*
W.M. DAWSON AND SONS LTD., Cannon House, *Folkestone, Kent CT19 5EE*
H. K LEWIS AND CO., 136 Gower Street, *London WC1E 6BS*

GREECE
KOSTARAKIS BROTHERS, International Booksellers, 2 Hippokratous Street, *Athens-143*

HOLLAND
MEULENHOFF-BRUNA B.V., Beulingstraat 2, *Amsterdam*
MARTINUS NIJHOFF B.V., Lange Voorhout 9—11, *Den Haag*
SWETS SUBSCRIPTION SERVICE, 347b Heereweg, *Lisse*

INDIA
ALLIED PUBLISHING PRIVATE LTD., 13/14 Asat Ali Road, *New Delhi 110001*
150 B-6 Mount Road, *Madras 600002*
INTERNATIONAL BOOK HOUSE PVT. LTD., Madame Cama Road, *Bombay 400039*
THE STATE TRADING CORPORATION OF INDIA LTD., Books Import Division, Chandralok, 36 Janpath, *New Delhi 110001*

ITALY
EUGENIO CARLUCCI, P.O. Box 252, *70100 Bari*
INTERSCIENTIA, Via Mazzé 28, *10149 Torino*
LIBRERIA COMMISSIONARIA SANSONI, Via Lamarmora 45, *50121 Firenze*
SANTO VANASIA, Via M. Macchi 58, *20124 Milano*
D. E. A., Via Lima 28, *00198 Roma*

JAPAN
KINOKUNIYA BOOK-STORE CO. LTD., 17-7, Shinjuku-ku 3 chome, Shinjuku-ku, *Tokyo 160-91*
MARUZEN COMPANY LTD., Book Department P.O. Box 5056 Tokyo International, *Tokyo 100-31*
NAUKA LTD., IMPORT DEPARTMENT, 2-30-19 Minami Ikebukuro, Toshima-ku, *Tokyo 171*

KOREA
CHULPANMUL, *Phenjan*

NORWAY
TANUM-CAMMERMEYER, Karl Johansgatan 41—43, *1000 Oslo*

POLAND
WĘGIERSKI INSTYTUT KULTURY, Marszałkowska 80, *Warszawa*
CKP I W ul. Towarowa 28 *00-958 Warsawa*

ROMANIA
D. E. P., *Bucureşti*
ROMLIBRI, Str. Biserica Amzei 7, *Bucureşti*

SOVIET UNION
SOJUZPETCHATJ — IMPORT, *Moscow*
and the post offices in each town
MEZHDUNARODNAYA KNIGA, *Moscow G-200*

SPAIN
DIAZ DE SANTOS, Lagasca 95, *Madrid 6*

SWEDEN
ALMQVIST AND WIKSELL, Gamla Brogatan 26, *101 20 Stockholm*
GUMPERTS UNIVERSITETSBOKHANDEL AB, Box 346, *401 25 Göteborg 1*

SWITZERLAND
KARGER LIBRI AG, Petersgraben 31, *4011 Base*

USA
EBSCO SUBSCRIPTION SERVICES, P.O. Box 1943, *Birmingham, Alabama 35201*
F. W. FAXON COMPANY, INC., 15 Southwest Park, *Westwood, Mass, 02090*
THE MOORE-COTTRELL SUBSCRIPTION AGENCIES, *North Cohocton, N. Y. 14868*
READ-MORE PUBLICATIONS, INC., 140 Cedar Street, *New York, N. Y. 10006*
STECHERT-MACMILLAN INC., 7250 Westfield Avenue, *Pennsauken N. J. 08110*

VIETNAM
XUNHASABA, 32, Hai Ba Trung, *Hanoi*

YUGOSLAVIA
JUGOSLAVENSKA KNJIGA, Terazije 27, *Beograd*
FORUM, Vojvode Mišića 1, *21000 Novi Sad*

20. XI. 1981 HU ISSN 0001—5407 Index: 26.007

ACTA CHIMICA

ACADEMIAE SCIENTIARUM HUNGARICAE

TOMUS 108 FASCICULUS 4

AKADÉMIAI KIADÓ, BUDAPEST

1981

ACTA CHIM. ACAD. SCI. HUNG. ACASA2 108 (4) 325–429 (1981)

ACTA CHIMICA

A MAGYAR TUDOMÁNYOS AKADÉMIA KÉMIAI TUDOMÁNYOK OSZTÁLYÁNAK IDEGEN NYELVŰ KÖZLEMÉNYEI

Acta Chimica is a journal for the publication of papers on all aspects of chemistry in English, German, French and Russian.

Acta Chimica is published in 3 volumes per year. Each volume consists of 4 issues of varying size.

Manuscripts should be sent to

Acta Chimica
Budapest, P.O. Box 67, H-1450, Hungary

Correspondence with the editors should be sent to the same address. Manuscripts are not returned to the authors.

Hungarian subscribers should order from Akadémiai Kiadó, 1363 Budapest, P.O.B. 24. Account No. 215 11488.

Orders from other countries are to be sent to "Kultura" Foreign Trading Company (H-1389 Budapest 62, P.O.B. 149. Account No. 218 10990) or its representatives abroad.

Acta Chimica Academiae Scientiarum Hungaricae, Tomus 108 (4), pp. 325—332 (1981)

MÖSSBAUER STUDY OF IRON(II) AND IRON(III) COMPLEXES OF SOME NITROGEN-, OXYGEN- AND SULPHUR DONOR LIGANDS. REDUCTION OF IRON(III) BY THE MERCAPTIDE GROUP

G. L. SAWHNEY,[1] J. S. BAIJAL,[1] S. CHANDRA[2]* and K. B. PANDEYA[3]

([1] *Department of Physics and Astrophysics, University of Delhi, Delhi,*
[2] *Department of Chemistry, Zakir Hussain College, Ajmeri Gate, Delhi,*
[3] *Department of Chemistry University of Delhi, Delhi, India*)

Received July 21, 1980

Accepted for publication December 12, 1980**

Complex formation reactions of iron(II) and iron(III) with semicarbazones and thiosemicarbazones of pyruvic acid and phenyl pyruvic acid have been studied by magnetic measurements and Mössbauer spectroscopy. With iron(II) all the ligands form hexa-coordinated octahedral complexes of the type Fe(ligand-H_2). With iron(III) semicarbazones the complexes of the composition [Fe(ligand-$H)_2$](OH) are formed. Thiosemicarbazones on the other hand, first reduce iron(III) to iron(II) and then form iron(II) complexes of the type Fe(ligand-$H)_2$.

Introduction

The Mössbauer spectra of iron complexes provide information about the iron configuration and have been progressively utilized in elucidating the structure and bonding [1, 2] in a large number of complexes. In particular, the isomer shift (δ) measures the electron density at the iron nucleus and the quadrupole splitting reflects the asymmetry of the iron electronic wave function. These two pieces of information can not be used to define the several molecular orbitals important in chemical bonding, but they may prove useful in deciding between various models of given molecule. The Mössbauer hyperfine parameters can be very useful when one studies a series of compounds in which a single group is varied systematically. The electronic structure of iron is influenced by steric rather than electronic effects induced by the substituents has been evidenced in recent studies on a series of iron(II) complexes [3].

Study on iron complexes of nitrogen, oxygen and sulphur donor ligands are important in view of these donor atoms being mainly encountered in the iron proteins; iron-sulphur proteins, in particular, being subject of immense interest. Transition metal complexes of semicarbazones and thiosemicarba-

* To whom correspondence should be addressed
** In final form accepted April 17, 1981

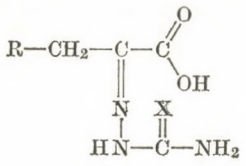

(I)

(a) R = H, X = O
(b) R = H, X = S
(c) R = Ph, X = O
(d) R = Ph, X = S

zones have drawn much attention recently [4]. This paper describes complexation reactions of iron(II) and iron(III) with pyruvic acid semicarbazone **Ia**, pyruvic acid thiosemicarbazone **Ib**, phenyl pyruvic acid semicarbazone **Ic** and phenyl pyruvic acid thiosemicarbazone **Id**.

In the course of reaction of iron(III) salts with pyruvic acid and phenyl pyruvic acid thiosemicarbazone it has been observed that the ligand first reduces iron(III) to iron(II) forming finally iron(II) complex, same as obtained from the reaction of iron(II) and pyruvic and phenyl pyruvic acid thiosemicarbazones.

To ascertain that the reduction is caused by the thiosemicarbazone moiety and not by the pyruvic acid part of the ligand molecules, reactions of the semicarbazones of pyruvic acid and phenyl pyruvic acid on iron(II) and iron(III) were also studied. In these cases no reduction of iron(III) occurred.

Experimental

Preparation of the ligands

Semicarbazones: Aqueous solution of semicarbazide hydrochloride and ethanolic solution of the ketone were mixed together in equimolar ratio. Equimolar amount of sodium acetate (aqueous) was also added and mixture was refluxed on a water bath and then concentrated. On cooling in ice bath white coloured semicarbazones precipitated out. The same was filtered, washed with water and recrystallized from hot ethanol.

Analysis for pyruvic acid semicarbazone ($C_4H_7N_3O_3$):

	% C	% H	% N
Found:	32.90	4.96	29.10
Calculated:	33.1	4.8	28.9

or p henyl pyruvic acid semicarbazone ($C_{10}H_{11}N_3O_3$):

	% C	% H	% N
Found:	54.45	5.54	19.20
Calculated:	54.3	5.43	19.00

Thiosemicarbazones: Aqueous solution of thiosemicarbazide and ethanolic solution of the ketone were mixed together in equimolar ratio. A small amount of glacial acetic acid was also mixed and the contents were refluxed on water bath for about 6 hrs and concentrated. On cooling in ice bath white coloured thiosemicarbazones separated out, which was worked out as above.

Analysis for pyruvic acid thiosemicarbazone ($C_4H_7N_3O_2S$):

	% C	% H	% N	% S
Found:	29.70	4.25	26.22	19.70
Calculated:	29.8	4.4	26.1	19.9

and for phenyl pyruvic acid thiosemicarbazone ($C_{10}H_{11}N_3O_2S$):

	% C	% H	% N	% S
Found:	50.8	4.20	17.45	13.20
Calculated:	50.6	4.6	17.7	13.5

Reactions with iron(II) salts

Hot ethanolic solutions of $FeCl_2 \cdot 4\,H_2O$ and the respective ligand were mixed together. Dark brown coloured complexes separated out instantaneously in the case of thiosemicarbazones. In case of semicarbazones the contents were refluxed for about 3 hrs and cooled when green coloured complexes separated out. These were filtered, washed with 50% ethanol and dried in electric oven at ~60 °C.

Reactions with iron(III) salts

With semicarbazones: A method similar to that in the case of iron(II) complexes was followed using anhydrous $FeCl_3$ in place of $FeCl_2 \cdot 4\,H_2O$. Dark brown coloured complexes were obtained.

With thiosemicarbazones: Reaction was carried out in the same way as in the case of iron(II) thiosemicarbazones using anhydrous $FeCl_3$ in place of $FeCl_2 \cdot 4\,H_2O$. Dark brown coloured complexes separated out instantaneously. When worked out these were found to be the same complexes as those obtained with iron(II) salt.

Physical measurements

Magnetic susceptibility measurements on powder form of the complexes were carried out by GOUY method using mercury tetrathiocyanatocobaltate(II) ($\chi_g = 20.71 \times 10^{-6}$ SI) as calibrant. The Mössbauer studies were carried out by using a 55.5×10^7 Bq (15 Cm) ^{57}Co (in Pd metrix) source held at room temperature on the powdered form of the complexes. The spectra were recorded on a 512 multichannel analyser in MSC mode. The data were analysed using a least square fitting programme on an IBM 360 computer. Infrared spectra of the complexes were recorded on Perkin–Elmer 621 automatic recording spectrophotometer in KBr medium.

Results and Discussion

Results of elemental analysis of the complexes obtained are given in Table I. Table IV presents the magnetic moments and Mössbauer data.

Table I

Elemental analysis

Reactants*	Complex obtained	Elemental analysis found/ (calcd.)%			
		Fe	C	H	N
$FeCl_2 \cdot 4\ H_2O$ + pysc	$Fe(pysc\text{-}H_2)$	15.90 (16.27)	27.80 (27.90)	3.62 (3.49)	24.34 (24.42)
$FeCl_2 \cdot 4\ H_2O$ + ppysc	$Fe(ppysc\text{-}H)_2$	11.51 (11.30)	48.30 (48.39)	4.13 (4.03)	16.64 (16.85)
$FeCl_2 \cdot 4\ H_2O$ + pytsc	$Fe(pytsc\text{-}H)_2$	14.90 (14.81)	25.73 (25.53)	3.29 (3.19)	22.56 (22.34)
$FeCl_2 \cdot 4\ H_2O$ + ppytsc	$Fe(ppytsc\text{-}H)_2$	10.61 (10.36)	45.65 (45.45)	3.99 (3.79)	15.60 (15.91)
$FeCl_3$(anhydrous) + pysc	$Fe(pysc\text{-}H)_2(OH)$	15.50 (15.42)	26.68 (26.59)	3.75 (3.60)	23.47 (23.27)
$FeCl_3$(anhydrous) + ppysc	$Fe(ppysc\text{-}H)_2(OH)$	10.92 (10.82)	46.53 (46.78)	4.03 (4.09)	16.52 (16.37)
$FeCl_3$(anhydrous) + pytsc	$Fe(pytsc\text{-}H)_2$	14.71 (14.81)	25.60 (25.53)	3.04 (3.19)	22.48 (22.34)
$FeCl_3$(anhydrous) + ppytsc	$Fe(ppytsc\text{-}H)_2$	10.40 (10.36)	45.36 (45.45)	3.72 (3.79)	15.78 (15.91)

* pysc = pyruvic acid semicarbazone,
ppysc = phenyl pyruvic acid semicarbazone,
pytsc = pyruvic acid thiosemicarbazone,
ppytsc = phenyl pyruvic acid thiosemicarbazone

The infrared spectra of all the complexes is provided direct information about the coordination of ligands. Pyruvic acid semicarbazone and thiosemicarbazone coordinate to the metal atom as a terdentate ligand [5, 6]. The infrared spectrum of phenyl pyruvic acid semicarbazone molecule shows bands due to the CO stretching vibrations of the semicarbazide moiety and the carboxyl groups and the ν(C=N) stretching vibrations at 1680—1750 cm^{-1} and 1620 cm^{-1}, respectively (Table II). On complex formation these bands are shifted towards lower side by 20—60 cm^{-1}. It indicates that phenyl pyruvic acid semicarbazone also behaves as a tridentate ligand, coordinates to the metal through oxygen of semicarbazide and carboxyl group and the ν(C=N). Infrared spectrum of phenyl pyruvic acid thiosemicarbazone shows bands at 1620 and 1700 cm^{-1} assignable to the ν(C=N) and COOH stretching frequencies, respectively. On complex formation these bands shifted towards lower side (Table II). Although definite assignment for νC=S vibration is difficult, it appears that the bands at 1090 cm^{-1} and 1025 cm^{-1} are due to ν(C=S) vibration as suggested earlier workers [7, 8]. The position of this band is also shifted towards lower side.

With iron(II) all the ligands form complexes of composition 1 : 2, metal-ligand. Hexacoordinate pseudo-octahedral structure of the type (**I**) is readily achieved with two tridentate ligand molecules per metal ion.

Table II

Important IR bands (cm^{-1})

Compound	$\nu_{C=O}$ semicarbazide moiety	$\nu_{C=O}$ carboxyl group	$\nu_{C=N}$	$\nu_{C=S}$
pysc	1680 (s)	1750 (s)	1620 (s)	—
ppysc	1680 (s)	1755 (s)	1610 (s)	—
$Fe(pysc\text{-}H)_2$	1650 (s)	1730 (s)	1605 (s)	—
$Fe(ppysc\text{-}H)_2$	1675 (s)	1755 (s)	1630 (s)	—
pytsc	—	1700 (s)	1620 (s)	1090 (m) 1025 (w)
$Fe(pytsc\text{-}H)_2$	—	1680 (s)	1600 (s)	1080 (m) 1020 (w)
ppytsc	—	1710 (s)	1625 (s)	1095 (m) 1020 (w)
$Fe(ppytsc\text{-}H)_2$	—	1695 (s)	1605 (s)	1085 (m) 1020 (w)

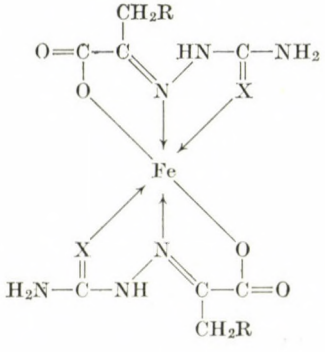

(I)

R = H or C_6H_5

X = O or S

All such complexes show magnetic moments corresponding to hexa-coordinate high-spin iron(II). Mössbauer parameters are also in conformity with such a structure. All the complexes exhibit isomer shift values in the range of high-spin iron(II) [9]. The isomer shift values for the semicarbazone complexes are larger than for the thiosemicarbazone complexes indicating that the S electron density on the iron atom is less in the semicarbazone complexes ($FeO_2N_2O_2$ core) than in thiosemicarbazone complexes ($FeO_2N_2S_2$ core). The replacement of sulphur by oxygen (a more electronegative atom) as a donor apparently leads to decrease in the S electron density of the centra

metal atom. Similar observations have been reported by GERBELEU *et al.* [10] for some iron(II) complexes of semicarbazide and thiosemicarbazide.

All the iron(II) complexes show quadrupole splitting values in the range for high-spin iron(II) [11—13]. Also all the complexes show strong temperature dependence of the quadrupole splitting value, with exception of the phenyl pyruvic acid thiosemicarbazone complex. Quadrupole splitting is dependent on the parameters Δ_1 and Δ_2, temperature and covalency coefficient α^2, as given by [14].

$$\Delta E_Q = 2/7 e^2 Q(1 - R) \langle r^{-3} \rangle \alpha^2 F(\Delta_1, \Delta_2, T, \alpha^2 \lambda_0) = 5.4 \alpha^2 F = 5.4 F \text{ mms}^{-1}$$

It may be noted that the parameter F takes into account the contribution by the lattice. For the complexes showing temperature dependent $Q.S.$ values the ligand field splittings Δ_1 and Δ_2 are of the same order as kT. The temperature independent value of the phenyl pyruvic acid complex is, however, intriguing.

The complexes obtained from the reaction of iron(III) salt and the thiosemicarbazone ligands also show composition Fe(ligand-H)$_2$. They also show magnetic moments and Mössbauer parameters almost identical to those of he correponding iron(II) complexes. It is obvious therefore that the thiosemicarbazone ligands first reduce iron(III) to iron(II) and then form the iron(II) complexes. The mercaptide group in the thiolo form (*b*) of the thiosemicarbazones is well known as a mild reducing agent [15].

(*a*) (*b*)

The suggested reduction of iron(III) to iron(II) may be represented as [6].

$$Fe^{3+} + -SH \rightleftharpoons Fe^{2+} + \frac{1}{2}(-S-S-) + H^+$$

The nujol mull electronic spectra of the complexes exhibit a broad 'd—d' band in the region 10,200—11,700 cm^{-1} (Table III). This band shows none of the splitting which is expected for high-spin iron(II) in the ligand field of less than *Oh* symmetry. It is assumed that this is due to a $^5T_{2g} \rightarrow {}^5E_g$ transition and that the broadness of the band is due to some splitting of the ^5E_g excited state. It is reasonable to suggests that all the complexes are hexacoordinate octahedral.

Table III

Electronic spectral bands (cm^{-1})

Compound	$^5T_{2g} \rightarrow {}^5E_g$ cm^{-1}
$Fe(pysc\text{-}H)_2$	10,200
$Fe(ppysc\text{-}H)_2$	10,400
$Fe(pytsc\text{-}H)_2$	10,600
$Fe(ppytsc\text{-}H)_2$	10,800

Table IV

Mössbauer and magnetic parameters

Complex**	Temp. (K)	Q.S. (mms^{-1})	I.S.* (mms^{-1})	μ_{eff} (BM)
$Fe(pysc\text{-}H)_2$	300	2.67	1.50	4.9
	78	3.16	1.63	
$Fe(ppysc\text{-}H)_2$	300	2.80	1.48	4.9
	78	3.34	1.56	
$Fe(pytsc\text{-}H)_2$	300	2.48	1.26	4.8
	78	3.14	1.36	
$Fe(ppytsc\text{-}H)_2$	300	3.28	1.17	5.1
	78	3.38	1.36	
$Fe(pysc\text{-}H)_2(OH)$	300	0.56	0.61	5.9
	78	0.60	0.68	
$Fe(ppysc\text{-}H)_2(OH)$	300	0.80	0.63	5.8
	78	0.83	0.66	
$^{**}Fe(pytsc\text{-}H)_2$	300	2.49	1.17	4.8
	78	3.21	1.33	
$^{**}Fe(ppytsc\text{-}H)_2$	300	3.33	1.17	5.3
	78	3.34	1.33	

* All values with respect to sodium nitroprusside
** These complexes were obtained by the reaction of $FeCl_3$ with the ligands

With the semicarbazone ligands, iron(III) forms complexes of composition $[Fe(ligand\text{-}H)_2]OH$. The following structure may be considered for these complexes. Both the complexes are of high-spin type showing magnetic moments in the range of 5.8—5.9 BM. Infrared spectra of these complexes show absorption at 3625 cm^{-1} indicating presence of free OH group in these complexes [16].

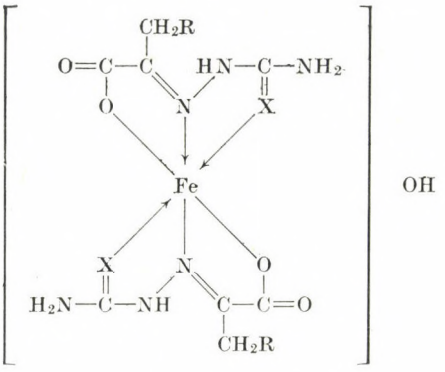

The two complexes show Mössbauer parameters corresponding to high-spin [17, 18] iron(III) (Table IV).

*

Our grateful thanks are due to CSIR, New Delhi for awarding a SRF to one of us (S. CHANDRA).

REFERENCES

[1] DANON, J.: Rev. Med. Phys., **36,** 459 (1963)
[2] GREENWOOD, N. N.: Mössbauer Spectroscopy, Chapman and Hill, London 1971
[3] SAITEVITCH, E., BAGGIS, K., PADI, M. A. de: Inorg. Chem. Acta, **17,** 59 (1976)
[4] CAMPBELL, M. J. M.: Coord. Chem. Rev., **15,** 279 (1975)
[5] ABLOV, A. V., BELICHUK, N. I., CHAPURINA, L. F.: Russ. J. Inorg. Chem., **15,** 57 (1970)
[6] ABLOV, A. V., GERBELEU, N. V.: Russ. J. Inorg. Chem., **15,** 952 (1970)
[7] BELLAMY, L. J., ROGASH, P. I.: J. Chem. Soc., **1960,** 2218
[8] YAMAGUCHI, A., PENCLAND, R. B. MIZUSHIMA, S., LANE, J. J., CARRAN, C., OUAGLIANE, J. B.: J. Am. Chem Soc., **80,** 527 (1958)
[9] BIRCHALL, T.: Can. J. Chem., **47,** 135 (1969)
[10] ABLOV, A. V., GERBELEU, N. V., GOLDANSKII, V. I., STUKAN, R. A., TURTA, K. I.: Russ. J. Inorg. Chem., **16,** 96 (1971)
[11] ERICKSEN, N. E.: Advan. Chem., Ser. No. **68,** 86 (1967)
[12] MAY, L.: Advan. Chem. Ser., No. **68,** 52 (1967)
[13] RILEY, D. P., MEWELL, P. H., STONE, J. A., BUSCH, D. H.: Inorg. Chem., **14,** 490 (1975)
[14] INGALLS, R.: Phys. Rev., **133A,** 787 (1964)
[15] (a) COTTELAIN, F.: Bull. Chem. Soc. Chim., **1945,** 49; (b) JENSEN, K. A., RAVEKE, E., MEDSEN, Z.: Anorg. Allgem. Chem., **219,** 243 (1934)
[16] NAKAMOTO, K.: "Infrared Spectra of Inorganic and Coordination Compounds" 229 p. New York Wiley-Interscience, 1970
[17] BANCROFT, G. M., MADDOCK, A. G., ONG, W. K., PRINCE, R. H.: J. Chem. Soc. (A), **1966,** 723
[18] RUSSO, Z., CALOGARO, S., BUNESCI, N., PETRERA, M.: J. Inorg. Nucl. Chem., **41,** 25 (1979)

G. L. SAWHNEY, J. S. BAIJAL — University of Delhi, Delhi—110007, India
S. CHANDRA — Zakir Husain College, Ajmeri Gate, Delhi—110006, India
K. B. PANDEYA — University of Delhi, Delhi—110007, India

Acta Chimica Academiae Scientiarum Hungaricae, Tomus 108 (4), pp. 333—342 (1981)

STEREOSELECTIVE HYDROGENOLYSIS OF DIOXOLANE-TYPE BENZYLIDENE ACETALS

PREPARATION OF MONO- AND DI-*O*-BENZYL ETHERS OF BENZYL β-L-ARABINOPYRANOSIDE

A. LIPTÁK, Z. SZURMAI, J. HARANGI and P. NÁNÁSI

(*Institute of Biochemistry, Kossuth Lajos University, Debrecen*)

Received November 4, 1980

Accepted for publication January 6, 1981

Both isomers (**2** and **3**) of benzyl 3,4-*O*-benzylidene-β-L-arabinopyranoside, their 2-*O*-benzyl- (**4** and **5**), 2-*O*-allyl- (**6** and **7**) and 2-*O*-*p*-toluenesulfonyl (**8** and **9**) derivatives were prepared and hydrogenolyzed with $LiAlH_4$–$AlCl_3$ reagent. The *exo*-isomers (**2**, **4**, **6**) transformed into the 3-*O*-benzyl derivatives (**10**, **14**, **16**), whereas the *endo*-isomers (**3**, **5**, **7**, **9**) gave predominantly the 4-*O*-benzyl ethers (**11**, **15**, **17**, **19**). As the only exception, compound **8** gave a 1 : 1 mixture of the corresponding 3-*O*- and 4-*O*-benzyl ethers.

Introduction

In continuation of our studies on the chemistry of dioxolane-type benzylidene acetals, we were interested in the synthesis of benzyl ethers of benzyl β-L-arabinopyranoside. Recently, we have shown that the hydrogenolysis of the isomers of benzyl 3,4-*O*-benzylidene-β-D-arabinopyranoside derivatives is a convenient route for the preparation of the benzyl ethers of benzyl β-D-arabinopyranoside [1]. Our efforts in extending this method to L-arabinose were motivated by (i) the difficulties in the synthesis of oligosaccharides containing L-arabinose due to the lack of suitably protected arabinose derivatives, and (ii) the fact that the preparation of the methyl ethers of L-arabinose is very laborious. Both difficulties could be eliminated by elaborating a simple method for the preparation of the benzyl ethers of benzyl β-L-arabinopyranoside.

Results and Discussion

The benzylidene acetals of different arabinopyranosides were among the first representatives when both isomers of the dioxolane-type benzylidene derivatives were prepared and isolated [2—5]. For our purposes the *exo*- and *endo*-isomers (**2** and **3**) of benzyl 3,4-*O*-benzylidene-β-L-arabinopyranoside served as the starting materials which were prepared from benzyl β-L-arabinopyranoside [6] (**1**) using α,α-dimethoxytoluene in the presence of *p*-toluene sulfonic acid catalyst. Compounds **2** and **3** were obtained in almost equal

quantities showing a thermodynamic control to operate under the reaction conditions used. The *exo*- and *endo*-isomers (**2** and **3**) could be separated by crystallization. Conventional benzylation, allylation and tosylation of **2** and **3** resulted in the 2-*O*-benzyl- (**4** and **5**), 2-*O*-allyl- (**6** and **7**) and 2-*O*-*p*-toluenesulfonyl (**8** and **9**) derivatives, respectively. It is to be noted that the *exo*-isomers have higher melting points than the *endo*-isomers, and the *exo*-isomers form readily crystals.

Comparison of the chemical shifts of the acetal protons of compounds **2**—**9** showed that — with the exception of compounds **8** and **9** — the rule proposed by BAGGETT *et al.* [3] is valid, *i.e.* the signal of the protons of the

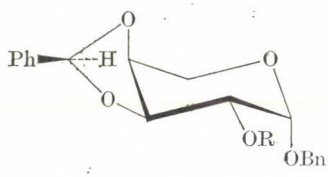

2 R = H
4 R = Bn
6 R = All
8 R = Ts

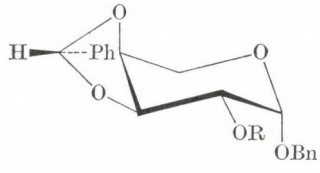

3 R = H
5 R = Bn
7 R = All
9 R = Ts

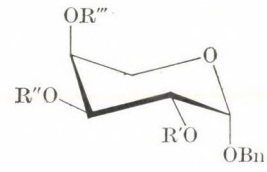

10 R′ = H, R″ = Bn, R‴ = H
11 R′ = H, R″ = H, R‴ = Bn
12 R′ = Ac, R″ = Bn, R‴ = Ac
13 R′ = Ac, R″ = Ac, R‴ = Bn
14 R′ = Bn, R″ = Bn, R‴ = H
15 R′ = Bn, R″ = H, R‴ = Bn
16 R′ = All, R″ = Bn, R‴ = H
17 R′ = All, R″ = H, R‴ = Bn
18 R′ = Ts, R″ = Bn, R‴ = H
19 R′ = Ts, R″ = H, R‴ = Bn
20 R′ = Bn, R″ = H, R‴ = H
21 R′ = All, R″ = H, R‴ = H
22 R′ = All, R″ = Bn, R‴ = Bn
23 R′ = H, R″ = Bn, R‴ = Bn

Ac = Acetyl, All = Allyl, Bn = Benzyl, Ts = Tosyl

exo-isomers appear at lower field compared with those of the *endo*-isomers. To our knowledge, this is the first exception to the rule mentioned above. Perhaps, this anomaly may be explained by the anisotropic shielding of the aromatic ring of the *p*-toluenesulfonyl group.

The ^{1}H-NMR spectra of compounds **2**—**9** in chloroform-*d* at 100 MHz were entirely first-order, and the magnitudes of the vicinal proton–proton

couplings observed, were, as expected, inconsistent with a chair conformation.

These skeleton proton resonances were analysed as follows. The signals near to 5 ppm were readily assigned to the anomeric protons, being the only signals with correct chemical shift which should be doublets. Additionally, the values of the $J_{1,2}$ coupling constants (3.0—3.8 Hz) were acceptable for *equatorial–axial* protons at C-1 and C-2 on a pyranoside ring. The mutual splitting patterns of the remaining protons permitted the assignments shown in Table I.

The observed values of $J_{2,3}$ in the spectra of the investigated acetal compounds were far too small for *axial–axial* orientation. These were extremely small in the case of the *endo*-isomer. The values of $J_{3,4}$ were found to be very large for *axial–equatorial* arrangement and these were larger in the case of the *endo*-isomers than for the *exo*-compounds. Evidently, the 3,4-*O*-benzylidene group causes gross distortion of the $^4C_1$ (L) conformation and this distortion is extremely strong at the bridgehead carbons. The values of the $^3J_{H,H}$ coupling constants show that the pyranoside ring has a strongly flattened conformation. This assumption has been also supported by X-ray measurements [7].

The reductive ring cleavage of compound **2** with chloroalane at 45 °C resulted in two compounds the ratio of which was found to be 72 : 28 by GLC. The main product was stable towards $NaIO_4$, so it must be benzyl 3-*O*-benzyl-β-L-arabinopyranoside (**10**). The minor product, benzyl 4-*O*-benyzl--β-L-arabinopyranoside (**11**) was removed from the reaction mixture by periodate oxidation. The oxidized reaction mixture was acetylated and purified by column chromatography to give the diacetate (**12**) of compound **10**. Catalytic deacetylation resulted in syrupy **10**. The hydrogenolysis of **2** at room temperature showed somewhat lower selectivity; the ratio of **10** and **11** was 2 : 1. Hydrogenolysis of the *endo*-isomer (**3**) at 45 °C gave a mixture of **10** and **11** in a ratio of 1 : 9. The di-*O*-acetyl derivative (**13**) of **11** crystallized from the reaction mixture after acetylation. Deacetylation of **13** resulted in **11**.

A similar result was obtained in the hydrogenolysis of the 2-*O*-benzyl derivative (**4**) of the *exo*-isomer (**2**), but in this case the ratio of the resulting 3-*O*-benzyl- (**14**) and 4-*O*-benzyl (**15**) derivatives did not depend on the reaction temperature; a 9 : 1 ratio of **14** and **15** was observed both at room temperature and at 45 °C. The ring cleavage of the *endo*-isomer (**5**) resulted in a 1 : 49 mixture of **14** and **15** at room temperature and a 1 : 7 ratio at 45 °C. Both **14** and **15** were purified by crystallization.

The reductive ring cleavage of the isomeric 2-*O*-allyl derivatives (**6** and **7**) showed high selectivity at 45 °C, the ratio of benzyl 2-*O*-allyl-3-*O*-benzyl- (**16**) and benzyl 2-*O*-allyl-4-*O*-benzyl-β-L-arabinopyranoside (**17**) being 9 : 1 and 1 : 13, respectively. Compound **17** was crystalline, but **16** proved to be a syrup, inseparable from **17**.

The hydrogenolysis of the *p*-toluenesulfonyl derivative (**8**) of the *exo*-

Table I

^{1}H-NMR *parameters for compounds* **2**—**9**

	H–1	$J_{1,2}$	H–2	$J_{2,3}$	H–3	$J_{3,4}$	H–4	$J_{4,5}$	H–$5_{a,e}$	PhC*H*	$PhCH_2$	Other protons
2	4.97	3.6	3.89	7.2	4.43	5.5	4.15	1.8	3.96	6.18	4.78 and 4.53	2.66 (HO-2), 7.50—7.20 (2Ph)
4	4.94	3.5	3.69	7.9	4.68	5.6	4.16	1.7	3.95	6.02	4.74, 4.51 1 4.80, 4.65 2	7.50—7.20 (3Ph)
6	4.98	3.4	3.65	8.0	4.59	5.4	4.10	2.0	3.92	6.13	473 and 4.52	4.20—4.06 (—CH_2—), 5.36—5.09 (=CH_2), 6.10—5.70 (—CH=), 7.50—7.20 (2Ph)
8	5.13	3.0	4.60—4.40	—		—	4.12	—	3.93	5.58	4.72 and 4.50	2.35 (CH_3), 7.90—7.20 (aromatic protons)
3	4.89	3.8	3.84	5.8	4.33	6.3	4.20	1.8	4.01	5.84	4.78 and 4.52	2.96 (HO—2), 7.60—7.10 (2Ph)
5	4.84	3.4	3.58	7.4	4.52	6.1	4.25	1.8	4.04	5.89	4.75, 4.50 1 4.68, 4.50 2	7.55—7.20 (3Ph)
7	4.90	3.3	3.54	7.5	4.43	5.9	4.24—3.86	2.5*a* 1.6*e*		5.85	473 and 4.50	4.24—3.86 (—CH_2—), 5.20—4.96 (=CH_2), 6.00—5.60 (—CH=), 7.55—7.20 (2Ph)
9	5.13	2.6	4.48—4.40	—		—	4.22	—	4.06	5.74	4.72 and 4.50	2.29 (CH_3), 7.70—7.00 (aromatic protons)

Table II

^{1}H-NMR *parameters for compounds* **10**, **11**, **14**, **15**, **17**—**20**, **23**

	H—1	H—2	H—3	H—4	H—$5_{a,e}$	$PhCH_2$	OH	$J_{H,OH}$	Aromatic protons	Other protons
10	4.90 (d)		4.04—3.55 (m, 5H)			4.82—4.41 (m, 4H)	2.89 (s, 2H)	—	7.50—7.00 (m, 10H)	—
11	4.96 (d)		3.92—3.60 (m, 5H)			4.78—4.42 (m, 4H)	2.82 (s, 2H)	—	7.50—7.10 (m, 10H)	—
14	4.93 (d)		4.02—3.77 (m, 5H)			4.83—4.49 (m, 6H)	2.69 (s, 1H)	—	7.60—7.20 (m, 15H)	—
15	4.97 (d)	3.87—3.74 (m, 1H)	4.26—4.06 (m, 1H)	3.87—3.74 (m, 3H)		4.83—4.45 (m, 6H)	2.52 (d, 1H)	7 Hz	7.60—7.20 (m, 15H)	—
17	4.87 (d)	3.72—3.48 (m, 1H)	4.09—3.82 (m, 1H)	3.72—3.48 (m, 3H)		4.70—4.37 (m, 4H)	2.47 (d, 1H)	7 Hz	7.30—6.90 (m, 10H)	5.90—5.53 (m, 1H, —CH=) 5.20—4.92 (m, 2H, $=CH_2$) 4.09—3.82 (m, 2H, $-CH_2-$)
18	4.94 (d)	4.76—4.30 (m, 1H)	3.95—3.64 (m, 4H)			4.76—4.30 (m, 4H)	2.48 (s, 1H)	—	7.75—7.05 (m, 14H)	2.30 (s, 3H, CH_3)
19	4.90 (d)	4.72—4.28 (m, 1H)	4.01 (m, 1H)	3.76—3.64 (m, 3H)		4.72—4.28 (m, 4H)	2.26 (d, 1H)	8 Hz	7.80—6.95 (m, 14H)	2.32 (s, 3H, CH_3)
20	4.91 (d)		4.09—3.57 (m, 5H)			4.76—4.36 (m, 4H)	3.08 (s, 2H)	—	7.50—7.15 (m, 10H)	—
23	5.02 (d)	3.76—3.68 (m, 1H)	4.22—4.10 (m, 1H)	3.76—3.68 (m, 3H)		4.80—4.45 (m, 6H)	2.35 (s, 1H)	—	7.60—7.10 (m, 15H)	—

isomer was not selective, the ratio of the 3-*O*-benzyl- (**18**) and the 4-*O*-benzyl (**19**) derivatives obtained was nearly 1 : 1 by TLC, and this ratio was found to be independent of the reaction temperature. At the same time, the hydrogenolysis of **9** resulted in an excellent product distribution; the ratio of **18** and **19** was 1 : 19.

The fact that the hydrogenolysis of dioxolane-type benzylidene derivatives can be performed in the presence of tosyloxy protecting groups affords the possibility of producing *trans* hydroxy-tosyloxy derivatives of pyranosides, serving as starting materials for the synthesis of several deoxy sugar derivatives [8].

Comparing the stereoselectivity of the ring cleavage reactions, it can be established that the *endo*-isomers gave higher selectivity than the *exo*-isomers. It can be presumed that under the conditions of ring cleavage isomerization is a competing reaction. If the rate of the isomerization is commensurable with the rate of reduction, the selectivity should be very poor. Investigating the isomerization of dioxolane-type benzylidene acetals [9] it was found that the rate of isomerization of the *exo*-isomers was higher than that of the *endo*-isomers. However, the rate of the isomerization is strongly dependent on the type of the substituents at the neighbouring hydroxyl groups of the pyranoside ring, so the selectivity of the ring cleavage, depending on the character of the neighbouring substituents, may be explained by the difference in the rates of isomerization.

The mono-*O*-benzyl ethers of **1** were prepared as follows: the hydrogenolysis of **2** and **3** resulted in the 3-*O*-benzyl ether (**10**) and 4-*O*-benzyl ether (**11**) of **1**, respectively. The 2-*O*-benzyl ether (**20**) was prepared by mild acid hydrolysis of either **4** or **5**.

The 2,3- (**14**) and 2,4-di-*O*-benzyl (**15**) ethers of **1** were prepared by the hydrogenolysis of **4** and **5**. The 3,4-di-*O*-benzyl derivative (**23**) of **1** was synthesized by the following route: benzyl 2-*O*-allyl-β-L-arabinopyranoside (**21**), prepared by the hydrolysis of either **6** or **7**, was benzylated to compound **22**. Deallylation of **22**, using Pd/C–acetic acid–ethanol–water system [10] gave **23** in good yield.

^{1}H-NMR data for compounds **10**, **11**, **14**, **15**, **17**—**20** and **23** are shown in Table II.

Experimental

M.p.'s were determined on a Kofler hot-stage apparatus and are uncorrected. Optical rotations were measured with a Perkin–Elmer 241 automatic polarimeter. ^{1}H-NMR spectra were obtained on a JEOL MH-100 (100 MHz) instrument using TMS as internal standard. GLC was performed with a Hewlett—Packard 5840 A instrument. Columns: (*a*) 10% of UCW-982 on Chromosorb WAW-DMCS (80—100 mesh), 2 ft, 220°/2.5°; (*b*) 20% of SE-30 on Chromosorb W (60—80 mesh), 4 ft, 300° isothermal; (*c*) 10% of UCW-982 on Chromosorb

WAW-DMCS (80—100 mesh), 4 ft, 250° isothermal; (*d*) 10% of UCW-982 on Chromosorb WAW-DMCS (80-100 mesh), 2 ft, 250°/2.5°; nitrogen flow-rate 20 mL/min. TLC examination was carried out on DC-Alurolle Kieselgel 60 F (Merck), detection with 50% sulfuric acid. Kieselgel G (Reanal) was used for column chromatography.

Benzyl *exo*-(2) and *endo*-3,4-*O*-benzylidene-β-L-arabinopyranoside (3)

To a solution of benzyl β-L-arabinopyranoside (**1**, 10.0 g) in DMF (60 mL) α,α-dimethoxytoluene (10 g) and toluene-*p*-sulfonic acid (200 mg) were added and the solution was stirred in vacuum at 60 °C for 3 h. After cooling, the mixture was diluted with dichloromethane (300 mL) washed with 5% $NaHCO_3$ solution (2×30 mL) and water (2×30 mL), dried over Na_2SO_4 and concentrated. Traces of DMF were removed by vacuum distillation. The syrupy residue solidified on treatment with *n*-hexane. Recrystallization from ethanol (80 mL) gave **2** (2.89 g; 27.5%), m.p. 142—144 °C, $[\alpha]_D$ +158° (*c* = 0.35, chloroform), R_f 0.27 (benzene–ethyl acetate, 9 : 1), R_T 5.87 min (*a*).

$C_{19}H_{20}O_5$ (328.37). Calcd. C 69.49; H 6.14. Found C 64.87; H 7.21%.

The mother liquor from the crystallization of **2** was concentrated to about 20 mL. The crystalline product (a mixture of **2** and **3**) was filtered off (2.05 g), and the filtrate was concentrated. The residue was twice recrystallized from cyclohexane (40 mL) to give **3** (2.17 g; 15.9%), m.p. 92—94 °C, $[\alpha]_D$ +162° (*c* = 1.37, chloroform), R_f 0.35 (benzene–ethyl acetate, 9 : 1), R_T 5.27 min (*a*).

$C_{19}H_{20}O_5$ (328.37). Calcd. C 69.49; H 6.14. Found C 64.29; H 6.34%.

Benzyl 2-*O*-benzyl-*exo*-3,4-*O*-benzylidene-β-L-arabinopyranoside (4)

A mixture of **2** (3.0 g) powdered KOH (6 g), and benzyl chloride (30 mL) was kept at 100 °C for 4 h. The cooled mixture was diluted with dichloromethane (150 mL). The resulting solution was washed with water (3×30 mL) and steam distilled in the presence of a small amount of $NaHCO_3$. The oily residue solidified under light petroleum and was recrystallized from ethanol to give **4** (2.79 g; 73.0%), m.p. 83—85 °C, $[\alpha]_D$ +114° (*c* = 0.98, chloroform), R_f 0.78 (benzene–methanol, 97 : 3), R_T 4.04 min (*b*).

$C_{26}H_{26}O_5$ (418.59). Calcd. C 74.62; H 6.26. Found C 72.70; H 6.68%.

Benzyl 2-*O*-benzyl-*endo*-3,4-*O*-benzylidene-β-L-arabinopyranoside (5)

Compound **3** (3.0 g) was benzylated, as described for **4**, to give **5** (2.72 g; 70.9%), m.p. 76—78 °C (from ethanol), $[\alpha]_D$ +152° (*c* = 1.01, chloroform), R_f 0.77 (benzene–methanol, 97 : 3), R_T 3.84 min (*b*).

$C_{26}H_{26}O_5$ (418.59). Calcd. C 74.62; H 6.26. Found C 72.53; H 6.44%.

Benzyl 2-*O*-allyl-*exo*-3,4-*O*-benzylidene-β-L-arabinopyranoside (6)

To a solution of **2** (3.28 g) in dry DMF (30 mL) was added NaH (1.2 g) in portions. The mixture was stirred at room temperature for 30 min, and cooled to 0 °C. Allyl bromide (6.05 g) was added to the cold solution which was then stirred for 1 h at 0 °C and 10 h at room temperature. The reaction mixture was cooled again and the excess of NaH was decomposed with dry methanol (5 mL). The solution was diluted with dichloromethane (150 mL), washed with water (3×30 mL), then dried over Na_2SO_4 and concentrated. Traces of DMF were removed by vacuum distillation. The residue was dissolved in dichloromethane (150 mL) and washed with water (5×10 mL), dried over Na_2SO_4 and concentrated to give syrupy **6** (3.14 g; 85.3%), $[\alpha]_D$ +180° (*c* = 0.98, chloroform), R_f 0.77 (benzene–methanol, 95 : 5), R_T 2.89 min (*d*).

Benzyl 2-*O*-allyl-*endo*-3,4-*O*-benzylidene-β-L-arabinopyranoside (7)

Compound **3** (3.28 g) was allylated, as described for **6**, to give **7** (3.34 g; 90.7%) as a syrup, $[\alpha]_D$ +149° (*c* = 1.01, chloroform)i R_f 0.77 (benzene–methanol, 95 : 5), R_T 2.66 min (*d*).

Benzyl *exo*-3,4-*O*-benzylidene-2-*O*-(*p*-toluenesulfonyl)-β-L-arabinopyranoside (8)

A solution of **2** (1.0 g) in dry pyridine (10 mL) was cooled to 0 °C. *p*-Toluenesulfonyl chloride (0.64 g) was added to the cool solution which was then stirred for 1 h at 0 °C and then at room temperature. After 30 h more *p*-toluenesulfonyl chloride (0.32 g) was added and stirring was continued for 60 h. The reaction mixture was poured into ice-water containing $NaHCO_3$ and mixed thoroughly; the water was five times decanted. The solid product was filtered off and then recrystallized from ethanol (40 mL) to give **8** (1.29 g; 87.8%), m.p. 124—126 °C, $[\alpha]_D$ +138° (c = 1.35, chloroform), R_T 0.86 (dichloromethane– ethyl acetate, 9 : 1).

$C_{26}H_{26}O_7S$ (482.56). Calcd. C 64.71; H 5.43. Found C 64.98; H 5.88%.

Benzyl *endo*-3,4-*O*-benzylidene-2-*O*-(*p*-toluenesulfonyl)-β-L-arabinopyranoside (9)

Compound **3** (2.0 g) was tosylated, as described for **8**, to give **9** (2.57 g; 87.4%), m.p. 102—104 °C (from 24 mL of ethanol), $[\alpha]_D$ +202° (c = 2.00, chloroform), R_f 0.86 (dichloromethane–ethyl acetate, 9 : 1).

$C_{26}H_{26}O_7S$ (482. 56). Calcd. C 64.71; H 5.43. Found C 65.46; H 5.70%.

Benzyl 3-*O*-benzyl-β-L-arabinopyranoside (10)

$LiAlH_4$ (0.80 g) was added to a solution of **2** (2.0 g) in a mixture of dry ether (10 mL) and dry dichloromethane (20 mL). A solution of $AlCl_3$ (2.0 g) in ether (10 mL) was then added dropwise during 1 min. The mixture was boiled under reflux and stirred for 5 min, and then cooled; the excess of reagent was decomposed with ethyl acetate (5 mL) and $Al(OH)_3$ was precipitated with water (10 mL). The solution was decanted and the combined organic layers were washed with water (2×30 mL), dried over Na_2SO_4 and concentrated. The residue (1.80 g; 89.5%) was a mixture of **10** and **11** in a ratio of 72 : 28 (GLC). It was oxidized with $NaIO_4$ (1 g) in 50% aqueous ethanol (50 mL) overnight at 4 °C. The mixture was filtered, concentrated and acetylated with acetic anhydride (20 mL) in pyridine (20 mL). The acetylated product was eluted from a column of Kieselgel G with benzene–ether (5 : 1) to give **12** (1.40 g). Saponification of **12** in dry methanol (20 mL) with methanolic 0.1*M* sodium methoxide (0.3 mL) gave pure **10** (0.96 g; 47.7%) as a syrup, $[\alpha]_D$ +147° (c = 1.26, chloroform), R_f 0.34 (benzene–methanol, 9 : 1), R_T 4.45 min (c).

$C_{19}H_{22}O_5$ (330.38). Calcd. C 69.08; H 6.71. Found C 65.10; H 6.57%.

Benzyl 4-*O*-benzyl-β-L-arabinopyranoside (11)

Reductive ring cleavage of **3** (2 0 g), as described for **10**, gave a mixture (1.77 g; 88.0%) of **10** and **11** in a ratio of 1 : 9 (GLC). The mixture was acetylated with acetic anhydride (25 mL) in pyridine (25 mL), and the crystalline product (2.22 g) was recrystallized from ether–*n*-hexane (3 : 1), to give **13** (1.14 g), m.p. 62—64 °C. Saponification of **13** in dry methanol (20 mL) with methanolic 0.1*M* sodium methoxide (0.3 mL) gave pure **11** (0.81 g; 40.3%) as a foam, $[\alpha]_D$ +171° (c = 1.38, chloroform), R_f 0.29 (benzene–methanol, 9 : 1), R_T 5.06 min (c).

$C_{19}H_{22}O_5$ (330.38), Calcd. C 69.08; H 6.71. Found C 65.17; H 6.07%.

Benzyl 2,3-di-*O*-benzyl-β-L-arabinopyranoside (14)

$LiAlH_4$ (220 mg) was added to a solution of **4** (1.20 g) in a mixture of dry ether (5 mL) and dry dichloromethane (15 mL). A solution of $AlCl_3$ (765 mg) in ether (10 mL) was then added dropwise during 1 min. The mixture was stirred at room temperature for 5 min. Work-up gave a syrupy mixture (1.08 g; 89.6%) of **14** and **15** in a ratio of 9 : 1 (GLC). The components were separated on Kieselgel G with benzene–ether (4 : 1) to give **14** (0.88 g; 73.0%). Recrystallization from cyclohexane (10 mL) yielded 0.49 g of **14** (40.6%), m.p. 58—60 °C, $[\alpha]_D$ +106° (c = 1.13, chloroform), R_f 0.31 (benzene–ether, 4 : 1), R_T 15.03 min (c).

$C_{26}H_{28}O_5$ (420.51). Calcd. C 74.26; H 6.71. Found C 72.26; H 6.64%.

Benzyl 2,4-di-*O*-benzyl-β-L-arabinopyranoside (15)

Reductive ring cleavage of **5** (1.70 g), as described for **14**, gave a crystalline mixture (1.60 g; 93.7%) of **14** and **15** in a ratio of 1 : 49. The mixture was recrystallized from cyclohexane (48 mL) to yield **15** (1.16 g; 67.9%), m.p. 78–80 °C, $[\alpha]_D$ +197° (c = 0.73, chloroform), R_f 0.36 (benzene–ether, 4 : 1), R_T 18.76 min (c).

$C_{26}H_{28}O_5$ (420.51). Calcd. C 74.26; H 6.72. Found C 71.84; H 6.80%.

Reductive ring cleavage of 6

$LiAlH_4$ (0.70 g) was added to a solution of **6** (2.14 g) in a mixture of dry ether (10 mL) and dry dichloromethane (20 mL). A solution of $AlCl_3$ (2.10 g) in ether (10 mL) was then added dropwise during 1 min. The stirred mixture was boiled under reflux for 10 min. Work-up gave a 9 : 1 mixture (1.96 g; 91.1%) of **16** and **17**; R_T 6.35 and 7.43 min (a). Compound **16** was inseparable from **17**.

Benzyl 2-*O*-allyl-4-*O*-benzyl-β-L-arabinopyranoside (17)

Reductive ring cleavage of **7** (3.0 g), as described above for the reaction of **6**, gave a 1 : 13 mixture (3.01 g; 99.8%) of **16** and **17**. Recrystallization from cyclohexane (13 mL) gave the major product **17** (1.57 g; 52.0%), m.p. 56–59 °C, $[\alpha]_D$ +175° (c = 0.89, chloroform), R_f 0.47 (benzene–methanol, 95 : 5), R_T 7.43 min (a).

Benzyl 3-*O*-benzyl-2-*O*-(*p*-toluenesulfonyl)-β-L-arabinopyranoside (18)

$LiAlH_4$ (0.20 g) was added to a solution of **8** in dry ether (5 mL) and dichloromethane (15 mL). A solution of $AlCl_3$ (0.75 g) in ether (10 mL) was added to the above mixture dropwise during 1 min. The mixture was then stirred at room temperature for 15 min. Work-up gave a 1 : 1 mixture (0.46 g; 97.5%) of **18** and **19**. The components were separated on Kieselgel G with dichloromethane–ethyl acetate (9 : 1) to give **18** (0.21 g; 44.5%) as a syrup, $[\alpha]_D$ +79° (c = 1.46, chloroform), R_f 0.58 (dichloromethane–ethyl acetate, 9 : 1).

Benzyl 4-*O*-benzyl-2-*O*-(*p*-toluenesulfonyl)-β-L-arabinopyranoside (19)

Reductive ring cleavage of **9** (2.0 g), as described for **18**, yielded a 1 : 19 mixture (1.91 g; 95.5%) of **18** and **19**. Recrystallization from cyclohexane (110 mL) gave pure **19** (1.57 g; 78.5%), m.p. 99–100 °C, $[\alpha]_D$ +145° (c = 1.60, chloroform), R_f 0.74 (dichloromethane–ethyl acetate, 9 : 1).

Benzyl 2-*O*-benzyl-β-L-arabinopyranoside (20)

A mixture of **4** and **5** (1.09 g), ethanol (30 mL) and 0.1*N* H_2SO_4 (30 mL) was boiled under reflux for 4 h. The hot solution was neutralized with $BaCO_3$, filtered and concentrated. The residue (0.73 g; 85.1%) was recrystallized from water (60 mL) to yield **20** (0.49 g; 57.1%), m.p. 128–130 °C, $[\alpha]_D$ +186° (c = 0.59, chloroform), R_f 0.25 (benzene–methanol, 9 : 1), R_T 4.23 min (c). *Lit.* m.p. 130–131 °C, $[\alpha]_D$ +194°.

$C_{19}H_{22}O_5$ (330.38). Calcd. C 69.07; H 6.71. Found C 65.77; H 6.28%.

Benzyl 2-*O*-allyl-β-L-arabinopyranoside (21)

A mixture of **6** and **7** (3.44 g) was hydrolyzed as described in the preparation of **20**. Work-up gave a crystalline product (2.8 g) which was recrystallized from *n*-hexane (400 mL) to yield **21** (1.52 g; 58.1%), m.p. 84–86 °C, $[\alpha]_D$ +225° (c = 0.72, chloroform), R_f 0.21 (benzene–methanol, 9 : 1), R_T 1.29 min (a).

$C_{15}H_{20}O_5$ (280.32). Calcd. C 64.27; H 7.19. Found C 62.95; H 6.95%.

Benzyl 2-*O*-allyl-3,4-di-*O*-benzyl-β-L-arabinopyranoside (22

A mixture of **21** (1.0 g), powdered KOH (2 g) and benzyl chloride (10 mL) was kept at 100 °C for 5 h. The cooled mixture was diluted with dichloromethane (150 mL). The resulting solution was washed with water (3×30 mL) and steam distilled. The residue was extracted

with dichloromethane (3×40 mL), the combined extracts were dried over Na_2SO_4 and concentrated. The syrupy product (0.92g; 69.8%) was crystallized from light petroleum (10 mL) to give **22** (0.43 g; 32.6%), m.p. 56—58 °C, $[\alpha]_D$ +116° (c = 1.00, chloroform), R_f 0.76 (benzene–methanol, 97 : 3), R_T 7.35 min (*a*).

$C_{29}H_{32}O_5$ (460.58). Calcd. C 75.63; H 7.00. Found C 72.14; H 6.41%.

Benzyl 3,4-di-*O*-benzyl-β-L-arabinopyranoside (23)

A solution of **22** (0.42 g) in 2 : 1 : 1 ethanol–acetic acid–water (20 mL) was added to a suspension of 10% Pd/C catalyst (0.21 g) in the same solvent mixture (5 mL), and the suspension was refluxed for 3 h. After cooling, the catalyst was filtered off and washed with ethanol (3×10 mL). The combined washings and filtrate were concentrated. The residue was eluted from a column of Kieselgel G with light petroleum–ethyl acetate (7 : 3) to obtain **23** (0.22 g; 57.4%). After recrystallization from cyclohexane the product had m.p. 49—52 °C, $[\alpha]_D$ +141° (c = 1.06, chloroform), R_f 0.63 (ligh petroleum–ethyl acetate, 7 : 3), R_T 18.28 min (*c*).

$C_{26}H_{28}O_5$ (420.51). Calcd. C 74.26; H 6.71. Found C 71.84; H 6.80%.

REFERENCES

[1] LITPÁK, A.: Carbohyd. Res., **63,** 69 (1978)
[2] OLDHAM, M. A., HONEYMAN, J.: J. Chem. Soc., **1946,** 986
[3] BAGGETT, N., BUCK, K. W., FOSTER, A. B., WEBBER, J. M.: J. Chem. Soc., **1965,** 3401
[4] GAREGG, P. J., MARON, L., SWAHN, C. G.: Acta Chem. Scand., **26,** 518 (1972)
[5] COLLINS, P. M., OPARAECHE, N. N.: Carbohyd. Res., **33,** 35 (1974)
[6] MCCORMICK, J. E.: Carbohyd. Res., **4,** 262 (1967)
[7] LOTTER, H., LIPTÁK, A.: Z. Naturforsch. B, **36,** 997 (1981)
[8] ALLERTON, R., OVEREND, W. G.: J. Chem. Soc., **1954,** 3629
[9] HARANGI, J., LIPTÁK, A., OLÁH, A., NÁNÁSI, P.: Carbohyd. Res., **98,** (1981) (In press)
[10] OGAWA, T., MATSUI, M.: Carbohyd. Res., **62,** Cl (1978)

András LIPTÁK
Zoltán SZURMAI
János HARANGI
Pál NÁNÁSI

H—4010 Debrecen P.O.Box 55.

Acta Chimica Academiae Scientiarum Hungaricae, Tomus 108 (4), pp. 343—349 (1981)

NATURE OF THE SPECIES FORMED ON THE SURFACE OF SUPPORTED PLATINUM AFTER ADSORPTION OF OLEFINS

A. PALAZOV[1]*, A. SÁRKÁNY,[2] CH. BONEV[1] and D. SHOPOV[1]

([1] *Institute of Organic Chemistry, Bulgarian Academy of Sciences, Sofia,*
[2] *Institute of Isotopes, Hungarian Academy of Sciences, Budapest*)

Received November 4, 1980

Accepted for publication January 6, 1981

Olefin chemisorption on platinum results in the formation of both π- and σ-bonded species, their ratio depending on the actual state of the catalyst surface (temperature, presence of hydrogen, *etc.*). The occurrence of π-bonded species is indicated by both the downward shift of the band of coadsorbed carbon monoxide and the reduced transmission in the 3000—3100 cm^{-1} region. The experimental results suggest that the reactive form, which is readily hydrogenated, is π-bonded to the surface. The remaining part, bonded by σ carbon-metal bonds, has no influence on the position of the CO band. A rearrangement of the surface metal atoms upon the action of the hydrocarbons is also proposed.

Introduction

A great number of infrared studies have been concerned with the adsorption of hydrocarbons on supported metals since useful information can be obtained about the surface species formed and its role in catalytic reactions. Recently, special experiments have been performed demonstrating the existence of a close relationship between spectroscopically observed surface species and intermediates of certain heterogeneous catalytic reactions [1]. Infrared spectroscopic studies involving coadsorption of hydrocarbons, carbon monoxide and hydrogen have also been carried out [2—5]. In the present study, making use of the coadsorption technique, a detailed picture of the nature of surface species formed after hydrocarbon adsorption on supported platinum is developed.

Experimental

The adsorption of some olefins and benzene on Pt/Al_2O_3 was studied by IR spectroscopy and gravimetric measurements. The catalyst (9 wt% Pt) was prepared by impregnation of alumina (Degussa) with H_2PtCl_6. The powder was dried at 60 °C and then pressed into thin pellets, 22×15 mm, each weighing about 100 mg. Prior to reduction in a flow of purified hydrogen the IR sample was heated in air at 500 °C in order to prevent NaCl windows of the IR cell from being contaminated due to H_2PtCl_6 decomposition.

The infrared cell and vacuum device have been described elsewhere [5].

All adsorption experiments were carried out at room temperature. It should be noted, however, that the catalyst was heated by the incident Rx radiation to a temperature of 35—

* To whom correspondence should be addressed

40 °C. During the coadsorption experiments carbon Imonoide was preadsorbed to obtain a definite surface coverage. Then the hydrocarbon was introduced into the IR cell and evacuated to a residual pressure of about 1×10^{-5} Torr (1 Torr = 133.3 Nm^{-2}).

After each experiment the catalyst sample was reactivated by oxidation and evacuation at 300 °C followed by reduction in purified hydrogen at 400 °C for 30 min and evacuation at 420 °C.

The spectrometer used was a Carl Zeiss (Jena) instrument, model UR-10; the infrared cell was mounted permanently in the sample compartment.

Hydrocarbons and carbon monoxide of "puriss" grade were supplied by Fluka (Switzerland). They were used without further purification. The hydrocarbons were outgassed by means of repeated freeze-thaw cycles.

The chemisorbed amounts of hydrocarbon were measured gravimetrically by a Sartorius Type 4102 electrobalance. For further details see Ref. [6]. The removability of the chemisorbed species was determined by hydrogen treatment in static conditions. The Pt/Al_2O_3 sample for gravimetric measurements weighed 0.121 g.

Results and Discussion

The infrared bands arising in the CH stretching region from hydrocarbons adsorbed on supported metals are not intense, which makes the unequivocal description of the structure of the surface species formed very difficult. At present, more definite conclusions about the nature of the adsorption bond can be drawn only for benzene and cyclohexane on platinum [4]. In this case the occurrence of a π complex was evidenced both by the IR spectra of chemisorbed benzene and cyclohexane and by the carbon monoxide coadsorption technique [4, 7]. However, two models have been proposed for the surface species formed after adsorption of olefins on supported metals. The first model suggested the formation of σ bonds between carbon atoms and the metal surface [8—10], while the other one predicted the occurrence of π-bonded surface species [11, 12] (hydrocarbon fragments only are shown for simplion):

(I)

where (*) denotes a surface site.

The failure to detect definite bands of measurable intensity above 3000 cm^{-1} was regarded as evidence against the presence of olefinic species (Ib). However, as can be seen in Fig. 1c—f, the transmission above 3000 cm^{-1} was reduced after adsorption of propylene, butene, pentene, and hexene. Earlier Shopov *et al.* [12] observed similar changes in the transmission of a Pt/Al_2O_3 sample covered by hexene-1. Taking into consideration this experimental fact and applying quantum chemical calculations, they suggested the formation of π-bonded surface species on the metallic surface. The absence of definite bands above 3000 cm^{-1} was explained by the assumption that adsorbed hydrocarbons have a different skeleton arrangement. Thus the observed broadening of the bands in the CH olefinic region (Fig. 1c—f) should

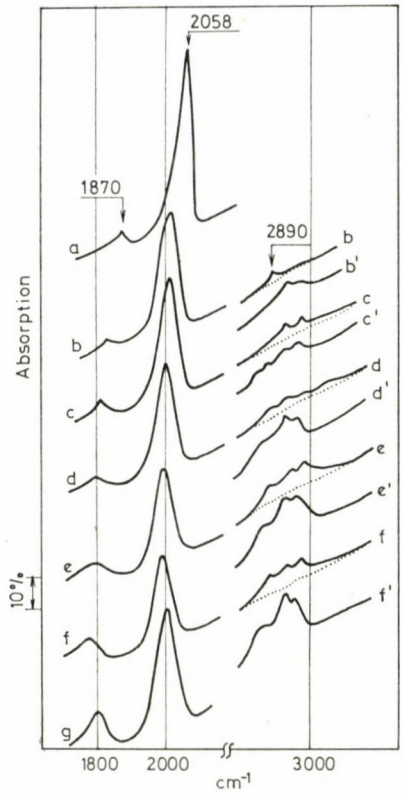

Fig. 1. Infrared spectra of the Pt/Al_2O_3 sample: a) After adsorption of CO ($\theta_{CO} = 0.17$) at 305 °C; b) ethylene coadsorbed; c) propylene coadsorbed; d) *trans*-butene-2 coadsorbed; e) pentene-1 coadsorbed; f) hexene-1 coadsorbed; g) benzene coadsorbed. Each hydrocarbon was coadsorbed at 35 °C and a pressure of about 5 Torr. *a′*–*f′*) hydrogen added ($p_{H_2} = 100$ Torr) at 35 °C after evacuation of the respective hydrocarbon from the IR cell. All the spectra were recorded at 35 °C

be attributed to the presence of adsorption complexes with a variety of configurations (*e.g. cis-* and *trans-*) and bond energies [12].

The weak bands in the CH stretching region with all hydrocarbons except ethylene (Fig. 1c–f) are due to CH_2 and CH_3 groups not connected with the surface, for example:

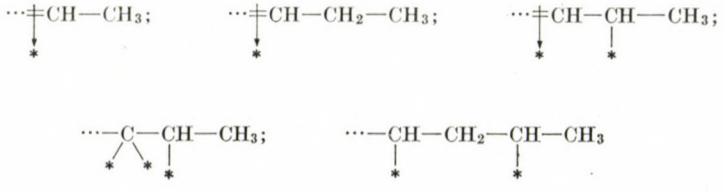

(II)

Recent IR experiments provide evidence that ethylene is linked to the surface of some transition metals by three bonds, one π and two σ bonds, giving rise to only one IR band below 2900 cm^{-1} [13]. This model is in agreement with data on C_2H_4 adsorption onto nickel single crystals, obtained by powerful physical techniques [14].

Applying the technique of carbon monoxide coadsorption with hydrocarbons, some additional data were obtained concerning the nature of bonding between olefins and platinum. Recently, it has been found that benzene adsorption on Pt/Al_2O_3 gives rise to a single band at 3050 cm^{-1} which is attributed to a π complex on the metal surface [4]. When benzene was admitted to a Pt/Al_2O_3 sample partially covered with carbon monoxide a downward shift of the CO band was observed [4]. Hence it can be deduced that compounds with π electron systems, if coadsorbed, shift the CO band to lower frequencies. In Fig. 1 and Table I it is seen that the low frequency shift is observed for all the hydrocarbons investigated in the present study. The only exception is methane which strongly supports the suggestion concerning the formation of π-bonded species with the other hydrocarbons, since it is relevant to assume

Table I

Infrared data on CO-hydrocarbon coadsorption and gravimetric measurements of hydrocarbon adsorption on Pt/Al_2O_3

Hydrocarbon	$\Delta\nu^1_{CO}$ (cm^{-1})	$\Delta\nu^2_{CO}$ (cm^{-1})	$G^{spectr.}_{des.}$ %	$G^{grav.}_{ads.}$ μg	$G^{grav.}_{des.}$ %
Ethylene	37	10	73	110	50
Propylene	39	10	74	—	—
trans-Butene-2	50	17	66	—	—
Pentene-1	52	25	52	—	—
Hexene-1	59	27	53	195	38
Benzene	48	18	63	165	30
Methane	no change		—	—	—

$\Delta\nu^1_{CO}$ — difference between the initial frequency of the CO band (2058 cm^{-1}, Fig. 1a) and the frequency of this band after coadsorption of a certain hydrocarbon (Fig. 1b—f);

$\Delta\nu^2_{CO}$ — difference between the initial frequency of the CO linear band (2058 cm^{-1}) and the frequency observed after hydrogen treatment and subsequent evacuation of the Pt/Al_2O_3 sample with coadsorbed CO and a certain hydrocarbon;

$G^{spectr.}_{des.}$ — amount of hydrocarbon desorbed after hydrogen treatment determined according to the equation:

$$G^{spectr.}_{des.} = \left(100 - \frac{\Delta\nu^2_{CO}}{\Delta\nu^1_{CO}} \times 100\right)\% ;$$

$G^{grav.}_{ads.}$ — gravimetrically measured amount of hydrocarbon adsorbed on Pt/Al_2O_3;

$G^{grav.}_{des}$ — desorbed amount of hydrocarbon after hydrogen treatment obtained by gravimetric measurements

that only σ-bonded species can occur with methane. Quantitative chemisorption measurements performed together with the spectroscopic study gave clear evidence for methane adsorption on Pt/Al_2O_3 partially covered with carbon monoxide.

The formation of conjugated double bonds in the π-adsorbed species (Ib) is suggested on the basis of a previously reported mechanism of dehydrocyclization of aliphatic hydrocarbons on platinum. For instance, the scheme of *n*-hexane dehydrocyclization proposes a stepwise elimination of hydrogen and the formation of hexenes, hexadienes, and hexatrienes [15, 16]. It is worth noting that coadsorption experiments with hexane on Pt/Al_2O_3 demonstrate that the CO band frequency is also decreased as in the case of olefins.

The model predicting the occurrence of surface species with conjugated double bonds does not suggest that hydrocarbons with conjugated double bonds, if adsorbed, would remain unchanged on the metal surface. For example, such a process, like self-hydrogenation, may cause the formation of adspecies with CH_2 and CH_3 groups not bonded to the surface and the appearance of σ bonds in the surface species (II).

Taking into consideration the conclusions made above, a correlation between the ionization potentials of hydrocarbons with definite structures on the surface and the CO band shift was found. It may be suggested that electrons from the highest occupied molecular π orbitals of the olefins will be transferred to the metal during adsorption. The first ionization potential appears to be a measure of the energy of the highest occupied orbital [17]. On the other hand, as was already discussed, the shift of ν(CO) depends on the electron donor ability of the coadsorbed hydrocarbon. Therefore, a correlation can be proposed between the ionization potential and the low frequency shift of the CO band. In Fig. 2, it is seen that this correlation is linear provided that π-bonded species

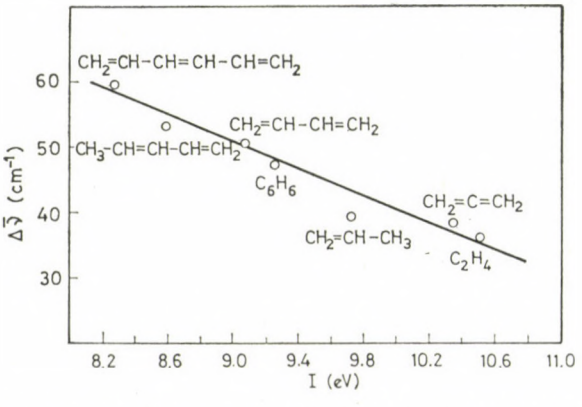

Fig. 2. A plot of the CO band shift *versus* the ionization potentials of coadsorbed hydrocarbons, which are suggested to be formed during adsorption of olefins on platinum. The values of the ionization potentials are taken from Ref. [18]

with conjugated double bonds occur on the surface. One exception is the case with propylene, when adsorbed allene is suggested to be formed in order to fit the point to the plot (Fig. 2).

As is already known [8—12], the addition of hydrogen to a Pt/Al_2O_3 sample with preadsorbed hydrocarbons results in an increase in the CH_2 and CH_3 band intensities (Fig. 1b'—f'). To explain this phenomenon, SHOPOV *et al.* [11, 12] proposed the conversion of the π-bonded adspecies (Ib) into a σ-bonded one:

(III)

It is very important to emphasize that after hydrogen addition both the intensity and frequency of the linear CO band (Fig. 1b—g) were restored (2058 cm^{-1}, Fig. 1a). This phenomenon can be predicted having in mind that hydrocarbons, if σ-bonded to the metal surface, will not affect the position of the CO band, as has been observed for carbon monoxide–methane coadsorption (Table I). Earlier experiments have shown that hydrogen coadsorption has no influence on the position of the high frequency band of CO, which is assigned to linear bonded species [2]. When the gas phase was removed from the IR cell, the CO band shifted again to lower frequencies. However, the shift from the initial position (Table I, $\Delta\nu^2_{CO}$) is much smaller than the one found in the case with CO-hydrocarbon coadsorption on a hydrogen-free metal surface (Table I, $\Delta\nu^1_{CO}$), probably due to the partial desorption of saturated hydrocarbons. For example, after hydrogen treatment and evacuation of a sample with coadsorbed carbon monoxide and ethylene, the CO band was shifted by only 10 cm^{-1} in comparison with the shift observed after ethylene coadsorption on a hydrogen-free platinum surface (37 cm^{-1}, Table I). On the basis of these data it can be estimated that 73% of the preadsorbed ethylene was converted into gaseous ethane (Table I, $G^{spectr.}_{des.}$). However, gravimetric measurements indicated that the treatment with hydrogen removed only 50% of the preadsorbed ethylene (Table I, $G^{grav.}_{des.}$). The difference between $G^{spectr.}_{des.}$ and $G^{grav.}_{des.}$ for hexene-1 and benzene was even greater (Table I). One reasonable explanation is that hydrogen treatment causes not only desorption of some part of the preadsorbed hydrocarbon but also decreases the concentration of the π bonds on the metal surface at the expense of σ bonds, which do not affect the CO band position, as was already discussed.

Another important finding concerning the IR data for carbon monoxide-hydrocarbon coadsorption is the behaviour of the 1870 cm^{-1} band (Fig. 1a). Usually the bands below 2000 cm^{-1} from CO adsorbed on transition metals are assigned to vibrations of multiply bonded species. Besides the frequency

fall, the intensity of this band is increased with the increase of the carbon atom number of the coadsorbed hydrocarbon; at the same time the intensity of the high frequency band is decreased (Fig. 1b—g). It can be suggested that upon hydrocarbon coadsorption the linearly bonded species is converted into a multiple bonded one. However, it is incorrect to assume that the more hydrocarbon is coadsorbed (*cf.* $G_{ads.}^{grav.}$ of ethylene, hexene-1, and benzene, Table I) the more linearly bonded species will be converted into multiple bonded CO molecules. On the contrary, the reverse assumption is more valid, bearing in mind the competition for sites on the metal surface. We believe that it is more correct to suggest a rearrangement of the surface metal atoms on the basis of the observed changes of CO adsorption modes. The new texture formed depends on the type of hydrocarbon which interacts with the metal surface. Applying a LEED technique, BARON *et al.* [19] have observed a temperature and pressure dependent structural rearrangement of the Pt(S)-[4(111)×(100)] surface in the presence of hydrocarbons.

REFERENCES

[1] PALAZOV, A. N., KHARSON, M. S., SHOPOV, D. M.: J. Catal., **36,** 251 (1975)
[2] PALAZOV, A., KADINOV, G., SHOPOV, D.: Commun. Dept. Chem. Bulg. Acad. Sci., **6,** 553 (1973)
[3] PRIMET, M., BASSET, J. M., MATHIEU, M. V., PRETTRE, M.: J. Catal., **29,** 213 (1973)
[4] PALAZOV, A.: J. Catal., **30,** 13 (1973)
[5] PALAZOV, A., BONEV, CH., SHOPOV, D.: React. Kinet. Catal. Lett., **9,** 383 (1978)
[6] SÁRKÁNY, A., TÉTÉNYI, P.: Acta Chim. Acad. Sci. Hung., **97,** 61 (1978)
[7] SHOPOV, D., PALAZOV, A.: Compt rend. Acad., bulg. Sci., **22,** 181 (1969)
[8] EISCHENS, R. P., PLISKIN, W. A.: Adv. Catal., **10,** 1 (1958)
[9] MORROW, B. A., SHEPPARD, N.: Proc. Roy. Soc., **Ä311,** 391 (1969)
[10] AVERY, N. R.: J. Catal., **19,** 15 (1970)
[11] SHOPOV, D., PALAZOV, A.: Kinet. Katal., **8,** 862 (1967)
[12] SHOPOV, D., ANDREEV, A., PALAZOV, A.: Commun. Dept. Chem. Bulg. Acad. Sci., **2,** 321 (1969)
[13] PALAZOV, A., BONEV, CH., SHOPOV, D., KHARSON, M. S., FIALKOVA, I. M., KIPERMAN, S. L.: Heterogeneous Catalysis, Proc. IVth Int. Symp., Varna, 1979, Part 1 p. 319, Publishing House Bulg. Acad. Sci., Sofia 1979
[14] BERTOLINI, J. C., ROUSSEAU, J.: Surface Sci., **83,** 531 (1979)
[15] PAÁL, Z., TÉTÉNYI, P.: I. Catal. **30,** 350 (1973)
[16] TÉTÉNYI, P., GUCZI, L., PAÁL, Z.: Acta Chim. (Budapest), **83,** 37 (1974)
[17] Progress in Physical Organic Chemistry, Vols **1** and **2,** S. COHEN, A. STREITWIESER and R. TAFT, (eds), p. 22, John Wiley and Sons, New York, London 1963
[18] Energii Razryva Khimicheskikh Sviazei. Potentsiali Ionizatsii i Srodstvo k Elektronu, Spravochnik, Nauka, Moscow 1974
[19] BARON, K., BLAKELY, D. W., SOMORJAI, G.: Surface Sci., **41,** 45 (1974)

Atanas PALAZOV
Chavdar BONEV
Dimitar SHOPOV
1113 Sofia, Bulgaria

Antal SÁRKÁNY H—1525 Budapest, P.O.Box 77

Acta Chimica Academiae Scientiarum Hungaricae, Tomus 108 (4), pp. 351—355 (1981)

MICRODETERMINATION OF MERCURY(II) AND SULFIDE IONS WITH A PYRIDINOL AZO DYE

O. S. CHAUHAN,[1] Y. S. VARMA,[1] I. SINGH,[2] B. S. GARG[1]* and R. P. SINGH[1]

([1] *Department of Chemistry, University of Delhi, Delhi*
[2] *Department of Chemistry, M. D. University, Rohtak*)

Received November 4, 1980

Accepted for publication January 6, 1981

The complexation equilibria of mercury(II) and (2'-amino-3'-hydroxypyridyl-4'-azo)benzene-4-sulfonic acid (AHP-4S), a water soluble pyridinol azo dye, has been studied spectrophotometrically. A selective and sensitive spectrophotometric method for the microdetermination of mercury(II) has been proposed. The composition, Beer's law and the optimum concentration range have been calculated using graphical methods. Using the principle of ligand exchange reaction, this complex has been used in the spectrophotometric determination of sulfide ions in aqueous solution. The method is simple, rapid and the sensitivity of sulfide ions determination is 0.67 ng/cm^2.

(2'-Amino-3'-hydroxypyridyl-4'-azo)benzene-4-sulfonic acid (AHP-4S), a water soluble pyridinol azo dye, has already been used in the determination of nitride [1], mercurimetric determination of iodide [2], titrimetric determination of lead(II) molybdate and tungstate [3], complexometric determination of Zn(II), Cd(II), Hg(II) [4], Co(II), Ni(II), Cu(II) [5] and as a visual indicator in the determination of ferrocyanide with zinc [6]. Up till now, heterocyclic azo dyes have not been used directly or indirectly in the determination of sulfide ions.

In the present communication, a sensitive and selective spectrophotometric method for the determination of mercury(II) and the use of the Hg(II)—(APH-4S) complex in the microdetermination of sulfide ions is proposed. The analytical principle is based on a ligand exchange reaction in aqueous medium and the visual comparative method has been adopted in which the decrease in absorbance of the Hg(II)—(AHP-4S) complex is proportional to the concentration of sulfide ions added. The method is simple, rapid and the sensitivity of sulfide ion determination is 0.67 ng/cm^2.

* To whom correspondence should be addressed

Experimental

Reagents

A stock solution of mercury(II) was prepared by dissolving the appropriate amount of metallic mercury in perchloric acid and standardized by conventional methods. AHP-4S was synthesized as reported earlier [1]. The purity was checked by elemental analysis and thin-layer chromatography. A 1×10^{-3} *M* stock solution was prepared in doubly distilled water. Dilute solutions of sodium hydroxide and perchloric acid were used for pH adjustments and a phosphate buffer of pH 4.8 was prepared. $Na_2S \cdot 9\,H_2O$ was dissolved in doubly distilled water and standardized iodometrically. The solution of sodium sulfide was prepared afresh to avoid its oxidation. All reagents used were of analytical grade.

Apparatus

A Unicam SP-600 spectrophotometer with matched 10 mm glass cells was used for recording the spectra. A Beckman Expandomatic SS-2 pH meter was used for pH adjustments.

Determination of mercury(II) ions

To a suitable aliquot containing 4.0—29.0 μg mercury(II), add 1 mL of 1×10^{-3} *M* AHP-4S solution, followed by 2.0 mL sodium hydrogen phosphate buffer (pH 4.8). Dilute to 10.0 mL and measure the absorbance at 535 nm against the corresponding reagent blank. The concentration of mercury(II) is determined from the calibration curve recorded under identical conditions.

Results and Discussion

AHP-4S forms a magenta coloured complex with mercury(II) with a maximum and constant absorbance at 535 nm in the pH range of 4.8—6.2. The complex is stable for 10 hrs. The molar composition (metal : ligand) of the complex are calculated by JOB's method of continuous variation and mole ratio plot is 1 : 2. Five moles of ligand are required for full colour development. Beer's law is valid upon 3.2 μg of mercury(II) and the optimum concentration of Hg(II) which can be accurately reproduced is 0.4—2.9 ppm. SANDELL' sensitivity (amount of mercury(II) corresponding to an absorbance of 0.001) as calculated from Beer's law plot is 0.0042 $\mu g/cm^2$ and the molar extinction coefficient is 4.76×10^4 1 $mole^{-1}\,cm^{-1}$ at 535 nm.

Effect of diverse ions

The effect of foreign ions was studied by taking 2.0 μg/mL of mercury(II), adding different amounts of foreign ions and determining the metal ion by the recommended procedure. It has been found that F^-, Cl^-, SCN^-, NO_2^-, NO_3^-, ClO_4^-, SO_3^{2-}, SO_4^{2-}, PO_4^{3-} and BO_3^{3-} do not interfere, neither do alkaline earths, lanthanides, Al(III), In(III), Ga(III), Ti(IV), V(V), Cr(V), Mn(II), UO_2(II), Mo(VI) and W(VI). The tolerance limits of the various ions (in ppm) which do not cause a deviation of $\pm2\%$ in absorbance at pH 4.8 are given in parentheses.

Oxalate, tartrate and citrate (1000, each), Br^- (100), Zn(II), Cd(II) (100, each), Co(II) (80), Ni(II) 60, Fe(II) (50), Ag(I) (20, masked with Cl^-).

I^-, CN^-, S^{2-}, $S_2O_3^{2-}$, thiourea, thiosemicarbazide, EDTA interfere seriously as did Cu(II).

Comparison of sensitivities with heterocyclic azo dyes

The present method using AHP-4S as a photometric reagent for the determination of Hg(II) compares favourably with heterocyclic azo dyes known for the purpose. PAR [7] is one of the most sensitive reagents for the determination of mercury(II) but various metal ions interfere. QAAc, though sensitive, involves serious interference of other metal ions [12]. The method using AHP-4S has the advantage that its determination can be carried out in the presence of a large excess of Zn(II), Cd(II), Co(II), Ni(II) and Fe(II). The method is rapid, simple, sensitive as well as selective. The sensitivities of other heterocyclic azo dyes used for the determination of mercury(II) are compared in Table I.

Determination of sulfide ions

Addition of sulfide ion solution to a known amount of Hg(II)—(AHP-4S) complex causes a decrease in absorbance which falls proportionally with the concentration of sulfide ions added, when recorded at 535 nm. This forms the basis of indirect determination of sulfide ions.

Table I

Comparison of sensitivities of heterocyclic azo dyes for the spectrophotometric determination of mercury(II)

No.	Mercury(II) complexed with	λ_{max} (nm)	Sensitivity ($\mu g/cm^2$)	References
1	4-(2-Pyridylazo)resorcinol) (PAR)	500	0.0029	[7]
2	*o*-(2-Thiazolylazo)-4-methoxy-phenol (TAMP)	638	0.0114	[8]
3	5-Hydroxy-4-(8-hydroxy-7-quinolylazo)--naphthalene-2,7-disulfonic acid (Azoxine H)	540	0.0055	[9]
4	3-(8-hydroxy-7-quinolylazo) naphthalene--1,5-disulfonic acid (Azoxine C)	540	0.0045	[9]
5	(2-Pyridylazo)-1-naphthol (PAN)	560	0.0111	[10]
6	1-(4-Methyl-2-thiazolylazo)-2-naphthol	580	0.0400	[10]
7	1-(2-Thiazolylazo)-2-naphthol	580	0.0345	[10]
8	2-(4-Antipyrylazo)-5-diethylaminophenol	600	0.1000	[11]
9	1-(2-Quinolylazo)-2-acenaphthylene-2-ol (QAAc)	540	0.0032	[12]
10	Ammonium(2'-amino-3'-hydroxypyridyl-4'--azo)benzene-4-arsonate	535	0.0055	[13]
11	(2'-Amino-3'-hydroxypyridyl-4'-azo)-benzene--4-sulfonic acid (AHP-4S)	535	0.0042	This work

Recommended procedure

To a solution containing 20.0 μg of mercury(II), add 0.5 mL of 1×10^{-3} *M* AHP-4S solution, followed by the sample solution containing up to 3.2 μg of sulfide ions. Shake well and adjust the pH 4.8 using a phosphate buffer. Dilute to 10.0 mL and measure the absorbance at 535 nm against the corresponding reagent blank.

Stoichiometry of mercury(II)—(AHP-4S) complex and sulfide ion reaction

To determine the stoichiometry of the mercury(II)—(AHP-4S) complex and sulfide reaction a mole ratio study was made. Various aliquots of sulfide ions were added to a known amount of mercury(II)—(AHP-4S) complex. The decrease in absorbance recorded at 535 nm reached the maximum value at a 1 : 1 ratio (Fig. 1), which shows that the displacement of AHP-4S ion

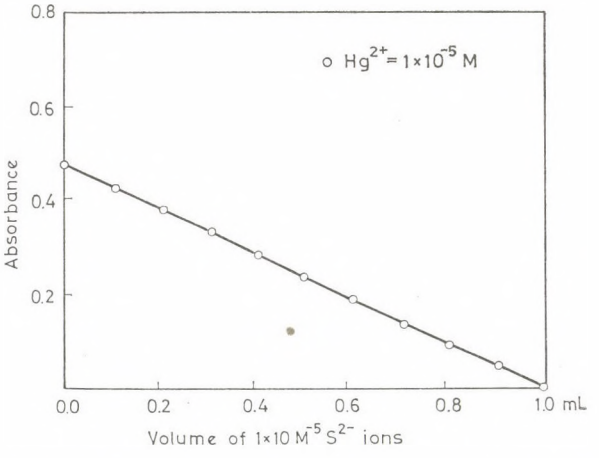

Fig. 1. Decomposition of mercury — (AHP-4S) complex by sulfide ions

by sulfide ions is stoichiometric with the formation of stable mercury sulfide. The overall reaction may be postulated as:

$$[Hg—(AHP\text{-}4S)_2] + S^{2-} \rightarrow HgS + 2(AHP\text{-}4S)^-$$

At certain instances, KNO_3 was used to coagulate mercuric sulfide.

This reaction was studied at different pH's varying the ligand concentration. The best results were obtained in the pH range 4.8—6.2, with a 5-fold molar excess of AHP-4S with mercury(II). The optimum concentration range of sulfide ions which can be reproduced accurately is 0.16—3.64 μg/10 mL using varying amounts of mercury(II). The relative standard deviation (5 ex-

periments) for the recovery of 0.16 μg of sulfide was found to be 0.1%. The effect of foreign ions was also studied and the interferences were found to be of the same order of magnitude as reported in the determination of mercury(II).

Comparison of sensitivities with other methods

The chloroanilate salt of mercury(II) has been reported in the spectrophotometric determination of sulfide ions in the visible [14] and UV region [15]. The optimum limit of 0.1—1.5 μg/mL sulfide ions has been determined by the latter method. The present method provides a simple, rapid and much more sensitive method for the determination of 0.16—3.64 μg/10 mL of sulfide ions. SANDELL's sensitivity (amount of sulfide ions corresponding to an absorbance of 0.001) is 0.67 ng/cm^2.

*

Two of the authors (O.S.C. and Y.S.V.) are thankful to U.G.C. and Centre of Advanced Study, University of Delhi, Delhi (India), for providing them with a teacher fellowship.

REFERENCES

[1] MEHTA, Y. L., GARG, B. S., KATYAL, M.: Talanta, **22,** 71 (1975)
[2] GUPTA, J. P., GARG, B. S., SINGH, R. P.: Ind. J. Chem., **16A,** 91 (1978)
[3] GUPTA, J. P., GARG, B. S., SINGH, R. P.: J. Ind. Chem. Soc., **54,** 1100 (1977)
[4] MEHTA, Y. L., GARG, B. S., KATYAL, M.: Anal. Chim. Acta, **86,** 323 (1976)
[5] GUPTA, J. P., MEHTA, Y. L., GARG, B. S., SINGH, R. P.: Ind. J. Chem., **15A,** 256 (1977)
[6] GUPTA, J. P., GARG, B. S., SINGH, R. P.: J. Ind. Chem. Soc., **54,** 983 (1977)
[7] UEDA, J.: J. Chem. Soc. Pure Chem. Sect., **92,** 418 (1971)
[8] KAI, F.: Anal. Chim. Acta, **44,** 242 (1969)
[9] CHERKISOV, A. I., TONKOSHUKUROV, V. S., POSTORONKO, A. I., RYZHEV, V. N.: Zh. Anal. Khim., **25,** 466 (1970); C.A. **73,** 31193b (1970)
[10] KOLOSOVA, I. V.: Tr. Perm. Cos. Med. Inst., **99,** 446 (1970); C.A. **78,** 37601h (1973)
[11] KOLOSOVA, I. V.: Izv. Vyss. Ucheb, Zaved. Khim. Khim. Tekhnol., **12,** 1329 (1969); C. A. **72,** 96358v (1970)
[12] SINGH, I., MEHTA, Y. L., GARG, B. S., SINGH, R. P.: Talanta, **23,** 617 (1976)
[13] VARMA, Y. S., SINGH, I., GARG, B. S., SINGH, R. P.: Microchim. Acta, **1979,** 445
[14] HOFFMAN, E.: Z. Anal. Chem., **195,** 372 (1965)
[15] HUMPHREY, R. E., HINZ, W.: Anal. Chem., **43,** 1100 (1971)

O. S. CHAUHAN
Y. S. VARMA
B. S. GARG
R. P. SINGH
Department of Chemistry, University of Delhi, Delhi—110007, India

I. SINGH
Department of Chemistry, M. D. University, Rohtak—124001, India

Acta Chimica Academiae Scientiarum Hungaricae, Tomus 108 (4), pp. 357—362 (1981)

COMPARATIVE NMR (^{1}H AND ^{13}C) STUDIES OF 3-ARYLIDENECHROMAN-4-ONES AND 3-BENZYLCHROMONES AND THEIR THIO ANALOGUES

Á. SZŐLLŐSY,[1] G. TÓTH[1] and A. LÉVAI[2]

([1]NMR Laboratory of the Institute for General and Analytical Chemistry, Technical University, Budapest and [2]Institute of Organic Chemistry, Kossuth Lajos University, Debrecen)

Received December 1, 1980

Accepted for publication January 6, 1981

^{1}H- and ^{13}C-NMR spectral properties of 3-arylidenechroman-4-ones and 3-benzylchromones and their thio analogues have been studied. It has been concluded that these techniques can help to differentiate between these structural isomers.

It is well known that reactions of chroman-4-one and 1-thiochroman-4-one with aromatic aldehydes give the corresponding 3-arylidenechroman-4-ones and -1-thiochroman-4-ones [1]. The product of condensation, obtainable with various *p*-substituted benzaldehydes, is in each case the *E* isomer, as it has been proved on the basis of NMR spectroscopic data [2]. Recently, it has been reported [3, 4] that in basic media the double bond in *exo*-position can be isomerized into *endo*-position, so that 3-benzylchromones and 3-benzyl-1-thiochromones are formed; in certain cases the condensation reactions effected under basic conditions directly yield these thermodynamically more stable products **VII**—**XII** [4].

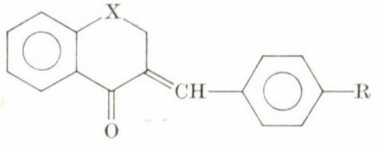

I—VI

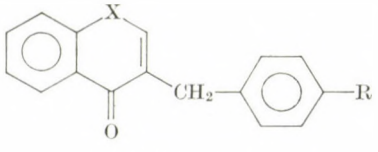

VII—XII

	X	R
I, VII	O	Br
II, VIII	O	CN
III, IX	O	NO_2
IV, X	S	Br
V, XI	S	CN
VI, XII	S	NO_2

Since our aim was to make detailed ^{1}H- and ^{13}C-NMR studies of compounds **I**—**VI** and **VII**—**XII**, it was thought advisable to effect, besides the structural identification of the condensation products, a pairwise comparison of the spectra of these compounds, and to determine the differences in their spectral parameters. Our experiences have shown that the formation of 3-benzyl chromones and 3-benzyl-1-thiochromones can be expected mainly in the reaction of benzaldehydes bearing electron-withdrawing *p*-substituents; therefore, the spectra of *p*-Br, *p*-CN and *p*-NO_2 derivatives will be discussed in the present paper.

Results and Discussion

^{1}H-NMR spectra

Characteristic data of the ^{1}H-NMR spectra are summarized in Table I. Several signals are suitable for differentiation between the structural isomers **I**—**VI** and **VII**—**XII**. As can be seen, distinction between structural isomers **I**—**III** and **VII**—**IX** is readily possible on the basis of the CH_2 signal, because its chemical shift is by about 1.4 ppm larger for the **I**—**III** isomers. At the same time, differentiation of structures **IV**—**VI** and **X**—**XII** on the basis of the chemical shift of the CH_2 signal is not feasible even by pairwise comparison. However, it is characteristic that in the spectra of the substances **I**—**VI** the methylene protons reveal allylic coupling with the =CH vinyl proton (^4J = 1.8 Hz and 1.1 Hz, respectively), while for compounds **VII**—**XII** no such a coupling can be detected.

A comparison of the data shows that the chemical shift of the H-5 aromatic proton, in *peri*-position with respect to the carbonyl group, is always larger in **I**—**VI** than in the case of the isomers **VII**—**XII**. The difference in the shielding effect of the carbonyl group in **IV**—**VI** and **X**—**XII** is due to the different molecular geometry, *i.e.* to the change of angle Θ in the McConnel equation [5] describing the diamagnetic anisotropic effect. (The other geometrical factor of the equation, the distance *r*, can be regarded as practically the same as shown by the Dreiding molecular models, taking into consideration all possible conformers.) In structures **I**—**III** and **VII**—**IX** all the geometrical factors are nearly identical, however, the conjugation of the carbonyl group is considerably different. (In the case of the *endo*-double bond, the planes of the two double bonds make a substantially smaller angle with each other, enhancing the conjugation.) The chemical shifts of the vinyl protons do not reveal characteristic differences and their signal is difficult to assign because of overlap with the signals of the aromatic protons.

Table I

^{1}H-NMR *data of the compounds investigated* (100 MHz, $\delta_{TMS} = 0$ ppm)

	=CH[a]	X—CH$_2$	H—5
I	7.76 t	5.27 d (^4J = 1.9 Hz)	7.99 m
II	7.82 t	5.27 d (^4J = 1.8 Hz)	8.02 m
III	7.87 t	5.29 d (^4J = 1.9 Hz)	8.01 m
IV	7.86 t	4.10 d (^4J = 1.1 Hz)	8.18 m
V	7.70 t	4.10 d (^4J = 1.1 Hz)	8.18 m
VI	7.66[b]	4.03 d (^4J = 1.2 Hz)	8.17 m
	=CH(H-2)	Ar—CH$_2$	H-5
VII	7.65[b]	3.73 s	8.19 m
VIII	7.78 s	3.83 s	8.18 m
IX	7.80 s	3.88 s	8.19 m
X	7.5—7.6[b]	4.01 s	8.53 m
XI	7.53—7.6[b]	4.05 s	8.51 m
XII	7.53[b]	3.91 s	8.54 m

[a] Confirmed by double-resonance experiments
[b] Overlapped

^{13}*C-NMR spectra*

^{13}C-NMR spectral data of chroman-4-one, chromone and their thio analogues are known [6, 7] hence the assignment of the ^{13}C-NMR spectra of the compounds under investigation can be performed on this basis, in the knowledge of the rules determining the chemical shifts of the carbon atoms of the phenyl ring [8a]. The data are summarized in Tables II and III. The assignments were confirmed by off-resonance spectra, non-decoupled ^{13}C-NMR spectra and selective proton decoupling. It has been found that the assignments of STILL *et al.* [7] are correct, though several data of their work were contested in a recent publication [9].

Comparing the ^{13}C-NMR data of compounds **I**—**VI** with the literature data for chroman-4-one and 1-thiochroman-4-one, it can be concluded that the change in the chemical shift of C-3 is very great. However, taking into consideration the circumstance that the hybridization of this carbon atom

Table II

^{13}C chemical shifts of compounds **I—VI** (25 MHz, $\delta_{TMS} = 0$ ppm)

	I	II	III	IV	V	VI
C2	67.5	67.3	67.3	29.1	29.1	29.2
C3	131.6	133.6	134.1	133.4*	135.3	136.0
C4	181.7	181.4	181.3	185.4	185.2	185.2
C5	127.9	128.0	127.9	130.4	130.5	130.6
C6	122.0	122.1	122.2	125.8	125.9	126.0
C7	135.8	136.1	136.3	133.0	133.3	133.4
C8	117.9	118.0	118.1	127.8	127.9	127.9
C4*a*	122.0	121.8	121.8	132.1	131.9	132.0
C8*a*	161.1	161.2	161.3	140.9	140.9	141.0
C1'	133.3	138.9	140.8	133.8*	139.5	141.7
C2', 6'	132.0	130.2	130.4	131.9	129.9	130.1
C3', 5'	131.3	132.4	123.3	130.9	132.4	124.0
C4'	123.8	112.9	148.1	123.1	112.2	147.7
CH=	135.8	134.6	134.1	136.1	134.8	134.3
CN		118.0			118.3	

* These values may be reversed

changes during "substitution", the downfield shift close to 100 ppm is not surprising. The chemical shift of the C-4 carbonyl carbon atom decreases by about 10 ppm as a result of further conjugation produced by the C=C double bond [10]. The upfield shift is larger in the case of 3-benzylidenechroman-4--ones than in their thio analogues since the angle made by the planes of the C=O and C=C double bonds is smaller, favouring conjugation, and a molecular geometry closer to coplanar is formed. Considerable change the chemical shift of the C-2 carbon atom was observed only in the case of the thio derivatives.

A comparison of the ^{13}C-NMR spectra of compounds **VII—XII** with the literature data shows that benzyl substitution causes at C-3 a downfield shift of 10 ppm, at C-2 an upfield shift of 2—3 ppm; that meets the expectations and is in good agreement with the literature data [8b].

The chemical shift of C-4 does not change considerably, because the 3-benzyl substitution does not markedly influence the conjugation of the carbonyl group.

Comparison of compounds **I—VI** containing the double bond in *exo*-position with their isomers **VII—XII** permits to draw the following conclusions:

Table III

^{13}C *chemical shifts of compounds* **VII—XII** (25 MHz, $\delta_{TMS} = 0$ ppm)

	VII	VIII	IX	X	XI	XII
C2	152.9	153.1	153.1	134.2	135.0	135.1
C3	123.9*	123.0	123.1	135.9	135.0	134.9
C4	177.1	177.0	177.0	178.6	178.4	178.6
C5	125.8	125.7	125.9	127.4	127.5	127.7
C6	124.9	125.1	125.3	126.3	126.4	126.5
C7	133.4	133.7	133.7	131.0	131.1	131.3
C8	117.9	118.0	118.1	128.9	128.8	128.9
C4*a*	123.7*	123.7	123.9	131.3	131.4	131.6
C8*a*	156.3	156.4	156.6	137.0	137.0	137.1
C1'	137.6	144.6	146.8	137.8	144.8	146.6
C2', 6'	131.5	130.1	129.0	131.6	129.7	123.7
C3', 5'	130.6	132.4	123.7	131.0	132.1	129.8
C4'	120.3	110.2	146.8	120.3	110.1	147.0
CH_2	31.2	32.0	31.9	37.3	38.2	38.1
CN		118.9			118.8	

* These values may be reversed

(1) The chemical shift of the only signal in the spectral range corresponding to the sp^3 C atoms (which is the only triplet in the off-resonance spectra) unequivocally indicates the structural isomer in question.

(2) Though the difference in the chemical shifts at C-4 are quite small, it is nevertheless a safe criterion of the appropriate structure.

(3) The chemical shift of the =CH carbon atom (or of C-2 in case of **VII—XII**) makes possible only a selection between structures **I—III** and **VII—IX**.

(4) The chemical shift of the C-1' carbon atom is by 4—6 ppm larger for **VII—XII** in accordance with the fact that in substituted benzene derivatives the vinyl group at direct position gives rise to a larger chemical shift than a methyl group [8a].

It should be noted that according to our experiences distinction between the structural alternatives is very easy on the basis of the first two differences, while the third and fourth characteristics can be recognized only after the complete assignment of the ^{13}C-NMR spectra. The differences offer a possibility for the determination of the ratio of isomers, within the limits of the application of ^{13}C-NMR for quantitative analysis [11].

Experimental

The spectra were recorded on a Jeol FX-100 spectrometer at 100 MHz or 25 MHz in deuterochloroform (internal standard TMS, $\delta = 0.0$ ppm) at room temperature. The assignments of the signals were supported by spectra obtained under ^1H off-resonance irradiation conditions.

REFERENCES

[1] LÉVAI, A., SCHÁG, J. B.: Pharmazie, **34,** 749 (1979) and references cited therein
[2] KEANE, D. D., MARATHE, K. G., O'SULLIVAN, W. J., PHILBIN, E. M., SIMONS, R. M., TEAGUE, P. C.: J. Org. Chem., **35,** 2286 (1970)
[3] MULVAGH, D., MEEGAN, M. J., DONNELLY, D.: J. Chem. Research (M), **1979,** 1710; (S), **1979,** 137
[4] LÉVAI, A., DINYA, Z., SCHÁG, J. B., TÓTH, G., SZŐLLŐSY, Á.: Pharmazie, **36,** 465 (1981)
[5] GÜNTHER, H.: NMR-Spektroskopie, p. 76. G. Thieme Verlag, Stuttgart 1973
[6] CHAUHAN, M. S., STILL, I. W. J.: Can. J. Chem., **53,** 2880 (1975)
[7] STILL, I. W. J., PLAVAC, N., MCKINNON, D. M., CHAUHAN, M. S.: Can. J. Chem., **54,** 280 (1976)
[8] PRETSCH, E., CLERC, T., SEIBL, J., SIMON, W.: Tabellen zur Strukturaufklärung organischer Verbindungen mit spektroskopischen Methoden, (*a*) p. C120; (*b*) p. C90. Springer Verlag, Berlin 1976
[9] WINKLER, T., FERRINI, P. G., HAAS, G.: Org. Magn. Res., **12,** 101 (1979)
[10] LEVY, G. C., NELSON, G. N.: Carbon-13 NMR for Organic Chemists, p. 112. Wiley-Interscience, New York 1972
[11] SHOOLERY, J. N.: Some quantitative applications of ^{13}C-NMR spectroscopy, in: Progress in Nuclear Magnetic Resonance Spectroscopy Vol. **11,** pp. 79—93. (Eds EMSLEY, J. W., FEENEY, J., SUTCLIFFE, L. H.), Pergamon Press, Oxford 1978

Áron SZŐLLŐSY
Gábor TÓTH } H—1111 Budapest, Gellért tér 4

Albert LÉVAI H—4010 Debrecen, P.O.Box 20

Acta Chimica Academiae Scientiarum Hungaricae, Tomus 108 (4), pp. 363—368 (1981)

FOTOMETRISCHE BLEIBESTIMMUNG MIT DITHIOPYRILMETHAN

A. I. Busev,[1] N. V. Trofimov[1] and P. Nenning[2]*

([1]*Lomonosov-Universität Moskau, Chemische Fakultät,*
[2]*Sektion Chemie der Karl-Marx-Universität Leipzig*)

Eingegangen am 22. März 1980

Zur Veröffentlichung angenommen am 10. Januar 1981

Es wird die Komplexbildungsreaktion von DTM mit Pb^{2+} untersucht. In essigsaurem Medium bildet sich ein gelber Komplex der Zusammensetzung Reagenz: Metall = 2 : 1 mit $\lambda_{max} = 390$ nm. Die Nachweisgrenze der Reaktion beträgt 1,1 μg/mL Pb^{2+}, das Beersche Gesetz gilt im Bereich 1,1—37,6 μg/mL Pb^{2+}. Die Bleibestimmung stören nicht: Li, Na, K, Ca, Sr, Ba, Mg, Y, La, Sc, Gd, Zn, Ni, Cr, Al, Cd, Be, Ti, Co, In, Ga, Cu. Es stören As, Sn, Mo, Te, Bi und Oxidationsmittel. Eine Bestimmungsmethode für Bleigehalte in chemischen Präparaten wurde ausgearbeitet. Der Variationskoeffizient der Methode beträgt 3,1—4,9%.

Bis-(2,3-dimethyl-1-phenylpyrazol-5-thion-4-yl)-methan (DTM) wurde schon zur fotometrischen Bestimmung von Te, Pd und Sb [1], Au und Bi [1; 2], Mo [1—3], Tl [4], As [5], Sb [6], Sn [7], Pt und Re [8] empfohlen. In [1] wird darauf hingewiesen, daß Pb(II) keine farbigen Komplexe mit DTM bildet. Wir haben festgestellt, daß in essigsäurem Medium Pb(II) mit DTM einen gelben Komplex bildet, der für die fotometrische Bleibestimmung Anwendung finden kann. Die vorliegende Arbeit ist dem Studium dieser Komplexbildungsreaktion und ihrer praktischen Anwendung gewidmet.

Experimenteller Teil

Bis-(2,3-dimethyl-1-phenylpyrazol-5-thion-4-yl)-methan (Dithiopyrilmethan, DTM) wird nach [8] hergestellt. Die Standardlösung wird durch genaue Einwaage und Auflösen des Reagenzes in verdünnter Essigsäure (1 : 1) erhalten. Verwendung finden eine $11{,}90 \cdot 10^{-3}$ *M* (= 0,5%-ige) und eine $5{,}64 \cdot 10^{-3}$ *M* Lösung.

Pb(II)-acetat-Standard erhalten wir durch Lösen einer $PbCO_3$-Einwaage in 60 mL verdünnter Essigsäure (1 : 1), Auffüllen auf 500 mL und kontrollierende Konzentrationsbestimmung durch Atomabsorption. Verwendet wird eine $1{,}88 \cdot 10^{-3}$ *M* Lösung.

Die Absorptionsspektren werden am SF-8 aufgenommen.

* Korrespondenz bitte an diesen Autor richten

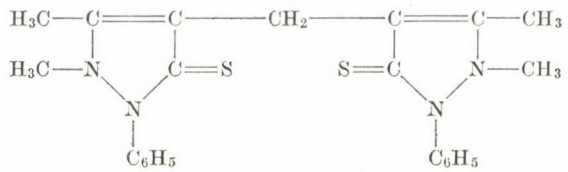

I

Ergebnisse

Im essigsäuren Medium bildet Pb^{2+} mit DTM einen stabilen gelben Komplex mit einem Absorptionsmaximum bei 390 nm. Bei dieser Wellenlänge adsorbiert DTM nicht. Die Absorbanz von Lösungen des Pb(II)-Komplexes mit DTM ist konstant im Intervall 4,4 bis 11,5 *N* Essigsäure. Bei geringerem Essigsäuregehalt der Lösung als 4,4 *N* fällt DTM aus.

Im optimalen Aciditätsbereich erreicht die Absorbanz der Lösung bei konstantem Pb^{2+}-Gehalt mit wachsender DTM-Konzentration einen konstanten Wert beim sechsfachen molaren Reagenzüberschuß.

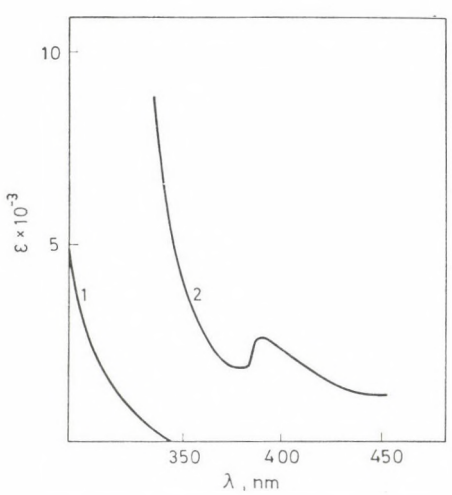

Abb. 1. Ausschnitt aus dem Absorptionsspektrum von 1. Bis-(2,3-dimethyl-1-phenyl-pyrazol--5-thion-4-yl)-methan, 2. Komplex des DTM mit Pb^{2+} in 9,6 *N* Essigsäure

Durch die Methode der Gleichgewichtsverschiebung wurde das Verhältnis Pb^{2+} : DTM = 1 : 2 bestimmt. Die Komplexbildungsreaktion findet im sauren Medium statt. Spektrofotometrisch läßt sich zeigen, daß das DTM

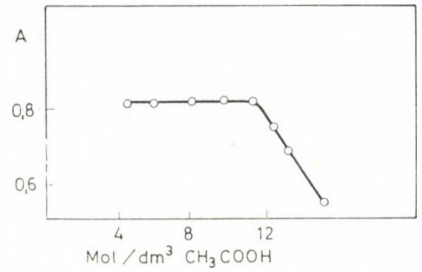

Abb. 2. Einfluß der Essigsäurekonzentration auf die Absorbanz des DMT-Pb-Komplexes. $\lambda = 390$ nm, $c_{Pb\,2+} = 0{,}38 \cdot 10^{-3}$ *M*, $c_{Reagenz} = 2{,}26 \cdot 10^{-3}$ *M*, $v = 50$ mL, $l = 1$ cm

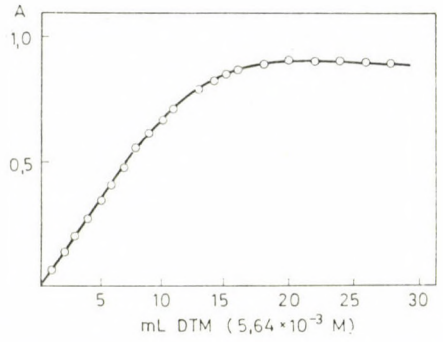

Abb. 3. Einfluß der DTM-Konzentration auf die Absorbanz des Komplexes. $\lambda = 390$ nm, $c_{Pb\,2+} = 0{,}38 \cdot 10^{-3}$ *M*, $v = 50$ mL, $l = 1$ cm

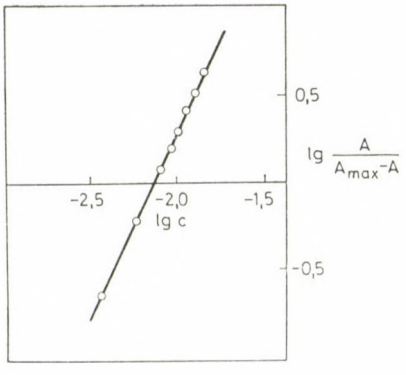

Abb. 4. Bestimmung der Komplexzusammensetzung nach der Methode der Gleichgewichtsverschiebung (zur Methode: [2]). $\lambda = 390$ nm, $c_{Pb\,2+} = 0{,}38 \cdot 10^{-3}$ *M*, 9,6 *M* Essigsäure

zweifach protonisiert ist. Mit der Hammetschen Aciditätsfunktion werden die Protonisierungskonstanten wie folgt bestimmt [9]:

$$pK_1 = 0{,}48 \pm 0{,}10 \text{ und } pK_2 = -1{,}13 \pm 0{,}08.$$

In [8] wird auf der Grundlage von IR- und NMR-Spektren des einfach protonisierten DTM-Moleküls darauf hingewiesen, daß das Proton nicht dem heterocyclischen Stickstoffatom zuzuordnen sei, sondern dem Schwefelatom und daß die Thiogruppen im protonisierten Molekül eine Wasserstoffbrückenbindung ausbilden. Demzufolge wäre der Prozeß der Protonisierung u.E. wie folgt vorstellbar:

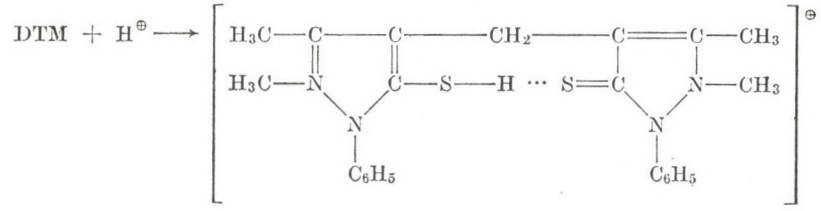

II

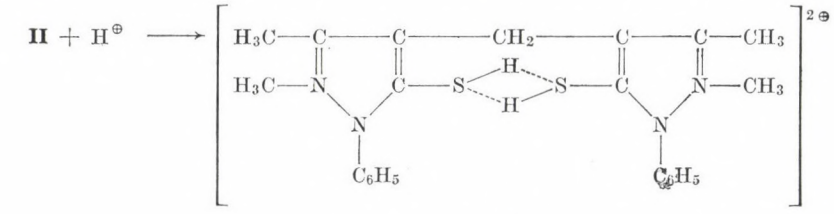

III

Unsere Vorstellungen unterscheiden sich damit von dem in [10] vorgeschlagenen Reaktionsablauf, wobei wir meinen, daß die Struktur der protonisierten Form des DTM nach [10] eine Reihe wesentlicher Nachteile hat.

Einmal werden in ihr die realen Valenzzustände einzelner Atome nicht richtig wiedergegeben. Zum zweiten sind beide Thiogruppen, die für die Komplexbildung verantwortlich sind, laut angegebener Formel blockiert durch eine starke Einfachbindung, die die Fähigkeit zur Komplexbildung wesentlich senken muß. Zum dritten fällt eine sehr widersprüchliche Ladungsverteilung auf: einmal ist die Ladung am heterocyclischen Stickstoffatom konzentriert, aber andererseits über das ganze Ion verteilt. Die Strukturen der protonisierten Formen, wie wir sie vorschlagen, ist frei von diesen Widersprüchen und entspricht früher erhaltenen experimentellen Daten [8].

Den Komplexbildungsprozeß des DTM mit Pb^{2+} kann man sich wie folgt vorstellen. In mäßig saurem Milieu wird das DTM an einer Thiogruppe protonisiert unter Bildung der Struktur **II**, die den Komplex **IV** bildet:

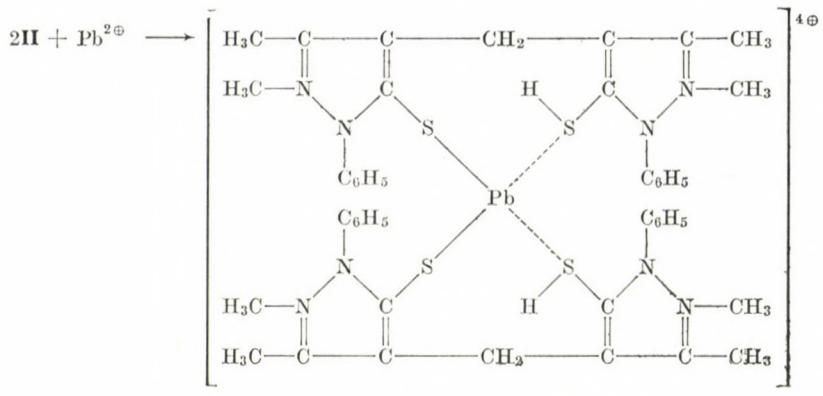

IV

Bei einer Essigsäurekonzentration >11.5 *N* wird die zweite Thiogruppe im DTM protonisiert, was mit der Zerstörung des Komplexes **IV** und einer dadurch bedingten Abnahme der Extinktion der Lösung verbunden ist. (Abb. 2)

$$\mathbf{IV} + 2\,H^+ \rightarrow 2\,\mathbf{III} + Pb^{2+}$$

Auch unter der Einwirkung von Oxidationsmitteln wie Cer(IV), Mn(VII), V(V), Cr(VI) u.a. wird der Komplex IV zerstört, was auf Oxidation der Thiogruppe zurückzuführen ist:

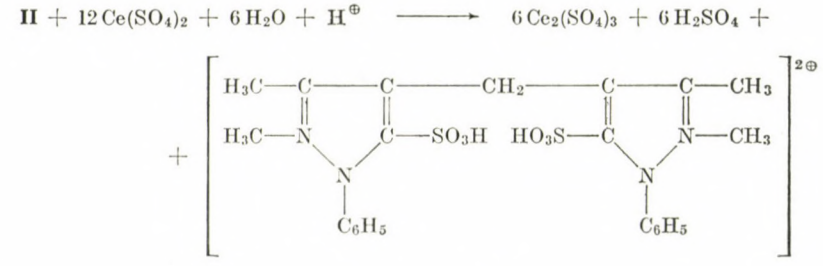

V

oder

$$\mathbf{IV} + 24\,Ce(SO_4)_2 + 12\,H_2O \rightarrow 2\,\mathbf{V} + 12\,Ce_2(SO_4)_3 + 11\,H_2SO_4 + PbSO_4$$

Die Pb-Bestimmung wird nicht gestört durch Li, Na, K, Ca, Mg, Sr, Ba, Y, La, Sc, Gd, Zn, Ni, Cd im Verhältnis 1 : 5000, Al 1 : 100, Cr 1 : 100, Be, Ti, Co 1 : 50, In, Ga 1 : 20, Cu, Fe 1 : 10. Es stören As, Sn, Mo, Te, Bi, Ce(IV), V(V), Cr(VI), Mn(VII), Cl^-.

Die Nachweisgrenze der Methode, bestimmt nach dem 3σ-Kriterium, beträgt 1,1 μg/mL Pb(II). Das Beersche Gesetz gilt im Intervall 1,1—37,6 μg/mL Pb(II). Damit ist diese Bleibestimmung nachweisstärker und selektiver als die Dithizonmethode [11].

Die Komplexbildungsreaktion wird zur Bestimmung von Bleiverunreinigungen in chemischen Spezies benutzt.

Dazu wird eine Einwaage desselben (1 g) in 6 *N* Essigsäure gelöst, in einen 50 mL-Maßkolben überführt, 5 mL 0,5%-ige DTM-Lösung in Essigsäure zugefügt, mit 6 *N* Essigsäure auf 50 mL aufgefüllt und die Absorbanz der Lösung bei 390 nm in einer Küvette mit 5 cm Schichtdicke gegen die Leerprobe gemessen. Der Bleigehalt ergibt sich aus einer Eichkurve. Durchgeführte Analysen sind in der Tabelle aufgeführt. Der Variationskoeffizient beträgt 3,1—4,9%.

Tabelle I

Analyse chemischer Präparate auf ihren Bleigehalt

Präparat	Pb zugefügt %	Pb gefunden %	Variationskoeffizient % ($n = 5$)
$CdCO_3$ "rein"	—	0,048	4,1
	0,025	0,076	4,2
	0,050	0,103	4,9
$CdCO_3$ "*p.a.*"	—	0,021	4,8
	0,010	0,032	3,8
	0,020	0,040	3,1
ZnO "rein"	—	0,036	3,7
	0,015	0,053	3,8
	0,030	0,064	3,7

LITERATUR

[1] DOLGOREV, A. V.: Urheberschein der UdSSR Nr. 51 57 47, veröffentlicht 30.5.1976, Bulletin Nr. 20
[2] DOLGOREV, A. V., LYSSAK, J. G.: J. analyt. chim. (russ.), **29** (9), 1766 (1974)
[3] TENIAKOVA, L. A., AKIMOV, V. K. im Sammelband "Zweite wissenschaftliche Konferenz der pribaltischen Republiken, der Belorussischen SSR und des Kaliningrader Gebietes, Analytische Chemie" (russ.), Band **1**, Riga 1976, Seite 13
[4] AKIMOV, V. K., BUSEV, A. I., SASSORINA, E. V.: *idem*, S. 7
[5] AKIMOV, V. K., RUDSIT, G. P., JEFREMOVA, L. E.: *idem*, S. 8
[6] RUDSIT, G. P., AKIMOV, V. K., JEFREMOVA, L. E.: *idem*, S. 9
[7] AKIMOV, V. K., TENIAKOVA, L. A., ANTONENKO, L. V.: *idem*, S. 15
[8] AKIMOV, V. K., SAIZEV, B. E., JEMELJANOVA, I. A., KLIOT, L. J., BUSEV, A. I.: J. anorg. Chem. (russ.), **21** (12), 3288 (1976)
[9] TROFIMOV, W. V.: "Untersuchung von Diantipyrilmethanderivaten (Redoxanen) als analytische Redoxreagentien" Dissertation, Gorki-Universität Perm, 1975
[10] DOLGOREV, A. V., LYSSAK, J. G., SIBAROVA, J. P. im Sammelband "Verwendung von Pyrazolonderivaten in der analytischen Chemie" (russ.), Perm. Gorki-Universität, 1977, S. 8
[11] FISCHER, H.: Z. angew. Chemie, **47**, 90 (1934); **50**, 919 (1937)
[12] ZOLOTOV, Iu. A.: Extraktion von Innerkomplexverbindungen (russ.), Verlag Nauka, Moskau 1968, Seite 127 und dort zitierte Literatur

Alexei Ivanovitsch BUSEV, Nikolai Vasilievitsch TROFIMOV } Lomonossov-Universität Moskau, Chemische Fakultät

Peter NENNING — Sektion Chemie der Karl-Marx-Universität, 7010 Leipzig, Liebigstraße 18

Acta Chimica Academiae Scientiarum Hungaricae, Tomus 108 (4), pp. 369—380 (1981)

PASSIVATION OF COPPER IN ACIDIC SULPHATES ELECTROLYTES

L. KISS,[1]* A. BOSQUEZ[2] and M. L. VARSÁNYI[1]

([1]*Department of Physical Chemistry and Radiology Eötvös L. University, Budapest,* [2] *National University of Panama*)

Received October 17, 1980

Accepted for publication January 14, 1981

The anodic behaviour of copper in galvanic baths containing sulphate is discussed. Diffusion plays a significant role in relevant kinetics. The diffusion of Cu^{2+} ions of the electrode surface is the most hindered step when anodic polarization is slight, diffusion of water towards this surface is the most impeded step when anodic polarization is high. A brownish-red coating by various copper oxides is developed on the surface of copper, it is passivated, when anodically polarized at high current density. Parameters which affect anodic passivation were tested, and a reaction mechanism for the passivation was suggested.

The anodic dissolution of copper consists of two consecutive steps [1, 2, 3]. This mechanism has been found to operate in sulphuric acid [2], perchloric acid [3] or diphosphate [4] media. At a sufficiently high positive electrode potential copper may be passivated also in acid media [5, 6]. This occurs for instance in a sulphuric acid solution and also in copper electrolytes generally used in the refining of this metal. It has been stated that passivation of copper in sulphuric acid media is enhanced by lowering the temperature, by increasing the acid [5] or the copper sulphate concentration [6]. Phosphorus, up to a concentration of 0.1 mass per cent, in the copper anode makes this to dissolve smoothly and with a high rate [6] while less anode mud is formed [7] and it contains only small amount of copper.

We have studied the passivation of copper with stationary plate, rotating disc and rotating ring disc electrodes in sulphuric acid solutions of copper sulphate. Our main aim was to gather experimental data which allow to draw conclusions on the mechnism of the passivation process of copper in the medium mentioned.

Experimental

0.7—1.2 *M* copper (II) sulphate and 0.5 *M* sulphuric acid solutions were prepared from A.G. chemicals with bidistilled water. In certain instances also the effect of additives was studied: sodium chloride, gelatin, or dimethylthiourea used for this purpose were all A.G. products. High-purity nitrogen was used to free the solution from oxigen.

The stationary plate electrodes were made of 99.9 electrolytically pure copper by means of rolling. The rotating disc as well as the rotating ring disc electrode (0.25 cm^2 surface) consisted of copper deposited from an acid sulphate copper bath; the ring electrode was platinum.

* To whom correspondence should be addressed

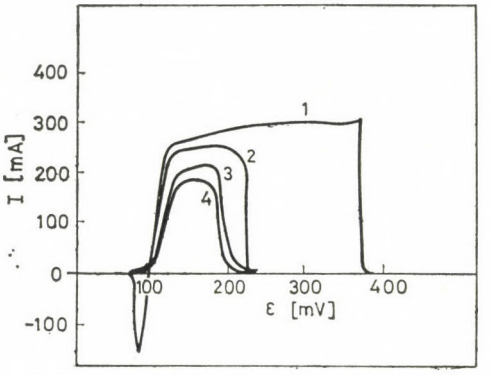

Fig. 1. Potentiodynamic curves for copper at various temperatures, in a solution of 1.1 mole dm^{-3} of $CuSO_4$ + 0.5 mole dm^{-3} of H_2SO_4, scan rate: 20 mV min^{-1}. (1) 38 °C, (2) 26 °C, (3) 13 °C, (4) 2 °C

Tests were carried out in glass apparatus described earlier [8, 9]. An OH-405 RADELKIS type, an AFKEL-415 type potentiostat and an AFKEL-413/1 type JATE bipotentiostat were used for potentiodynamic measurements; the recording of data was done with a RADELKIS OH-815/1 type and a BRYANS 26000-A3 type Y_1Y_2X recorder. The first two types of potentiostats allow the elimination of the ohmic potential drop.

A saturated calomel electrode served as a reference electrode.

Results

Figure 1 shows the effect of temperature on the passivation of copper. Polarization curves are recorded on a stationary plate electrode; the solution is composed of 1.1 mole dm^{-3} $CuSO_4$ + 0.5 mole dm^{-3} H_2SO_4; the rate of potential change is 20 mV · min^{-1}; ohmic potential drop is prevented. As the results show the maximum polarization current for passivation is greater when

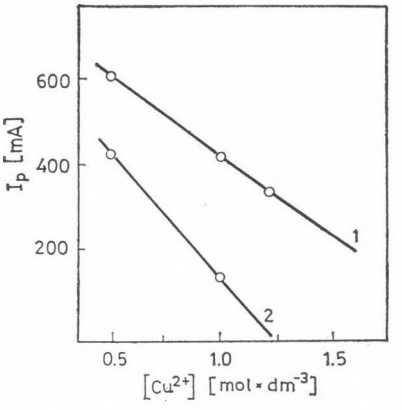

Fig. 2. Change of critical maximum current intensity I_p for passivation of copper at 25 °C and at 2 °C, as a function of copper sulphate concentration

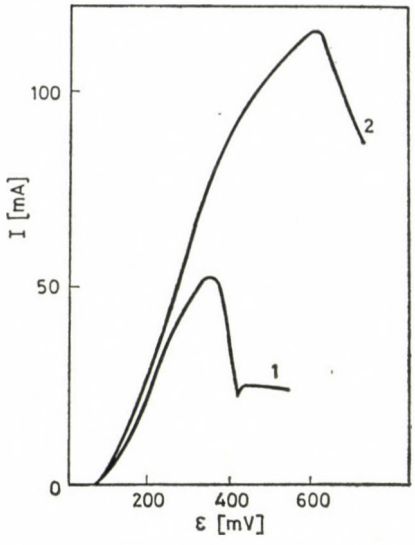

Fig. 3. Potentiodynamic curves at room temperature and at various r.p.m. of the copper disc electrode in a solution of 0.7 mole dm^{-3} of $CuSO_4$ + 0.5 mole dm^{-3} of H_2SO_4 scan rate: 100 mV min^{-1}. (1) r.p.m. = 610 (2) r.p.m. = 2340

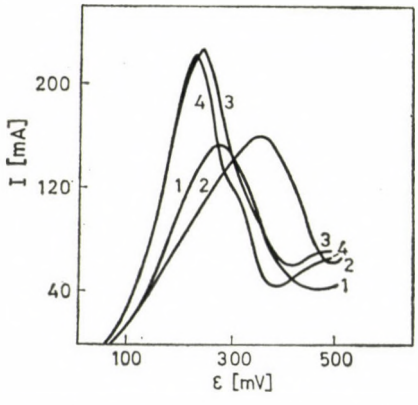

Fig. 4. Potentiodynamic curves for copper in the presence of Cl^- ions at room temperature in a solution of 0.5 mole dm^{-3} of H_2SO_4 + 0.88 mole dm^{-3} of $CuSO_4$, scan rate: 100 mV min^{-1}. Concentrations of the additive: (1) *nil*, (2) 100 mg dm^{-3}, (3) 300 mg dm^{-3}, (4) 600 mg dm^{-3}

the temperature is raised and the potential at the break (diminution) of the current is shifted towards the more positive values.

Figure 2 shows that the maximum current intensity I_p for passivation becomes less when the concentration of copper(II) sulphate in the solution is increased.

In Fig. 3 potentiodynamic curves recorded on a rotating disc electrode show the effect of the r.p.m. of this electrode. These curves are determined

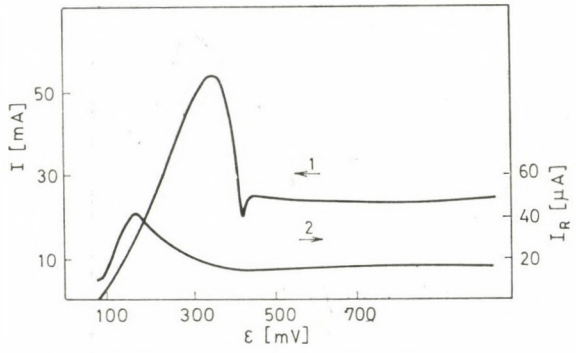

Fig. 5. (1) Potentiodynamic curve I *vs.* ε for a copper disc electrode at 610 r.p.m. (2) Change of the ring current as a function of disc potential, I_R *vs.* ε, on the platinum ring electrode at 600 mV

without a compensation for ohmic potential drop, at room temperature, the rate of potential change is 100 mV · min^{-1}. It is to be seen that when r.p.m. of the electrode is increased the current intensity for passivation is substantially greater. Also the potential at which the intensity drop supervenes will more positive when r.p.m. is increased, however, part of the shift of potential shown in Fig. 3 is due to ohmic potential drop. The quantitative interpretation of experimental data obtained by means of a rotating disc as well as by that of the rotating ring disc electrode to be discussed presently, is generally difficult since the geometry of the electrode changes in time because currents at comparatively high intensity pass through it and some of its mass is dissolved rather rapidly.

Figure 4 shows the effect, on a stationary copper electrode plate, of chloride ions added to the electrolyte which contains 0.9 mole dm^{-3} $CuSO_4$ and 0.5 mole dm^{-3} of H_2SO_4. The maximum of the potentiodynamic curve is shifted by about 70 to 80 mV toward positive potentials when NaCl is present in a 100 mg dm^{-3} concentration. An increase in NaCl concentration shifts the maximum in the negative direction and the current intensity here recorded is much greater than that found for chloride-free media.

Figure 5 gives characteristic data pertinent to tests with rotating ring disc electrodes. The disc is copper, the ring platinum. Composition of the solution is 0.7 mole dm^{-3} of $CuSO_4$ + 0.5 mole dm^{-3} of H_2SO_4. Speed: 610 r.p.m. At the anodic polarization of copper the Cu(I) ions formed as intermediates are oxidized on the ring electrode. At the beginning when anodic polarization increases also the limiting current of the oxidation of Cu(I) ions measurable on the ring increases and attains a maximum when the disc current is about 10 mA (40 mA · cm^{-2}); with a further increase of the anodic polarization of the copper disc the ring current decreases.

Discussion

In accord with literature data [5, 6] our experimental results suggest that — other conditions being the same — lowering the temperature or increasing the concentration of copper sulphate in the solution decreased the critical current density j_p for passivation (*cf.* Figs 1 and 2). In other words, the farther away we are from the concentration of a saturated solution of copper sulphate the higher the figure for j_p will be. According to Fig. 3 in the case of a rotating copper disc electrode, higher r.p.m. of it goes with higher figures also of j_p. Figure 3 reveals also that increasing the r.p.m. of the disc electrode the current across the electrode is increased significantly in every section of the polarization curve. This suggests that diffusion plays an important role in the kinetics of this process. Former results [2] show that the diffusion of Cu(II) ions from the electrode surface determines the kinetics of the anodic dissolution of in sulphuric acid. When a rotating disc electrode is used with an increase in r.p.m. the domain of mixed transfer-diffusion kinetics can be reached.

On the basis of the preceding it can be said that the processes in the initial (active) section of the potentiokinetic curves may be, for instance, the following:

1. $$Cu + H_2O \underset{k_{k_1}}{\overset{k_{a_1}}{\rightleftharpoons}} (CuOH)_{ads} + H^+ + e$$

2. $$(CuOH)_{ads} \underset{k_{k_2}}{\overset{k_{a_2}}{\rightleftharpoons}} (CuOH^+)_{ads} + e$$

3. $$(CuOH^+)_{ads} + H^+ \underset{k_{k_3}}{\overset{k_{a_3}}{\rightleftharpoons}} (Cu^{2+})_{ads} + H_2O$$

4. $$(Cu^{2+})_{ads} + x\ H_2O \underset{k_{k_4}}{\overset{k_{a_4}}{\rightleftharpoons}} [Cu^{2+}_{(aqu)}]_0$$

5. $$[Cu^{2+}_{(aqu)}]_0 \xrightarrow{X_5} Cu^{2+}_{(aqu)}.$$

Scheme 1

In the equations also the rate constants of the processes are marked. Reactions 1 and 2 are electrode reactions, therefore these rate constants as it is well known [2], depend exponentially on the electrode potential.

Scheme 1 corresponds to the two-step mechanism formerly proposed [2]. Then we did not include into the scheme reactions 3, 4 and 5, further we supposed that adsorption occurred but on a negligibly small part of the surface. With the conditions which obtained in earlier tests (not too concentrated solution of acid, no copper sulphate present in the electrolyte), reactions 3 and 4 did not affect the kinetics; the diffusion of the hydrated Cu(II) ions was taken into consideration in the kinetic correlations.

According to Scheme 1 the diffusion of the hydrated copper ions from the electrode surface is the most impeded step, up to a not too high anodic current density; for the preceding steps equilibrium is set in. At high anodic current densities, however, and especially in concentrated sulphuric acid or concentrated copper sulphate solutions, according to Scheme 1, it is possible that there is not enough water available for the adequate hydratation of copper, then the diffusion of water towards the electrode surface governs the rate of anodic dissolution. This means that formation of salt may begin on the surface of the electrode and an anodic limiting current intervenes.

When the anodic dissolution of copper occurs according to Scheme 1 then the kinetics of this process can be written as follows,

$$j_I = X_5(c_{20} - c_2) \tag{1}$$

where c_{20} and c_2 represent the respective concentrations of hydrated Cu(II) ions at the electrode surface and in the bulk of the solution, and X_5 stands for the rate of diffusion of the same ions. The c_{20} concentration of hydrated Cu(II) ions at the electrode surface can be expressed by means of the rate constants for the approximate equilibria which precede the fifth step. Therefrom

$$c_{20} = \frac{k_{a_1} k_{a_2} k_{a_3} k_{a_4}}{k_{k_1} k_{k_2} k_{k_3} k_{k_4}} c^x_{H_2O,0}. \tag{2}$$

Here $c^x_{H_2O}$ stands for the concentration of unbound water (not coordinated to an ion) at the electrode surface. For (1) we have thus

$$j_I = X_5(k c_{H_2O,0} - c_2) \tag{3}$$

where

$$k = \frac{k_{a_1} k_{a_2} k_{a_3} k_{a_4}}{k_{k_1} k_{k_2} k_{k_3} k_{k_4}}$$

and where, to simplify matters, we suppose that $x = 1$.

In the present case current density j_I can be expressed also by the rate of diffusion of water towards the electrode surface.

$$j_I = x_{H_2O}(c_{H_2O} - c_{H_2O,0}) \tag{4}$$

where x_{H_2O} is the rate constant of the diffusion of water (the dimension is the same as for rate constant X_5), c_{H_2O} is the concentration of the unbound water molecules in the bulk of the solution. *I.e.*

$$c_{H_2O} = c'_{H_2O} - (x c_{CuSO_4} + y c_{H_2SO_4}) \tag{5}$$

when the numbers of water molecules bonded by one $CuSO_4$ or by one H_2SO_4 molecule are represented by x and y, respectively, and c'_{H_2O} stands for the total concentration of water in the electrolyte solution.

Combining Eqs (3) and (4) gives the expression

$$j_I = \frac{X_5(kc_{H_2O} - c_2)}{1 + \frac{X_5 k}{X_{H_2O}}}. \tag{6}$$

Thus, at low anodic polarization, when

$$1 \gg \frac{X_5 k}{X_{H2O}} \tag{7}$$

we obtain Eq (3), *i.e.* the kinetics of the process is not affected by the diffusion of water. We arrive at the same conclusion when the water concentration in the solution is high.

At high anodic polarization

$$1 \ll \frac{X_5 k}{X_{H_2O}} \tag{8}$$

Then, if $kc_{H_2O} \gg c_2$, from correlation (6) we deduce that

$$j_I = X_{H_2O} c_{H_2O} \tag{9}$$

i.e. in this case the rate of the anodic dissolution of the metal is governed by the limiting current for the diffusion of water. Separation of salt can begin on the electrode surface, with a further anodic polarization of the electrode the anodic current does not increase; in a stationary case the limiting current for the diffusion of water equals the migration by diffusion of the salt away from the electrode surface. The concentration of the salt at the surface is saturation concentration.

A further increase in current density is possible when copper is oxidized by other reaction besides Scheme 1. A brownish-red coating is formed on the electrode surface when copper is anodically polarized at high current density. Also literature data [5] confirm that this is an indication for the appearance of various copper oxides. Therefore, we suppose that at sufficiently positive potentials in the course of the recording of potentiodynamic polarization curves several other reactions proceed beside Scheme 1 at a rate commensurable with these. These other reactions are

6. $$Cu(CuOH)_{ads} \xrightarrow{k_{a_6}} (Cu_2O)_{ads} + H^+ + e$$

7. $$(Cu_2O)_{ads} \underset{k_{k_7}}{\overset{k_{a_7}}{\rightleftharpoons}} Cu(CuO)_{ads}$$

8. $$(CuOH^+)_{ads} \underset{k_{k_8}}{\overset{k_{a_8}}{\rightleftharpoons}} (CuO)_{ads} + H^+.$$

Scheme 2

In Scheme 2 also the rate constants are marked. Reaction 6 is an electrode process, thus k_{a_6} varies exponentially with the electrode potential [2]. Reaction 6 effects the current that passes through the electrode, only at sufficiently positive potentials (in practice most probably when the rate of processes of Scheme 1 becomes independent of the potential), thus when current densities are low, the role of reactions of Scheme 2 in the electrode processes can be disregarded. Let j_{II} symbolize the contribution of reactions in Scheme 2 to current density j across the electrode then

$$j + j_I + j_{II} \tag{10}$$

and

$$j_{II} = k_{a_6}\theta_1 \tag{11}$$

where θ_1 stands for the part of copper covered with CuOH. In order to get a value for j_{II} first should be calculated.

Taking into consideration the reactions in Schemes 1 and 2 (equilibria 1, 2, 3, 7 and 8) for θ_1 we get [10, 11]:

$$\theta_1 = \left[\frac{k_{k_1} c_{H^+}}{k_{a_1}} + \left(\frac{k_{a_5} c_{H^+}}{k_{k_3}} + \frac{k_{k_7} k_{a_8}}{k_{a_7} k_{k_8} c_{H^+}} + \frac{k_{a_8}}{k_{k_8} c_{H^+}} \right) \frac{k_{a_2}}{k_{k_2}} \right]^{-1}. \tag{12}$$

According to our supposition in current-free state, or at low anodic polarization $k_{k_1} c_{H^+} \gg k_{a_1}$. Therefore, when anodic polarization is not too high the second term on the right hand side of Eq. (12) can be disregarded and we obtain

$$\theta_1 = \frac{k_{a_1}}{k_{k_1} c_{H^+}}. \tag{13}$$

An increase in anodic polarization increases θ_1 (because process 1 is an electrode reaction). However, with the increase of polarization the terms of the right hand side of Eq. (12) become commensurable, moreover, at further anodic polarization, the first term becomes negligible in comparison to the second one, thus θ_1 decreases when the positive potential grows. (Also process 2 is an electrode reaction!) In other words: θ_1 changes according to a curve that passes through a potential maximum. However, we assume that $\theta_1 \ll 1$.

Keeping in mind that electrode reactions are exponential functions of electrode potentials, and on the basis of Eq. (3) and Eqs (10), (11), (12) we can write

$$j = \frac{X_5 \left(k' c_{H_2O} \exp \frac{2F\varepsilon}{RT} - c_2 \right)}{1 + \frac{X_5 k' \exp \frac{2F\varepsilon}{RT}}{X_{H_2O}}} + \frac{k'_{a_6} \exp \frac{\alpha_6 F\varepsilon}{RT}}{K_1 \exp - \frac{F\varepsilon}{RT} + K_2 \exp \frac{F\varepsilon}{RT}} \tag{13}$$

where

$$k' = \frac{k'_{a_1} k'_{a_2} k'_{a_3} k_{a_4}}{k'_1 k'_{k_2} k_{k_3} k_{k_4}},$$

$$K_1 = \frac{k_{k_3} c_{H^+}}{k'_{a_1}}$$

$$K_2 = \frac{k_{a_3} c_{H^+}}{k_{k_3}} + \frac{k_{k_7} k_{a_8}}{k_{a_7} k_{k_8} c_{H^+}} + \frac{k_{a_8}}{k_{k_8} c_+} \cdot \frac{k'_{a_2}}{k'_{k_2}}$$

ε = electrode potential, k'_{a_1}, k'_{k_1}, k'_{a_2}, k'_{k_2} and k'_{a_6} stand for the rate constants of the corresponding electrode reactions when $\varepsilon = 0$, α_6 is the transfer coefficient in reaction 6, the other symbols are the usual ones.

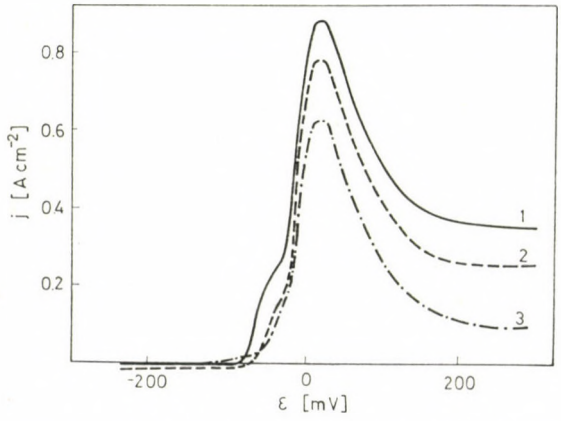

Fig. 6. Potentiodynamic curves calculated according to Eq (13) $k' = 3$; $k'_{a_6} = 1$ A dm^{-2}; $\alpha_6 = 0.5$; $K_1 = K_2 = 1$; (1) $-X_5 = X_{H_2O} = 0.01$ A dm mole^{-1}, $c_2 = 0.5$ mole dm^{-3}, $c_{H_2O} =$ $= 35$ mole dm^{-3}, (2) $-X_5 = X_{H_2O} = 0.01$ A dm mole^{-1}, $c_2 = 1.5$ mole dm^{-3}, $c_{H_2O} = 25$ mole dm^{-3}; (3) $X_5 = X_{H_2O} = 0.0025$ A dm mole^{-1}, $c_2 = 0.5$ mole dm^{-3}, $c_{H_2O} = 35$ mole dm^{-3}

Figure 6 shows curves calculated with parameters arbitrarily taken. These show that Eq. (13) approximately describes the character of a potentiodynamic curve experimentally obtained, and changes in this character when various parameters (concentration of $CuSO_4$, r.p.m. of the electrode) are altered. This makes it highly probable that reaction Schemes 1 and 2 indeed describe the processes which proceed on the copper electrodes under the conditions here studied, processes which essentially affect kinetics.

Further, with the help of Eq. (13) it can be interpreted how temperature, concentrations of H_2SO_4 and $CuSO_4$, affect the critical current density j_p for passivation.

When temperature is raised the concentration of unbound water increases, and it decreases when the concentrations of sulphuric acid and copper sulphate increase. Thus it is clear that raising the temperature increases j_p and that it decreases when concentrations of sulphuric acid and copper sulphate increase.

Measurements with rotating copper disc — platinum ring electrodes show that hydrated Cu^+ ions migrate away from the surface of the electrode and are oxidized to Cu^{2+} ions on the platinum ring. Accordingly the following processes occur:

9. $$(CuOH)_{ads} + H^+ + x\,H_2O \rightleftharpoons [Cu^+_{(aqu)}]_0$$

10. $$[Cu^+_{(aqu)}]_0 \rightarrow Cu^+_{(aqu)}$$

Scheme 3

Reaction 9 (possibly a series of consecutive steps) produces Cu^+ ions capable to migrate off the electrode. The limiting current I_R of oxidation, which can be measured on the ring electrode, is

$$I_R = r_1^2 \pi N X_1 c_{10} \tag{14}$$

when the solution does not contain any Cu^+ ions (*cf.* [11], p. 103); here N is a constant depending on the geometry of the ring disc electrode, r_1 is the radius of the electrode disc, X_1 is the rate constant of the diffusion of Cu^+ ions, c_{10} is the concentration of hydrated Cu^+ ions at the surface of the disc electrode. From 9. at equilibrium, when concentrations of H^+ and H_2O are constant and anodic polarization is not too high, c_{10} becomes proportional to θ_1, *i.e.*

$$c_{10} = k_1 \theta_1 \tag{15}$$

where k_1 is constant.

On the basis of (12), (14) and (15) we get

$$I_R = \frac{r_1^2 \pi N X_1 k_1}{K_1 \exp -\dfrac{F\varepsilon}{RT} + K_2 \exp \dfrac{F\varepsilon}{RT}}. \tag{16}$$

According to (16), and in accord with experimental results, when I_R is plotted as a function of electrode potential ε, a curve that passes a maximum results and this maximum on the I_R *vs.* ε curve appears at more negative potentials than the maximum of the j *vs.* ε curve. This can be seen in Fig. 5 which show the experimental data as well as in Fig. 7 which shows the curves calculated with parameters arbitrarily chosen on the basis of Eqs (13) and (16).

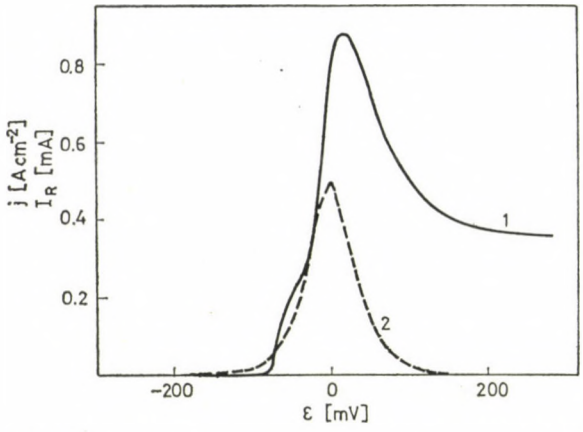

Fig. 7. (1) I *vs.* ε potentiodynamic curve calculated on the basis of Eq (13). The parameters adopted are the same as those pertinent to curve 1) in Fig. 6. (2) correlation I_R *vs.* ε, at constant ring potential, calculated according to Eq (16); $r_1^2 \pi N = 10^{-2}$ dm^2; $k_1 = 2.10^{-3}$ A dm^2; $K_1 = K_2 = 1$

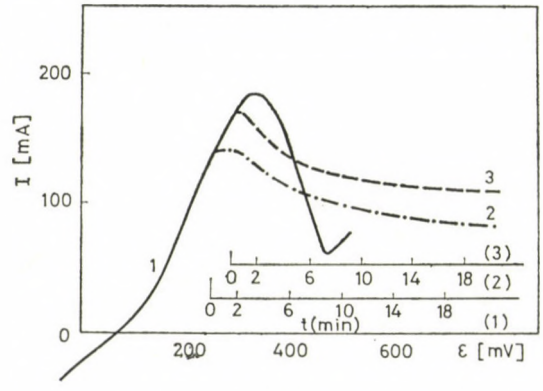

Fig. 8. Potentiodynamic curve for copper at 25 °C in a solution of 0.88 mole dm^{-3} of $CuSO_4$ + 0.5 mole dm^{-3} of H_2SO_4 100 mV min^{-1}. (1) Change of current intensity with time, at constant potential, (2) 250 mV, (3) 280 mV

The correlations here discussed describe the curves pertinent to the potentiodynamics which lead to the passivation of copper. A copper electrode held at a sufficiently positive potential allows the accumulation of Cu_2O and CuO on its surface. Therefore when, for instance, the potential change is stopped before the maximum on the potentiodynamic curve the current intensity that passes through the electrode decreases. This can be seen in Fig. 8. Cu_2O and CuO formed give [12] copper, copper(I)-sulphate, respectively, copper(II) sulphate in sulphuric acid solution. Consequently, on the surface in contact with sulfuric acid solution only insignificant amount of reducible oxide can be present.

Addition of chloride alters the reaction scheme. At low chloride concentration (100 mg dm^{-3}), the concentration of Cu^+ ions formed in process of Scheme 3 is increased and chloride stabilized Cu^+, as can be shown by tests using the rotating disc ring electrode. Therewith θ_1 decreases at a given potential and this causes the passivation potential to shift toward more positive values. A similar effect is due to the addition of dimethylthiourea (0.2 g · dm^{-3}) to copper baths [11]. At higher chloride concentration CuCl is deposited on the surface and this enhances the deposition of salt and oxides on it.

REFERENCES

[1] MATTSON, F., BOCKRIS, J. O'M.: Trans. Faraday. Soc., **55,** 1586 (1959)
[2] KISS, L., FARKAS, J.: Magy. Kém. Folyóirat, **76,** 395 (1970) Acta Chim. Acad. Sci. Hung., **66,** 395 (1970)
[3] MOLODOV, A. I., MARKOSZYAN, G. N., LOSEV, V. V.: Elektrohimiya, **7,** 263 (1971)
[4] ASTAKHOVA, R., SZALMA, J., FARKAS, J., KISS, L.: Magy. Kém. Folyóirat, **85,** 315 (1979)
[5] LECKIE, H. P.: J. Electrochem. Soc., **117,** 1478 (1970)
[6] SADAKOV, G. A., BELYANIYA, T. V.: Zash. Met., **10,** 197 (1974)
[7] BUKAVYATSKAS, V. K., STULGENIE, S. P., STACKYAVICHENE, A. V., MATULIS, YU., YU.: Tr. A N Lit.S.S.R. Seriya B, t. **4** (113) 11 (1979)
[8] KISS, L., DO NGOC LIEN, VARSÁNYI, M. L.: Magy. Kém. Folyóirat, **76,** 371 (1970)
[9] KISS, K., FARKAS, J., KŐRÖSI, A., MANDL, J.: Magy. Kém. Folyóirat, **69,** 127 (1973)
[10] KISS, L.: Kinetics of the Electrochemical Dissolution of Metals (in Hungarian), Akadémiai Kiadó, Budapest 1980, p. 131, 145
[11] BOSQUEZ, A.: Ph. D. Thesis, Budapest, 1980
[12] NÁRAY SZABÓ, I.: Inorganic Chemistry, Vol. III (in Hungarian), Akadémiai Kiadó, Budapest 1958, p. 56

László KISS
Magda VARSÁNYI } H—1088 Budapest Puskin u. 11—13.

Ágnes BOSQUEZ National University of Panama

Acta Chimica Academiae Scientiarum Hungaricae, Tomus 108 (4), pp. 381—388 (1981)

AN ELECTROCHEMICAL STUDY OF PALLADIUM-COPPER CATALYSTS

T. MALLÁT and J. PETRÓ*

(*Department of Organic Chemical Technology, Technical University, Budapest*)

Received November 17, 1980

Accepted for publication January 22, 1981

Sorption of hydrogen by Pd—Cu catalysts prepared by co-precipitation has been studied by means of electrochemical potentiodynamic polarization. When the copper content increases, the amount of sorbed hydrogen decreases, the bonding between metal and hydrogen becomes weaker, the energy distribution of metal — hydrogen bonding becomes ever more homogeneous. At copper contents of 42—44 atom % the β-phase dissolution of hydrogen in dispersed, powdery Pd—Cu catalysts stops; this is shown by the free enthalpy changes pertinent to the $\beta \rightarrow \alpha$-phase transition and by the hydrogen to metal atomic ratios observed. The activity in the hydrogenation of various functional groups of catalysts containing 10—30 atom % copper is better than that of unalloyed palladium.

Introduction

The hydrogen sorption power and the catalytic activity of Pd—Cu alloys is the topic of many scientific papers. It has been found that copper diminishes the solubility of hydrogen and the energy content of the metal–hydrogen bond; the measure of this decrease, however, is rather different according to the data given by various authors [1—4]. Even relatively great amounts, *e.g.* 40 to 60 atom % of copper do hardly diminish the activity; or in some cases the activity *vs.* copper content curve has a maximum at low copper contents. Deactivation of the catalyst occurs only at copper contents above 60 to 70 atom % [5—8]. The introduction of copper affects not only the rate of hydrogenation but also influences its direction: an aldehyde can be made with high selectivity from an acid chloride with a suitably prepared Pd—Cu catalyst [9, 10].

The authors of the papers mentioned above believe that changes in hydrogen sorption or activity are due partly to changes in the electronic structure and partly to those in the crystal lattice parameters. Lattice constants decrease, and the ratio of electrons to atoms increases with an increase of copper content [2, 11].

When at equilibrium, palladium with copper up to 40 atom % forms a homogeneous, face-centered cubic lattice: a substitution alloy. With a greater

* To whom correspondence should be addressed

participation of copper the formation of intermetallic compounds like PdCu or $PdCu_3$ [2] or, according to other authors [12], $PdCu_5$ or Pd_3Cu_5 can be noted.

In this work we used highly active Pd—Cu catalysts prepared under conditions usually employed in catalyst manufacture, *i.e.* catalysts at non-equilibrium composition. The metal-hydrogen system was studied by an electrochemical (potentiodynamic) method, the applicability of which had been proven in earlier work [13, 14] with Pd and Pd—Hg catalyst powders.

Experimental

Catalysts and electrolyte were prepared from analytically pure chemicals.

Pd—Cu catalysts with 0, 10, 20, 30, 40, 60 and 80 atom % copper were prepared by means of hydrogenation. A solution (60 cm^3) of H_2PdCl_4 and $CuSO_4$ in suitable proportions was allowed to fall dropwise on $NaHCO_3$ (100 g) at 370—380 K. The dry powder thus obtained was reduced at 370 K for 30 min in a current of hydrogen. Then the inorganic salts were removed by dissolving in water. Filtration followed and copious rinsing with water till no ions remained. Drying at room temperature under reduced pressure produced the finished catalyst.

The three-electrode cell used for potentiodynamic polarization has been described in an earlier paper [15]. 4 mg portions of the catalyst were placed upon the measuring electrode. The cell, without the reference and polarizing electrodes, was flushed with argon for 15 min, with hydrogen for 15 min, and again with argon for 2 to 4 min, in order to remove excess hydrogen. Then the cell was filled with a 0.5 *M* solution of sulfuric acid.

The potential of Pd—Cu catalyst after the addition of the electrolyte was less than 30 mV; recording started upon anodic polarization.

Flushing with hydrogen, *i.e.* reduction, was needed because part of the metal in the dry catalyst stored in air (with some oxygen adsorbed on its surface) dissolves when sulfuric acid is poured onto it [16].

An AMEL SU 551 type potentiostat was used. Recordings proceeded at polarization rates between 2 and 40 mV min^{-1}, at room temperature.

The hydrogen content of the catalysts was determined from the hydrogen region of the potentiodynamic curves by graphical integration of the area under the curve, with correction for the capacity of the double layer. Hydrogen contents were found to be unaffected by the rates of polarization.

The hydrogen contents of 2 to 10 mg portions of a Pd catalyst were determined in separate tests, and it was found that (within systematic errors of $\pm 5\%$) hydrogen contents were unaffected by variation of the sample mass. This suggests and proves that the contact between the blank Pt-foil of the measuring electrode and the catalyst powder was good. Such results are to be found also in the literature [7]. It has also been shown that the surface of a catalyst powder in a similar system determined electrochemically on the basis of hydrogen content and according to the BET method do not differ from each other by more than 10—20% [18].

The potentials pertinent to hydrogen ionization maxima were determined on fresh samples every time because upon anodic polarization above 300 mV the metals dissolve and thus the composition at the surface is substantially altered. The rate of polarization was decreased till the peak potential did not change (± 2 mV) any more, taking into account also the approximate ohmic potential drop. At less than 30 mV the location of the peak was rather uncertain because adsorption and desorption processes assumed ever greater importance.

The *activity* of the catalyst was studied by means of hydrogenation in the liquid phase of cyclohexene, acetophenone, nitrobenzene, and phenylacetylene. 20 mg portions of the catalyst and 10 cm^3 portions of ethanol were placed in a hydrogenation flask of 50 cm^3 capacity. The air above this liquid was replaced by hydrogen, then the catalyst was saturated with hydrogen whilst the flask was shaken (298 K, 101 kPa, 330 min^{-1}). After injection of 2 cm^3 of a solution of the reagent in ethanol into the closed system the consumption of hydrogen was followed with a gas burette. 1 cm^3 of this reagent solution contained an amount of the organic reagent whose complete reduction required 1 mmol of hydrogen. The activity was characterized by the initial consumption of hydrogen referred to 1 g of the catalyst.

Results and Discussion

The potentiodynamic curves for a Pd catalyst and for Pd—Cu catalysts containing 10, 20, 30, 40, and 60 atom % copper are shown in Fig. 1. Within the hydrogen region, *i.e.* from 0 to about 300—350 mV, there are two characteristic maxima on the curve for Pd. The first, somewhat higher, peak is attributable principally to the ionization of hydrogen dissolved in the β-phase; the second pertains to strongly bound, mainly adsorbed hydrogen. In this latter interval the slight amount of dissolved (α-phase) hydrogen can be disregarded. The error in this differentiation is not greater than 10% on Pd with a large surface area [18.] Further maxima can be observed when the rate of hydrogen consumption is kept low, as reported earlier [13].

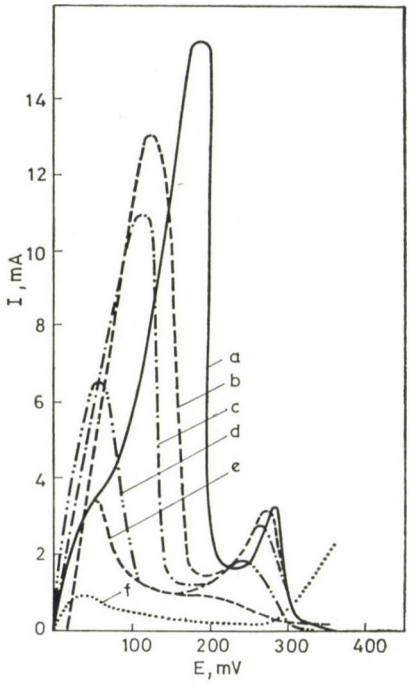

Fig. 1. Potentiodynamic curves of Cu—Pd alloy catalysts ($v = 40$ mV min^{-1}). a) Pd; b) 10 at.% Cu—Pd; c) 20 at.% Cu—Pd; d) 30 at.% Cu—Pd; e) 40 at.% Cu—Pd; f) 60 at.% Cu—Pd

Introduction of copper causes a shift of the peaks towards lower potentials and a decrease of their heights. Hydrogen contents determined from the areas under the curves are collected in Table I. With the increase of copper content, the greater amount of loosely bonded hydrogen and total hydrogen decreases monotonically. The amount of strongly bonded hydrogen decreases

Table I

Hydrogen content of Pd—Cu *catalysts determined by a potentiodynamic method*

Copper (at. %)	Hydrogen $\left(\frac{cm^3}{g\ catalyst}\right)$		
	tota	loosely bonded I	strongly bonded II
0	73.1	62.9	10.1
10	66.5	52.3	14.2
20	51.0	37.8	13.2
30	29.3	19.3	10.0
40	16.9	10.3	6.6
60	2.9	—	—
80	—	—	—

slowly after a maximum. The two types of hydrogen cannot be distinguished from each other when a Pd—Cu catalyst with 60 atom % copper is used; with a Cu—Pd catalyst with 80 atom % copper no hydrogen sorption occurs at all.

On the basis of the amount of strongly bonded adsorbed hydrogen, an approximate figure for the surface area of palladium can be deduced, if monolayer coverage is assumed and the number of metal atoms per unit surface area is known [18, 19]. In this way the figure 42 $m^2\ g^{-1}$ is found as the specific surface area of palladium. When copper is introduced also copper atoms are present on the surface besides palladium atoms and since under these circumstances no hydrogen sorption by copper occurs (supposing that spill-over is not significant), the amount of adsorbed hydrogen will be proportional to the amount of palladium at the surface. With this in mind, and disregarding changes in the stoichiometry of hydrogen chemisorption and in the lattice constant, Figure 1 also suggests that the specific surface areas of catalysts with 10, 20 and 30 atom % copper are greater than that of a Pd catalyst.

A plot of the ratio of β-phase hydrogen to the overall number of metal atoms as a function of copper concentration produces, to a good approximation, a straight line (Fig. 2). The intercept of this line indicates the copper content (44 atom %) when hydrogen ceases to be dissolved. This figure is quite near to that calculated from data published by BURCH and BUSS [2]. The slope of the line shows that one atom of copper is equivalent to 1.25 atom of hydrogen. Data in the literature [1, 2, 3] do not give an answer to the question whether copper is equivalent to one or two hydrogen atoms.

Table II presents peak potentials determined by means of decreasing the rate of polarization; they characterize the strength of the metal–hydrogen bonding. Altogether five characteristic peaks can be distinguished for palla-

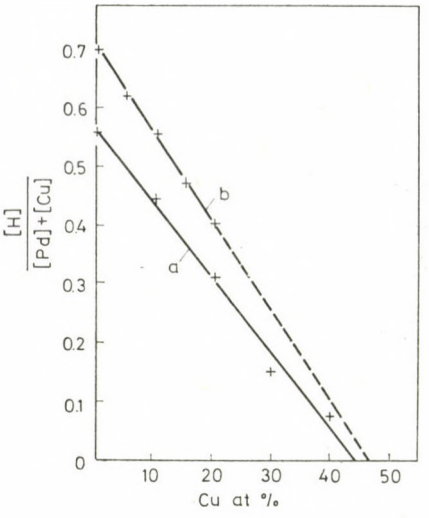

Fig. 2. Dissolution of hydrogen in Cu—Pd alloys. a) This work; b) Ref. [2]

Table II

Locations of maxima on the potentiodynamic curves of Pd—Cu *catalysts*

Copper (at. %)	Hydrogen ionization maxima (mV)			Metal dissolution	
				beginning (mV)	maximum (mV)
0	64, x	175	258, *x*	—	—
10	46, x		246	525	610
20	35		238	505	600
30	18		230	480	600
40	—		220	420	600
60	—		y	290	595
80	—		—	290	580

x = not an independent peak, only a shoulder
y = diffuse peak, maximum indeterminable

dium at low rates of potential change. On samples containing 10 atom % copper, there are three such peaks; samples containing greater amounts of copper have only two characteristic peaks. At 60 atom % copper, even the two principal forms of hydrogen cease to be distinct. The potentials pertinent to these two hydrogen peaks monotonically decrease with the increase of copper content; this means that the energy of the metal–hydrogen bond decreases.

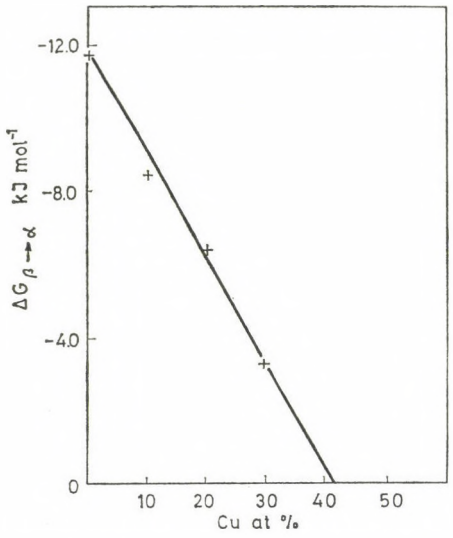

Fig. 3. Free enthalpy change of hydrogen dissolution in Cu—Pd alloys as a function of the composition

From 40 atom % upwards, the location of loosely bonded hydrogen cannot be determined accurately because of the rather low potentials.

The change of free enthalpy, ΔG, pertinent to the phase transition $\beta \rightarrow \alpha$ was determined by means of the equation $\Delta G = -2\ FE$, from peak potentials, E, at quasi-equilibrium states. They are plotted as a function of the copper content in Fig. 3. The intercept of the straight line corresponds to a copper content of 42 atom %. This means that β-phase dissolving of hydrogen at higher copper contents is possible only if extraneous work is invested. The figure just given is in good agreement with that obtained from the hydrogen to metal atomic ratios shown in Fig. 2.

Figure 1 shows that also on the potentiodynamic curve for a catalyst with 60 atom % copper there is a maximum below 100 mV though no dissolved hydrogen in this sample seems to be possible if what has been written in connection with Figs 2 and 3 is true. An explanation of this contradiction may be found in the possibility that the composition of the catalyst grains oscillates around an average value and may significantly differ from it. Further, in this case the approximation that hydrogen below 100 mV can be considered to be dissolved mostly in the β-phase may cause greater errors.

The lattice constants of the catalysts determined by X-ray diffraction decrease monotonically with the increase of copper content (Table III), in other words, an alloy is formed at least inside the grains. Palladium lines are broadened in every case, indicating that the dispersity is very great indeed, but a new phase cannot be detected at all.

Table III

Lattice constants of Pd—Cu *catalysts as a function of copper content*

Copper (at. %)	a_0 (nm)
0	0.389
10	0.387
20	0.385
30	0.382
40	0.379
60	0.373
80	0.372

These findings accord quite well with the picture obtainable when the dissolving of hydrogen is studied, *i.e.* the alloying of copper decreases the lattice constant and adsorption. It is interesting to note that, in contrast to the literature [2, 12], a homogeneous alloy is formed also above 40 atom % of copper. This is quite understandable since these are thermodynamically labile, active catalysts.

The activity of the catalysts in the liquid phase hydrogenation of carbon–carbon double and triple bonds, of model compounds which contain a nitro group or carbonyl group, has a maximum which is a function of copper content (Table IV). A catalyst with 80 atom % copper, on which, according to what

Table IV

Relative activity of Pd—Cu *catalysts as a function of copper content*

Copper (at. %)	Activity $\left(\frac{\text{cm}^3\ \text{H}}{\text{min g of catalyst}}\right)$			
	cyclohexene	acetophenone	phenylacetylene	nitrobenzene
0	1.0	1.0	1.0	1.0
10	1.06	1.25	1.46	1.12
20	0.87	1.28	1.34	0.97
30	0.87	1.66	1.31	0.99
40	0.62	0.94	1.11	0.79
60	0.11	0.16	0.55	0.12
80	—	—	—	—

has been said before, no hydrogen sorption occurs, is inactive also in hydrogenation.

Several cases are quoted in the literature [14, 20] in order to show that the activity of platinum metals alloyed with 10 to 30 atom % inactive component is better than that of the pure metal. Several attempts, to explain how activities of Pd—Cu alloys are affected by the composition, are known, as mentioned in the introductory part of this paper. In this instance the simplest interpretation of the activity maxima might be that the initial increase of activity is due to an increase of surface area. Substitution of copper atoms for palladium atoms gradually compensates this effect and the alloy becomes inactive at a certain composition. Unequivocal deductions, however, require that we know also the surface composition of catalysts. This we propose to determine, also by means of electrochemical techniques, in studies closely connected with the one reported here.

*

Our thanks are due to Dr. A. KÁLMÁN, Central Research Institute for Chemistry of the Hungarian Academy of Sciences, Budapest, for the X-ray diffractograms.

REFERENCES

[1] KARPOVA, R. A., TVERDOVSKII, I. P.: Zh. Fiz. Khim., **33,** 1393 (1959)
[2] BURCH, R., BUSS, R. G.: J. Chem. Soc. Faraday Trans., I, **71,** 913, 922 (1975)
[3] BURCH, BUSS, R. G.: Solid State Commun., **15,** 407 (1974)
[4] FLANAGAN, T. B., CHISDES, D. M.: Solid State Commun., **16,** 529 (1975)
[5] BIZHANOVA, N. B., ERZHANOVA, M. S., SOKOLSKII, D. V.: Izv. Akad. Nauk Kazah. SSR., Ser. Khim., **19,** 15 (1949)
[6] TVERDOVSKII, I. P., VERT, ZH. L., KARPOVA, P. A.: Tr. Gosud. Inst. Prikl. Khim., **46,** 207 (1960)
[7] CADENHEAD, D. A., MASSE, N. G.: J. Phys. Chem., **70,** 3558 (1966)
[8] ALCHUDZHAN, A. A., KRISTOSTYRYAN, E. T.: Izv. Akad. Nauk Arm. SSR, **10,** 333 (1957)
[9] PETRÓ, J., MÁTHÉ, T., TUNGLER, A., CSŰRÖS, Z.: Hung. 168,073 (1977); Brit. 1,510,195 (1978); U.S. 4,021,374 (1977)
[10] PETRÓ, J., MÁTHÉ, T., TUNGLER, A.: Hung. 169,835 (1978); Ger. 2,506,157 (1977)
[11] TVERDOVSKII, I. P., VERT, ZH. L., KONDRASHEV, YU. D:. Dokl. Akad. Nauk SSSR, **127** 835 (1959)
[12] SAVITSKII, E. M., POLYAKOVA, V. P., TYLKINA, M. A.: Splavy palladiya. Nauka, Moscow, 1967
[13] MALLÁT, T., POLYÁNSZKY, É., PETRÓ, J.: J. Catal., **44,** 345 (1976)
[14] PETRÓ, J., MALLÁT, T.: Acta Chim. Acad. Sci. Hung., **95,** 253 (1977)
[15] POLYÁNSZKY, É., MALLÁT, T., PETRÓ, J.: Acta Chim. Acad. Sci. Hung., **92,** 147 (1977)
[16] POURBAIX, M.: Atlas of Electrochemical Equilibria in Aqueous Solution. Pergamon Press, London 1966
[17] KUTYUKOVA, G. G., FASMAN, A. B., TUNGATBAEV, S. T.: Elektrokhimiya, **11,** 1357 (1957)
[18] BURSHTEIN, R. H., TARASEVICH, M. R., VILINSKAYA, V. S.: Elektrokhimiya, **3,** 349 (1967)
19] ABEN, P. C.: J. Catal., **10,** 224 (1958)
20] BOND, G. C.: Catalysis by Metals. Acad. Press, London 1962

Tamás MALLÁT
József PETRÓ
H—1521 Budapest, Műegyetem rkp. 3.

Acta Chimica Academiae Scientiarum Hungaricae, Tomus 108 (4), pp. 389—394 (1981)

REACTIONS OF *O,O*-DIETHYLPHOSPHONO DITHIOCARBAMATE WITH TITANIUM(IV), ZIRCONIUM(IV) AND OXOMOLYBDENUM(VI) DERIVATIVES

G. S. SODHI and N. K. KAUSHIK*

(*Department of Chemistry, University of Delhi, India*)

Received September 10, 1980

In revised form December 12, 1980

Accepted for publication January 27, 1981

Some *O,O*-diethylphosphono/dithiocarbamate complexes of the type $(\eta^5\text{-R})_2$ M$\{S_2CNHPO(OEt)_2\}Cl$ [R = C_5H_5, $CH_3C_5H_4$, C_9H_7, M = Ti(IV), Zr(IV) and OMo(VI)] have been prepared. Various physical measurements reveal that these complexes are nonelectrolytes in which the dithiocarbamate ligand is bidentate. The complexes are fairly stable in inert atmosphere, but decompose on standing in air.

Introduction

Dithiocarbamate derivatives often exhibit unusual coordination phenomena. This is the outcome of the fact that in some complexes, the dithiocarbamate ligand behaves as a monodentate group [1, 2], while in others it acts as a bidentate group [3—6]. In order to investigate the bonding mode of the *O,O*-diethylphosphono dithiocarbamate group, we report in this communication the synthesis of a few complexes of the type $(\eta^5\text{-R})_2$M $\{S_2CNHPO(OEt)_2\}Cl$ where *R* = cyclopentadienyl (C_5H_5); methylcyclopentadienyl ($CH_3C_5H_4$), indenyl (C_9H_7), M = Ti(IV), Zr(IV) and OMo(VI). These complexes have been characterized on the basis of elemental analysis, electrical conductivity and magnetic susceptibility measurements, and by IR, NMR and electronic spectral studies. Infrared and UV spectral studies demonstrate that in these complexes the dithiocarbamate group behaves as a bidentate ligand, similar to those reported earlier [3—6]. Conductivity measurements in nitrobenzene solution indicate that these complexes are nonelectrolytes. The complexes are fairly stable in inert atmosphere but decompose on standing in air.

* To whom correspondence should be addressed

Table I

Analytical data and physical characteristics of the complexes

Compound	Colour	Dec. temp. °C (a)	Conductivity data λ(b) (molarity × 10^3=0.3)	% of Elements found (Calc.)				
				M	S	P	Cl	N
$(\eta^5\text{-}C_5H_5)_2Ti(DPD)Cl$	Orange	208	0.52	10.93 (10.85)	14.40 (14.49)	7.11 (7.02)	8.09 (8.04)	3.25 (3.11)
$(\eta^5\text{-}CH_3C_5H_4)_2Ti(DPD)Cl$	Reddish brown	202	0.55	10.29 (10.20)	13.74 (13.63)	6.69 (6.60)	7.65 (7.56)	2.88 (2.98)
$(\eta^5\text{-}C_9H_7)_2Ti(DPD)Cl$	Brown	215	0.52	8.93 (8.84)	11.91 (11.82)	5.65 (5.72)	6.62 (6.55)	2.63 (2.58)
$(\eta^5\text{-}C_5H_5)_2Zr(DPD)Cl$	Pale yellow	218	0.50	18.81 (18.92)	13.20 (13.30)	6.39 (6.28)	7.32 (7.39)	2.88 (2.95)
$(\eta^5\text{-}CH_3C_5H_4)_2Zr(DPD)Cl$	White	211	0.55	17.78 (17.85)	12.48 (12.56)	6.04 (6.11)	6.92 (6.84)	2.73 (2.80)
$(\eta^5\text{-}C_9H_7)_2Zr(DPD)Cl$	Pale yellow	225	0.53	15.59 (15.64)	10.94 (10.86)	5.30 (5.42)	6.07 (6.11)	2.39 (2.29)
$(\eta^5\text{-}C_5H_5)_2MoO(DPD)Cl$	Yellowish green	221	0.52	18.89 (18.98)	12.75 (12.66)	6.20 (6.13)	7.10 (7.02)	2.81 (2.76)
$(\eta^5\text{-}CH_3C_5H_4)_2MoO(DPD)Cl$	Yellow	213	0.51	17.90 (17.98)	11.89 (11.99)	5.90 (5.81)	6.72 (6.65)	2.68 (2.62)
$(\eta^5\text{-}C_9H_7)_2MoO(DPD)Cl$	Yellow	238	0.52	15.90 (15.84)	10.48 (10.57)	5.20 (5.12)	5.75 (5.86)	2.21 (2.31)

(DPD) *O,O*-diethylphosphono dithiocarbamato
(a) Uncorrected values
(b) in $ohm^{-1}\ cm^2\ mole^{-1}$

Results and Discussion

The complexes can be prepared by the reaction of potassium *O,O*-diethylphosphono dithiocarbamate with equimolar proportions of the transition metal derivatives of the type $(\eta^5\text{-R})_2MCl_2$ in refluxing dichloromethane in accordance with the following equation:

$$(\eta^5\text{-R})_2MCl_2 + (EtO)_2PONHCS_2K^+ \rightarrow (\eta^5\text{-R})_2M\{S_2CNHPO(OEt)_2\}Cl + KCl.$$

Table I lists the analytical data and physical characteristics of the complexes. All the complexes are soluble in acetone, DMSO, THF and partly soluble in halogenated hydrocarbons. The molar conductances of 10^{-3} *M* solution of these complexes in nitrobenzene were found to be of the order of 0.5 $ohm^{-1}\,cm^2\,mole^{-1}$. These conductivity results indicate the covalent nature of the compounds and the absence of ionic species in solution. Though the complexes are thermally quite stable, they are kinetically reactive and decompose on standing in air.

Whether the dithiocarbamate group is monodentate or bidentate, is reflected in the $\nu(C\cdots S)$ stretching frequency [1, 7]. The present complexes show only one medium absorption band at $\sim$1000 cm^{-1} which supports the bidentate nature of the dithiocarbamate group in all the complexes.

The band around 1350 cm^{-1} is assigned to the $\nu(C\cdots N)$ stretching frequency. When compared with the complexes reported earlier [3—6], this band occurs at a lower energy indicating considerably less double-bond character of the $(C\cdots N)$ bond in these complexes. The infrared frequencies, together with the assignments for the $(\eta^5\text{-R})_2M\{S_2CNHPO(OEt)_2\}Cl$ complexes are listed in Table II.

Table II

Characteristic infrared frequencies (cm^{-1}) *of the complexes*

Compound	ν(M—S)	ν(M—Cl)	$\nu(C\cdots N)$	$\nu(C\cdots S)$	ν(P=O)	ν(C—O)
$(\eta^5\text{-}C_5H_5)_2Ti(DPD)Cl$	345 (m)	380 (m)	1370 (s)	995 (s)	1260 (m)	1110 (s)
$(\eta^5\text{-}CH_3C_5H_4)_2Ti(DPD)Cl$	350 (m)	375 (m)	1375 (s)	1000 (s)	1250 (m)	1120 (s)
$(\eta^5\text{-}C_9H_7)_2Ti(DPD)Cl$	345 (m)	370 (m)	1350 (s)	1010 (s)	1265 (m)	1105 (s)
$(\eta^5\text{-}C_5H_5)_2Zr(DPD)Cl$	355 (m)	385 (m)	1360 (s)	990 (s)	1255 (m)	1115 (s)
$(\eta^5\text{-}CH_3C_5H_4)_2Zr(DPD)Cl$	360 (m)	375 (m)	1355 (s)	1005 (s)	1250 (m)	1110 (s)
$(\eta^5\text{-}C_9H_7)_2Zr(DPD)Cl$	345 (m)	380 (m)	1375 (s)	1015 (s)	1265 (m)	1115 (s)
$(\eta^5\text{-}C_5H_5)_2MoO(DPD)Cl$	355 (m)	370 (m)	1370 (s)	995 (s)	1270 (m)	1105 (s)
$(\eta^5\text{-}CH_3C_5H_4)_2MoO(DPD)Cl$	360 (m)	375 (m)	1380 (s)	1020 (s)	1260 (m)	1120 (s)
$(\eta^5\text{-}C_9H_7)_2MoO(DPD)\,Cl$	358 (m)	375 (m)	1375 (s)	1005 (s)	1255 (m)	1125 (s)

(s) = strong, (m) = medium

Absorptions owing to the P=O stretching vibrations occur at $\sim$1260 cm^{-1}. The free ligand shows this absorption at $\sim$1250 cm^{-1}. Since there is no significant shift of ν(P=O) in the complexes, it is unlikely that the atom attached directly to the phosphorus could act as a coordinating centre.

The strong absorption at $\sim$1110 cm^{-1} is characteristic of the C—O stretching vibration in the C_2H_5OP group, while that at $\sim$3075 cm^{-1} are due to N—H stretching frequency. The medium, intensity bands in the range 365—345 cm^{-1} are assigned to the metal–sulphur vibrational frequencies [8]. The presence of the Mo=O group in molybdenum derivatives is confirmed by the appearance of a sharp absorption band at $\sim$990 cm^{-1}.

Table III lists the position of the resonance signals observed in the NMR spectra of the complexes. The NMR spectra are simple and easily interpreted. The intensities were determined by planimetric integration of these spectra and the integrated proton ratios correspond to the formula

$$(\eta^5\text{-R})_2\text{M}\{S_2CNHPO(OEt)_2\}\text{Cl}.$$

Table III

Proton chemical shifts (δ) and coupling constant data of the complexes

Compound	R	—NH	—$POCH_2$—	—CH_3
$(\eta^5\text{-}C_5H_5)_2$Ti(DPD)Cl	R=C_5H_5	4.82	4.18 (m)	1.35 (t)
	6.0 (s)			J = 7.0 Hz
$(\eta^5\text{-}CH_3C_5H_4)_2$Ti(DPD)Cl	R=$CH_3C_5H_4$	4.85	4.22 (m)	1.33 (t)
	5.8 (s), 2.22 (s)			J = 7.0 Hz
$(\eta^5\text{-}C_9H_7)_2$Ti(DPD)Cl	R=C_9H_7	4.80	4.20 (m)	1.31 (t)
	6.85—7.30 (m)			J = 7.2 Hz
$(\eta^5\text{-}C_5H_5)_2$Zr(DPD)Cl	R=C_5H_5	4.82	4.23 (m)	1.34 (t)
	6.08 (s)			J = 7.0 Hz
$(\eta^5\text{-}CH_3C_5H_4)_2$Zr(DPD)Cl	R=$CH_3C_5H_4$	4.80	4.25 (m)	1.32 (t)
	5.85 (s), 2.15 (s)			J = 6.8 Hz
$(\eta^5\text{-}C_9H_7)_2$Zr(DPD)Cl	R=C_9H_7	4.83	4.17 (m)	1.35 (t)
	6.73—7.35 (m)			J = 7.2 Hz
$(\eta^5\text{-}C_5H_5)_2$MoO(DPD)Cl	R=C_5H_5	4.85	4.21 (m)	1.34 (t)
	6.12 (s)			J = 6.7 Hz
$(\eta^5\text{-}CH_3C_5H_4)_2$MoO(DPD)Cl	R=$CH_3C_5H_4$	4.83	4.17 (m)	1.36 (t)
	5.92 (s), 2.21 (s)			J.=.7.0 Hz
$(\eta^5\text{-}C_9H_7)_2$MoO(DPD)Cl	R=C_9H_7	4.82	4.19 (m)	1.32 (t)
	6.80—7.25 (m)			J = 7.1 Hz

(s) = singlet, (t) = triplet, (m) = multiplet

Although the ethoxy protons are distant from the sulphur atoms in the present complexes they are shifted to a lower field than that for the free ligand [9]. The signals of NMR spectra are sharp, without being split.

Whereas the resonance due to C_5H_5 proton occurs as a sharp singlet, that due to the C_5H_4 portion of η^5-$CH_3C_5H_4$ is observed is a comparatively broad peak.

The electronic spectra of the complexes, exhibit a single band in the 24,700—24,350 cm^{-1} region which may be assigned to the charge-transfer band [10, 11] in accord with the electronic configuration $(n\text{-}1)d^\circ$, ns° of the metal atom in each case. Magnetic susceptibility values at room temperature show that all complexes are diamagnetic. The diamagnetic dithiocarbamates are of particular interest since they do not absorb in much of the visible region of the spectrum. Hence the absorption in the UV region arising due to internal transitions among the chromophoric groups present in the ligand can be studied. All the complexes show an intense band at $\sim$35,000 cm^{-1} due to $\pi \rightarrow \pi^*$ transition of the N····C····S group [12, 13]. The position of this band is shifted to a lower energy due to the electron-withdrawing ability of the amine group in the ligand. Another band which is expected to occur at $\sim$30,000 cm^{-1} due to $\pi \rightarrow \pi^*$ transition in the S····C····S group and is associated with the non-equivalence of the C—S bonds, is not observed as a prominent band in these complexes, showing that the dithiocarbamate ligand is bidentate. This fact is also confirmed by IR spectroscopy.

Experimental

The metal content, phosphorus, nitrogen and sulphur were determined by standard methods [14]. Nitrobenzene was purified for conductance measurements by the method described by FAY and Lowry [15]. Various transition metal derivatives, $(\eta^5\text{—R})_2TiCl_2$ [16—18] $(\eta^5\text{—R})_2ZrCl_2$, [18—20] and $(\eta^5\text{—R})_2MoOCl_2$ [21], (R = C_5H_5, $CH_3C_5H_4$ and C_9H_7) were prepared by standard methods. Potassium *O,O*-diethylphosphono dithiocarbamate was prepared by the method described by ADDOR [22].

Preparation of complexes. Potassium salt of *O,O*-diethylphosphono/dithiocarbamate was refluxed separately with equimolar quantities of the transition metal derivatives of the type $(\eta^5\text{—R})_2MCl_2$ [R = C_5H_5, $CH_3C_5H_4$, C_9H_7, M = Ti(IV), Zr(IV) and OMo(IV)] in dichloromethane for about 10 hrs. The solution was filtered hot and its volume reduced to about one-fourth of the original. The products were obtained by adding petroleum ether to the concentrated filtrate and allowing the mixture to stand overnight.

Conductance measurements were made in nitrobenzene at 30.00 $\pm$ 0.05 °C using a Beckmann Conductivity Bridge (Model RC—18A). Solid state IR spectra were recorded in KBr pellets in the 4000—200 cm^{-1} region on a Perkin—Elmer 621 grating spectrophotometer. Magnetic measurements were carried out by GOUY's method using mercury(II) tetrathiocyanatocobaltate(II) as a calibrant. Visible and UV spectra were recorded on a CØ Russian recording spectrophotometer and Beckmann DU-2 spectrophotometer. Proton NMR spectra were recorded at a sweep width of 900 Hz on a Perkin–Elmer R-32 spectrophotometer. Chemical shifts are expressed relative to an internal reference, TMS (1% by volume).

*

The authors are thankful to the University Grants Commission, New Delhi for providing financial assistance to a research project under which the present work was carried out.

REFERENCES

[1] JOHNSON, B. F. G., ALOBAIDI, K. H., MCCLEVERTY, J. A.: J. Chem. Soc., **1969,** 1668
[2] DOMENICANO, A., VACIAGO, A., ZAMBONELLI, L., LOADER, P. L., VENANZI, L. M.: Chem. Commun., **1966,** 476
[3] KAUSHIK, N. K., BHUSHAN, B., CHHATWAL, G. R.: Synth. React. Inorg., Met. Org. Chem., **8,** 567 (1978)
[4] BHUSHAN, B., MITTAL, I. P., CHHATWAL, G. R., KAUSHIK, N. K.: J. Inorg. Nucl. Chem., **41,** 159 (1979)
[5] KAUSHIK, N. K., BHUSHAN, B., CHHATWAL, G. R.: Transition Metal Chem., **3,** 215 (1978)
[6] KAUSHIK, N. K., BHUSHAN, B., CHHATWAL, G. R.: Z. Naturforsch., **34**b. 949 (1979)
[7] BONATI, F., UGO, R.: J. Organomet. Chem., **10,** 257 (1967)
[8] BRADLEY, D. C., GITLITZ, M. H.: J. Chem. Soc. (A), **1969,** 1152
[9] BIBLER, J. P., KARRAKEV, D. G.: Inorg. Chem., **7,** 982 (1968)
[10] DUNN, T. M., NYHOLM, R. S., YAMAD, S.: J. Chem. Soc., **1962,** 1564
[11] DORAIN, P. B., PATTERSON, H. H., JORDON, P. C.: J. Chem., Phys. **49,** 3845 (1968)
[12] JORGENSEN, C. K.: J. Inorg. Nucl. Chem., **24,** 1571 (1962)
[13] TAKAMI, F., WAKHARA, S., MAEDA, T.: Tetrahedron Letters **28,** 2645 (1971)
[14] VOGEL, A. I.: A Textbook of Quantitative Inorganic Analysis, 3rd ed. Longmans London 1964
[15] FAY, R. C., LOWRY, R. N.: Inorg. Chem., **6,** 1512 (1967)
[16] WILKINSON, G., BIRGINGHAM, J.: J. Am. Chem. Soc., **76,** 4281 (1959)
[17] REYNOLDS, L. T., WILKINSON, G.: J. Inorg. Nucl. Chem., **9,** 86 (1959)
[18] SAMUEL, E., SETTON, R.: J. Organomet. Chem., **4,** 156 (1965)
[19] WAILES, P. C.: WEIGOLD, H., BELL, A. P.: J. Organomet. Chem., **33,** 181 (1971)
[20] SAMUEL, E.: Bull. Soc. Chim. Fr., **1966,** 3548
[21] ANAND, S. P., MULTANI, R. K. JAIN, B. D.: Curr. Sci., **37,** 487 (1968)
[22] ADDOR, R. W.: J. Heterocyclic Chem., **7,** 381 (1970)

G. S. SODHI
N. K. KAUSHIK
University of Delhi, Department of Chemistry, Delhi—110007, India

Acta Chimica Academiae Scientiarum Hungaricae, Tomus 108 (4), pp. 395—400 (1981)

BIS(η^5-FLUORENYL) *N*-ARYL DITHIOCARBAMATO CHLORO ZIRCONIUM(IV) COMPLEXES

A. K. SHARMA and N. K. KAUSHIK*

(*Department of Chemistry, University of Delhi, India*)

Received January 7, 1981

Accepted for publication January 27, 1981

Some bis(η^5-fluorenyl) *N*-aryl dithiocarbamato chloro zirconium(IV) complexes of the type $(\eta^5\text{-}C_{13}H_9)_2Zr(S_2CNHR)Cl$ (where R = different aryl groups) have been prepared. Various physical measurements reveal that these complexes are diamagnetic, monomeric and nonelectrolytes in which dithiocarbamate ligand is bidentate. The complexes are fairly stable in inert atmosphere and dry air but decompose in moist air.

Introduction

Dithiocarbamate derivatives often ehxibit unusual coordination. For instance in zirconium chemistry 8-coordination occurs in $Zr(S_2CNR_2)_4$ [1], 7-coordination occurs in $CpZr(S_2CNR_2)_3$ [2] and $MeCpZr(S_2CNR_2)_3$ [3]. Some 5-coordinated dithiocarbamate derivatives have also been reported. For instance GARG *et al.* have reported preparation of $Cp_2Zr(S_2CNR_2)Cl$ [4] and KAUSHIK *et al.* have synthesized $Cp_2Zr(S_2CNHR)Cl$ [5]. They have assigned the monomeric penta-coordinated structure to all these complexes in which dithiocarbamate ligand is bidentate.

In the present communication some bis(η^5-fluorenyl) *N*-aryl dithiocarbamato chloro zirconium(IV) compounds of the type $(\eta^5\text{-}C_{13}H_9)_2Zr(S_2CNHR)Cl$, (where, R = -phenyl, *o*-, *m*-, *p*-tolyl, *o*-, *p*-, *m*-chlorophenyl, *p*-bromophenyl, *p*-iodophenyl and *p*-methoxyphenyl groups) have been synthesized. Molecular weight conductance and infrared spectral studies show that these complexes are monomeric, nonelectrolytes in which dithiocarbamate group acts as a bidentate ligand similar to those reported earlier [1—5]. Therefore a coordination number of five may be assigned to zirconium(IV) in all these complexes.

Results and Discussion

It is evident from analytical data that one mole of bis(η^5-fluorenyl)-zirconium(IV) dichloride reacts with one mole of ammonium dithiocarbamates according to the following equation:

* To whom correspondence should be addressed

$$(\eta^5\text{-}C_{13}H_9)_2ZrCl_2 + NH_4(S_2CNHR) \rightarrow (\eta^5\text{-}C_{13}H_9)_2Zr(S_2CNHR) + NH_4Cl$$

The method described above gives products of high purity as can be judged by their elemental analysis, molecular weight determination and infrared spectral studies. Conductance measurements show that all the complexes are essentially nonelectrolytes in nitrobenzene. From molecular weight determination, it is concluded that these complexes are monomeric. Magnetic susceptibility values at room temperature show that the complexes are diamagnetic.

All these complexes are quite stable in inert atmosphere and also in dry air but they decomposes in moist air. The compounds are soluble in methanol, ethanol and benzene and are insoluble in carbon tetrachloride, chloroform, carbon disulphide, dichloromethane and acetone.

In recent years the infrared spectra of numerous dithiocarbamates have been reported [1, 6, 7]. In general, these spectra are fairly complex. Fortunately from structural point of view it is necessary to distinguish between unidentate and bidentate dithiocarbamate groups. A coordination number of five may be assigned to zirconium atom in these complexes if dithiocarbamate ligand is bidentate and each fluorenyl group occupies one coordination site, however,

Table I

Analytical data of $(\eta^5\text{-}C_{13}H_9)_2Zr(S_2CNHR)Cl$ *complexes*

Sr. No.	Compound	Found (calc.) %					
		C	H	N	S	Zr	Cl
1.	$(\eta^5\text{-}C_{13}H_9)_2Zr[S_2CNHC_6H_5]Cl$	63.0 (63.30)	3.8 (3.84)	2.1 (2.24)	10.0 (10.26)	14.4 (14.60)	5.7 (5.86)
2.	$(\eta^5\text{-}C_{13}H_9)_2Zr[S_2CNH(o\text{-}CH_3C_6H_4)]Cl$	63.7 (63.88)	3.8 (4.07)	2.0 (2.19)	9.9 (10.02)	14.0 (14.28)	5.5 (5.56)
3.	$(\eta^5\text{-}C_{13}H_9)_2Zr[S_2CNH(m\text{-}CH_3C_6H_4)]Cl$	64.0 (63.88)	4.0 (4.07)	2.1 (2.19)	9.9 (10.02)	14.1 (14.28)	5.6 (5.56)
4.	$(\eta^5\text{-}C_{13}H_9)_2Zr[S_2CNH(p\text{-}CH_3C_6H_4)]Cl$	63.4 (63.88)	3.9 (4.07)	2.0 (2.19)	9.8 (10.02)	14.2 (14.28)	5.4 (5.56)
5.	$(\eta^5\text{-}C_{13}H_9)_2Zr[S_2CNH(o\text{-}ClC_6H_4)]Cl$	60.1 (60.07)	3.5 (3.49)	2.1 (2.12)	9.5 (9.71)	13.7 (13.84)	10.6 (10.77)
6.	$(\eta^5\text{-}C_{13}H_9)_2Zr[S_2CNH(m\text{-}ClC_6H_4)]Cl$	60.0 (60.07)	3.5 (3.49)	2.2 (2.12)	9.6 (9.71)	13.6 (13.84)	10.5 (10.77)
7.	$(\eta^5\text{-}C_{13}H_9)_2Zr[S_2CNH(p\text{-}ClC_6H_4)]Cl$	60.0 (60.07)	3.6 (3.49)	2.1 (2.12)	9.5 (9.71)	13.7 (13 84)	10.4 (10.77)
8.	$(\eta^5\text{-}C_{13}H_9)_2Zr[S_2CNH(p\text{-}BrC_6H_4)]Cl$	56.0 (56.28)	3.3 (3.27)	1.8 (1.98)	9.0 (9.09)	12.7 (12.96)	4.9 (5.04)
9.	$(\eta^5\text{-}C_{13}H_9)_2Zr[S_2CNH(p\text{-}IC_6H_4)]Cl$	52.4 (52.76)	3.1 (3.06)	1.9 (1.87)	8.3 (8.52)	12.0 (12.15)	4.5 (4.73)
10.	$(\eta^5\text{-}C_{13}H_9)_2Zr[S_2CNH(p\text{-}OCH_3C_6H_5)]Cl$	60.7 (60.48)	3.9 (3.97)	2.1 (2.14)	9.6 (9.77)	13.6 (13.93)	5.3 (5.42)

Table II

Yields and physical data (λ *in* ohm^{-1} cm^2 mole^{-1})

Sr. No.	Compound	Colour	Dec. temp. °C	Yield (%)	Conductance		Mol. wt. Found (Calc.)
					$\times 10^3 M$	λ	
1.	$(\eta^5\text{-}C_{13}H_9)_2Zr[S_2CNHC_6H_5]Cl$	Light brown	88—90	72	0.50	0.22	620 (624.72)
2.	$(\eta^5\text{-}C_{13}H_9)_2Zr[S_2CNH(o\text{-}CH_3C_6H_4)]Cl$	Light brown	76—79	70	0.50	0.24	635 (638.72)
3.	$(\eta^5\text{-}C_{13}H_9)_2Zr[S_2CNH(m\text{-}CH_3C\ H_4)]Cl$	Light brown	110—114	68	0.50	0.28	632.4 (638.72)
4.	$(\eta^5\text{-}C_{13}H_9)_2Zr[S_2CNH(p\text{-}CH_3C_6H_4)]Cl$	Brownish white	100—102	64	0.50	0.32	633 (638.72)
5.	$(\eta^5\text{-}3C_{13}H_9)_2Zr[S_2CNH(o\text{-}ClC_6H_4)]Cl$	White	60—64	68	0.50	0.20	652.8 (659.22)
6.	$(\eta^5\text{-}C_{13}H_9)_2Zr[S_2CNH(m\text{-}ClC_6H_4)]Cl$	White	80—84	70	0.50	0.32	654.2 (659.22)
7.	$(\eta^5\text{-}C_{13}H_9)_2Zr[S_2CNH(p\text{-}ClC_6H_4)]Cl$	White	90—93	68	0.50	0.30	654 (659.22)
8.	$(\eta^5\text{-}C_{13}H_9)_2Zr[S_2CNH(p\text{-}BrC_6H_4)]Cl$	Yellowish white	100—102	64	0.50	0.34	700.8 (703.62)
9.	$(\eta^5\text{-}C_{13}H_9)_2Zr[S_2CNH(p\text{-}IC_6H_4)]Cl$	White	99—103	60	0.50	0.38	746.5 (750.62)
10.	$(\eta^5\text{-}C_{13}H_9)_2Zr[S_2CNH(p\text{-}OCH_3C_6H_5)]Cl$	White	136—140	62	0.50	0.22	650.4 (654.72)

coordination number four would result if the dithiocarbamate ligand behaved as a *S*-bonded monodentate ligand. These two possibilities can be distinguished by infrared spectral studies. BONATI and UGO [6] showed that if dithiocarbamate ligand is bidentate, a single band at $\sim$1000 cm^{-1} is found which is due to two equivalent C—S stretching vibrations. In the case of unidentate dithiocarbamates as in EtS_2CNEt_2, a doublet arise at $\sim$1005 and $\sim$983 cm^{-1} which is due to two nonequivalent C—S stretching vibrations. All the complexes prepared possess one medium intensity band at $\sim$1000 cm^{-1} (apart from the C—H derivatives). This indicates the presence of a four-membered ring system in the complexes and support the bidentate nature of dithiocarbamate ligands.

Table III lists the characteirstic infrared frequencies for

$$(\eta^5\text{-}C_{13}H_9)_2Zr(S_2CNHR)Cl$$

(where R = different aryl groups). The thiouride band (C$\cdots$N) near 1510 cm^{-1} is very characteristic of the dithiocarbamates. The frequency of this band lies between 1250 and 1380 cm^{-1} for C—N and between 1640 and 1690 cm^{-1} for C=N which suggests that the band possesses some double-bond character. Bands occurring around $\sim$995, $\sim$385 and $\sim$360 in these complexes have been assigned to ν(C$\cdots$S), ν(Zr—Cl) and ν(Zr—S) vibrations, respectively.

Table III

Characteristic infrared bands of $(\eta^5\text{-}C_{13}H_9)_2Zr(S_2CNHR)Cl$

Sr. No.	Compound	Peak position cm^{-1}							
		(Zr—Cl)	(Zr—S)	(C⋯N)	(C⋯S)	(C—H) stretching	(C—H) asym.	(C—H) in plane	(C—H) put of plane
1.	$(\eta^5\text{-}C_{13}H_9)_2Zr[S_2CNHC_6H_5]Cl$	382 (m)	368 (m)	1510 (s)	998 (s)	3110 (m)	1430 (m)	1020 (s)	810 (vs)
2.	$(\eta^5\text{-}C_{13}H_9)_2Zr[S_2CNH(o\text{-}CH_3C_6H_4)]Cl$	378 (m)	365 (m)	1510 (s)	995 (s)	3110 (m)	1440 (m)	1030 (s(	815 (vs)
3.	$(\eta^5\text{-}C_{13}H_9)_2Zr[S_2CNH(m\text{-}CH_3C_6H_4)]Cl$	372 (m)	358 (m)	1505 (s)	1000 (s)	3120 (m)	1440 (m)	1040 (s)	815 (vs)
4.	$(\eta^5\text{-}C_{13}H_9)_2Zr[S_2CNH(p\text{-}CH_3C_6H_4)]Cl$	380 (m)	355 (m)	1510 (s)	1000 (s)	3115 (m)	1440 (m)	1045 (s)	805 (vs)
5.	$(\eta^5\text{-}C_{13}H_9)_2Zr[S_2CNH(o\text{-}ClC_6H_4)]Cl$	372 (m)	360 (m)	1500 (s)	1000 (s)	3115 (m)	1430 (m)	1040 (s)	820 (vs)
6.	$(\eta^5\text{-}C_{13}H_9)_2Zr[S_2CNH(m\text{-}ClC_6H_4)]Cl$	380 (m)	362 (m)	1500 s()	998 (s)	3120 (m)	1435 (m)	1040 (s)	820 (vs)
7.	$(\eta^5\text{-}C_{13}H_9)_2Zr[S_2CNH(p\text{-}ClC_6H_4)]Cl$	385 (m)	360 (m)	1510 (s)	998 (s)	3110 (m)	1435 (m)	1030 (s)	815 (vs)
8.	$(\eta^5\text{-}C_{13}H_9)_2Zr[S_2CNH(p\text{-}BrC_6H_4)]Cl$	375 (m)	365 (m)	1510 (s)	1000 (s)	3100 (m)	1440 (m)	1035 (s)	810 (vs)
9.	$(\eta^5\text{-}C_{13}H_9)_2Zr[S_2CNH(p\text{-}IC_6H_4)]Cl$	380 (m)	364 (m)	1510 (s)	1000 (s)	3110 (m)	1430 (m)	1025 (s)	820 (vs)
10.	$(\eta^5\text{-}C_{13}H_9)_2Zr[S_2CNH(p\text{-}OCH_3C_6H_5)]Cl$	375 (m)	360 (m)	1515 (s)	1005 (s)	3110 (m)	1435 (m)	1030 (s)	810 (vs)

(m) = medium, (s) = strong, (vs) = very strong

The bands occurring at ~3100, ~1440 and ~810 cm^{-1} in all these complexes show the presence of π-bonded fluorenyl groups.

From the above discussion it is evident that if fluorenyl groups are assumed to occupy single coordination sites then IR data would favour a five-coordinated structure for all these complexes.

The electronic spectra of all these complexes recorded in nujol exhibit a single band in the region of 24,980—24,300 cm^{-1}. This band may be assigned to a charge-transfer band [8].

Experimental

Zirconium, chlorine, nitrogen and sulphur in these compounds were determined by standard methods [9].

Carbon and hydrogen contents of the complexes were measured in the microanalytical laboratories of the Department of Chemistry, University of Delhi. Table I lists the analytical data of the complexes. Nitrobenzene was purified for conductance measurements by the method described by FAY and LOWRY [10].

Bis(η^5-fluorenyl)zirconium(IV) dichloride was prepared by reacting zirconium tetrachloride with fluorene in dimethoxyethane for 16—18 hours as described by SAMUEL and SELTON [11].

Preparation of ligands. Ammonium salts of the *N*(aryl) dithiocarbamate ligand $NH_4(S_2CNHR)$ were prepared by the reaction of equimolar amounts of the appropriate amine, carbon disulphide and ammonium hydroxide [12]. Since the ammonium salts contain water of crystallization, it was necessary to dry them in vacuum over P_2O_5, first at room temperature and than at 110 °C until their infrared spectra showed no water or only traces of water.

Preparation of the complexes. All the complexes were prepared by similar methods. Bis(η^5-fluorenyl)zirconium(IV) dichloride was stirred in dimethoxyethane *ca.* 100 mL with stoichiometric amounts of appropriate ammonium dithiocarbamate for 18—20 hours under dry nitrogen. The solution was then filtered and its volume was reduced to *ca.* 20 mL. Crystalline product was obtained by adding an excess of petroleum ether and allowing the mixture to stand overnight. The excess solvent was removed in vacuum and the compounds dried over P_2O_5 (~2 hrs).

Conductance measurements were made in nitrobenzene at 30.00 ± 0.05 °C using a Beckmann Conductivity Bridge (Model RC-18A). Solid state IR spectra were recorded in KBr pellets in the 4000—200 cm^{-1} region on a Perkin—Elmer 621 grating spectrophotometer. Magnetic measurements were carried out by GOUY's method using mercury(II) tetrathiocyanatocobaltate(II) as a calibrant. Electronic spectra of these complexes were run on a Perkin–Elmer 4000 Å instrument in the 400—750 nm range. Molecular weights were determined ebulliometrically in refluxing benzene. Table II lists yields and physical data of the complexes.

Attempts to prepare these complexes by reacting bis(η^5-fluorenyl)zirconium(IV) dichloride with ammonium salt of the respective dithiocarbamate in such solvents as THF and benzene gave poor yields and impure products.

REFERENCES

[1] BRADLEY, D. C., GITLITZ, M. H.: J. Chem. Soc. A, **1969,** 1152
[2] JAIN, V. K., GARG, B. S., SINGH, R. P.: Aust. J. Chem., **30,** 2545 (1977)
[3] JAIN, V. K., GARG, B. S.: J. Inorg. Nucl. Chem., **40,** 239 (1976)
[4] JAIN, V. K., KUMAR, V., GARG, B. S.: Inorg. Chem. Acta, **26,** 197 (1978)
[5] KAUSHIK, N. K., BHUSHAN, B., CHHATWAL, G. R.: J. Inorg. Nucl. Chem., **42,** 457 (1980)
[6] BONATI, F., UGO, R.: J. Organometal. Chem., **10,** 257 (1967)
[7] DOMENICANO, A., VACIAGO, A., ZAMBONELLI, L., LOADER, P. L., VENANZI, L. M.: Chem. Comm., **1966,** 476
[8] DORAIN, P. B., PETTERSON, H. S., JORDON, .P C.: J. Chem. Phys., **49,** 3845 (1968)

[9] VOGEL, A. I.: A Textbook of Quantitative Inorganic Analysis, 3rd ed. Longmans, London 1964
[10] FAY, R. C., LOWRY, R. N.: Inorg. Chem., **6**, 1512 (1967)
[11] SAMUEL, E., SELTON, R.: J. Organometal. Chem., **4**, 156 (1965)
[12] KLOPPING, H. L., VANDERKERK, G. J. M.: Rec. Trav. Chem., **70**, 917 (1951)

Anand Kumar SHARMA
N. K. KAUSHIK
University of Delhi, Department of Chemistry, Delhi—110007, India

Acta Chimica Academiae Scientiarum Hungaricae, Tomus 108(4) pp. 401-412 (1981)

SEMIEMPIRICAL QUANTUM CHEMICAL CALCULATIONS ON THE CONFORMATIONS OF γ-BUTYROLACTONE AND CYCLOPENTANONE

P. NAGY

(Chemical Works of Gedeon Richter Ltd., Budapest)

Received November 13, 1980

In revised form January 21, 1981

Accepted for publication February 4, 1981

CNDO/2 and PCILO semiempirical quantum chemical methods have been used to calculate the relative stabilities of the conformers of cyclopentanone and γ-butyrolactone. The molecular geometries have been optimized at two levels: total geometry optimization and optimization of bond and torsion angles, using fixed bond lengths. The latter method gives the better results. The most stable conformer of cyclopentanone is the twisted form, the second stable form is planar. The γ-butyrolactone is most stable in a structure corresponding to a twisted form. The second stable form seems to be planar. The interconversion of the twisted forms of different configurations may take place through inversion.

Introduction

The conformations of many five-membered rings — having a double bond or being saturated — have been investigated in detail experimentally or/and theoretically [1—6]. Cyclopentanone and γ-butyrolactone are two examples of five-membered saturated rings differing not too strongly from each other in structure.

The conformations of cyclopentanone were studied both theoretically [3b] and experimentally [7, 8]. However, only some limited investigations have been carried out on the conformation of γ-butyrolactone [9—12]. Quantum chemical calculations on the relative stabilities of the possible conformers have not yet been made to our knowledge.

It is our aim in this work to calculate the total energies of the different conformers of γ-butyrolactone and to obtain information about their relative stabilities. For calculating the molecular energies, the CNDO/2 [13, 14] and PCILO [15—18] semiempirical methods were chosen. Both methods have been widely used in calculations of conformer energies (see *e.g.* refs [5,6, 19—22]).

The calculations for the cyclopentanone molecule have been made here only to test whether the CNDO/2 and PCILO methods are capable of reproducing the most stable conformation of five-membered saturated rings, in accordance with experiment.

Calculations and results

The calculated values of the total energies of the different conformers refer to their geometry optimized structures. To optimize the molecular geometry PULAY's CNDO/force method and program have been used [23, 24].

The geometry iterations have been repeated until the change in the total energy has become less than about 0.00002 a. u. in two subsequent steps[a]. At the same time, the CARTESIAN components of the remaining forces acting on the atoms (with the exception of the carbonyl oxygen) had values of about 10^{-10} N.

Two levels of geometry optimization have been considered. In the complete optimization of structural parameters all the bond lengths, bond and torsion angles vary. In the version of partial optimization only the bond and torsion angles change, the bond lengths are kept fixed.

Having the optimized molecular geometries from the CNDO/2 calculations, these geometries have been used in the PCILO computations, too, to calculate the total energies of conformers. The corresponding QCPE program [25] has been modified by WELLER.

To the geometry optimization of cyclopentanone the starting structural parameters have been taken from microwave results [7]. Due to the limited amount of structural information referring to γ-butyrolactone, data on similar molecules have been used for the starting molecular structure [11, 26—28].

Two sets of fixed bond lengths have been applied at the level of angle optimization to γ-butyrolactone. In set I, the "average" bond lengths were assumed on the basis of ref. [28]. In set II, the bond lengths were taken from X-ray diffraction data [11]. To calculate the starting CARTESIAN coordinates of the atoms in some puckered conformations (not given in ref. [11]) ROZSONDAI's [29] program has been used.

At angle optimization level the constancy of the bond lengths has been assured in first order. This has led to slight changes in some bond lengths after a great number of geometry iterations. The changes have not exceeded 0.2 pm with one exception. Here the change reached 0.6 pm in a C—C bond of cyclopentanone. However, it is supposed that this extent of increase in the bond length has no influence on the qualitative conclusions.

The starting molecular forms investigated are given in Fig. 1.

The classification to planar (P), envelope (E) or twisted (T) conformation is based on the position of the C_5 and C_6 atoms relative to the 2,1,3 plane. The C_4 atom remained in this plane during the geometry optimization process. If both the C_5 and C_6 atoms are practically in the plane, the conformation is considered planar. In the non-planar conformations the convention of KLYNE and PRELOG [30] has been accepted for the sign of torsion angles. In the

[a] 1 a. u. = 2625.707 kJ/mol

Cyclopentanone

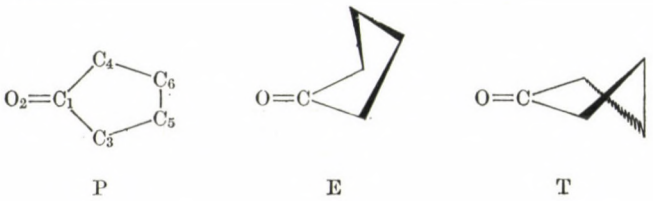

P E T

γ-Butyrolactone

P T

E1 E2 E3 E4

Fig. 1. The symbols P,E,T refer to planar, envelope, twisted conformations, respectively. The thicker lines point to atoms being out of the 2,1,3,4 plane

twisted form the sign of the 6413 and 5314 torsion angles are identical. However, the signs of the above torsion angle are different in the envelope conformations. Four envelope conformations have been considered. E1 and E2 conformations have the C_6 and C_5 atoms, respectively, as the single ones being out of the plane of the ring. In the E3 and E4 conformations both C_5 and C_6 are out of plane atoms. In E3 the C_6, in E_4 the C_5 atom is nearer to the plane, as compared with the other out-of-plane atom.

The optimized geometry parameters are given in Tables I, II, III. In these and the subsequent Tables symbols of the starting conformation are given in parentheses according to Fig. 1. For example, T(E2) means twisted conformation that has been obtained from an E2 starting structure during the geometry optimization.

The puckering amplitude is a characteristic parameter of the non-planar rings. DUNITZ [31] gave an approximate formula to calculate it in five-membered rings:

$$540 - \sum_i \varphi_i = 240\, q_D^2 \qquad (1)$$

Table I

CNDO/2 *optimized structural parameters for the cyclopentanone conformers*
Bond lengths in pm, bond angles in degrees

	P		E		T	
	A	*B*	*A*	*B*	*A*	*B*
Bond lengths						
12	127.2	122.2	127.1	122.2	127.1	122.2
13	146.9	150.4	146.8	151.2	147.0	150.5
35	148.1	155.7	148.1	155.8	148.1	155.7
56	148.5	155.7	148.5	155.7	148.5	155.7
Bond angles						
213	124.6	124.2	125.4	124.8	124.7	124.6
314	110.8	111.6	109.2	110.4	110.6	110.8
135	106.2	106.8	105.7	105.3	106.1	105.4
356	108.4	107.4	107.9	107.3	108.0	104.7
Torsion angles						
3564	0.0	0.0	0.0	0.0	12.0	30.4
1356	0.0	0.0	−11.5	−12.4	−9.5	−24.6
4135	0.0	0.0	19.1	21.1	3.6	9.5
STO-3G[a]						
3564			0.0		35.55	
1356			−13.56		−28.51	
4135			22.55		10.94	
exp.[b]						
3564					37.6	
1356					−30.5	
4135					11.8	

Sets *A* and *B* correspond to total and angle optimized geometries, respectively
[a] The *ab initio* values are taken from [3b]
[b] The values are taken from [3b], calculated on the basis of experimental data of [7]

where q_D is the puckering amplitude, φ_i the "i"-th bond angle.

In order to have a comparison with the more complicated method of CREMER and POPLE [3b], the puckering amplitude of cyclopentanone has been computed here by the method of DUNITZ using data given is [3b]. Since DUNITZ's approximation refers to a pentagon of equal bond lengths, the average length of the ring bonds has been chosen. However, q_{CP} refers to the original geometry. The results are given in Table IV.

The agreement is satisfactory, so q values have been calculated for our optimized geometries of cyclopentanone and γ-butyrolactone, too, using the DUNITZ method (Table V).

The total energies for the different forms of cyclopentanone and γ-butyrolactone are shown in Tables VI and VII. The different starting geometries result in more or less different equilibrium angles and relative energies, even if the type of the conformation obtained agrees (*c.f.* Tables III, VII). Possible reasons of the differences will be discussed later.

Table II

CNDO/2 *optimized structural parameters for the γ-butyrolactone conformers*
Bond lengths in pm, bond angles in degrees

	P	T(E2)	T(T)	E4(E1)	E4(E4)
Bond lengths					
12	126.8	126.8	126.8	126.9	126.7
13	136.5	136.7	136.5	136.6	136.6
14	146.1	146.3	146.1	146.2	146.2
35	138.7	138.8	138.6	138.7	138.7
46	147.8	147.8	147.8	147.8	147.7
56	148.0	147.9	148.0	148.0	147.8
Bond angles (φ)					
413	113.6	113.8	113.5	113.2	113.4
213	116.8	116.4	116.4	116.6	116.4
214	129.6	129.8	130.1	130.2	130.2
146	103.9	102.7	103.8	101.3	101.8
135	106.4	102.5	106.5	104.6	105.4
356	111.5	109.9	111.2	109.8	110.2
564	104.6	101.8	104.6	101.5	103.2
Torsion angles (τ)					
4653	0.2	30.6	6.8	−30.3	−23.3
6413	−0.3	0.9	2.4	−20.1	−17.8
5314	0.5	17.6	1.8	1.7	3.7
5641	0.1	−17.7	−5.2	28.3	23.2
6531	−0.4	−29.9	−5.3	18.3	12.5

Discussion

Cyclopentanone

The two levels of geometry optimization have led to similar bond angles in general, however, the torsion angles differ significantly in the twisted conformation. Our calculated torsion angles are compared with STO-3G *ab initio* and experimental results (Table I.)

The agreement is satisfactory in the envelope conformation, but in the twisted one the total geometry optimization has led to an excessively flat ring structure. The calculated puckering amplitudes even in the fixed bond length approximation are only in moderate accordance with the *ab initio*

Table III

CNDO/2 *optimized bond and torsion angles in γ-butyrolactone, accepting fixed bond lengths*
Bond lengths in pm, bond angles in degrees

R	P		T(E2)	E3(E2)	T(T)	E4(E1)		E3(E3)
	I	II	I	II	I	I	II	I
12	122.0	122.2	122.2	122.1	122.0	122.1	122.4	122.0
13	136.5	138.2	136.9	138.1	137.1	136.8	138.4	137.1
14	150.6	150.6	150.8	150.5	150.9	150.6	150.8	150.9
35	144.2	148.0	143.9	148.1	144.0	144.1	148.1	144.0
46	152.2	156.3	152.3	156.3	152.2	152.1	156.2	152.2
56	152.4	157.6	152.5	157.6	152.5	152.3	157.6	152.5
φ								
413	113.8	114.9	113.9	115.1	113.6	113.4	114.6	113.8
213	117.1	116.5	117.3	116.6	117.3	117.4	116.6	117.5
214	129.1	128.6	128.8	128.3	129.0	129.2	128.8	128.7
146	104.0	104.6	102.9	103.7	102.5	101.3	101.2	102.7
135	107.5	107.5	103.8	104.0	104.7	105.5	105.3	102.7
356	110.3	109.5	109.0	108.0	108.7	108.8	108.0	109.8
564	104.3	103.4	101.4	100.8	101.2	101.2	100.3	102.8
τ								
4653	0.2	−0.5	29.8	28.1	31.4	−30.0	−30.3	21.9
6413	−0.3	2.6	1.4	−0.2	9.2	−20.6	−24.6	−12.8
5314	0.4	−3.0	17.1	18.2	10.2	2.1	5.5	26.2
5641	0.1	−1.1	−18.0	−16.5	−23.1	28.5	30.8	−5.8
6531	−0.4	2.1	−29.3	−28.9	−26.2	18.0	16.4	−29.5

The starting values of the bond lengths in sets I and II have been accepted on the basis of data [28], [11], respectively. Explanation of the difference in the corresponding bond lengths at the different conformations is given in the text

and experimental values (see Tables IV, V). The total geometry optimization has led to an unsatisfactorily small value for q in the twisted conformation.

The results given in Table VI show that our semiempirical calculations find the twisted form to be of the highest stability, in accordance with the *ab initio* predictions. The only exception is the CNDO/2 result after total geometry optimization. As far as the second stable form is concerned, the *ab initio* results are contradictory. Our PCILO results and the CNDO/2 ones at angle optimization level support the *ab initio* 4-31G and 6-31G prediction: the planar form is the second stable one.

Table IV

Comparison of the puckering amplitudes calculated with different methods for cyclopentanone

Values in pm

	STO-3G geom.[a]		Exp. geom.[b]
	E	T	T
Puckering ampl.			
q_D[c]	22.5	34.5	37.8
q_{CP}[d]	22.2	34.4	37.5

[a] Taken from [3b]

[b] Taken from [3b], calculated on the basis of data given in ref. [7]

[c] q_D is the puckering amplitudes, calculated with the DUNITZ method

[d] The q_{CP} value was calculated with the CREMER—POPLE method, taken from [3b]

Our test calculations on cyclopentanone show that a qualitatively correct picture may be gained carrying out angle optimization using fixed bond lengths. The PCILO method, however, even at total geometry optimization level gives the most stable conformation properly. This suggests that the use of the PCILO method in our calculations is superior to the application of CNDO/2.

Table V

Puckering amplitudes for cyclopentanone and γ-butyrolactone, calculated at CNDO/2 *optimized geometry*

Values in pm

Cyclopentanone	E	T			
Total opt.	18.0	10.5			
Angle opt	20.8	29.8			
γ-butyrolactone	**E4(E1)**	**T(E2)**	**E4(E4)**	**E3(E3)**	**T(T)**
Total opt.	28.7	28.3	22.7		5.9
Angle opt.	29.7	28.5		27.4	29.0

Table VI

Total energies of the cyclopentanone conformers relative to the planar form
ΔE in kJ/mol

	E	T
Total opt. geom.		
CNDO/2[a]	−1.92	− 1.37
PCILO[b]	1·19	− 0.57
Angle opt. geom.		
CNDO/2[c]	3.00	− 3.24
PCILO[d]	2.96	− 2.08
STO-3G opt. geom[e].	−1.13	−10.05
4-31 G opt. geom[e].	0.29	−10.97
exp.[f]		− 9.00

The total energy of the planar form in kJ/mol: [a] −158129.26, [b] −158690.74, [c] −157996.58, [d] −158557.21, [e] ref. [3b], [f] ref. [8]

Table VII

Total energies of γ-butyrolactone conformers relative to the planar form
ΔE in kJ/mol

Total opt. geom.	E4(E1)		E4(E4)	T(E2)		T(T)
CNDO/2[a]	0.50		−0.71	1.23		−0.21
PCILO[b]	4.69		1.76	4.26		−0.12
Angle opt. geom.	**E4(E1)**		**E3(E3)**	**T(E2)**	**E3(E2)**	**T(T)**
	I.	II.	I.	I.	II.	I.
CNDO/2[c]	−1.33	0.21	2.36	−2.59	−0.44	2.33
PCILO[d]	0.20	−0.25	3.83	−2.42	−1.38	3.16

The symbols in parantheses refer to the starting conformation. The parameters of sets I and II are given in Table III. The total energy of the planar form is given in kJ/mol: [a] −183773.86, [b] −184317.59, [c] −183688.88 (I), −183605.40 (II), [d] −184229.32 (I), −184163.26 (II)

γ-Butyrolactone

Though it is clear from the calculations for cyclopentanone that the angle optimization level gives the better result, total geometry optimization has also been carried out here. It was intended to see the difference between the predictions of the two geometry optimization levels for a molecule having no symmetry.

From MW spectra a puckered ring was established [9, 10] though no actual conformation could be assigned. Comparison of the measured and calculated KERR constants also supports the non-planar form [12]. Calculations in [10] using the method of PITZER and DONATH [32] found the twisted form to be probable. On the basis of FRIDRICHSONS's and MATHIESON's [11] X-ray investigations on butyrolactone, as a substructure in himbacine, the ring is puckered similarly to the E4 conformation of the present work. So these preliminary results show considerable differences. Their only common element is that the most stable form is not planar.

To calculate the total energy of the planar conformation, some of the ring atoms were slightly out of the plane in the starting arrangement. So with lack of restrictions to C_S symmetry, the geometry optimization would have led to non-planar conformation if it were not a local energy minimum. The results of the geometry optimizations (Tables II, III) show the following main features:

1. The total geometry optimization has led practically to the same length of a given bond in any conformation. This was strong support for using identical values for a given bond lengths in the different conformations, if only the angles were to be optimized. The ring bonds are generally too short. The difference of the C_1O_3 and O_3C_5 equilibrium bond lengths has been found to be significantly less than in open-chained esters [28] or lactones [11, 33, 34].

2. The resulting values of the corresponding bond angles have been near to each other using either total or angle optimization. Slightly different values have been obtained using set I or II.

3. The calculated torsion angles are generally independent of the level of optimization, but show a significant dependence on their starting values at a given level. The values obtained for P, T(E2) and E4(E1) conformations are very similar at the two levels. The dependence on the starting values may be seen in the resulting values obtained for the E4(E1) and E4(E4) pair and in the significant difference between the T(E2) and T(T) values in Table II. Furthermore, different values have been obtained for the T(E2)—T(T) pair, too, using bond angle optimization (Table III).

The T(E2) structure may be considered twisted only on the basis of the positive sign of the 6413 torsion angle. The value of this angle has been found so small at both levels that the conformation is much nearer to E2 than to a really twisted form. (The 6413 torsion angle is zero in E2 and has a negative value in E3).

The differences of some degrees in the torsion angles of the E4(E1) and E4(E4) forms may be interpreted by that the energy hypersurface of γ-butyrolactone has many local minima near to each other. The differences of these energy minima may be small, as it is the case with the E4 forms, or may be considerable, as has been found for the T(E2)—T(T) pair.

The puckering amplitudes are generally of similar magnitude at both levels. The only significant exception has been found at the T(T) form in the total optimized structure. The differences of the amplitudes in the twisted and envelope forms are significantly smaller than in the case of cyclopentanone (Tables IV, V).

The total energies of the structures investigated show different orders depending on the level of the geometry optimization as well as on the semiempirical method used (Table VII).

Among the total optimized structures, the PCILO method finds the twisted form to be the most stable. The second stable form is planar, the third stable form is E4 envelope. The energy differences, as compared with the twisted form, are 0.12 kJ/mol and 1.88 kJ/mol, respectively.

The CNDO/2 method finds the E4 envelope form as the most stable one, similarly as in the case of cyclopentanone. This prediction is probably due to the unreliable flat ring geometry obtained for the twisted form.

At angle optimization level the CNDO/2 and PCILO results differ only in that they predict a reversed order for the second and third stable forms. Both methods find the T(E2) conformation to be of the lowest total energy with set I. The second stable conformation is E4(E1) or planar, calculated by CNDO/2 or PCILO, respectively. The calculated total energy differences between the two most stable conformations are not too large: 1.26 kJ/mol by CNDO/2, 2.42 kJ/mol by PCILO. The third stable form has been found higher in energy than T(E2) by about 2.6 kJ/mol in both semiempirical methods. However, these conformation energies may also be underestimated, as was the case with the conformers of cyclopentanone.

The E3(E3) and T(T) structures are found to be much less stable than the T(E2) form.

Both CNDO/2 and PCILO find E3 to be the most stable conformation using set II. The optimized angles of T(E2) and E3(E2) are very close to each other, disregarding the sign of the 6413 torsion angle (Table III). The absolute value of the 6413 torsion angle hardly differs from zero in either conformation. So it is very difficult to decide on this basis which form corresponds to the most stable conformation. Moreover, at angle optimization level the decision should not be made, since the different sets of fixed bond lengths impose different restriction on the equilibrium angles. As a result, small differences may arise.

The two semiempirical methods give the reversed order for the second and third stable conformer as compared with set I. This means that the results are sensitive to the set used. However, almost the same values have been obtained for the structural parameters of the most stable form with any set. The bond lengths of set I seem more reliable, so for the second stable conformation, the planar form is accepted on the basis of PCILO calculations.

Conclusions

The level of geometry optimization and the semiempirical method chosen influence the predicted order of the total energies of conformers. Thus relative stabilities may be considered reliable only in cases where the total energy difference is great enough.

The CNDO/2 total geometry optimization does not give reasonable bond lengths and torsion angles in the saturated rings investigated. More promising results may be obtained at angle optimization level, which leads to a qualitatively proper order of conformer energy in cyclopentanone.

The most stable conformation of γ-butyrolactone is found to be twisted. The $O_2C_1O_3C_4$ atoms are coplanar, the C_6 atom is also near to his plane. The torsion about the C_1O_3 bond is significant. This means that the smaller number of eclipsed C—H bonds or oxygen lone pairs in a non-planar conformation is favoured as compared with the greater delocalization and the smaller strain in bond angles in the planar form. The second stable form is planar; the energy difference is about 2.4 kJ/mol, calculated with the PCILO method.

The interconversion of the two configurations of the twisted form *via* pseudorotation or inversion is questioned, since the E4(E1) form is predicted to be less stable than the planar only by 0.2 kJ/mol. Nevertheless, the PCILO results support the proposal in [10] concerning the inversion path.

*

The author would like to express his gratitude to Dr. Á. I. Kiss for valuable discussions, to Dr. P. Pulay and to Dr. B. Rozsondai for using their computer programs.

REFERENCES

[1] Starck, B., Mutter, R., Spretter, C., Kettemann, K., Boggs, A., Botskor, M., Jones, M.: Bibliography of Microwave Spectroscopy 1945—1975. Physics Data 9—1, 1977
[2] Landolt, H. H., Börnstein, R.: Neue Serie **II**/7, Springer-Verlag, Berlin—Heidelberg—New York 1976
[3a] Cremer, D., Pople, J. A.: J. Am. Chem. Soc., **97,** 1354 (1975)
[3b] Cremer, D., Pople, J. A.: J. Am. Chem. Soc., **97,** 1358 (1975)
[4] Cremer, D.: J. Chem. Phys., **70,** 1898, 1911, 1928 (1979)
[5] De Alti, G., Declava, P.: J. Mol. Struct., **31,** 319 (1976)
[6] De Alti, G., Declava, P.: J. Mol. Struct., **41,** 299 (1977)
[7] Kim, H., Gwinn, W. D.: J. Chem. Phys., **51,** 1815 (1969)
[8] Ikeda, T., Lord, R. C.: J. Chem. Phys., **56,** 4450 (1972)
[9] Legan, A. C.: J. Chem. Soc., *D.*, **1970,** 838
[10] Durig, J. R., Li, Y. S., Tong, C. C.: J. Mol. Struct., **18,** 269 (1973)
[11] Fridrichsons, J., McL. Mathieson, A.: Acta Cryst., **15,** 119 (1962)
[12] Chia, L. H. L., Huang. H. H., Wong, Y. F.: J. Chem. Soc., *B*, **1970,** 1138
[13] Pople, J. A., Santry, D. P., Segal, G. A.: J. Chem. Phys., **43,** S129, S136 (1965)
[14] Pople, J. A., Segal, G. A.: J. Chem. Phys., **44,** 3289 (1966)
[15] Diner, S., Malrieu, J. P., Claverie, P.: Theor. Chim. Acta, **13,** 1 (1969)
[16] Malrieu, J. P., Claverie, P., Diner, S.: Theor. Chim. Acta, **13,** 18 (1969)
[17] Diner, S., Malrieu, J. P., Jordan, F., Gilbert, M.: Theor. Chim. Acta, **15,** 100 (1969)

[18] JORDAN, F., GILBERT, M., MALRIEU, J. P., PINCELLI, U.: Theor. Chim. Acta, **15,** 221 (1969)
[19] WELLER, TH., KLÖPPER, D., KÖHLER, H.-J.: Z. Chem., **14,** 278 (1974)
[20] KÖHLER, H.-J., WELLER, TH., KLÖPPER, D.: Z. Chem., **15,** 224 (1975)
[21] REMKO, M.: Z. Phys. Chem., Neue Folge, Bd. **106,** 125, 249 (1977)
[22] BARBIER, C., VINCENT, C.: Gazz. Chim. Ital., **108,** 373 (1978)
[23] PULAY, P.: Mol. Phys., **17,** 197 (1969)
[24] PULAY, P., TÖRÖK, F.: Mol. Phys., **25,** 1153 (1973)
[25] QCPE Program No. 220, Indiana Univ., Bloomington, Indiana
[26] BEVAN, J. W., LEGAN, A. C.: J. Chem. Soc. Faraday Trans. II, **69,** 902 (1973)
[27] WHITE, W. F., BOGGS, J. E.: J. Chem. Phys., **54,** 4714 (1971)
[28] SUTTON, L. E.: Tables of Interatomic Distances. The Chemical Society, London 1965
[29] ROZSONDAI, B.: Acta Chim. (Budapest) **93,** 47 (1977)
[30] KLYNE, W., PRELOG, V.: Experientia, **16,** 521 (1960)
[31] DUNITZ, J. D.: Tetrahedron, **28,** 5459 (1972)
[32] PITZER, K. S., DONATH, W. E.: J. Am. Chem. Soc., **81,** 3213 (1959)
[33] MC CONNELL, J. F., MCL. MATHIESON, A., SCHOENBORN, B. P.: Tetrahedron Lett., **1962,** 445
[34] MCL. MATHIESON, A. TAYLOR, J. C.: Tetrahedron Lett., **1961,** 590

Péter NAGY H—1475 Budapest, P.O.Box 27.

Acta Chimica Academiae Scientiarum Hungaricae, Tomus 108 (4) pp. 413-423 (1981)

ANODIC DISSOLUTION OF METALS, II

ANODIC DISSOLUTION OF INDIUM IN AQUEOUS PERCHLORATE SOLUTIONS

J. SZALMA,[1] J. FARKAS,[1] L. KISS[1]* and P. JOÓ[2]

([1] Department of Physical Chemistry and Radiology, Eötvös L. University, Budapest, [2] Isotope Laboratory, Kossuth L. University, Debrecen)

Received November 4, 1980

Accepted for publication February 4, 1981

The investigated problem was whether the anodic dissolution of indium in perchlorate medium proceeds in two or three consecutive charge transfer steps. A rotating indium disc electrode and a rotating indium disc electrode fitted with a platinum ring were used in the study. On the basis of criteria established earlier [5] it could be decided unequivocally that the dissolution of indium takes place in three consecutive one-electron steps.

In the past two decades the anodic dissolution of indium was discussed in many papers, which have been summarized in some comprehensive publications [1—3]. All investigations concluded definitely that the anodic dissolution of indium proceeds by a multi-stage mechanism, that is, *via* several consecutive charge transfer steps. Utilizing various methods, the In^+ ion has been identified as the intermediate of the ionization process [1—3]. It also appears probable that the In^+ ion is further oxidized to In^{3+} in the form of a complex with hydroxide ions or other anions present in the solution, by the electrochemical path, or in a homogeneous reaction in the bulk of the solution. In^{++} ions as intermediates could not be identified in the anodic dissolution process.

For this reason, it is an unsettled question whether the further oxidation of the In^+ ion proceeds in a single two-electron step or in two one-electron steps (through In^{++} ion), since most of the kinetic results can be interpreted on the basis of both mechanisms [1, 2].

The objective of our work was to decide whether the anodic dissolution of indium in an acidic perchlorate medium proceeds by two or three consecutive one-electron transfer reactions.

The two mechanisms which we wish to distinguish are as follows:

1. $$In \underset{k_{k_1}}{\overset{k_{a_1}}{\rightleftarrows}} In^+ + e$$

2. $$In^+ \underset{k_{k_2}}{\overset{k_{a_2}}{\rightleftarrows}} In^{++} + e \qquad (I)$$

* To whom correspondence should be addressed

3. $$In^{++} \underset{k_{k_2}}{\overset{k_{a_2}}{\rightleftarrows}} In^{+++} + e$$

or

4. $$In \underset{k_{k_1}}{\overset{k_{a_1}}{\rightleftarrows}} In^{+} + e$$

5. $$In^{+} \underset{k^*_{k_2}}{\overset{k^*_{a_2}}{\rightleftarrows}} In^{+++} + 2e \qquad \text{(II)}$$

For simplicity, we did not indicate in the above reactions that the indium ions always react in some sort of complex. On the arrows we indicated the rate constants of the corresponding electrode processes changing exponentially with the electrode potential ε [4].

In our previous paper [5] we discussed the methods in detail, on the basis of which it can be decided whether an electrochemicl process follows the reaction path (I) or (II). Accordingly, the problem can be settled (i) by determining coefficient b of the anodic TAFEL line for indium; (ii) by the analysis of the polarization curves measured on a rotating indium disc electrode at different rpm values; (iii) from experimental data obtained with an indium disc electrode and an indifferent ring electrode [4—6].

We therefore measured the anodic polarization curves on a rotating indium electrode at different rpm values and the limiting current on an indifferent ring electrode, controlled by the In^+ ions. All measurements were carried out in acidic perchlorate solution.

Experimental

The rotating disc electrode was made of 99.93% indium containing metal manufactured by BDH. The ring electrode was smooth platinum. The radius of the disc electrode was 0.25 cm, the thickness of the insulating teflon ring was 0.03 cm, that of the platinum ring 0.03 cm. The geometry factor of this rotating annular electrode was $N = 0.22$ [4].

The solutions were made of analytical grade MERCK perchloric acid and sodium perchlorate, using triply distilled water. The measurements were carried out in solutions saturated with oxigen-free nitrogen.

The glass apparatus did not differ from the one described earlier [7]. The measurements were carried out potentiostatically, using a double potentiostat [7]. The reference electrode was a calomel electrode prepared with 1.0 mol/dm^3 sodium chloride. The electrode potentials indicated in the following refer to the potential measured against this electrode.

Results

The polarization curves measured on the rotating indium disc electrode at 25 °C in a 1.0 mol/dm^3 $HClO_4$ + 2.0 mol/dm^3 $NaClO_4$ solution are presented in Fig. 1. As demonstrated by the figure, the TAFEL lines are shifted towards negative potentials with increasing rpm values of the disc. Coefficient b of the straight lines has a value of 52—55 mV, practically independently of the rpm of the electrode. These data indicate that in the given conditions the kinetics of the process are significantly affected by the diffusion of In^+ ions.

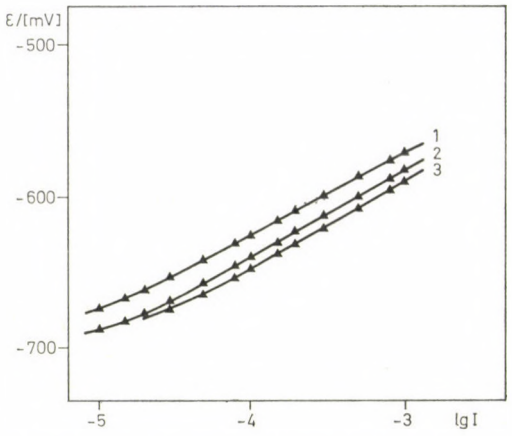

Fig. 1. Anodic polarization curves of indium measured with a rotating indium disc electrode Solution: 1.0 mol/dm³ $HClO_4$ + 2.0 mol/dm³ $NaClO_4$ in water. Temperature: 25 °C. 1 — 140 rpm; 2 — 520 rpm; 3 — 1030 rpm

The rate constants of the investigated process depend characteristically on the composition of the electrolyte solution and on its temperature. The subsequent experiments were therefore carried out under conditions where the data obtained would allow to answer the question exposed in the introduction. The dependence of the anodic dissolution of indium on the temperature and composition of the electrolyte solution will be discussed in a following paper.

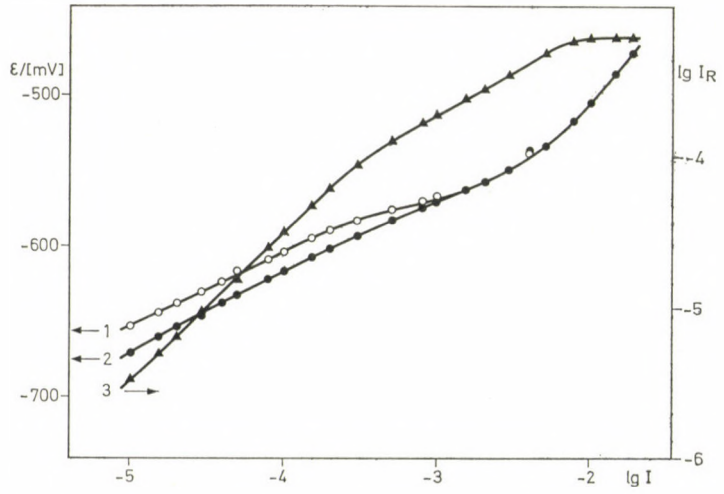

Fig. 2. Anodic polarization curves of indium measured with a rotating indium disc electrode (ε *vs.* lg I) and oxidative limiting current measured on the platinum ring electrode (lg I_R *vs.* lg I). Solution: 2.0 mol/dm³ $HClO_4$ + 1.0 mol/dm³ $NaClO_4$ in water. Temperature: 0 °C. 1 — lg I *vs.* ε, 140 rpm; 2 — lg I *vs.* ε, 1030 rpm; 3 — lg I_R *vs.* lg I, 1030 rpm

Figure 2 shows the anodic polarization curves measured at 0 °C in a 2 mol/dm^3 $HClO_4$ + 1 mol/dm^3 $NaClO_4$ solution and the oxidative limiting current measured on the ring electrode. On the polarization curve measured at 140 rpm (curve 1) three sections approaching linearity can be observed. The constant b for the first section (at low current densities) is ~60 mV, that of the second section ~35 mV, that of the third section (at high current densities) ~115 mV. At high rpm values of the electrode (curve 2, 1030 rpm), only a slight curveture appears instead of the medium (35 mV) section.

In the same figure we also plotted the logarithm of the oxidative limiting current I_R of the In^+ intermediate of indium dissolution measured on the ring electrode *versus* the logarithm of the disc current I (curve 3). It is apparent from the Figure that I_R increases with the disc current I up to currents where the current densities correspond to the steep section of the polarization curve. From there on, the limiting current I_R measured on the ring electrode appears independent of the disc current.

To demonstrate this in a more effective way, we plotted the same data linearly in Fig. 3. This Figure clearly demonstrates how the ring current becomes independent of the disc current.

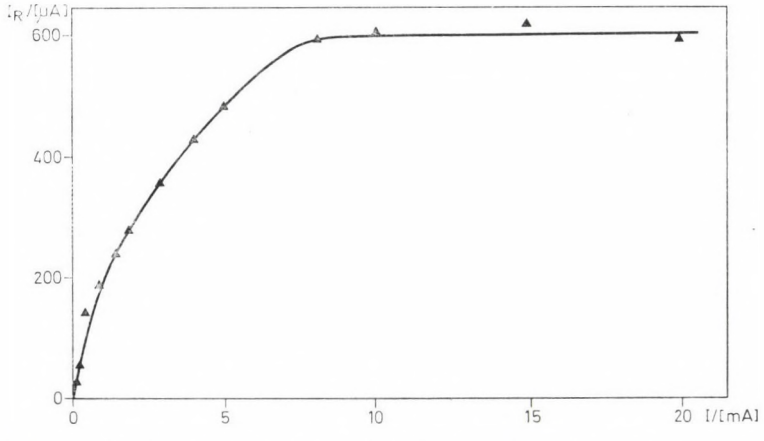

Fig. 3. Oxidative limiting current measured on the ring electrode *vs.* current measured on the disc electrode (*cf.* curve 3, Fig. 2)

Interpretation of the experimental results

The constants b of the anodic polarization curves presented in Figs 1 and 2 yield no solution to our problem. In our earlier paper [5] we demonstrated that $b \cong 60$ mV and dependence on the rmp value of the disc indicates that the kinetics are controlled above all by the diffusion of the In^+ ions. Therefore, neither portion of the curves gives any information on the further oxidation

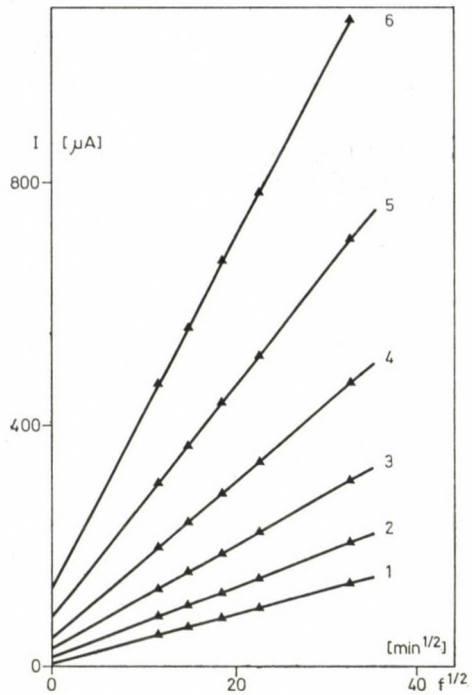

Fig. 4. Interpretation of the rpm dependence of the polarization curves measured on the indium disc electrode according to Eq. (1) (*cf.* Fig. 1). 1 — $\varepsilon = -640$ mV; 2 — $\varepsilon = -630$ mV; 3 — $\varepsilon = -620$ mV; 4 — $\varepsilon = -610$ mV; 5 — $\varepsilon = -600$ mV; 6 — $\varepsilon = -590$ mV

of the In^+ ion. The slope $b \simeq 120$ mV and independence of rpm indicates that the kinetics are controlled by the $In \rightarrow In^+ + e^-$ process. In principle, one could conclude on our problem from section with slopes of 30 or 40 mV [5]. Such a section appears on curve 1 in Fig. 2, but the measured slope is around 35 mV, and is therefore unsuited to solve the problem.

The dependence of the polarization curves on rpm can be interpreted by Eq. (38) of our earlier paper [5]. According to this equation, at constant electrode potential

$$I = A + Bf^{1/2} \tag{1}$$

where

$$A = r_1^2 \pi \frac{3}{n_2} \cdot \frac{k_{a_1} \cdot k_{a_2}}{k_{k_1}} \tag{2}$$

$$B = r_1^2 \pi \frac{k_{a_1}}{k_{k_1}} \cdot X_1' \tag{3}$$

where r_1 is the radius of the disc electrode; n_2 is 2 in the case of a two-step process, and 1 in the case of a three-step process; X_1' is a quantity depending

on the diffusion coefficient of the In^+ ion and on the kinematic viscosity of the solution, but independent of the electrode potential [5].

From the data in Fig. 4 it may be seen that I *vs.* $f^{1/2}$ values actually yield straight lines. The values of A and B defined by Eq. (1) increase with increasing potential. As shown by Eqs (2) and (3), the values of A and B also depend on the rate constants depending on the electrode potential. Since k_{a_1} and k_{k_1} do not differ for the two mechanisms, the following are valid for both reaction paths:

$$k_{a_1} = k'_{a_1} \exp\left\{\frac{\alpha_1 F \varepsilon}{RT}\right\} \tag{4}$$

$$k_{k_1} = k'_{k_1} \exp\left\{-\frac{(1-\alpha_1) F \varepsilon}{RT}\right\} \tag{5}$$

where k'_{a_1} and k'_{k_1} are the rate constants of the corresponding steps for the case $\varepsilon = 0$; α_1 is the anodic transfer coefficient for the 1st (or 4th) reaction step; ε is the electrode potential; the other symbols are those in general use.

However, k_{a_2} figuring in Eq. (2) differs for the two reactions paths. For three-step processes

$$k_{a_2} = k'_{a_2} \exp\left\{\frac{\alpha_2 F \varepsilon}{RT}\right\} \tag{6}$$

and for two-step processes

$$k_{a_2} = k'_{a_2} \exp\left\{\frac{2\alpha_2^* F \varepsilon}{RT}\right\} \tag{7}$$

the symbols being analogous to the former ones. Utilizing these relationships, one obtains from Eq. (2)

$$\lg A = C + \frac{(1 + n_2 \alpha_2) F \varepsilon}{2.303\, RT} \tag{8}$$

where

$$C = \lg\left\{r_1^2 \pi \frac{3}{n_2} \cdot \frac{k'_{a_1} k'_{a_2}}{k'_{k_1}}\right\} \tag{9}$$

It follows from Eq. (8) that a linear relationship must exist between $\lg A$ and ε, with a coefficient for ε of 0.025 V^{-1} in the case of reaction path (I), that is, $n_2 = 1$, if the calculations are made for 25 °C and $\alpha_2 \cong 0.5$. Calculating with the same conditions, the value for path (II) is 0.033 V^{-1}. The relationship $\lg A$ *versus* ε based on experimental data is plotted in Fig. 5. The slope of the straight line is 0.024 V^{-1}.

$$\lg B = D + \frac{F}{2.303\, RT} \varepsilon \tag{10}$$

where

$$D = \lg\left\{r_1^2 \pi \frac{k'_{a_1}}{k'_{k_1}} X'_1\right\} \tag{11}$$

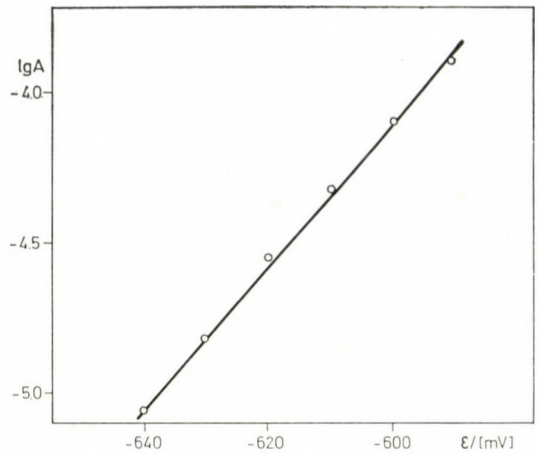

Fig. 5. Experimental data lg A *vs.* ε plotted according to Eq. (8)

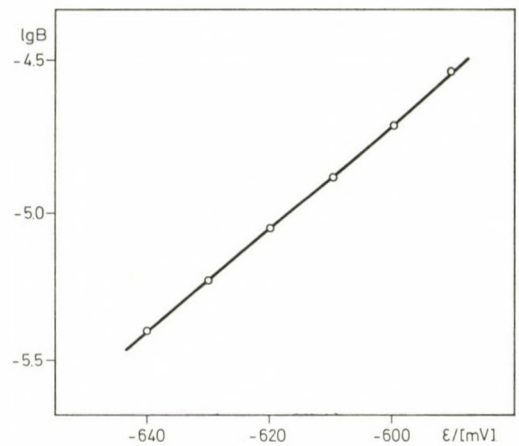

Fig. 6. Experimental data lg B *vs.* ε plotted according to Eq. (10)

Consequently, the relationship lg B *versus* ε is also linear, with an identical slope for both reaction paths. Its value for the above experimental conditions in 0.017 V^{-1}. The experimental data plotted in Fig. 6 yield a slope of 0.017 V^{-1}.

Combining the above equations, one obtains

$$\lg\left(\frac{A}{B}\right) = (C - D) + \frac{n_2 \alpha_2 F}{2.303\,RT}\,\varepsilon \tag{12}$$

The slope of the relationship lg A/B *versus* ε for reaction path (I) is 0.0083 V^{-1}, that for the two-step recation path (II) is 0.017 V^{-1}. The experimental data lg (A/B) *vs.* ε are plotted in Fig. 7. The slope of the straight line is 0.0071 V^{-1}.

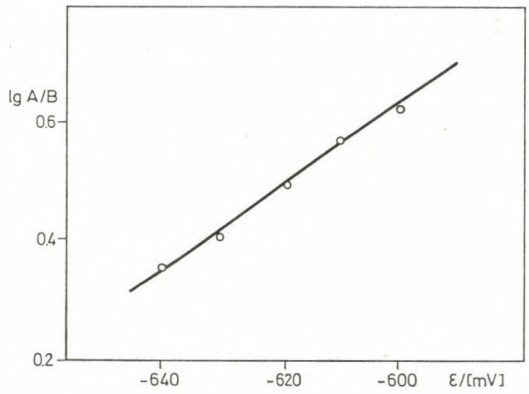

Fig. 7. Experimental data lg A/B *vs* ε plotted according to Eq. (12)

The calculated theoretical slopes and the experimental slopes are summarized in Table I (the data are rounded to two-digit numbers). The reciprocals of these data are listed in Table II since they are analogous values to the TAFEL b constants common in the electrochemical literature.

The data in Tables I and II prove that the anodic dissolution of indium in acidic perchlorate solutions proceeds by the reaction path (I), that is, *via* three one-electron steps.

The analysis of the results obtained with the rotating disc electrode fitted with a ring leads to similar conclusions. At high current densities the curve lg I_R *versus* lg I and the curve I_R *versus* I shown in Figs 2 and 3 become parallel to the abscissa. As reported in our previous paper [5], this unequivocally demonstrates the three-step mechanism.

Table I

Calculated and experimental slopes of the relationships expressed by Eqs (8), (10) *and* (12)

Slope	Calcd. for reaction path		Experimental
	(I)	(II)	
$\frac{\partial \lg A}{\partial \varepsilon}$	0.025 V^{-1}	0.033 V^{-1}	0.024 V^{-1}
$\frac{\partial \lg B}{\partial \varepsilon}$	0.017 V^{-1}	0.017 V^{-1}	0.017 V^{-1}
$\frac{\partial \lg (A/B)}{\partial \varepsilon}$	0.0083 V^{-1}	0.017 V^{-1}	0.0071 V^{-1}

Table II

Reciprocal of the values in Table I

	Calcd. for reaction path		Experimental
	(I)	(II)	
$\frac{\partial \varepsilon}{\partial \lg A}$	40 mV	30 mV	42 mV
$\frac{\partial \varepsilon}{\partial \lg B}$	58 mV	58 mV	58 mV
$\frac{\partial \varepsilon}{\partial \lg (A/B)}$	120 mV	58 mV	130 mV

Plotting I/I_R *versus* $f^{-1/2}$ yields further data to decide between the two mechanisms. According to Eq. (49) in [5].

$$\frac{I}{I_R} = A' + B' f^{-1/2} \tag{13}$$

Here

$$A' = \frac{1}{2N} \tag{14}$$

$$B' = B'' \exp\left\{\frac{n_2 \alpha_2 F \varepsilon}{RT}\right\} \tag{15}$$

$$B'' = \frac{3k'_{a_1}}{2 n_2 N X'_1} \tag{16}$$

From Eq. (15)

$$\lg B' = \lg B'' + \frac{n_2 \alpha_2 F \varepsilon}{2.303\, RT} \tag{17}$$

The slope of the lines corresponding to Eq. (17) (at 25 °C, and $\alpha_2 \simeq 0.5$) is 0.0083 V^{-1} for the three-step mechanism, and 0.017 V^{-1} for the two-step mechanism.

The lines constructed from the experimental data according to Eq. (13) are presented in Fig. 8. As may be seen, the lines obtained at different electrode potentials intersect the ordinate as expected from the equation, in one point, and their slope changes with the potential. The relationship lg B' *versus* ε is presented in Fig. 9. The slope of the line is 0.0084 V^{-1}. The slopes calculated from the equations and the experimental data (and, similarly to Table III, their reciprocals) are summarized in Table III. The interpreted data also prove that reaction path (I) is the one followed in the anodic dissolution of indium.

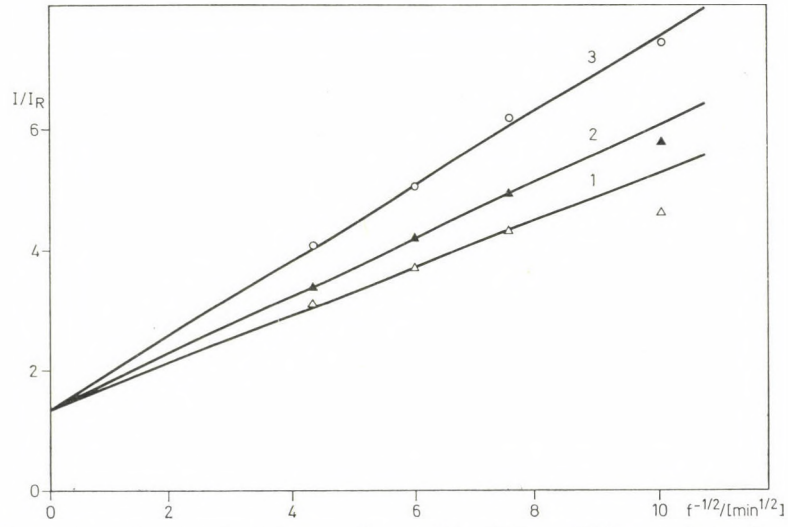

Fig. 8. Experimental data plotted according to Eq. (13) at different electrode potentials. $1 - \varepsilon = -580$ mV; $2 - \varepsilon = -560$ mV; $3 - \varepsilon = -540$ mV

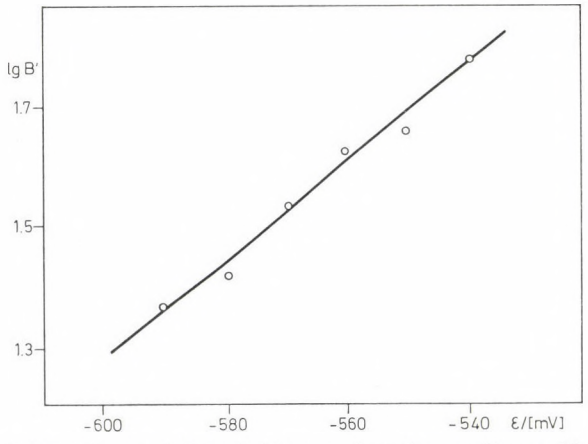

Fig. 9. Experimental data lg B' *vs.* ε plotted according to Eq. (17)

Table III

Calculated and experimental values for the slopes of the relationship expressed by Eq. (17) *and their reciprocals*

	Calcd. for reaction path		Experimental
	(I)	(II)	
$\frac{\partial \lg B'}{\partial \varepsilon}$	0.0083 V^{-1}	0.017 V^{-1}	0.0084 V^{-1}
$\frac{\partial \varepsilon}{\partial \lg B'}$	120 mV	58 mV	120 mV

REFERENCES

[1] Losev, V. V., Molodov, A. I.: Itogi nauki i tekhniki, Elektrokhimiya, **8**, 25 (1972)
[2] Losev, V. V., Molodov, A. I.: Encyclopedia of Electrochemistry of the Elements. Vol. **1**, p. 1. Dekker, New York, Basel 1976
[3] Piercy, R., Hampson, N. A.: J. Appl. Electrochem., **5**, 1 (1975)
[4] Kiss, L.: Kinetics of Electrochemical Dissolution of Metals (in Hungarian), Akadémiai Kiadó, Budapest 1980
[5] Kiss, L., Farkas, J.: Acta Chim. Acad. Sci. Hung., **107**, 181 (1981)
[6] Kiss, L., Farkas, J., Varsányi, M. L.: Ann. Univ. Sci., Budapestiensis, Sectio Chim., **15**, 95 (1979)
[7] Farkas, J., Dobos, L., Kovács, P., Kiss, L.: Acta Chim. Acad. Sci. Hung. (In press)

József Szalma
József Farkas
László Kiss
H—1088 Budapest, Puskin u. 11—13.

Pál Joó
H—4010 Debrecen, Egyetem tér 1.

RECENSIONES

GILLIES, M. T.: *Water-Based Industrial Finishes Recent Developments*

Chemical Technology Review, No. 167
Noyes Data Corporation, Park Ridge, New Jersey, 1980, pp. 435

This book, volume 167 of the popular Chemical Technology Review Series, reports on patents concerning water-based coatings, issued in the USA between January 1, 1978, and December 31, 1979.

Interest in water-based coatings has been intensified considerably all over the world in the past few years because over and above the ever more strict environmental and health regulations, and economical aspects in the use of energy carriers.

Of course, this book does not deal exclusively with coating substances that have no organic solvent content: in order to be made suitable for specific applications, water-based coating compositions practically always contain certain organic solvents, mostly those with high boiling points.

However, these cosolvents can be present only in low concentration in the system and by using them the safety measures are carefully taken into consideration, with special regard to the health protection of the workers which become manifest only after a long latency period.

The application of water-based systems instead of conventional industrial finishes prepared with organic solvents implies the elaboration of new techniques. The progress is so rapid in this field that adequate up-to-date information about it can not be obtained through the conventional channels. In order to overcome difficulties arising from this fact, the Publisher employs special methods (typesetting, binding *etc.*); due to these the time between final acceptance of the manuscript and the completed book is significantly shortened. Thus up-to-date information is made available very quickly indeed.

The aim of this book is twofold: to provide detailed technical information for those who are working in this field, and to assist the study of the patent literature.

Every patent specification relevant to this topic and issued within the period defined before is cited without selection. Altogether 277 patents are published. However, this volume should not be considered to be merely and simply a collection of patents, by eliminating the official style and juristic phraseology, it offers all the important technological information, details the latest trends and the energy and health advantages to be gained.

The patents discussed are ordered in nine main chapters which are subdivided into several groups. The main and sub-chapters are introduced by short reviews of the particular field, it is followed by the description of the patents in the sequence of their publication.

The main chapters are as follows:

Thermally Cured Organic Coatings
Electrodeposited Coatings
Organic Corrosion Resistant Coatings
Nonstick and Can Coatings
Coatings for Automotive and Electrical Uses
Autodepositing and Air-Dried Coatings
Coatings for Special Applications
Inorganic and Metallic Coatings
Special Processes

A triple index completes the volume: a list of the patent numbers (277 data); a list of the inventors (380 names); and a list of the patentees (122 companies).

The table of contents is arranged in such a way that it serves also as a subject index. The space devoted to the various fields and the number of specifications thus confined, ade-

quately characterize the tendency of progress and the extent of interest in any directions in the mentioned period.

The speedy publication of this volume will certainly help to avoid parallel research and development. This book may serve as a source of new ideas and offers methods of over coming problems. Both technological and research staff can use this book advantageously.

F. HORKAY

Eckhart BUDDECKE: *Grundriss der Biochemie*

Für Studierende der Medizin, Zahnmedizin und Naturwissenschaften

Sechste, neubearbeitete Auflage

Walter der Gruyter Verlag, Berlin—New York, 1980, 616 pages, about 400 formulae, and collection on processes and diagrams.

The textbook is well compiled, its language is concise, easy to comprehend and it can be used by those who know German at least at medium level.

The introductory part of the book lists the nomenclature, abbreviations and SI units used in biochemical studies, and these are they consistently referred to throughout the book.

The first 309 pages comprise a review of general biochemistry (kinetics and energetics of biochemical reactions, enzymes and coenzymes), the role and metabolism of compounds participating in the structure of living organisms and data on the topics of biological oxidation and the citrate cycle, and water and ion equilibria.

This first part of the textbook may prove useful for university students, who wish to acquire basic biochemical knowledge, and it is especially suitable for the teaching of medical students, as the author draws special attention to the clinical and pathological aspects.

The next approx. 100 pages deal with the fundamental elements of biochemical regulations and with the role of hormones and vitamins in the metabolism. These chapters do not endeavour to discuss physiology in detail, but they provide absolutely correct information regarding the current knowledge of the biochemical mode of action of hormones and vitamins, and their metabolism, rendering the book suitable for use by medical students.

In the third part, the role of different tissues and organs and their metabolisms are described. This part requires the student to master the biochemical knowledge discussed in the former chapters to comprehend the relation and characteristics of metabolic processes playing a part in the different tissues and organs. It bears special significance on the education of medical students because of the pathobiochemical reviews on the various tissues and organs.

It is worth emphasizing that today, when the lengths of the average textbooks are ever increasing, the author has succeeded in providing a short yet complete presentation of the facts in the individual chapters in this book. The formulae and processes are well arranged and their understanding is facilitated by the colored typography for emphasis. The appendix contains selected examination tests providing a possibility to draw up written examination questions.

L. VODNYÁNSZKY and I. HORVÁTH

Cement and Mortar Technology and Additives

Edited by M. H. GUTCHO

Noyes Data Corporation, Park Ridge, New Jersey, U.S.A., 1980, 540 pages

This book gives a brief and factual description of all patents issued in the United States in 1978 and 1979 and covering the following technical areas: manufacture of cement clinker, cement additives and compositions, non-portland inorganic cements and binders, oil-well cementing, reinforced products, shaped building products, lightweight and foamed products,

refractory products, gypsum products, anchoring and reinforcing elements, solidification of hazardous wastes, and finally specialty products and processes. From this brief summary it can be seen that the topics covered are essential for the readers of this journal.

It is a data-based publication, providing information retrieved from the patent literature of the U.S. This, however, means that the book is non-critical: it can only be used as detailed source of technical information as the material published, regardless of whether or not the described process is technically or economically feasible, remains on the reader's judgment.

Obviously not full patents, only condensates are given in this volume. This, however, emphasizes the responsibility of the editor concerning whether the description is really concentrating on the essence of the topic. In the reviewer's opinion, the editor has served well this purpose: it is evident that the information published is really significant, avoiding the legal jargon and juristic phraseology which sometimes makes the study of a patent very tiresome.

The book contains 256 patents and 3 re-issues; it is thought that this coverage is complete and unbiased. Detailed company and author indexes, and also numerical index (where the patents appear in their order of issuing) are presented. However, no subject index is included, but this omission is counteracted by a very detailed table of contents, which can be well used instead. A short extract from the table of contents will show that this is really a workable tool of information retrieval.

The main heading "Cement additives and compositions" is divided into the following sub-headings: set control, accelerated hardening, strengtheners and set accelerators, early high-strength portland cement, additives for high-strength concrete, water reducers for concrete, water reducers for wet-process cement manufacture, improvers of workability, plasticity, *etc.*, especially in fiber-containing compositions, fluidizing agents, air-entraining agents, expanding and shrinkage-inhibiting additives, freeze-thaw resistant additives. Eeach of these subheadings contains 2—4 patents of the field so topically similar patents are easy to find.

Perhaps the most important feature of the volume is its timeliness. The book was published, in 1980, while the last covered patent was issued December 18, 1979. This is a very short lag indeed, as it is definitely less than the lag between the invention and patent granting, or patent granting and commercial practice. The well-edited book is durably bound, with easy-to-read letters. It is recommended to all who are interested in recent technical development in the field of cement — mortar technology, as it establishes a sound background before launching into new research.

As appears from the imprint, this book is already a second of the series (there was a similar volume, in 1976, by the same publisher, edited by A. J. FRANKLIN). Let us hope that the publication of this valuable data-based series will continue in the future.

F. TAMÁS

Advances in Chemistry, Vol. 49

Akadémiai Kiadó, Budapest 1980, 174 pages

Volume **49** of the series *Advances in Chemistry* contains two reviews of monograph character. The first is the work of József DÉVAY "Determination of the corrosion rate of metals by the measurement of polarization resistance", the other, written by Ferenc GAIZER is "The application of electronic computers for the calculation of complex equilibria".

It is well known that parallel to the development of metal materials of construction and to stricter demands, the role of corrosion and its prevention gains in importance. Within this field, it is of basic importance to establish the exact corrosion rate under various conditions, and together with it, for the very reason to find suitable methods of protection and to predict corrosion, to elucidate the given corrosion mechanism. For this several methods were and are available, however, of these not all can be applied under all conditions or to purposes. The possibility to determine the corrosion rate of metals on the basis of polarization resistance is just one of the most up-to-date and most exact methods to attain this double purpose. Therefore, the modern review of József DÉVAY is of particular value, and there is no similar work even in the foreign literature. The author deals over 102 pages with the general description of the methods and the possibilities of its applications, discusses the simple and special cases of application, the experimental determination of the so-called. Tafel slopes in connection with the polarization curve, needed for the calculation of the corrosion current, and briefly describes also other methods for the determination of that.

The bibliography comprises 141 references and can be practically considered as complete up to 1976. The review written in a clear style is easily understandable, and at the same time, the discussion is kept at a high level. The work is a now and valuable contribution to the steadily growing Hungarian corrosion literature, covering novel information on theory, corrosion prevention practice and measuring techniques.

The other monograph is somewhat shorter than the first, which is justified also by the nature of the subject. In this part Ferenc GAIZER presents the possibilities, modes and processes of the computerized calculations of complex equilibria.

The computation of equilibrium and other constants can be considered already as actually solved, and in certain fields even a selection between reliable programs is possible. Some monographs on the complex chemical application of computerized methods were published already, though not in Hungarian, but in spite of this the present review, discussing up to 1975 the processes developed, is a new, valuable, truly comprehensive work. Thus, its chief merit is to make also the Hungarian reader acquainted with this sphere of problems and its methods, important also from the aspect of chemical practice. The author first discusses the complex formation itself and its more important basic equations, then the principles of computerized processes elaborated for the evaluation of complex equilibria, and of these more detailed the so-called non-statistical programs, the processes based on the least squares method, and briefly presents also other processes of evaluation. The brief monograph closes with a valuable chapter of 7 pages, dealing with conclusions, in which the author gives his opinion on the performance of computer methods, on the efficiency of existing programs, on the effect of the systematic errors of the measurements, and in general, on the possible applications of the methods mentioned, on running times, and on the fundamental fact that results obtained by computerized methods must be supported in each case by conclusive chemical considerations to actually acquire true knowledge of the given system investigated. The review is complete with a bibliography containing 162 references, which is an unequivocal proof of the detailed and comprehensive compilation, as the subject itself dates back only to fifteen years. The work will be of assistance to all research and industrial chemists interested in the study of complex equilibria, and in general, of chemical equilibria.

Finally, a remark of general character, not addressed to the authors. Both monographs would increase in value, if the period between the delivery and the publishing of the manuscript could be shortened. Indeed, it is now 1981, while the closing date of the first monograph is 1976, that of the other 1975. Five and six years are a long time in both rapidly developing fields of science, bringing many new results, which indubitably should be already included in an up-to-date monograph.

E. BERECZ

Structure and Bonding, Vol. 42
Luminescence and Energy Transfer

Springer Verlag, Berlin—Heidelberg—New York, 1980
133 pages, 64 figures, 10 tables

The book consists of three main chapters. The author of the first one is G. BLASSE Professor of the State University of Utrecht. It is entitled: "The luminescence of closed-shell transition metal complexes. New developments". This chapter (42 pages) contains 32 line drawings and 74 references.

Oxyanions of closed-shell transition metals (from titanium to molybdenum, from zirconium to ruthenium and from tantalum to osmium, are in general luminescent except chromate and permanganate. The mechanism can be explained by two singlets and two triplets: the complex is excited between the two singlet states and emits between the two triplets. The splitting of the level pairs depends on the crystal field effect or on the spin-orbit interaction. The life-time of the excited state is between several μs and several ms, and depends on the magnitude of the spin-orbit interaction, the temperature and the accompanying cation. The mechanism of luminescence is mostly influenced by cations with close energy levels of the s^2 configuration (Pb^{2+}, Bi^{3+}). The sub-chapters of the chapter are: *The electronic structure of closed-shell transition metal complexes* (tetrahedral and octahedral). *The luminescence of closed-shell transition metal complexes* (listing the individual complexes). *The influence of surrounding cations with low-lying energy levels. Conclusions and proposals for further research.*

The authors of the second main chapter are R.C. POWELL, Professor of the Oklahoma State University, and G. BLASSE. Its title is "Energy transfer in concentrated systems". It consists of 54 pages with 4 tables, 15 line drawings, and contains 182 references.

The general mechanism of energy transfer is that a sensitizer absorbs energy, gives it over to an activator, which emits this energy. Depending on whether the sensitizer belongs to the lattice or is an impurity, so-called host sensitization or impurity sensitization is realized. If the activator is of the same type of particles it is called energy migration, if it is a different one, the name is energy transfer. The mechanism of the transfer itself can be photoconduction, in the case of which absorption causes electron excess in the conduction band or electron deficiency in the valence band, it can be emission or reabsorption by another sensitizer, or it can be a radiationless transfer without charge transfer. The excited sensitizers can exchange energy in the form of excitons. The titles of the sub-chapters are: *Single-step resonant energy transfer. Phonon-assisted energy transfer. Multistep energy migration. Models to describe trapping in multistep energy transfer. Thermal effects on exciton migration. Experimental measurements. Characteristics of materials. Conclusions and suggestions for further work.*

The third chapter is written by K. C. BLEIJENBERG, also of the State University of Utrecht. It is entitled: "Luminescence properties of uranate centres in solids." It consists of 36 pages with 5 tables, 17 line drawings and 71 references.

The luminescence of uranates depends on the coordination number and on the surrounding of the uranate colour centers. In this chapter the luminescence of oxyanions with octahedral coordination is discussed. The most interesting type of these is the luminescence excited by uranates built into a sodium fluoride lattice, in which four uranate centers may take part. The titles of the sub-chapters are: *Charge transfer transitions within the octahedral uranate group. Luminescence properties of uranate groups in oxidic compounds. Luminescence properties of uranate centers in sodium fluoride single crystals.*

The aim of the book is to give a survey on this subject and to introduce those into it who intend to do research in this field. The book fulfills this goal completely, thus giving most valuable information for the researcher.

Gy. VARSÁNYI

INDEX

PHYSICAL AND INORGANIC CHEMISTRY

ORGANIC CHEMISTRY

ANALYTICAL CHEMISTRY

PRINTED IN HUNGARY
Akadémiai Nyomda, Budapest

Les Acta Chimica paraissent en français, allemand, anglais et russe et publient des mémoires du domaine des sciences chimiques.

Les Acta Chimica sont publiés sous forme de fascicules. Quatre fascicules seront réunis en un volume (3 volumes par an).

On est prié d'envoyer les manuscrits destinés à la rédaction à l'adresse suivante:

Acta Chimica
Budapest, P.O.B. 67, H-1450, Hongrie

Toute correspondance doit être envoyée à cette même adresse.

La rédaction ne rend pas de manuscript.

Abonnement en Hongrie à l'Akadémiai Kiadó (1363 Budapest, P.O.B. 24, C. C. B. 215 11488), à l'étranger à l'Entreprise du Commerce Extérieur « Kultura » (H-1389 Budapest 62, P.O.B. 149 Compte-courant No. 218 10990) ou chez représentants à l'étranger.

Die Acta Chimica veröffentlichen Abhandlungen aus dem Bereich der chemischen Wissenschaften in deutscher, englischer, französischer und russischer Sprache.

Die Acta Chimica erscheinen in Heften wechselnden Umfanges. Vier Hefte bilden einen Band. Jährlich erscheinen 3 Bände.

Die zur Veröffentlichung bestimmten Manuskripte sind an folgende Adresse zu senden

Acta Chimica
Budapest, Postfach 67, H-1450, Ungarn

An die gleiche Anschrift ist jede für die Redaktion bestimmte Korrespondenz zu richten.

Manuskripte werden nicht zurückerstattet.

Bestellbar für das Inland bei Akadémiai Kiadó (1363 Budapest, Postfach 24, Bankkonto Nr. 215 11488), für das Ausland bei »Kultura« Außenhandelsunternehmen (H-1389 Budapest 62, P.O.B. 149. Bankkonto Nr. 218 10990) oder seinen Auslandsvertretungen.

«Acta Chimica» издают статы по химии на русском, английском, французском и немецком языках.

«Acta Chimica» выходит отдельными выпусками разного объема, 4 выпуска составляют один том и за год выходят 3 тома.

Предназначенные для публикации рукописи следует направлять по адресу:

Acta Chimica
Budapest, P.O.B. 67, H-1450, ВНР

Всякую корреспонденцию в редакцию направляйте по этому же адресу.

Редакция рукописей не возвращает.

Отечественные подписчики направляйте свои заявки по адресу Издательства Академии Наук (1363 Budapest, P.O.B. 24. Текущий счет 215 11488), а иностранные подписчики через организацию по внешней торговле «Kultura» (H-1389 Budapest 62, P.O.B. 149. Текущий счет 218 10990) или через ее заграничные представительства и уполномоченных.

Reviews of the Hungarian Academy of Sciences are obtainable at the following addresses:

AUSTRALIA
C.B.D. LIBRARY AND SUBSCRIPTION SERVICE, Box 4886, G.P.O., *Sydney N.S.W. 2001*
COSMOS BOOKSHOP, 145 Ackland Street, *St. Kilda (Melbourne), Victoria 3182*

AUSTRIA
GLOBUS, Höchstädtplatz 3, *1200 Wien XX*

BELGIUM
OFFICE INTERNATIONAL DE LIBRAIRIE, 30 Avenue Marnix, *1050 Bruxelles*
LIBRAIRIE DU MONDE ENTIER, 162 Rue du Midi, *1000 Bruxelles*

BULGARIA
HEMUS, Bulvar Ruski 6, *Sofia*

CANADA
PANNONIA BOOKS, P.O. Box 1017, Postal Station "B", *Toronto, Ontario M5T 2T*

CHINA
CNPICOR, Periodical Department, P.O. Box 50, *Peking*

CZECHOSLOVAKIA
MAD'ARSKÁ KULTURA, Národni třida 22, *115 33 Praha*
PNS DOVOZ TISKU, Vinohradská 46, *Praha 2*
PNS DOVOZ TLAČE, *Bratislava 2*

DENMARK
EJNAR MUNKSGAARD, Norregade 6, *1165 Copenhagen*

FINLAND
AKATEEMINEN KIRJAKAUPPA, P.O. Box 128, *SF-00101 Helsinki 10*

FRANCE
EUROPERIODIQUES S. A., 31 Avenue de Versailles, *78170 La Celle St.-Cloud*
LIBRAIRIE LAVOISIER, 11 rue Lavoisier, *75008 Pari*
OFFICE INTERNATIONAL DE DOCUMENTATION ET LIBRAIRIE, 48 rue Gay-Lussac, *75240 Paris Cedex 05*

GERMAN DEMOCRATIC REPUBLIC
HAUS DER UNGARISCHEN KULTUR, Karl-Liebknecht-Strasse 9, *DDR-102 Berlin*
DEUTSCHE POST ZEITUNGSVERTRIEBSAMT, Strasse der Pariser Kommüne 3—4, *DDR-104 Berlin*

GERMAN FEDERAL REPUBLIC
KUNST UND WISSEN ERICH BIEBER, Postfach 46, *7000 Stuttgart 1*

GREAT BRITAIN
BLACKWELL'S PERIODICALS DIVISION, Hythe Bridge Street, *Oxford OX1 2ET*
BUMPUS, HALDANE AND MAXWELL LTD., Cowper Works, *Olney, Bucks MK46 4BN*
COLLET'S HOLDINGS LTD., Denington Estate. *Wellingborough, Northant NN8 2QT*
WM. DAWSON AND SONS LTD., Cannon House, *Folke tone, Kent CT19 5EE*
H. K. LEWIS AND CO., 136 Gower Street, *London WC1E 3BS*

GREECE
KOSTARAKIS BROTHERS, International Booksellers, 2 Hippokratous Street, *Athens-143*

HOLLAND
MEULENHOFF-BRUNA B.V., Beulingstraat 2, *Amsterdam*
MARTINUS NIJHOFF B.V., Lange Voorhout 9—11, *Den Haag*
SWETS SUBSCRIPTION SERVICE, 347b Heereweg, *Lisse*

INDIA
ALLIED PUBLISHING PRIVATE LTD., 13/14 Asaf Ali Road, *New Delhi 110001*
150 B-6 Mount Road, *Madras 600002*
INTERNATIONAL BOOK HOUSE PVT. LTD., Madame Cama Road, *Bombay 400039*
THE STATE TRADING CORPORATION OF INDIA LTD., Books Import Division, Chandralok, 36 Janpath, *New Delhi 110001*

ITALY
EUGENIO CARLUCCI, P.O. Box 252, *70100 Bari*
INTERSCIENTIA, Via Mazzé 28, *10149 Torino*
LIBRERIA COMMISSIONARIA SANSONI, Via Lamarmora 45, *50121 Firenze*
SANTO VANASIA, Via M. Macchi 58, *20124 Milano*
D. E. A., Via Lima 28, *00198 Roma*

JAPAN
KINOKUNIYA BOOK-STORE CO. LTD., 17-7 Shinjuku-ku 3 chome, Shinjuku-ku, *Tokyo 160-91*
MARUZEN COMPANY LTD., Book Department, P.O. Box 5050 Tokyo International, *Tokyo 100-31*
NAUKA LTD. IMPORT DEPARTMENT, 2-30-19 Minami Ikebukuro, Toshima-ku, *Tokyo 171*

KOREA
CHULPANMUL, *Phenjan*

NORWAY
TANUM-CAMMERMEYER, Karl Johansgatan 41—43, *1000 Oslo*

POLAND
WĘGIERSKI INSTYTUT KULTURY, Marszałkowska 80, *Warszawa*
CKP I W ul. Towarowa 28 *00-95 Warsawa*

ROUMANIA
D. E. P., *Bucureşti*
ROMLIBRI, Str. Biserica Amzei 7, *Bucureşti*

SOVIET UNION
SOJUZPETCHATJ — IMPORT, *Moscow*
and the post offices in each town
MEZHDUNARODNAYA KNIGA, *Moscow G-200*

SPAIN
DIAZ DE SANTOS, Lagasca 95, *Madrid 6*

SWEDEN
ALMQVIST AND WIKSELL, Gamla Brogatan 26, *101-20 Stockholm*
GUMPERTS UNIVERSITETSBOKHANDEL AB, Box 346, *401 25 Göteborg 1*

SWITZERLAND
KARGER LIBRI AG, Petersgraben 31, *4071 Basel*

USA
EBSCO SUBSCRIPTION SERVICES, P.O. Box 1943, *Birmingham, Alabama 35201*
F. W. FAXON COMPANY, INC., 15 Southwest Park, *Westwood, Mass, 02090*
THE MOORE-COTTRELL SUBSCRIPTION AGENCIES, *North Cohocton, N.Y. 14868*
READ-MORE PUBLICATIONS, INC., 140 Cedar Street, *New York, N. Y. 10006*
STECHERT-MACMILLAN, INC., 7250 Westfield Avenue, *Pennsauken N.J. 08110*

VIETNAM
XUNHASABA, 32, Hai Ba Trung, *Hanoi*

YUGOSLAVIA
JUGOSLAVENSKA KNJIGA, Terazije 27, *Beograd*
FORUM, Vojvode Mišića 1, *21000 Novi Sad*

HU ISSN 0001—5407 Index: 26.007